DISS. ETH NO. 27312

POLAR MICROPOLLUTANTS AND THEIR TRANSFORMATION PRODUCTS IN GROUNDWATER: IDENTIFICATION WITH LC-HRMS AND THEIR ABATEMENT IN WATER TREATMENT

A thesis submitted to attain the degree of

DOCTOR OF SCIENCES of ETH ZURICH

(Dr. sc. ETH Zurich)

presented by

KARIN KIEFER

M.Sc. Geoecology, Karlsruhe Institute of Technology

born on 25.10.1989

citizen of Germany

accepted on the recommendation of

Prof. Dr. Juliane Hollender (examiner)

Prof. Dr. Thorsten Reemtsma (co-examiner)

Prof. Dr. Urs von Gunten (co-examiner)

Prof. Dr. Bernhard Wehrli (co-examiner)

2021

Contents

Summary v

Zusammenfassung vii

Chapter 1: Introduction 1

1.1 Groundwater – a Major Drinking Water Resource 2
1.2 Analytical Methods to Identify Contaminants 4
1.3 Drinking Water Treatment 7
1.4 Objectives and Thesis Contents 9
References 11

Chapter 2: New Relevant Pesticide Transformation Products in Groundwater Detected Using Target and Suspect Screening for Agricultural and Urban Micropollutants with LC-HRMS 19

Abstract 20
2.1 Introduction 21
2.2 Methods 22
2.2.1 Groundwater Samples 22
2.2.2 Sampling 23
2.2.3 Sample Enrichment 23
2.2.4 LC-HRMS/MS 23
2.2.5 Target Screening 24
2.2.6 Suspect Screening 24
2.3 Results and Discussion 26
2.3.1 Target Screening 26
2.3.2 Suspect Screening 26
2.3.3 New Pesticide TPs 30
2.3.4 Agricultural vs. Urban Pollution 32
2.4 Conclusions 35
Acknowledgement 36
References 37

Chapter SI2: Supporting Information to Chapter 2 41

Chapter 3: Identification of LC-HRMS Nontarget Signals in Groundwater After Source Related Prioritization 103

Abstract 104
3.1 Introduction 105
3.2 Methods 106
3.2.1 Groundwater Samples 106
3.2.2 Sample Preparation via Vacuum-Assisted Evaporation 107

3.2.3 LC-HRMS/MS Analysis 107
3.2.4 Target Screening 108
3.2.5 Suspect and Nontarget Screening 108
3.3 Results and Discussion 111
3.3.1 Sample Classification based on Targets 111
3.3.2 Classification of Nontargets 113
3.3.3 Characterization of Groundwater Quality at Monitoring Sites 116
3.3.4 Identification of Nontargets and Suspects 118
3.4 Conclusions 123
Acknowledgements 123
References 124

Chapter SI3: Supporting Information to Chapter 3 131

Chapter 4: Chlorothalonil Transformation Products in Drinking Water Resources: Widespread and Challenging to Abate 197

Abstract 198
4.1 Introduction 199
4.2 Materials and Methods 200
4.2.1 Drinking Water Resources and Waterworks 200
4.2.2 Stock Solutions and Chemicals 201
4.2.3 Laboratory and Pilot-Scale Experiments 201
4.2.4 Analytical Methods 204
4.3 Results and Discussion 206
4.3.1 Chlorothalonil TPs in Drinking Water Resources 206
4.3.2 Abatement of Chlorothalonil TPs during Drinking Water Treatment 208
4.3.3 Laboratory Experiments 210
4.3.4 Practical Implications 214
4.4 Conclusions 214
Acknowledgements 215
References 216

Chapter SI4: Supporting Information to Chapter 4 221

Chapter 5: Conclusions and Outlook 241

5.1 Comprehensive Screening for Micropollutants and its Limitations 242
5.2 Chlorothalonil TPs: Widespread and Challenging to Abate 245
5.3 Practical Implications and General Outlook 246
References 248

Acknowledgements 251

Curriculum Vitae 253

Summary

Groundwater is a major drinking water resource, providing on average 50% of domestic water supply worldwide; in several European countries, this can even be as high as 70-100%. Although groundwater is better protected from anthropogenic influences than surface waters, a broad variety of chemicals used in agriculture, households, and industry have been detected in groundwater in the ngL^{-1} to μgL^{-1} range. Chemicals may enter groundwater via seepage after pesticide application to agricultural soils, from leaky sewers, or from the infiltration of wastewater-impacted surface waters. Natural attenuation processes such as sorption and (bio)transformation do not sufficiently retain polar, mobile, and persistent micropollutants (MPs) and may even lead to the formation of polar transformation products (TPs). Compared to the large number of chemicals potentially released into the aquatic environment, previous research and monitoring programs focused only on a few compounds so that groundwater quality with regard to organic MPs is largely unknown.

Therefore, this work aimed to comprehensively screen groundwater for polar MPs from agricultural and urban sources. The majority of investigated groundwater samples originated from areas with intense agricultural use and/or densely populated areas in Switzerland. To ensure a sensitive detection of polar compounds, samples were enriched using vacuum-assisted evaporation followed by reversed-phase liquid chromatography coupled to high-resolution tandem mass spectrometry (RPLC-HRMS/MS). Target, suspect, and nontarget screening approaches enabled analysis of the samples (i) for MPs, for which reference material was available (targets), (ii) for MPs that were expected to be present (suspects), and (iii) for the remaining signals without prior information (nontargets).

First, 31 groundwater samples were systematically screened for pesticides and their TPs, primarily originating from agriculture. The screening included all pesticides (>300) approved in Switzerland from 2005 to 2017 and more than 1100 TPs, which were mostly experimentally observed in the European pesticide registration. 169 pesticides and 67 pesticide TPs were covered by target screening; the remaining pesticides and TPs were detected with suspect screening. To identify additional contamination sources, 283 target compounds (such as pharmaceuticals and food additives) from urban sources were quantified. Suspect hits were assessed for plausibility based on intensity, isotope pattern, retention time prediction, and in silico fragmentation. Finally, 22 suspects were identified unequivocally with reference material and five suspects were tentatively identified. The occurrence of 13 pesticide TPs in groundwater was reported for the first time. Among these novel pesticide TPs were six TPs of the fungicide chlorothalonil. Chlorothalonil TP R471811 had highest concentrations among all investigated MPs (up to 2700 ngL^{-1}) and was the only MP detected in all samples. As previously observed, pesticide TPs showed higher concentrations than the applied pesticides, demonstrating their importance for a comprehensive assessment of groundwater quality.

After the systematic screening for pesticides and their TPs, we focused on potential MPs from urban origin. Using a target screening for 269 urban MPs and 229 agricultural MPs, each of the 60 groundwater samples was classified with regard to the extent of urban and agricultural influence (high or low influence). Next, all LC-HRMS signals were categorized as (i) potential

urban MP, (ii) potential urban and/or agricultural MP, (iii) potential agricultural MP, and (iv) not classifiable, depending on their occurrence and intensity in the classified samples. According to this, the 498 target compounds would explain 4-72% of estimated concentrations of potential urban and/or agricultural MPs in individual samples (8-28% based on detections). Additionally, the most intense nontargets were annotated with proposed structures with an automated method using two in silico fragmenters (MetFrag and SIRIUS4/CSI:FingerID) and a list of >988,000 potentially environmentally relevant compounds. To avoid missing important urban MPs, nontarget screening was complemented with a suspect screening for 1162 polar compounds, primarily from urban origin. Finally, 22 compounds were identified unequivocally with reference material and 18 compounds were tentatively identified; among these were 13 compounds that were reported in groundwater for the first time. In addition, the nontarget screening showed that one monitoring site was far more contaminated than the other sites, demonstrating the importance of broad screening approaches.

Finally, the occurrence of chlorothalonil TPs in drinking water resources (i.e. 73 groundwater and four surface water samples) and their fate in water treatment were investigated. After the re-evaluation of approval of the fungicide chlorothalonil in the European Union and Switzerland, Swiss authorities declared all TPs of chlorothalonil to be “relevant”, implying a drinking water standard of 100 ngL^{-1}. The chlorothalonil sulfonic acid TPs (R471811, R417888, R419492) were detected at higher concentrations and more frequently in the investigated drinking water resources (>100 ngL^{-1} in up to 52% of samples) than the phenolic TPs (SYN507900, SYN548580, R611968; >100 ngL^{-1} in up to 3% of samples). Moreover, the sulfonic acid TPs are more challenging to abate in water treatment. The sulfonic acid TPs persist in UV disinfection, ozonation, and advanced oxidation processes, whereas the phenolic TPs are abated in these processes (partially or below detection limit). Reverse osmosis and activated carbon were found to successfully abate all TPs. However, the reverse osmosis process produces large volumes of reject water and activated carbon needs to be regenerated or exchanged very frequently to sufficiently abate the TP with highest concentrations (R471811).

The presented groundwater screening revealed several MPs that were not previously reported, but many potential MPs remained unknown because they could not be elucidated or were not detected. Gaps in the screening included compounds (i) which were not part of the compound lists such as novel TPs, (ii) which were not detectable with the applied analytical approach (e.g. too polar/apolar, too small, not ionizable), and (iii) which could not be elucidated due to issues in data analysis or unavailable reference material. MPs, which are mobile and persistent in the environment, may also persist in waterworks, thereby posing a risk to the water supply, as illustrated by the example of chlorothalonil TPs. With future progress in analytics, more MPs will be detected in groundwater, but their evaluation in the regulatory context and their fate in water treatment are still unknown. This situation highlights the importance of precautionary measures, preventing the release of chemicals to the aquatic cycle, to preserve groundwater resources.

Zusammenfassung

Grundwasser ist eine wichtige Trinkwasserressource, welche weltweit 50% des Wasserbedarfs von Haushalten bereitstellt und in mehreren europäischen Ländern sogar 70-100%. Obwohl Grundwasser besser vor anthropogenen Einflüssen geschützt ist als Oberflächengewässer, wurden im Grundwasser zahlreiche Chemikalien aus der Landwirtschaft, Haushalten und Industrie im ngL^{-1} bis μgL^{-1} Bereich nachgewiesen. Chemikalien können mit dem Sickerwasser ins Grundwasser eingetragen werden infolge der Anwendung von Pestiziden auf landwirtschaftlichen Böden, aufgrund undichter Abwasserkanäle oder durch die Infiltration von mit Abwasser belasteten Oberflächengewässern. Natürliche Prozesse wie Sorption und (Bio-) Transformation halten polare, mobile und persistente Spurenstoffe nicht ausreichend zurück und können sogar zur Bildung polarer Transformationsprodukte (TPs) führen. Im Vergleich zur grossen Zahl an Chemikalien, die möglicherweise in den Wasserkreislauf freigesetzt werden, umfassten bisherige Untersuchungen und Monitoringprogramme nur wenige Verbindungen, so dass die Grundwasserqualität in Bezug auf organische Spurenstoffe weitgehend unbekannt ist.

Ziel dieser Arbeit war es daher, das Grundwasser umfassend auf polare Spurenstoffe aus landwirtschaftlichen und urbanen Quellen zu untersuchen. Der Grossteil der untersuchten Grundwasserproben stammte aus landwirtschaftlich intensiv genutzten und/oder dicht besiedelten Gebieten der Schweiz. Um polare Substanzen empfindlich nachzuweisen, wurden die Proben mittels Verdampfung unter Vakuum angereichert und anschliessend mit Umkehrphasen-Flüssigchromatographie gekoppelt an die hochauflösende Tandem-Massenspektrometrie (RPLC-HRMS/MS) analysiert. Target-, Suspect- und Nontarget-Screening-Ansätze ermöglichten die Analyse der Proben (i) auf Spurenstoffe, für die Referenzmaterial zur Verfügung stand (Targets), (ii) auf erwartete Spurenstoffe (Suspects), und (iii) auf die verbleibenden Signale ohne vorherige Informationen (Nontargets).

Zunächst wurden 31 Grundwasserproben systematisch auf Pestizide und deren TPs untersucht, welche hauptsächlich aus der Landwirtschaft stammen. Das Screening umfasste alle von 2005 bis 2017 in der Schweiz zugelassenen Pestizide (> 300) und mehr als 1100 TPs, die grösstenteils experimentell in der europäischen Pestizidzulassung beobachtet wurden. 169 Pestizide und 67 Pestizid-TPs wurden mittels Target-Screening abgedeckt, die verbleibenden Pestizide und TPs mittels Suspect-Screening. Um zusätzliche Kontaminationsquellen zu identifizieren, wurden 283 Target-Substanzen aus urbanen Quellen quantifiziert (beispielsweise Pharmazeutika und Lebensmittelzusatzstoffe). Suspect-Treffer wurden basierend auf Intensität, Isotopenmuster, Vorhersage der Retentionszeit und In-Silico-Fragmentierung auf Plausibilität überprüft. Schliesslich wurden 22 Suspects eindeutig mit Referenzmaterial identifiziert und fünf Suspects wurden vorläufig identifiziert. Das Auftreten von 13 Pestizid-TPs im Grundwasser wurde zum ersten Mal erwähnt. Unter diesen neuen Pestizid-TPs befanden sich sechs TPs des Fungizids Chlorothalonil. Chlorothalonil TP R471811 wies die höchsten Konzentrationen unter allen untersuchten Spurenstoffen auf (bis zu 2700 ngL^{-1}) und wurde als einziger Spurenstoff in allen Proben nachgewiesen. Wie bereits zuvor beobachtet, zeigten Pestizid-TPs höhere Konzentrationen als die angewandten Pestizide, was ihre Bedeutung für eine umfassende Bewertung der Grundwasserqualität hervorhebt.

Nach dem systematischen Screening auf Pestizide und deren TPs konzentrierten wir uns auf potenzielle Spurenstoffe urbaner Herkunft. Mittels eines Target-Screenings nach 269 urbanen Spurenstoffen und 229 landwirtschaftlichen Spurenstoffen wurde jede der 60 Grundwasser-Proben hinsichtlich des Ausmasses des urbanen und landwirtschaftlichen Einflusses klassifiziert (hoher oder geringer Einfluss). Als nächstes wurden alle LC-HRMS-Signale basierend auf ihrem Auftreten und ihrer Intensität in den klassifizierten Proben in folgende Kategorien eingeteilt: (i) potenziell urbane Spurenstoffe, (ii) potenziell urbane und/oder landwirtschaftliche Spurenstoffe, (iii) potenziell landwirtschaftliche Spurenstoffe und (iv) nicht klassifizierbar. Demnach würden die 498 Target-Substanzen 4-72% der geschätzten Konzentrationen potenziell urbaner und/oder landwirtschaftlicher Spurenstoffe in den einzelnen Proben erklären (8-28% basierend auf Detektionen). Anschliessend wurden die intensivsten Nontargets in automatisierter Weise mit Strukturvorschlägen annotiert, wobei zwei In-Silico-Fragmentierungstools (MetFrag and SIRIUS4/CSI:FingerID) mit einer Liste von >988'000 potenziell umweltrelevanter Verbindungen verwendet wurden. Um wichtige urbane Spurenstoffe nicht zu übersehen, wurde das Nontarget-Screening durch ein Suspect-Screening auf 1162 polare Substanzen, hauptsächlich aus urbanen Quellen, ergänzt. Schliesslich wurden 22 Substanzen eindeutig mit Referenzmaterial und 18 Substanzen vorläufig identifiziert, von denen 13 Substanzen erstmals im Grundwasser nachgewiesen wurden. Zudem zeigte das Nontarget-Screening, dass eine Messstelle weitaus stärker kontaminiert war als die anderen, was die Bedeutung von Screening-Ansätzen mit breitem Anwendungsbereich veranschaulicht.

Schliesslich wurde das Auftreten von Chlorothalonil-TPs in Trinkwasserressourcen (73 Grundwasser- und vier Oberflächenwasserproben) und deren Verhalten in der Wasseraufbereitung untersucht. Nach der Neubewertung der Zulassung des Fungizids Chlorothalonil in der Europäischen Union und der Schweiz stuften die Schweizer Behörden alle TPs von Chlorothalonil als „relevant" ein, was einen Trinkwasserhöchstwert von 100 ngL^{-1} impliziert. Die Chlorothalonil-Sulfonsäure-TPs (R471811, R417888, R419492) wurden in höheren Konzentrationen und häufiger in den untersuchten Trinkwasserressourcen (>100 ngL^{-1} in bis zu 52% der Proben) nachgewiesen als die phenolischen TPs (SYN507900, SYN548580, R611968; >100 ngL^{-1} in bis zu 3% der Proben). Darüber hinaus ist es schwieriger, die Sulfonsäure-TPs in der Wasseraufbereitung zu entfernen. Die Sulfonsäure-TPs sind in der UV-Desinfektion, Ozonung und erweiterten Oxidationsverfahren persistent, während die phenolischen TPs bei diesen Prozessen entfernt werden (teilweise oder bis unterhalb der Nachweisgrenze). Umkehrosmose und Aktivkohle können die Konzentration von allen TPs verringern. Die Umkehrosmose verursacht jedoch grosse Mengen an Konzentrat und die Aktivkohle muss sehr häufig regeneriert oder ausgetauscht werden, um das TP mit den höchsten Konzentrationen (R471811) ausreichend zu entfernen.

Das vorgestellte Grundwasserscreening zeigte mehrere Spurenstoffe auf, die vorher nicht bekannt waren. Dennoch blieben viele potenzielle Spurenstoffe unbekannt, da sie nicht aufgeklärt werden konnten oder nicht nachgewiesen wurden. Lücken im Screening umfassten Substanzen, (i) die nicht Teil der Substanzlisten waren, wie neuartige TPs, (ii) die mit dem angewandten analytischen Ansatz nicht nachweisbar waren (z.B. zu polar/unpolar, zu klein, nicht ionisierbar), und (iii) die aufgrund von Problemen bei der Datenanalyse oder fehlendem Referenzmaterial nicht aufgeklärt werden konnten. Spurenstoffe, die mobil und in der Umwelt persistent sind, können auch in Wasserwerken bestehen bleiben und so ein Risiko für die Wasserversorgung darstellen, wie das Beispiel der Chlorothalonil-TPs zeigt. Mit zukünftigen

Fortschritten in der Analytik werden mehr Spurenstoffe im Grundwasser entdeckt werden, aber ihre Bewertung im regulatorischen Kontext und ihr Verhalten in der Wasseraufbereitung sind noch unbekannt. Dies unterstreicht die Bedeutung von Vorsorgemassnahmen, um die Freisetzung von Chemikalien in den Wasserkreislauf zu verhindern und so die Grundwasserressourcen zu schützen.

Chapter 1: Introduction

1.1 Groundwater – a Major Drinking Water Resource

Groundwater is in many regions the **major drinking water resource**, providing worldwide approximately 50% of domestic water supply, in Germany and Switzerland 70-80%, and in some countries such as Denmark and Austria even 100% (FAO 2016, Zektser and Everett 2004). The high importance of groundwater for drinking water production compared to surface water results mainly from its better protection from contamination (Zektser and Everett 2004), minimizing the need for water treatment. Nevertheless, a broad variety of chemicals used in agriculture, households and industry has been reported in groundwater at concentrations in the ngL^{-1} to μgL^{-1} range, e.g. pesticides, personal care products, pharmaceuticals, food additives, hormones, stimulants, plasticisers, or industrial chemicals, and associated transformation products (TPs) (Lapworth et al. 2012). These micropollutants (MPs) originate from various sources such as manure and pesticide application in agriculture (Postigo and Barcelo 2015), leachate from landfills (Holm et al. 1995, Müller et al. 2011), industrial sites (Postigo and Barcelo 2015), or sewer systems (Wolf et al. 2012), and the infiltration of possibly contaminated surface waters, either naturally or via managed aquifer recharge (Díaz-Cruz and Barceló 2008, Hamann et al. 2016) (Figure 1). Compared to the large number of chemicals registered worldwide (>350,000; Wang et al. (2020)), monitoring studies cover only a very small fraction; e.g. the Swiss National Groundwater Monitoring NAQUA monitored approximately 200-300 organic MPs from 2007-2016 (BAFU 2019). Therefore, groundwater quality is largely unknown.

The MP composition and concentrations detected in groundwater depend, on the one hand, on the amounts of each compound that are released from their respective sources and, on the other hand, on the relevant transport processes. **Transport of MPs** is linked to MP properties and aquifer/top layers characteristics, both influencing the extent of MP attenuation by dilution, sorption to organic matter or mineral surfaces, or chemical and biological transformation. Sorption is highly dependent on substance properties (charge, hydrophobicity), the

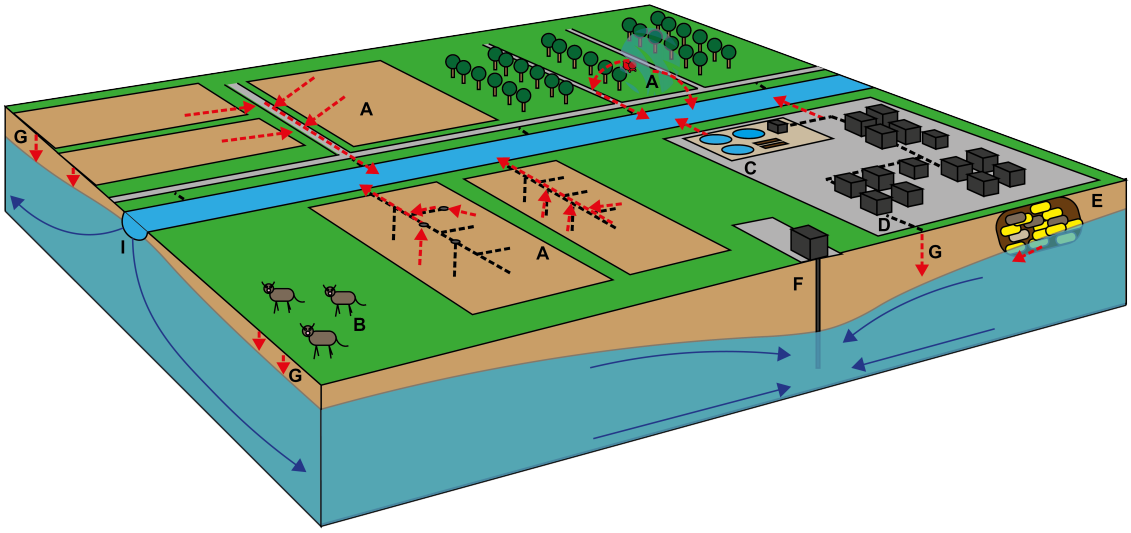

Figure 1: Pesticide application (A), livestock farming (B), municipal and industrial wastewater treatment plants (C), leaky sewers (D), or landfills (E) threaten groundwater quality. Pollutants may reach the groundwater abstraction well (F) or spring either via seepage (G) or infiltrating surface water (I). Figure: Urs Schönenberger & Karin Kiefer, Eawag.

hydrogeological setting (clay and organic matter content of aquifer and top layers), and groundwater characteristics (ionic strength) (Lapworth et al. 2012, Postigo and Barcelo 2015). For example, the artificial sweetener acesulfame has a negative net charge and low hydrophobicity and biodegradability, resulting in low sorption and high mobility, and is subsequently nearly ubiquitous in groundwater (Postigo and Barcelo 2015, Scheurer et al. 2009). Conversely, polychlorinated biphenyls (PCBs) are also persistent but hydrophobic, and therefore are readily removed by adsorption (Reemtsma et al. 2016). Furthermore, degradation reduces MP concentrations in the water phase but can lead to the formation of TPs that may be even more persistent and mobile, thereby increasing the number of xenobiotics present in groundwater. Several studies reported higher concentrations of the TPs compared to the corresponding parent compounds, especially in the case of pesticides (Buttiglieri et al. 2009, Kolpin et al. 1998, Kormos et al. 2011). Transport processes and degradation favour the presence of persistent and mobile organic compounds, so-called PMOCs (Reemtsma et al. 2016), and lead to higher vulnerability of shallow alluvial, unconfined or karstic aquifers compared to confined and deep aquifers (Lapworth et al. 2012). On the other hand, long water residence times and poor microbial activity in deep groundwater bodies may result in aquifer systems acting as MP reservoirs (Postigo and Barcelo 2015).

Therefore, to protect aquatic systems including aquifers, various measures have already been or are currently being implemented in Switzerland. Selected wastewater treatment plants will be upgraded with advanced treatment including ozonation or activated carbon, reducing the MP load released to the aquatic environment (WPA 814.20). **Groundwater protection** zones were designated in the proximity of drinking water abstraction wells, restricting land use to a varying extent, depending on the distance to the well. Groundwater protection zone S1 (immediate surrounding of the well) only allows activities connected to water supply (WPO 814.201); protection zone S2 (groundwater flow >10 days from outer border to the well) limits constructions and excavations and prohibits the use of wood preservatives, liquid farm manures, and selected plant protection products (ORRChem 814.81 , PPPO 916.161 , WPO 814.201); protection zone S3 (distance from outer border of S3 to S2 at least as great as from outer border of S2 to S1) should guarantee enough time to take measures to protect the drinking water well, e.g. in the case of accidents with hazardous substances (WPO 814.201).

In addition to reducing the input of chemicals to groundwater via improved wastewater treatment or restrictions in land use, the use of certain chemicals is regulated on a European as well as a national level. Chemicals used above 1 ton per year (t a^{-1}) on the European market are registered and authorised under the European Union (EU) **regulation REACH** (Registration, Evaluation, Authorisation and Restriction of Chemicals) (Regulation (EC) 1907/2006), affecting also most chemicals used in Switzerland due to the tight economic exchange with the EU. For chemicals used at quantities >10 t a^{-1}, REACH requires that chemicals be assessed if they are persistent, bioaccumulative, and toxic or very persistent and very bioaccumulative (PBT/vPvB) (Regulation (EC) 1907/2006). A comparable assessment for being mobile (i.e. persistent, mobile and toxic or very persistent and very mobile, PMT/vPvM) is expected to be implemented in REACH (EC 2020, Hale et al. 2020). The industry could then replace chemicals identified as PMT/vPvM compounds or implement risk mitigation measures to reduce their release to the environment. Moreover, water suppliers could even enforce the polluter to remediate drinking water resources (Neumann and Schliebner 2017).

Specific chemicals such as **pesticides** are regulated by the Plant Protection Products Ordinance (PPPO 916.161) and the Biocidal Products Ordinance (BPO 813.12), depending on their use on plants or on other applications, respectively. Corresponding regulations exist as well on the EU level (Regulation (EC) 1107/2009 , Regulation (EU) 528/2012). The **registration** of active substances in plant protection products requires a risk assessment performed by the industry concerning the toxicology to mammals, ecotoxicological impacts on non-target organisms, the formation of TPs in the environment, and the fate of the active substance and its TPs in the environment (Regulation (EC) 1107/2009). Pesticide TPs are classified as "relevant" if they are considered to be toxic, to have pesticidal effects, or if the active substance is classified as carcinogen category 1A or 1B; if none of these criteria are met, compounds are considered "non-relevant", as described in the EU guidance document Sanco/221/2000 –rev.10- final (European Commission 2003). For pesticides and their relevant TPs, a drinking water standard of 100 ngL^{-1} applies in Switzerland and the EU (EDI 2016, European Commission 1998). Except for pesticides and TPs and few selected pollutants (e.g. polycyclic aromatic hydrocarbons), the European drinking water directive does not regulate organic MPs (European Commission 1998). In contrast, the Swiss drinking water directive provides maximum values for compounds with unknown toxicity but with structural hints to a genotoxic potential (100 ngL^{-1}) and for compounds with unknown toxicity and without structural hints to a genotoxic potential (10 μgL^{-1}) (EDI 2016).

Various studies used data from chemicals regulation to monitor these compounds in the aquatic environment, demonstrating the high value of regulatory data (Gago-Ferrero et al. 2018, Schulze et al. 2019, Singer et al. 2016). Especially, a target screening for pesticide TPs revealed blind spots in surface and groundwater quality (Reemtsma et al. 2013a). However, some pesticide TPs might have been overlooked due to restrictions in analytics and limited access to reference material (Reemtsma et al. 2013b).

1.2 Analytical Methods to Identify Contaminants

High-performance liquid chromatography coupled by electrospray ionization to **high-resolution tandem mass spectrometry** (HPLC-ESI-HRMS/MS) is widely used today to detect known and unknown pollutants at trace level concentrations. The first environmental applications of LC-HRMS were published around 1999/2000 using time-of-flight instruments; since 2008 additionally using Orbitrap mass spectrometers (Hernandez et al. 2012). In contrast to triple quadrupole mass spectrometers with unit resolution, HRMS enables the simultaneous detection of thousands of molecules at high sensitivity and high precision, including determination of the mass-to-charge ratio (m/z) of a molecular ion to the third or even fourth decimal place, without the preselection of analytes (Krauss et al. 2010). Samples measured by HRMS can even be screened retrospectively, years after the analysis, thus facilitating the creation of digital sample archives (Alygizakis et al. 2019). Unknown nontarget compounds can be assigned with molecular formulae and proposed structures, using fragments generated during MS/MS experiments. Depending on the type of MS/MS experiments, i.e. data-dependent or data-independent acquisition, either selected analytes (e.g. based on a mass list and/or intensity ranking) or all analytes (within larger isolation windows) are fragmented. Data-dependent acquisition produces high-quality MS/MS spectra, but only for a limited amount of analytes. In contrast, data-independent acquisition covers all analytes, facilitating retrospective screenings (Renaud

et al. 2017). However, the elucidation of unknown compounds requires the assignment of MS/MS fragments to its precursor, which remains challenging in data-independent acquisition (Zhang et al. 2020).

Although HRMS can simultaneously detect a large number of molecules, the compounds reaching the detector depend on the **chromatographic approach** and the ionization interface applied. Most studies focusing on polar to semi-polar compounds use reversed-phase (RP) LC in combination with ESI (Leendert et al. 2015), a soft ionization method suitable for a wide polarity range including very polar compounds (Rosenberg 2003). However, Reemtsma et al. (2016) recently pointed out that current RPLC-based analytics do not sufficiently cover very polar compounds and proposed to close this analytical gap by using additional chromatographic approaches such as ion-exchange chromatography (IC) (Barron and Gilchrist 2014), hydrophilic interaction LC (HILIC) (Jandera 2011), supercritical fluid chromatography (SFC) (Lesellier and West 2015), or mixed mode (MM) LC, combining RPLC or HILIC with ion exchange properties (Zhang et al. 2016). Schulze et al. (2019) recently compared different chromatographic systems by targeting 64 PMOCs. Seven PMOCs were detected with only one approach, while 37 were detected by all approaches. The number of analytes detected in each approach was rather similar; RPLC and MMLC covered up to 47 PMOCs, SFC covered up to 50 PMOCs, and HILIC 55. Consequently, the choice of a chromatographic system excludes certain analytes; however, the tradeoff of using several chromatographic approaches is an increase in time and effort for both analysis and data evaluation.

MPs are generally present at low concentrations in groundwater and sensitive detection requires **enrichment** of samples prior to analysis. Analogous to selection of the chromatographic method, the selected method of enrichment also discriminates against certain analytes (Köke et al. 2018, Mechelke et al. 2019, Schulze et al. 2019). Solid-phase extraction (SPE) is widely used in environmental studies (Huntscha et al. 2012, Loos et al. 2010, Sjerps et al. 2016), additionally acting as sample clean-up. To enrich a wide scope of analytes with different physicochemical properties, mixed-bed multi-layer SPE cartridges can be beneficial (Mechelke et al. 2019). Alternatives to SPE are freeze-drying (Montes et al. 2017) or evaporation (Köke et al. 2018, Mechelke et al. 2019). Vacuum-assisted evaporation reduces not only the loss of polar compounds but also the need of solvents, being therefore a more environmentally friendly alternative to SPE. However, with this method matrix components such as salts are also enriched, leading to significant signal suppression in ESI (Köke et al. 2018, Mechelke et al. 2019) or adduct formation.

Sophisticated **data analysis workflows** have been and are still being developed to extract as much as possible from the huge amounts of data acquired using LC-HRMS/MS. Three major data analysis approaches are differentiated, i.e. target, suspect, and nontarget screening (Krauss et al. 2010). First, **target screening** includes compounds for which reference standards are available in the laboratory. For these compounds not only the exact mass but also MS/MS fragments and the retention time on the relevant chromatographic system are known. The availability of reference material confirms that the target compound can be analysed with the selected analytical approach and also allows for quantification. Second, **suspect screening** can be used to search for compounds expected in the sample based on the exact mass (obtained from the molecular structure). Possible hits can be checked for plausibility by comparing measured MS/MS fragments with in silico predicted MS/MS fragments and by predicting

retention time from molecular structure (Aalizadeh et al. 2019, Kern et al. 2009, Moschet et al. 2013). Suspect screening is a valuable supplement to target screening for cases where the reference material of a compound of interest is either unavailable or too expensive, as shown by a nearly complete pesticide screening in Swiss surface waters (Moschet et al. 2014). Third, **nontarget screening** refers to all remaining LC-HRMS signals or peaks about which no prior information is known. Whereas target and suspect screening aim to elucidate individual peaks based on a target or suspect list, nontarget screening is more and more understood as a pattern analysis tool, providing a deeper understanding of the dataset, followed by the elucidation of prioritized peaks (Hollender et al. 2017).

Prior to the suspect or nontarget screening, LC-HRMS data need to be pre-processed, using vendor or open-source software or workflows (Bletsou et al. 2015, Hohrenk et al. 2019, Menger et al. 2020). **Data pre-processing** can include peak detection ("peak picking"), grouping of peaks originating from the same compound such as isotopologues, adducts, or in-source fragments ("componentization"), retention time alignment, intensity normalization, replicate filtering, and blank subtraction or annotation (Bader et al. 2016, Hollender et al. 2017, Katajamaa and Orešič 2007). The success of the pre-processing is evaluated using target compounds (Moschet et al. 2013). The final peak or compound table with the intensities in individual samples is then annotated with suspects based on their exact mass or is used for the prioritization of nontargets of interest.

Prioritization strategies in the subsequent data analysis depend on the experimental set-up, sampling approach and thereby the underlying research question. Peak intensity is a major criterion for prioritization, assuming that intensity correlates with concentration. Some studies focused on peaks with a characteristic isotope pattern, indicating e.g. Cl or Br and therefore a likely anthropogenic origin (Hug et al. 2014, Ruff et al. 2015). Underlying patterns in a dataset can be analysed to find compounds that are (i) persistent in drinking water supply (Müller et al. 2011), (ii) being discharged along a river course (Ruff et al. 2015), (iii) being discharged by industry but not by households (Anliker et al. 2020), (iii) being discharged in the past but still detectable in bank filtrate or sediments (Albergamo et al. 2019, Chiaia-Hernandez et al. 2017), or (iv) being formed in wastewater treatment plants (Schollée et al. 2015, Schollée et al. 2018). The applied prioritization strategies range from determining the absence/presence or intensity decrease/increase of a peak in specific samples or determining the intensity variation in temporally related samples, to applying multivariate statistics such as hierarchical cluster analysis or principal component analysis. The challenge of differentiating between anthropogenic and natural compounds is probably common to all studies focusing on MPs.

Compared to the high number of nontarget peaks detected or prioritized (often >1000), environmental studies so far only result in the elucidation of a few nontarget peaks with high confidence (e.g. Müller et al. (2011), Gago-Ferrero et al. (2015), Ruff et al. (2015), Koppe et al. (2020); all <20 unequivocal identifications), demonstrating that **structure elucidation** is still a major bottleneck in nontarget screening. The first step is generally to assign a molecular formula to the nontarget of interest. However, often several formulae can be assigned (Gago-Ferrero et al. 2015, Hug et al. 2014), depending on assumed mass accuracy and the elements included. Next, to propose a structure, databases such as ChemSpider (RSC 2020), PubChem (Kim et al. 2019), CompTox Chemistry Dashboard (Williams et al. 2017), and NORMAN Suspect List exchange (www.norman-network.com/nds/SLE) can be searched for the assigned molecular

formulae or the assumed monoisotopic mass. However, these searches regularly result in hundreds or even thousands of candidate structures (Müller et al. 2011, Ruff et al. 2015). To rank the candidates, database searches can be combined with in silico fragmentation tools such as MetFrag (Ruttkies et al. 2016), SIRIUS4/CSI:FingerID (Dührkop et al. 2015, Dührkop et al. 2019), or CFM-ID (Allen et al. 2014). These software search the databases using the measured accurate mass or suggested molecular formulae for candidates and subsequently check if the measured MS/MS spectra can be explained by the structure. Different software use different approaches to rank candidates. For example, MetFrag applies a bond dissociation approach to predict fragments, while SIRIUS4/CSI:FingerID uses a fragmentation tree approach to predict a molecular fingerprint from the measured spectrum. In addition, MetFrag incorporates additional information such as metadata (e.g. reference counts in databases), retention time prediction, or similarity to MS/MS spectra in the library MassBank of North America (MoNA, http://mona.fiehnlab.ucdavis.edu/). Measured MS/MS spectra can also be directly compared to experimental spectra in libraries such as MoNA, mzCloud (www.mzcloud.org), or the European MassBank (Horai et al. 2010, Schulze et al. 2012). A match in an MS/MS library offers higher confidence structural assignment than in silico prediction (Schymanski et al. 2014), but the number of compounds covered by experimental MS/MS spectra in libraries is limited (Vinaixa et al. 2016). Some recent studies applied in silico fragmenters in more automated methods to cover not only a few individual peaks of interest but several hundred (Albergamo et al. 2019, Tian et al. 2020), thereby achieving slightly more confirmations with high confidence compared to former environmental studies. The elucidation of true unknowns, i.e. compounds that are not present in any database (for example TPs that have not yet been observed), is probably rather unlikely, except if additional information is available as e.g. in the case of transformation experiments (Huntscha et al. 2014, Nika et al. 2017, Zahn et al. 2019).

When assigning proposed structures to nontargets it is important to carefully communicate the **confidence in the elucidation**. In 2014, Schymanski et al. (2014) proposed a classification scheme with five confidence levels. Unequivocal confirmation (Level 1) is only achieved if a reference standard is measured in the laboratory with the same analytical method, enabling comparison of retention time and MS/MS fragments of the peak of interest with retention time and MS/MS fragments of the reference standard. Probable structures are assigned based on an MS/MS match in the literature or libraries (Level 2a) or diagnostic evidence (e.g. experimental context, no other structure possible; Level 2b). Level 3 describes tentative candidates and may also include the possibility of several isomers. Level 4 and Level 5 represent peaks of interest, for which either an unequivocal molecular formula can be reported or only the measured accurate mass, respectively.

With the large advances recently in analytical chemistry, a huge array of compounds can be measured. However, these methods still only include compounds that are amenable to measurement. Furthermore, progress in the areas of data analysis and structure elucidation are continually increasing the number of compounds that can be identified. However, it remains critical that confidence in identification is communicated clearly.

1.3 Drinking Water Treatment

So far, drinking water treatment in Switzerland primarily targets the removal of particles and microbiological contaminants, although some of the applied treatment processes may also

abate MPs. Surface water and karstic spring water (ca. 20-30% of Swiss drinking water, SVGW (2016)) require a multi-step treatment comprising of e.g. flocculation and sand filtration for suspended solids removal, ozonation or chlorination for disinfection, and activated carbon filtration for reducing taste/odour impairments and potential oxidation by-products. Membrane processes such as micro- or ultrafiltration offer an alternative to multi-step treatments (Moel et al. 2006, Pianta et al. 2000). Furthermore, surface water quality can be improved by managed aquifer recharge (ca. 15% of Swiss drinking water, considered to be groundwater in the statistics, SVGW (2016)). Strategies include the infiltration of surface water into the aquifer via bank filtration or infiltration ponds, which leads to full or partial removal of suspended solids, bacteria, and viruses (Hiscock and Grischek 2002, Moel et al. 2006). Groundwater from porous (or slightly fissured) aquifers is usually either directly used as drinking water (ca. 30% of drinking water) or after basic treatment such as UV disinfection (ca. 30% of drinking water) or chemical disinfection (e.g. chlorination, ca. 10% of drinking water) (SVGW 2016). Currently, only a few site-specific cases exist, where more complex treatment trains were installed to abate MPs (<10% of drinking water, SVGW (2016)). However, the detection of new MPs may require an upgrade of waterworks with suitable treatment processes, which depend strongly on the physicochemical properties of the MP.

Managed aquifer recharge artificially increases the amount of groundwater available for drinking water supply, but also introduces wastewater-borne MPs to the aquifer. These MPs will be partially abated by sorption or degradation (Hiscock and Grischek 2002, Maeng et al. 2011), but degradation might result in more persistent and mobile TPs. **UV irradiation** is widely used for disinfection, requiring a minimum UV dose of 400 Jm^{-2} according to German, Austrian, and Swiss legislation (DVGW 2006, ÖNORM 2001, SVGW 2010). Even at such low UV doses, some MP abatement was reported, as in the case of acesulfame (Scheurer et al. 2014); but this depends on the reactivity of the MP (Wols and Hofman-Caris 2012). MP abatement is explained by direct and/or indirect photo transformation (Canonica et al. 2008) and can be enhanced by increasing the UV dose and/or the addition of hydrogen peroxide (H_2O_2) to generate hydroxyl radicals (Hessler et al. 1993). **Ozonation** can be used for disinfection and for the abatement of MPs with electron-rich moieties. Also during ozonation, hydroxyl radicals are formed, which may lead to the abatement of ozone-refractory compounds such as atrazine (von Sonntag and von Gunten 2012). In contrast to other oxidants, hydroxyl radicals react rather unselectively with a broad range of MPs but also natural organic matter compounds, leading to lower MP transformation efficiency (Lee and von Gunten 2010). Alternative **advanced oxidation processes (AOPs)** include UV/ozone (O_3), UV/Cl_2, or O_3/H_2O_2 (Miklos et al. 2018, Stefan 2018). All oxidation processes can lead to the formation of TPs and byproducts, which are in some cases even more toxic than the precursors (Sharma et al. 2018, von Gunten 2018). TPs and byproducts are often partially removed by a post-treatment such as sand or activated carbon filtration, due to biodegradation and/or adsorption (Hammes et al. 2006, Hollender et al. 2009).

Non-destructive treatment processes such as **activated carbon**, either in powdered or granular form, can offer an alternative to avoid the formation of TPs. Sorption to activated carbon strongly depends on the properties of the MP and correlates to some extent with hydrophobicity (Delgado et al. 2012, Westerhoff et al. 2005). **Nanofiltration** especially retains larger, anionic MPs (through electrostatic repulsion due to negative surface charge of membranes), while **reverse osmosis** rejects nearly all solutes to a large extent (Taheran et al. 2016). Rejection mechanisms in nanofiltration and reverse osmosis are still not fully understood but are probably

dominated by size-exclusion and electrostatic repulsion (Bellona et al. 2004). However, MP removal by non-destructive treatment processes requires frequent regeneration or exchange of the activated carbon, and disposal of the highly-concentrated reject water, resulting in high financial and ecological costs (Snyder et al. 2007).

1.4 Objectives and Thesis Contents

Groundwater is an essential resource for water supply but its quality is threatened by polar compounds originating (i) from pesticide application in agriculture and (ii) from municipal and industrial wastewater entering the aquifers via either bank filtration or leaky sewers. Furthermore, many MPs present in groundwater might still be unknown. Therefore, the overall **goal of this study** was to comprehensively assess groundwater quality with regard to polar MPs and their TPs. The applied analytical approach was optimized for the sensitive detection of a wide range of polar compounds, using vacuum-assisted evaporation followed by RPLC-ESI-HRMS/MS. The subsequent data analysis combined target, suspect, and nontarget screening approaches. Chapter 2 and 3 describe a systematic screening for polar MPs from agricultural and urban sources. The detection of TPs of the fungicide chlorothalonil at high concentrations (chapter 2) together with a new drinking water standard for these compounds motivated chapter 4. The monitoring sites investigated are part of the Swiss National Groundwater Monitoring NAQUA. The Federal Office for the Environment (FOEN) provided a rough characterization for each site of the land use in the catchment. This work was funded to a large extent by the FOEN.

Chapter 2 focused on pesticides and their TPs. Therefore, most investigated monitoring sites were located in intensively used agricultural areas. The target and suspect screening was designed to cover all pesticides registered in Switzerland from 2005-2017 and their TPs. Structural information of more than 1100 pesticide TPs was gathered from various sources; most were experimentally observed in the EU pesticide registration. We aimed to evaluate the suspect hits in a detailed and systematic way to prioritize the most promising hits for confirmation and quantification with reference material.

Chapter 3 aimed to identify urban MPs and to comprehensively assess groundwater quality by taking into account all detected LC-HRMS peaks. Samples originated from monitoring sites with very different land use in their catchments. We intended to estimate the fraction of still unknown groundwater contamination from urban or agricultural sources, by characterizing detected LC-HRMS peaks with regard to their potential origin (urban, agricultural, natural). Moreover, an automated method with in silico fragmentation tools was incorporated to increase the number of successful compound identifications.

Chapter 4 was motivated by the detection of TPs of the fungicide chlorothalonil at high concentrations (chapter 2). In parallel to our findings, chlorothalonil was re-evaluated by the European Commission, which subsequently recommended classifying chlorothalonil as carcinogen category 1B. This reclassification subsequently resulted in the Swiss authorities declaring all chlorothalonil TPs as relevant, leading to the drinking water standard of 100 ngL^{-1} to apply to these compounds, challenging water suppliers in agriculturally intensively used areas. To support water suppliers in their decision-making with regard to removal of these compounds, we investigated the abatement of chlorothalonil TPs in water treatment. First, we

analysed the extent of chlorothalonil TPs contamination in a larger sample set (same as used for chapter 3). Then, the fate of chlorothalonil TPs in UV disinfection, ozonation, AOP treatment, activated carbon filtration, and reverse osmosis was examined in lab-scale, pilot-scale, and/or full-scale.

References

Aalizadeh, R., Nika, M.C. and Thomaidis, N.S., 2019. Development and application of retention time prediction models in the suspect and non-target screening of emerging contaminants. J Hazard Mater 363, 277-285.

Albergamo, V., Schollée, J.E., Schymanski, E.L., Helmus, R., Timmer, H., Hollender, J. and de Voogt, P., 2019. Nontarget Screening Reveals Time Trends of Polar Micropollutants in a Riverbank Filtration System. Environ Sci Technol 53(13), 7584-7594.

Allen, F., Greiner, R. and Wishart, D., 2014. Competitive fragmentation modeling of ESI-MS/MS spectra for putative metabolite identification. Metabolomics 11(1), 98-110.

Alygizakis, N.A., Oswald, P., Thomaidis, N.S., Schymanski, E.L., Aalizadeh, R., Schulze, T., Oswaldova, M. and Slobodnik, J., 2019. NORMAN digital sample freezing platform: A European virtual platform to exchange liquid chromatography high resolution-mass spectrometry data and screen suspects in "digitally frozen" environmental samples. TrAC Trends in Analytical Chemistry 115, 129-137.

Anliker, S., Loos, M., Comte, R., Ruff, M., Fenner, K. and Singer, H., 2020. Assessing Emissions from Pharmaceutical Manufacturing Based on Temporal High-Resolution Mass Spectrometry Data. Environmental science & technology 54(7), 4110-4120.

Bader, T., Schulz, W., Kummerer, K. and Winzenbacher, R., 2016. General strategies to increase the repeatability in non-target screening by liquid chromatography-high resolution mass spectrometry. Anal Chim Acta 935, 173-186.

BAFU, 2019. State and development of groundwater in Switzerland. Results of the National Groundwater Monitoring NAQUA, status as of 2016 (Zustand und Entwicklung Grundwasser Schweiz. Ergebnisse der Nationalen Grundwasserbeobachtung NAQUA, Stand 2016), Bundesamt für Umwelt, Bern.

Barron, L. and Gilchrist, E., 2014. Ion chromatography-mass spectrometry: a review of recent technologies and applications in forensic and environmental explosives analysis. Anal Chim Acta 806, 27-54.

Bellona, C., Drewes, J.E., Xu, P. and Amy, G., 2004. Factors affecting the rejection of organic solutes during NF/RO treatment--a literature review. Water Res 38(12), 2795-2809.

Bletsou, A.A., Jeon, J., Hollender, J., Archontaki, E. and Thomaidis, N.S., 2015. Targeted and non-targeted liquid chromatography-mass spectrometric workflows for identification of transformation products of emerging pollutants in the aquatic environment. TrAC Trends in Analytical Chemistry 66, 32-44.

BPO 813.12, Swiss Regulation No. 813.12 concerning the placment on the market and handling of biocidal products, Biocidal Products Ordinance, BPO (Verordnung über das Inverkehrbringen von und den Umgang mit Biozidprodukten, Biozidprodukteverordnung, VBP).

Buttiglieri, G., Peschka, M., Fromel, T., Muller, J., Malpei, F., Seel, P. and Knepper, T.P., 2009. Environmental occurrence and degradation of the herbicide n-chloridazon. Water research 43(11), 2865-2873.

Canonica, S., Meunier, L. and von Gunten, U., 2008. Phototransformation of selected pharmaceuticals during UV treatment of drinking water. Water research 42, 121-128.

Chiaia-Hernandez, A.C., Gunthardt, B.F., Frey, M.P. and Hollender, J., 2017. Unravelling Contaminants in the Anthropocene Using Statistical Analysis of Liquid Chromatography-High-Resolution Mass Spectrometry Nontarget Screening Data Recorded in Lake Sediments. Environ Sci Technol 51(21), 12547-12556.

Delgado, L.F., Charles, P., Glucina, K. and Morlay, C., 2012. The removal of endocrine disrupting compounds, pharmaceutically activated compounds and cyanobacterial toxins during drinking water preparation using activated carbon--a review. Sci Total Environ 435-436, 509-525.

Díaz-Cruz, M.S. and Barceló, D., 2008. Trace organic chemicals contamination in ground water recharge. Chemosphere 72(3), 333-342.

Dührkop, K., Shen, H., Meusel, M., Rousu, J. and Bocker, S., 2015. Searching molecular structure databases with tandem mass spectra using CSI:FingerID. Proc Natl Acad Sci U S A 112(41), 12580-12585.

Dührkop, K., Fleischauer, M., Ludwig, M., Aksenov, A.A., Melnik, A.V., Meusel, M., Dorrestein, P.C., Rousu, J. and Bocker, S., 2019. SIRIUS 4: a rapid tool for turning tandem mass spectra into metabolite structure information. Nat Methods 16(4), 299-302.

DVGW, 2006. W 294-2 Worksheet 06/2006: UV devices for disinfection in water supply; part 2: testing the quality, function and effectiveness of disinfection (W 294-2 Arbeitsblatt 06/2006: UV-Geräte zur Desinfektion in der Wasserversorgung; Teil 2: Prüfung von Beschaffenheit, Funktion und Desinfektionswirksamkeit).

EC, 2020. Communication from the commission to the European parliament, the council, the European economic and social committee and the committee of the regions. Chemicals Strategy for Sustainability. Towards a Toxic-Free Environment. COM(2020) 667 final. https://ec.europa.eu/environment/pdf/chemicals/2020/10/Strategy.pdf. Accessed: 13/02/2021.

EDI, 2016. Swiss regulation No. 817.022.11 concerning drinking water and water in public swimming pools and shower facilities (Verordnung des EDI über Trinkwasser sowie Wasser in öffentlich zugänglichen Bädern und Duschanlagen (TBDV) vom 16. Dezember 2016 (Stand am 1. Mai 2018)), Eidgenössisches Departement des Innern.

European Commission, 1998. Council Directive 98/83/EC of 3 November 1998 on the quality of water intended for human consumption. Official Journal of the European Communities (L330).

European Commission, 2003. Guidance document on the assessment of the relevance of metabolites in groundwater of substances regulated under council directive 91/414/EE. Sanco/221/2000 –rev.10- final.

FAO, 2016. Global Diagnostic on Groundwater Governance. Food and Agriculture Organization of the United Nations. http://www.fao.org/3/a-i5706e.pdf.

Gago-Ferrero, P., Schymanski, E.L., Bletsou, A.A., Aalizadeh, R., Hollender, J. and Thomaidis, N.S., 2015. Extended Suspect and Non-Target Strategies to Characterize Emerging Polar Organic Contaminants in Raw Wastewater with LC-HRMS/MS. Environ Sci Technol 49(20), 12333-12341.

Gago-Ferrero, P., Krettek, A., Fischer, S., Wiberg, K. and Ahrens, L., 2018. Suspect Screening and Regulatory Databases: A Powerful Combination To Identify Emerging Micropollutants. Environ Sci Technol 52(12), 6881-6894.

Hale, S.E., Arp, H.P.H., Schliebner, I. and Neumann, M., 2020. What's in a Name: Persistent, Mobile, and Toxic (PMT) and Very Persistent and Very Mobile (vPvM) Substances. Environ Sci Technol.

Hamann, E., Stuyfzand, P.J., Greskowiak, J., Timmer, H. and Massmann, G., 2016. The fate of organic micropollutants during long-term/long-distance river bank filtration. Science of The Total Environment 545-546, 629-640.

Hammes, F., Salhi, E., Köster, O., Kaiser, H.-P., Egli, T. and von Gunten, U., 2006. Mechanistic and kinetic evaluation of organic disinfection by-product and assimilable organic carbon (AOC) formation during the ozonation of drinking water. Water research 40(12), 2275-2286.

Hernandez, F., Sancho, J.V., Ibanez, M., Abad, E., Portoles, T. and Mattioli, L., 2012. Current use of high-resolution mass spectrometry in the environmental sciences. Anal Bioanal Chem 403(5), 1251-1264.

Hessler, D.P., Gorenflo, V. and Frimmel, F.H., 1993. Degradation of Aqueous Atrazine and Metazachlor Solutions by UV and UV/H202 - Influence of pH and Herbicide Concentration. Acta hydrochimica et hydrobiologica 21(4), 209-214.

Hiscock, K.M. and Grischek, T., 2002. Attenuation of groundwater pollution by bank filtration. Journal of Hydrology 266(3), 139-144.

Hohrenk, L.L., Itzel, F., Baetz, N., Tuerk, J., Vosough, M. and Schmidt, T.C., 2019. Comparison of Software Tools for Liquid Chromatography-High-Resolution Mass Spectrometry Data Processing in Nontarget Screening of Environmental Samples. Anal Chem.

Hollender, J., Zimmermann, S.G., Koepke, S., Krauss, M., McArdell, C.S., Ort, C., Singer, H., von Gunten, U. and Siegrist, H., 2009. Elimination of Organic Micropollutants in a Municipal Wastewater Treatment Plant Upgraded with a Full-Scale Post-Ozonation Followed by Sand Filtration. Environmental science & technology 43(20), 7862-7869.

Hollender, J., Schymanski, E.L., Singer, H.P. and Ferguson, P.L., 2017. Nontarget Screening with High Resolution Mass Spectrometry in the Environment: Ready to Go? Environ Sci Technol 51(20), 11505-11512.

Holm, J.V., Rügge, K., Bjerg, P.L. and Christensen, T.H., 1995. Occurrence and Distribution of Pharmaceutical Organic Compounds in the Groundwater Downgradient of a Landfill (Grindsted, Denmark). Environmental science & technology 29(5), 1415-1420.

Horai, H., Arita, M., Kanaya, S., Nihei, Y., Ikeda, T., Suwa, K., Ojima, Y., Tanaka, K., Tanaka, S., Aoshima, K., Oda, Y., Kakazu, Y., Kusano, M., Tohge, T., Matsuda, F., Sawada, Y., Hirai, M.Y., Nakanishi, H., Ikeda, K., Akimoto, N., Maoka, T., Takahashi, H., Ara, T., Sakurai, N., Suzuki, H., Shibata, D., Neumann, S., Iida, T., Tanaka, K., Funatsu, K., Matsuura, F., Soga, T., Taguchi, R., Saito, K. and Nishioka, T., 2010. MassBank: a public repository for sharing mass spectral data for life sciences. Journal of Mass Spectrometry 45(7), 703-714.

Hug, C., Ulrich, N., Schulze, T., Brack, W. and Krauss, M., 2014. Identification of novel micropollutants in wastewater by a combination of suspect and nontarget screening. Environmental pollution 184, 25-32.

Huntscha, S., Singer, H.P., McArdell, C.S., Frank, C.E. and Hollender, J., 2012. Multiresidue analysis of 88 polar organic micropollutants in ground, surface and wastewater using online mixed-bed multilayer solid-phase extraction coupled to high performance liquid chromatography-tandem mass spectrometry. J Chromatogr A 1268, 74-83.

Huntscha, S., Hofstetter, T.B., Schymanski, E.L., Spahr, S. and Hollender, J., 2014. Biotransformation of benzotriazoles: insights from transformation product identification and compound-specific isotope analysis. Environ Sci Technol 48(8), 4435-4443.

Jandera, P., 2011. Stationary and mobile phases in hydrophilic interaction chromatography: a review. Anal Chim Acta 692(1-2), 1-25.

Katajamaa, M. and Orešič, M., 2007. Data processing for mass spectrometry-based metabolomics. Journal of chromatography A 1158(1), 318-328.

Kern, S., Fenner, K., Singer, H.P., Schwarzenbach, R.P. and Hollender, J., 2009. Identification of Transformation Products of Organic Contaminants in Natural Waters by Computer-Aided Prediction and High-Resolution Mass Spectrometry. Environmental science & technology 43(18), 7039-7046.

Kim, S., Chen, J., Cheng, T., Gindulyte, A., He, J., He, S., Li, Q., Shoemaker, B.A., Thiessen, P.A., Yu, B., Zaslavsky, L., Zhang, J. and Bolton, E.E., 2019. PubChem 2019 update: improved access to chemical data. Nucleic Acids Res 47(D1), D1102-D1109.

Köke, N., Zahn, D., Knepper, T.P. and Fromel, T., 2018. Multi-layer solid-phase extraction and evaporation-enrichment methods for polar organic chemicals from aqueous matrices. Anal Bioanal Chem 410(9), 2403-2411.

Kolpin, D.W., Thurman, E.M., Linhart, S.M.J.A.o.E.C. and Toxicology, 1998. The Environmental Occurrence of Herbicides: The Importance of Degradates in Ground Water. 35(3), 385-390.

Koppe, T., Jewell, K.S., Dietrich, C., Wick, A. and Ternes, T.A., 2020. Application of a non-target workflow for the identification of specific contaminants using the example of the Nidda river basin. Water Res 178, 115703.

Kormos, J.L., Schulz, M. and Ternes, T.A., 2011. Occurrence of Iodinated X-ray Contrast Media and Their Biotransformation Products in the Urban Water Cycle. Environmental science & technology 45(20), 8723-8732.

Krauss, M., Singer, H. and Hollender, J., 2010. LC-high resolution MS in environmental analysis: from target screening to the identification of unknowns. Anal Bioanal Chem 397(3), 943-951.

Lapworth, D.J., Baran, N., Stuart, M.E. and Ward, R.S., 2012. Emerging organic contaminants in groundwater: A review of sources, fate and occurrence. Environmental pollution 163, 287-303.

Lee, Y. and von Gunten, U., 2010. Oxidative transformation of micropollutants during municipal wastewater treatment: Comparison of kinetic aspects of selective (chlorine, chlorine dioxide, ferrateVI, and ozone) and non-selective oxidants (hydroxyl radical). Water research 44(2), 555-566.

Leendert, V., Van Langenhove, H. and Demeestere, K., 2015. Trends in liquid chromatography coupled to high-resolution mass spectrometry for multi-residue analysis of organic micropollutants in aquatic environments. TrAC Trends in Analytical Chemistry 67, 192-208.

Lesellier, E. and West, C., 2015. The many faces of packed column supercritical fluid chromatography--a critical review. J Chromatogr A 1382, 2-46.

Loos, R., Locoro, G., Comero, S., Contini, S., Schwesig, D., Werres, F., Balsaa, P., Gans, O., Weiss, S., Blaha, L., Bolchi, M. and Gawlik, B.M., 2010. Pan-European survey on the occurrence of selected polar organic persistent pollutants in ground water. Water research 44(14), 4115-4126.

Maeng, S.K., Sharma, S.K., Lekkerkerker-Teunissen, K. and Amy, G.L., 2011. Occurrence and fate of bulk organic matter and pharmaceutically active compounds in managed aquifer recharge: a review. Water Res 45(10), 3015-3033.

Mechelke, J., Longree, P., Singer, H. and Hollender, J., 2019. Vacuum-assisted evaporative concentration combined with LC-HRMS/MS for ultra-trace-level screening of organic micropollutants in environmental water samples. Analytical and Bioanalytical Chemistry 411, 2555–2567.

Menger, F., Gago-Ferrero, P., Wiberg, K. and Ahrens, L., 2020. Wide-scope screening of polar contaminants of concern in water: A critical review of liquid chromatography-high resolution mass spectrometry-based strategies. Trends in Environmental Analytical Chemistry 28.

Miklos, D.B., Remy, C., Jekel, M., Linden, K.G., Drewes, J.E. and Hübner, U., 2018. Evaluation of advanced oxidation processes for water and wastewater treatment – A critical review. Water research 139, 118-131.

Moel, P.J.d., de Moel, P.J., Dijk, J.C.v. and Verberk, J.Q.J.C., 2006. Drinking Water: Principles And Practices.

Montes, R., Aguirre, J., Vidal, X., Rodil, R., Cela, R. and Quintana, J.B., 2017. Screening for Polar Chemicals in Water by Trifunctional Mixed-Mode Liquid Chromatography-High Resolution Mass Spectrometry. Environ Sci Technol 51(11), 6250-6259.

Moschet, C., Piazzoli, A., Singer, H. and Hollender, J., 2013. Alleviating the reference standard dilemma using a systematic exact mass suspect screening approach with liquid chromatography-high resolution mass spectrometry. Analytical chemistry 85(21), 10312-10320.

Moschet, C., Wittmer, I., Simovic, J., Junghans, M., Piazzoli, A., Singer, H., Stamm, C., Leu, C. and Hollender, J., 2014. How a complete pesticide screening changes the assessment of surface water quality. Environ Sci Technol 48(10), 5423-5432.

Müller, A., Schulz, W., Ruck, W.K. and Weber, W.H., 2011. A new approach to data evaluation in the non-target screening of organic trace substances in water analysis. Chemosphere 85(8), 1211-1219.

Neumann, M. and Schliebner, I., 2017. Position // october 2017: Protecting the sources of our drinkin water: A revised proposal for implementing criteria and an assessment procedure to identify Persistent, Mobile and Toxic (PMT) and very Persistent, very Mobile (vPvM) substances registered under REACH. German Environment Agency.

https://www.umweltbundesamt.de/sites/default/files/medien/1410/publikationen/171027_uba_pos_pmt_substances_engl_2aufl_bf.pdf.

Nika, M.C., Bletsou, A.A., Koumaki, E., Noutsopoulos, C., Mamais, D., Stasinakis, A.S. and Thomaidis, N.S., 2017. Chlorination of benzothiazoles and benzotriazoles and transformation products identification by LC-HR-MS/MS. J Hazard Mater 323(Pt A), 400-413.

ÖNORM, 2001. M 5873-1: Water disinfection systems using ultraviolet rays - requirements and testing (Anlagen zur Desinfektion von Wasser mittels Ultraviolett-Strahlen - Anforderungen und Prüfung).

ORRChem 814.81, Ordinance on the Reduction of Risks relating to the Use of Certain Particularly Dangerous Substances, Preparations and Articles (Chemical Risk Reduction Ordinance, ORRChem) of 18 May 2005 (Status as of 23 June 2020) (Verordnung zur Reduktion von Risiken beim Umgang mit bestimmten besonders gefährlichen Stoffen, Zubereitungen und Gegenständen (Chemikalien-Risikoreduktions-Verordnung, ChemRRV) vom 18. Mai 2005 (Stand am 23. Juni 2020)). Swiss Federal Council (ed).

Pianta, R., Boller, M., Urfer, D., Chappaz, A. and Gmünder, A., 2000. Costs of conventional vs. membrane treatment for karstic spring water. Desalination 131(1), 245-255.

Postigo, C. and Barcelo, D., 2015. Synthetic organic compounds and their transformation products in groundwater: occurrence, fate and mitigation. Science of The Total Environment 503-504, 32-47.

PPPO 916.161, Ordinance concerning the placment of plant protection products on the market (Plant Protection Products Ordinance, PPPO) of 12 May 2010 (Status as of 1 July 2020) ((Verordnung über das Inverkehrbringen von Pflanzenschutzmitteln (Pflanzenschutzmittelverordnung, PSMV) vom 12. Mai 2010 (Stand am 1. Juli 2020)). Swiss Federal Council (ed).

Reemtsma, T., Alder, L. and Banasiak, U., 2013a. Emerging pesticide metabolites in groundwater and surface water as determined by the application of a multimethod for 150 pesticide metabolites. Water research 47(15), 5535-5545.

Reemtsma, T., Alder, L. and Banasiak, U., 2013b. A multimethod for the determination of 150 pesticide metabolites in surface water and groundwater using direct injection liquid chromatography-mass spectrometry. Journal of chromatography A 1271(1), 95-104.

Reemtsma, T., Berger, U., Arp, H.P., Gallard, H., Knepper, T.P., Neumann, M., Quintana, J.B. and Voogt, P., 2016. Mind the Gap: Persistent and Mobile Organic Compounds-Water Contaminants That Slip Through. Environmental science & technology 50(19), 10308-10315.

Regulation (EC) 1107/2009, Regulation (EC) No 1107/2009 of the European Parliament and of the Council of 21 October 2009 concerning the placing of plant protection products on the market and repealing Council Directives 79/117/EEC and 91/414/EEC.

Regulation (EC) 1907/2006, Regulation (EC) No 1907/2006 of the European Parliament and of the Council of 18 December 2006 concerning the Registration, Evaluation, Authorisation and Restriction of Chemicals (REACH), establishing a European Chemicals Agency.

Regulation (EU) 528/2012, Regulation (EU) No 528/2012 of the European Parliament and of the Council of 22 May 2012 concerning the making available on the market and use of biocidal products Text with EEA relevance.

Renaud, J.B., Sabourin, L., Topp, E. and Sumarah, M.W., 2017. Spectral Counting Approach to Measure Selectivity of High-Resolution LC-MS Methods for Environmental Analysis. Anal Chem.

Rosenberg, E., 2003. The potential of organic (electrospray- and atmospheric pressure chemical ionisation) mass spectrometric techniques coupled to liquid-phase separation for speciation analysis. Journal of chromatography A 1000(1), 841-889.

RSC, 2020. ChemSpider, Royal Society of Chemistry. http://www.chemspider.com/.

Ruff, M., Mueller, M.S., Loos, M. and Singer, H.P., 2015. Quantitative target and systematic non-target analysis of polar organic micro-pollutants along the river Rhine using high-

resolution mass-spectrometry--Identification of unknown sources and compounds. Water Res 87, 145-154.

Ruttkies, C., Schymanski, E.L., Wolf, S., Hollender, J. and Neumann, S., 2016. MetFrag relaunched: incorporating strategies beyond in silico fragmentation. Journal of Cheminformatics 8(3).

Scheurer, M., Brauch, H.-J. and Lange, F.T., 2009. Analysis and occurrence of seven artificial sweeteners in German waste water and surface water and in soil aquifer treatment (SAT). Analytical and Bioanalytical Chemistry 394(6), 1585-1594.

Scheurer, M., Schmutz, B., Happel, O., Brauch, H.J., Wulser, R. and Storck, F.R., 2014. Transformation of the artificial sweetener acesulfame by UV light. Sci Total Environ 481, 425-432.

Schollée, J., Schymanski, E., Avak, S., Loos, M. and Hollender, J., 2015. Prioritizing Unknown Transformation Products from Biologically-Treated Wastewater Using High-Resolution Mass Spectrometry, Multivariate Statistics, and Metabolic Logic. Analytical chemistry 87(24), 12121-12129.

Schollée, J.E., Bourgin, M., von Gunten, U., McArdell, C.S. and Hollender, J., 2018. Non-target screening to trace ozonation transformation products in a wastewater treatment train including different post-treatments. Water Res 142, 267-278.

Schulze, S., Zahn, D., Montes, R., Rodil, R., Quintana, J.B., Knepper, T.P., Reemtsma, T. and Berger, U., 2019. Occurrence of emerging persistent and mobile organic contaminants in European water samples. Water Res 153, 80-90.

Schulze, T., Schymanski, E., Stravs, M.A., Neumann, S., Krauss, M., Singer, H., Hug, C., Gallampois, C.M., Hollender, J., Slobodnik, J. and Brack, W., 2012. NORMAN MassBank: Towards a community-driven, open-access accurate mass spectral database for the identification of emerging pollutants. Norman Network Bulletin, www.norman-network.net (3), 9-11.

Schymanski, E.L., Jeon, J., Gulde, R., Fenner, K., Ruff, M., Singer, H.P. and Hollender, J., 2014. Identifying small molecules via high resolution mass spectrometry: communicating confidence. Environmental science & technology 48(4), 2097-2098.

Sharma, A., Ahmad, J. and Flora, S.J.S., 2018. Application of advanced oxidation processes and toxicity assessment of transformation products. Environ Res 167, 223-233.

Singer, H., Wössner, A., McArdell, C. and Fenner, K., 2016. Rapid Screening for Exposure to "Non-Target" Pharmaceuticals from Wastewater Effluents by Combining HRMS-Based Suspect Screening and Exposure Modeling. Environmental science & technology 50(13), 6698-6707.

Sjerps, R.M., Vughs, D., van Leerdam, J.A., ter Laak, T.L. and van Wezel, A.P., 2016. Data-driven prioritization of chemicals for various water types using suspect screening LC-HRMS. Water Res 93, 254-264.

Snyder, S.A., Adham, S., Redding, A.M., Cannon, F.S., DeCarolis, J., Oppenheimer, J., Wert, E.C. and Yoon, Y., 2007. Role of membranes and activated carbon in the removal of endocrine disruptors and pharmaceuticals. Desalination 202(1), 156-181.

Stefan, M.I. (ed) 2018. Advanced Oxidation Processes for Water Treatment: Fundamentals and Applications, IWA Publishing, London.

SVGW, 2010. W13d: Guideline for UV disinfection in water supply (Richtlinie zur UV-Desinfektion in der Wasserversorgung). Schweizerischer Verein des Gas- und Wasserfaches.

SVGW, 2016. W15001: Statistical surveys of water supplies in Switzerland operating year 2015 (W15001: Statistische Erhebungen der Wasserversorgungen in der Schweiz Betriebsjahr 2015).

Taheran, M., Brar, S.K., Verma, M., Surampalli, R.Y., Zhang, T.C. and Valero, J.R., 2016. Membrane processes for removal of pharmaceutically active compounds (PhACs) from water and wastewaters. Sci Total Environ 547, 60-77.

Tian, Z., Peter, K.T., Gipe, A.D., Zhao, H., Hou, F., Wark, D.A., Khangaonkar, T., Kolodziej, E.P. and James, C.A., 2020. Suspect and Nontarget Screening for Contaminants of Emerging Concern in an Urban Estuary. Environ Sci Technol 54(2), 889-901.

Vinaixa, M., Schymanski, E.L., Neumann, S., Navarro, M., Salek, R.M. and Yanes, O., 2016. Mass spectral databases for LC/MS- and GC/MS-based metabolomics: State of the field and future prospects. TrAC Trends in Analytical Chemistry 78, 23-35.

von Gunten, U., 2018. Oxidation Processes in Water Treatment: Are We on Track? Environ Sci Technol 52(9), 5062-5075.

von Sonntag, C. and von Gunten, U., 2012. Chemistry of Ozone in Water and Wastewater Treatment: From Basic Principles to Applications, IWA Publisher, London.

Wang, Z., Walker, G.W., Muir, D.C.G. and Nagatani-Yoshida, K., 2020. Toward a Global Understanding of Chemical Pollution: A First Comprehensive Analysis of National and Regional Chemical Inventories. Environmental science & technology 54(5), 2575-2584.

Westerhoff, P., Yoon, Y., Snyder, S. and Wert, E., 2005. Fate of Endocrine-Disruptor, Pharmaceutical, and Personal Care Product Chemicals during Simulated Drinking Water Treatment Processes. Environmental science & technology 39, 6649-6663.

Williams, A.J., Grulke, C.M., Edwards, J., McEachran, A.D., Mansouri, K., Baker, N.C., Patlewicz, G., Shah, I., Wambaugh, J.F., Judson, R.S. and Richard, A.M., 2017. The CompTox Chemistry Dashboard: a community data resource for environmental chemistry. J Cheminform 9(1), 61.

Wolf, L., Zwiener, C. and Zemann, M., 2012. Tracking artificial sweeteners and pharmaceuticals introduced into urban groundwater by leaking sewer networks. Science of The Total Environment 430, 8-19.

Wols, B.A. and Hofman-Caris, C.H.M., 2012. Review of photochemical reaction constants of organic micropollutants required for UV advanced oxidation processes in water. Water research 46(9), 2815-2827.

WPA 814.20, Federal Act on the Protection of Waters (Waters Protection Act, WPA) of 24 January 1991 (Status as of 1 January 2016) (Bundesgesetz über den Schutz der Gewässer (Gewässerschutzgesetz, GSchG) vom 24. Januar 1991 (Stand am 1. Januar 2016)). Federal Assembly of the Swiss Confederation (ed).

WPO 814.201, Waters Protection Ordinance (WPO) of 28 October 1998 (Status as of 1 April 2020) (Gewässerschutzverordnung (GSchV) vom 28. Oktober 1998 (Stand am 1. April 2020). Swiss Federal Council (ed).

Zahn, D., Mucha, P., Zilles, V., Touffet, A., Gallard, H., Knepper, T.P. and Fromel, T., 2019. Identification of potentially mobile and persistent transformation products of REACH-registered chemicals and their occurrence in surface waters. Water Res 150, 86-96.

Zektser, I.S. and Everett, L.G., 2004. Groundwater resources of the world and their use, United Nations Educational, Scientific and Cultural Organization, Paris.

Zhang, F., Ge, W., Ruan, G., Cai, X. and Guo, T., 2020. Data-Independent Acquisition Mass Spectrometry-Based Proteomics and Software Tools: A Glimpse in 2020. Proteomics 20(17-18), e1900276.

Zhang, L., Dai, Q., Qiao, X., Yu, C., Qin, X. and Yan, H., 2016. Mixed-mode chromatographic stationary phases: Recent advancements and its applications for high-performance liquid chromatography. TrAC Trends in Analytical Chemistry 82, 143-163.

Chapter 2: New Relevant Pesticide Transformation Products in Groundwater Detected Using Target and Suspect Screening for Agricultural and Urban Micropollutants with LC-HRMS

Karin Kiefer[1,2], Adrian Müller[1], Heinz Singer[1], Juliane Hollender[1,2]*

[1] Eawag: Swiss Federal Institute of Aquatic Science and Technology, Ueberlandstrasse 133, 8600 Dübendorf, Switzerland
[2] Institute of Biogeochemistry and Pollutant Dynamics, Universitätstrasse 16, ETH Zurich, 8092 Zurich, Switzerland

*Corresponding author: juliane.hollender@eawag.ch

Published in Water Research, DOI: 10.1016/j.watres.2019.114972

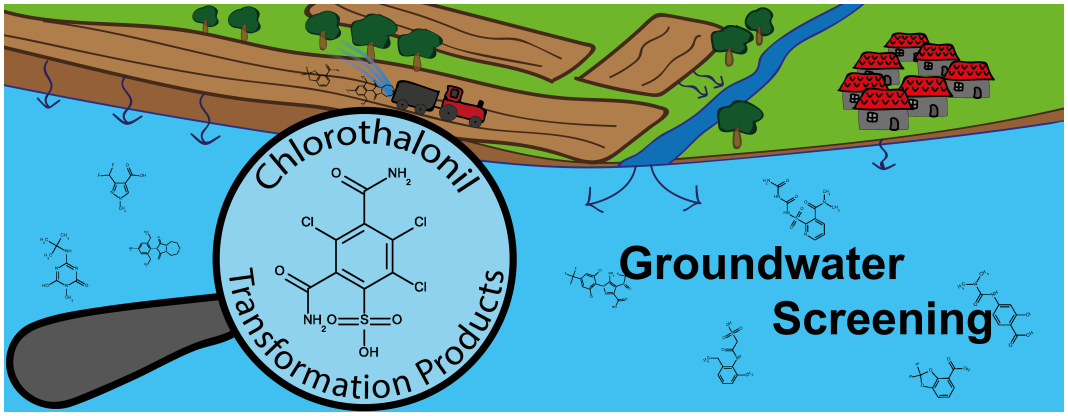

Abstract

Groundwater is a major drinking water resource, but its quality is threatened by a broad variety of anthropogenic micropollutants (MPs), originating from agriculture, industry, or households, and undergoing various transformation processes during subsurface passage. To determine a worst-case impact of pesticide application in agriculture on groundwater quality, a target and suspect screening for more than 300 pesticides and more than 1100 pesticide transformation products (TPs) was performed in 31 Swiss groundwater samples which predominantly originated from areas with intensive agriculture. To assess additional urban contamination sources, more than 250 common urban MPs were quantified. Most of the screened pesticide TPs were experimentally observed by the pesticide producers within the European pesticide registration. To cover very polar pesticide TPs, vacuum-assisted evaporative concentration was used for enrichment, followed by liquid chromatography high-resolution tandem mass spectrometry (LC-HRMS/MS). Based on intensity, isotope pattern, retention time, and in silico fragmentation, the suspect hits were prioritised and verified. We identified 22 suspects unequivocally and five tentatively; 13 TPs are reported here for the first time to be detected in groundwater. In 13 out of 31 groundwater samples, the total concentration of the 20 identified and quantified suspects (1 pesticide and 19 pesticide TPs) exceeded the total concentration of the 519 targets (236 pesticides and TPs; 283 urban MPs) for which we screened. Pesticide TPs had higher concentrations than the parent pesticides, illustrating their importance for groundwater quality. The newly identified very polar chlorothalonil TP R471811 was the only compound detected in all samples with concentrations ranging from 3 to 2700 ng/L. Agricultural MP concentration and detection frequency correlated with agricultural land use in the catchment, except for aquifers, where protective top layers reduced MP transport from the surface. In contrast to agricultural MPs, urban MPs displayed almost no correlation with land use. The dominating entry pathway of urban MPs was river bank filtration.

Keywords: pesticides metabolites; high resolution mass spectrometry; MetFrag; micropollutants; monitoring; land use

2.1 Introduction

Groundwater is in many countries the major source for drinking water; in Switzerland, 80% of drinking water originates from groundwater (Freiburghaus 2012). However, especially in densely populated areas, human activities threaten groundwater quality. Pharmaceuticals, sweeteners, or industrial chemicals (here referred to as urban MPs) are predominantly released to the aquatic environment via wastewater (Daughton and Ternes 1999), and consequently may enter groundwater along wastewater impacted streams (Heberer et al. 2004, Lewandowski et al. 2011) or leaky sewers (Wolf et al. 2012). Agricultural MPs, such as pesticides and their TPs, are intentionally spread into the environment and reach groundwater mainly via seepage from agricultural soils (Postigo and Barcelo 2015).

During subsurface passage, MPs may undergo natural attenuation processes such as sorption or degradation (Lapworth et al. 2012, Postigo and Barcelo 2015). However, the TPs formed are often more persistent and more mobile than the parent compound, as shown for several pesticides (Buttiglieri et al. 2009, Kolpin et al. 2004). Reemtsma et al. (2016) and Arp et al. (2017) highlighted the risks that so-called PMOCs (persistent and mobile organic contaminants) pose to drinking water supplies. PMOCs easily migrate in the water cycle, reach water works, and may even pass through more advanced technologies such as activated carbon filtration or ozonation. Shallow aquifers with well-permeable top layers and interactions with surface waters are highly vulnerable to contamination with polar and persistent MPs. Due to the lack of appropriate analytical methods, Reemtsma et al. (2016) expect that most PMOCs have been so far overlooked.

While many urban MPs so far are not considered in Swiss and European drinking water regulation, a drinking water limit of 100 ng/L applies to pesticides and their relevant TPs (EDI 2016, European Commission 1998). Pesticide TPs are defined as relevant if they either i) still exhibit pesticidal activity, ii) show severe toxicological effects (European Commission 2003), or iii) if their toxicity is unknown but the parent is considered to be toxic. The relevance is only classified if the pesticide TPs are predicted to exceed 100 ng/L after 1 m soil passage. So far, pesticide TPs are insufficiently monitored for three reasons: i) reference material for TPs is often not available, ii) analytical methods are not appropriate, and iii) many pesticide TPs are not known because pesticide registration data is either not easily accessible or not at all available. Currently available pesticide TP lists (Banning et al. 2019, Reemtsma et al. 2013b) represent the result of a prioritization process, meaning that the lists are possibly not comprehensive. The insufficient monitoring is especially concerning as pesticide TPs often occur more frequently and at higher concentrations than the active substance, as was reported e.g. for acetochlor, alachlor, metolachlor and chloridazon (Buttiglieri et al. 2009, FOEN 2019, Kolpin et al. 2004, Kolpin et al. 1998, Weber et al. 2007).

Reemtsma et al. (2013a) addressed this data gap with a target screening for 150 pesticide TPs in German surface and groundwater with triple-quadrupole mass spectrometry and detected 17 so far unpublished pesticide TPs. However, the 150 pesticide TPs were selected based on expert judgement about their occurrence in the aquatic environment, availability of reference material, toxcicological assessment, and their ability to be analysed with the chosen method. Some pesticide TPs, which were already known to be widespread in the environment (e.g. chloridazon-desphenyl, N,N-dimethylsulfamide) could not be included due to their polarity (Reemtsma et al. 2013b).

To overcome the lack of reference material, high resolution mass spectrometry followed by a suspect screening approach has in recent years been successfully used in environmental analytics (Brunner et al. 2019, Kern et al. 2009, Moschet et al. 2013). Briefly, HRMS data is searched against the suspect list containing the monoisotopic masses of expected compounds. Then, the suspect hits are checked for plausibility. For this, different criteria have been applied: i) absence / low intensity in background, ii) retention time (RT), iii) isotope pattern, iv) ionization potential, and v) MS/MS fragmentation. Measured MS/MS fragments may be used to search MS/MS libraries such as the European MassBank (Horai et al. 2010), MassBank of North America (MoNA 2019) and METLIN (Smith et al. 2005), to predict molecular fingerprints or to compare with predicted fragments by applying in silico tools such as CSI:FingerID (Duhrkop et al. 2015) and MetFrag (Ruttkies et al. 2016). However, certainty in the true identity of a suspect hit can only be obtained with reference material.

This study aimed to comprehensively assess the impact of pesticide application in agriculture on groundwater quality. Therefore, we applied a target and suspect screening approach to cover more than 300 pesticides and more than 1100 TPs. Most TPs were experimentally observed by the pesticide producers within the European pesticide registration. The analytical method was optimised for very polar compounds using vacuum-assisted evaporative concentration as enrichment method. To ensure that as many pesticide TPs as possible were detected, 21 groundwater monitoring sites were chosen which were known to be polluted with several pesticides or known TPs. In addition, ten groundwater monitoring sites were sampled which were more influenced by urban MPs or relatively pristine, to investigate how widespread the occurrence of pesticide TPs is in groundwater. To compare the contamination from agriculture to the overall contamination with MPs in the investigated groundwater monitoring sites, we analyzed additionally more than 250 MPs known to originate from urban sources. The MP pattern was then compared to land use and hydrogeological settings.

2.2 Methods

2.2.1 Groundwater Samples

The 31 groundwater samples originated from nine springs and 22 abstraction wells (referred to as monitoring sites) regularly monitored within the Swiss National Groundwater Monitoring NAQUA, operated by the Federal Office for the Environment in close collaboration with the cantonal authorities (https://www.bafu.admin.ch/bafu/en/home/topics/water/info-specialists/state-of-waterbodies/state-of-groundwater.html). The data presented shows rather a worst-case scenario, and therefore, is not representative of Swiss groundwater quality.

The monitoring sites were selected based on the land use in the catchments and long-term monitoring data: i) 21 monitoring sites showed high concentrations or frequent detections of pesticides or their TPs in the past, or their catchment was dominated by agriculture; ii) seven monitoring sites were impaired by wastewater tracers such as acesulfame, benzotriazole, carbamazepine and sulfamethoxazole; and iii) three monitoring sites were relatively pristine with regards to MP concentrations and/or anthropogenic activities in their catchments. For each monitoring site, the catchment was estimated based on abstraction volume / spring discharge, hydrogeological maps and reports on the designation of groundwater protection zones. The so-defined catchments were then compared to land-use statistics. Land use classes were as follows: i) agriculture (cropland, orchards, vineyards), ii) settlement (settlement, transport infrastructure), and iii) grassland/forest/other (summer pastures, grazing and

livestock, forest, unproductive areas). This data set on the land use, size and location of the catchments was provided by the Swiss Federal Office for the Environment.

2.2.2 Sampling

Groundwater samples were collected in May 2017 within the routine sampling of NAQUA. The samples were filled in laboratory glass bottles (which were previously annealed at 500 °C; 500 mL and 1000 mL bottles, SIMAX Kavalier, Czech Republic), stored for up to one week at <10 °C in the dark, and then kept frozen at -20 °C until measurement. To assess possible contamination from sample handling, ultrapure water was analogously frozen, enriched and analysed as blank samples.

2.2.3 Sample Enrichment

To avoid the loss of very polar compounds during enrichment, the samples were concentrated via vacuum-assisted evaporative concentration using the Syncore® Analyst (BÜCHI, Switzerland) with slight modifications to the method validated by Mechelke et al. (2019): 60 mL sample volume was filled into BÜCHI glass vials (0.3 mL appendix volume), spiked with 224 isotope labelled internal standards (ILIS) and evaporated at 20 mbar and 45 °C to 1-5 mL using the back-flush unit. The BÜCHI glass vials were rinsed with 1.5 mL H_2O/methanol mix (85:15) to reduce analyte losses by sorption on the glass surface. Then, the samples were evaporated to ~0.3 mL, the sample volume was adjusted to 0.4 mL with ultrapure water, and centrifuged at 10621 g for five minutes in flat bottom glass inserts (0.5 mL, 110506, BGB Analytik AG, Switzerland). The supernatant was transferred using glass Pasteur pipettes (747715, Brand GmbH, Germany) to HPLC vials (1.5 mL vials: 080400-XL; screw caps: 090301; BGB Analytik, Switzerland) equipped with conical glass inserts (0.34 mL, 110503, BGB Analytik AG, Switzerland), kept at 8 °C and analysed within 4 days.

For target quantification and quality control, 22 calibration standards ranging from 0.1-1000 ng/L, six spiked samples (3x10 / 3x100 ng/L) and nine blank samples, i.e. ultrapure water spiked with internal standards, were enriched and analysed analogously to the samples (SI2-A1).

2.2.4 LC-HRMS/MS

A volume of 100 µL, corresponding to 15 mL of the original water sample, was injected on a reverse phase C18 column (Atlantis® T3 3 µm, 3.0x150 mm; Waters, Ireland) which retains polar compounds well. To improve the retardation of very polar compounds, the gradient started with 100% eluent A (water + 0.1% concentrated formic acid), then eluent B (methanol + 0.1% concentrated formic acid) was increased from 1.5 to 18.5 min to 95%, held for 10 min, and lowered again to the starting conditions. The column was re-equilibrated for 4 min. The flow rate was 0.3 mL/min. The HPLC system comprised a PAL autosampler (CTC Analytics, Switzerland) and a Dionex UltiMate3000 RS pump (Thermo Fisher Scientific, U.S.).

Samples were measured (in sequence) first in positive, then in negative electrospray ionization mode on a high-resolution mass spectrometer (Q Exactive Plus, Thermo Fisher Scientific, U.S.). After ionization with electrospray (spray voltage 4/-3 kV), an MS1 full-scan (m/z 100-1000, mass resolution 140 000 at m/z 200) was performed followed by five data-dependent fragmentation experiments (mass resolution 17 500 at m/z 200) using higher energy collision-induced dissociation (HCD). MS/MS acquisition was triggered by the m/z of the target ions with normalised collision energies (NCE) 15-120 depending on the m/z. Isolation window was 1 Da.

If no target ion was detected, the most intense ions in the MS1 were fragmented at NCE 15, 60, and 105 (further details in SI2-A1). To confirm suspects with reference material, samples were re-measured with adjusted MS/MS settings (section 2.2.6.4 and SI2-A4).

2.2.5 Target Screening

TraceFinder 4.1 (Thermo Fisher Scientific, U.S.) was used for quantification of 519 target analytes with an extraction window of 5 ppm. The RT and MS/MS fragments of the target analytes (SI2-B4) were compared to RT and fragments of reference material. Most analytes were quantified with a linear calibration curve (weighting 1/x) using the peak area ratio of analyte and ILIS. If a structurally identical ILIS was not available (70% of targets), data was exported to R (R Core Team 2016) and an in-house script (https://github.com/dutchjes/TFAnalyzeR/blob/master/RelativeRecoveryCalculation.R) was used to select the ILIS which eluted at similar RT as the analyte and which resulted in the best relative recovery (close to 100% in all spiked samples, SI2-B4). For compounds without structurally identical ILIS, concentrations were corrected by the relative recovery (for details see SI2-A2).

2.2.6 Suspect Screening

2.2.6.1 Suspect List

We aimed to screen for all organic molecules and their TPs which were registered as pesticides (active substances, safeners, synergists) in Switzerland from 2005 to 2017 according to the Ordinance on Plant Protection Products; pesticides only registered according to the Ordinance on Biocidal Products were not included. Pesticides with undefined composition such as natural mixtures (e.g. essential oils) or technical products (e.g. alkyl-dimethyl-benzyl-ammoniumchloride) were excluded from the screening or replaced by representative molecules. As groundwater may be polluted by compounds applied decades ago, eight pesticides, only approved before 2005 but sold in high amounts, were additionally included in the screening. In total, the pesticide list comprised 396 organic molecules. A list of 1120 TPs, covering 74% of these pesticides, was collected from different sources, such as Latino et al. (2017), Lewis et al. (2016), Reemtsma et al. (2013b), BLW (2019), Agroscope (personal communication) or in-house data. The majority of the TPs (85%) originated from the database Eawag-Soil (www.envipath.org/package) containing pesticide transformation pathways assessed in aerobic laboratory soil experiments by the pesticide producers within the European registration process (Latino et al. 2017). Of the pesticides for which no transformation data could be gathered, 23% were pheromones or phytoregulators, and 33% were sold in low amounts (<1 t/a), and therefore, their TPs were expected to be less important. For 5% of pesticides without transformation data, sales volumes ranged from 1-10 t/a, and for 39% sales data was not available. Refer to SI2-B1 and SI2-B2 for a list of pesticides and TPs. Finally, the suspect list contained 223 pesticides and 1033 TPs, which were not yet covered by the target screening applied (section 2.2.5) and had a monoisotopic mass >99 Da (Figure 2-1).

2.2.6.2 Automated Screening

Automated screening with Compound Discoverer 2.1 (CD 2.1; Thermo Fisher Scientific, U.S.) included a peak picking step, RT alignment, and grouping of isotopologues and adducts (to form compounds) as well as grouping of compounds across samples (Figure 2-1). Compounds were marked as background if their peak area in the samples was less than three times larger than the maximum peak area in the blanks. Suspects were annotated based on the exact mass,

and targets using exact mass and RT with a RT window of 2 min. Parameter settings were optimised and tested with ILIS data (Figure SI2-A2); ILIS detection rate was 97%. See Table SI2-A2 for details on parameter settings.

2.2.6.3 Suspect Filtering and Prioritization

As the parameters were set to avoid false negative detections, most suspect hits represented noise compounds that could not be removed automatically with CD 2.1. Therefore, compounds annotated as suspects were checked visually and excluded if the signal to noise (S/N) was below 10. Suspect hits which were likely a false positive were excluded using the following criteria: i) peak height $<10^5$, ii) unrealistic RT based on predicted hydrophobicity (SI2-A3), iii) missing Cl/Br isotopologue although expected due to molecular formula and detection limit estimated by CD 2.1, iv) very noisy extracted ion chromatogram (EIC), v) no MS/MS fragment explained by the structure using the in silico fragmenter MetFrag (Ruttkies et al. 2016) if MS/MS scans were acquired (46% of suspect hits with S/N>10). MetFrag CL 2.4.2 was run in an automated way for all suspect hits using an R script. MetFrag retrieved candidate structures from the suspect list (SI2-B1, SI2-B2) and the web database ChemSpider (RSC 2018), and compared the predicted fragments of each candidate with the measured one (SI2-A3). Then, reference material was obtained either commercially or via the European Crop Protection Agency (ECPA) for the most promising suspect hits according to MetFrag results, peak shape and intensity, plausibility of RT and mass accuracy.

2.2.6.4 Suspect Confirmation and Quantification

To confirm the suspects, seven samples were re-measured with adjusted MS/MS settings (SI2-A4). The MS/MS fragments (m/z, intensity) and RT of the suspect hit were compared to the MS/MS fragments and RT of reference material by plotting EICs and head to tail plots using the R packages MSnbase (Gatto and Lilley 2012) and MSMSsim (Schollée 2017). Refer to SI2-A4 for details on the R script and to SI2-C for the resulting plots. Then, the identification confidence was classified following the scheme in Schymanski et al. (2014).

The confirmed suspects were quantified in the 31 samples by applying the calibration model determined later with the same LC-HRMS/MS system. For quantification, seven samples were enriched and analysed again, together with twelve calibration standards and three spiked samples. Then the confirmed suspects were quantified in the 31 measurement files from the first analysis and the seven measurement files from the second analysis, using the calibration standards from the second analysis (section 2.5 and SI2-A4). In case of three suspect hits, reference material could only be obtained for their isomer or structurally similar TP, so that concentrations were estimated assuming the same ionization efficiency as their isomer or structurally similar TP.

Data analysis was performed in RStudio with R version 3.4.1 (R Core Team 2016) if not stated otherwise. The HRMS measurement data files were converted to the open .mzXML data format using the msconvert tool from ProteoWizard (Chambers et al. 2012). JChem for Office (Version 17.1.2300.1455; ChemAxon Ltd.) was used for chemical structure illustration and logD prediction. The 90^{th} percentiles of concentrations were reported if more than 10% of the samples showed a detection.

2.3 Results and Discussion

2.3.1 Target Screening

The LOQ was ≤10 ng/L for 78% of the 519 targets, including more than 100 very polar compounds with $logD_{pH7}$ ranging from -5 to 0, showing the excellent sensitivity and broad applicability of the analytical setup comprised of vacuum-assisted evaporation followed by LC-HRMS/MS analysis. In the 31 groundwater samples, we detected 33 of 169 pesticides, 30 of 67 pesticide TPs and 42 of 283 urban MPs (16 of 175 pharmaceuticals, seven of 46 pharmaceutical TPs, one of seven industrial chemicals, three of five sweeteners and 15 of 50 others). Individual samples contained four to 44 targets (Figure 2-4, SI2-B4). Two pesticides (atrazine, bentazone) and one relevant pesticide TP (atrazine-desethyl) exceeded the European / Swiss drinking water limit for pesticides and relevant pesticide TPs of 100 ng/L. For comparison, one pesticide TP with unclear relevance, four non-relevant pesticide TPs, one non-relevant biocide TP and five urban MPs also exceeded 100 ng/L (without regulatory consequences, Table SI2-A3). The herbicide TP chloridazon-desphenyl showed the highest concentration (1800 ng/L) followed by another herbicide TP, metolachlor-ESA with 970 ng/L. Both TPs have been known to be widespread in groundwater for more than 10 years (Buttiglieri et al. 2009, Kolpin et al. 1998, Loos et al. 2010, Weber et al. 2007), and therefore are part of many routine monitoring programmes.

2.3.2 Suspect Screening

2.3.2.1 Suspect List

The suspect list comprised 223 pesticides and 1033 TPs with a monoisotopic mass >99 Da; most pesticide TPs were observed in aerobic soil degradation experiments or in lysimeter and field studies by the pesticide producers within the European pesticide registration. In order to minimize false negative findings, the suspect list was not reduced beforehand by evaluating the suspects' likelihood of being present in groundwater (polarity, sales volume), of being retained by LC method (polarity) or ionized in electrospray (presence of functional groups). Nevertheless, their amenability to LC-electrospray-MS was evaluated: more than 95% have a similar polarity as the analytes quantified with the applied analytical method (Figure 2-1) and 99.5% contain a heteroatom, increasing the electrospray ionization potential (Figure SI2-A1).

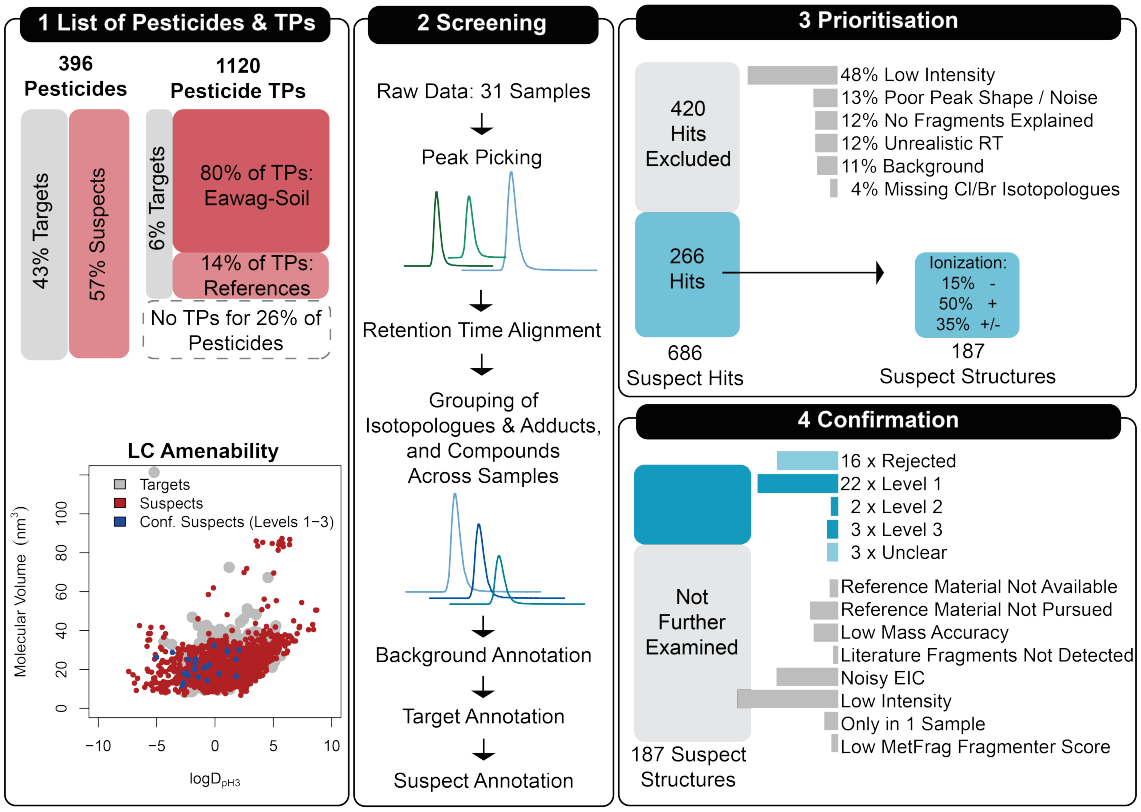

Figure 2-1: The compiled list of pesticides and TPs comprised 396 pesticides (43% targets, 57% suspects) and 1120 TPs (6% targets, 94% suspects). 1256 suspects (223 pesticides, 1033 TPs) had a monoisotopic mass >99 Da; 95% of these suspects had a similar logD as the target compounds and 99.5% included a heteroatom (box 1). After the automated screening (box 2), the suspect hits were prioritised (box 3, blue color) and the most promising suspects were further examined with reference material if available (box 4, blue color).

2.3.2.2 Prioritisation and Identification

After background, target and noise removal, 686 suspect hits, annotated with 430 suspect structures, remained. The 686 suspect hits were reduced to 266 by excluding hits with low intensity (48%), poor peak shape / noise (13%), no MS/MS fragments explained by the suspect according to the in silico fragmenter MetFrag (12%), unrealistic RT (12%), background (11%), or missing Cl/Br isotopologues if expected from the formula (4%). The 266 suspect hits corresponded to only 187 different suspect structures as some compounds were grouped insufficiently across samples, even though m/z and RT deviated only slightly; others were detected in positive and negative ionization mode or the EICs exhibited several peaks with different RTs. The 187 suspect structures were then further prioritised by taking e.g. peak intensity and shape, detection frequency, mass accuracy and MetFrag results into account (Figure 2-1, SI2-B3).

Reference material could be obtained for the 43 most promising suspects, either commercially (twelve reference standards) or from the pesticide producers via the European Crop Protection Agency (31 reference standards). For details on suspects which were not further investigated, see SI2-A3 and SI2-B3. We confirmed 21 TPs and one pesticide (Level 1) and rejected nine TPs and seven pesticides. Two TPs were identified as probable (Level 2, no reference standard), three TPs as tentative structure (Level 3), either because reference material was not available

(2 TPs) or due to analytical problems (1 TP, reference material impure or unstable), and three suspects remained unclear (details in SI2-C) and could not be classified following Schymanski et al. (2014), although reference material was available (Figure 2-1). The confirmed suspect hits (Levels 1-3, Table 2-1) included among others TPs from the fungicides chlorothalonil (7 TPs), fluxapyroxad / bixafen (2 TPs), metalaxyl (1 TP), and fludioxonil (1 TP), TPs from the herbicides terbuthylazine (4 TPs), dimethachlor (1 TP), acetochlor / metolachlor (2 TPs), nicosulfuron (2 TPs), and TPs from the insecticide fipronil (2 TPs). 13 TPs (Level 1: 10; Level 2: 1, Level 3: 2) are reported here for the first time in groundwater. SI2-B5 and SI2-C provide detailed information for each confirmed or rejected suspect. MS/MS spectra of the confirmed suspects were uploaded to the European MassBank (Horai et al. 2010).

Confirmed suspects tended to have higher peak intensity than rejected suspects (Figure SI2-A4a; median intensity $3.5x10^5$ vs. $5x10^4$). This difference was expected since intense peaks provide more information about the candidate, and therefore, facilitate the correct evaluation of the suspect hit before confirmation with reference material. Interestingly, sales data was not a strong indicator for the likelihood of a positive suspect hit (Figure SI2-A4c).

In silico fragmentation was especially useful for the correct prioritization of intense peaks with relatively large m/z (>300), such as in the cases of chlorothalonil and fipronil TPs. Intense precursor peaks improve the quality of MS/MS spectra, showing less interfering peaks, and the larger molecules may produce more information-rich spectra. Conversely, if precursor intensity is low, as is the case for many suspect hits, acquiring meaningful MS/MS spectra is challenging because the high number of interfering peaks leads to many fragments that are not related to the compound of interest. For example, for one compound 83 MS/MS peaks were detected, of which 26 could be explained by the annotated suspect fenazaquin (Figure SI2-A5). For this suspect, 2122 candidates were retrieved from ChemSpider, and, up to 47 fragments could be explained by ChemSpider hits. The suspect fenazaquin was then rejected with reference material due to different retention time.

Using broad suspect lists or even web databases such as ChemSpider for compound elucidation proves often to be less successful for TP identification compared to high quality suspect lists. In our case, 13 out of the confirmed suspects (Levels 1-3) were not part of ChemSpider, while ten were in ChemSpider but based on expert knowledge were not expected to originate from pesticides, based on their names. Compounds that cannot be traced back to specific sources are less likely to be prioritized for elucidation in suspect and nontarget screenings. This highlights the need for high quality suspect lists, comprising e.g. experimentally observed TPs as in this study, to increase the number of identifications of compounds that are so far not known to be of environmental relevance.

Table 2-1: Confirmed pesticide TPs (Levels 1-3) except for Level 3 candidates with analytical problems (cymoxanyl TPs: reference material impure / unstable) ordered according to novelty and spread. TP names from European pesticide registration. Ident. Level = Identification Level; LOQ = limit of quantification; c_{90th} = 90th percentile of concentrations; c_{max} = maximum concentration.

Reported in Groundwater for the First Time	**Ident. Level**	**LogD$_{pH7}$**	**LOQ (ng/L)**	**Detections (31 Samples)**	**C$_{90th\ percentile}$ (ng/L)**	**C$_{max}$ (ng/L)**
 Chlorothalonil TP R471811	1	-1.7	3	31	1100	2700
Terbuthylazine TP CSCD692760 	1	-1.5	3	27	27	32
 Terbuthylazine TP CSAA036479	1	-2.7	0.6	25	6.4	27
Chlorothalonil TP R417888 Isomers 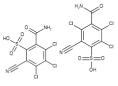	3	-0.7	-	18/19	~18/~39	~49/~120
 Chlorothalonil TP R419492	1	-4.5	-	18	Not Quantified	
Chlorothalonil TP SYN548580 	1	0.0	-	13	Not Quantified	
 Chlorothalonil TP SYN507900	1	0.4	1.3	13	33	150
Fipronil TP RPA 106681 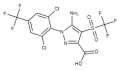	2b	1.0	-	11	14	~120
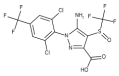 Fipronil TP RPA 200761	1	1.1	1	6	6.6	71
Fluxapyroxad & Bixafen TP CSCD465008 	1	-2.8	15	1	-	~60
 Fluxapyroxad & BixafenTP CSAA798670	1	-2.7	10	1	-	13
Cycloxydim TP BH 517-TSO E/Z isomer* 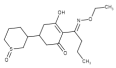	1	-0.1	1.3	1	-	1.3
Rarely Mentioned in Literature						
 Terbuthylazine TP CSCD648241 *Valsecchi et al. (2017), LfU (2018)*	1	-2.5	0.5	29	54	190
Terbuthylazine TP MT23/GS16984 *Valsecchi et al. (2017), LfU (2018)* 	1	1.8	0.5	29	52	78
 Chlorothalonil TP R417888 *LUBW (2011)*	1	-0.7	1	28	470	1300
Dimethachlor TP CGA 369873 *Reemtsma et al. (2013a)* 	1	-0.9	0.5	28	67	95
 Nicosulfuron TP UCSN *Steverkooperation (2016)*	1	-2.3	0.2	27	24	75
Metolachlor TP NOA413173 *Reemtsma et al. (2013a)* 	1	-3.6	1.7	22	130	430
 Metolachlor TP CGA 368208 / Acetochlor sulfonic acid *Reemtsma et al. (2013a)*	1	-0.5	1	20	46	150
Nicosulfuron TP AUSN *Steverkooperation (2016)* 	1	-1.6	3	17	27	47
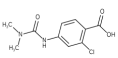 Chlorotoluron TP CGA15140 *Reemtsma et al. (2013a)*	2a	-1.8	-	9	No Standard	
Pinoxaden TP NOA 407854* *Reemtsma et al. (2013a)* 	1	2.1	0.3	4	0.3	5.5
 Fludioxonil TP CGA 192155 *Reemtsma et al. (2013a)*	1	-0.7	3	2	-	200
Metalaxyl-M TP CGA108906 *Reemtsma et al. (2013a)* 	1	-5.0	7	1	-	8.8

*Possibly, formation during sample enrichment / analysis, see SI-C for details.

2.3.3 New Pesticide TPs

Within the suspect screening, one pesticide (oxadixyl) and 26 pesticide TPs (Levels 1-3) were identified. Table 2-1 presents the confirmed TPs, except for Level 3 candidates with analytical problems (cymoxanil TPs). For details, see SI2-B5 and SI2-C. The most prominent pesticide TPs regarding their novelty, concentration, or spread are discussed in the following section.

2.3.3.1 Chlorothalonil TPs

To the best of our knowledge, we report here the detection of the chlorothalonil TP R471811 for the first time in environmental samples. TP R471811 was the only MP detected in all samples, exceeding 100 ng/L in 20 out of 31 samples. Additionally, this compound had the highest maximum concentration of all compounds, detected at 2700 ng/L in a single sample (average in all samples 520 ng/L, 90th percentile c_{90th} 1100 ng/L). In future, concentrations of R471811 might still increase due to its high persistence (DT_{50}: 98-1000 d) and further formation from the parent TP R417888 (Figure 2-2), whereby the removal of R471811 in drinking water production may prove challenging. Due to the high polarity and the electron-withdrawing functional groups, even more advanced treatment technologies such as activated carbon and ozonation are expected to hardly retain or degrade the compound (Matsushita et al. 2018, Von Sonntag and Von Gunten 2012). This is especially concerning because the toxicological relevance of the TPs has not been sufficiently assessed; however, the active substance is classified as carcinogenic, as reported within the current re-approval process in the EU (EFSA 2018). Therefore, TP R471811 should provisionally be classified as relevant (EFSA 2018) implying a drinking water limit of 100 ng/L (EDI 2016, European Commission 1998).

The classification as relevant pesticide TPs applies as well to the other chlorothalonil TPs detected in this study (Figure 2-2). Whereas monitoring data from Germany is available for TP R417888 (LUBW 2011), we present here as well the first detection of TP SYN507900 (Level 1) and of two isomers of R417888 (Level 3) in groundwater. Two more TPs were detected later by a manual exact mass screening, because a recent EFSA report (2018) noted that additional chlorothalonil TPs are expected in groundwater. Therefore, the exact masses of these suspects were manually screened for to avoid false negatives. For TP R419492 we detected a broad and early-eluting peak ($[M-H]^-$ & $[M-2H]^{2-}$; RT 4-6 min) in 18 samples. The CD 2.1 workflow also successfully picked features (defined by their m/z and RT) but unsuccessfully merged these features into a compound. Another TP, SYN548580, was detected in 13 samples (RT 10 min); this TP was not on the suspect list. As reference material was received later, both TPs (R419492 and SYN548580) could only be confirmed (Level 1) and quantified in new samples from the same or other sites. In these samples, both TPs showed lower concentrations than R471811.

The high concentrations and detection frequencies of chlorothalonil TPs is explained by their mobility and the broad application of the fungicide chlorothalonil, e.g. for grain and vegetable cultivation but also on non-agricultural land such as golf courses (BLW 2018a). Chlorothalonil was not analysed in this study as chlorothalonil does not sufficiently ionise in electrospray. However, in German groundwater samples with high concentrations of TP R417888 (c_{max} 1700 ng/L) chlorothalonil has never been detected (LUBW 2011) because chlorothalonil adsorbs strongly to soil particles (EFSA 2018). Recently, the EU banned chlorothalonil due to the carcinogenic properties of chlorothalonil, the risk to fish and amphibians and the expected groundwater contamination with TPs (European Commission 2019).

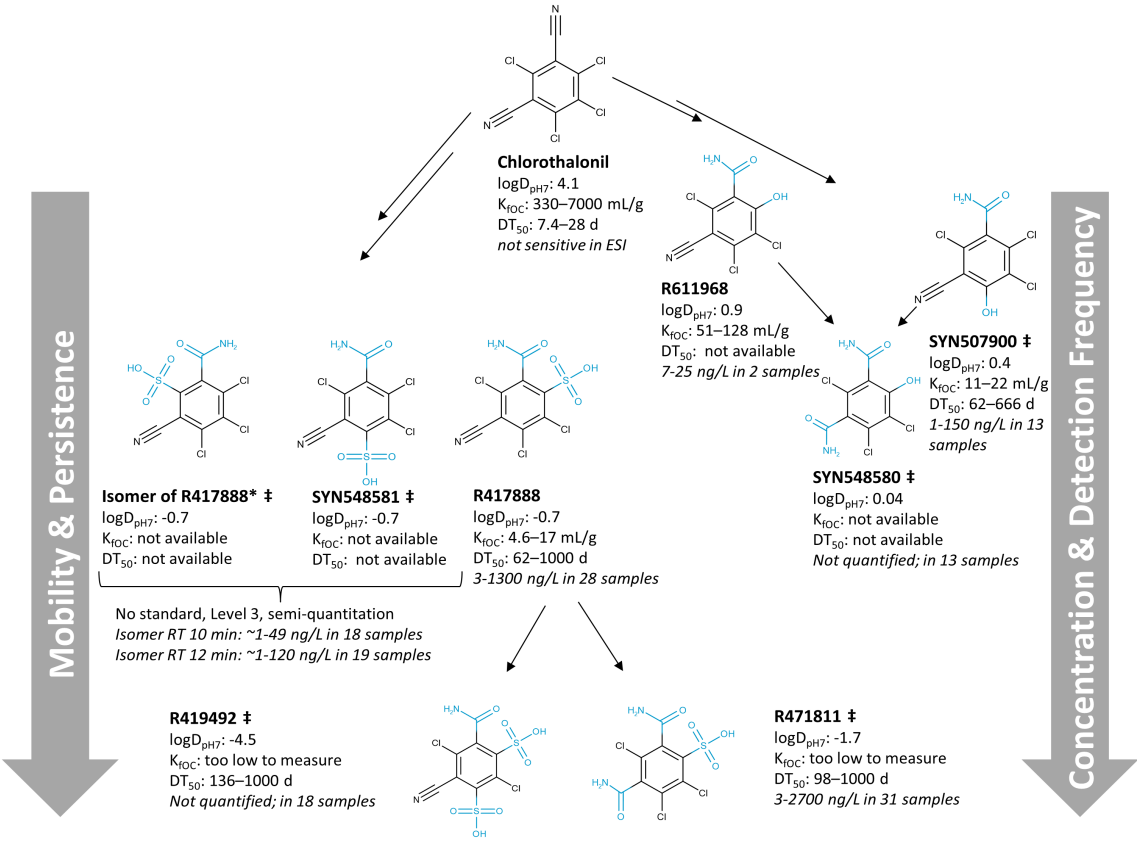

Figure 2-2: Chlorothalonil and its TPs detected in groundwater; concentrations and frequency of detection increase with mobility and persistence. K_{foC} and DT_{50} from EFSA (2018); *isomer is not included in EFSA (2018); ‡ detection in groundwater is reported here for the first time.

2.3.3.2 Fipronil TPs

The suspect screening provided four suspect hits for fipronil TPs: RPA 200761 (logD$_{pH7}$: 1.1), RPA 106681 (logD$_{pH7}$: 1.0), MB 46233 (logD$_{pH7}$: 2.2) and RPA 105320 (logD$_{pH7}$: 3.6), none of which has previously been reported to be detected in groundwater. RPA 200761 was confirmed with reference material (6 detections, 1-70 ng/L). For the remaining TPs, reference material could not be obtained. However, the reference material for RPA 200761 was not pure, i.e. further peaks were detected for the $[M+H]^+$ and $[M-H]^-$ of the other TPs, the RTs of which matched with the detections of other TPs in the samples. MS/MS data could be acquired for RPA 106681, most fragments were annotated with structure proposals (Figure SI2-A6) so that RPA 106681 was identified as probable structure (Level 2b). Semi-quantitative concentrations ranging from 0.7 to 120 ng/L (c_{90th} ~14 ng/L) in 11 samples were estimated assuming the same ionization efficiency as for RPA 200761.

The detection of fipronil TPs is surprising, because it is expected that relatively low amounts of the insecticide have been released to the environment. The insecticide fipronil was sold in Switzerland for seed treatment from 2009 to 2011 in low amounts (<5 t/a) (BLW 2018b), but is not approved anymore due to high toxicity to bees. In addition, fipronil has been used as biocide, but sales data is not available. Fipronil and its less mobile, but well-known, TPs fipronil-sulfide (MB 45950), fipronil-sulfone (MB 46136) and fipronil-desulfinyle (MB 46513) were not detected, which may be related to the high LOQs (10-50 ng/L), to their low mobility (logD$_{pH7}$: >4), and to the low application amounts several years ago.

2.3.3.3 Terbuthylazine TPs

In many European countries, the triazine herbicide terbuthylazine has replaced atrazine (Alvarez et al. 2016), which was banned in the EU in 2005 (2004/248/EC 2004) and in Switzerland in 2009. While terbuthylazine and its well-known and relevant TP terbuthylazine desethyl were only detected in 12 and 19 samples, respectively, at low concentrations (c_{90th} 5 / 6.1 ng/L, c_{max} 22 / 38 ng/L), the suspect screening revealed four additional TPs: CSAA036479 (LM2), CSCD692760 (LM3), MT23 (LM5), and CSCD648241 (LM6). The four TPs were detected in 80 - 90% of the samples with c_{90th} ranging from 6.4 to 54 ng/L. While the TPs LM2 and LM3 were only reported in groundwater within field studies performed for the European pesticide registration (EFSA 2017), Valsecchi et al. (2017) and LfU (2018) detected LM5 and LM6 in an Italian aquifer and German drinking water, respectively.

2.3.3.4 Nicosulfuron TPs

We identified two non-relevant nicosulfuron TPs, UCSN and AUSN. The more persistent UCSN was measured more frequently and at higher concentrations than the less persistent AUSN (UCSN: DT_{50} 126-308 d, 27 detections, c_{90th} 24 ng/L, c_{max} 75 ng/L; AUSN: DT_{50} 74-218 d, 17 detections, c_{90th} 27 ng/L, c_{max} 47 ng/L) (EFSA 2008). Suspect hits for two other nicosulfuron TPs, MU-466 and HMUD, were not further examined with reference material due to very low peak intensity. In German surface waters, the TPs AUSN, UCSN and ASDM were detected at concentrations of up to 150 ng/L; HMUD was below LOQ (Steverkooperation 2016). The herbicide nicosulfuron is used as post-emergence herbicide in maize cultivation (BLW 2018a, Lewis et al. 2016); sales in Switzerland are 1-5 t/a (BLW 2018b). Nicosulfuron is low to moderately persistent (DT_{50} 7-46 d) in aerobic soils (EFSA 2008), and accordingly, was only detected in four samples at concentrations <5 ng/L.

2.3.4 Agricultural vs. Urban Pollution

The target and suspect screening showed clearly that not only pesticides but also their TPs need to be monitored to comprehensively assess the impact of pesticide application in agriculture on groundwater quality. Although we quantitatively analysed more pesticides than pesticide TPs (176 vs. 97), the total concentration of pesticide TPs exceeded the total concentration of the active substances in 30 samples. This holds also true for individual pesticides: most active substances were detected less frequently and at lower concentrations than the sum of their TPs (Figure 2-3) as was also reported in the Swiss National Groundwater Monitoring NAQUA (FOEN 2019, Reinhardt et al. 2017) and research studies (Buttiglieri et al. 2009, Kolpin et al. 2004, Weber et al. 2007). These findings coincide with substance properties such as DT_{50} and K_{foC} (EFSA peer review reports, if available) and predicted $logD_{pH7}$ values. The pesticide TPs often show higher persistence and mobility than the active substance.

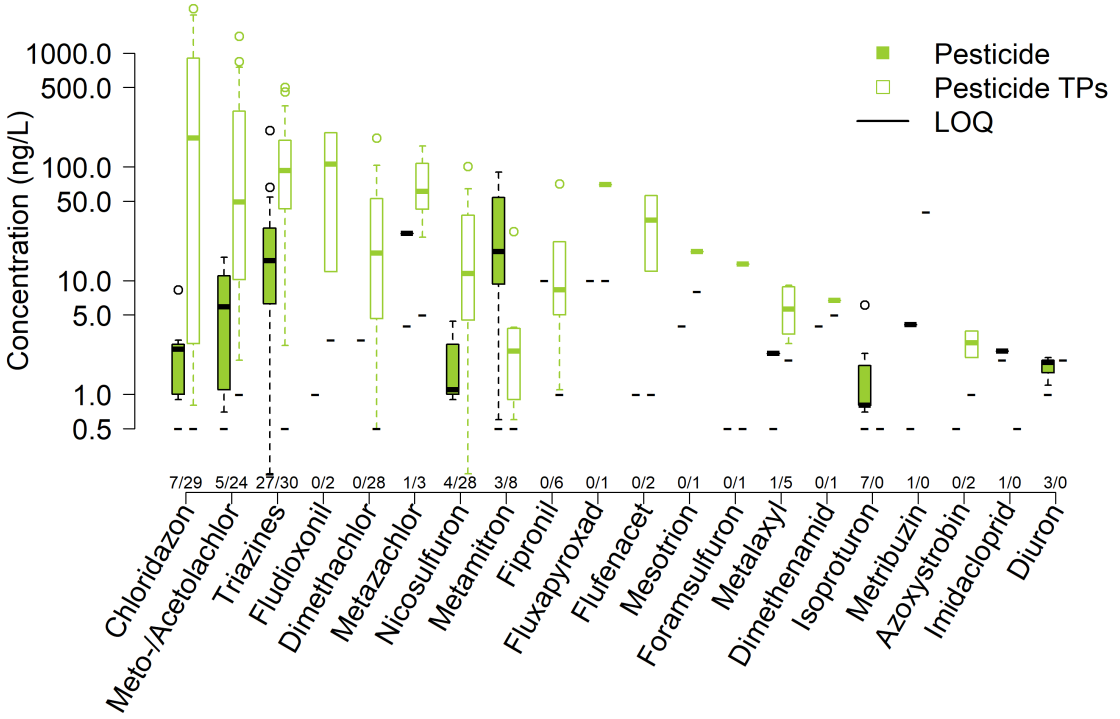

Figure 2-3: The total concentration of active substance (in filled boxes) compared to the pesticide TPs (in open boxes). In almost all cases the total concentration of TPs is higher than the concentration of the active substance. Numbers above x-axis indicate the detection frequency of the active substance / TPs in the 31 samples. Total concentration is plotted on the y-axis on a logarithmic scale. Compounds are ordered by decreasing maximum concentration. Triazines were summarised, as many TPs may originate from different triazines. Pesticides for which only TPs could be analysed with the analytical method are not included (e.g. chlorothalonil). Metolachlor-ESA was not analysed in all samples due to RT shifts.

To assess to what extent the selected groundwater samples were polluted by agricultural and/or urban influences, we screened additionally for 283 MPs from predominantly urban sources. Although the quantitative screening comprised approximately as many agricultural as urban MPs (273 vs. 283), the total concentration and detection frequency of agricultural MPs exceeded the concentration and detection frequency of urban MPs in 26 and 28 samples, respectively. The dominance of agricultural MPs was expected, as we predominantly selected groundwater monitoring sites which were known to be impacted by agricultural MPs, to cover groundwater contamination with pesticide TPs as comprehensively as possible. Nevertheless, eleven samples were clearly impacted by urban contamination sources, revealing at least ten different urban MPs. Figure 2-4 illustrates the MP pattern and land use in the catchment of the 31 sampled aquifers.

The presence of agricultural and urban MPs in the individual groundwater samples is partly explained by the land use within the catchments. The percentage of agricultural land in the catchments correlated weakly with the total concentration of agricultural MPs (Pearson's ρ 0.50) and with detection frequency (ρ 0.34), respectively (see Figure SI2-A7). Land use probably correlated more strongly with concentration than with detection frequency, as the agricultural area influences more the amount than the number of applied pesticides. Surprisingly, the groundwater monitoring site with the highest percentage of agriculture in the catchment showed only a low concentration of agricultural MPs (220 ng/L, Figure 2-4

Figure 2-4, Figure SI2-A7). Total MP concentration at this location was dominated by the widespread and highly mobile chlorothalonil TP R471811, accounting for 84% of total MP concentration. The low contamination with agricultural MPs may be explained by the hydrogeological setting. According to borehole logs, the groundwater well abstracts water from a heterogeneous aquifer consisting of sand-loam layers with gravel lentils / channels. Furthermore, the borehole logs show less permeable loam-clay top layers, which may act as a protective barrier, reducing MP transport from the surface. This explains both the low MP concentration, low nitrate concentration (10 mg/L), and the low oxygen content (oxygen content during sampling: 0.5 mg/L, dissolved organic carbon content: <0.5 mg/L). If this sample is excluded as outlier, the correlation between percentage of agricultural land and agricultural MP concentration increases from ρ 0.50 to ρ 0.64.

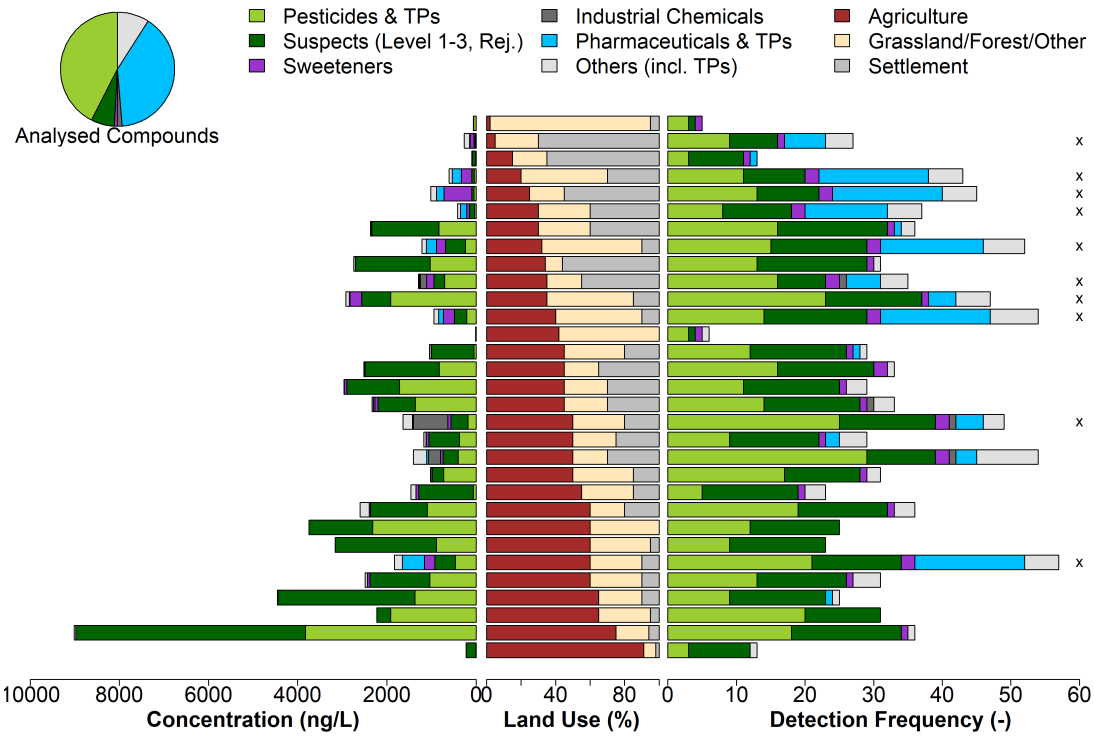

Figure 2-4: Total concentration (left) and detection frequency (right) per compound class and sample compared to land use. In the centre, land use in the catchment of each groundwater monitoring site. In the upper left, pie chart with the distribution of all quantitatively analysed substances in compound classes. Suspects: pesticides and pesticide TPs which were confirmed and quantified (Levels 1-3) or rejected with reference standards. Agricultural MPs: pesticides and suspects. Urban MPs: sweeteners, industrial chemicals, pharmaceuticals and others. "X" marks groundwater monitoring sites close to wastewater impacted streams (<700m, river bank filtration). Monitoring sites are ordered from top to bottom by increasing agricultural land use. The pesticide TP metolachlor-ESA could not be analysed in all samples due to RT shift.

While agricultural pollution seems to be related to agricultural land use area, no or only a very weak correlation was found between urban MP concentration/detection frequency, and percentage of settlement in the catchment (Pearson's ρ 0.14/0.21, see Figure SI2-A7). The low correlation shows the different entry pathways for agricultural and urban MPs. Pesticides and their TPs predominantly enter groundwater diffuse via seepage from agricultural soils, whereas, urban MPs enter groundwater primarily along wastewater impacted streams or leaky sewer systems. While streams are not considered in the land use characterisation of the monitoring sites, sewer systems are covered by the land use class "settlement". Ten out of eleven samples with at least ten different urban MPs originated from groundwater monitoring sites which are located 30 to 700 m from a wastewater impacted stream (river bank filtration, Figure 2-4). The groundwater monitoring site without river bank filtration influence, however, drains a catchment with a sewer, which may explain the presence of 16 different urban MPs in addition to the 40 agricultural MPs. Especially in urban areas, leaky sewer systems were shown to present a major contamination source for groundwater (Wolf et al. 2012). Similar observations were made by Ter Laak et al. (2012) in a Dutch groundwater screening study comprising 42 pumping wells differing in the hydrogeological setting (river bank filtration, phreatic, and (semi-) confined) and the land use. Ter Laak et al. (2012) detected more compounds in groundwater from rural than from urban areas. However, most of these compounds found in rural areas could not be identified, possibly because the target screening was only comprised of a few pesticides and TPs. See SI2-A6 for further discussion of site-specific MP contamination.

2.4 Conclusions

- Suspect screening with a high-quality suspect list comprising more than 1000 experimentally observed pesticide TPs revealed the presence of several so far overseen pesticide TPs in groundwater. The suspect list presented is currently the most comprehensive pesticide TP data set which is publicly accessible and is recommended for screening surface and groundwaters worldwide.
- The suspect screening identified 27 pesticides and pesticide TPs (Levels 1-3). The TPs of chlorothalonil, nicosulfuron, fipronil, terbuthylazine, bixafen and fluxapyroxad were so far rarely mentioned in literature or not known at all. Spectra for future screening studies are available on MassBank (www.massbank.eu).
- Chlorothalonil TPs were widely present in groundwater. Chlorothalonil TP R471811 was detected in all samples, even in aquifers with low anthropogenic impact. In 20 out of 31 samples, concentrations exceeded 100 ng/L. The human-toxicological risk needs to be assessed as well as the fate in drinking water treatment.
- Total MP concentrations ranged from 60 to 9000 ng/L. The MPs with the highest concentration and detection frequency were pesticide TPs followed by parent pesticides (detection frequency) and sweeteners (concentration). Concentrations of 15 TPs originating from nine different pesticides exceeded 100 ng/L in at least one sample.
- Land use in the catchment and hydrogeological setting (river bank filtration, top layers) strongly drove the MP pattern. Urban MPs were predominantly detected in aquifers that interact with wastewater impacted streams. Agricultural MPs were found in aquifers with agriculture in the catchment.

Acknowledgement

This study was funded by the Swiss Federal Office for the Environment FOEN and the Swiss National Science Foundation (grant number 205320_165935). Samples of the National Groundwater monitoring NAQUA were provided by the Federal Office for the Environment FOEN and the cantonal authorities. Groundwater monitoring sites were selected by Miriam Reinhardt. We are grateful to all those involved in sample collection and transport and to the Eawag AuA laboratory for analysing various hydrochemical parameters. The comprehensive list of pesticides approved in Switzerland 2005-2017 was provided by the Swiss Water Pollution Control Association platform (VSA-Platform). Additionally, we thank Kathrin Fenner, Diogo Latino and co-workers for the extensive list of pesticide TPs that were extracted manually from European pesticide registration dossiers in a labour-intensive process. We especially thank Philipp Longrée for his support in lab work, LC-HRMS measurement and target quantification. Furthermore, we acknowledge Emma Schymanski for her support in compiling the suspect list and for providing an R script to run MetFrag in an automated way for all suspect hits. We thank Jennifer Schollée and Michael Stravs for their help with R, and additionally, Jennifer Schollée and Miriam Reinhardt for proofreading the manuscript and their critical feedback. Finally, we acknowledge Syngenta, BASF, Dupont and Bayer for providing reference material.

References

2004/248/EC, 2004. Commission decision of 10 March 2004 concerning the non-inclusion of atrazine in Annex I to Council Directive 91/414/EEC and the withdrawal of authorisations for plant protection products containing this active substance. Official Journal of the European Union 78, 1-3.

Alvarez, P.M., Quinones, D.H., Terrones, I., Rey, A. and Beltran, F.J., 2016. Insights into the removal of terbuthylazine from aqueous solution by several treatment methods. Water research 98, 334-343.

Arp, H.P.H., Brown, T.N., Berger, U. and Hale, S.E., 2017. Ranking REACH registered neutral, ionizable and ionic organic chemicals based on their aquatic persistency and mobility. Environmental Science: Processes & Impacts 19(7), 939-955.

Banning, H., Bialek, K., Czub, G., Müller, A., Pickl, C., Scheithauer, M., Straus, G. and Tüting, W., 2019. Recommendation list for the monitoring of pesticide metabolites in German groundwaters (Empfehlungsliste für das Monitoring von Pflanzenschutzmittel-Metaboliten in deutschen Grundwässern). UBA. https://www.umweltbundesamt.de/dokument/empfehlungsliste-fuer-das-monitoring-von. Accessed: 25/06/2019.

BLW, 2018a. List of approved plant protection products (Pflanzenschutzmittelverzeichnis). Federal Office for the Agriculture. https://www.psm.admin.ch/de/produkte. Accessed: 18/12/2018.

BLW, 2018b. Sales per active ingredient (Verkaufsmengen je Pflanzenschutzmittel-Wirkstoff). Federal Office for the Agriculture. https://www.blw.admin.ch/blw/de/home/nachhaltige-produktion/pflanzenschutz/pflanzenschutzmittel/verkaufsmengen-der-pflanzenschutzmittel-wirkstoffe.html. Accessed: 18/01/2019.

BLW, 2019. Relevance of plant protection product metabolites in groundwater and drinkingwater (Relevanz von Pflanzenschutzmittel-Metaboliten im Grund- und Trinkwasser). Federal Office for the Agriculture, Agroscope, Federal Food Safety and Veterinary Office. https://www.blw.admin.ch/blw/de/home/nachhaltige-produktion/pflanzenschutz/pflanzenschutzmittel/nachhaltige-anwendung-und-risikoreduktion.html. Accessed: 18/01/2019.

Brunner, A.M., Vughs, D., Siegers, W., Bertelkamp, C., Hofman-Caris, R., Kolkman, A. and ter Laak, T., 2019. Monitoring transformation product formation in the drinking water treatments rapid sand filtration and ozonation. Chemosphere 214, 801-811.

Buttiglieri, G., Peschka, M., Fromel, T., Muller, J., Malpei, F., Seel, P. and Knepper, T.P., 2009. Environmental occurrence and degradation of the herbicide n-chloridazon. Water research 43(11), 2865-2873.

Chambers, M.C., Maclean, B., Burke, R., Amodei, D., Ruderman, D.L., Neumann, S., Gatto, L., Fischer, B., Pratt, B., Egertson, J., Hoff, K., Kessner, D., Tasman, N., Shulman, N., Frewen, B., Baker, T.A., Brusniak, M.-Y., Paulse, C., Creasy, D., Flashner, L., Kani, K., Moulding, C., Seymour, S.L., Nuwaysir, L.M., Lefebvre, B., Kuhlmann, F., Roark, J., Rainer, P., Detlev, S., Hemenway, T., Huhmer, A., Langridge, J., Connolly, B., Chadick, T., Holly, K., Eckels, J., Deutsch, E.W., Moritz, R.L., Katz, J.E., Agus, D.B., MacCoss, M., Tabb, D.L. and Mallick, P., 2012. A cross-platform toolkit for mass spectrometry and proteomics. Nature Biotechnology 30, 918.

Daughton, C.G. and Ternes, T.A., 1999. Pharmaceuticals and personal care products in the environment: agents of subtle change? Environmental health perspectives 107 Suppl 6, 907-938.

Duhrkop, K., Shen, H., Meusel, M., Rousu, J. and Bocker, S., 2015. Searching molecular structure databases with tandem mass spectra using CSI:FingerID. Proc Natl Acad Sci U S A 112(41), 12580-12585.

EDI, 2016. Swiss regulation No. 817.022.11 concerning drinking water and water in public swimming pools and shower facilities (Verordnung des EDI über Trinkwasser sowie Wasser in öffentlich zugänglichen Bädern und Duschanlagen (TBDV) vom 16. Dezember 2016 (Stand am 1. Mai 2018)), Eidgenössisches Departement des Innern.

EFSA, 2008. Conclusion regarding the peer review of the pesticide risk assessment of the active substance nicosulfuron. EFSA Journal 120, 1-91.

EFSA, 2017. Peer review of the pesticide risk assessment for the active substance terbuthylazine in light of confirmatory data submitted. EFSA Journal 15(6), 1-20.

EFSA, 2018. Peer review of the pesticide risk assessment of the active substance chlorothalonil. EFSA Journal 16(1), 1-40.

European Commission, 1998. Council Directive 98/83/EC of 3 November 1998 on the quality of water intended for human consumption. Official Journal of the European Communities (L330).

European Commission, 2003. Guidance document on the assessment of the relevance of metabolites in groundwater of substances regulated under council directive 91/414/EEC. Sanco/221/2000 –rev.10- final.

European Commission, 2019. SANTE/10186/2018 Rev 1: Final Renewal report for the active substance chlorothalonil finalised in the Standing Committee on Plants, Animals, Food and Feed at its meeting on 22 March 2019 in view of the non-renewal of the approval of chlorothalonil as active substance in accordance with Regulation (EC) No 1107/20091. https://ec.europa.eu/food/plant/pesticides/eu-pesticides-database/public/?event=activesubstance.ViewReview&id=1720. Accessed: 05/08/2019.

FOEN, 2019. Plant protection products in groundwater. Federal Office for the Environment. https://www.bafu.admin.ch/bafu/de/home/themen/wasser/fachinformationen/zustand-der-gewaesser/zustand-des-grundwassers/grundwasser-qualitaet/pflanzenschutzmittel-im-grundwasser.html. Accessed: 15/08/2019.

Freiburghaus, M., 2012. Statistical overview of water supply in Switzerland 2010 (Statistische Übersicht über die Wasserversorgung in der Schweiz 2010). Aqua & Gas 3, 54-59.

Gatto, L. and Lilley, K.S., 2012. MSnbase - an R/Bioconductor package for isobaric tagged mass spectrometry data visualization, processing and quantitation. Bioinformatics (28), 288-289.

Heberer, T., Mechlinski, A., Fanck, B., Knappe, A., Massmann, G., Pekdeger, A. and Fritz, B., 2004. Field studies on the fate and transport of pharmaceutical residues in bank filtration. Ground Water Monitoring and Remediation 24(2), 70-77.

Horai, H., Arita, M., Kanaya, S., Nihei, Y., Ikeda, T., Suwa, K., Ojima, Y., Tanaka, K., Tanaka, S., Aoshima, K., Oda, Y., Kakazu, Y., Kusano, M., Tohge, T., Matsuda, F., Sawada, Y., Hirai, M.Y., Nakanishi, H., Ikeda, K., Akimoto, N., Maoka, T., Takahashi, H., Ara, T., Sakurai, N., Suzuki, H., Shibata, D., Neumann, S., Iida, T., Tanaka, K., Funatsu, K., Matsuura, F., Soga, T., Taguchi, R., Saito, K. and Nishioka, T., 2010. MassBank: a public repository for sharing mass spectral data for life sciences. Journal of Mass Spectrometry 45(7), 703-714.

Kern, S., Fenner, K., Singer, H.P., Schwarzenbach, R.P. and Hollender, J., 2009. Identification of Transformation Products of Organic Contaminants in Natural Waters by Computer-Aided Prediction and High-Resolution Mass Spectrometry. Environmental science & technology 43(18), 7039-7046.

Kolpin, D.W., Schnoebelen, D.J. and Thurman, E.M., 2004. Degradates Provide Insight to Spatial and Temporal Trends of Herbicides in Ground Water. Ground Water 42(4), 601-608.

Kolpin, D.W., Thurman, E.M., Linhart, S.M.J.A.o.E.C. and Toxicology, 1998. The Environmental Occurrence of Herbicides: The Importance of Degradates in Ground Water. 35(3), 385-390.

Lapworth, D.J., Baran, N., Stuart, M.E. and Ward, R.S., 2012. Emerging organic contaminants in groundwater: A review of sources, fate and occurrence. Environmental pollution 163, 287-303.

Latino, D.A., Wicker, J., Gutlein, M., Schmid, E., Kramer, S. and Fenner, K., 2017. Eawag-Soil in enviPath: a new resource for exploring regulatory pesticide soil biodegradation pathways and half-life data. Environmental Science Processes and Impacts 19, 449-464.

Lewandowski, J., Putschew, A., Schwesig, D., Neumann, C. and Radke, M., 2011. Fate of organic micropollutants in the hyporheic zone of a eutrophic lowland stream: Results of a preliminary field study. Science of The Total Environment 409(10), 1824-1835.

Lewis, K.A., Tzilivakis, J., Warner, D.J. and Green, A., 2016. An international database for pesticide risk assessments and management. Human and Ecological Risk Assessment: An International Journal 22(4), 1050-1064.

LfU, 2018. Development of PPP pollution in Bavarian waters - balance after 30 years of PSM monitoring. (Entwicklung der PSM-Belastung in bayerischen Gewässern – Bilanz nach 30 Jahren PSM-Monitoring). Bayerisches Landesamt für Umwelt. http://www.bestellen.bayern.de/shoplink/lfu_all_00146.htm.

Loos, R., Locoro, G., Comero, S., Contini, S., Schwesig, D., Werres, F., Balsaa, P., Gans, O., Weiss, S., Blaha, L., Bolchi, M. and Gawlik, B.M., 2010. Pan-European survey on the occurrence of selected polar organic persistent pollutants in ground water. Water research 44(14), 4115-4126.

LUBW, 2011. Groundwater monitoring programme - results from sampling campaign 2010 (Grundwasserüberwachungsprogramm - Ergebnisse der Beprobung 2010). Reihe Grundwasserschutz. 42, 1-98. http://www4.lubw.baden-wuerttemberg.de/servlet/is/208632/.

Matsushita, T., Morimoto, A., Kuriyama, T., Matsumoto, E., Matsui, Y., Shirasaki, N., Kondo, T., Takanashi, H. and Kameya, T., 2018. Removals of pesticides and pesticide transformation products during drinking water treatment processes and their impact on mutagen formation potential after chlorination. Water research 138, 67-76.

Mechelke, J., Longree, P., Singer, H. and Hollender, J., 2019. Vacuum-assisted evaporative concentration combined with LC-HRMS/MS for ultra-trace-level screening of organic micropollutants in environmental water samples. Analytical and Bioanalytical Chemistry.

MoNA, 2019. MoNA - MassBank of North America. http://mona.fiehnlab.ucdavis.edu/. Accessed: 21/01/2019.

Moschet, C., Piazzoli, A., Singer, H. and Hollender, J., 2013. Alleviating the reference standard dilemma using a systematic exact mass suspect screening approach with liquid chromatography-high resolution mass spectrometry. Analytical chemistry 85(21), 10312-10320.

Postigo, C. and Barcelo, D., 2015. Synthetic organic compounds and their transformation products in groundwater: occurrence, fate and mitigation. Science of The Total Environment 503-504, 32-47.

R Core Team, 2016. R: A language and environment for statistical computing. R Foundation for Statistical Computing, Vienna, Austria. https://www.R-project.org/.

Reemtsma, T., Alder, L. and Banasiak, U., 2013a. Emerging pesticide metabolites in groundwater and surface water as determined by the application of a multimethod for 150 pesticide metabolites. Water research 47(15), 5535-5545.

Reemtsma, T., Alder, L. and Banasiak, U., 2013b. A multimethod for the determination of 150 pesticide metabolites in surface water and groundwater using direct injection liquid chromatography-mass spectrometry. Journal of chromatography A 1271(1), 95-104.

Reemtsma, T., Berger, U., Arp, H.P., Gallard, H., Knepper, T.P., Neumann, M., Quintana, J.B. and Voogt, P., 2016. Mind the Gap: Persistent and Mobile Organic Compounds-Water Contaminants That Slip Through. Environmental science & technology 50(19), 10308-10315.

Reinhardt, M., Kozel, R., Hofacker, A. and Leu, C., 2017. Monitoring of pesticide residues in groundwater (Monitoring von PSM-Rückständen im Grundwasser). Aqua & Gas 6, 78-89.

RSC, 2018. ChemSpider, Royal Society of Chemistry. http://www.chemspider.com/.

Ruttkies, C., Schymanski, E.L., Wolf, S., Hollender, J. and Neumann, S., 2016. MetFrag relaunched: incorporating strategies beyond in silico fragmentation. Journal of Cheminformatics 8(3).

Schollée, J.E., 2017. MSMSsim: Functions for processing HRMS2 spectra from output from RMassBank, mainly for calculating spectral similarity. https://github.com/dutchjes/MSMSsim.

Schymanski, E.L., Jeon, J., Gulde, R., Fenner, K., Ruff, M., Singer, H.P. and Hollender, J., 2014. Identifying small molecules via high resolution mass spectrometry: communicating confidence. Environmental science & technology 48(4), 2097-2098.

Smith, C.A., Maille, G.O., Want, E.J., Qin, C., Trauger, S.A., Brandon, T.R., Custodio, D.E., Abagyan, R. and Siuzdak, G., 2005. METLIN: A Metabolite Mass Spectral Database. Therapeutic Drug Monitoring 27(6), 747-751.

Steverkooperation, 2016. Cooperation agriculture and water management in the catchment of the Sterver dam (Kooperation Landwirtschaft und Wasserwirtschaft im Einzugsgebiet der Stevertalsperre - Ein Bericht über die Ergebnisse der Beratung in 2015). Kooperation Land- und Wasserwirtschaft im Einzugsgebiet der Stevertalsperre. http://www.acker-saatbau.de/images/PDF/Steverakte2015.pdf. Accessed: 18/01/2019.

Ter Laak, T.L., Puijker, L.M., van Leerdam, J.A., Raat, K.J., Kolkman, A., de Voogt, P. and van Wezel, A.P., 2012. Broad target chemical screening approach used as tool for rapid assessment of groundwater quality. Science of The Total Environment 427-428, 308-313.

Valsecchi, S., Mazzoni, M., Rusconi, M., Polesello, S., Sala, A., Longoni, O. and Rusconi, M., 2017. Spread and risk assessment of LM6, a non-chlorinated metabolite of terbuthylazine, in groundwater (Diffusione e valutazione di rischio di LM6, metabolita non clorurato della terbutilazina, nelle falde acquifere). Ingegneria dell'Ambiente 4(2), 131-141.

Von Sonntag, C. and Von Gunten, U., 2012. Chemistry of Ozone in Water and Wastewater Treatment: From Basic Principles to Applications, IWA Publisher, London.

Weber, W.H., Seitz, W. and Schulz, W., 2007. Detection of the metabolites desphenyl-chloridazone and methyl-desphenyl-chloridazone in surface, ground and drinking water (Nachweis der Metaboliten Desphenyl-Chloridazon und Methyldesphenyl-chloridazon in Oberflächen-, Grund- und Trinkwasser). Vom Wasser 105, 7-14.

Wolf, L., Zwiener, C. and Zemann, M., 2012. Tracking artificial sweeteners and pharmaceuticals introduced into urban groundwater by leaking sewer networks. Science of The Total Environment 430, 8-19.

Chapter SI2: Supporting Information to Chapter 2 New Relevant Pesticide Transformation Products in Groundwater Detected Using Target and Suspect Screening for Agricultural and Urban Micropollutants with LC-HRMS

SI2-B can be found under:
doi.org/10.1016/j.watres.2019.114972

SI2-A1: Analytical Methods

Spike solutions: Reference material was dissolved in ethanol, methanol, acetonitrile, ethanol/water mix, methanol/water mix, dimethyl sulfoxide, ethyl acetate, toluene, acetone, water, ethanol + 0.1 M HCl, or methanol + 0.1 M HCl at concentrations ranging from 100 to 1000 mg/L, depending on solubility and stability. Then, mix solutions were prepared in ethanol or acetonitrile at 10 mg/L which were combined for the final spike solutions (0.0001, 0.001, 0.01, 0.1 mg/L).

Sample preparation: The groundwater samples were thawed (pH ~7). The BÜCHI vials were rinsed with the sample, then, filled with 60.0 g of the sample. The sample was spiked with 60 µL isotope labelled internal standard (ILIS) solution (0.1 mg/L) at 100 ng/L. The sample was evaporated to 1-5 mL in the Syncore Analyst using the back-flush unit at 20 mbar and 45 °C within ~3.5 h. To reduce analyte losses, the BÜCHI vials were rinsed with 1.5 mL methanol:water (15:85). Then, the sample was evaporated to 0.3 mL, and transferred to a 0.5 mL vial. The sample volume was adjusted to 0.4 mL using ultrapure water. After centrifuging (10 000 rpm, 5 min; Eppendorf centrifuge 5415D) the supernatent was transferred to the measurement vial.

For quantification and quality control, 22 calibration standards at eleven concentration levels (0.1, 0.5, 1, 5, 10, 25, 50, 100, 250, 500, 1000 ng/L) prepared in ultrapure water, nine blank samples (ultrapure water, either freshly withdrawn from the purifier station or frozen for several weeks in the laboratory glass bottles) and six groundwater samples spiked at 10 or 100 ng/L were processed analogously to the groundwater samples. X-ray contrast media were spiked 5x higher due to the lower sensitivity. Perfluorinated carbons (PFCs) were calibrated from 0.1 to 50 ng/L. PFC-ILIS were spiked at 10 ng/L.

BÜCHI vials were cleaned with diluted HCl, hot tap water, deionised water, ultrapure water and finally methanol.

LC-HRMS/MS: To cover late-eluting perfluorocarbons (PFCs), the isocratic phase (95% eluent B) was prolonged from 10 to 12 min in negative ionization. In addition, a black carbon cartridge was installed directly after the pump to remove PFCs released from the pump.

Table SI2-A1: ESI-HRMS/MS settings

Parameter	
Spray voltage (kV)	4 / -3
Capillary temperature (°C)	320
Sheath gas (AU)	40
Auxiliary gas (AU)	10
S-lens RF level (AU)	50
Automatic gain control (AGC) target MS1	10^6
Maximum injection time MS1 (ms)	100
Scan range MS1 (m/z)	100 - 1000
Resolution MS1 (at m/z 200)	140 000
Data-dependent trigger	Ions of target compounds; if idle pick most intense
Isolation window (m/z)	1
Number of dd-MS/MS	Top 5
Resolution MS2 (at m/z 200)	17 500
Automatic gain control (AGC) target MS/MS	2×10^5
Maximum injection time MS/MS (ms)	80
Dynamic exclusion time (s)	8

SI2-A2: Target Quantification

ILIS Selection: Quantification was based on the peak area ratio of analyte and ILIS. If a structurally identical ILIS was not available, ILIS selection was supported by an internal R script using the R functions published at https://github.com/dutchjes/TFAnalyzeR/blob/master/RelativeRecoveryCalculation.R.

First, the TraceFinder 4.1 export was imported to R (R Core Team 2016) and all ILIS co-eluting with the analyte within the given RT window (generally ±1.5 min) were selected (function selectISTDs()). Then, a linear calibration model was calculated for each combination of analyte and ILIS (function calibrationCalc()), and finally, sample concentrations were determined based on each calibration model (function predictConc()). Using the concentration c in the spiked / not spiked samples and the theoretical spike level, relative recoveries as defined in equation SI2-1 were calculated,

$$\text{Relative Recovery} = \frac{\left(c_{\text{spiked sample}} - c_{\text{not spiked sample}}\right)}{\text{Theoretical Spike Level}} \qquad \text{(SI2-1)}$$

if the following equation was true (function recoveryCalc()):

$$c_{\text{not spiked sample}} < \left(c_{\text{spiked sample}} - c_{\text{not spiked sample}}\right) \cdot 1.7 \qquad \text{(SI2-2)}$$

This check ensured that relative recoveries were only determined if the concentration difference in the spiked and not spiked samples was large enough, to avoid cases where the relative recoveries were dominated by measurement uncertainty, and therefore, misleading. Finally, an ILIS was selected for which the mean relative recovery was close to 100% and the standard deviation of the relative recoveries across the spiked samples was low. Final analyte

concentrations were corrected by the relative recovery, if a structurally identical ILIS was not available.

Limit of Quantification (LOQ): The LOQ in ultrapure water ($LOQ_{Ultrapure}$) was defined as the lowest calibration standard with at least five data points along the chromatographic peak (MS1 full scan mode) and a peak area ratio (analyte vs. ILIS) of at least twice the peak area ratio in all blank samples. To estimate the LOQ in matrix (LOQ_{Matrix}), the $LOQ_{Ultrapure}$ was divided by the absolute recovery:

$$LOQ_{Matrix} = \frac{LOQ_{Ultrapure}}{\text{Absolute Recovery}} \quad \text{(SI2-3)}$$

If the sample concentration was in the range of the LOQ_{Matrix}, the so-defined LOQ_{Matrix} was lowered if the chromatographic peaks in the samples were defined by at least five data points.

Absolute recoveries were determined for each analyte by comparing the peak area in the matrix to the peak area in ultrapure water, as described in the following. If a structurally identical ILIS was available, the peak area of the ILIS in the matrix (environmental samples) was divided by the peak area of the ILIS in ultrapure water (median of all enriched calibration standards) according to equation SI2-4:

$$\text{Absolute Recovery}_{\substack{\text{Identical}\\\text{ILIS}}} = \text{Median}\frac{\text{Peak Area ILIS}_{Matrix}}{\text{Median (Peak Area ILIS}_{Ultrapure})} \quad \text{(SI2-4)}$$

If a structurally identical ILIS was not available, the peak area of the analyte in the spiked sample (after subtracting the peak area in the not spiked sample) was compared to the peak area of the analyte in the calibration standard that corresponded to the spike level:

$$\text{Absolute Recovery}_{\substack{\text{No Identical}\\\text{ILIS}}} = \frac{\text{Peak Area}_{\substack{\text{Spiked}\\\text{Sample}}} - \text{Peak Area}_{\substack{\text{Not Spiked}\\\text{Sample}}}}{\text{Peak Area}_{\substack{\text{Calibration}\\\text{Standard}}}} \quad \text{(SI2-5)}$$

SI2-A3: Suspect Screening

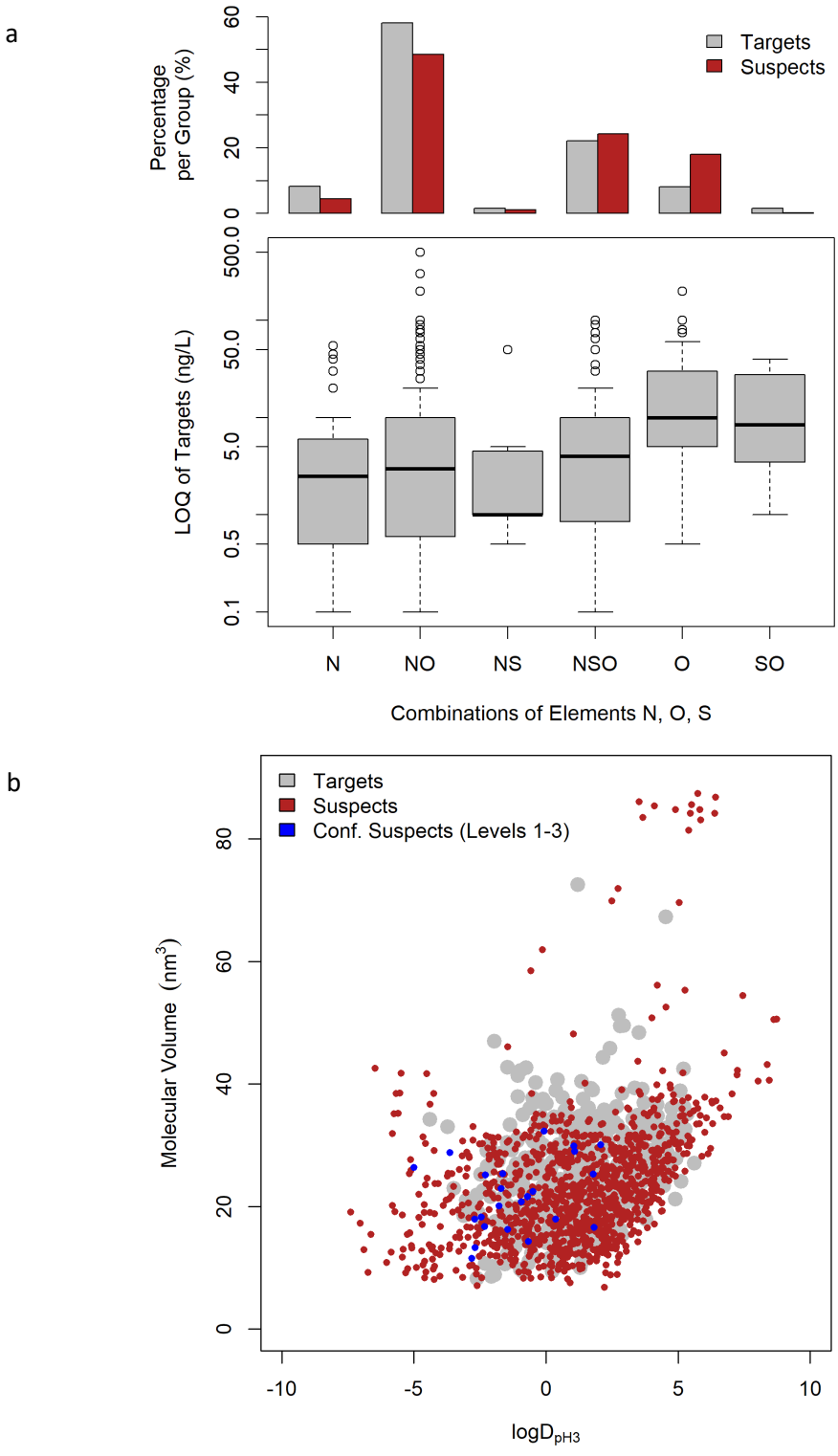

Figure SI2-A 1: a) Bar plots: distribution of heteroatoms in targets and suspects; boxplots: LOQ of targets depending on heteroatoms; 0.5% of suspects do not contain any heteroatoms (not shown). b) Molecular volume vs. $logD_{pH3}$ of the targets (grey), suspects (red) and confirmed suspects (blue). The theoretical pH of the LC eluent was 3.

Automated Screening: The suspect screening with Compound Discoverer (CD 2.1) was performed separately for positive and negative electrospray ionization. To optimize parameter settings, mass accuracy and RT shift of ILIS were analysed. The accurate mass of the ILIS deviated less than 5 ppm from their exact mass. Furthermore, ILIS shifted not more than 1.5 min within the measurement sequence (except for metolachlor-esa-d11: more than 15 min, Figure SI2-A2). Table SI2-A2 lists the used nodes and most important parameter settings for CD 2.1.

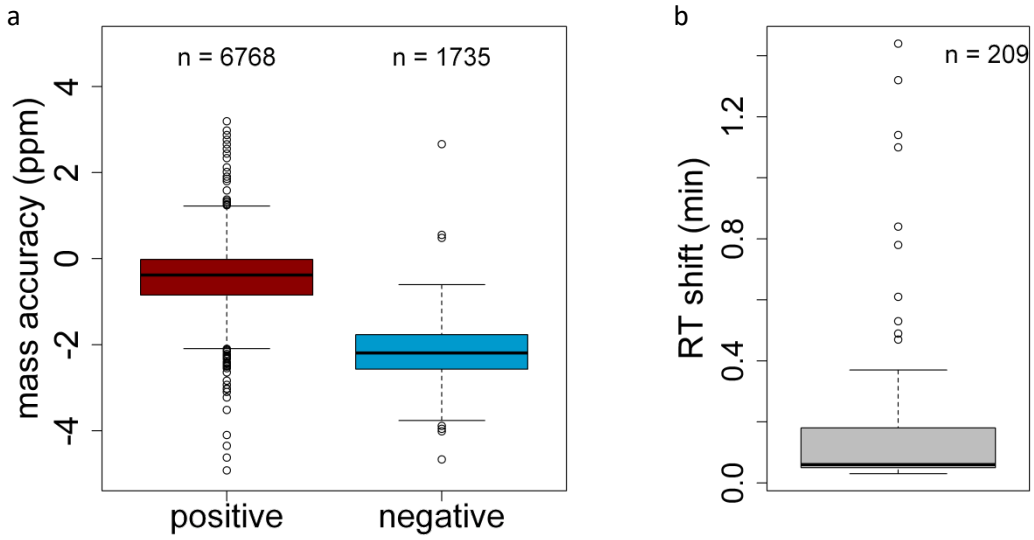

Figure SI2-A2: a) Mass accuracy of ILIS in positive and negative ionization mode; b) maximum RT shift of ILIS within measurement sequence.

Table SI2-A2: Nodes and parameter settings used for the CD 2.1 workflow.

Node	**Settings**
Input Files	
Select Spectra	• Precursor mass 100 – 1000 Da • Unrecognized mass analyser: FTMS • Unrecognized activation: HCD
RT Alignment	• Maximum shift 0.75 min • Mass tolerance 3 ppm (pos) / 5 ppm (neg)

Detect unknown compounds	• 3 ppm (pos); 5 ppm (neg)
	• 30% intensity tolerance
	• S/N threshold 3
	• Min peak intensity 1000 (pos) and 500 (neg) Ions
	  ○ Positive: [M+H]+1, [M+K]+1, [M+Na]+1, [M+NH4]+1, [2M+H]+1, [M+2H]+2, [M-e]+1
	  ○ Negative: [M+FA-H]-1, [2M+FA-H]-1, [M-H]-1, [M-2H]-2, [2M-H]-1
	• Base Ions
	  ○ [M+H]+1, [M+NH4]+1 (pos) / [M-H]-1 (neg)
	• Filter Peaks: True
	• Max. Peak Width: 0.8 min
	• Remove Singlets: **False**
	• Min Scans per Peak: 5
	• Min. Isotopes: **1**
	• Max. element counts: C90 H190 Br3 Cl4 F6 K2 N10 Na2 O18 P3 S5

Merge Features	• 3 ppm (pos), 5 ppm (neg) • RT Tolerance 0.75 min
Group Unknown compounds	• 3 ppm (pos), 5 ppm (neg) • 0.75 min RT Tolerance • Preferred Ions [M+H]+1, [M+K]+1, [M+Na]+1, [M+NH4]+1 (pos) / [M-H]-1 (neg)
Search Mass Lists	• Lists with targets, ILIS and suspects • RT TRUE • RT Tolerance 2 min • Mass Tolerance 3 ppm (pos), 5 ppm (neg)
Assign Compound Annotations	• 3 ppm (pos), 5 ppm (neg)
Mark Background Compounds if…	• Max. Sample/Blank 3 • Hide Background: False
Predict Compositions	• Mass tolerance 3 ppm (pos), 5 ppm (neg) • S/N Threshold 3 • Mass tolerance for fragments matching: 10 ppm

RT Prediction: Each suspect hit was evaluated regarding the plausibility of the RT using a simple RT prediction model based on the logD. The logD values were predicted at pH 3 (theoretical pH of LC eluents) with JChem for Excel (Version 17.1.2300.1455; ChemAxon Ltd.) for 615 targets and ILIS. Then, a linear model was fitted (Figure SI2-A3) and suspect RTs were predicted from their $logD_{pH3}$ using R (R Core Team 2016). Suspect hits were considered as unlikely, and therefore, excluded, if measured and predicted RT differed more than 10 min.

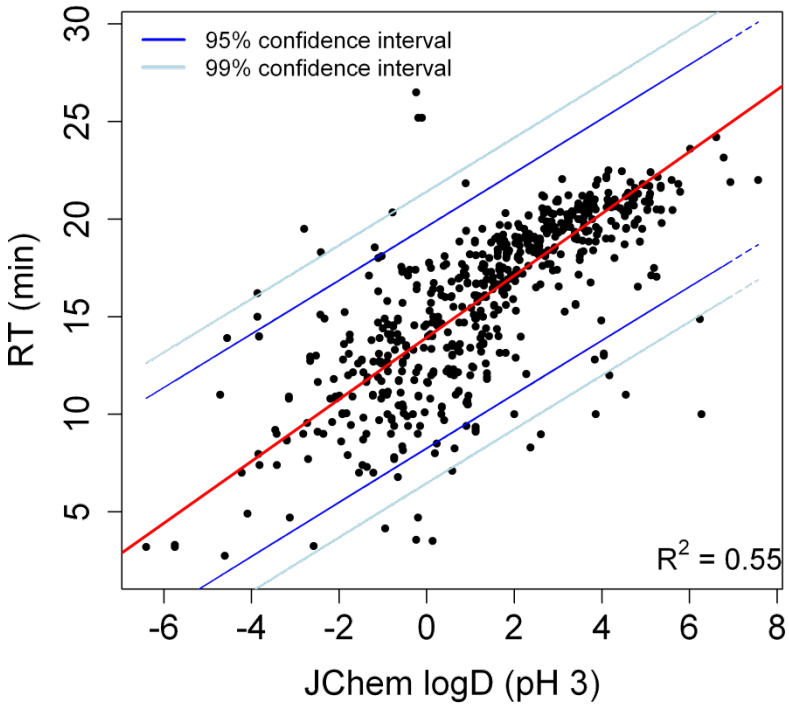

Figure SI2-A3: Linear RT prediction model based on logD values of 615 target compounds.

In silico Fragmentation with MetFrag: The in silico fragmenter MetFrag was used to test if the annotated suspect structures could explain measured MS/MS fragments. Using an internal R script, MetFrag CL 2.4.2 was run in batch mode. First, the MS/MS spectra were extracted from .mzXML files for each suspect hit using the RMassBank package (Stravs et al. 2013). For this, the m/z of the [M+H]+ / [M-H]- were calculated from the annotated suspect formula (RChemMass package, https://github.com/schymane/RChemMass/), and then, the most intense MS/MS scan triggered by the calculated m/z and acquired in the sample with the largest MS1 intensity was written to a .txt file. To reduce noise signals, peaks with intensity less than 1% relative to the base peak were removed. Next, MetFrag retrieved all structures from ChemSpider and the suspect list matching the measured m/z within 3 or 5 ppm (positive / negative mode). Salts and stereoisomers were removed using the unconnected compound and InChIKey filter. FragmenterScore, RetentionTimeScore, ChemSpider data (ChemSpiderDataSourceCount, ChemspiderReferenceCount, ChemSpiderPubMedCount, ChemSpiderRSCCount, ChemSpiderExternalReferenceCount), and OfflineMetFusionScore were weighted equally. MetFrag results are summarized in SI2-B 3 comprising fragmenter score of the suspect, number and formulae of explained peaks by the suspect, number of ChemSpider hits, the compound from Chemspider that explains most fragments, that has highest fragmenter score, and the one that has the highest total score.

Suspect Hits not Further Investigated: 143 suspects were not further investigated using reference material. Some suspects will remain unclear, e.g. for 21 suspects reference material could not be obtained or was not pursued as they were considered to be of lower priority. Eight suspects were not further investigated because they were only detected in one sample. Some suspects were disregarded as they showed a noisy EIC (35 suspects) or low intensity (57 suspects) hampering confirmation (area $<5x10^4$). 22 suspects were excluded as they were relatively unlikely to represent a positive hit: One suspect hit, annotated both as TP of various sulfurons and as terbuthylazine TP, was identified as terbuthylazine TP; in the case of three suspects the measured fragments did not match the main fragments reported by Reemtsma et al. (2013); 14 hits showed low mass accuracy (averaged over isotopologues/adducts: >2.5 ppm; for four suspects, the maximum fragmenter score of the ChemSpider candidates was more than three times larger than the fragmenter score of the suspect and therefore the suspects were deemed as unlikely to be the correct structure.

SI2-A4: Suspect Confirmation and Quantification

Seven samples comprising all suspects (sample aliquots which were not thawed previously), three spiked samples (10, 100, 1000 ng/L) and two blanks were enriched and measured as described in SI2-A1 with the following slight modifications. Calibration levels were 0.1, 0.5, 1, 5, 10, 25, 50, 100, 500, 1000, 2000 and 3000 ng/L. The dynamic exclusion time and number of dd-MS/MS experiments were reduced to 3 s and top 3, respectively, to increase the number of MS/MS scans along a chromatographic peak.

Suspects were confirmed based on retention time and matching MS/MS spectra in standard and sample with the following method. Using the R package MSnbase (Gatto and Lilley 2012), the EICs of the most intense adduct in standard, sample and spiked sample were extracted (mass window 5 ppm) and plotted to check the retention time. Then, the most intense fragments in the standard were determined, and the EICs of these fragments (in standard and samples) were plotted. Head to tail plots were created with the R package MSMSsim (https://github.com/dutchjes/MSMSsim). In addition, retention time was checked on a second chromatographic system using a reverse phase biphenyl column (Raptor Biphenyl, 2.7 µm, 100x3.0 mm; Restek, Bellefonte, U.S.). The gradient started with 100% eluent A (water + 0.1% concentrated formic acid + 2.5 mM ammonium formate) for 1.5 min, then eluent B (90% / 10% acetonitrile / water + 0.1% concentrated formic acid + 2.5 mM ammonium formate) was increased to 100% within 25 min, and held for 2 min. The column was re-equilibrated for 4 min.

Suspect concentrations were determined in the 31 samples by applying the calibration model determined later with the same LC-HRMS system. For this, seven samples were analysed twice, once in the first analysis, and once in the same measurement sequence as the calibration standards used for quantification. For this second sample preparation and measurement, the same ILIS spike solution was used as for the first sample preparation and measurement. The determined concentrations of both analyses matched within measurement accuracy.

SI2-A5: Results of Target and Suspect Screening

Table SI2-A 3: Micropollutants (MPs) detected at least once with concentrations >100 ng/L in the 31 groundwater samples. MPs identified in suspect screening: italic. Median (c_{median}), 90th percentile (c_{90th}) and maximum (c_{max}) of concentrations in 31 samples.

MP	MP Class	$logD_{pH7}$	LOQ (ng/L)	No. Of Detec-tions	C_{median} (ng/L)	C_{90th} (ng/L)	C_{max} (ng/L)
Atrazine	Pesticide	2.2	0.5	25	7.1	37	180
Bentazone	Pesticide	-0.2	0.1	18	0.5	23	260
Atrazine-desethyl	Pesticide TP	1.5	0.5	29	11	59	150
Atrazine-desethyl-desisopropyl	Pesticide TP	0.5	0.3	30	17	78	120
Chloridazon-desphenyl	Pesticide TP	-0.7	1	28	120	1200	1800
Chloridazon-methyl-desphenyl	Pesticide TP	-0.6	0.5	22	32	220	670
Chlorothalonil TP R417888	Pesticide TP	-0.7	1	28	33	470	1300
Chlorothalonil TP Isomer of R417888, **Level 3**	Pesticide TP	-0.7	no standard	19	~21	~39	~120
Chlorothalonil TP R471811	Pesticide TP	-1.7	3	31	300	1100	2700
Chlorothalonil TP SYN507900	Pesticide TP	0.4	1.3	13	<1.3	33	150
Dimethachlor-ESA	Pesticide TP	-1.1	5	9	<5		120
Fipronil-TP RPA 106681, Level 2b	Pesticide TP	1.0	no standard	11	~1.9	14	~120
Fludioxonil TP CGA 192155	Pesticide TP	-0.7	3	2	-	-	200
Metolachlor TP CGA 368208 (=Acetochlor sulfonic acid)	Pesticide TP	-0.5	1	20	3.2	46	150
Metolachlor TP NOA413173	Pesticide TP	-3.4	1.7	22	7	130	430
Metolachlor-ESA*	Pesticide TP	-0.3	35	9*	69*	642*	970*
Terbuthylazine TP CSCD648241	Pesticide TP	-2.5		29	9.5	54	190
N-N-dimethylsulfamide	Biocide TP	-1.5	5	18	7.8	67	>200
Benzotriazole	Corrosion inhibitor	1.3	5	13	-	59	210
Melamine	Industrial chemical	-2.0	5	4	-	32	770
Diatrizoate	Pharmaceutical	-0.6	15	4	-	64	340
Acesulfame	Sweetener	-1.5	0.5	26	37	120	260
Sucralose	Sweetener	-0.5	10	7	-	93	520

* Metolachlor-ESA could only be analysed in 13 samples due to shifting RT.

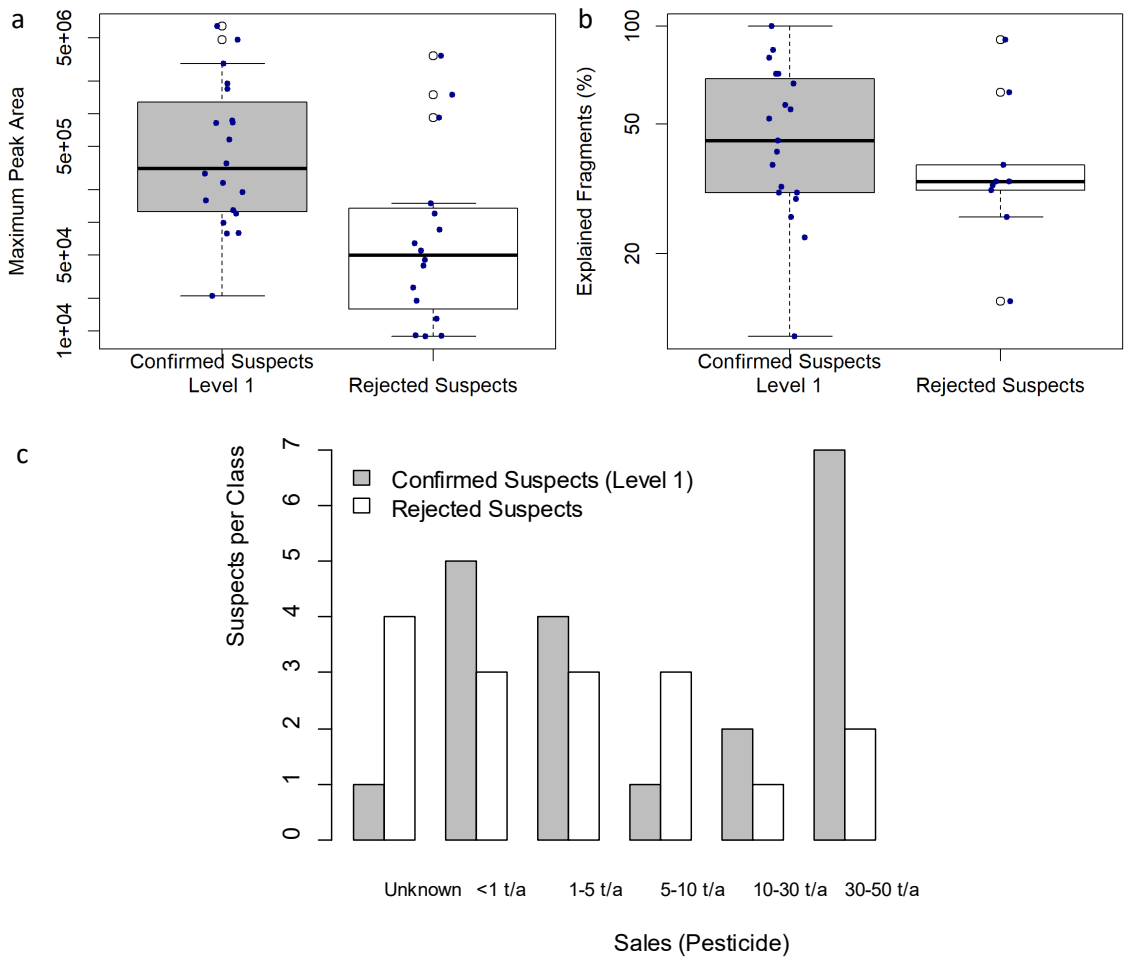

Figure SI2-A 4: Comparison of maximum peak area (a), explained fragments from MetFrag (b) and sale volumes (c) of suspects which were confirmed or rejected using reference material.

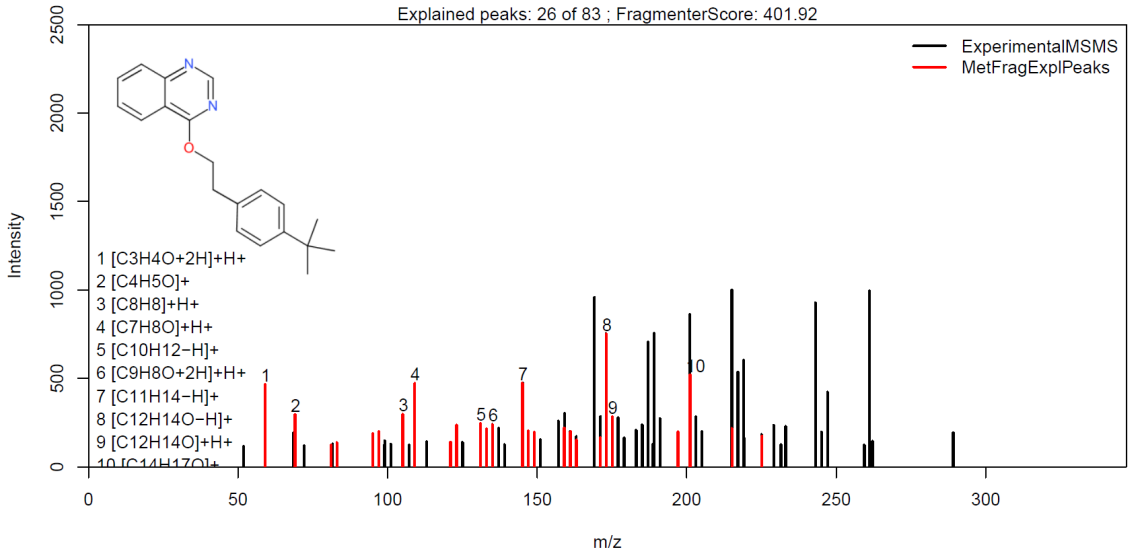

Figure SI2-A 5: HRMS/MS spectrum of the suspect hit fenazaquin with peaks which could be explained by the structure marked in red; fenazaquin was rejected using reference material due to different RT.

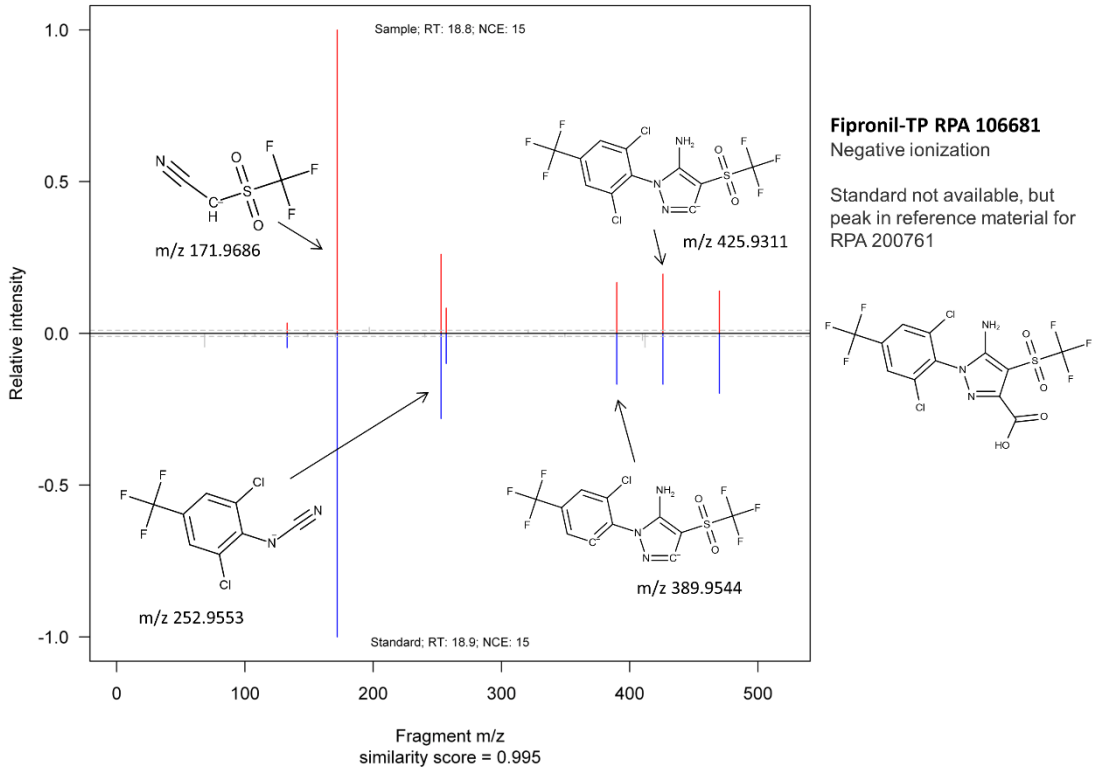

Figure SI2-A 6: HRMS/MS spectra of fipronil TP RPA 106681 in sample (above, red) and reference material (below, blue) with structure proposals for four fragments. For RPA 106681, reference material was not available, but the obtained reference material for RPA 200761 revealed a peak at the precursor m/z of RPA 106681 ($[M+H]^+$ & $[M-H]^-$). RT matches with peaks in sample.

SI2-A6: Impact of Land Use on Groundwater Quality

Land use drives not only total concentrations of MP classes, as discussed in section 3.4, but explains also the presence of site-specific MPs. One sample was noticeable for the high contamination with the industrial chemical melamine (770 ng/L), which explained 47% of total MP concentration. Melamine is a transformation product (TP) of the biocide cyromazine but also a high production volume chemical used for the fabrication of a wide range of materials, such as laminate, paper, textiles, or glues (Europe: 250000 t/a). Melamine is well-degradable in wastewater treatment plants with adapted microbial community but relatively persistent in the environment (OECD 1999). We expect that the high amounts of melamine enter the aquifer via seepage from nearby landfills or from bank filtrate from the Rhone River, which acts as a receiving water for numerous municipal and, most importantly, industrial wastewater treatment plants. This explanation was supported by the detection of typical wastewater tracers such as benzotriazole (210 ng/L) and acesulfame (70 ng/L) at the same monitoring site. Seitz and Winzenbacher (2017) reported for melamine median concentrations of 360 ng/L in groundwater and 610 ng/L in stream water in Germany due to seepage from a nearby landfill and the discharge of treated wastewater, respectively.

The highest MP concentration (9000 ng/L) was detected in a spring draining intensively cultivated arable land. TPs of chlorothalonil, chloridazon and metolachlor explained 90% of total MP concentration. In contrast, the sample with the lowest MP concentration (60 ng/L) was dominated by the herbicide asulam (54 ng/L). Asulam concentration was more than five times higher than in all other groundwater wells. The herbicide has not been approved in the EU since 2012 (European Commission 2011), but is still used in Switzerland to combat dock and fern species, e.g. on pastures (*Rumex obtusifolius, Rumex alpinus, Pteridium aquilinum, Dryopteris filix-mas*). The catchment of the spring is dominated by grassland / pastures (63%) and forest (30%); wastewater impacted streams do not influence groundwater recharge. Consequently, the catchment explained both the generally low MP and the high asulam contamination.

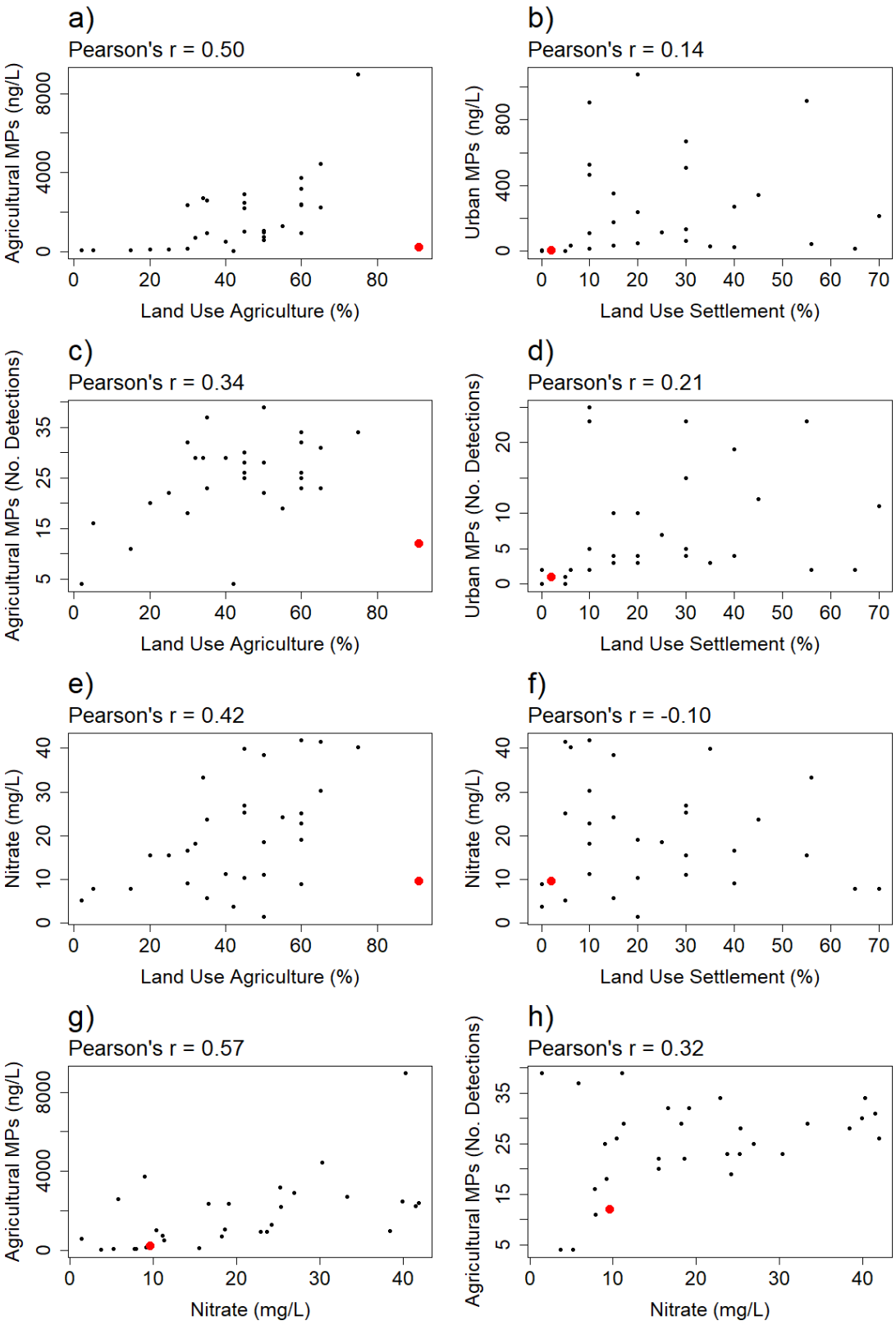

Figure SI2-A7: a, c, e: Correlation between total agricultural MP concentration / agricultural MP detections / nitrate concentration and percentage of agricultural land use in catchment (cropland, orchards, vineyards); b, d, f: correlation between total urban MP concentration / urban MP detections / nitrate concentration and percentage of settlement in catchment; g, h: correlation between total agricultural MP concentration / agricultural MP detections and nitrate concentration; "pesticides" = pesticides and TPs. Red dots: groundwater monitoring site with catchment dominated by agriculture, but low MP and nitrate contamination (section 3.4).

References

European Commission, 2011. Commission Implementing Regulation (EU) No 1045/2011 of 19 October 2011 concerning the non-approval of the active substance asulam, in accordance with Regulation (EC) No 1107/2009 of the European Parliament and of the Council concerning the placing of plant protection products on the market, and amending Commission Decision 2008/934/EC. Official Journal of the European Union 275.

Gatto, L. and Lilley, K.S., 2012. MSnbase - an R/Bioconductor package for isobaric tagged mass spectrometry data visualization, processing and quantitation. Bioinformatics (28), 288-289.

OECD, 1999. Screening Information Dataset (SIDS) Initial Assessment Report (SIAR): Melamine CAS N°:108-78-1. UNEP Publications, 110-198.

R Core Team, 2016. R: A language and environment for statistical computing. R Foundation for Statistical Computing, Vienna, Austria. https://www.R-project.org/.

Reemtsma, T., Alder, L. and Banasiak, U., 2013. A multimethod for the determination of 150 pesticide metabolites in surface water and groundwater using direct injection liquid chromatography-mass spectrometry. Journal of chromatography A 1271(1), 95-104.

Seitz, W. and Winzenbacher, R., 2017. A survey on trace organic chemicals in a German water protection area and the proposal of relevant indicators for anthropogenic influences. Environmental Monitoring Assessment 189, 1-17.

Stravs, M.A., Schymanski, E.L., Singer, H.P. and Hollender, J., 2013. Automatic recalibration and processing of tandem mass spectra using formula annotation. J Mass Spectrom 48(1), 89-99.

SI2-C: Analytical Information for Identified Suspects

Tables SI2-C1 and SI2-C2 present the suspects, which were confirmed, tentatively identified or rejected using reference material or expert knowledge. The identification confidence is communicated using the classification method of Schymanski et al. 2014. Figure SI2-C1 summarises the identification confidence levels. We confirmed 19 transformation products (TPs) and one pesticide (Level 1) and rejected nine TPs and seven pesticides. Two TPs were identified as probable (Level 2, no reference standard), three TPs as tentative structure (Level 3), either because reference material was not available (2 TPs) or due to analytical problems (1 TPs), and three suspects remained unclear and could not be classified following Schymanski et al. (2014).

Extracted ion chromatograms (EICs) and MS/MS spectra of confirmed suspects (Level 1-3) are illustrated on page 72-101. In addition, EICs of the most intense fragments were plotted to avoid that background ions are mistakenly annotated as MS/MS fragments (see e.g. Fludioxonil–TP CGA 192155, Fluxapyroxad (BAS 700 F)–TP CSAA798670).

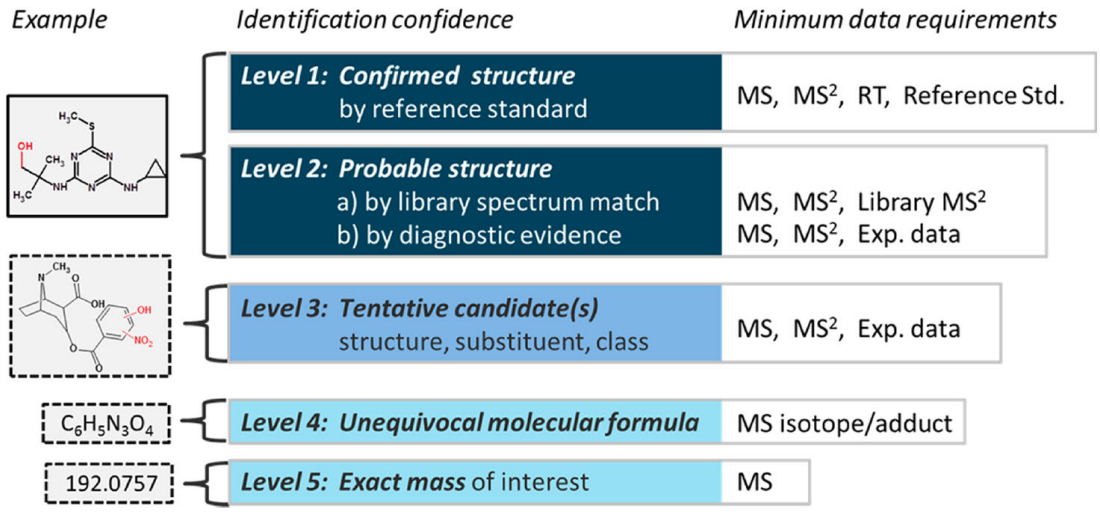

Figure SI2-C1: Identification confidence levels (Schymanski et al. 2014).

References

Schymanski, E.L., Jeon, J., Gulde, R., Fenner, K., Ruff, M., Singer, H.P. and Hollender, J. 2014. Identifying small molecules via high resolution mass spectrometry: communicating confidence. Environ Sci Technol 48(4), 2097-2098, 10.1021/es5002105.

BLW, 2018. Sales per active ingredient (Verkaufsmengen je Pflanzenschutzmittel-Wirkstoff). Federal Office for the Agriculture. https://www.blw.admin.ch/blw/de/home/nachhaltige-produktion/pflanzenschutz/pflanzenschutzmittel/verkaufsmengen-der-pflanzenschutzmittel-wirkstoffe.html. Accessed: 18/01/2019.

Reemtsma, T., Alder, L. and Banasiak, U., 2013. Emerging pesticide metabolites in groundwater and surface water as determined by the application of a multimethod for 150 pesticide metabolites. Water research 47(15), 5535-5545.

Table SI2-C1: Pesticide TPs

Suspect	Structure	Parent	Sales amount (t/a) (BLW 2018)	Log D (pH 7)	RT (min)	Refe-rence material from	Reemtsma et al. 2013: 75th percentile (ng/L)	Nr. Of Detects	Max. conc. (ng/L)	LOQ (ng/L)	Comment
Chlorothalonil-TP SYN507900 [M-H]- Level 1	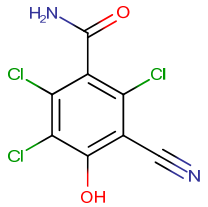	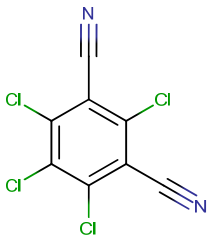	30-50	0.4	12.9	Syngenta	Not included in study	13	150	1.3	• MS/MS okay • Biphenyl column: confirmed
Chlorothalonil-TP R417888 [M-H]- Level 1	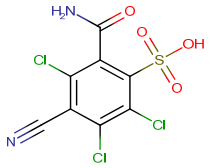	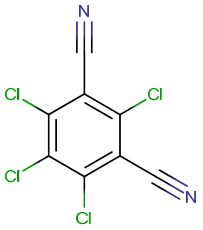	30-50	-0.7	15.3	Syngenta	55	28	1300	1	• MS/MS okay • Biphenyl column: confirmed
Chlorothalonil-TP R471811 [M-H]- Level 1	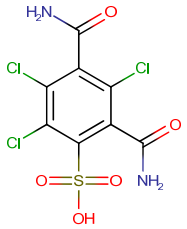	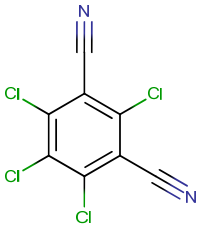	30-50	-1.7	7.5	Syngenta	Not included in study	31	2700	3	• MS/MS okay • Biphenyl column: confirmed but RTs are not perfectly stable

Suspect	Structure	Parent	Sales amount (t/a) (BLW 2018)	Log D (pH 7)	RT (min)	Refe-rence material from	Reemtsma et al. 2013: 75th percentile (ng/L)	Nr. Of Detects	Max. conc. (ng/L)	LOQ (ng/L)	Comment
Chlorothalonil-TP R419492 [M-2H]2- Level 1	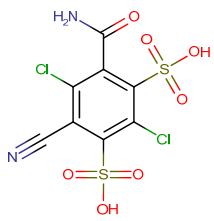	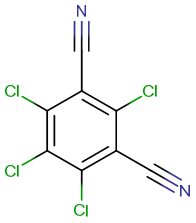	30-50	-4.5	5	Syngenta	Not included in study	18	-	-	• Compound was detected later and could therefore not be confirmed and quantified in the here presented samples. Compound was confirmed (Level 1) in other groundwater samples.
Chlorothalonil-TP SYN548580 [M-H]- Level 1	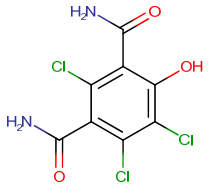	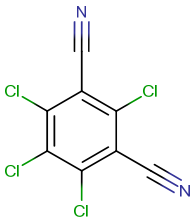	30-50	0.0	10	Syngenta	Not included in study	13	-	-	• Compound was detected later and could therefore not be confirmed and quantified in the here presented samples. Compound was confirmed (Level 1) in other groundwater samples.
Cycloxydim-TP BH 517-TSO E/Z-isomer [M+H]+ Level 1	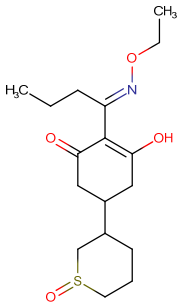	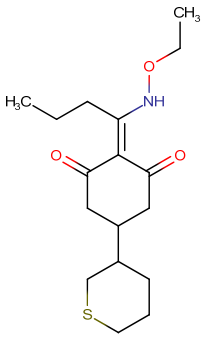	<1	-0.1	15.5 & 19	BASF	Not included in study	1	1.3	1	• 2 peaks in standard (RT 15.5 & 19 min); peak 19 min is more intense, different fragment ratios → E/Z isomers • MS/MS okay • Possibly, concentrations are overestimated as TP may be formed during LC by hydrolysis of cycloxydim: pH~3 →single injection of cycloxydim contains 5-10% of TP (estimation based on peak areas) • Biphenyl column: confirmed

Suspect	Structure	Parent	Sales amount (t/a) (BLW 2018)	Log D (pH 7)	RT (min)	Refe-rence material from	Reemtsma et al. 2013: 75th percentile (ng/L)	Nr. Of Detects	Max. conc. (ng/L)	LOQ (ng/L)	Comment
Dimethachlor-TP CGA 369873 [M-H]- Level 1	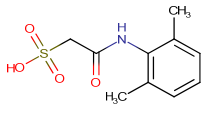	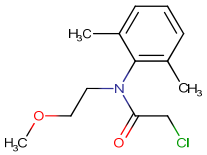	5-10	-0.9	15	Syngenta	39	28	95	0.5	• MS/MS okay • Biphenyl column: confirmed
Fipronil-TP RPA 200761 [M+H]+ Level 1	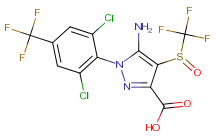	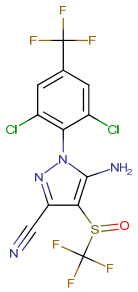	<1	1.1	18.9	BASF	Not included in study	6	71	1	• MS/MS okay • Reference standard contains also fipronil-TP 106681 (intensity <1% relative to intensity of fipronil-TP RPA 200761) • reference standard: certificate of analysis is expired since May 2013 • Biphenyl column: TP is not in samples analysed with biphenyl column
Fludioxonil-TP CGA 192155 [M-H]- Level 1	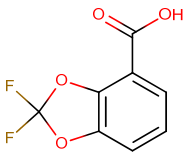	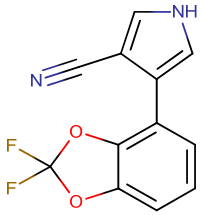	1-5	-0.7	18	Syngenta	3	2	200	3	• MS/MS okay • Biphenyl column: confirmed
Fluxapyroxad (BAS 700 F) & bixafen-TP CSCD465008 [M-H]- Level 1	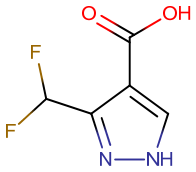	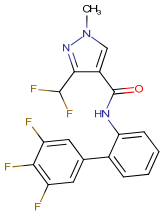	1-5	-2.8	10.4	BASF	Not included in study	1	~60	15	• MS/MS okay • Shoulder peak in matrix sample possibly due to tautomerism or carboxylic acid (protonated / deprotonated form; predicted pKa 3.3)

Suspect	Structure	Parent	Sales amount (t/a) (BLW 2018)	Log D (pH 7)	RT (min)	Refe-rence material from	Reemtsma et al. 2013: 75th percentile (ng/L)	Nr. Of Detects	Max. conc. (ng/L)	LOQ (ng/L)	Comment
		fluxapyroxad (BAS 700) 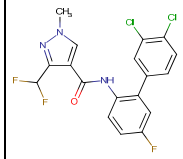 bixafen									• concentrations are semiqantitative due to poor peak shape on Atlantis column • ChemSpider hit elutes 1.3 min later: 1-(Difluoromethyl)-1H-pyrazole-3-carboxylic acid • Biphenyl column: confirmed (better peak shape than on Atlantis column)
Fluxapyroxad (BAS 700 F)-TP CSAA798670 & bixafen-TP M42 [M+H]+ Level 1	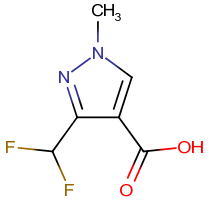	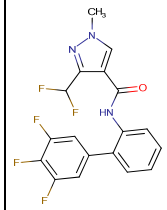 Fluxapyroxad (BAS 700) 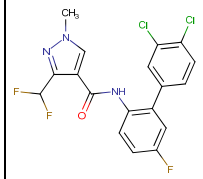 bixafen	1-5	-2.7	12	BASF	Not included in study	1	13	10	• MS/MS okay • Shoulder peak in matrix sample possibly due to carboxylic acid (protonated / deprotonated form; predicted pKa 3.3) • Biphenyl column: confirmed

Suspect	Structure	Parent	Sales amount (t/a) (BLW 2018)	Log D (pH 7)	RT (min)	Refe-rence material from	Reemtsma et al. 2013: 75th percentile (ng/L)	Nr. Of Detects	Max. conc. (ng/L)	LOQ (ng/L)	Comment
Metalaxyl-M-TP CGA108906 [M+H]+ Level 1	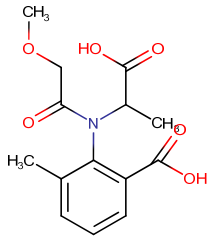	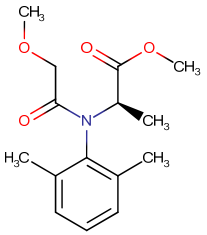	1-5	-5	16	Syngenta	4	1	8.8	7	• MS/MS okay • Double peak possibly due to acid group (protonated / deprotonated form; predicted pKa 3.2) • Both peaks have same fragments • noisy -> high LOQ • according to MS/MS, compound is in several samples • Biphenyl column: TP is not in samples analysed with biphenyl column
Metolachlor-TP CGA 368208 / Acetochlor sulfonic acid [M-H]- Level 1	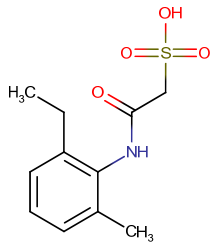	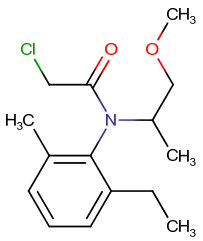	10-30	-0.5	17	Syngenta	9	20	150	1	• MS/MS okay • TP of metolachlor-ESA & acetochlor • Biphenyl column: confirmed
Metolachlor-TP NOA413173 [M-H]- Level 1	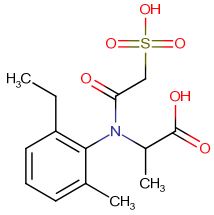	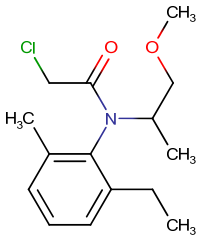	10-30	-3.6	22	Syngenta	290	22	430	1.7	• MS/MS okay • Double peak like metolachlor-ESA • TP of metolachlor-ESA • Biphenyl column: confirmed

Suspect	Structure	Parent	Sales amount (t/a) (BLW 2018)	Log D (pH 7)	RT (min)	Refe-rence material from	Reemtsma et al. 2013: 75th percentile (ng/L)	Nr. Of Detects	Max. conc. (ng/L)	LOQ (ng/L)	Comment
Nicosulfuron-TP AUSN [M+H]+ Level 1	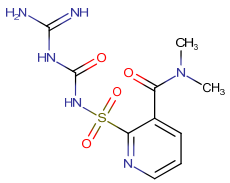	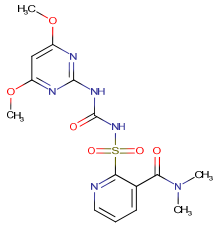	1-5	-1.6	8.5	Dupont	Not included in study	17	47	3	• MS/MS okay • Blind: up to 1 ng/L • Biphenyl column: confirmed
Nicosulfuron-TP UCSN [M+H]+ Level 1	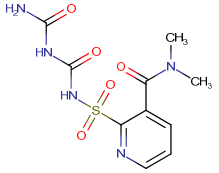	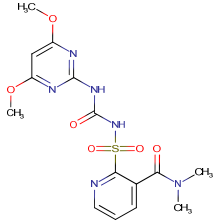	1-5	-2.3	9.4	Dupont	Not included in study	27	75	0.2	• MS/MS okay • Biphenyl column: confirmed
Pinoxaden-TP NOA 407854 [M+H]+ Level 1	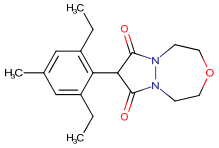	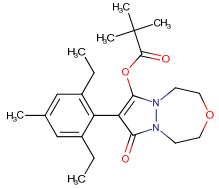	<1	2.1	18.2	Syngenta	2	4	5.5	0.3	• Possibly, concentrations are overestimated as metabolite may be formed during LC by hydrolysis of pinoxaden: pH~3 →single injection of pinoxaden contains 10-20% of TP (estimation based on peak areas) • Noisy • Biphenyl column: confirmed
Terbuthylazine-TP CSAA036479 [M+H]+ Level 1	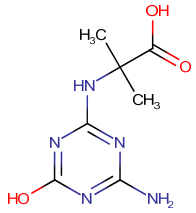	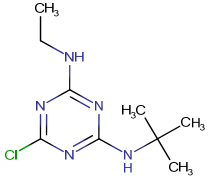	30-50	-2.7	8	Syngenta	Not included in study	25	27	0.6	• MS/MS okay • Biphenyl column: confirmed

Suspect	Structure	Parent	Sales amount (t/a) (BLW 2018)	Log D (pH 7)	RT (min)	Refe-rence material from	Reemtsma et al. 2013: 75th percentile (ng/L)	Nr. Of Detects	Max. conc. (ng/L)	LOQ (ng/L)	Comment
Terbuthylazine-TP CSCD648241 [M+H]+ Level 1	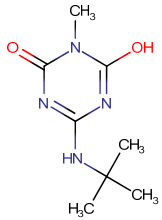	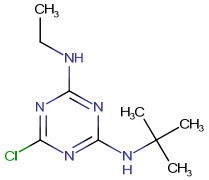	30-50	-2.5	14	Syngenta	Not included in study	29	190	0.5	• MS/MS okay • Biphenyl column: confirmed
Terbuthylazine-TP CSCD692760 [M+H]+ Level 1	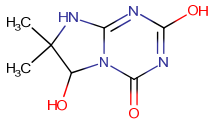	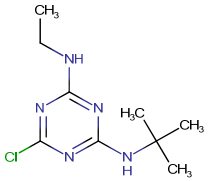	30-50	-1.5	8.3	Syngenta	Not included in study	27	32	3	• MS/MS okay • Noisy • Biphenyl column: confirmed
Terbuthylazine-TP MT23-GS16984 [M+H]+ Level 1	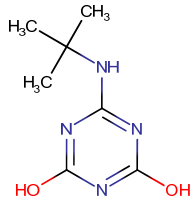	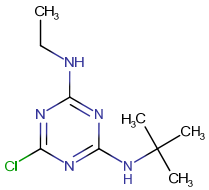	30-50	1.8	12.7	Syngenta	Not included in study	29	78	0.5	• MS/MS okay • Many samples contain further isobaric peaks: RT 10.5, 11.8 min • Biphenyl column: confirmed
Chlorotoluron TP CGA 15140 [M-H]- Level 2a	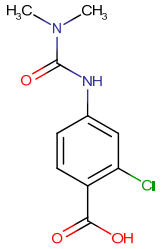	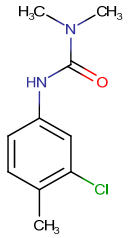	10-30	-1.8	15		11	9	No STD	-	• **No standard** • Cl isotope pattern fits in samples with intense peaks • Fragments 197 & 152 detected (Reemtsma et al. 2013)

Suspect	Structure	Parent	Sales amount (t/a) (BLW 2018)	Log D (pH 7)	RT (min)	Refe-rence material from	Reemtsma et al. 2013: 75th percentile (ng/L)	Nr. Of Detects	Max. conc. (ng/L)	LOQ (ng/L)	Comment
Fipronil-TP RPA 106681 [M+H]+ Level 2b	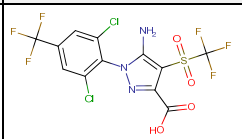	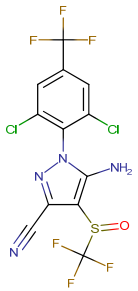	<1	1	19	BASF no STD synthetisized	Not included in study	11	120	-	• **No standard** • **semiquantitative**, same calibration model as for fipronil-TP RPA 200761; • standard RPA200761 seems to be not pure, i.e. contains as well RPA 106681 → fragments in standard & sample match perfectly
Chlorothalonil-TP 4-carbamoyl-2,3,5-trichloro-6-cyanobenzenesulfonic acid / 2-carbamoyl-3,4,5-trichloro-6-cyanobenzenesulfonic acid [M-H]- Level 3	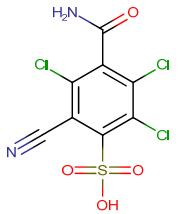 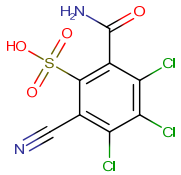	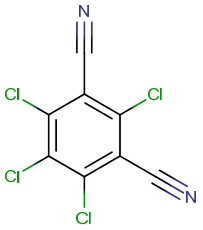	30-50	-0.7 and -0.7	10.3 & 12		Not included in study	RT 10 min: 18 RT 12 min: 19	RT 10 min: 49 RT 12 min: 120	-	• Isomers of R417888 • **No standard** → **semi-quantitative,** conservative estimation, same calibration model as for chlorothalonil-TP R417888
Cymoxanil-TPs: IN-JX915 and IN-U3204 [M+H]+ Level 3	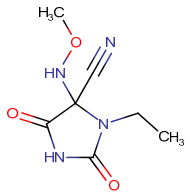 TP IN-JX915 or	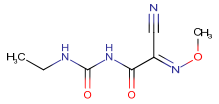 logD (pH7): 0.1	5-10	-2.3 and -0.3	11.5	Dupont	Not included in study	2	5.3	1	• Compounds are isobaric to cymoxanil **Cymoxanil:** • 2 peaks: 11.5, 15.3 min; highest intensity: 15.3 min **TP IN-JX915:** • 3 peaks (7.7, 11.5, 15.3 min); highest intensity: 11.5 min

Suspect	Structure	Parent	Sales amount (t/a) (BLW 2018)	Log D (pH 7)	RT (min)	Refe-rence material from	Reemtsma et al. 2013: 75th percentile (ng/L)	Nr. Of Detects	Max. conc. (ng/L)	LOQ (ng/L)	Comment
	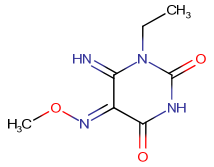 TP IN-U3204										• Peak at 15.3 min is probably cymoxanil (cymoxanil is not stable during analysis → cymoxanil standard: 2 peaks (11.5 & 15.3 min) **TP IN-U3204:** • 2 peaks (7.7, 11.5); highest intensity: 11.5 min ➔ Equilibrium between 3 structures? According to logD (pH3): o 7.7 min: IN-JX915 o 11.5 min: IN-U3204 o 15.3 min: cymoxanil **Samples:** • Only peak at 11.5 min • Noisy • MS/MS okay Biphenyl column: concentration in samples was too low to be confirmed with biphenyl column
Azole-TP 1,2,4 triazole acetic acid [M+H]+ Rejected	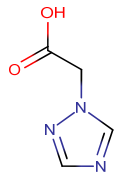	Different azoles	5-10	-4.2	6	Bayer	Not included in study	0		10	• RT does not match • Biphenyl column: no clear peak in sample

Suspect	Structure	Parent	Sales amount (t/a) (BLW 2018)	Log D (pH 7)	RT (min)	Refe-rence material from	Reemtsma et al. 2013: 75th percentile (ng/L)	Nr. Of Detects	Max. conc. (ng/L)	LOQ (ng/L)	Comment
Cymoxanil-TP IN-KQ960 [M+H]+ Rejected	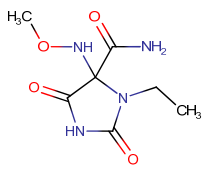	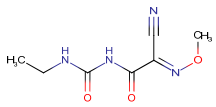	5-10	-1.4	9.9	Dupont	Not included in study	0		15	• RT does not match • Noisy • Biphenyl column: rejected
Cyprodinil-TP CGA 249287 [M+H]+ Rejected	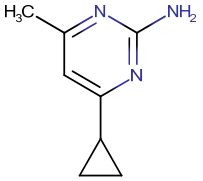	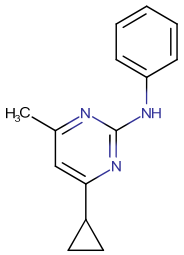	5-10	0.9	10	Syngenta	Not included in study	0		5	• Noisy • Small peak (<5 ng/L) in 2 samples with similar RT as in standard, but fragment intensity ratios do not fit well in sample & standard • Spiked sample: double peak → probably different compound in sample • Biphenyl column: rejected (peak in sample elutes 0.5 min earlier)
Ethofumesate-2-hydroxy Rejected	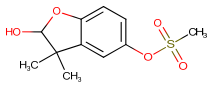	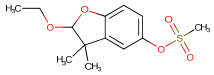	10-30	1.3		Dr. Ehrenstorfer	Not included in study	0		Not determined	• RT does not match • Low ionizability
Methiocarb-TP methiocarb sulfone phenol [M-H]- Rejected	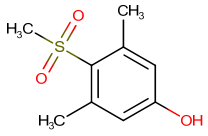	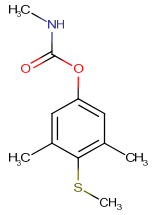	1-5	1.5	14.5	Bayer	Not included in study	0		6	• RT does not match • Biphenyl column: rejected

Suspect	Structure	Parent	Sales amount (t/a) (BLW 2018)	Log D (pH 7)	RT (min)	Refe-rence material from	Reemtsma et al. 2013: 75th percentile (ng/L)	Nr. Of Detects	Max. conc. (ng/L)	LOQ (ng/L)	Comment
Pirimicarb-desamido (R031805) [M+H]+ Rejected	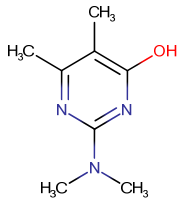	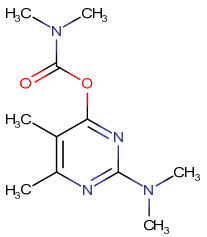	1-5	1.8	8.5	Dr. Ehrenstorfer	Not included in study	0		0.5	• RT does not match • Biphenyl column: not tested
Pymetrozine-TP CGA371075 [M+H]+ Rejected	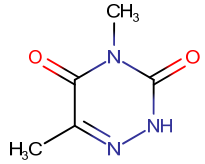	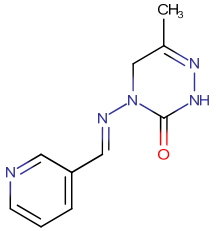	<1	-0.6	11	Syngenta	Not included in study	0		-	• Reference standard: 2 peaks (10.7 & 11 min) • Samples: 1 peak (~10.8 min) • Different fragments • LOQ cannot be defined • Biphenyl column: no peak in STD
Spiroxamin aminodiol [M+H]+ Rejected	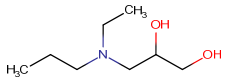	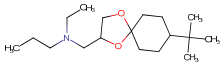	5-10	-2.3	7	Bayer	Not included in study	0		2	• RT does not match • • Biphenyl column: rejected
Terbuthylazine-TP MT24 G35713 [M+H]+ Rejected	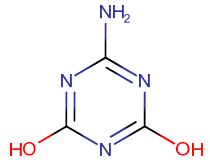	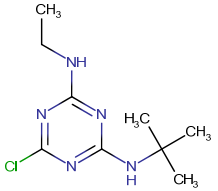	30-50	0.5	3.8	Syngenta	Not included in study	0		Not determined	• RT does not match • Peak at 12.6 min in EIC is In-source fragment of Terbuthylazine-TP MT23-GS16984

Suspect	Structure	Parent	Sales amount (t/a) (BLW 2018)	Log D (pH 7)	RT (min)	Refe-rence material from	Reemtsma et al. 2013: 75th percentile (ng/L)	Nr. Of Detects	Max. conc. (ng/L)	LOQ (ng/L)	Comment
Asulam-TP Sulfanilamide [M+NH4]+ Unclear	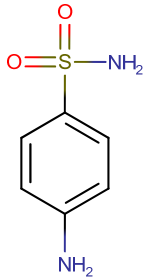	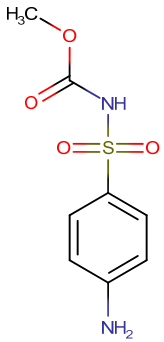	10-30	-0.2	7.5	LGC	Not included in study	3	14	10	• [M+H]+ and [M+NH4]+ of similar intensity • No MS/MS due to low intensity? • RT okay • Biphenyl column: concentration in samples was too low to be confirmed with biphenyl column
Pymetrozine-TP CGA294849 [M+H]+ Unclear	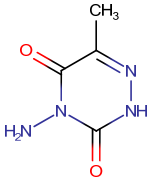	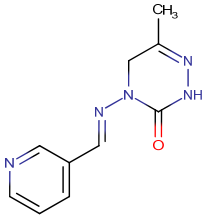	<1	-1.2	7.5	Syngenta	Not included in study	1	~LOQ	15	• No MS/MS in samples due to low intensity • noisy • low ionization efficiency • only in 1 sample with urban catchment • Standard was pursued due to later-eluting, more intense peaks • Biphenyl column: concentration in samples was too low to be confirmed with biphenyl column
Trifluoroacetic-acid [M-H]- Unclear	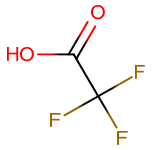	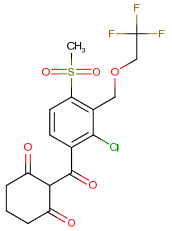 Tembotrione	<1	-2.6	5	Sigma-Aldrich	Not included in study	31		-	• in all samples • Only 1 fragment • Quantification not possible with applied LC method • Tembotrione is probably not the major source of trifluoroacetic acid • High background

Table SI2-C2: Pesticides

Suspect	Structure	Sales amount (t/a) (BLW 2018)	Log D (pH 7)	RT (min)	Refe-rence material from	Reemtsma et al. 2013: 75th percentile (ng/L)	Nr. Of Detects	Max. conc. (ng/L)	LOQ (ng/L)	Comment
Oxadixyl [M+H]+ Level 1	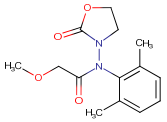	No data	1.8	16	Riedel-de Haën	Not included in study	1	41	1	• MS/MS okay • Not approved as pesticide since 2011 • Biphenyl column: oxadixyl <LOQ in samples which were analysed with biphenyl column
Captan Rejected	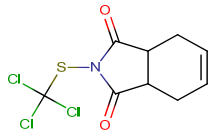	30-50	3.2		Riedel-de Haën	Not included in study	0		-	• No ionization / not stable in water?
Chlorpropham (CIPC) [M+H]+ Rejected	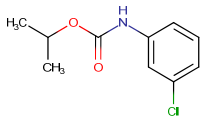	1-5	3.2	20	Sigma-Aldrich	Not included in study	0		1000	• RT does not match • Low ionizability
Fenazaquin [M+H]+ Rejected	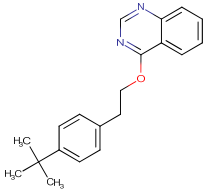	<1	5.4	24	Sigma-Aldrich	Not included in study	0		10	• RT does not match • Biphenyl column: no peaks in analysed samples
Heptenophos [M+H]+ Rejected	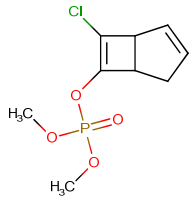	No data	1.1	18	Riedel-de Haën	Not included in study	0		50	• Ionization only in positive mode → no peak in samples

Suspect	Structure	Sales amount (t/a) (BLW 2018)	Log D (pH 7)	RT (min)	Refe-rence material from	Reemtsma et al. 2013: 75th percentile (ng/L)	Nr. Of Detects	Max. conc. (ng/L)	LOQ (ng/L)	Comment
Metaldehyde [M+NH4]+ Rejected	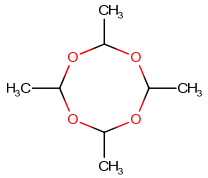	30-50	1.2	13.5	Dr. Ehrenstorfer	Not included in study	0		100	• High background • [M+NH4]+ more sensitive • Biphenyl column: rejected
Pyrifenox [M+H]+ Rejected	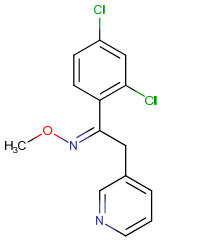	No data	3.7	18.5	Dr. Ehrenstorfer	Not included in study	0		3	• RT does not match • Biphenyl column: rejected
Vinclozolin [M+H]+ Rejected	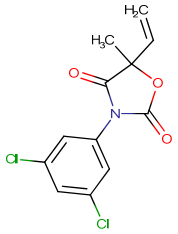	No data	3.7	20.5	Dr. Ehrenstorfer		0		100	• RT does not match • Low ionizability

Chlorothalonil-TP R417888
Level 1
[M-H]- 326.88063
(STD 100 ng/L)

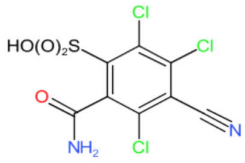

Normalized Extracted Ion Chromatogram (MS1)

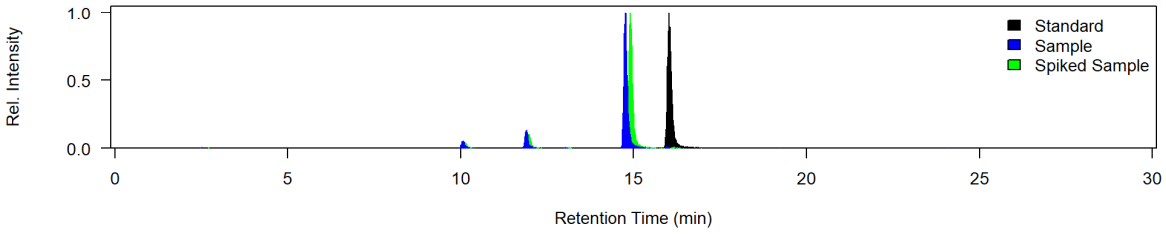

Extracted Ion Chromatogram (MS1)

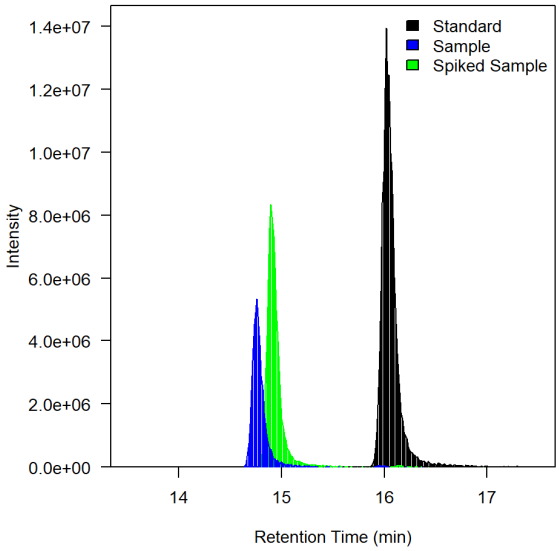

Most Intense Fragments in Sample

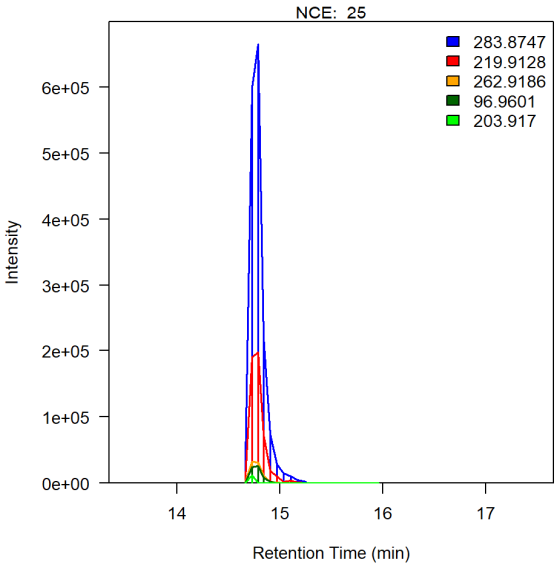

Most Intense MS2 Scan

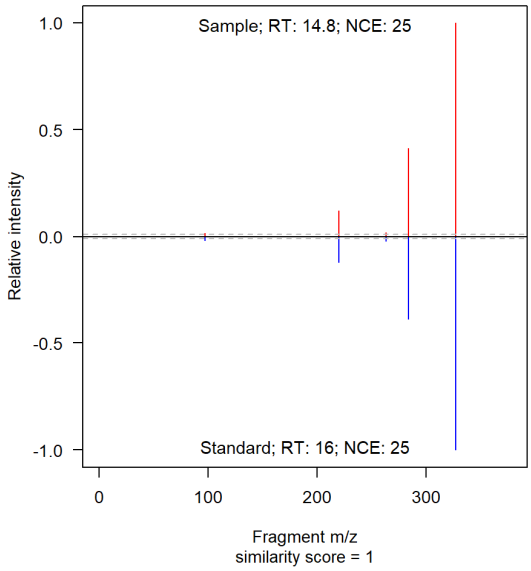

Most Intense Fragments in Standard

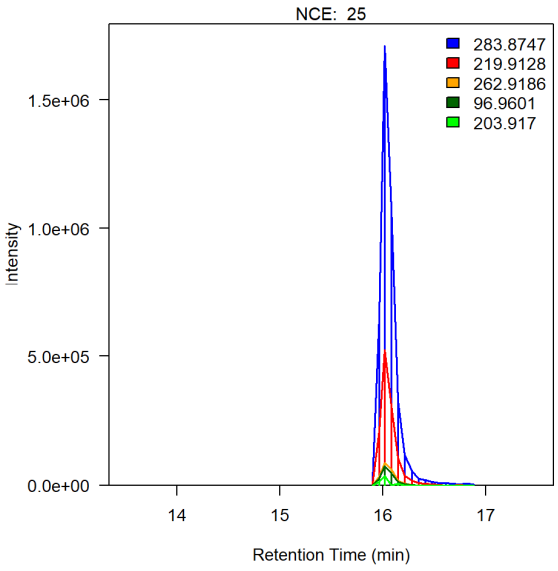

Chlorothalonil-TP R471811
Level 1
[M-H]- 344.8912
(STD 500 ng/L)

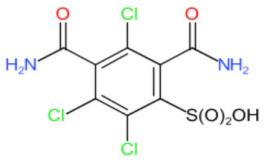

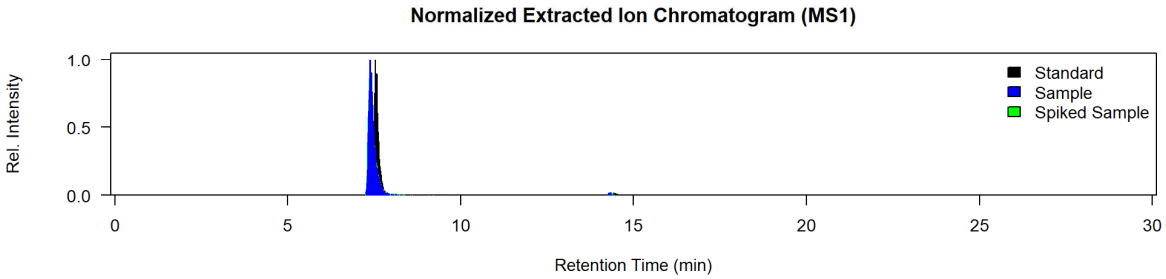

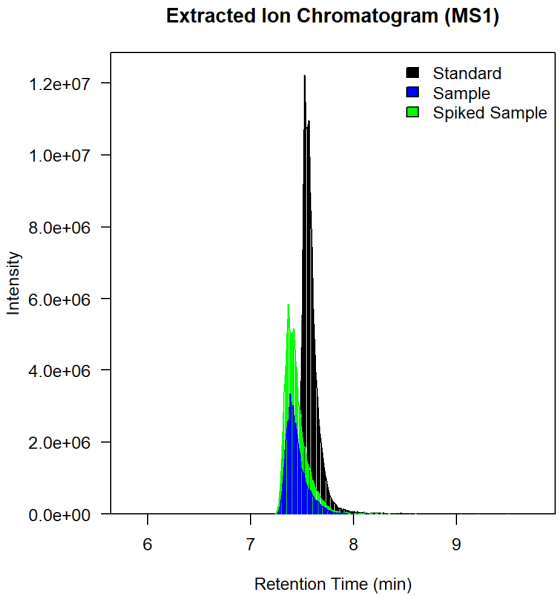

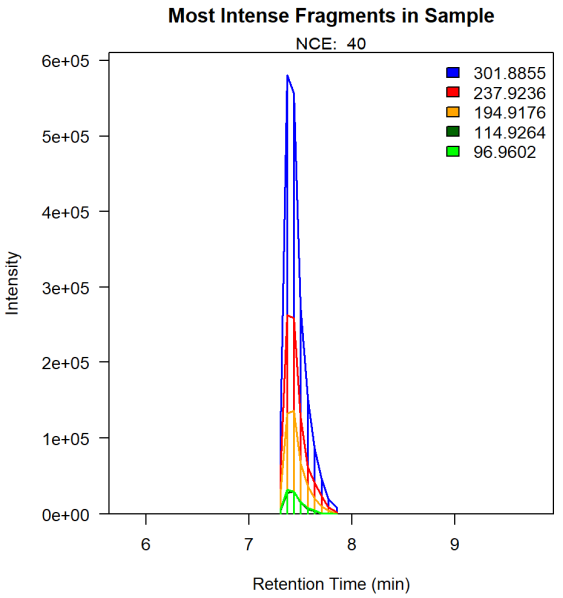

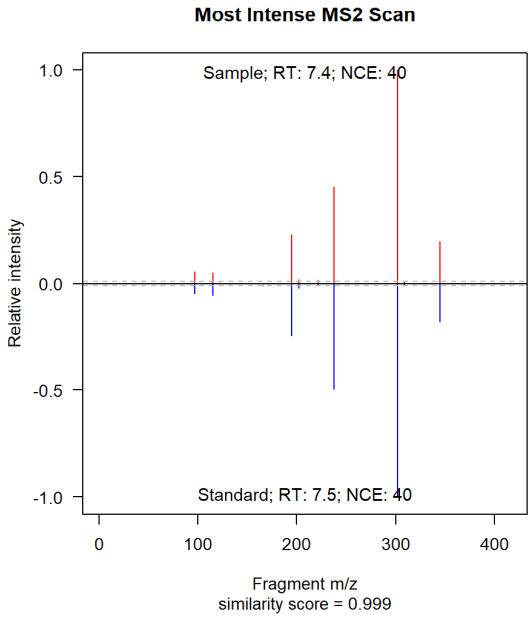

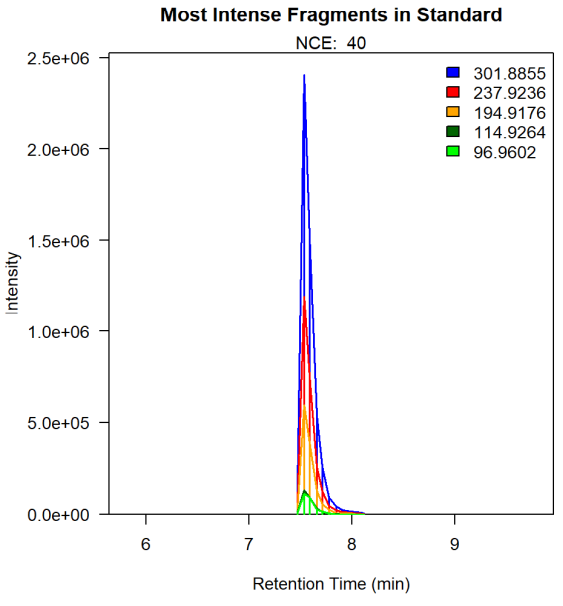

Chlorothalonil-TP SYN507900
Level 1
[M-H]- 262.91873
(STD 50 ng/L)

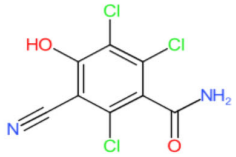

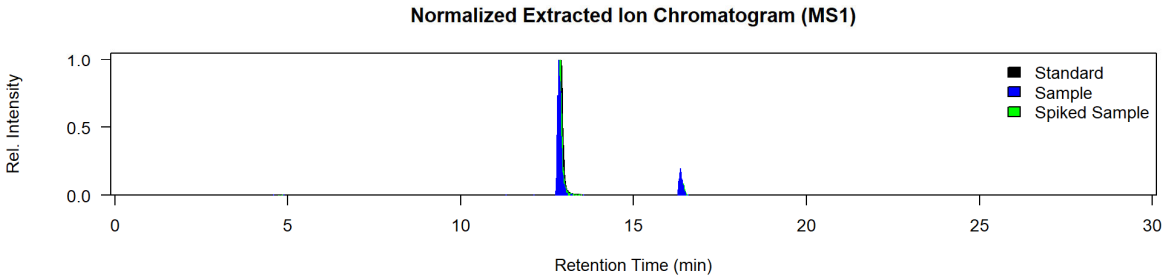

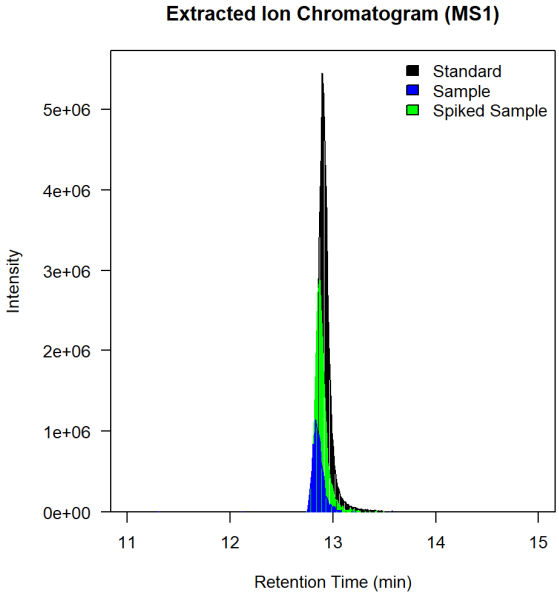

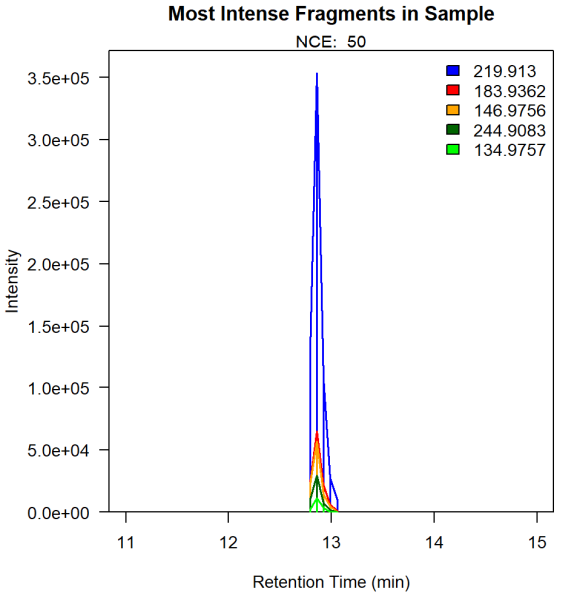

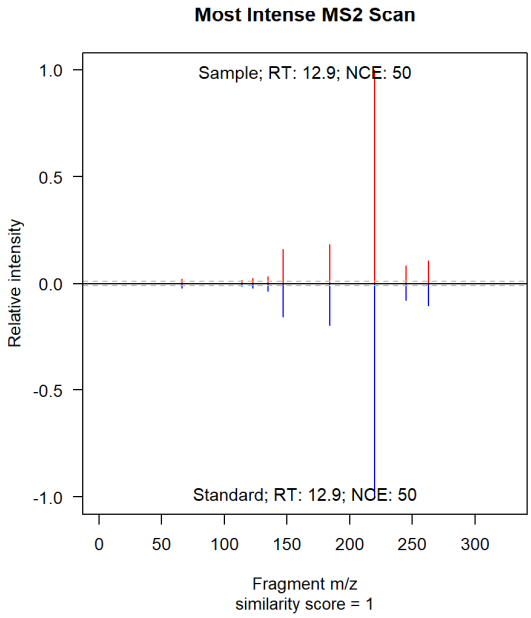

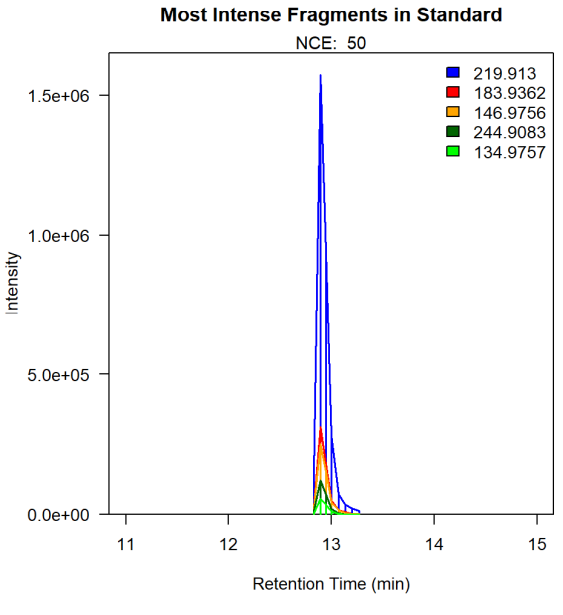

Chlorothalonil-TP R419492
Level 1
[M-2H]2- 185.934572
(STD 100 ng/L)

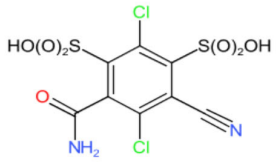

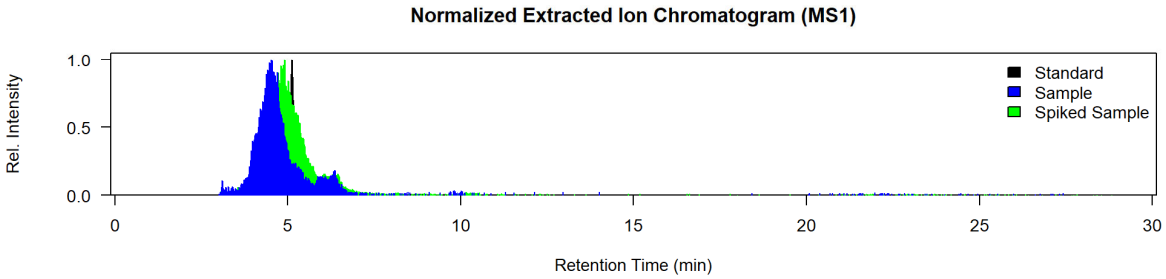

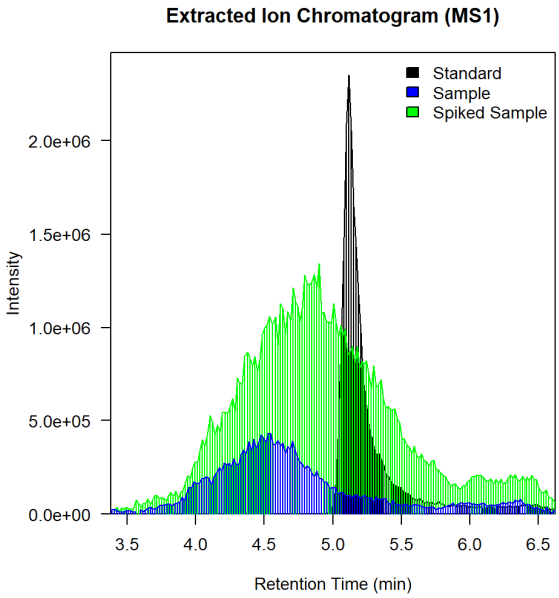

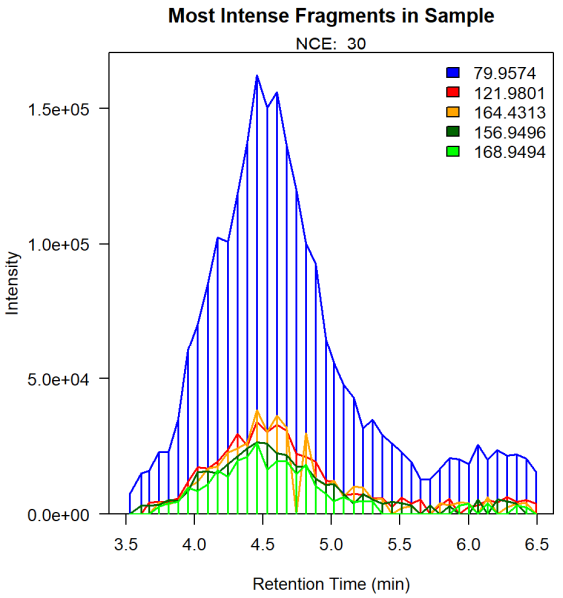

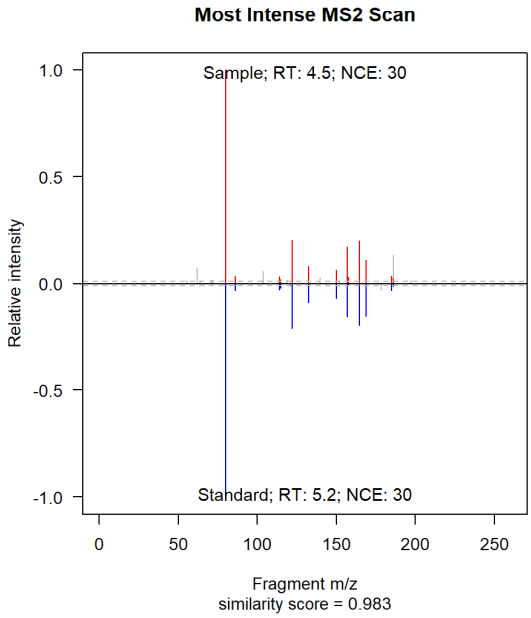

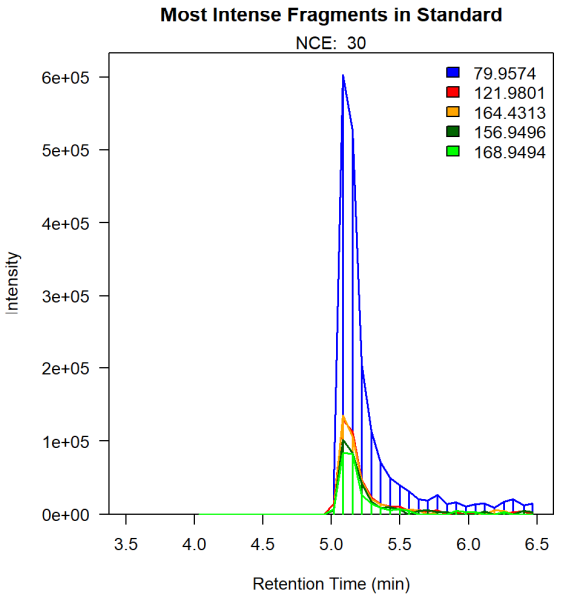

Chlorothalonil-TP R419492
Level 1
[M-H]- 372.87642
(STD 100 ng/L)

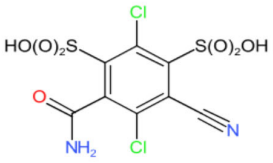

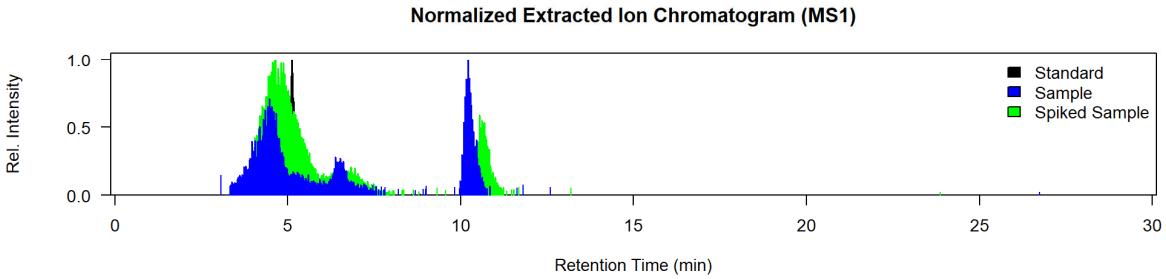

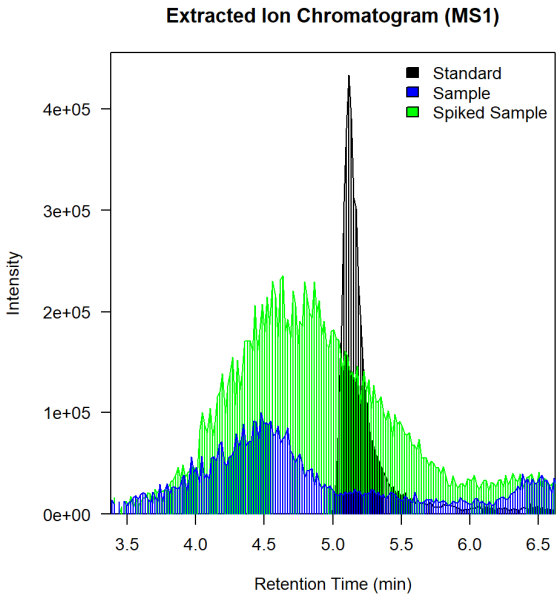

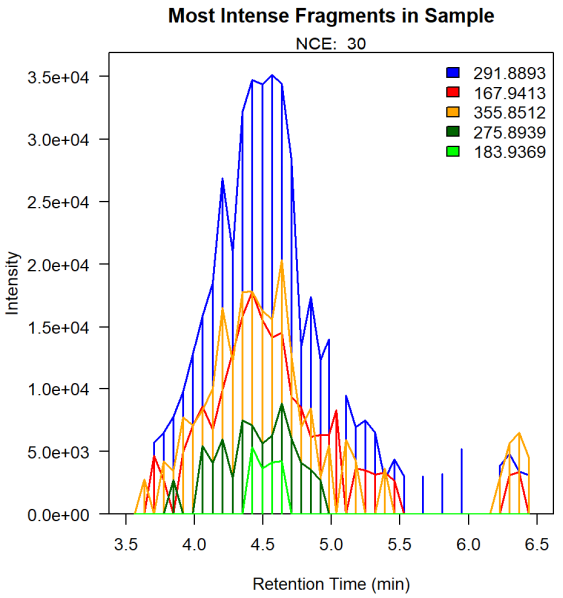

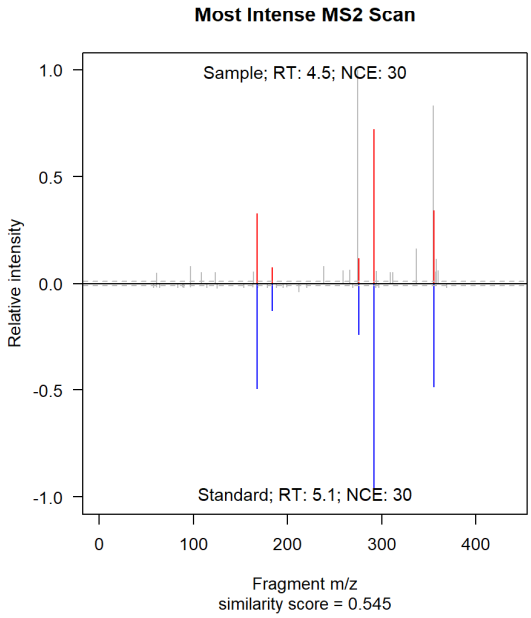

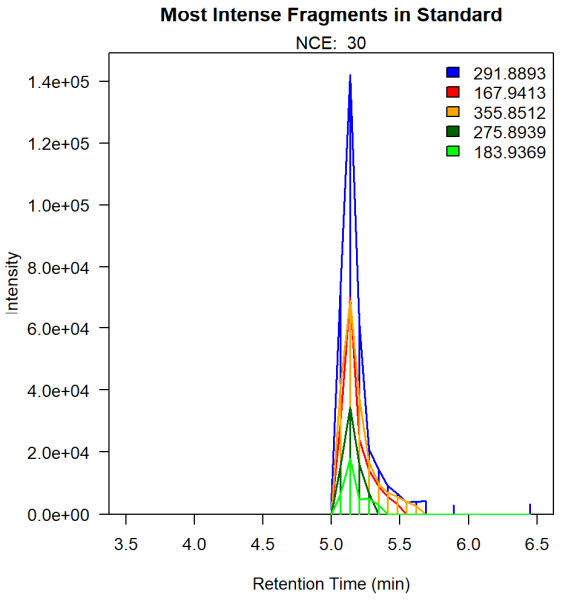

Chlorothalonil-TP SYN548580
Level 1
[M-H]- 280.9293
(STD 100 ng/L)

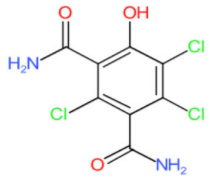

Normalized Extracted Ion Chromatogram (MS1)

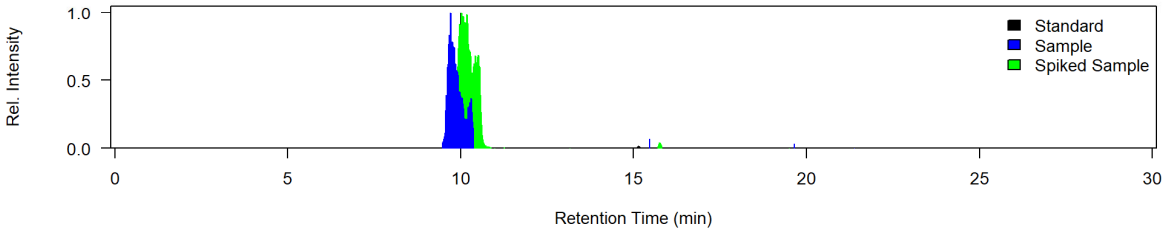

Extracted Ion Chromatogram (MS1)

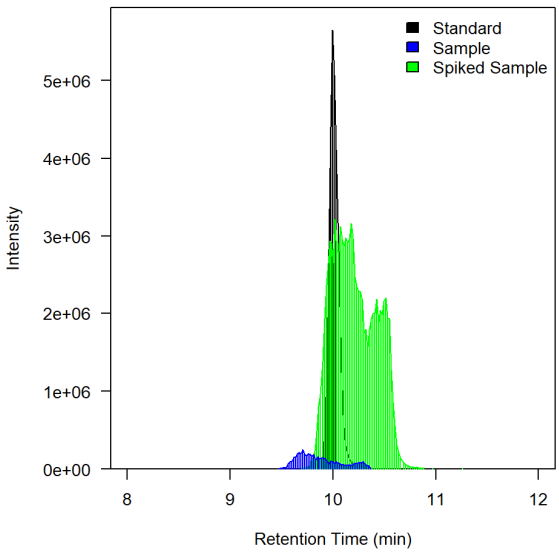

Most Intense Fragments in Sample

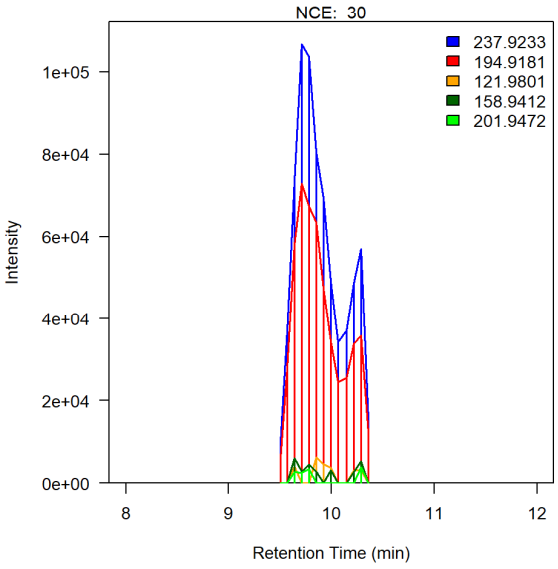

Most Intense MS2 Scan

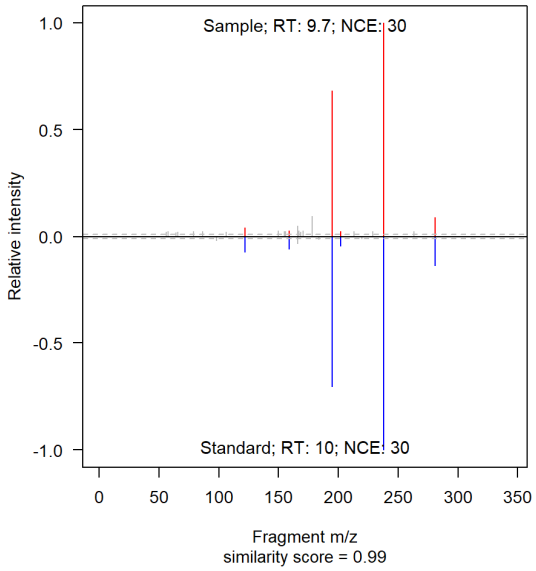

Most Intense Fragments in Standard

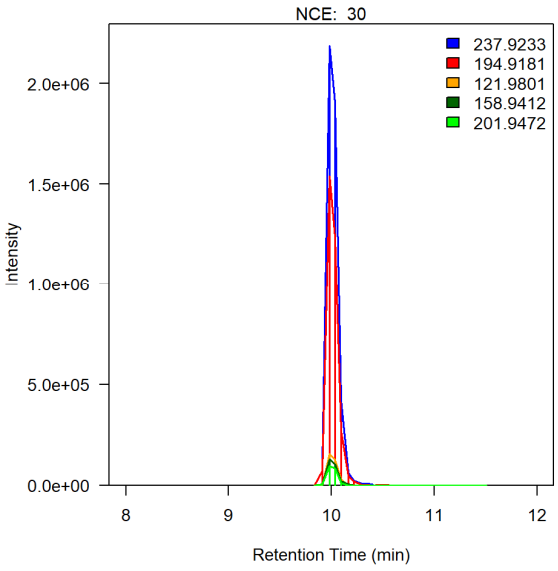

Cycloxydim-TP BH 517-TSO E/Z-isomer
Level 1
[M+H]+ 342.17336
(STD 25 ng/L)

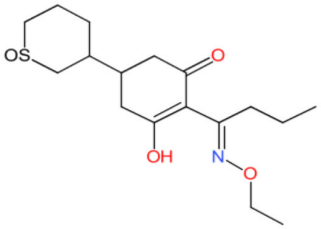

Normalized Extracted Ion Chromatogram (MS1)

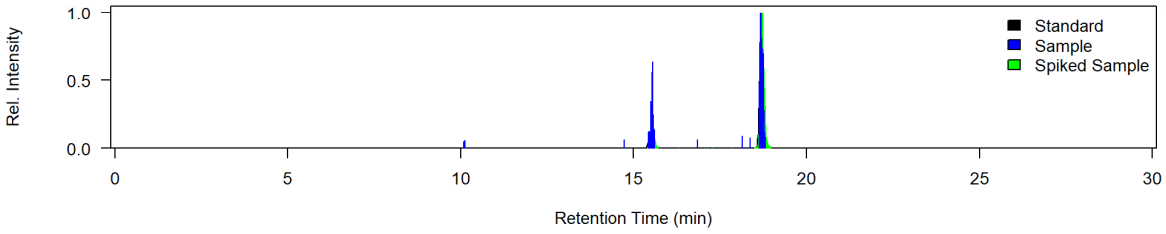

Extracted Ion Chromatogram (MS1)

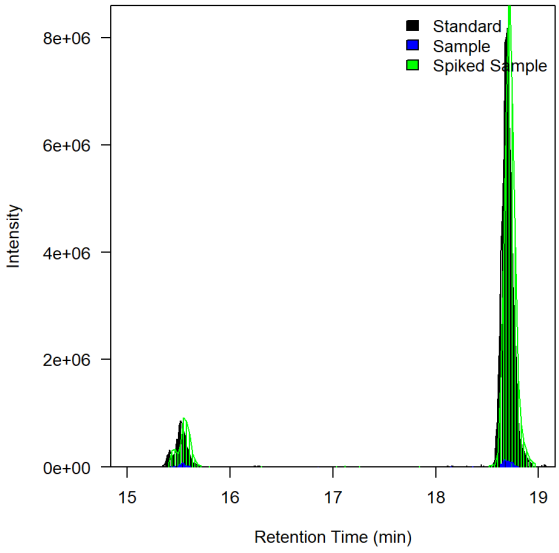

Most Intense Fragments in Sample

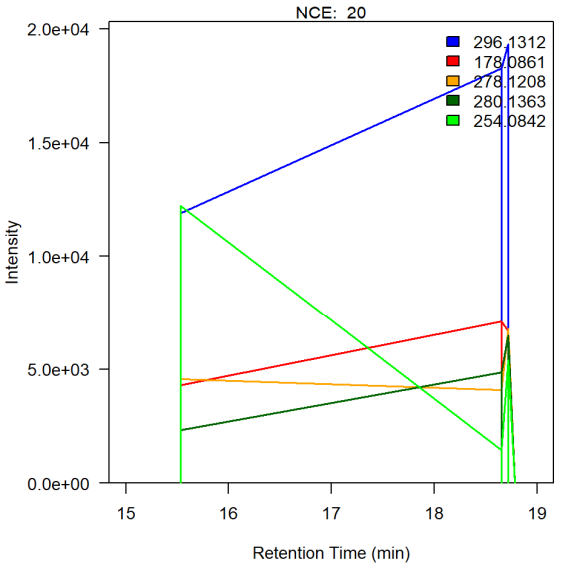

Most Intense MS2 Scan

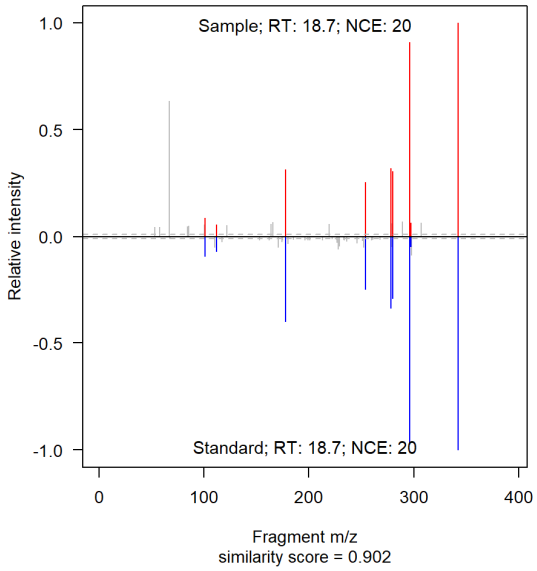

Most Intense Fragments in Standard

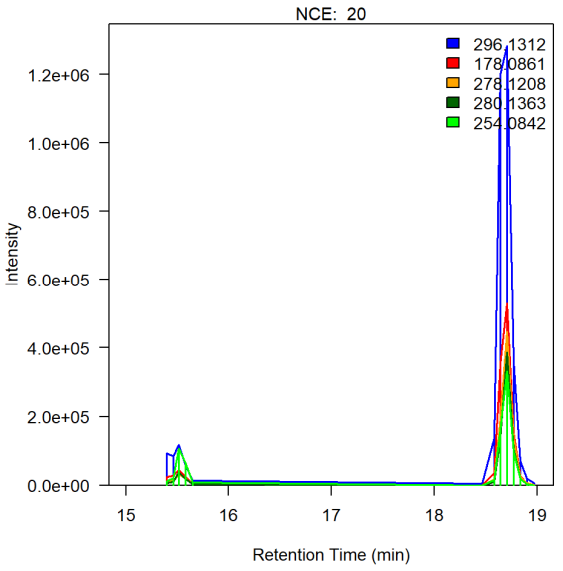

Dimethachlor-TP CGA 369873
Level 1
[M-H]- 242.04925
(STD 25 ng/L)

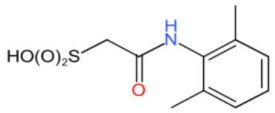

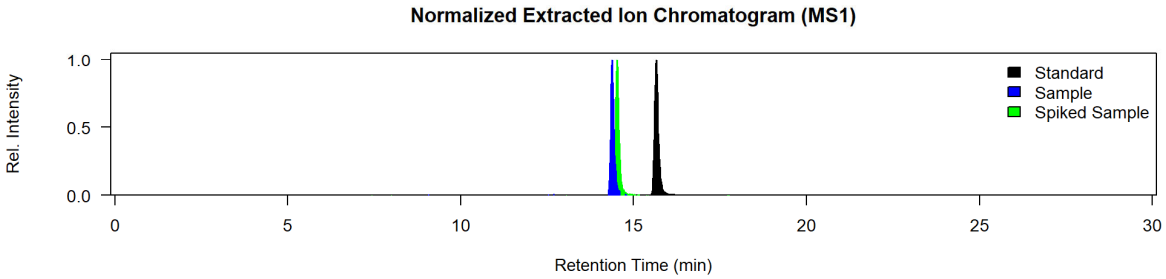

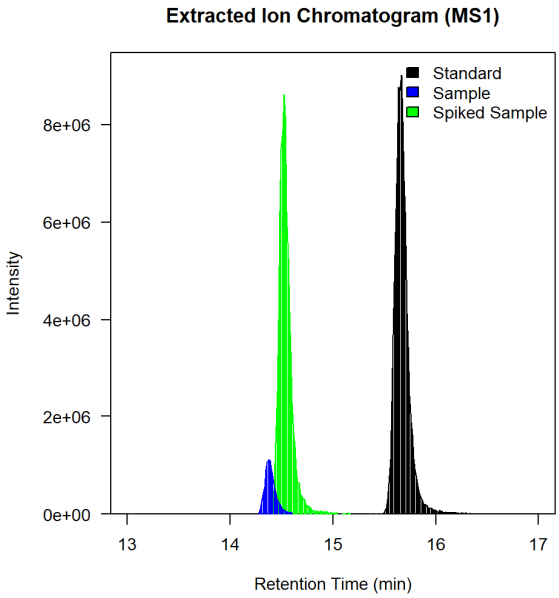

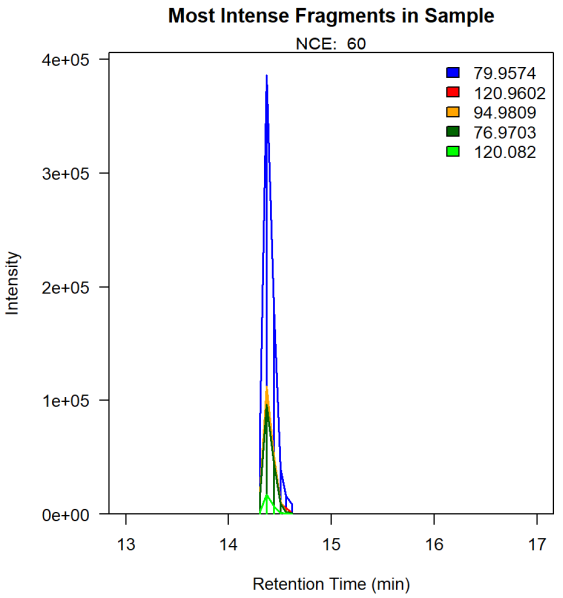

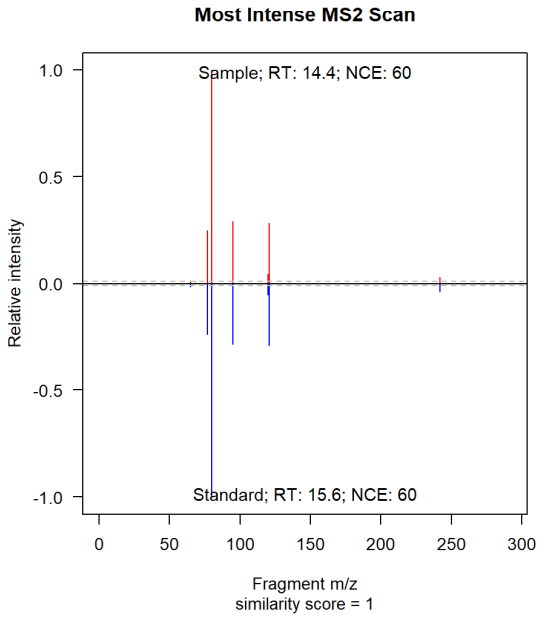

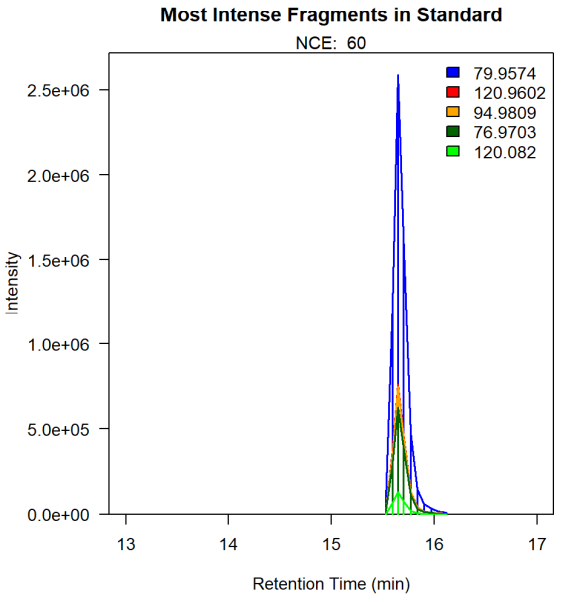

Fipronil-TP RPA 200761
Level 1
[M+H]+ 455.94056
(STD 25 ng/L)

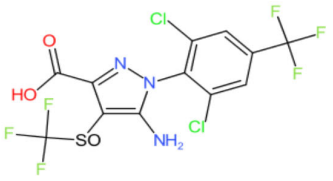

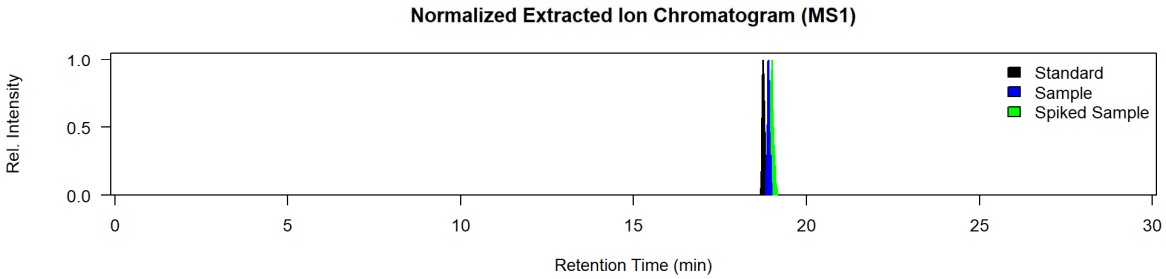

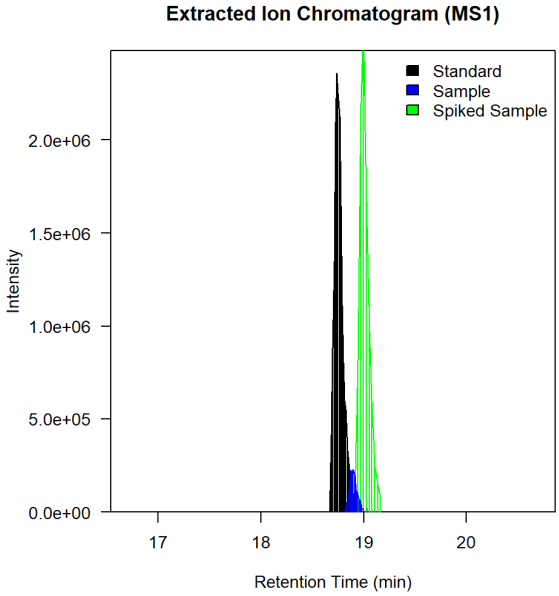

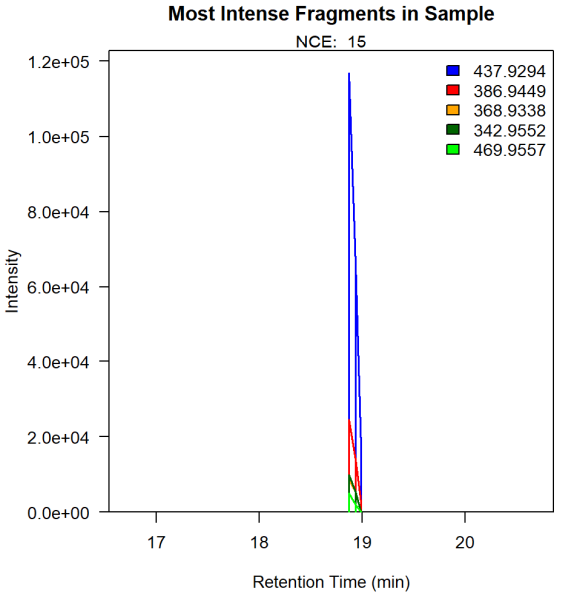

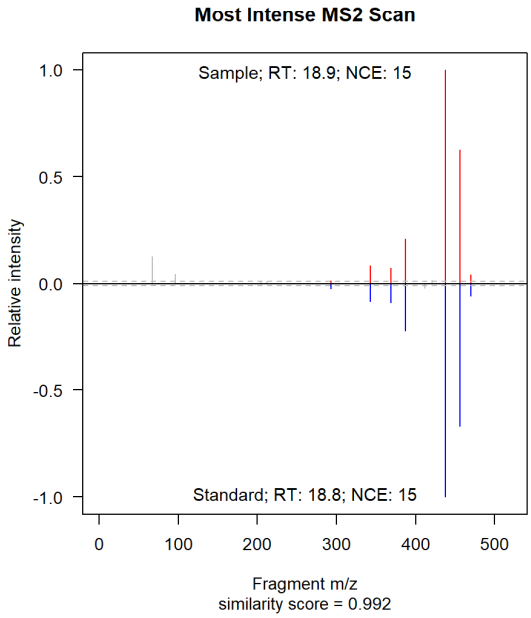

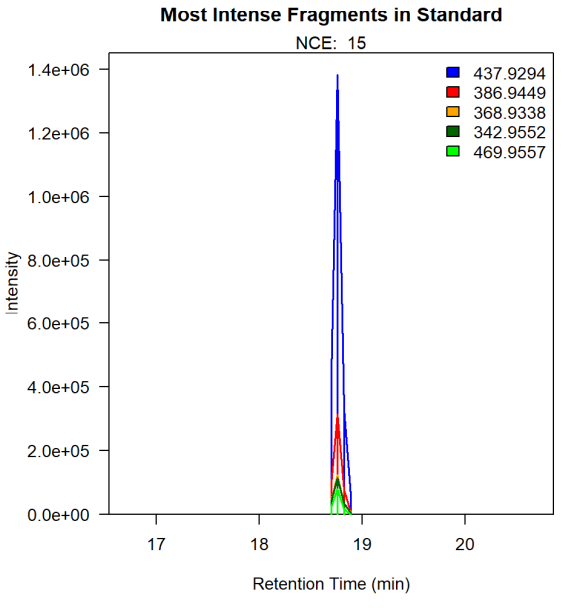

Fludioxonil-TP CGA 192155
Level 1
[M-H]- 201.00048
(STD 25 ng/L)

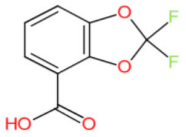

Normalized Extracted Ion Chromatogram (MS1)

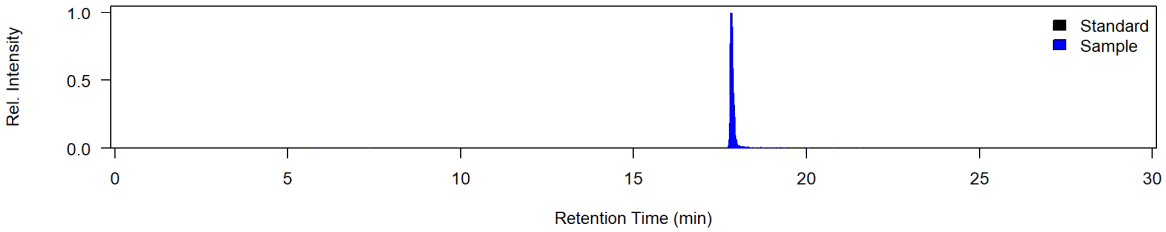

Extracted Ion Chromatogram (MS1)

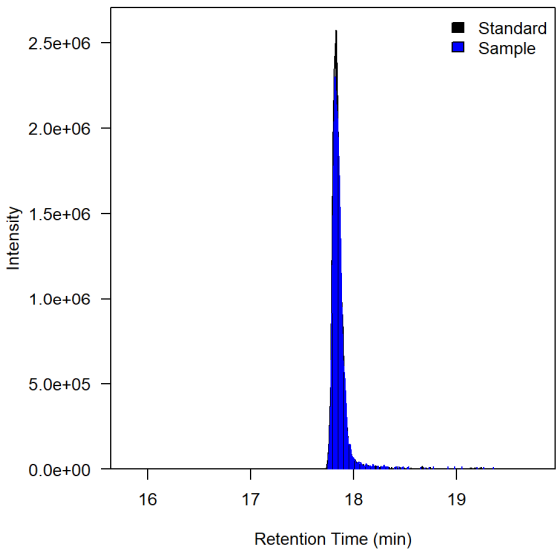

Most Intense Fragments in Sample

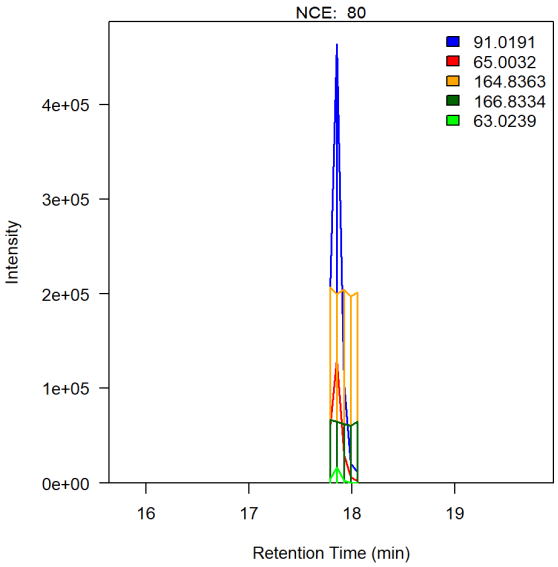

Most Intense MS2 Scan

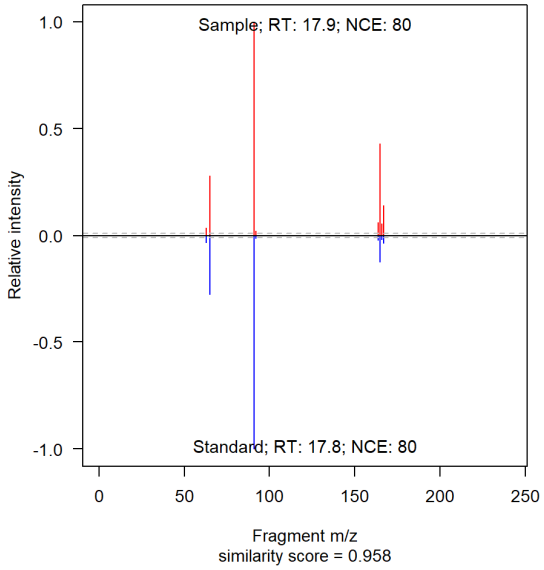

Most Intense Fragments in Standard

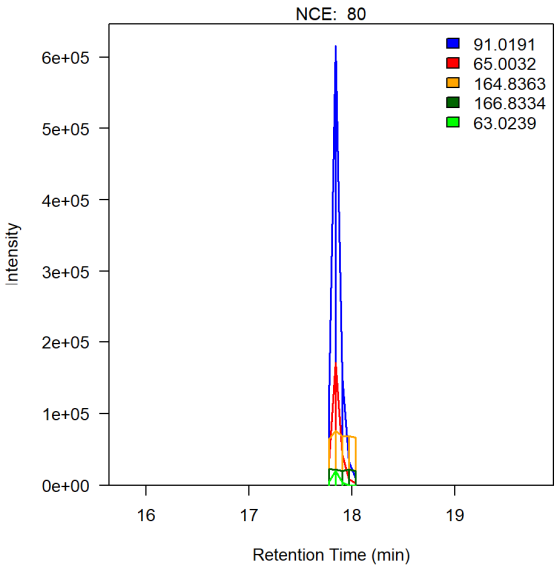

Fluxapyroxad (BAS 700 F)-TP CSAA798670
Level 1
[M+H]+ 177.04701
(STD 25 ng/L)

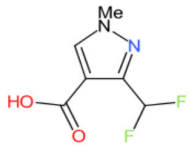

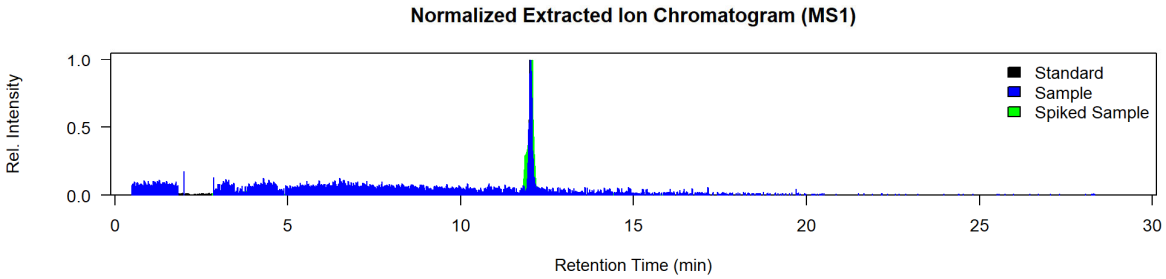

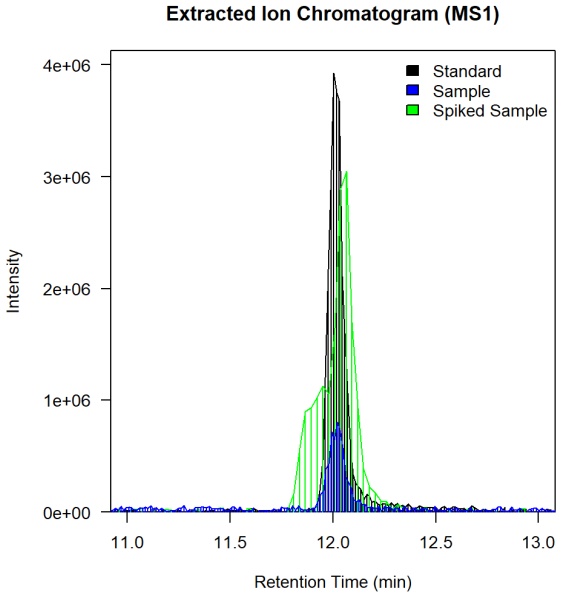

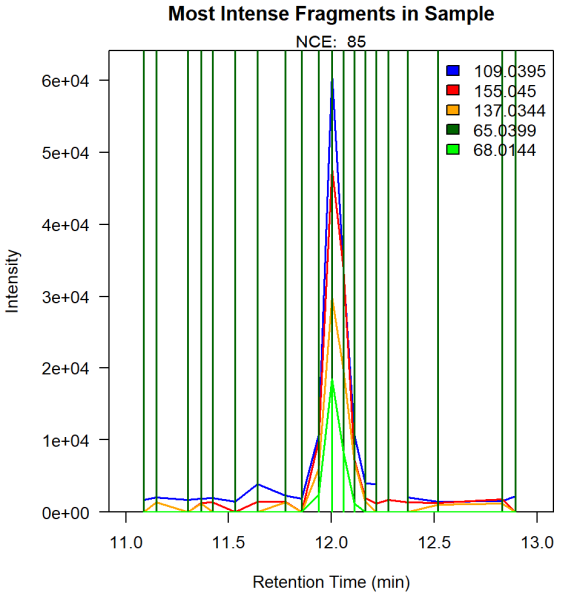

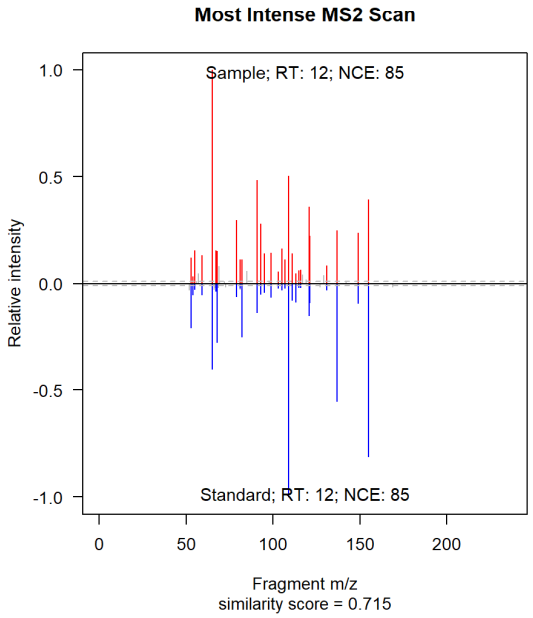

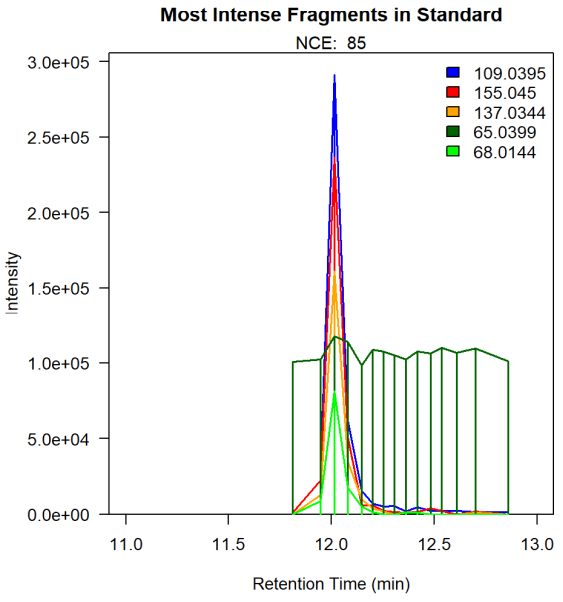

Fluxapyroxad (BAS 700 F)-TP CSCD465008
Level 1
[M-H]- 161.01681
(STD 25 ng/L)

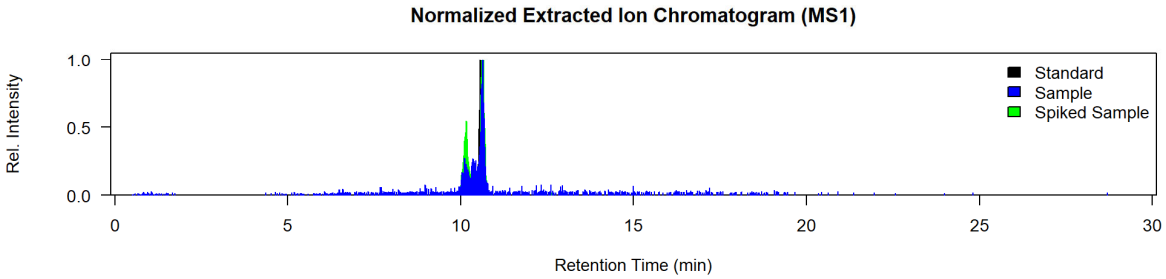

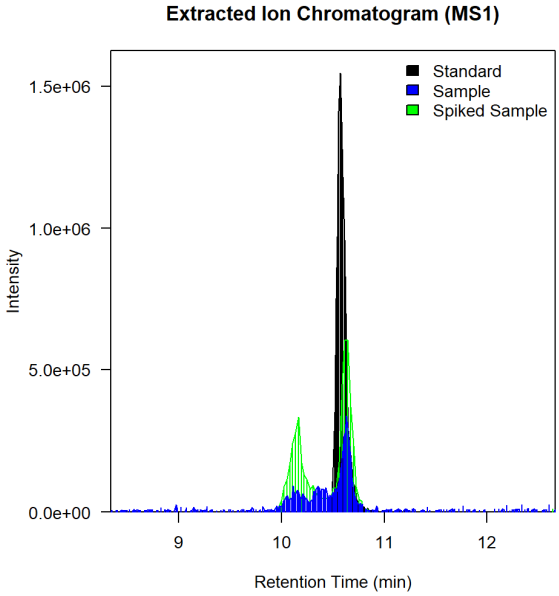

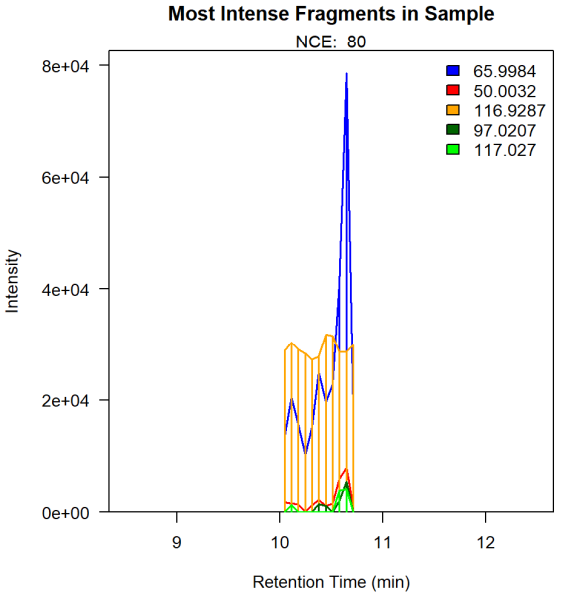

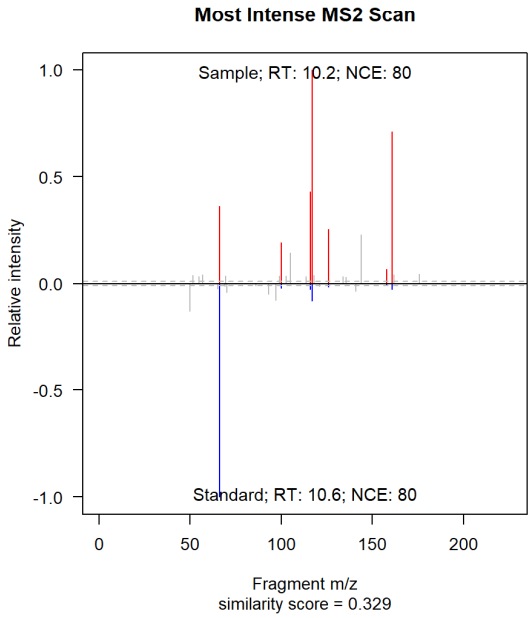

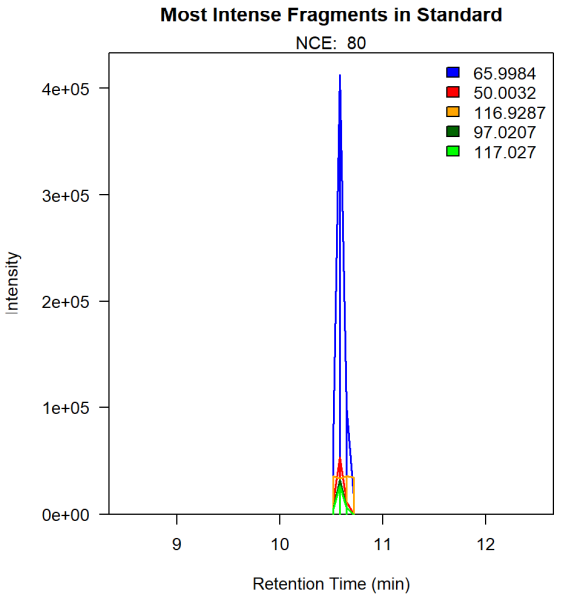

Metalaxyl-M-TP CGA108906
Level 1
[M+H]+ 296.11286
(STD 25 ng/L)

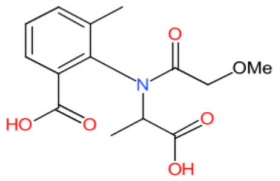

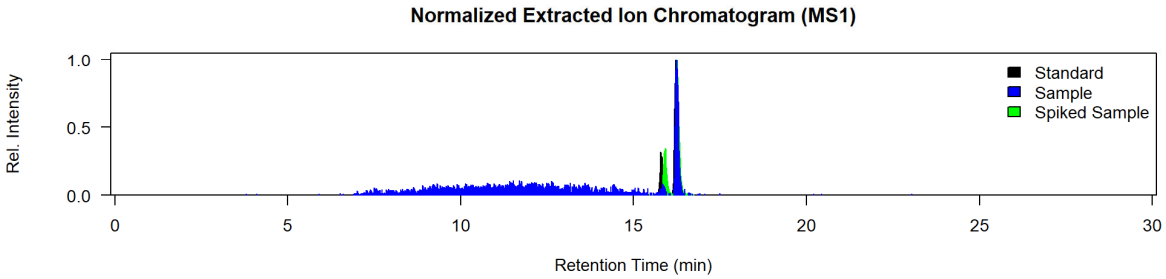

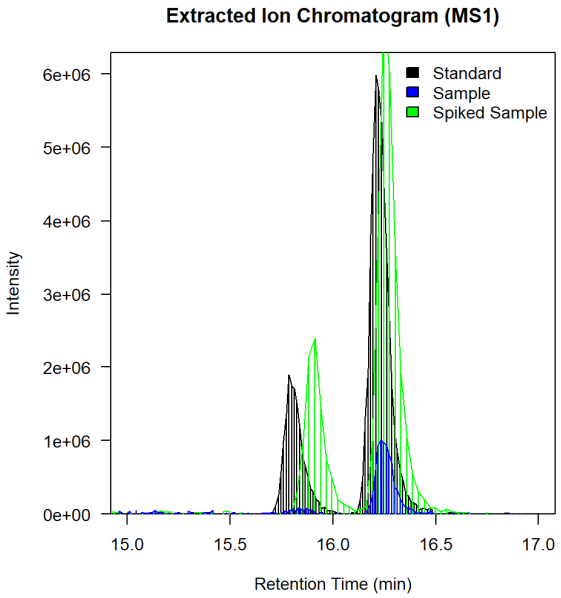

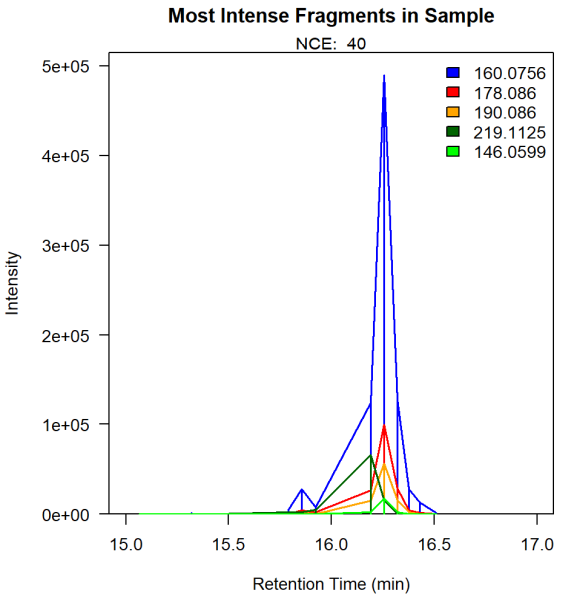

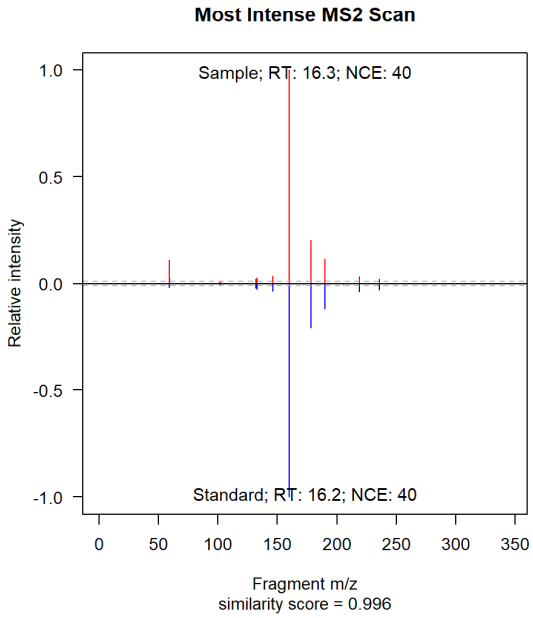

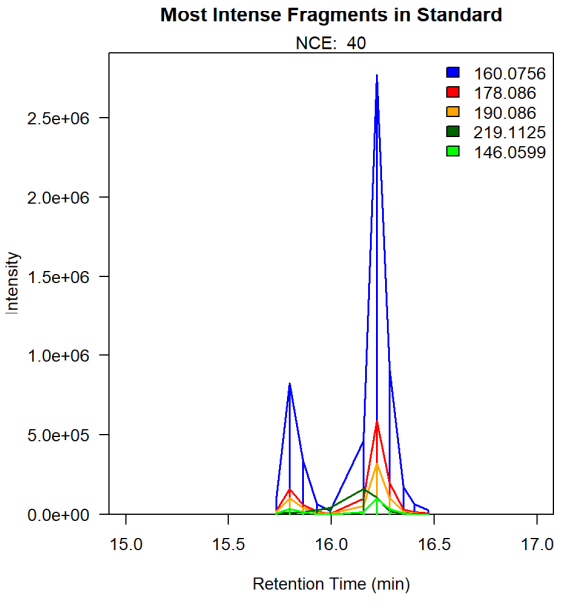

Metolachlor-TP CGA 368208 / Acetochlor sulfonic acid
Level 1
[M-H]- 256.0649
(STD 50 ng/L)

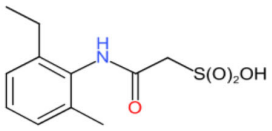

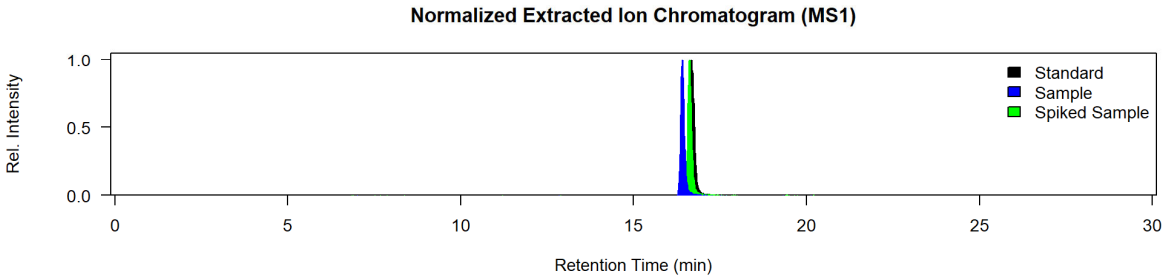

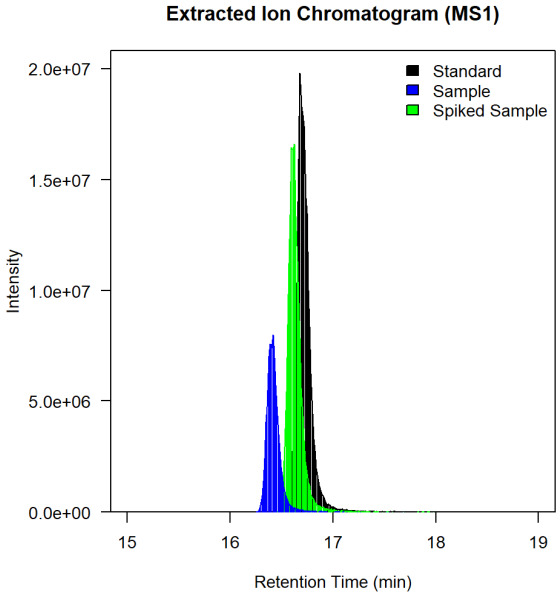

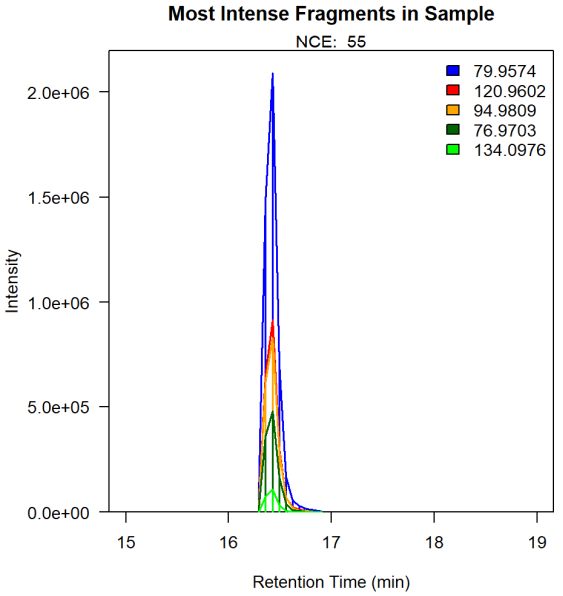

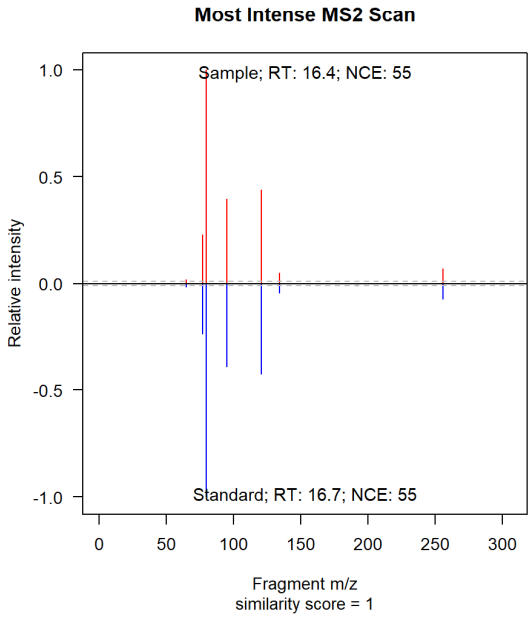

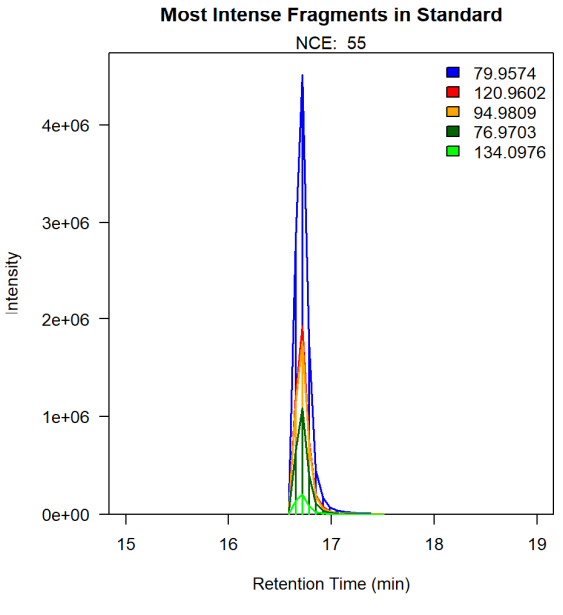

Metolachlor-TP NOA413173
Level 1
[M-H]- 328.08603
(STD 500 ng/L)

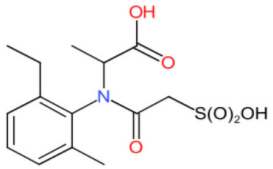

Normalized Extracted Ion Chromatogram (MS1)

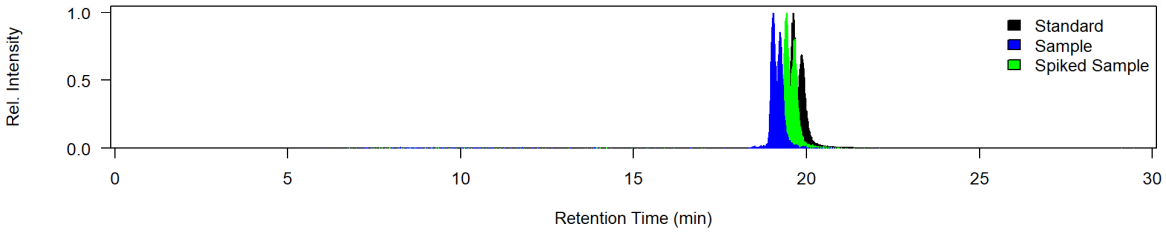

Extracted Ion Chromatogram (MS1)

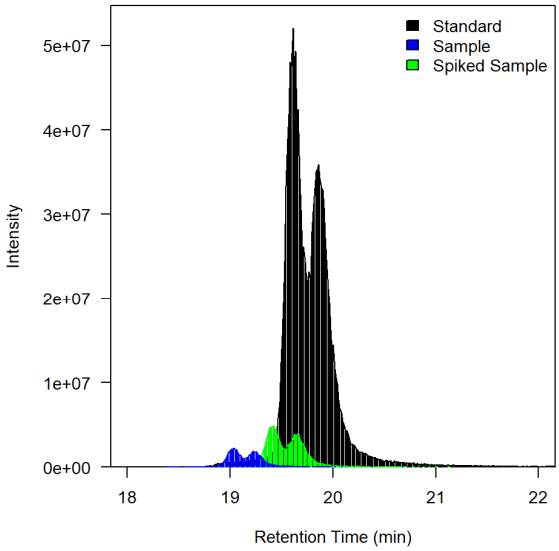

Most Intense Fragments in Sample

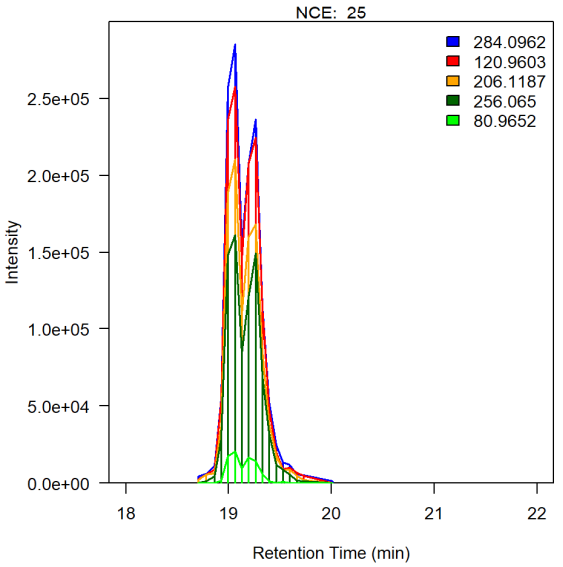

Most Intense MS2 Scan

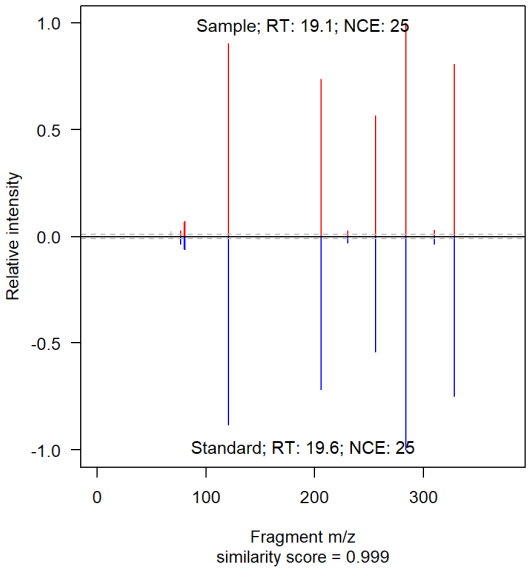

Most Intense Fragments in Standard

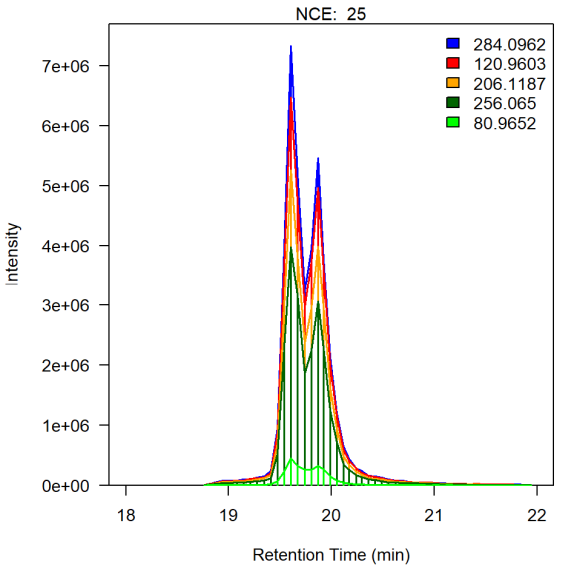

Nicosulfuron-TP AUSN
Level 1
[M+H]+ 315.087
(STD 50 ng/L)

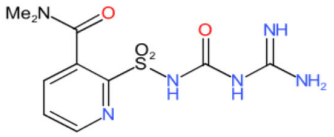

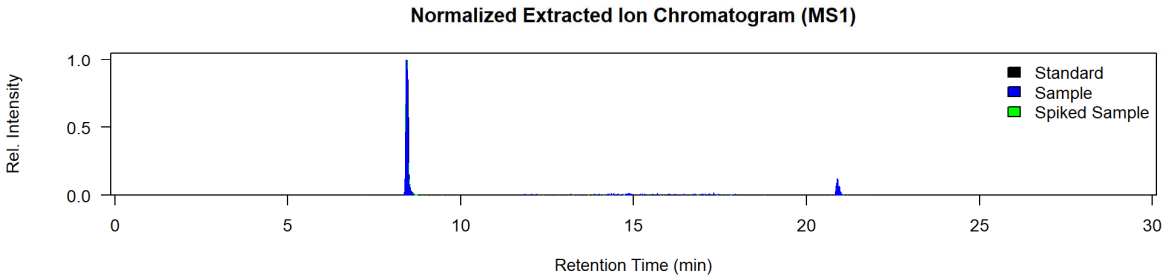

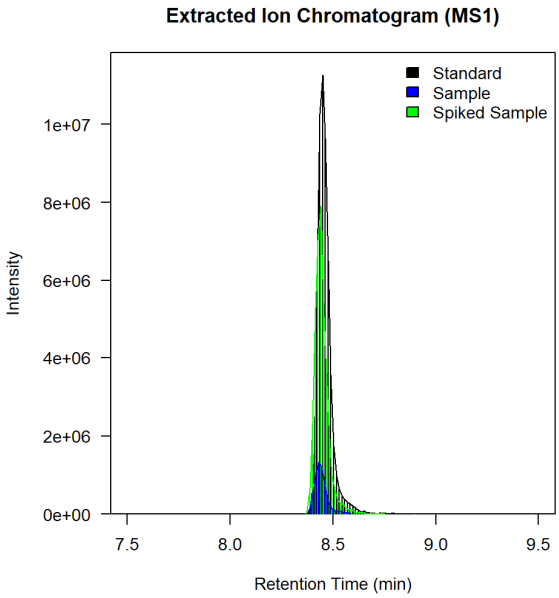

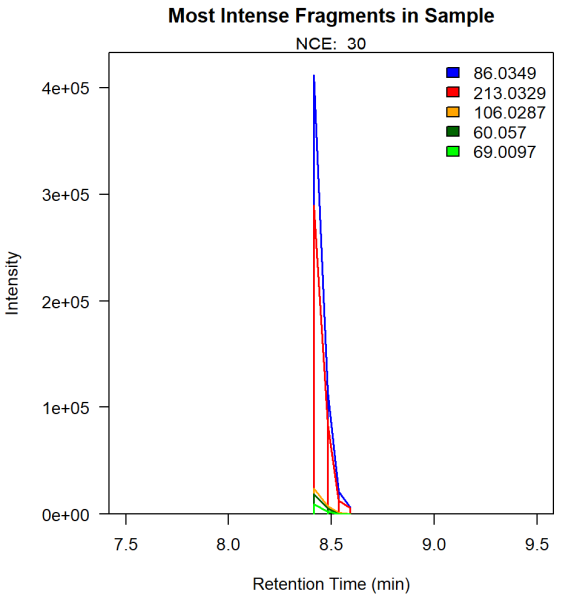

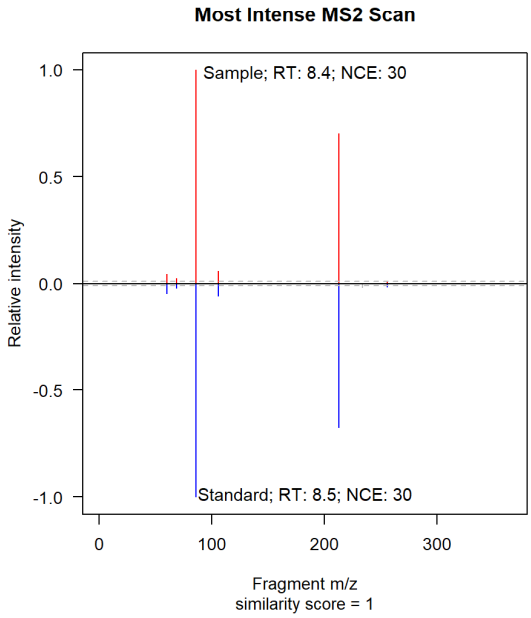

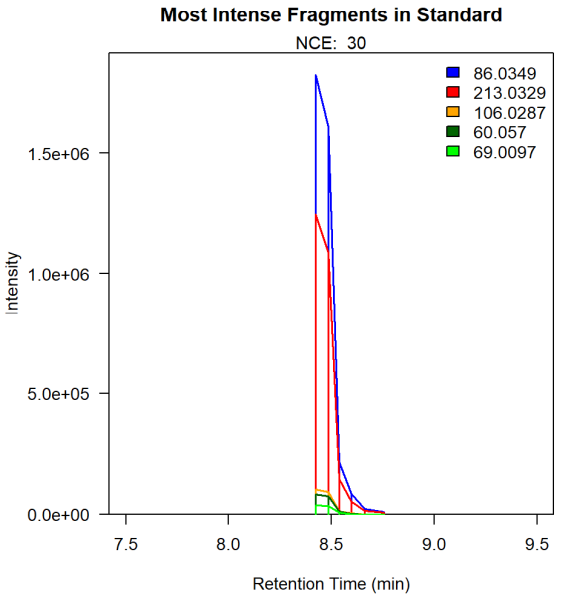

Nicosulfuron-TP UCSN
Level 1
[M+H]+ 316.07102
(STD 50 ng/L)

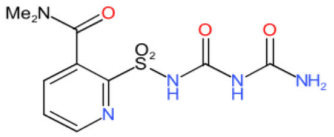

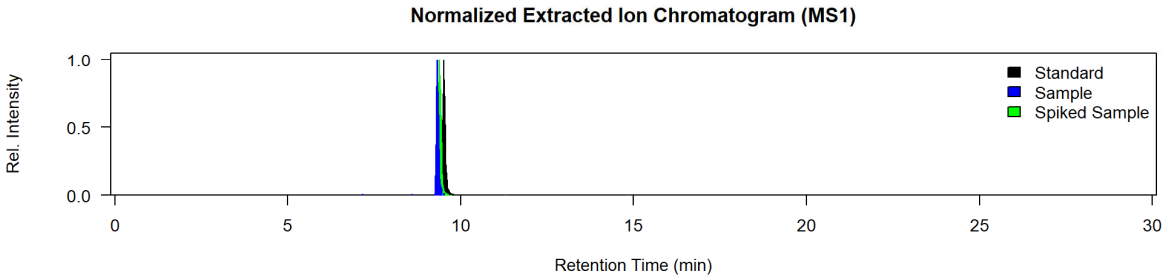

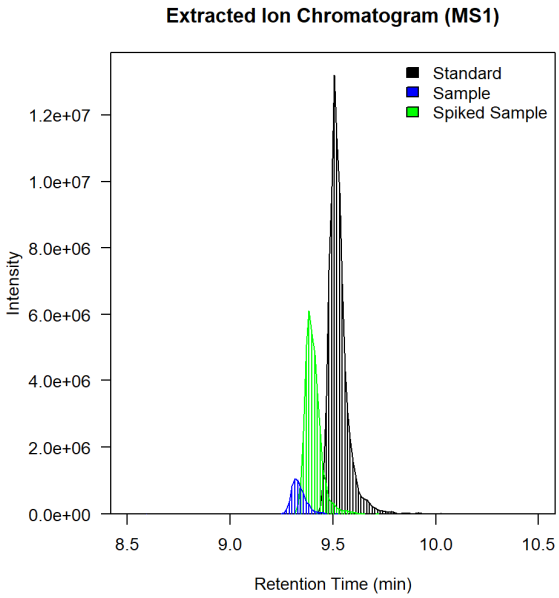

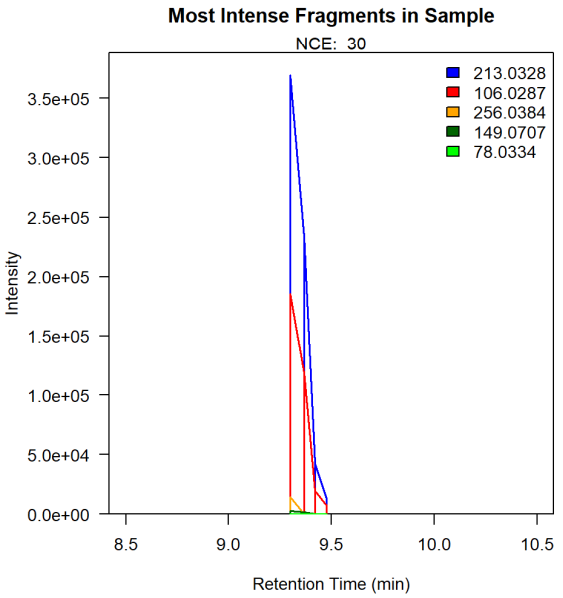

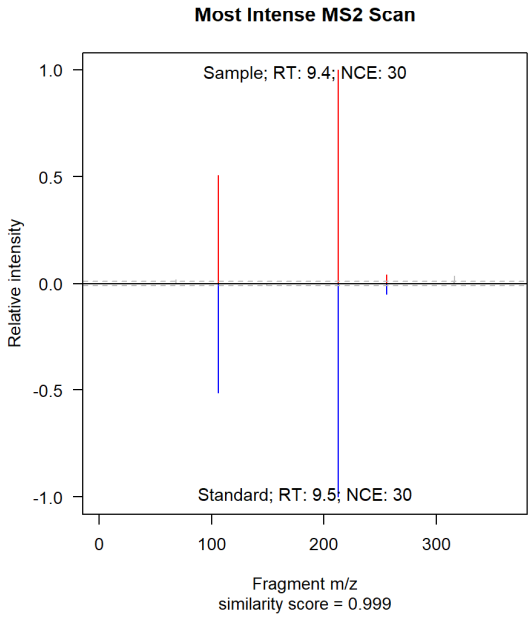

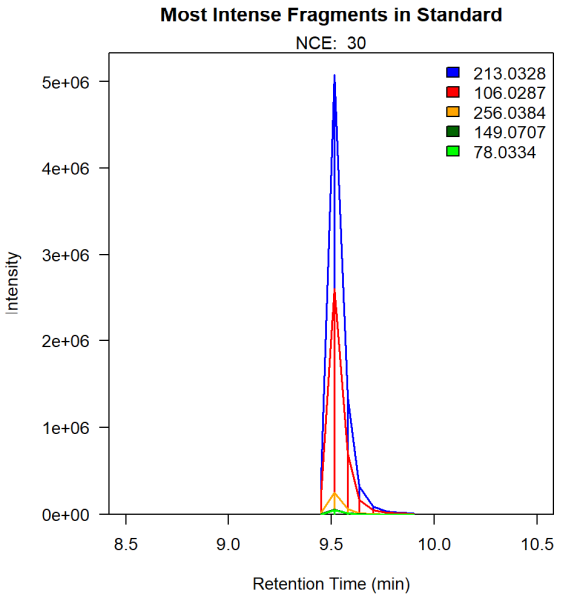

Oxadixyl
Level 1
[M+H]+ 279.13393
(STD 25 ng/L)

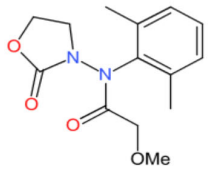

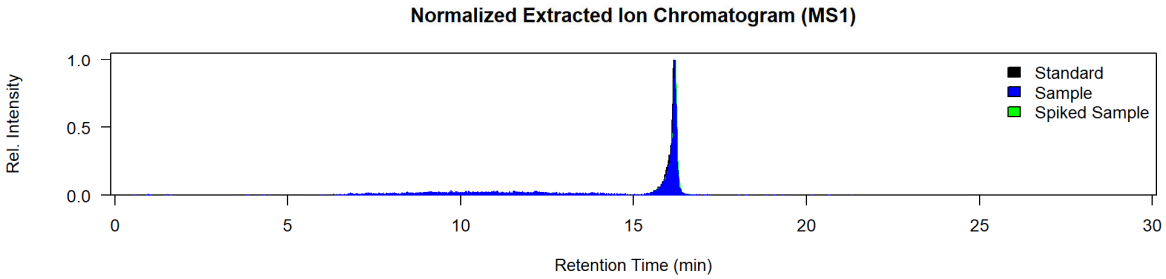

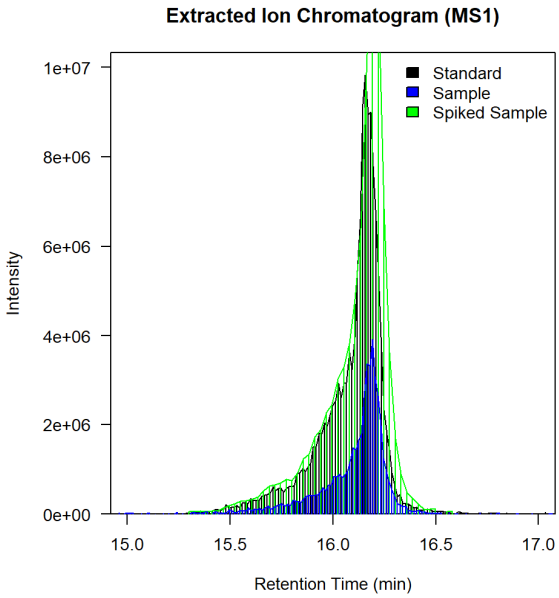

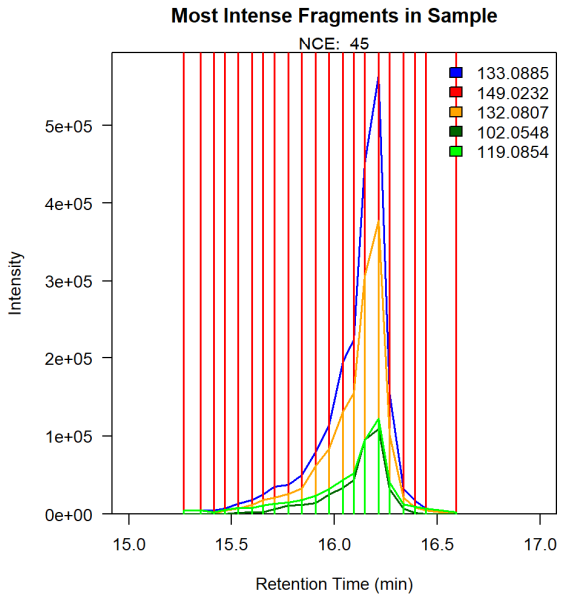

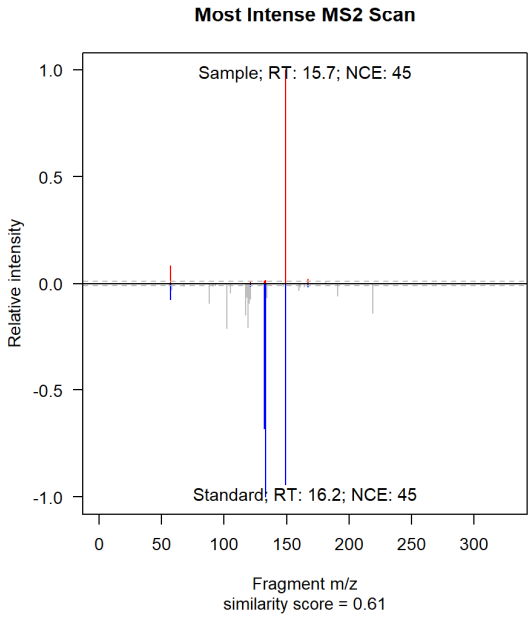

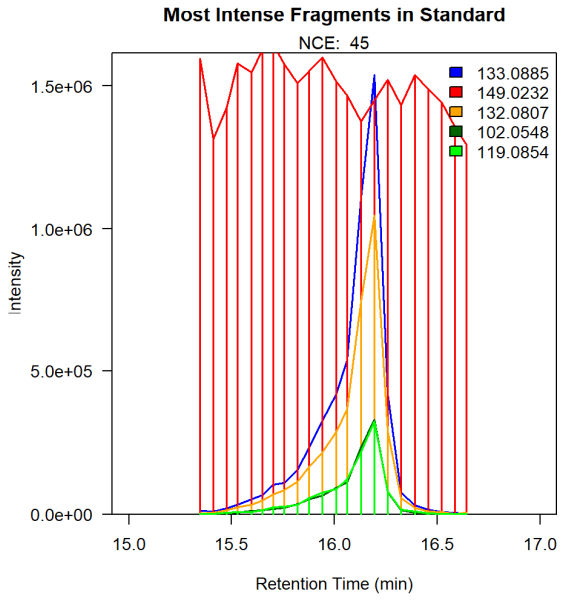

Pinoxaden-TP NOA 407854
Level 1
[M+H]+ 317.18597
(STD 25 ng/L)

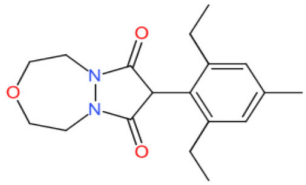

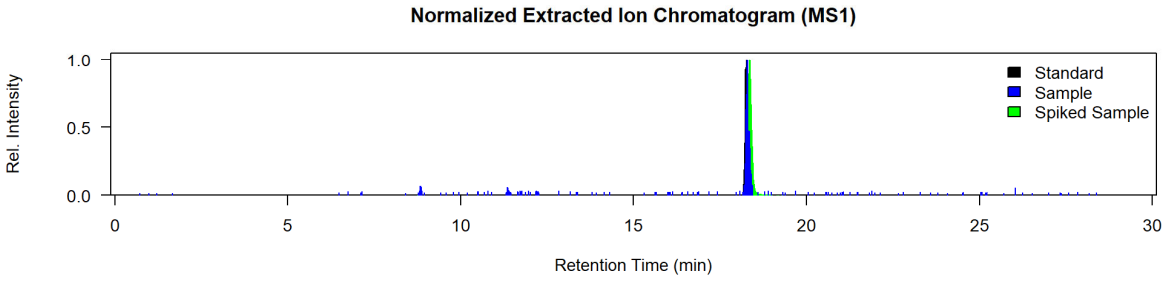

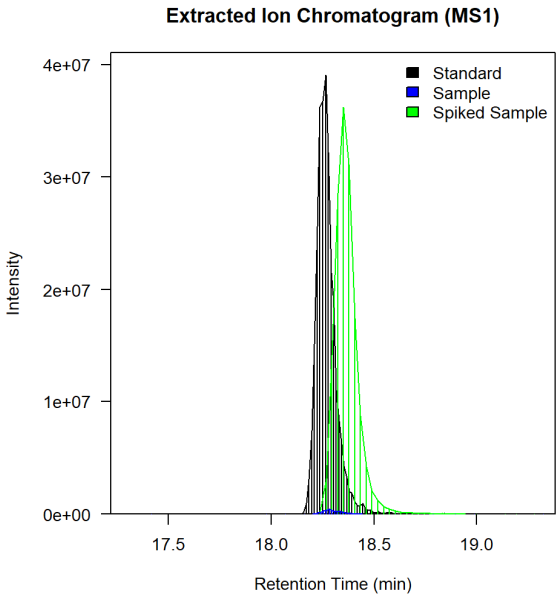

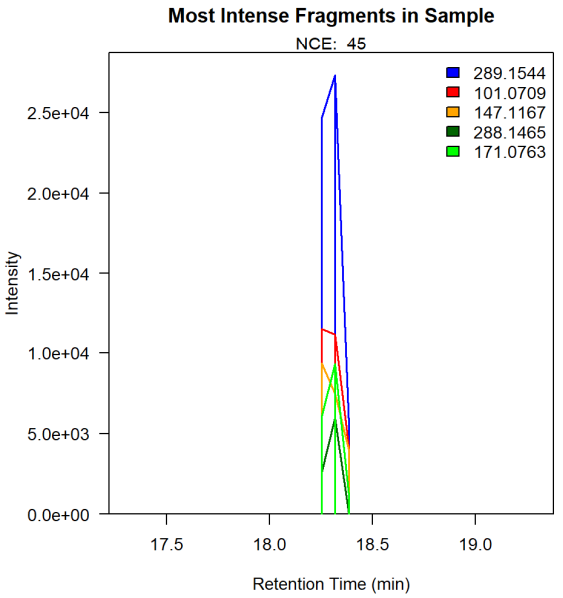

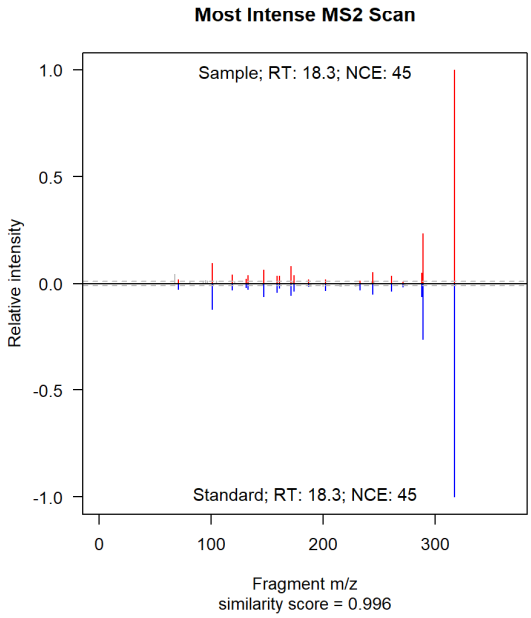

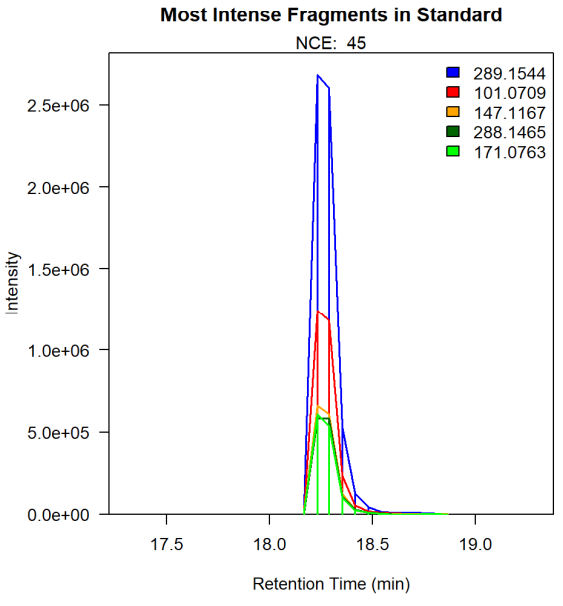

Terbuthylazine-TP CSAA036479
Level 1
[M+H]+ 214.09347
(STD 25 ng/L)

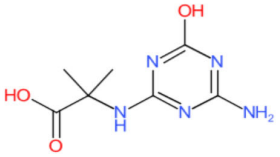

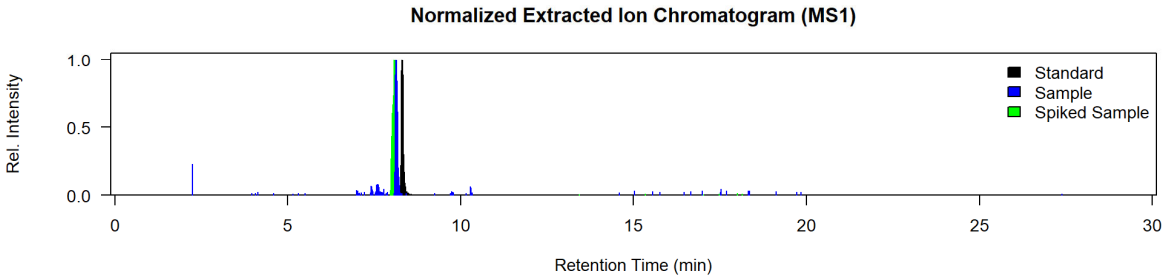

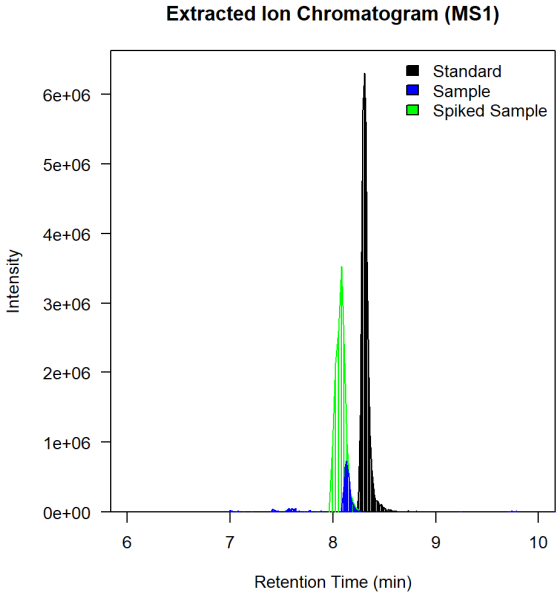

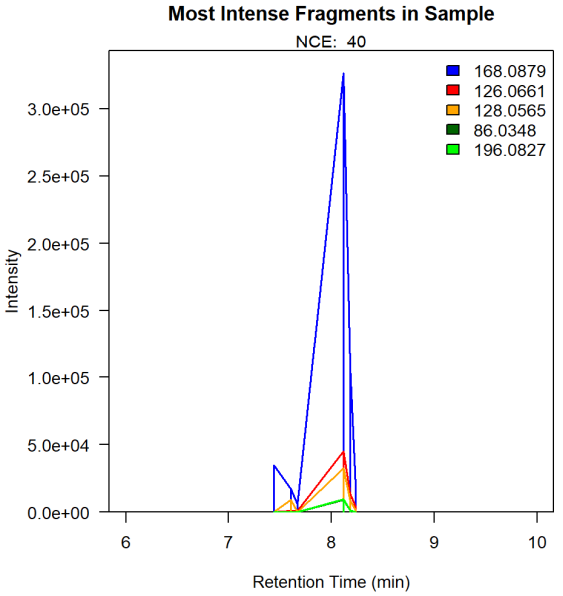

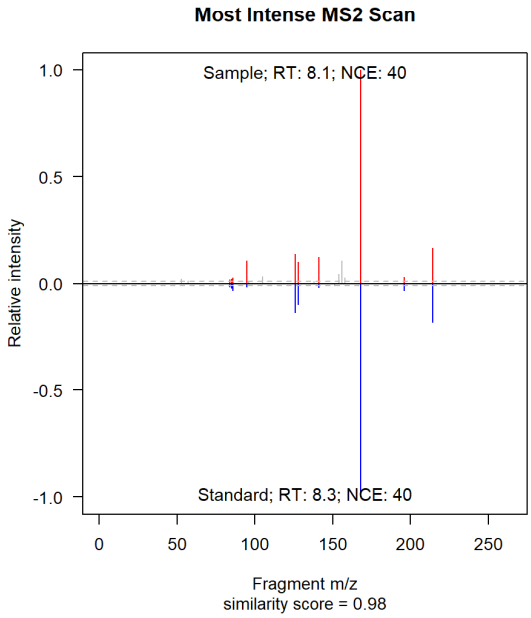

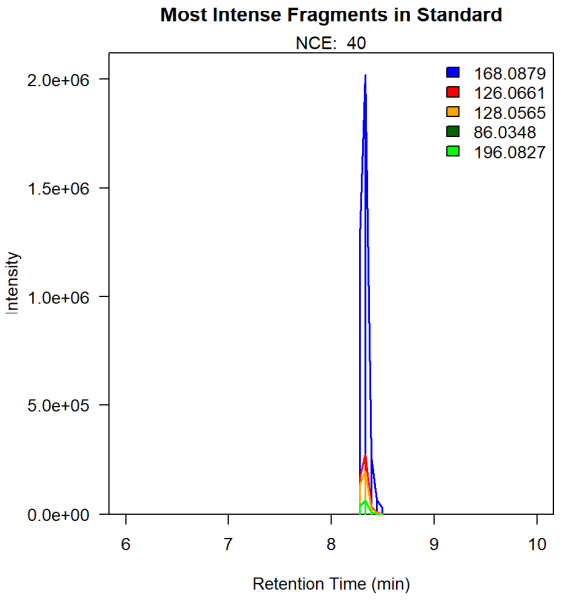

Terbuthylazine-TP CSCD648241
Level 1
[M+H]+ 199.11895
(STD 100 ng/L)

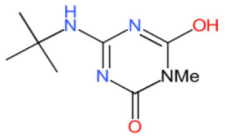

Normalized Extracted Ion Chromatogram (MS1)

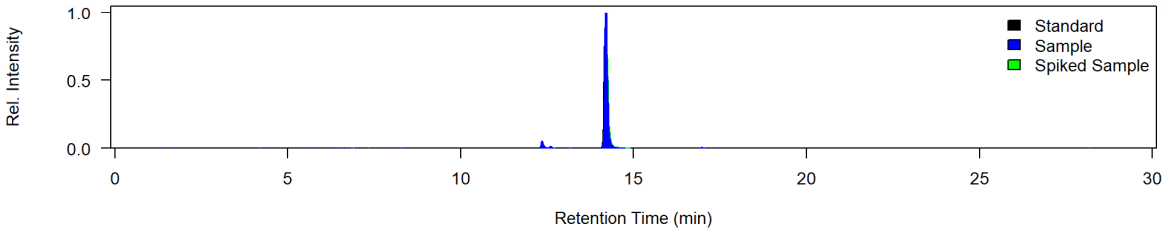

Extracted Ion Chromatogram (MS1)

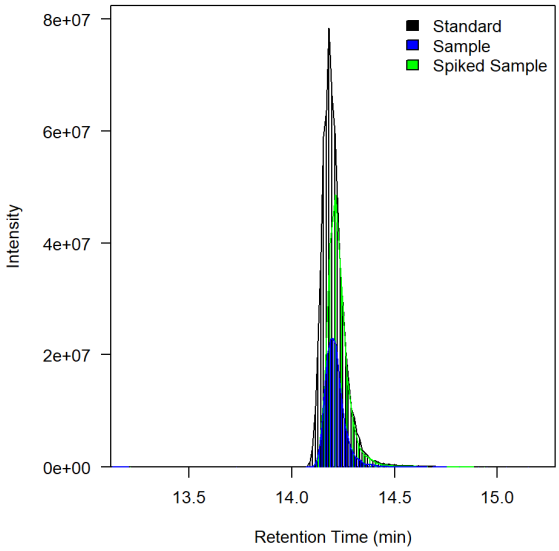

Most Intense Fragments in Sample

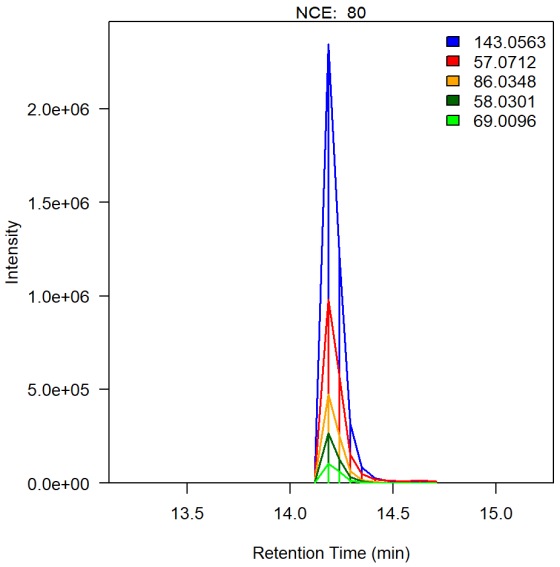

Most Intense MS2 Scan

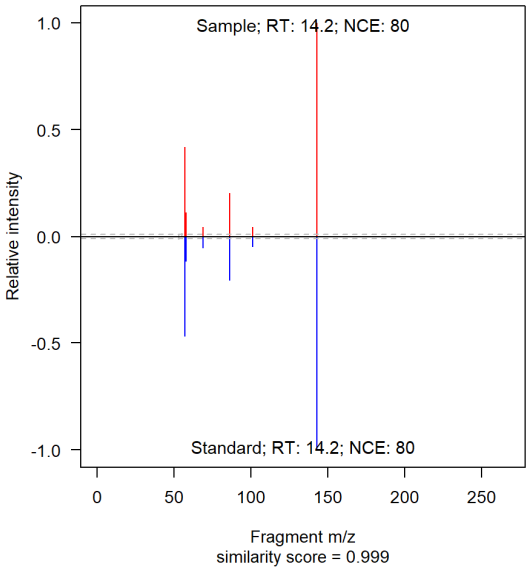

Most Intense Fragments in Standard

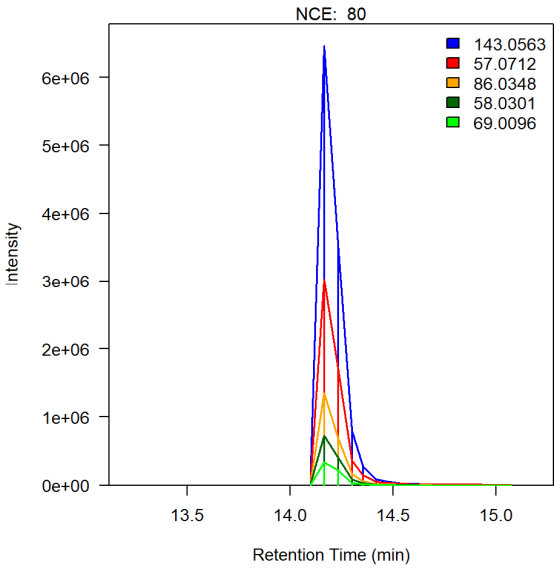

Terbuthylazine-TP CSCD692760
Level 1
[M+H]+ 199.08257
(STD 25 ng/L)

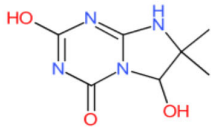

Normalized Extracted Ion Chromatogram (MS1)

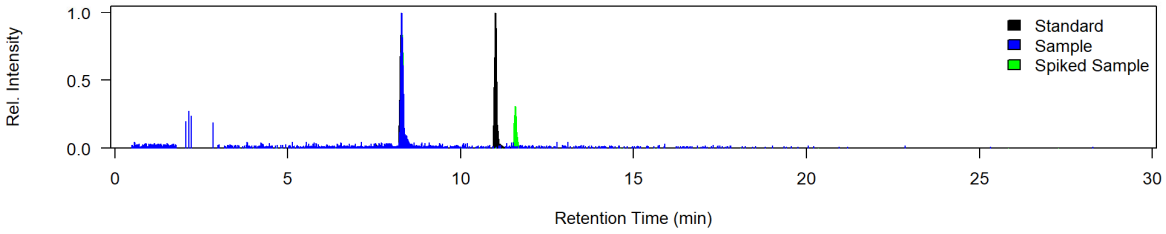

Extracted Ion Chromatogram (MS1)

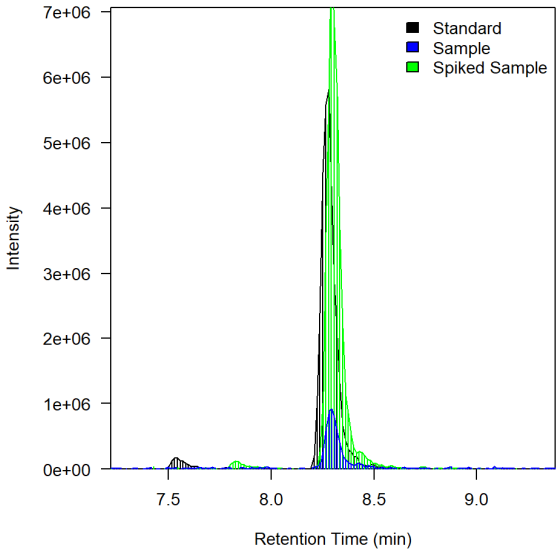

Most Intense Fragments in Sample

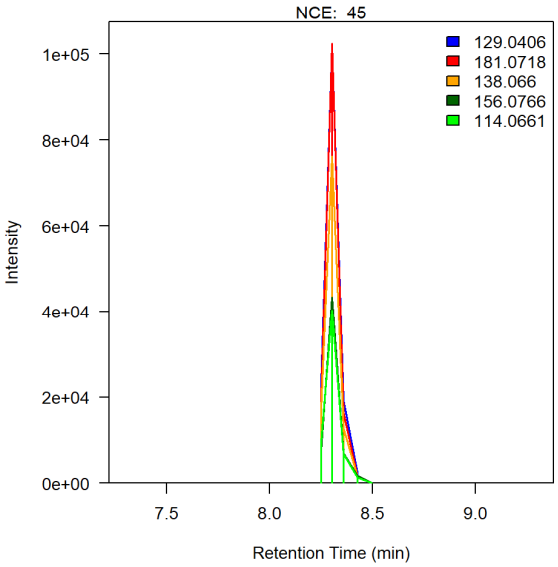

Most Intense MS2 Scan

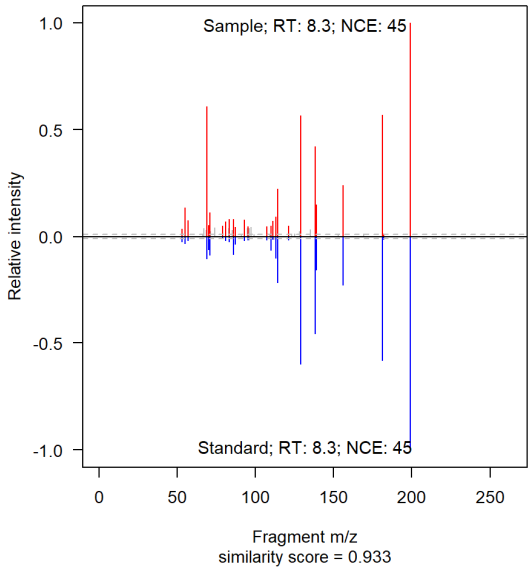

Most Intense Fragments in Standard

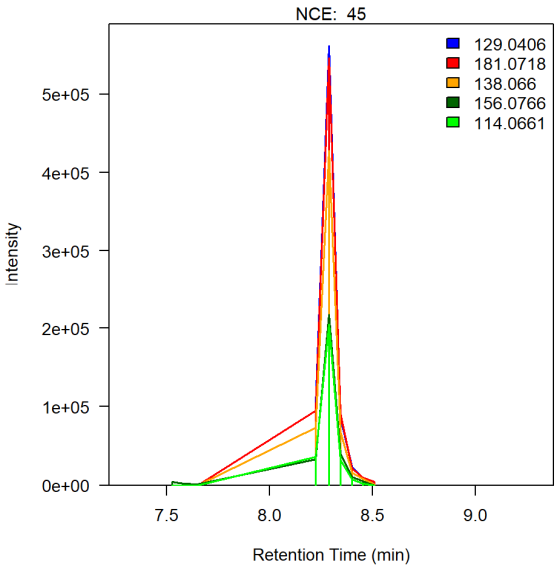

Terbuthylazine-TP MT23_GS16984
Level 1
[M+H]+ 185.1033
(STD 25 ng/L)

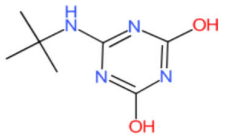

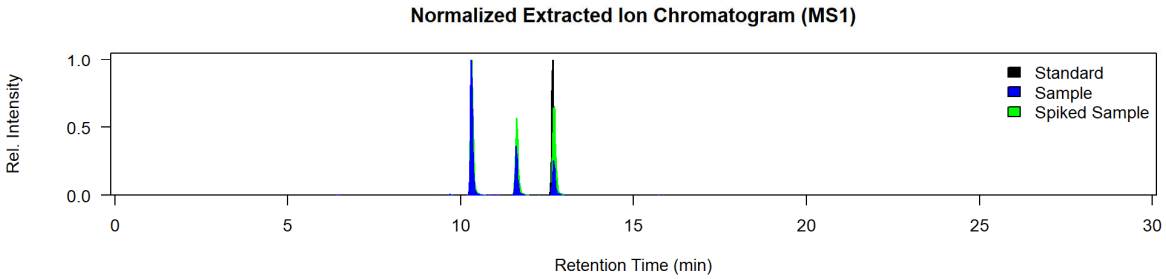

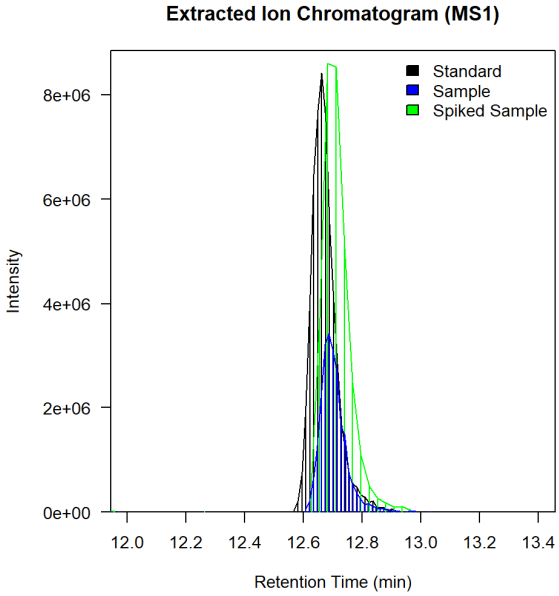

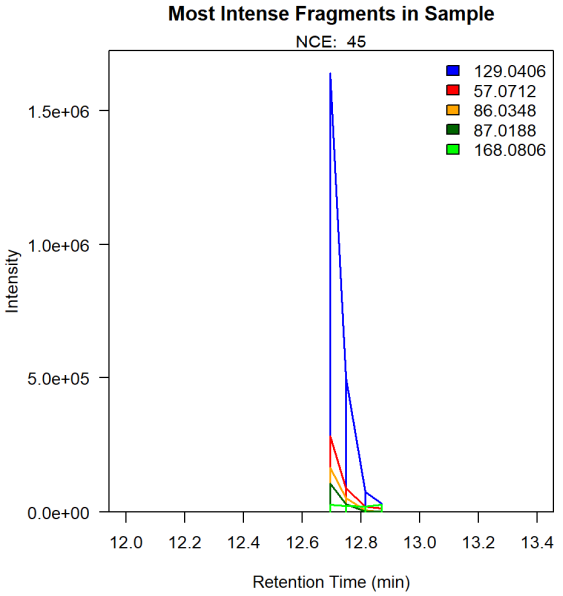

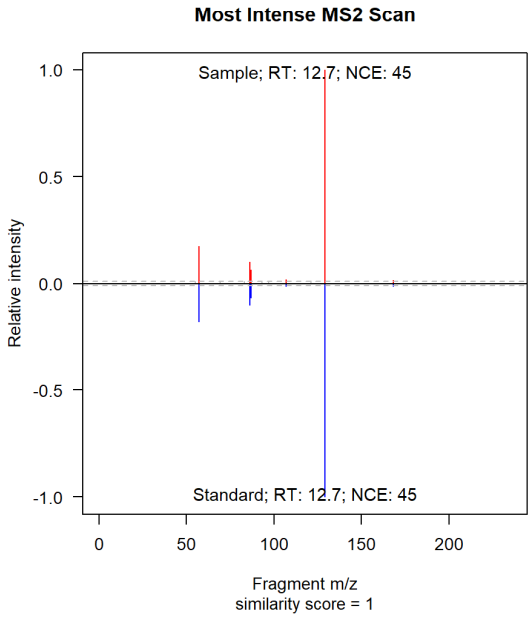

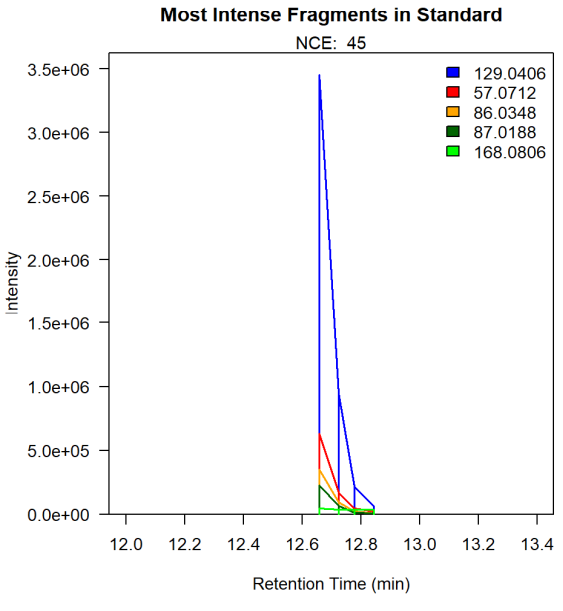

Cymoxanil-TP IN-JX915 / U3204
Level 3
[M+H]+ 199.08257
(STD 50 ng/L)

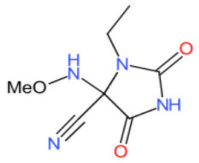

Normalized Extracted Ion Chromatogram (MS1)

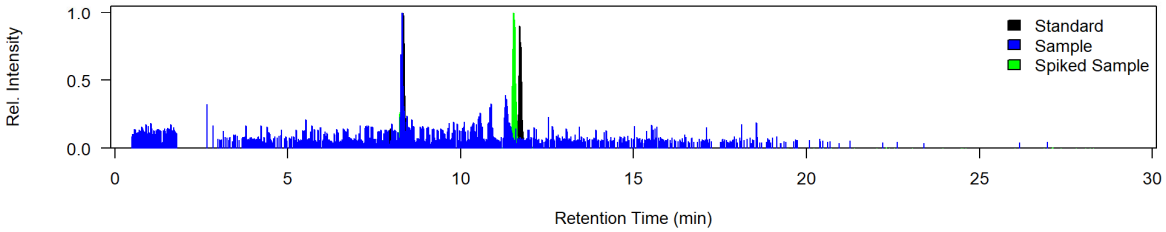

Extracted Ion Chromatogram (MS1)

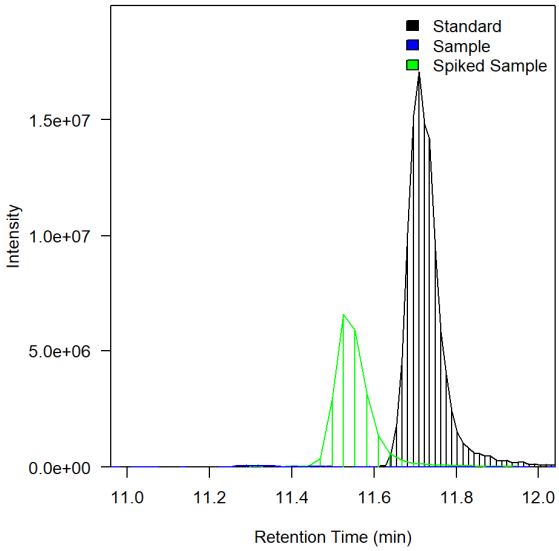

Most Intense Fragments in Sample

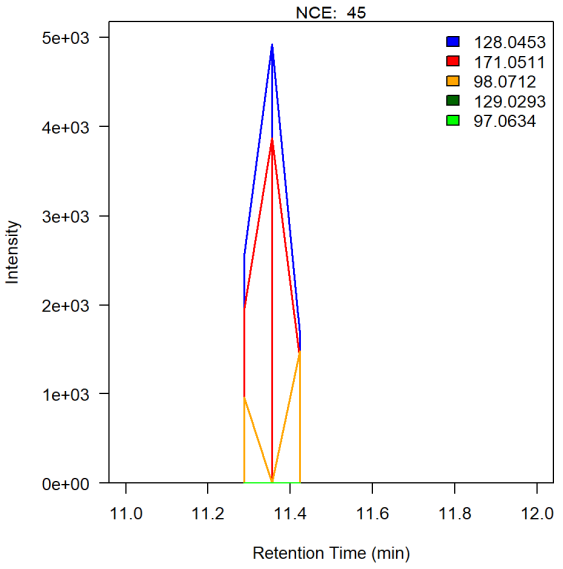

Most Intense MS2 Scan

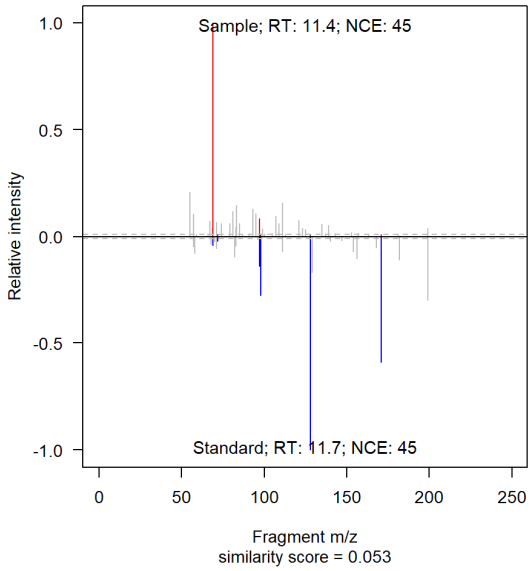

Most Intense Fragments in Standard

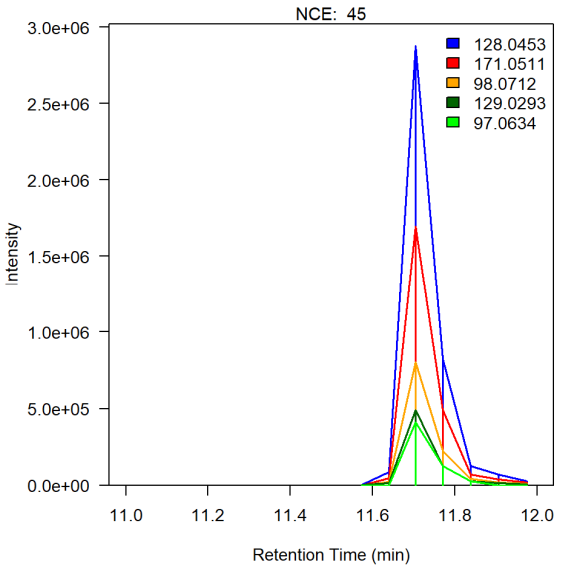

Chlorotoluron-TP CGA 15140
Level 2a
[M-H]- 241.038543

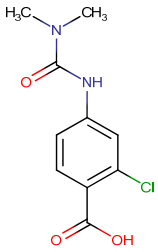

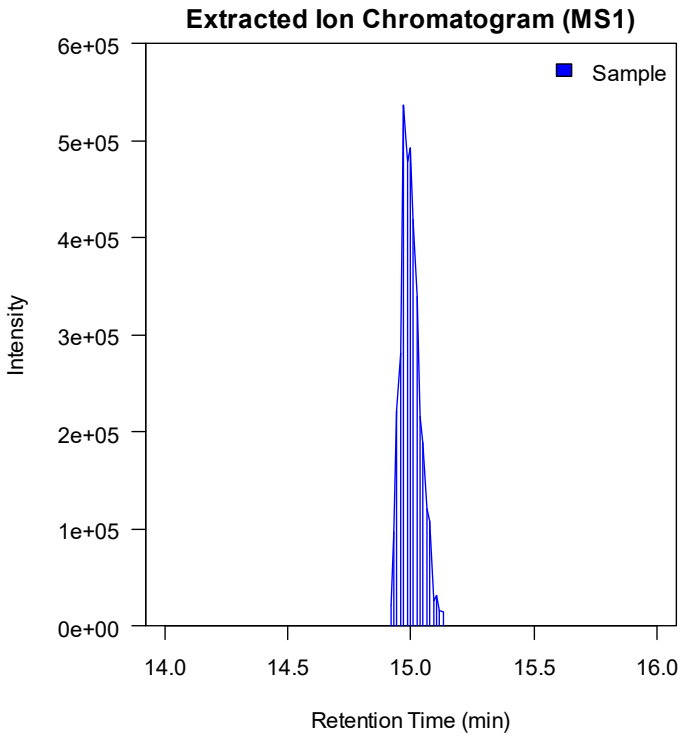

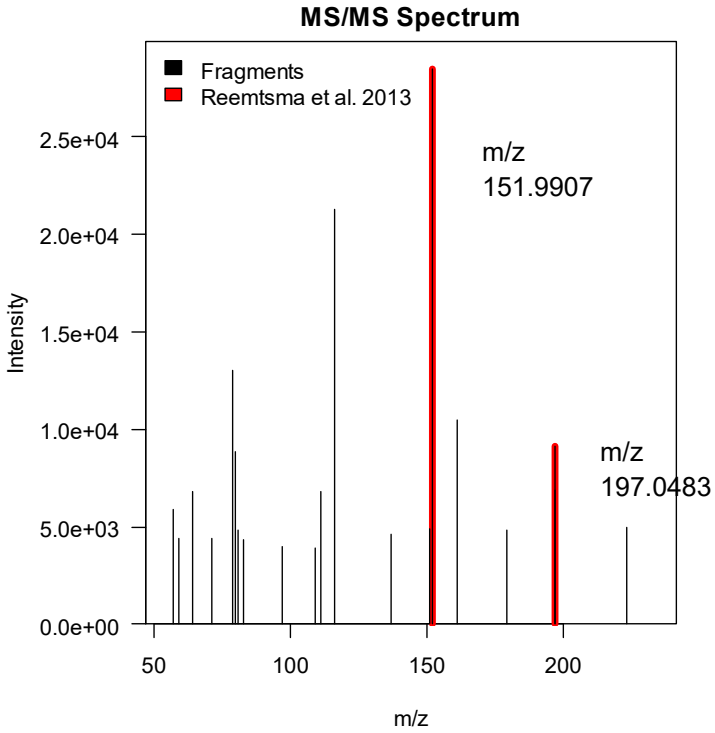

Fipronil-TP RPA 106681
Level 2b
[M-H]- 469.920924
Standard RPA 200761

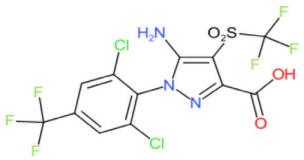

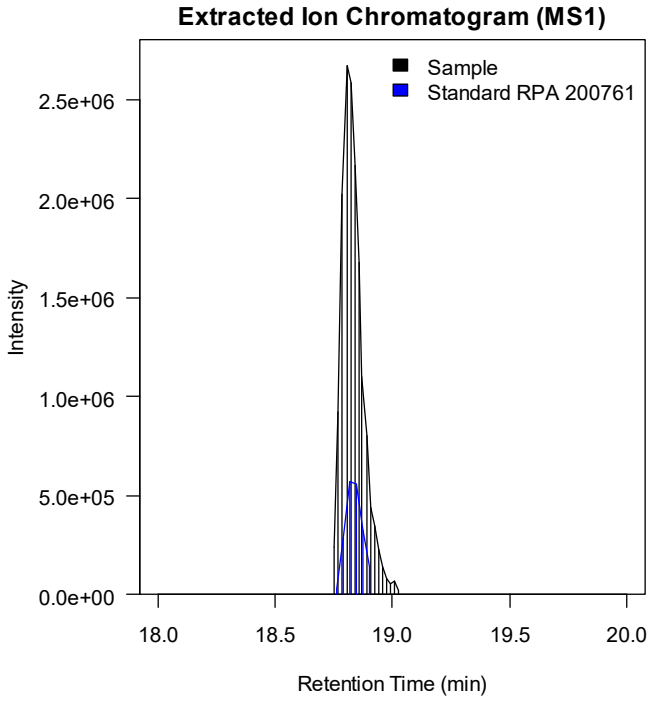

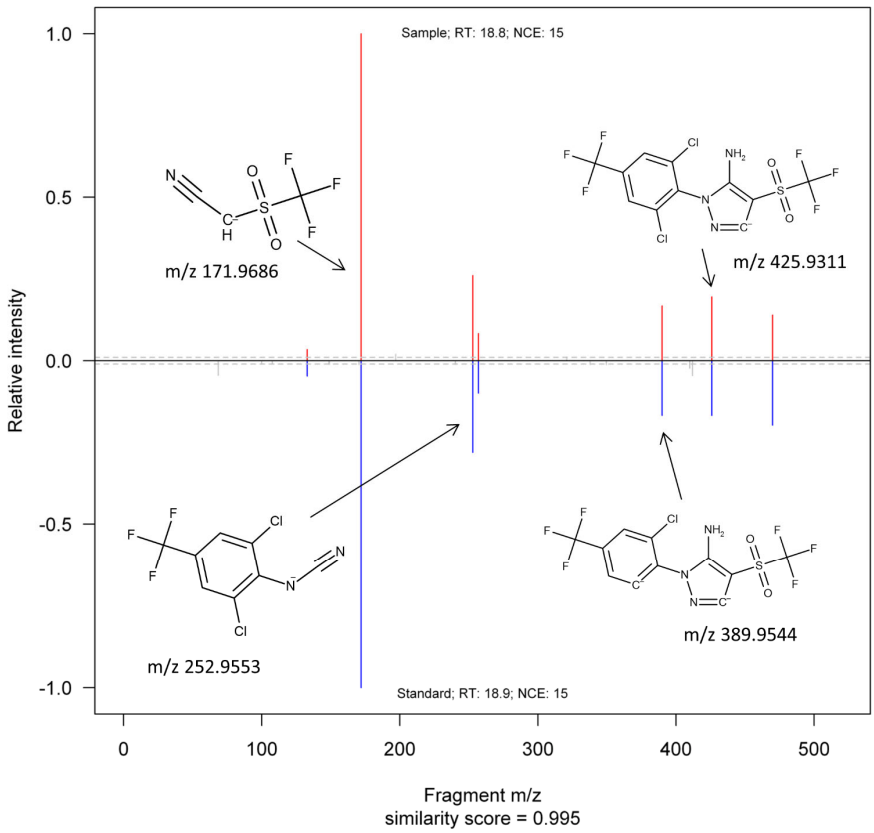

Cymoxanil-TP IN-JX915 / U3204
Level 3
[M+H]+ 199.08257
(STD 50 ng/L)

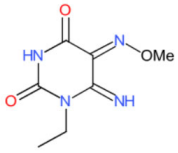

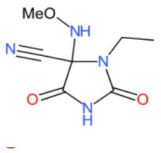

Normalized Extracted Ion Chromatogram (MS1)

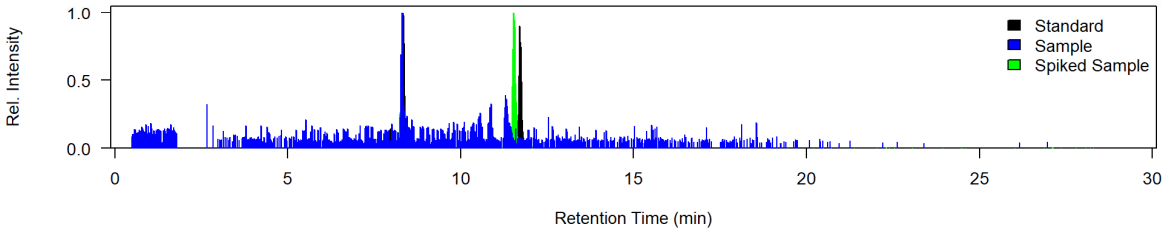

Extracted Ion Chromatogram (MS1)

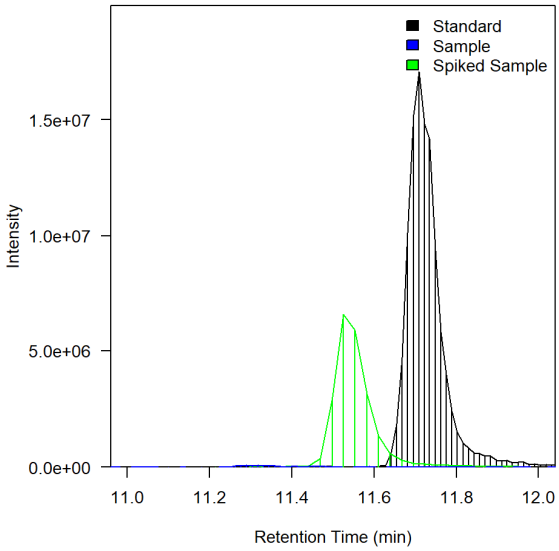

Most Intense Fragments in Sample

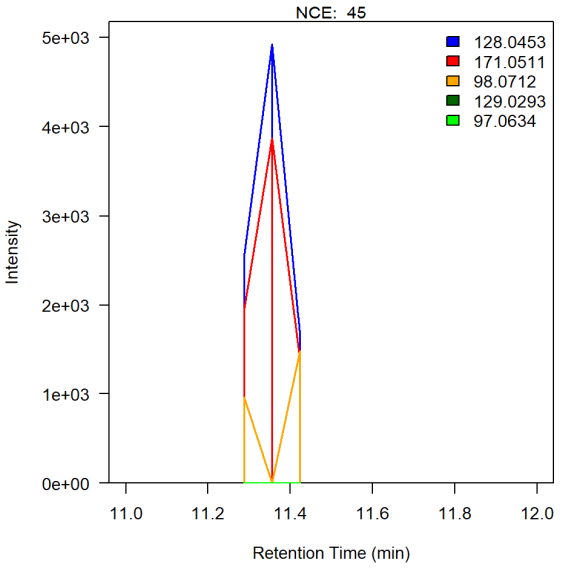

Most Intense MS2 Scan

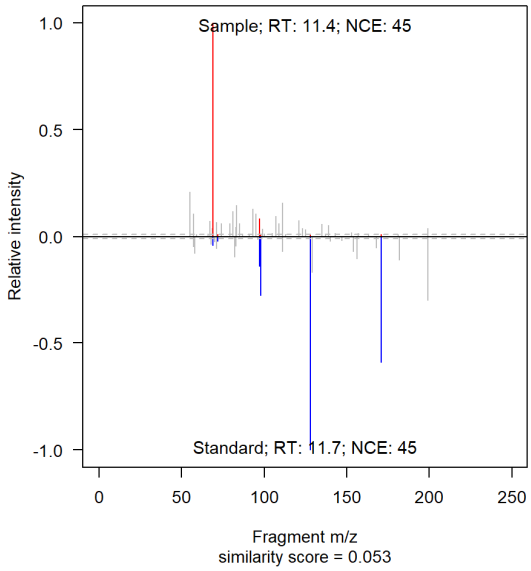

Most Intense Fragments in Standard

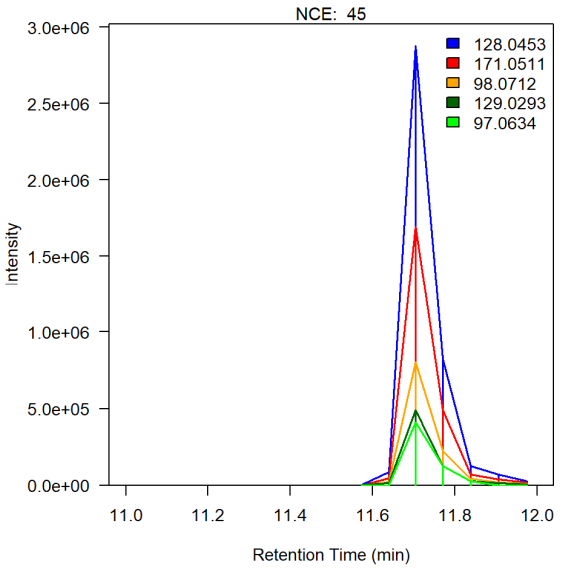

Chlorothalonil-TPs 4-carbamoyl-2,3,5-trichloro-6-cyanobenzenesulfonic acid /2-carbamoyl-3,4,5-trichloro-6-cyanobenzenesulfonic acid
Level 3
[M-H]- 326.88063

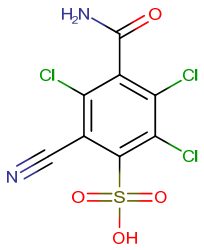

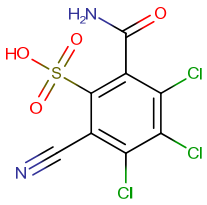

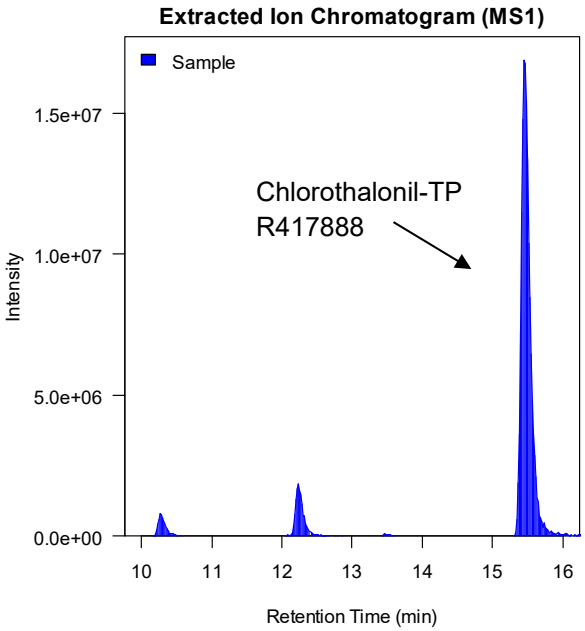

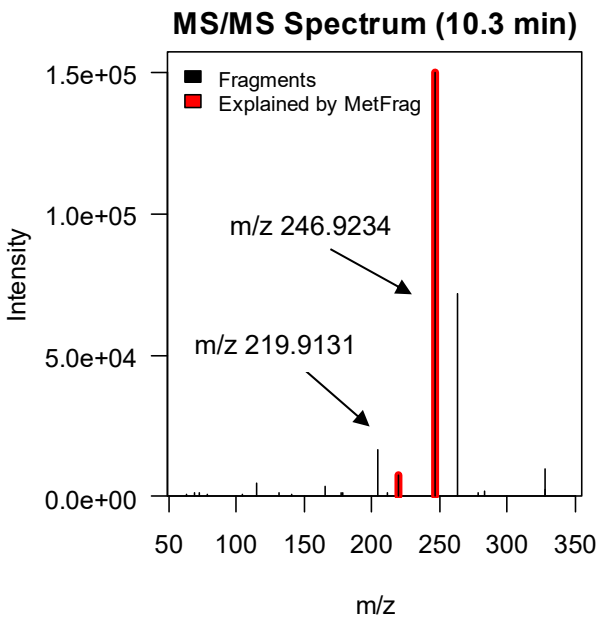

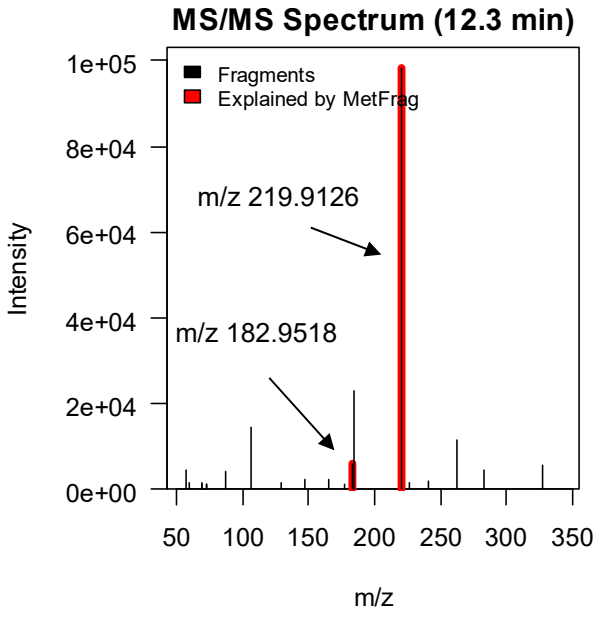

Asulam-TP Sulfanilamide
Unclear
[M+NH4]+ 190.06447
STD 25 ng/L

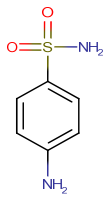

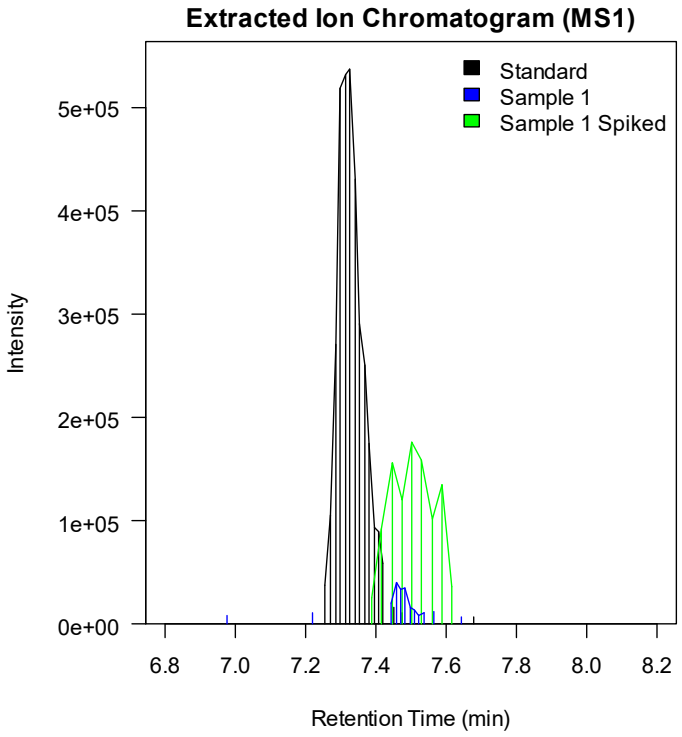

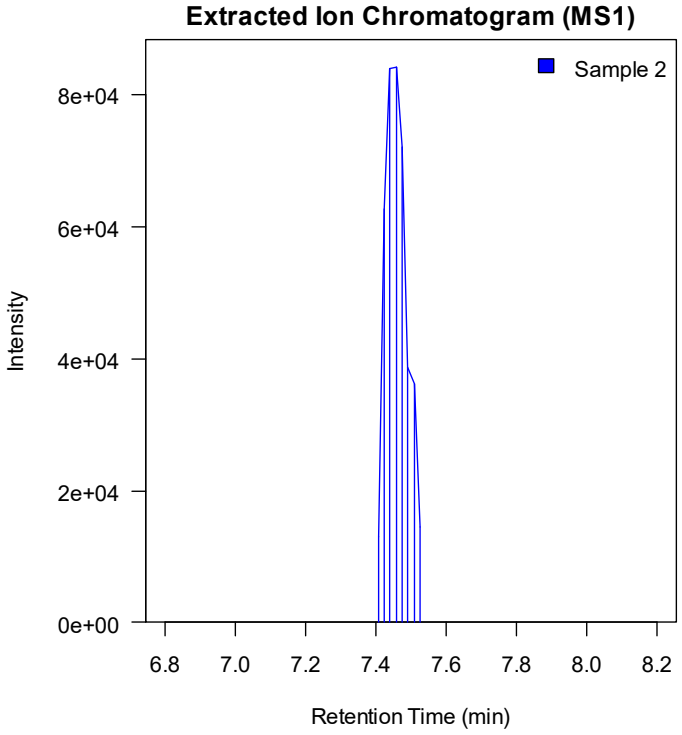

Remark: Sample 2 was not measured in the same sequence as standard, sample 1 and sample 1 spiked.

Pymetrozine-TP CGA294849
Unclear
[M+H]+ 143.05635
STD 100 ng/L

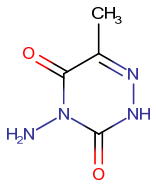

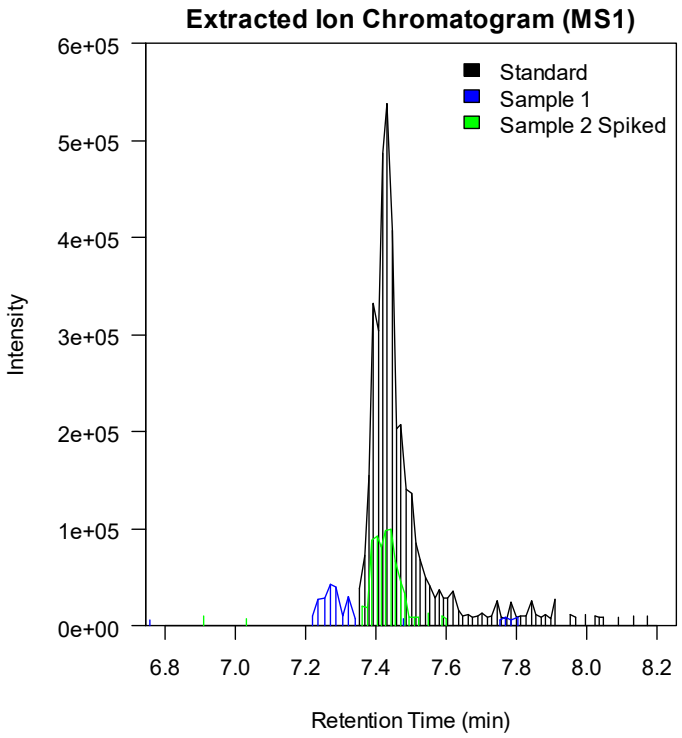

Remark: Sample 1 was not measured in the same sequence as standard & sample 2 spiked; no peak in sample 2.

Chapter 3: Identification of LC-HRMS Nontarget Signals in Groundwater After Source Related Prioritization

Karin Kiefer[1,2], Letian Du[1,2], Heinz Singer[1], Juliane Hollender[1,2]*

[1] Eawag, Swiss Federal Institute of Aquatic Science and Technology, 8600 Dübendorf, Switzerland

[2] Institute of Biogeochemistry and Pollutant Dynamics, ETH Zurich, 8092 Zurich, Switzerland

* Corresponding author: juliane.hollender@eawag.ch

Published in Water Research, DOI: 10.1016/j.watres.2021.116994.

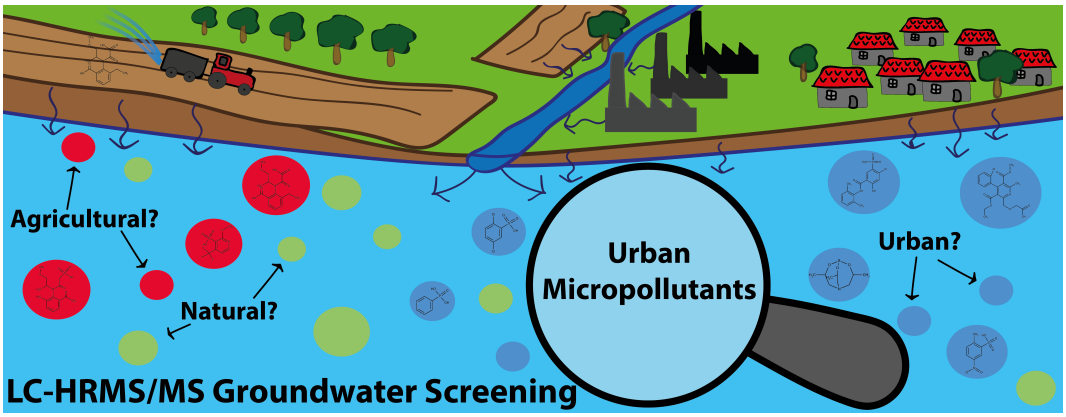

Abstract

Groundwater is a major drinking water resource but its quality with regard to organic micropollutants (MPs) is insufficiently assessed. Therefore, we aimed to investigate Swiss groundwater more comprehensively using liquid chromatography high-resolution tandem mass spectrometry (LC-HRMS/MS). First, samples from 60 sites were classified as having high or low urban or agricultural influence based on 498 target compounds associated with either urban or agricultural sources. Second, all LC-HRMS signals were related to their potential origin (urban, urban and agricultural, agricultural, or not classifiable) based on their occurrence and intensity in the classified samples. A considerable fraction of estimated concentrations associated with urban and/or agricultural sources could not be explained by the 139 detected targets. The most intense nontarget signals were automatically annotated with structure proposals using MetFrag and SIRIUS4/CSI:FingerID with a list of >988,000 compounds. Additionally, suspect screening was performed for 1162 compounds with predicted high groundwater mobility from primarily urban sources. Finally, 12 nontargets and 11 suspects were identified unequivocally (Level 1), while 17 further compounds were tentatively identified (Level 2a/3). Among these were 13 pollutants thus far not reported in groundwater, such as: the industrial chemicals 2,5-dichlorobenzenesulfonic acid (19 detections, up to 100 ng L^{-1}), phenylphosponic acid (10 detections, up to 50 ng L^{-1}), triisopropanolamine borate (2 detections, up to 40 ng L^{-1}), O-des[2-aminoethyl]-O-carboxymethyl dehydroamlodipine, a transformation product (TP) of the blood pressure regulator amlodipine (17 detections), and the TP SYN542490 of the herbicide metolachlor (Level 3, 33 detections, estimated concentrations up to 100-500 ng L^{-1}). One monitoring site was far more contaminated than other sites based on estimated total concentrations of potential MPs, which was supported by the elucidation of site-specific nontarget signals such as the carcinogen chlorendic acid, and various naphthalenedisulfonic acids. Many compounds remained unknown, but overall, source related prioritisation proved an effective approach to support identification of compounds in groundwater.

Keywords

Target screening, nontarget screening, micropollutant, persistent and mobile compounds, PMOC, AcquireX

3.1 Introduction

Groundwater is a major drinking water resource and therefore its quality is of high interest. Various micropollutants (MPs) from agriculture, households, or industry, entering aquifers via different pathways, affect groundwater quality (Loos et al. 2010). Whereas pesticides are applied in high amounts to agricultural soils (Pimentel 2009) and then enter aquifers mainly via seepage, pharmaceuticals, household and industrial chemicals may contaminate aquifers predominantly via leaky sewers (Wolf et al. 2012) or via bank filtration from wastewater impacted surface waters (Heberer et al. 2004). Consequently, the land use in the catchment and/or hydrogeological setting (e.g. bank filtration, characteristics of top layers) influence the MP pattern at the groundwater monitoring site (Stuart et al. 2014, Ter Laak et al. 2012). Given that (i) >350,000 chemicals, and mixtures thereof, are registered in national and regional inventories (Wang et al. 2020), (ii) compounds undergo transformations in the environment and engineered systems (Kolpin et al. 2009), and (iii) "new" MPs are regularly reported to be in the water cycle, e.g. Weber et al. (2007), Schmidt and Brauch (2008), Reemtsma et al. (2013), Schlüsener et al. (2015), Zahn et al. (2016), Gago-Ferrero et al. (2018), Schulze et al. (2019), or Zahn et al. (2019), it seems insufficient to evaluate water quality only on the basis of selected analytes.

Liquid chromatography high-resolution tandem mass spectrometry (LC-HRMS/MS) enables the detection of possibly thousands of small molecules in a water sample, both from natural and anthropogenic sources. Some of these compounds can be elucidated by broad-scope target screening where reference standards are available in the laboratory, while others are detected as part of suspect screening, i.e. searching for specific structures without having reference material at hand (Krauss et al. 2010). However, usually most LC-HRMS/MS signals remain unknown (so-called nontargets), and should therefore be further investigated. Spectral libraries such as the European MassBank (Horai et al. 2010), MassBank of North America (MoNA; http://mona.fiehnlab.ucdavis.edu/), and mzCloud (www.mzcloud.org) allow structural annotation of nontarget signals with high confidence level (Schymanski et al. 2014b), though their use is limited to compounds for which MS/MS spectra were made accessible by other laboratories. For compounds not present in spectral libraries, in silico fragmentation tools, e.g. MetFrag (Ruttkies et al. 2016), SIRIUS4/CSI:FingerID (Dührkop et al. 2015, Dührkop et al. 2019), and CFM-ID (Allen et al. 2014), in combination with large chemical compound databases such as PubChem (Kim et al. 2019), CompTox Chemistry Dashboard (Williams et al. 2017), or the NORMAN Suspect List Exchange (www.norman-network.com/nds/SLE) are promising alternatives for structural annotation. These tools enable the high-throughput annotation of thousands of nontargets, however, with often hundreds or even thousands of candidates. Thus, the final identification with reference material remains a major bottleneck so that so far only few nontargets have been elucidated with high confidence in water samples (Albergamo et al. 2019, Gago-Ferrero et al. 2015, Schymanski et al. 2014a, Tian et al. 2020).

As a consequence, nontargets of interest need to be prioritized before investing time and resources into structure elucidation or even purchasing reference material, using one or a combination of several approaches depending on the study context. Most studies apply filters for analytical quality control, e.g. excluding compounds detected in procedural blanks and including only compounds with high reproducibility in replicate and pooled samples (Broadhurst et al. 2018, Sangster et al. 2006). The use of pooled samples (i.e. samples comprising aliquots of all samples) is more common in metabolomics than in environmental studies. Intensity is a

crucial parameter in most studies (Hug et al. 2014, Schymanski et al. 2014a), as intense signals may provide higher-quality MS/MS data supporting elucidation. Additionally, intensity correlates to some extent with concentration, though it is important to highlight that high intensity or concentration does not necessarily mean high toxicological risk. Furthermore, Cl and Br isotope patterns may point to compounds from anthropogenic origins (Chiaia-Hernandez et al. 2014, Hug et al. 2014) and homologues to larger groups of related compounds such as surfactants (Schymanski et al. 2014a). Comparing related samples such as raw water and final drinking water (Müller et al. 2011) or road dust and surface water (Seiwert et al. 2020) facilitate prioritization of persistent signals originating from a specific source. In this regard, multivariate statistical tools such as principal component analysis and hierarchical clustering can be applied, for example to samples collected along a wastewater treatment plant (Schollée et al. 2015, Schollée et al. 2018) or a riverbank transect (Albergamo et al. 2019), to determine nontargets with specific trends.

The goal of this study was to comprehensively evaluate the quality of water derived from 60 groundwater monitoring sites in Switzerland. To do so, all detected LC-HRMS signals were to be related to their potential sources (urban, agricultural), followed by structural elucidation of the most prominent ones, focusing in particular on potential MPs from urban sources. Our hypothesis was that by combining an appropriate nontarget prioritization strategy with a highly automated structure elucidation workflow, we would find previously unreported compounds in groundwater. First, we performed an extensive target screening for 498 MPs to classify the samples according to their dominating urban and agricultural pollutants. Next, all LC-HRMS signals were classified based on their pre-dominating occurrence in urban or agricultural sources, which was assessed by comparing samples with high vs. low urban or high vs. low agricultural influence. Structure elucidation focused on nontargets from potentially urban sources because we investigated already in detail major agricultural MPs, i.e. pesticides and their transformation products (TPs), in a similar sample set (Kiefer et al. 2019). Accordingly, most intense nontargets from potentially urban sources and, in addition widespread nontargets, were annotated with candidate proposals using MetFrag and SIRIUS4/CSI:FingerID and finally elucidated with reference standards, if commercially available. To not overlook important urban MPs with lower signal intensity, we applied additionally a suspect screening for 1162 polar, and therefore mobile, compounds from mainly urban sources.

3.2 Methods

3.2.1 Groundwater Samples

The applied nontarget screening approach aimed to classify nontargets with regards to their origin (urban, agricultural), based on their occurrence at monitoring sites that are i) urban impacted, ii) agriculturally impacted, or iii) show only low anthropogenic impact. Therefore, 60 monitoring sites (44 abstraction wells, 16 springs) were selected out of >500 sites from the Swiss National Groundwater Monitoring NAQUA (www.bafu.admin.ch/naqua) based on long-term monitoring data collected within NAQUA. Twenty sites contained MPs from pre-dominantly urban sources (pharmaceuticals, sweeteners), while 20 other sites showed high frequency or concentrations of MPs from agricultural sources (pesticides and their TPs). A further 20 sites exhibited comparably low anthropogenic contamination. Several sites were not clearly

classifiable as urban- or agriculturally–impacted due to the occurrence of pollutants from both source types.

The 60 groundwater samples were collected in laboratory glass bottles (previously annealed at 500 °C; 1 L bottles, SIMAX Kavalier, Czech Republic) in May and August 2018 within the routine sampling of NAQUA. Samples were stored cooled for up to four weeks and then frozen at -20 °C until measurement. For quality control, pooled samples were prepared, i.e. samples consisting of an equal amount of each sample. For this, aliquots (5 or 10 mL) of each groundwater sample were transferred to laboratory glass bottles (0.5 L or 1 L) using a 5 mL brown glass vial before samples were frozen. To determine contaminations from sampling, sample storage or handling, ultrapure water (>18 MΩcm, Barnstead Nanopure Diamond system) was filled into laboratory glass bottles, transferred during sampling into another bottle (at five monitoring sites), and then stored and processed analogously to the groundwater samples as blank samples.

3.2.2 Sample Preparation via Vacuum-Assisted Evaporation

To avoid losses of polar compounds during sample enrichment, samples were concentrated via vacuum-assisted evaporation, analogously to Mechelke et al. (2019) though with slight modifications. Samples were transferred to BÜCHI glass vials (1 mL appendix, previously annealed at 450 °C) at a volume of 120 mL and spiked with 35 isotope-labelled internal standards at 100 ng L^{-1}. Samples were evaporated on a Syncore® Analyst (BÜCHI, Switzerland) for 7-8 hours to approximately 1 mL at 20 mbar and 45 °C (appendix cooled at 7-10 °C) using the back-flush unit. The concentrate volume was adjusted to 1.6 mL by adding ultrapure water using annealed glass Pasteur pipettes (747715, Brand GmbH, Germany). The BÜCHI vials were rinsed thoroughly with the concentrate to reduce analyte losses due to sorption. Finally, the concentrate was centrifuged at 3720 g (Heraeus Megafuge 1.0 R, Thermo Fisher Scientific, U.S.) in annealed vials and transferred to 1.5 mL vials (previously annealed at 500 °C; vials: 080400-XL; screw caps: 090301; BGB Analytik, Switzerland). Analogously to the samples, four calibration standards (1, 10, 100, 1000 ng L^{-1} in ultrapure water), four spiked samples (1, 10, 100, 250 ng L^{-1}), six pooled samples (i.e. replicates) and seven field and laboratory blank samples (ultrapure water spiked with internal standards) were prepared for quality control and target quantification. For details on spike solutions, see SI3-A1.

3.2.3 LC-HRMS/MS Analysis

Samples were measured in triplicate in a randomized order. After nine sample injections (three triplicates), a blank was injected, followed by a pooled sample for quality control. The concentrated samples (140 µL, i.e. 10.5 mL of the original sample) were injected to a LC system consisting of a PAL RTC autosampler (CTC Analytics, Switzerland), a reversed phase C18 column (Atlantis T3, 3 µm, 3 × 150 mm; Waters, Ireland), and a Dionex UltiMate 3000 RS pump (Thermo Fisher Scientific RS). The gradient elution started with 100% water (containing 0.1% formic acid) to achieve an optimal retention of polar compounds. Then, methanol (containing 0.1% formic acid) was added and increased to 95% from 1.5 to 18.5 min, and finally kept constant for 10 min. The flow rate was 0.3 mL min^{-1}. For details, see Table SI3-A1.

Analytes were ionized in electrospray (3.5/-2.5 kV) and detected on an Orbitrap mass spectrometer (Fusion Lumos, Thermo Fisher Scientific, U.S.) with a resolution R of 240,000 (at m/z 200, full width at half maximum (FWHM)) in MS1 full-scan mode (m/z 100-1000), followed by three to four data-dependent MS/MS full-scans (high-resolution product scans; R 30,000 FWHM at m/z 200; cycle time 1 s; isolation window of precursor 1 m/z). Internal calibration

(EASY-IC™) ensured a mass accuracy of <±2 ppm in MS1 scans for 99.8% of detected target compound peaks and internal standard peaks (<±1 ppm for 98.4% of peaks). AcquireX software (Deep Scan; Thermo Fisher Scientific, U.S.) was used to increase MS/MS coverage. In the first triplicate injection, data-dependent MS/MS full-scans were triggered based on a mass list containing target compounds. Then, AcquireX performed peak picking and added detected features (m/z and retention time) to the mass list so that in the second triplicate injection, data-dependent MS/MS full-scans were triggered based on the mass list modified by AcquireX. Before the third injection, AcquireX shifted features, for which MS/MS scans were already acquired during the second injection, from the mass to the exclusion list so that these features were not triggered again. If no features from the mass list were detected, the MS/MS scans for the most intense signals were acquired. Triggered features were excluded dynamically for 3 s. For details, see SI3-A2.

3.2.4 Target Screening

For each target compound, extracted ion chromatograms were plotted with the MSnbase R package (Gatto and Lilley 2012) and visually inspected. If the target compound was detected in groundwater samples, the concentration was determined using Trace Finder 4.1 (Thermo Fisher Scientific, U.S.) based on the peak area ratio of the target compound to that of corresponding internal standard. If no structurally identical isotope-labelled internal standard was available, an internal standard was selected with similar retention time as the analyte and resulting in a relative recovery close to 100% in the spiked samples using an in-house R script (Schollée 2018). For details on target quantification including determination of limit of quantification (LOQ), see SI3-A3.

3.2.5 Suspect and Nontarget Screening

Measurement files were converted to mzXML format using MSConvert 3.0, ProteoWizard (Chambers et al. 2012) and then processed in the enviMass workflow (envibee GmbH, Switzerland). Data post-processing was conducted in the R environment, version 3.6.3 (R Core Team 2020).

3.2.5.1 Data Pre-Processing

Data pre-processing was performed using the enviMass workflow (version 4.2633) including peak picking, mass recalibration, retention time alignment, intensity normalization based on median intensity of internal standards, replicate filtering, and target and suspect annotation. Features, i.e. chromatographic peaks defined by their m/z and retention time, that likely resulted from the same compound (adducts, isotopologues) were grouped into so called components based on intensity correlation and m/z distance. The most intense feature within a component was used for further data analysis. Settings (e.g. m/z and retention time tolerances) were optimized until 87% of target peaks (detected with Trace Finder 4.1, section 3.2.4) were found. 62% of target peaks that were not detected were <10 ng L^{-1} or exceeded the LOQ (section 3.2.4) by less than factor 5; other non-detects were mostly related to large retention time shifts (i.e. exceeding the retention time tolerance for targets) or poor peak shape. For final settings, see SI3-A4.

Finally, a table containing the peak height intensity pattern of each component across the samples (so-called profiles) was exported. Profiles were prioritized for further inspection by excluding those with a retention time <3 min, average sample/blank intensity ratio <5, and maximum peak intensity <10^6. For comparison, a peak height intensity of 10^6 corresponded to a

concentration of ≥10 ng L^{-1} for approximately 90% of targets ionizing in positive ionization mode and 35% of targets ionizing in negative ionization mode.

It should be noted that for some compounds several components might exist (e.g. positive and negative ionization, in-source fragments). Moreover, for some target compounds, two or three profiles were observed, often related to shifting retention times or peak picking artefacts. Therefore, profiles differing in m/z by <2 ppm and retention time <30 s were grouped using an in-house R function (Schollée et al. in preparation). Peak intensities were averaged across replicates.

3.2.5.2 Prioritization of Profiles Using Sample Classification

To classify nontarget compounds according to their potential origin (urban, agricultural), groundwater samples were first classified based on the sum concentration of 269 targets from predominantly urban origin (pharmaceuticals and their TPs, sweeteners, industrial chemicals, biocides, illicit drugs, personal care products, and others, SI3-B1) and 229 targets from predominantly agricultural origin (pesticides and their TPs, SI3-B1). Samples were defined as having high urban influence if the sum concentration of urban targets was >100 ng L^{-1}; otherwise, they were defined as samples with low urban influence. Likewise, samples for which the sum concentration of agricultural targets exceeded 100 ng L^{-1} were defined as having high agricultural influence, and otherwise as having low agricultural influence. The cut-off of 100 ng L^{-1} was guided by the European Union's drinking water standard for single pesticides and relevant pesticide TPs (European Commission 1998). The sum concentration (instead of concentrations of single compounds) was used so that the classification depended not only on single targets with high concentrations.

Next, the ratio of a compound's average intensity in samples with high urban/agricultural influence to that of its average intensity in samples with low urban/agricultural influence was calculated as a measure for the likelihood that the compound originated from urban sources or agricultural sources, respectively:

$$\text{Measure for urban origin} = \frac{\text{average intensity in samples with high urban influence}}{\text{average intensity in samples with low urban influence}} \quad (1)$$

$$\text{Measure for agricultural origin} = \frac{\text{average intensity in samples with high agricultural influence}}{\text{average intensity in samples with low agricultural influence}} \quad (2)$$

If the compound was not detected in one of the sample groups, it was assumed that the compound was detected in one sample with the minimum intensity observed in the whole dataset to avoid dividing by 0.

Profiles were classified as follows:

- potential urban MP: measure for urban origin >5 and measure for agricultural origin ≤5,
- potential agricultural MP: measure for urban origin ≤5 and measure for agricultural origin >5,
- potential urban and agricultural MP: measure for urban origin >5 and measure for agricultural origin >5,
- not classifiable: remaining profiles.

Here, the decision to use a factor of five as threshold was guided by profiles annotated as target compounds, i.e. >80% of profiles of urban targets and >90% of profiles of agricultural targets, respectively, showed on average more than five times higher intensities in samples with high urban/agricultural influence vs. samples with low urban/agricultural influence. However, it should be pointed out that some target compounds, which would be classified as "potential urban and agricultural MP", likely originate only from urban sources (e.g. x-ray contrast agent diatrizoic acid).

To gather more information on potential sources, the most intense profiles in each group (urban, urban/agricultural, agricultural profiles with maximum intensity $>5 \times 10^6$; not classifiable profiles with maximum intensity $>10^7$ and ≥30 detections) were retrospectively screened for in the effluent of two Swiss municipal wastewater treatment plants (24 h composite samples, dry-weather conditions). For this, extracted ion chromatograms (EICs) were generated for blank and effluent samples, measured with a comparable method (without enrichment), using the R package MSnbase (Gatto and Lilley 2012). The EICs were then checked for peaks with intensity $>10^5$ and deviating <1 min from the average retention time of the corresponding profiles (SI3-C2).

Total concentrations in each sample were estimated assuming that the compounds ionize either less efficiently than, as efficiently as, or more efficiently than the 113 targets compounds (92 in positive ionization mode, 21 in negative ionization mode) spiked in to groundwater samples (1, 10, 100, 250 ng L^{-1}). Here "less efficiently than", "as efficiently as", and "more efficiently than" correspond to the 25th, 50th and 75th percentile of target compound peak intensities. For details, see SI3-A5.

3.2.5.3 Elucidation of Suspects and Nontargets

Nontargets: Structural elucidation of nontargets focused on profiles that were classified as potentially of urban or urban and agricultural origin and that had maximum intensity $>5 \times 10^6$, and on all profiles that had maximum intensity $>10^7$ and ≥30 detections. For each profile, MS1 and MS/MS data were extracted from the sample with highest precursor intensity using the RMassBank package (Stravs et al. 2013). Structural proposals were then assigned using both MetFrag CL 2.4.5 (using functions from the R package ReSOLUTION, Schymanski (2020)) and SIRIUS4/CSI:FingerID. Both in silico fragmenters were used with a list of >988,000 compounds of potential environmental relevance, including those in CompTox (Schymanski 2019), PubChemLite tier1 (Bolton and Schymanski 2020), NORMAN SusDat (Norman Network et al. 2020), STOFF-IDENT (Letzel et al. 2017), the original dataset used for UBAPMT (Arp and Hale 2020), i.e. Extended PMT (H.-P. Arp and S.E. Hale, personal communication), SwissPest19 (Kiefer et al. 2020b), as well as 71 additional potentially mobile pesticide transformation products (T. Poiger, personal communication). For details, see SI3-A6.

Nontargets were prioritized for confirmation based on multiple lines of evidence as in the following: (i) a positive hit in the MS/MS libraries NIST17 (National Institute of Standards and Technology, U.S. Department of Commerce), MoNA (LC-MS/MS spectra obtained from https://mona.fiehnlab.ucdavis.edu/downloads in December 2019) or MassBank (obtained from https://github.com/MassBank/MassBank-data in December 2019) using the NIST Mass Spectral Search Program (version 2.3) or in mzCloud (selected hits manually checked), (ii) performance of in silico fragmentation, (iii) peak shape, (iv) intensity and detection frequency, (v) plausibility of retention time, and (vi) availability of reference material.

Suspects: The suspect list comprised 1162 MS-ready structures, all with heteroatoms and exact masses >100, and was compiled from Schulze et al. (2019), KEMI Market List (Fischer 2017), UBAPMT (Arp and Hale 2020), and Extended PMT (H.-P. Arp and S.E. Hale, personal communication). The Extended PMT dataset was filtered for compounds classified as very mobile (vM) and "highly expected in the environment" (H.-P. Arp, personal communication, e.g. due to high production volumes). The KEMI Market List, containing >25,000 chemicals that are expected on the EU market (e.g. industrial chemicals, pharmaceuticals, pesticides), was restricted to compounds that are more likely to occur in groundwater. Therefore, only compounds were selected that exhibited a high water exposure index (>15; water exposure index ranges from 1 to 27) and were classified as (potentially) mobile or very mobile (pot M/vM, M/vM, or vM) based on speciation and $\log D_{OW}$ (predicted by JChem for Office, version 19.22.0.548; ChemAxon Ltd.)), as described by Arp and Hale (2019).

Profiles annotated with the suspect list by enviMass (section 3.2.5.1) were prioritized in a similar workflow as nontarget profiles. MetFrag and SIRIUS4/CSI:FingerID were run using both the suspect list and PubChemLite tier1 (Bolton and Schymanski 2020) as databases to check how well the measured MS/MS spectrum fits to the suspect compared to other candidates (SI3-A6). Only suspects ranked among the top 3 candidates of SIRIUS4/CSI:FingerID were checked manually, as described for nontargets.

Prioritized suspects and nontargets were classified, in accordance with Schymanski et al. (2014b), (i) as confirmed structures where reference material was available for identity confirmation (Level 1), (ii) as probable structures where an MS/MS library match was achieved (Level 2a) or (iii) as tentative structures where tentative identifications were based solely on MS/MS interpretation (Level 3). The annotation of MS/MS fragments with structural proposals for tentatively identified compounds was supported by CFM-ID 3.0. Level 1 candidates were identified and quantified as follows. Ten selected samples were enriched and measured together with four calibration standards (1, 10, 100, 1000 ng L^{-1}) and six spiked samples (100, 250, 1000 ng L^{-1}) with adjusted MS/MS settings. The determined calibration model was applied to the previously measured samples for quantification. The quality of quantification was evaluated for each compound based on relative recoveries in spiked samples and the reproducibility of concentrations in the samples, which were each measured twice. Not every compound could be quantified satisfactorily so that in some cases, either concentration ranges or no concentrations are reported. Further details regarding structural confirmation, quantification and associated MS/MS spectra can be found in SI3-A7, SI3-A12, and SI3-B4, respectively.

3.3 Results and Discussion

3.3.1 Sample Classification based on Targets

The extent of urban and/or agricultural influence on the 60 groundwater monitoring sites was evaluated based on the sum concentration of 269 urban and 229 agricultural target compounds (for concentrations of individual targets see SI3-B1, and for targets with detections ≥ 100 ng L^{-1} see Table SI3-A7). Accordingly, 17 sites showed only low urban and agricultural influence, 18 sites were predominantly influenced by agricultural targets, 22 sites were influenced by agricultural and urban targets and three sites were predominantly impacted by urban targets (Figure 3-1). These classifications, which were based on the here presented target screening, were consistent with classifications based on long-term monitoring data for 53 out of 60

monitoring sites (for details see SI3-A8). For most monitoring sites the classification was also consistent with the land use of the catchment, i.e. sites with high urban influence were often close to settlements or to wastewater impacted surface waters (bank filtration), sites with high agricultural influence were usually in areas with intensive agricultural land use, and the catchments of sites with low urban and agricultural influence were usually dominated by grassland or forest.

Urban classification was primarily associated with the sweetener acesulfame, the biocide TP N,N-dimethylsulfamide (may also originate from the banned plant protection product tolylfluanid), the industrial chemical melamine, and the corrosion inhibitor benzotriazole, i.e. if one of these targets is removed from the dataset, then two to five sites are no longer classified as having "high urban influence" or "high urban and agricultural influence" (Figure 3-1). Analogously, the agricultural classification was most driven by a TP of the fungicide chlorothalonil (R471811), which was the only target compound detected in each sample (maximum concentration 2200 ng L^{-1}; Kiefer et al. (2020a)). For further details, see Figure SI3-A2. If samples were classified based on detection frequency of urban or agricultural targets, using a cut-off of e.g. 10 detections, then 44 sites would be classified in the same way (Figure SI3-A3). Here it should be noted that some pesticides may also be used as biocides (e.g. N,N-dimethylsulfamide (TP), triazine herbicides) and some pharmaceuticals are also used as veterinary drugs. Therefore, these targets may be related to urban and agricultural activities, potentially resulting in a wrong classification of some sites.

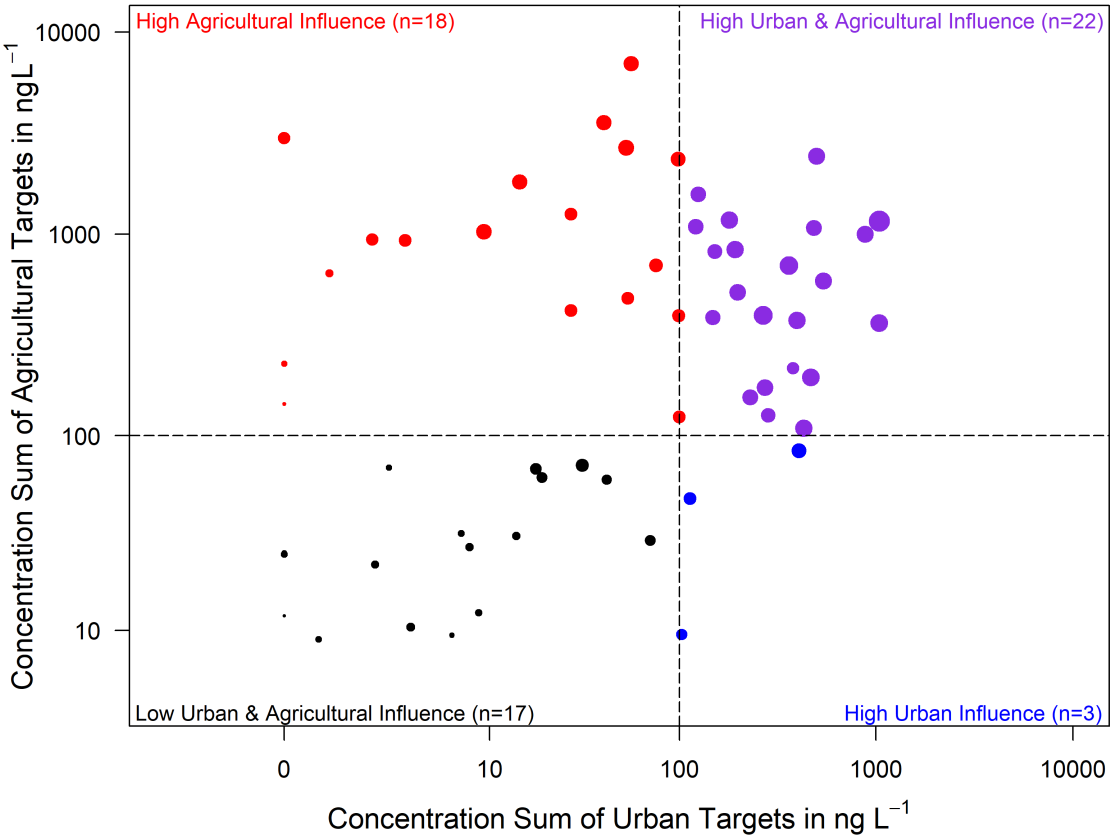

Figure 3-1: Classification of samples according to the concentration sums of urban and agricultural targets. Dashed lines mark the threshold of 100 ng L^{-1} used for classification. Size of circles correlates with number of detected targets (1-74 per sample). Axes are log-scaled.

3.3.2 Classification of Nontargets

In the 60 groundwater samples, 6504 intensity profiles across samples (hereafter "compounds") were detected with maximum intensity $>10^6$ (Table 3-1), including 4800 nontargets and 98 targets in positive ionization mode and 1573 nontargets and 33 targets in negative ionization mode. The total number of compounds was likely slightly lower, due to ambiguities that arise during componentisation of isotopologues and adducts, e.g. ten target compounds were associated with several profiles. Furthermore, some compounds might be detected in both ionization modes, such as 15 target compounds. Of the 6373 nontargets, 4027 (63%) were found in less than five out of six pooled sample replicates or the intensity showed a relative standard deviation of >50% (in pooled samples with detections, see Table 3-1), indicating that either the concentration was too low to be reproducibly detected (potentially due to dilution during mixing of sample aliquots) or that the peak shape was not reproducible. Moreover, for 296 compounds, the maximum intensity in the pooled samples was even higher than the maximum intensity in the groundwater samples. This may be related to contamination during sample handling or peak picking artefacts (e.g. noise).

From the 6373 nontargets, 331 (5%) were classified as potential urban MPs, 945 (15%) as potential agricultural MPs, and 1892 (30%) as potential MPs from urban and agricultural sources. The remaining 3205 (50%) could not be assigned to one of these groups (not classifiable) and might be compounds of natural origins (Table 3-1, Figure 3-2). More than 90% of profiles annotated as target compound were classified correctly, which was expected because classification criteria (>5 times higher intensity in contaminated samples) were guided by the target compounds.

The "not classifiable" target compounds (centre of Figure 3-2) were unclassified due to one or more of the following reasons: (i) a compound was incorrectly annotated (different compound with similar retention time); (ii) a compound had a noisy EIC, resulting in too many detections by enviMass; (iii) a compound originates from multiple sources (the sweetener saccharin may originate from wastewater or from pig manure (Buerge et al. 2011) and can therefore occur at less contaminated sites); (iv) a compound was detected in only one sample with low urban and agricultural influence (site-specific); (v) a compound had shifting retention time and was therefore not correctly grouped; (vi) compounds that have probably been spread ubiquitously, such as banned triazine pesticides and their TPs; and (vii) a compound eluted very early and was therefore affected by ion suppression. This early-eluting compound was melamine, an industrial chemical and TP of the larvicide cyromazine, which is often applied to manure (ECHA 2015). Based on concentrations (determined with a structurally identical internal standard), melamine would be correctly classified as an MP from urban and agricultural sources. This compound was, however, hardly retained by the applied chromatographic method (retention time 3.4 min), eluting together with salts and other highly polar compounds, leading to strong ion suppression effects and, in turn, low intensity (which is used for automatic classification), which hampered proper classification. In total, 20% of all detected compounds eluted between 3 and 4 min. Half of these compounds are located in the centre of Figure 3-2, indicating either their ubiquitous occurrence or their possible misclassification, as in the case of melamine.

In addition, many compounds with broad late-eluting peaks, positive mass defect values and higher m/z were located in the centre of Figure 3-2. Many were assigned as potential natural

organic matter and occurred either at each site or were randomly distributed (see SI3-A9 for details; Table 3-1).

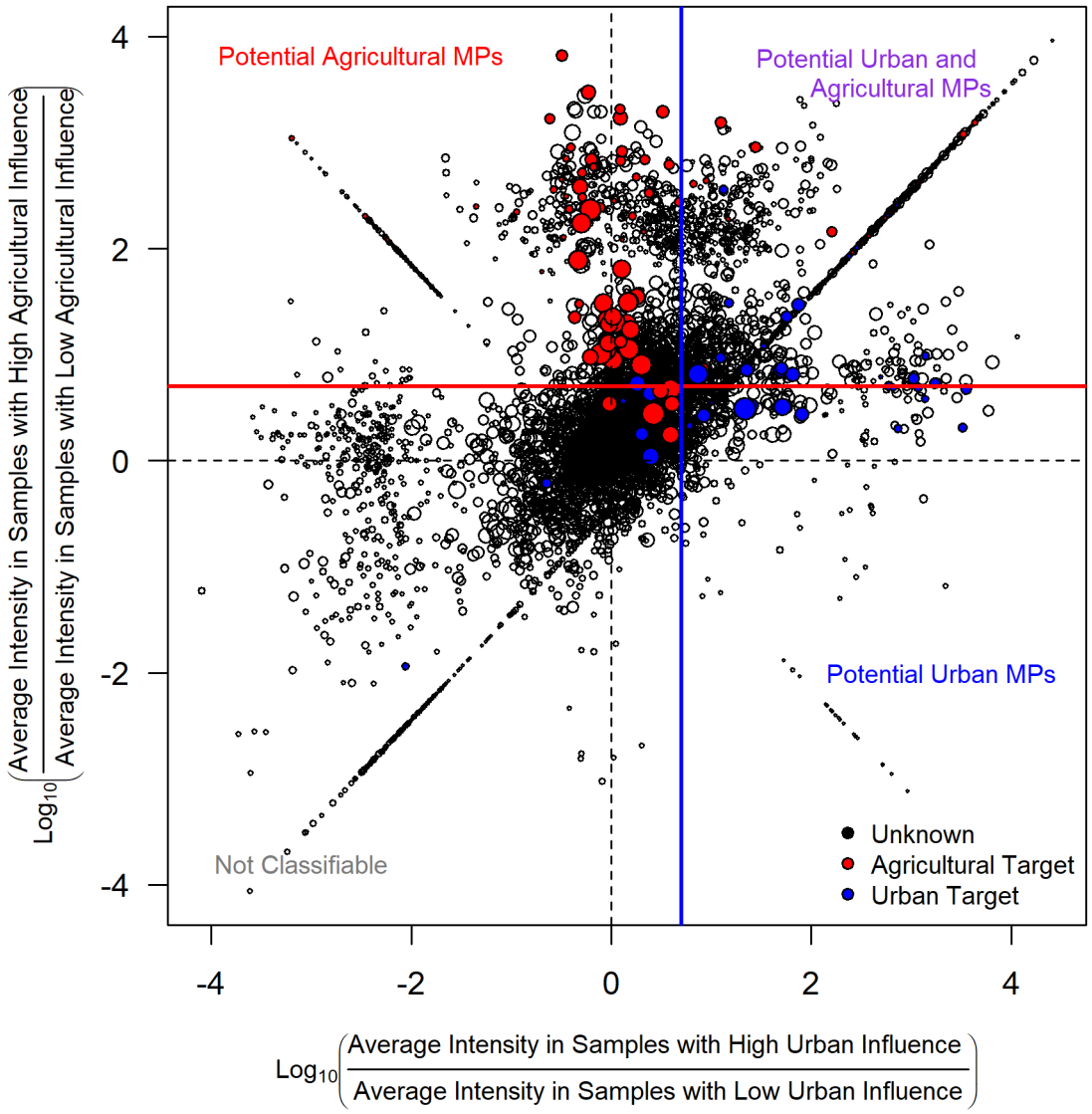

Figure 3-2: Compounds were classified based on their occurrence and intensity in samples with urban or agricultural influence. Each circle represents one compound; size of circle correlates with detection frequency in samples (1-60). Compounds to the right of/above the blue/red lines ($log_{10}(5)$) show, on average, more than five times higher intensities in samples with high urban/agricultural influence than in samples with low urban/agricultural influence. Compounds on the diagonals are artefacts resulting from the replacement of non-detects with the minimum intensity observed across the whole dataset (see section 3.2.5.2).

Table 3-1: Classification of target and nontarget compounds as well as characterisation of nontarget compounds regarding maximum intensity, retention time, and detections in the 60 groundwater samples. Numbers in brackets correspond to the percentage of profiles that are less relevant for structure elucidation (e.g. false positives): (i) profiles with early retention time (3-4 min, i.e. salts and very polar compounds), (ii) profiles, for which a very broad (>5 min) peak shape is likely (i.e. if >2 profiles with retention time >10 min were grouped; potential natural organic matter (NOM), see SI3-A9 for explanation), or (iii) profiles, for which the maximum intensity in the pooled samples was higher than the maximum intensity in the samples. The category "reproducible in pooled samples" provides the number of nontargets detected in at least five out of six pooled sample replicates with relative standard deviation <50% (calculated in pooled samples with detections).

	Urban	**Urban and Agricultural**	**Agricultural**	**Not Classifiable**	**Total**
All Compounds	345 (26%)	1929 (8%)	1013 (21%)	3217 (48%)	6504 (30%)
Targets					
Urban Targets	14 (0%)	21 (0%)	1 (0%)	6 (17%)	42 (2%)
Agricultural Targets	0	16 (0%)	67 (1%)	6 (0%)	89 (1%)
Nontargets					
Total (without Targets)	331 (27%)	1892 (8%)	945 (22%)	3205 (48%)	6373 (31%)
Retention Time <4 min	68 (100%)	81 (100%)	140 (100%)	1127 (100%)	1416 (100%)
Reproducible in Pooled Samples	122 (20%)	517 (9%)	318 (19%)	1389 (43%)	2346 (31%)
Potential NOM	9 (100%)	34 (100%)	44 (100%)	244 (100%)	327 (100%)
Intensity $>5 \times 10^6$	56 (38%)	323 (12%)	86 (24%)	394 (72%)	859 (42%)
Intensity $>10^7$	21 (19%)	156 (15%)	30 (30%)	191 (76%)	398 (46%)
Intensity $>5 \times 10^7$	2 (0%)	11 (0%)	3 (33%)	38 (82%)	54 (59%)
≥30 Detections	10 (40%)	24 (17%)	51 (24%)	862 (44%)	947 (43%)
Intensity $>10^7$ & ≥30 Detections	6 (33%)	12 (25%)	14 (21%)	97 (86%)	129 (71%)
Intensity $>10^7$ & <30 Detections	15 (13%)	144 (14%)	16 (38%)	94 (67%)	269 (34%)
Site-specific (1 Detection)	23 (17%)	727 (6%)	110 (39%)	106 (65%)	873 (16%)

Further characterization and elucidation focused on the more intense compounds classified as potential MPs from urban or urban and agricultural sources (maximum intensity $>5 \times 10^6$) and the most prominent compounds from the remaining dataset ($>10^7$, ≥30 detections). From the resulting 488 compounds in the positive and negative mode (SI3-B2), 480 compounds had at least one MS/MS spectrum, demonstrating the effectiveness of AcquireX (section 3.2.3). AcquireX increased the MS/MS coverage for the 488 nontargets by 39% (for suspects an increase of 73% was observed; detailed discussion in SI3-A10). Overall, 409 compounds were annotated with between 1 and 576 candidate proposals using MetFrag and/or SIRIUS4/CSI:FingerID. Most compounds without candidate proposals (80%) eluted before 4 min and therefore might be artefacts from the LC-HRMS/MS analysis.

To get further evidence for an anthropogenic origin, 562 compounds were checked for characteristic isotope patterns such as Cl (SI3-C1) and for their occurrence in effluent samples of two municipal wastewater treatment plants (SI3-C2, including 74 agricultural compounds with maximum intensity $>5 \times 10^6$, which were not part of the 488 compounds). At least 39 of the 488 compounds contained one or more Cl atoms (see SI3-B2 and discussion in SI3-A9) based on their isotope pattern. In terms of occurrence, 38% of the 56 urban compounds were detected in at least one of the two effluent samples, only 12% of the 323 urban/agricultural compounds and 12% of the 86 agricultural compounds showed a peak in the effluent samples. Interestingly, also

a high percentage of the 97 not classifiable compounds (39%) were found in the wastewater effluents (SI3-B2). However, the majority of these not classifiable compounds (70%) eluted between 3 and 4 min, i.e. they were possibly misclassified or occur naturally (e.g. salts).

3.3.3 Characterization of Groundwater Quality at Monitoring Sites

Figure 3-3 illustrates the total estimated concentrations of detected compounds at the 60 monitoring sites, after excluding potential false positives (see figure caption). The total concentrations were estimated assuming that the compounds ionize, on average, as efficiently as the target compounds (section 3.2.5.2).

The target screening, shown for comparison, demonstrates that anthropogenic activities affect the monitoring sites to very different extents. Total target concentrations ranged from 12 to 7000 ng L^{-1}. For most monitoring sites, the nontarget screening confirmed the contamination trend observed in the target screening. Monitoring sites with few target detections also had less nontarget detections than sites where several targets were found (Figure SI3-A7). Most not classifiable nontargets were detected in positive ionization mode (Figure SI3-A8). To estimate which percentage of total contamination was explained by the target screening for 498 MPs, we compared the estimated concentration of targets with the estimated concentration of nontargets from each source (without not classifiable/site-specific nontargets, i.e. only 1 detection, and without potential false positives). According to this approximation, the targets would explain 4 to 72% of the total contamination in individual samples (median: 34%; pooled samples: 30-33%; based on detections: 8-28%, median: 16%, pooled samples 10-11%). Assuming that nontargets ionize as efficiently as target compounds, 46 nontargets had concentrations >100 ng L^{-1} in at least one groundwater sample. However, it should be kept in mind that these estimates are subject to various uncertainties: (i) the classification might be erroneous; (ii) the true ionization efficiency of individual compounds might differ considerably from the ionization efficiency assumed by our quantification approach (same ionization efficiency for all compounds); (iii) matrix effects (ion suppression and enhancement) may influence signal intensities and thus the estimated concentrations in individual samples; (iv) some potential MPs might have been detected several times, e.g. in both ionization modes or due to insufficient componentisation (see section 3.3.2).

Despite these uncertainties, nontarget screening indicated that the contamination from agriculture at sites with high agricultural influence might be considerably higher than assumed based solely on target screening. Indeed, based on the roughly estimated compound concentrations, 21-96% of potential agricultural MPs, detected at sites with high agricultural influence, would not be explained by targets (median: 49%, pooled samples: 48-52%; based on detections: 62-89%, median 77%, pooled samples: 81%). This was at first glance surprising since we had previously performed a suspect screening for most registered pesticides, including their TPs, using samples from partially the same monitoring sites (Kiefer et al. 2019). The suspect list comprised more than 1000 pesticide TPs, compiled from various sources and mostly observed within the European pesticide registration. However, for many pesticides applied in Switzerland between 2005 and 2017, relatively few TPs could be gathered for the suspect list; for 26% of pesticides transformation data was unavailable or inaccessible. Considering that for some pesticides, e.g. chlorothalonil, more than 20 TPs are known (EFSA 2018), it is likely that the suspect list lacked important TPs, which were therefore not detected using the suspect screening approach.

Whether groundwater quality is indeed more affected by agriculture than by urban activities (as indicated by the target screening) remains unclear. Many nontarget compounds were jointly assigned to both urban and agricultural sources ("potential urban and agricultural MPs"; Figure 3-3: purple), though some of these probably originate from only urban sources, as shown for some identified compounds (see Table 3-2 and section 3.3.4.2). One monitoring site differed strongly from the remaining sites in terms of estimated concentrations, total number of nontarget compounds and the number of site-specific compounds (Figure 3-3, Figure SI3-A6 to Figure SI3-A11). Strikingly, this site was not suspicious in the target screening, except for high concentrations of the pesticide cycluron (140 ng L^{-1}; SI3-B1), which was banned in Switzerland in 2005 and in the EU in 2003 (European Commission 2002). The elucidation of some nontargets supports the hypothesis that this monitoring site is highly contaminated (section 3.3.4).

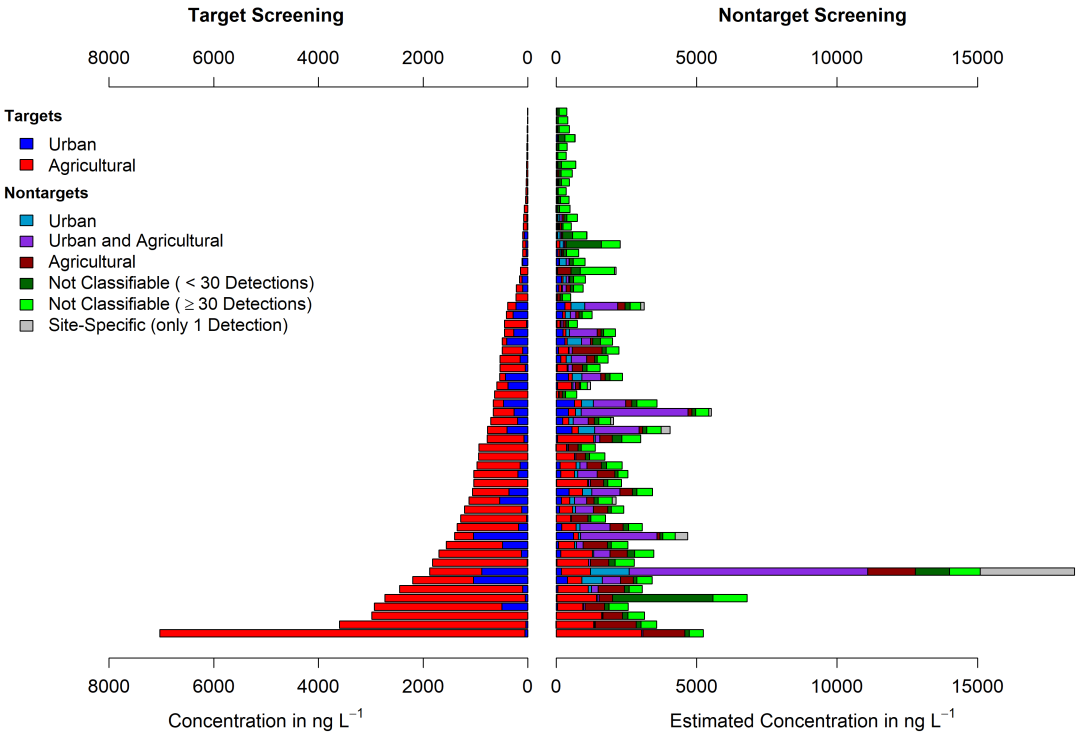

Figure 3-3: Total concentrations determined in target screening (left) and estimated total concentrations determined from nontarget screening (right) for each monitoring site. The colour code indicates the potential source of the contamination. Concentrations were estimated assuming that the nontargets ionize on average as efficiently as target compounds (same ionization efficiency for each nontarget). Therefore, concentrations of urban and agricultural targets determined in the target screening may differ from estimated concentrations of targets determined in the nontarget screening. To reduce false positives, compounds were excluded if they (i) were identified as potential natural organic matter (broad peak, retention time >10 min, SI3-A9), (ii) had retention time <4 min, (iii) had a maximum intensity in the pooled samples that was larger than the maximum intensity in the samples (296 compounds), or (iv) were not reproducibly detected in the pooled samples (<5 detections or relative standard deviation >50%). The early-eluting compounds were excluded because they are likely to be misclassified (intensity does not necessarily correlate with concentration) or to be of natural origins (e.g. salts). The exclusion of compounds not reproducibly detected in the pooled samples may lead to an underestimation of site-specific pollution. See Figure SI3-A6 to Figure SI3-A11 for similar plots based on detections or estimated concentrations, with and without excluded compounds.

3.3.4 Identification of Nontargets and Suspects

Structural elucidation efforts were especially successful where (i) nontargets were annotated with relatively few structural candidates (12 of 21 unequivocally or tentatively identified nontargets had <10 candidates), (ii) MS/MS spectra of the correct candidate were available in libraries or literature (13 nontargets), (iii) useful metadata was accessible (e.g. information on field of application for candidates), and finally (iv) reference material could be purchased.

Using 29 reference standards, we confirmed 11 suspects and 12 nontargets (Level 1) and rejected three suspects and three nontargets. Moreover, five nontargets and two suspects could be identified as probable structures by a library spectrum match (Level 2a), while a further five nontargets and five suspects were assigned tentative structures (Level 3). Figure 3-4 presents novel compounds (Level 1 or Level 3) and Table 3-2 compounds, which were already reported to be detected in environmental samples. Further details, including quantification results and MS/MS spectra, are given in SI3-A12 and SI3-B4. In addition, MS/MS spectra will be uploaded to MassBank (www.massbank.eu).

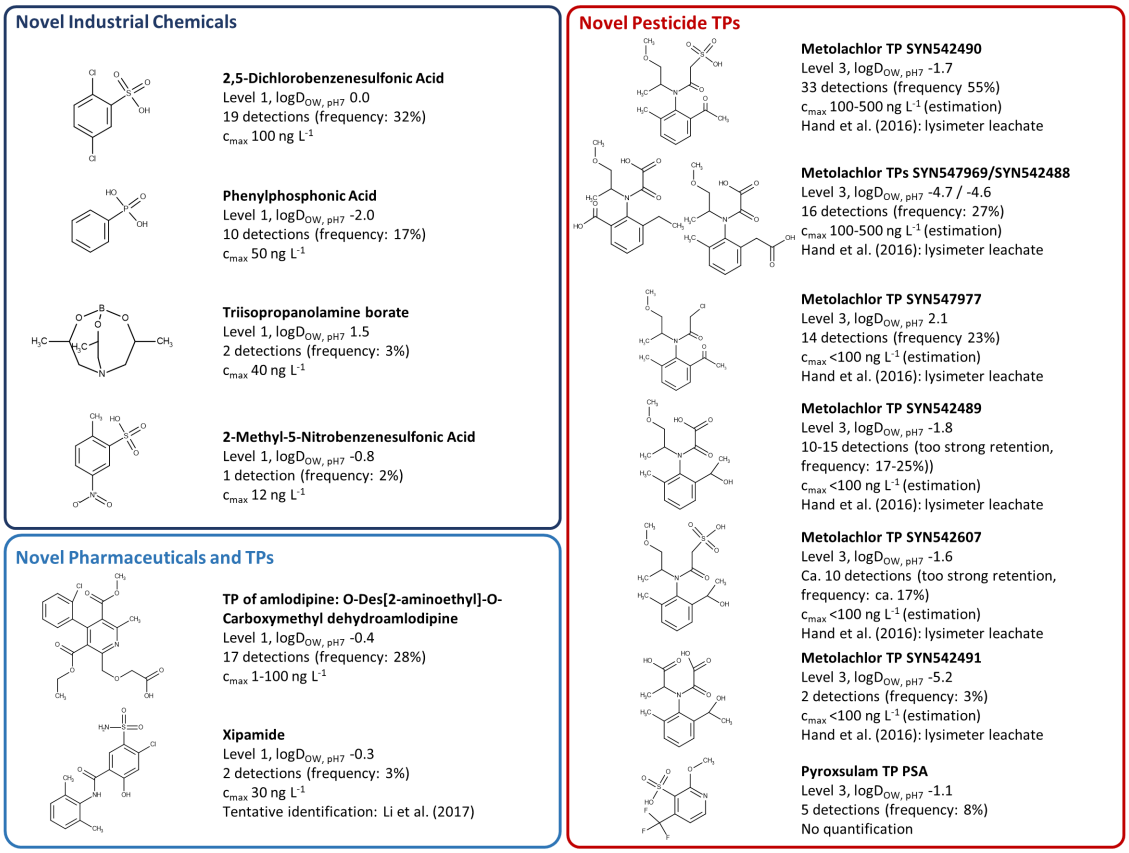

Figure 3-4: Novel MPs elucidated through nontarget and suspect screening. For more details, including structural identifiers and quantification results in individual samples, see SI3-B4. For MS/MS fragments, see SI3-A12. Two metolachlor TPs were too strongly retained by LC, i.e. partially eluting in subsequent samples. $logD_{OW,\ pH7}$ (water-n-octanol distribution coefficient considering the speciation at pH 7) was predicted with JChem for Office (Version 17.1.2300.1455; ChemAxon Ltd.).

Table 3-2: Identified suspects and nontargets, reported previously in literature and ordered according to confirmation confidence and detection frequency in groundwater. The PubChem Compound ID (CID) is provided as identifier. Further identifiers (InChIKey, SMILES) and quantification results are listed in SI3-B4. For MS/MS fragments, see SI3-A12. See SI3-B2 and SI3-B3 for all prioritized nontargets and suspects, including annotated candidates. References point to studies reporting prior detections in environmental samples; n.q. = no quantification.

Compound	Screening	Classification	Maximum Concentration in ng L^{-1}	No. Of Detections	Use/ Sources	Literature on Environmental Occurrence
Trifluoroacetic acid* Level 1, CID 6422	Suspect	Not Classifiable	>5000	60	Various sources	Berg et al. (2000), Scheurer et al. (2017)
Trifluoromethanesulphonic acid* Level 1, CID 62406	Suspect	Agricultural	90	53	Industrial chemical	Zahn et al. (2016)
Atrazine-desethyl-desisopropyl Level 1, CID 18831	Nontarget	Agricultural	90	51	Pesticide TP	BMASGK (2018)
Perfluoropropanesulfonic acid Level 1, CID 9859771	Nontarget	Urban & Agricultural	5-30	51	Perfluorinated compound	Mak et al. (2009)
Oxypurinol* Level 1, CID 135398752	Nontarget	Urban	300	20	Pharmaceutical TP	Funke et al. (2015)
Methyldiphenylphosphine oxide** Level 1, CID 75041	Nontarget	Urban & Agricultural	n.q.	23	Industrial chemical	Brand et al. (2018)
Edetic acid (EDTA)* Level 1, CID 6049	Suspect	Urban	n.q.	20	Industrial chemical	Schmidt et al. (2004)
2-Acrylamido-2-methyl-1-propanesulfonic acid (AMPS)* Level 1, CID 65360	Suspect	Urban & Agricultural	90	13	Wide-spread use (industry and households)	Schulze et al. (2019)
Perfluorobutylsulphon-amide Level 1, CID 10958205	Nontarget	Urban & Agricultural	n.q.	13	Perfluorinated compound	Chu et al. (2015) in fish
Methenamine* Level 1, CID 4101	Suspect	Urban	<200	11	Wide-spread use (industry and household)s	Knepper et al. (1999)
Dimethylbenzenesulfonic acid (isomers)* Level 1	Suspect	Urban & Agricultural	80	10	Industrial chemical	Betowski et al. (1996)
p-Toluenesulfonic acid* Level 1, CID 6101	Suspect	Not Classifiable	200-700	7	Industrial chemical	Crathorne et al. (1984)
5-Methoxy-2H-benzotriazole Level 1, CID 119717	Nontarget	Urban & Agricultural	3	7	Benzotriazole derivate or TP thereof	Liu et al. (2013), Huntscha et al. (2014): tentative structure
Propyphenazone Level 1, CID 3778	Nontarget	Urban & Agricultural	10	5	Pharmaceutical	Heberer (2002)
Pyrimidinol (2-Isopropyl-6-methyl-4-pyrimidone) Level 1, CID 135444498	Nontarget	Urban & Agricultural	60	2	Pesticide / biocide TP (diazinon TP)	Diaz-Cruz and Barcelo (2006)
Fluometuron Level 1, CID 16562	Suspect	Urban & Agricultural	40	2	Pesticide / biocide	Herrero Hernández et al. (2012)
Sulisobenzone Level 1, CID 19988	Suspect	Site-specific	50-100	1	UV filter, various uses	Rodil et al. (2008)

Compound	Screening	Classifi-cation	Maximum Concen-tration in ng L^{-1}	No. Of Detec-tions	Use/ Sources	Literature on Environmental Occurrence
Iopromide TP 643 Level 2a, CID 139597923	Nontarget	Urban & Agricultural	n.q.	26	Pharmaceutical TP	Schulz et al. (2008)
Iopromide TP 701 A Level 2a, CID 139596314	Nontarget	Urban & Agricultural	n.q.	23	Pharmaceutical TP	Schulz et al. (2008)
Iomeprol TP 629 Level 2a, CID 23189998	Nontarget	Urban	n.q.	18	Pharmaceutical TP	Kormos et al. (2009)
Triphenylphosphine oxide* Level 2a, CID 13097	Nontarget	Urban & Agricultural	n.q.	16	Industrial chemical (synthesis by-product)	Knepper et al. (1999)
Hexa(methoxymethyl)-melamine Level 2a, CID 62479	Suspect	Not Classifiable	n.q.	7	Industrial chemical	Dsikowitzky and Schwarzbauer (2015), Bobeldijk et al. (2002)
Metolachlor TP CGA357704 Level 2a, CID 71312482			<100	6	Pesticide TP	Reemtsma et al. (2013)
Chlorendic acid Level 2a, CID 8266	Nontarget	Site-specific	n.q.	1	Industrial chemical, TP of organochlorine pesticides	Ying et al. (1986), IPCS (1996)
Isomer of 5,6-Dimethyl-2H-benzotriazole Level 3	Nontarget	Urban	1-10	15	Benzotriazole derivate or TP thereof	Huntscha et al. (2014), Trcek et al. (2018)
Isomer of 5-Methoxy-2H-benzotriazole Level 3	Nontarget	Urban & Agricultural	10-30	14	Benzotriazole derivate or TP thereof	Liu et al. (2013), Huntscha et al. (2014): tentative structure
Naphthalenedisulfonic acids (various isomers)* Level 3	Nontarget	Urban & Agricultural	>500	1	Industrial chemical	Jekel and Gruenheid (2005), Knepper et al. (1999)

*Contamination during sample processing cannot be fully excluded. Only detections are reported, meaning that the concentration in groundwater samples was at least twice as high as the maximum concentration in 18 blank samples. Where quantification was not possible, an intensity threshold was instead applied, requiring a sample intensity at least five times higher than the maximum intensity recorded in blank samples. **The METLIN MS/MS library reports different MS/MS fragments than recorded in this study.

3.3.4.1 Novel Micropollutants

2,5-dichlorobenzenesulfonic acid is pre-registered under REACH and was predicted as likely to be carcinogenic and persistent in the environment (ECHA 2020). 2,5-dichlorobenzenesulfonic acid was detected in 19 out of 60 samples, mostly in the low ng L^{-1} range, in one sample at 100 ng L^{-1}. We did not find evidence for a prior detection in environmental samples in available literature.

Phenylphosphonic acid is registered under REACH (10-100 t/a, ECHA (2020)) and was detected at 10 monitoring sites with concentrations of up to 50 ng L^{-1}. Schulze et al. (2019) compared various analytical approaches for the analysis of polar compounds. Phenylphosphonic acid could only be analysed by reversed-phase LC, but the tested enrichment methods, all based on solid

phase extraction, were unsuitable for this industrial chemical. The occurrence in environmental samples after evaporative enrichment is here reported for the first time.

O-des[2-aminoethyl]-O-carboxymethyl dehydroamlodipine is a TP of the blood pressure regulator amlodipine, which is approved in Switzerland. The TP was detected in nearly one third of the samples at concentrations <100 ng L^{-1} and is probably reported here for the first time in environmental samples.

Triisopropanolamine borate was detected at two monitoring sites at concentrations of up to 40 ng L^{-1} and was to our knowledge not reported before in the environment. The sulphonamide diuretic drug **xipamide** was found in two samples at 30 ng L^{-1}. Previously, Li et al. (2017) identified xipamide only tentatively in European wastewater-impacted rivers. Interestingly, xipamide is not approved in Switzerland and was therefore also not on the target list (PharmaWiki 2020). One nontarget compound, detected at five monitoring sites and classified as a potential urban and agricultural MP, was tentatively identified as the pesticide TP **pyroxsulam TP PSA** (reference standard not available).

Amongst the top ten most intense potential agricultural MPs with a detection frequency >50%, we tentatively identified **metolachlor TP SYN542490** (reference standards not available). Assuming a similar ionization efficiency as metolachlor-ESA and metolachlor TP CGA 368208, maximum concentrations were estimated to be in the range of 100-500 ng L^{-1}, which is comparable to the concentrations of the target compounds metolachlor-ESA and metolachlor TP CGA 368208. S-metolachlor is currently under review for renewal in the EU. In contrast to our previously performed target and suspect screening (Kiefer et al. 2019), which included nine metolachlor TPs, here we had access to nine further metolachlor TPs (including TP SYN542490; T. Poiger, personal communication). They were previously observed in a lysimeter study by the pesticide producer (Hand et al. 2016). After the detection of SYN542490, we manually screened for the remaining TPs and tentatively identified the TPs CGA357704 (reported previously by Reemtsma et al. (2013)), SYN542607, SYN547977, SYN542489, SYN542491, and one or both of the isomers, namely SYN547969 and SYN542488; all of which were detected at lower intensity and lower frequency compared to SYN542490.

3.3.4.2 Evaluation of Pre-Classification of Elucidated Compounds

The identification efforts focused on compounds classified as potential MPs from urban sources and urban and agricultural sources. Probably all elucidated compounds with this pre-classification originate from urban or industrial sources, except for the tentatively identified TP of the herbicide pyroxsulam, namely pyroxsulam TP PSA. Furthermore, we investigated the most intense and wide-spread potential agricultural pollutants leading to the identification of TPs of the pesticides metolachlor and atrazine, confirming the correct pre-classification. Interestingly, in addition to the mentioned pesticide TPs, we also detected the short-chain perfluorinated compound trifluoromethanesulfonic acid (53 detections), which has previously been reported by Zahn et al. (2016) and Schulze et al. (2019) as a wide-spread MP with concentrations in the ng L^{-1} to µg L^{-1} range. The highest concentrations in our study (up to 90 ng L^{-1}) were detected in samples with high agricultural influence, explaining its classification as a potential agricultural MP. In contrast to another short-chain perfluorinated compound, trifluoroacetic acid, for which various sources have been reported including the degradation of pesticides (Scheurer et al. 2017), trifluoromethanesulfonic acid is to our knowledge not known as being of potential agricultural origin.

Four elucidated suspects could not be related to urban and/or agricultural sources, i.e. were "not classifiable". The industrial chemical hexa(methoxymethyl)melamine showed, on average, only four times higher intensity in samples with high urban influence compared to the average intensity in samples with low urban influence and was therefore "not classifiable" (threshold was five, section 3.2.5.2). In the case of p-toluenesulfonic acid, contamination during sample handling or analysis led to false positive detections in a few samples, including the blank samples. This compound is a known background contaminant (Schulze et al. 2019). On average its intensity was 28 times higher in samples than in blanks, meaning it was not removed during pre-processing (section 3.2.5.1). Similarly, 1,3-diphenylguanidine was detected in all samples and in 19 of these had an intensity five times greater than in blanks. However, in spiking experiments (100 ng L^{-1}) we observed 3-4 times higher intensities in the sample matrix than in ultrapure water (ion enhancement), suggesting that the detections with relatively high intensity might represent contaminations. Therefore, 1,3-diphenylguanidine is not reported in Table 3-2. A further "not classifiable" compound was trifluoroacetic acid, which is a ubiquitously spread pollutant and may enter groundwater via diffuse sources (atmospheric deposition, pesticide application) or point sources (industrial emissions to rivers) (Berg et al. 2000, Freeling et al. 2020, Scheurer et al. 2017). Accordingly, trifluoroacetic acid was detected in all samples, though reliable quantification was not possible.

Many identified nontargets and suspects were pre-classified as "potential urban and agricultural MP", although they likely originate only from urban sources (e.g. TPs of x-ray contrast agent iopromide, benzotriazole derivates, Table 3-2). This imprecise classification results from the large number of monitoring sites, which were influenced by both urban and agricultural activities, whereas only few sites showed a high urban but low agricultural influence (Figure 3-1). To achieve a better classification of urban MPs, more monitoring sites with primarily urban influence would be needed for the workflow, but this was difficult to obtain due to the Swiss small-scale structured landscape.

The characterization of the monitoring sites (section 3.3.3) highlighted one site in particular, due to its especially high contamination in terms of both the number and estimated concentrations of detected nontargets (Figure 3-3, Figure SI3-A6 to Figure SI3-A11). Out of 46 nontargets with estimated concentrations >100 ng L^{-1} (section 3.3.3; 10 of the 46 were identified), 23 were detected at this site. The hypothesis that this site might be highly contaminated was further supported by the elucidation of various compounds, being either site-specific or showing highest concentrations at this site, such as the industrial chemicals naphthalenedisulfonic acids (various isomers, >500 ng L^{-1}) and p-toluenesulfonic acid (200-700 ng L^{-1}), the diazinone TP pyrimidinol (60 ng L^{-1}), the industrial chemicals dimethylbenzenesulfonic acids (various isomers, 80 ng L^{-1}) and 2,5-dichlorobenzenesulfonic acid (100 ng L^{-1}), and chlorendic acid (Level 2a). The ECHA classifies chlorendic acid as a carcinogen category 1B (ECHA 2020). Potential sources include the degradation of flame-retardant polyesters or organochlorine pesticides such as endosulfan, heptachlor, or aldrin (IPCS 1996). The reason for this contamination is unknown, but the groundwater from this site is not currently used for drinking water production.

3.4 Conclusions

By combining an appropriate compound prioritization strategy with a highly automated structural elucidation workflow, we were able to characterize groundwater quality in a more comprehensive manner than previously possible using targeted methods and in doing so, to identify as yet unreported MPs.

- Nontargets were prioritized based on their potential origin for structural elucidation. Categorisation of nontargets also provided rough estimates of the number and the concentrations of thus far overlooked contaminants.
- A combination of computational tools supported the structural elucidation process. AcquireX improved MS/MS coverage for nontargets and suspects, while MetFrag and SIRIUS4/CSI:FingerID (together with an extensive compound database) resulted in 23 unequivocally identified and 17 tentatively identified compounds. 13 of these compounds are novel.
- Structural elucidation was most successful for compounds (i) with MS/MS spectra in libraries or literature, (ii) that were assigned limited numbers of candidate structures, (iii) that had accessible metadata, and (iv) for which available reference material was available.
- Despite the high degree of automation of the structural elucidation workflow, structural elucidation itself remains a major bottleneck in transforming unknowns into known compounds. Moreover, elucidation of compounds not presently in any database, e.g. so far not observed TPs, is highly challenging and was not covered at all by our elucidation approach.
- One groundwater sample was revealed to be much more polluted than assumed based on target screening, highlighting the relevance of comprehensive screening approaches for evaluating water quality.

Acknowledgements

This study was funded by the Swiss Federal Office for the Environment (FOEN). Samples were provided by the Swiss cantons and by the Swiss National Monitoring NAQUA. We thank Miriam Reinhardt, FOEN, project management NAQUA, and all those involved in sample collection and transport. Furthermore, we are grateful to Philipp Longrée and Bernadette Vogler, Eawag, for their excellent support in the laboratory. We are especially thankful to Emma Schymanski, Luxembourg Centre for Systems Biomedicine, for an overview on available compound lists, to Martin Loos, envibee GmbH, for his support with enviMass, and to Jennifer Schollée and Michael Stravs, Eawag, for sharing R functions and helpful discussions. Besides, we received valuable feedback to the manuscript from Miriam Reinhardt and Ronald Kozel, FOEN. Special thanks go to Jennifer Schollée and Martin Jones, Eawag, for proofreading and critical comments.

References

Albergamo, V., Schollée, J.E., Schymanski, E.L., Helmus, R., Timmer, H., Hollender, J. and de Voogt, P., 2019. Nontarget Screening Reveals Time Trends of Polar Micropollutants in a Riverbank Filtration System. Environ Sci Technol 53(13), 7584-7594.

Allen, F., Greiner, R. and Wishart, D., 2014. Competitive fragmentation modeling of ESI-MS/MS spectra for putative metabolite identification. Metabolomics 11(1), 98-110.

Arp, H.P. and Hale, S.E., 2020. S36 | UBAPMT | Potential Persistent, Mobile and Toxic (PMT) substances (Version NORMAN-SLE-S36.0.2.0) [Data set], Zenodo. http://doi.org/10.5281/zenodo.3637611.

Arp, H.P.H. and Hale, S.E., 2019. UBA Texte 126/2019: REACH: Improvement of guidance methods for the identification and evaluation of PM/PMT substances, German Environment Agency (UBA), Dessau-Roßlau, Germany.

Berg, M., Müller, S.R., Mühlemann, J., Wiedmer, A. and Schwarzenbach, R.P., 2000. Concentrations and Mass Fluxes of Chloroacetic Acids and Trifluoroacetic Acid in Rain and Natural Waters in Switzerland. Environmental Science and Technology 34(13), 2675-2683.

Betowski, L.D., Kendall, D.S., Pace, C.M. and Donnelly, J.R., 1996. Characterization of groundwater samples from superfund sites by gas chromatagraphy/mass spectrometry and liquid chromatography/mass spectrometry. Environmental Science and Technology 30(12), 3558-3564.

BMASGK, 2018. Austrian Report on Drinking Water 2017 (Österreichischer Trinkwasserbericht 2017). https://www.verbrauchergesundheit.gv.at/lebensmittel/trinkwasser/Trinkwasserbericht_2017.pdf?7i5641.

Bobeldijk, I., Stoks, P.G.M., Vissers, J.P.C., Emke, E., van Leerdam, J.A., Muilwijk, B., Berbee, R. and Noij, T.H.M., 2002. Surface and wastewater quality monitoring: combination of liquid chromatography with (geno)toxicity detection, diode array detection and tandem mass spectrometry for identification of pollutants. Journal of chromatography A 970(1), 167-181.

Bolton, E. and Schymanski, E.L., 2020. PubChemLite tier0 and tier1 (Version PubChemLite.0.2.0) [Data set], Zenodo. http://doi.org/10.5281/zenodo.3611238.

Brand, S., Schlüsener, M.P., Albrecht, D., Kunkel, U., Strobel, C., Grummt, T. and Ternes, T.A., 2018. Quaternary (triphenyl-) phosphonium compounds: Environmental behavior and toxicity. Water Res 136, 207-219.

Broadhurst, D., Goodacre, R., Reinke, S.N., Kuligowski, J., Wilson, I.D., Lewis, M.R. and Dunn, W.B., 2018. Guidelines and considerations for the use of system suitability and quality control samples in mass spectrometry assays applied in untargeted clinical metabolomic studies. Metabolomics 14(6), 72.

Buerge, I.J., Keller, M., Buser, H.R., Muller, M.D. and Poiger, T., 2011. Saccharin and other artificial sweeteners in soils: estimated inputs from agriculture and households, degradation, and leaching to groundwater. Environmental Science and Technology 45(2), 615-621.

Chambers, M.C., Maclean, B., Burke, R., Amodei, D., Ruderman, D.L., Neumann, S., Gatto, L., Fischer, B., Pratt, B., Egertson, J., Hoff, K., Kessner, D., Tasman, N., Shulman, N., Frewen, B., Baker, T.A., Brusniak, M.-Y., Paulse, C., Creasy, D., Flashner, L., Kani, K., Moulding, C., Seymour, S.L., Nuwaysir, L.M., Lefebvre, B., Kuhlmann, F., Roark, J., Rainer, P., Detlev, S., Hemenway, T., Huhmer, A., Langridge, J., Connolly, B., Chadick, T., Holly, K., Eckels, J., Deutsch, E.W., Moritz, R.L., Katz, J.E., Agus, D.B., MacCoss, M., Tabb, D.L. and Mallick, P., 2012. A cross-platform toolkit for mass spectrometry and proteomics. Nature Biotechnology 30, 918.

Chiaia-Hernandez, A.C., Schymanski, E.L., Kumar, P., Singer, H.P. and Hollender, J., 2014. Suspect and nontarget screening approaches to identify organic contaminant records in lake sediments. Analytical and Bioanalytical Chemistry 406(28), 7323-7335.

Chu, S., Letcher, R.J., McGoldrick, D.J. and Backus, S.M., 2015. A New Fluorinated Surfactant Contaminant in Biota: Perfluorobutane Sulfonamide in Several Fish Species. Environmental science & technology 50(2), 669-675.

Crathorne, B., Fielding, M., Steel, C.P. and Watts, C.D., 1984. Organic compounds in water: analysis using coupled-column high-performance liquid chromatography and soft-ionization mass spectrometry. Environmental science & technology 18(10), 797-802.

Diaz-Cruz, M.S. and Barcelo, D., 2006. Highly selective sample preparation and gas chromatographic-mass spectrometric analysis of chlorpyrifos, diazinon and their major metabolites in sludge and sludge-fertilized agricultural soils. J Chromatogr A 1132(1-2), 21-27.

Dsikowitzky, L. and Schwarzbauer, J., 2015. Hexa(methoxymethyl)melamine: An Emerging Contaminant in German Rivers. Water Environment Research 87(5), 461-469.

Dührkop, K., Shen, H., Meusel, M., Rousu, J. and Bocker, S., 2015. Searching molecular structure databases with tandem mass spectra using CSI:FingerID. Proc Natl Acad Sci U S A 112(41), 12580-12585.

Dührkop, K., Fleischauer, M., Ludwig, M., Aksenov, A.A., Melnik, A.V., Meusel, M., Dorrestein, P.C., Rousu, J. and Bocker, S., 2019. SIRIUS 4: a rapid tool for turning tandem mass spectra into metabolite structure information. Nat Methods 16(4), 299-302.

ECHA, 2015. Opinion of the Biocidal Products Committee on the application for approval of the active substance cyromazine for product type 18; ECHA/BPC/087/2015. https://echa.europa.eu/documents/10162/a281e819-013d-40f5-aae3-719aac9489b7. 21/07/2020.

ECHA, 2020. European Chemicals Agancy. https://www.echa.europa.eu/information-on-chemicals. Accessed: Sep 2020.

EFSA, 2018. Peer review of the pesticide risk assessment of the active substance chlorothalonil. EFSA Journal 16(1), 1-40.

European Commission, 1998. Council Directive 98/83/EC of 3 November 1998 on the quality of water intended for human consumption. Official Journal of the European Communities (L330).

European Commission, 2002. Commission regulation (EC) No 2076/2002 of 20 November 2002 extending the time period referred to in Article 8(2) of Council Directive 91/414/EEC and concerning the non-inclusion of certain active substances in Annex I to that Directive and the withdrawal of authorisations for plant protection products containing these substances. Official Journal of the European Communities 319(4).

Fischer, S., 2017. S17 | KEMIMARKET | KEMI Market List MS-ready (12/05/2017) (Version NORMAN-SLE-S17.0.1.3) [Data set], Zenodo. http://doi.org/10.5281/zenodo.3653175.

Freeling, F., Behringer, D., Heydel, F., Scheurer, M., Ternes, T.A. and Nodler, K., 2020. Trifluoroacetate in Precipitation: Deriving a Benchmark Data Set. Environ Sci Technol.

Funke, J., Prasse, C., Lutke Eversloh, C. and Ternes, T.A., 2015. Oxypurinol - A novel marker for wastewater contamination of the aquatic environment. Water Res 74, 257-265.

Gago-Ferrero, P., Schymanski, E.L., Bletsou, A.A., Aalizadeh, R., Hollender, J. and Thomaidis, N.S., 2015. Extended Suspect and Non-Target Strategies to Characterize Emerging Polar Organic Contaminants in Raw Wastewater with LC-HRMS/MS. Environ Sci Technol 49(20), 12333-12341.

Gago-Ferrero, P., Krettek, A., Fischer, S., Wiberg, K. and Ahrens, L., 2018. Suspect Screening and Regulatory Databases: A Powerful Combination To Identify Emerging Micropollutants. Environ Sci Technol 52(12), 6881-6894.

Gatto, L. and Lilley, K.S., 2012. MSnbase - an R/Bioconductor package for isobaric tagged mass spectrometry data visualization, processing and quantitation. Bioinformatics (28), 288-289.

Hand, L.H., Marshall, S.J., Saeed, M., Earll, M., Hadfield, S.T., Richardson, K. and Rawlinson, P., 2016. High-resolution accurate mass spectrometry as a technique for characterization of complex lysimeter leachate samples. Environ Toxicol Chem 35(6), 1401-1412.

Heberer, T., 2002. Tracking persistent pharmaceutical residues from municipal sewage to drinking water. Journal of hydrology (Amsterdam) 266(3-4), 175-189.

Heberer, T., Mechlinski, A., Fanck, B., Knappe, A., Massmann, G., Pekdeger, A. and Fritz, B., 2004. Field studies on the fate and transport of pharmaceutical residues in bank filtration. Ground Water Monitoring and Remediation 24(2), 70-77.

Herrero Hernández, E., Pose Juan, E., Álvarez Martín, A., Andrades, M., Rodríguez Cruz, M. and Sánchez-Martín, M.J., 2012. Pesticides and degradation products in groundwaters from a vineyard region: Optimization of a multiresidue method based on SPE and GC-MS. Journal of Separation Science 35(24), 3492-3500.

Horai, H., Arita, M., Kanaya, S., Nihei, Y., Ikeda, T., Suwa, K., Ojima, Y., Tanaka, K., Tanaka, S., Aoshima, K., Oda, Y., Kakazu, Y., Kusano, M., Tohge, T., Matsuda, F., Sawada, Y., Hirai, M.Y., Nakanishi, H., Ikeda, K., Akimoto, N., Maoka, T., Takahashi, H., Ara, T., Sakurai, N., Suzuki, H., Shibata, D., Neumann, S., Iida, T., Tanaka, K., Funatsu, K., Matsuura, F., Soga, T., Taguchi, R., Saito, K. and Nishioka, T., 2010. MassBank: a public repository for sharing mass spectral data for life sciences. Journal of Mass Spectrometry 45(7), 703-714.

Hug, C., Ulrich, N., Schulze, T., Brack, W. and Krauss, M., 2014. Identification of novel micropollutants in wastewater by a combination of suspect and nontarget screening. Environmental pollution 184, 25-32.

Huntscha, S., Hofstetter, T.B., Schymanski, E.L., Spahr, S. and Hollender, J., 2014. Biotransformation of benzotriazoles: insights from transformation product identification and compound-specific isotope analysis. Environ Sci Technol 48(8), 4435-4443.

IPCS, 1996. Environmental Health Criteria 185, Chlorendic Acid and Anhydride. International Programme on Chemical Safety. World Health Organization.

Jekel, M. and Gruenheid, S., 2005. Bank filtration and groundwater recharge for treatment of polluted surface waters. Water Supply 5(5), 57-66.

Kiefer, K., Müller, A., Singer, H. and Hollender, J., 2019. New Relevant Pesticide Transformation Products in Groundwater Detected Using Target and Suspect Screening for Agricultural and Urban Micropollutants with LC-HRMS. Water research 165.

Kiefer, K., Bader, T., Minas, N., Salhi, E., Janssen, E.M.L., von Gunten, U. and Hollender, J., 2020a. Chlorothalonil transformation products in drinking water resources: Widespread and challenging to abate. Water research 183.

Kiefer, K., Müller, A., Singer, H. and Hollender, J., 2020b. S60 | SWISSPEST19 | Swiss Pesticides and Metabolites from Kiefer et al 2019 (Version S60.0.1.1) [Data set], Zenodo. http://doi.org/10.5281/zenodo.3766352.

Kim, S., Chen, J., Cheng, T., Gindulyte, A., He, J., He, S., Li, Q., Shoemaker, B.A., Thiessen, P.A., Yu, B., Zaslavsky, L., Zhang, J. and Bolton, E.E., 2019. PubChem 2019 update: improved access to chemical data. Nucleic Acids Res 47(D1), D1102-D1109.

Knepper, T.P., Sacher, F., Lange, F.T., Brauch, H.J., Karrenbrock, F., Roerden, O. and Lindner, K., 1999. Detection of polar organic substances relevant for drinking water. Waste Management 19(2), 77-99.

Kolpin, D.W., Battaglin, W.A., Conn, K.E., Furlong, E.T., Glassmeyer, S.T., Kalkhoff, S.J., Meyer, M.T. and Schnoebelen, D.J., 2009. Transformation Products of Synthetic Chemicals in the Environment. Boxall, A.B.A. (ed), 83-100, Springer, Berlin, Heidelberg.

Kormos, J.L., Schulz, M., Wagner, M. and Ternes, T.A., 2009. Multistep Approach for the Structural Identification of Biotransformation Products of Iodinated X-ray Contrast Media by Liquid Chromatography/Hybrid Triple Quadrupole Linear Ion Trap Mass Spectrometry and 1H and 13C Nuclear Magnetic Resonance. Analytical chemistry 81(22), 9216-9224.

Krauss, M., Singer, H. and Hollender, J., 2010. LC-high resolution MS in environmental analysis: from target screening to the identification of unknowns. Anal Bioanal Chem 397(3), 943-951.

Letzel, T., Grosse, S. and Sengel, M., 2017. S2 | STOFFIDENT | HSWT/LfU STOFF-IDENT Database of Water-Relevant Substances (Version NORMAN-SLE-S2.0.1.0) [Data set], Zenodo. http://doi.org/10.5281/zenodo.2621452.

Li, Z., Kaserzon, S.L., Plassmann, M.M., Sobek, A., Gomez Ramos, M.J. and Radke, M., 2017. A strategic screening approach to identify transformation products of organic micropollutants formed in natural waters. Environ Sci Process Impacts 19(4), 488-498.

Liu, Y.S., Ying, G.G., Shareef, A. and Kookana, R.S., 2013. Biodegradation of three selected benzotriazoles in aquifer materials under aerobic and anaerobic conditions. J Contam Hydrol 151, 131-139.

Loos, R., Locoro, G., Comero, S., Contini, S., Schwesig, D., Werres, F., Balsaa, P., Gans, O., Weiss, S., Blaha, L., Bolchi, M. and Gawlik, B.M., 2010. Pan-European survey on the occurrence of selected polar organic persistent pollutants in ground water. Water research 44(14), 4115-4126.

Mak, Y.L., Taniyasu, S., Yeung, L.W.Y., Lu, G., Jin, L., Yang, Y., Lam, P.K.S., Kannan, K. and Yamashita, N., 2009. Perfluorinated Compounds in Tap Water from China and Several Other Countries. Environmental science & technology 43(13), 4824-4829.

Mechelke, J., Longree, P., Singer, H. and Hollender, J., 2019. Vacuum-assisted evaporative concentration combined with LC-HRMS/MS for ultra-trace-level screening of organic micropollutants in environmental water samples. Analytical and Bioanalytical Chemistry 411, 2555–2567.

Müller, A., Schulz, W., Ruck, W.K. and Weber, W.H., 2011. A new approach to data evaluation in the non-target screening of organic trace substances in water analysis. Chemosphere 85(8), 1211-1219.

Norman Network, Aalizadeh, R., Alygizakis, N.A., Schymanski, E.L., Slobodnik, J. and Fischer, S., 2020. S0 | SUSDAT | Merged NORMAN Suspect List: SusDat (Version NORMAN-SLE-S0.0.2.2) [Data set], Zenodo. http://doi.org/10.5281/zenodo.3695732.

PharmaWiki, 2020. Xipamid. https://www.pharmawiki.ch/wiki/index.php?wiki=Xipamid. Accessed: 14/11/2020.

Pimentel, D., 2009. Integrated Pest Management: Innovation-Development Process: Volume 1. Peshin, R. and Dhawan, A.K. (eds), 83-87, Springer Netherlands, Dordrecht.

R Core Team, 2020. R: A Language and Environment for Statistical Computing. R Foundation for Statistical Computing, Vienna, Austria. https://www.R-project.org/.

Reemtsma, T., Alder, L. and Banasiak, U., 2013. Emerging pesticide metabolites in groundwater and surface water as determined by the application of a multimethod for 150 pesticide metabolites. Water research 47(15), 5535-5545.

Rodil, R., Quintana, J.B., López-Mahía, P., Muniategui-Lorenzo, S. and Prada-Rodríguez, D., 2008. Multiclass Determination of Sunscreen Chemicals in Water Samples by Liquid Chromatography−Tandem Mass Spectrometry. Analytical chemistry 80(4), 1307-1315.

Ruttkies, C., Schymanski, E.L., Wolf, S., Hollender, J. and Neumann, S., 2016. MetFrag relaunched: incorporating strategies beyond in silico fragmentation. Journal of Cheminformatics 8(3).

Sangster, T., Major, H., Plumb, R., Wilson, A.J. and Wilson, I.D., 2006. A pragmatic and readily implemented quality control strategy for HPLC-MS and GC-MS-based metabonomic analysis. Analyst 131(10), 1075-1078.

Scheurer, M., Nödler, K., Freeling, F., Janda, J., Happel, O., Riegel, M., Müller, U., Storck, F.R., Fleig, M., Lange, F.T., Brunsch, A. and Brauch, H.-J., 2017. Small, mobile, persistent: Trifluoroacetate in the water cycle – Overlooked sources, pathways, and consequences for drinking water supply. Water research.

Schlüsener, M.P., Kunkel, U. and Ternes, T.A., 2015. Quaternary Triphenylphosphonium Compounds: A New Class of Environmental Pollutants. Environ Sci Technol 49(24), 14282-14291.

Schmidt, C.K., Fleig, M., Sacher, F. and Brauch, H.-J., 2004. Occurrence of aminopolycarboxylates in the aquatic environment of Germany. Environmental pollution 131(1), 107-124.

Schmidt, C.K. and Brauch, H.-J., 2008. N,N-Dimethylsulfamide as Precursor for N-Nitrosodimethylamine (NDMA) Formation upon Ozonation and its Fate During Drinking Water Treatment. Environmental science & technology 42(17), 6340-6346.

Schollée, J., Schymanski, E., Avak, S., Loos, M. and Hollender, J., 2015. Prioritizing Unknown Transformation Products from Biologically-Treated Wastewater Using High-Resolution Mass Spectrometry, Multivariate Statistics, and Metabolic Logic. Analytical chemistry 87(24), 12121-12129.

Schollée, J.E., 2018. TFAnalyzeR, version 1.0.1, Analysis of TraceFinder Target Screening, Zenodo, DOI: 10.5281/zenodo.3234748.

Schollée, J.E., Bourgin, M., von Gunten, U., McArdell, C.S. and Hollender, J., 2018. Non-target screening to trace ozonation transformation products in a wastewater treatment train including different post-treatments. Water Res 142, 267-278.

Schollée, J.E., Hollender, J. and McArdell, C.S., in preparation. Characterizing advanced treatment with ozone and activated carbon at multiple wastewater treatment plants through non-target screening.

Schulz, M., Loffler, D., Wagner, M. and Ternes, T.A., 2008. Transformation of the X-ray contrast medium iopromide in soil and biological wastewater treatment. Environ Sci Technol 42(19), 7207-7217.

Schulze, S., Zahn, D., Montes, R., Rodil, R., Quintana, J.B., Knepper, T.P., Reemtsma, T. and Berger, U., 2019. Occurrence of emerging persistent and mobile organic contaminants in European water samples. Water Res 153, 80-90.

Schymanski, E., Singer, H., Longrée, P., Loos, M., Ruff, M., Stravs, M., Ripollés Vidal, C. and Hollender, J., 2014a. Strategies to Characterize Polar Organic Contamination in Wastewater: Exploring the Capability of High Resolution Mass Spectrometry. Environmental science & technology 48(3), 1811-1818.

Schymanski, E.L., Jeon, J., Gulde, R., Fenner, K., Ruff, M., Singer, H.P. and Hollender, J., 2014b. Identifying small molecules via high resolution mass spectrometry: communicating confidence. Environmental science & technology 48(4), 2097-2098.

Schymanski, E.L., 2019. MetFrag Local CSV: CompTox (7 March 2019 release) Wastewater MetaData File (Version WWMetaData_4Oct2019) [Data set], Zenodo. http://doi.org/10.5281/zenodo.3472781.

Schymanski, E.L., 2020. ReSOLUTION: SOLUTIONS for High ReSOLUTION Mass Spectrometry. R package. https://rdrr.io/github/schymane/ReSOLUTION/.

Seiwert, B., Klockner, P., Wagner, S. and Reemtsma, T., 2020. Source-related smart suspect screening in the aqueous environment: search for tire-derived persistent and mobile trace organic contaminants in surface waters. Anal Bioanal Chem.

Stravs, M.A., Schymanski, E.L., Singer, H.P. and Hollender, J., 2013. Automatic recalibration and processing of tandem mass spectra using formula annotation. J Mass Spectrom 48(1), 89-99.

Stuart, M.E., Lapworth, D.J., Thomas, J. and Edwards, L., 2014. Fingerprinting groundwater pollution in catchments with contrasting contaminant sources using microorganic compounds. Sci Total Environ 468-469, 564-577.

Ter Laak, T.L., Puijker, L.M., van Leerdam, J.A., Raat, K.J., Kolkman, A., de Voogt, P. and van Wezel, A.P., 2012. Broad target chemical screening approach used as tool for rapid assessment of groundwater quality. Science of The Total Environment 427-428, 308-313.

Tian, Z., Peter, K.T., Gipe, A.D., Zhao, H., Hou, F., Wark, D.A., Khangaonkar, T., Kolodziej, E.P. and James, C.A., 2020. Suspect and Nontarget Screening for Contaminants of Emerging Concern in an Urban Estuary. Environ Sci Technol 54(2), 889-901.

Trcek, B., Zigon, D., Zidar, V.K. and Auersperger, P., 2018. The fate of benzotriazole pollutants in an urban oxic intergranular aquifer. Water Res 131, 264-273.

Wang, Z., Walker, G.W., Muir, D.C.G. and Nagatani-Yoshida, K., 2020. Toward a Global Understanding of Chemical Pollution: A First Comprehensive Analysis of National and Regional Chemical Inventories. Environmental science & technology 54(5), 2575-2584.

Weber, W.H., Seitz, W. and Schulz, W., 2007. Detection of the metabolites desphenyl-chloridazone and methyl-desphenyl-chloridazone in surface, ground and drinking water

(Nachweis der Metaboliten Desphenyl-Chloridazon und Methyldesphenyl-chloridazon in Oberflächen-, Grund- und Trinkwasser). Vom Wasser 105, 7-14.

Williams, A.J., Grulke, C.M., Edwards, J., McEachran, A.D., Mansouri, K., Baker, N.C., Patlewicz, G., Shah, I., Wambaugh, J.F., Judson, R.S. and Richard, A.M., 2017. The CompTox Chemistry Dashboard: a community data resource for environmental chemistry. J Cheminform 9(1), 61.

Wolf, L., Zwiener, C. and Zemann, M., 2012. Tracking artificial sweeteners and pharmaceuticals introduced into urban groundwater by leaking sewer networks. Science of The Total Environment 430, 8-19.

Ying, W.-C., Bonk, R.R., Lloyd, V.J. and Sojka, S.A., 1986. Biological treatment of a landfill leachate in sequencing batch reactors. 5(1), 41-50.

Zahn, D., Fromel, T. and Knepper, T.P., 2016. Halogenated methanesulfonic acids: A new class of organic micropollutants in the water cycle. Water Res 101, 292-299.

Zahn, D., Mucha, P., Zilles, V., Touffet, A., Gallard, H., Knepper, T.P. and Fromel, T., 2019. Identification of potentially mobile and persistent transformation products of REACH-registered chemicals and their occurrence in surface waters. Water Res 150, 86-96.

Chapter SI3: Supporting Information to Chapter 3 Identification of LC-HRMS Nontarget Signals in Groundwater After Source Related Prioritization

SI3-B and SI3-C can be found under:
doi.org/10.1016/j.watres.2021.116994

SI3-A1 Spike Solutions

For calibration standard preparation and spiking of samples, reference material was dissolved in ethanol, methanol, acetonitrile, ethanol/water mix, methanol/water mix, dimethyl sulfoxide, ethyl acetate, toluene, acetone, water, ethanol + 0.1 M HCl, or methanol + 0.1 M HCl at concentrations ranging from 100 to 1000 mgL^{-1}, depending on solubility and stability. Then, mix solutions were prepared in ethanol or acetonitrile at 10 mgL^{-1} which were combined for the final spike solutions (0.001, 0.01, 0.1 mgL^{-1}). The isotope labelled internal standard spike solution, containing 35 compounds, was prepared in ethanol at 0.1 mgL^{-1}.

SI3-A2: LC-HRMS Settings

Table SI3-A1: HPLC method

Autosampler: PAL RTC (CTC Analytics, Switzerland) **Pump: Dionex UltiMate3000 RS (Thermo Fisher Scientific, U.S.)** **Column: Atlantis T3 3 µm, 3.0 x 150 mm (Waters, Ireland)**	
Injection volume	140 µL
Flow rate	0.3 mL min^{-1}
Eluent A	Water + 0.1% formic acid
Eluent B	Methanol + 0.1% formic acid
Gradient	0 min: 100% eluent A, 0% eluent B 1.5 min: 100% eluent A, 0% eluent B 18.5 min: 5% eluent A, 95% eluent B 28.5 min: 5% eluent A, 95% eluent B 29 min: 100% eluent A, 0% eluent B 33 min: 100% eluent A, 0% eluent B

Table SI3-A2: ESI-HRMS/MS settings

Mass Spectrometer: Fusion Lumos (Thermo Fisher Scientific, U.S.)	
Spray voltage (kV)	3.5 / -2.5
Capillary temperature (°C)	300
Sheath gas (AU)	40
Auxiliary gas (AU)	10
S-lens RF level (AU)	60
Automatic gain control (AGC) target MS1	5×10^4
Maximum injection time MS1 (ms)	50
Scan range MS1 (m/z)	100 - 1000
Resolution MS1 (at m/z 200)	240,000
Internal calibration	Yes (EASY-IC™)
AcquireX enabled	TRUE
Cycle time	1 s
MS/MS activation type	Higher energy collisional dissociation (HCD)
Data-dependent trigger	Ions of mass list; if idle pick most intense
Min. precursor intensity to trigger MS/MS	10^4
Isolation window (m/z)	1
Resolution MS/MS (at m/z 200)	30,000
Automatic gain control (AGC) target MS/MS	1×10^4
Maximum injection time MS/MS (ms)	54
Dynamic exclusion time (s)	3
Normalized collision energy (NCE)	Stepped: 15, 30, 60

SI3-A3: Quantification

Quantification was performed in two steps. First, extracted ion chromatograms (EICs) were plotted to check if the compound was detected in groundwater samples. The detected compounds were then identified and quantified using Trace Finder 4.1 (Thermo Fisher Scientific, U.S.).

To check for detections, the EIC of the compound (most intense ion: $[M+H]^+$, $[M+NH4]^+$, $[M+Na]^+$, $[M-H]^-$, $[M+FA-H]^-$ or in-source fragment according to in-house database) was extracted and plotted with a 5 ppm window and a 4 min retention time window for calibration standards, spiked samples, blank samples and groundwater samples using the R package MSnbase (Gatto and Lilley 2012). If the compound was not detected, the limit of quantification (LOQ) was defined as the smallest spike level in the spiked samples (1, 10, 100 or 250 ngL^{-1}), which resulted in a chromatographic peak, i.e. at least five consecutive data points.

Detected compounds were further identified by comparing the measured MS/MS fragments to the MS/MS fragments in the in-house library or mzVault. Quantification was based on the peak area ratio of analyte and isotope labelled internal standard (ILIS) using a linear calibration model (weighting 1/x). If a structurally identical ILIS was not available, an ILIS was selected eluting at similar retention time as the analyte and resulting in a relative recovery close to 100% in the spiked samples. Relative recoveries were calculated based on the concentration in the spiked and not spiked samples:

$$\text{Relative Recovery} = \frac{\left(c_{\text{spiked sample}} - c_{\text{not spiked sample}}\right)}{\text{Theoretical Spike Level}} \quad \text{(SI-1)}$$

ILIS selection was supported by an internal R script using the functions published on Zenodo (Schollée 2018). For a detailed description of the R script, see SI2-A2. Concentrations determined in Trace Finder 4.1 were corrected with the relative recovery, if a structurally identical ILIS was not available.

For compounds detected in groundwater, the LOQ in matrix (LOQ_{Matrix}) was estimated according to equation (SI-2) from the LOQ in ultrapure water ($LOQ_{Ultrapure}$) defined as the lowest calibration standard with at least five data points along the chromatographic peak (MS1 full scan mode).

$$LOQ_{Matrix} = \frac{LOQ_{Ultrapure}}{\text{Absolute Recovery}} \quad \text{(SI-2)}$$

If the sample concentration was in the range of the LOQ_{Matrix}, the so-defined LOQ_{Matrix} was lowered if the chromatographic peaks in the samples were defined by at least five data points. Furthermore, the LOQ_{Matrix} was set at least twice higher than the concentration in all blank samples.

Absolute recoveries were determined for each analyte by comparing the peak area in the matrix to the peak area in ultrapure water, as described in the following. If a structurally identical ILIS was available, the peak area of the ILIS in the matrix was divided by the peak area of the ILIS in ultrapure water (median of all enriched calibration standards):

$$\text{Absolute Recovery}_{\substack{\text{Identical}\\\text{ILIS}}} = \text{Median}\frac{\text{Peak Area ILIS}_{Matrix}}{\text{Median (Peak Area ILIS}_{Ultrapure})} \quad \text{(SI-3)}$$

If a structurally identical ILIS was not available, the peak area of the analyte in the spiked sample (after subtracting the peak area in the not spiked sample) was compared to the peak area of the analyte in the calibration standard that corresponded to the spike level (10 and 100 ngL^{-1}):

$$\text{Absolute Recovery}_{\substack{\text{No Identical}\\\text{ILIS}}} = \frac{\text{Peak Area}_{\substack{\text{Spiked}\\\text{Sample}}} - \text{Peak Area}_{\substack{\text{Not Spiked}\\\text{Sample}}}}{\text{Peak Area}_{\substack{\text{Calibration}\\\text{Standard}}}} \quad \text{(SI-4)}$$

SI3-A4: enviMass Settings

Data pre-processing for suspect and nontarget screening was performed using the enviMass workflow (v4.2633). Table SI3-A3 and Table SI3-A4 list the workflow options and settings.

Table SI3-A3: Workflow options

Preprocessing	
Mass recalibration	Yes
Retention time alignment	Yes
Median intensity normalization	No
Blank / blind peak detection	Yes
Replicate filter	Yes
LOD interpolation	Yes
Targets	
Compound screening ILIS	Yes
Compound screening target	Yes
Intensity normalization using ILIS-profiles	Yes
Nontargets	
Peak shape correlation	Yes
File-wise componentization isotopologue	Yes
File-wise componentization adduct	Yes
File-wise componentization homologue series	No
Profile componentization	Yes
Watch list screening	No
Concentrations	
Calibration	No
Quantification	No
Recovery	No
Profiling	
Profile extraction	Yes
Profile filtering	Remove peaks from blinds: yes; remove peaks from spiked files: no
Profile blind detection	Yes
Trend detection	No
Comparisons	No

Table SI3-A4: Workflow settings

Peak Picking	
Filter RT range?	No
Filter mass range?	No
Parameter estimation	No
Maximum retention time gap in an EIC in s	300
Maximum m/z deviation of a centroid data in ppm	8.5
Minimum number of centroid data points per peak	3
…within a given a given RT window in s	3.8
Maximum RT gap length to be interpolated in s	10
Maximum RT width of a single peak ± from apex in s	120
Minimum log10(intensity) threshold	-10
Minimum Signal/Noise	3
Minimum Signal/Base	2
Maximum possible number of peaks within a single EIC	5
Peak area or peak intensoid?	Intensoid (max int.)
Instrument/Resolution	OT_Fusion, QExactiveHF_240000@200
Tolerances	
+/- m/z tolerance	1 ppm
Maximum RT deviation between peaks of the same analyte in s	1.5
Intensity tolerance in %	30
Mass Recalibration	
Reference compounds:	both
m/z tolerance	1 mmu
Maximum allowable m/z correction …	1 mmu
RT tolerance in s	30
Alignment	
reference file to align all other files	pos: 201811_pos_189_QC_4_R1; neg: 201811_neg_213_QC_2_R2
m/z tolerance	1 ppm (pos), 1 ppm (neg)
Reference peaks/masses	All peaks (recommended)
Maximum permissible (or expected) RT shift correction in s	30
Maximum number of most intense reference peaks to include	1000
Maximum number of iteration for match window adaption	4
Only include replicable peaks (if applicable)?	Yes
Only plot but do not apply alignment results?	No

Table SI3-A4 (continued)

Blind	
Factor by which the sample peak intensity must exceed the blank/blind peak intensity to not be subtracted	10
m/z tolerance in ppm	3
RT tolerances in s	60
Subtract with the blank/blind file(s) specified in the tag1 entry of each file (=comma-separated blind file IDs, otherwise set to FALSE)?	Yes
Replicates	
+/- m/z tolerance in ppm	2
RT tolerance window of peaks caused by the same analyte in s	30
Absolute log intensity tolerance X	10
Screening ILIS	
RT tolerance in s	60
Restriction to latest files	No
Cutoff score	0.8
Screen for MS/MS fragments	No
Screening Targets	
RT tolerance in s	60
Restriction to latest files	No
Cutoff score	0.8
Screen for MS/MS fragments	No
Screening Adducts	
Positive adducts	M+H, M+NH4, M+Na, M+K
Negative Adducts	M-H
Quantification	Not done
Normalization	Yes (positive & negative)
Minimum of screened files covered by each ILIS profile in %	90
Screening threshold	0.8
Minimum number of ILIS profile peaks per file (= ensures coverage):	15
Use subsampling	Yes
Number of blank/blind profiles in subsample:	100
Number of sample profiles in subsample:	100
Profiles	
Peak mass deviation within profiles: +/- m/z tolerance in ppm	3
Peak deviation within profiles: RT tolerance in s	60
Omit files with table entry profiled=FALSE from profiling?	TRUE

Table SI3-A4 (continued)

Trends	Not done
File wise Componentization Isotopologues	
Run atom bound estimation?	FALSE
File wise Componentization Adducts	
Positive Adducts	M+H, M+NH4, M+Na, M+K, M+DMSO+H, 2M+H
Negative Adducts	M-H, 2M-H, M+FA-H, M+Cl, M-2H
File wise Componentization Peak Shape Correlation	
Min. number of MS1 scans over which peak pairs co-elute to check for their peak shape correlation:	10
Min. Spearman correlation [0,1] coefficient:	0.9
Profile Componentization	
Restrict profile componentization to a set of latest files only?	FALSE
Filtering of outliers in profile component relations (recommended):	TRUE
Allow searching for additional adducts for peak shape correlated profiles?	FALSE
Restrict profile componentization to isotopologue and selected adduct relations only?	FALSE
Restrict profile componentization to top 100 most intense & trend profiles only?	FALSE

SI3-A5: Estimation of Nontarget Concentrations

The concentration of nontargets was estimated from peak height intensities of target compounds in spiked samples. First, peak height intensities were determined using Trace Finder 4.1. Then, the 25th, 50th, and 75th percentiles of peak height intensities were calculated for each spiking level (1, 10, 100, 250 ngL^{-1}) and for positive and negative ionization mode separately. Target compounds which were detected at concentrations of >20% of the spiking level in one of the spiked samples were excluded. Then, linear calibration models (Figure SI3-A1) were calculated to estimate nontarget concentrations assuming that nontargets (i) ionize on average less efficiently than targets (25th percentile), (ii) ionize on average as efficiently as targets (50th percentile), or (iii) ionize on average more efficiently than targets (75th percentile).

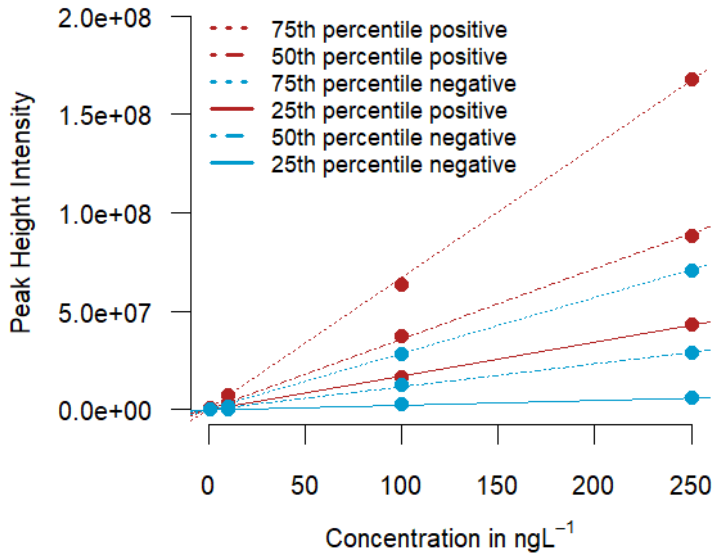

Figure SI3-A1: Linear regression models between spiking levels (1, 10, 100, 250 ngL^{-1}) and 75th, 50th, and 25th percentiles of peak height intensities of target compounds in four groundwater samples. Regression was forced through the origin.

SI3-A6: Structure Elucidation with MetFrag and SIRIUS4/CSI:FingerID

MetFrag (Ruttkies et al. 2016) and SIRIUS4/CSI:FingerID (Dührkop et al. 2015, Dührkop et al. 2019) were used (i) in the nontarget screening to support structure elucidation and (ii) in the suspect screening to test if the experimental MS/MS spectrum fits to the suspect structure.

First, MS1 and MS/MS spectra were extracted for each nontarget/suspect profile for the monoisotopic ion from the mzXML files using the RMassBank package (Stravs et al. 2013). The most intense MS1 and MS/MS scans at given retention time (±30 s) were written to txt files after removing peaks with intensity <1% relative to the base peak to reduce noise signals. The enviMass workflow (version 4.2633) exports the m/z of the most intense feature within a component. However, the most intense feature is not necessarily the monoisotopic ion (e.g. brominated or multiple chlorinated compounds). Therefore, the isotope pattern of profiles with mass defect <0 (Br, Cl have a negative mass defect) were checked manually and the m/z of the monoisotopic ion was selected for MS1 and MS/MS spectra extraction. For further processing with MetFrag and SIRIUS4/CSI:FingerID, the spectra from the mzXML file, where the

nontarget/suspect was detected at highest intensity, was used and it was assumed that the m/z represents the $[M+H]^+$ or $[M-H]^-$.

MetFrag CL 2.4.5 was run in batch mode using the R functions MetFragConfig and runMetFrag adapted from the R package ReSOLUTION (Schymanski 2020). For each profile, MetFrag retrieved candidates matching the m/z within 2 ppm from a local csv file. For details on the compound lists used in suspect and nontarget screening, respectively, refer to the manuscript and Table SI3-A5. Salts and stereoisomers were removed using the unconnected compound and InChIKey filters implemented in MetFrag. The candidates were fragmented in silico using a bond dissociation approach. In silico fragments were compared to experimental fragments with a relative mass deviation of 7 ppm (mass accuracy in MS/MS scan mode was lower than in MS1 scan mode). The maximum tree depth was 2. Finally, candidates were ranked using different scoring terms (Table SI3-A6).

MS1 and MS/MS spectra were converted to ms and msp format, and then imported in batch mode to SIRIUS4/CSI:FingerID or the NIST Mass Spectral Search Program (version 2.3). SIRIUS4/CSI:FingerID was operated with the same local compound lists as used with MetFrag. Molecular formula prediction was limited to formulae available in the compound lists as otherwise for many nontarget/suspect profiles unrealistic formulae were suggested.

Table SI3-A5: Number of compounds originating from various lists used for structure elucidation in nontarget and suspect screening. Stereoisomers were removed by filtering for the first block of the InChIKey. The column "Additional Compounds" refers to the number of compounds, which are not included in lists above; e.g. NORMAN SusDat comprises 65,596 compounds (without stereoisomers), but 51,887 are part of CompTox.

Compound List in Nontarget Screening	**No. of Compounds**	**Additional Compounds**
CompTox (Schymanski 2019)	773,232	773,232
NORMAN SusDat (Norman Network et al. 2020)	65,596	13,709
PubChemLite tier1 (Bolton and Schymanski 2020)	363,911	200,698
Extended PMT (H.-P. Arp and S.E. Hale, personal communication)	2,124	215
STOFF-IDENT (Letzel et al. 2017)	11,071	95
SwissPest19 (Kiefer et al. 2020)	1,472	521
Further pesticide transformation products (T. Poiger, personal communication)	618	71
Compound List in Suspect Screening	**No. of Compounds**	**Additional Compounds****
Extended PMT (H.-P. Arp and S.E. Hale, personal communication)*	607	548
UBAPMT (Arp and Hale 2020)	215	38
Schulze et al. (2019)	64	21
KEMI Market List (Fischer 2017)*	796	555

*Original lists contain more compounds. Lists were filtered for compounds that are more likely to occur in groundwater (see details in manuscript). **Only compounds with heteroatoms and exact mass >100.

Table SI3-A6: MetFrag scoring terms and their weightings used for nontarget and suspect screening.

Scores in Nontarget Screening	**Weighting**
FragmenterScore	1
AutomatedPeakFingerPrintAnnotationScore (Ruttkies et al. 2019)	1
AutomatedLossFingerPrintAnnotationScore (Ruttkies et al. 2019)	1
RetentionTimeScore →retention time prediction based on target compounds	1
OfflineMetFusionScore (Gerlich and Neumann 2013)	1
OfflineIndividualMoNAScore → similarity with candidate in MassBank of North America (MoNA; built into MetFrag)	1
PatentCountScore → patent count from PubChem	0.25
CompTox DATA_SOURCES	0.25
KEMI_ExposureScore_Water_0to1	0.25
PMT_Emission_likely → emission likely? Yes or no (according to H.-P. Arp, personal communication)	0.25
Scores in Suspect Screening	**Weighting**
FragmenterScore	1
RetentionTimeScore →retention time prediction based on target compounds	1
SuspectListScore → higher ranking if structure on suspect list	1
PatentCountScore → patent count from PubChem	1

SI3-A7: Suspect/Nontarget Confirmation and Quantification

Ten samples and one pooled sample comprising all prioritized suspects and nontargets (sample aliquots which were not thawed previously), five spiked samples (100, 250, 1000 ngL^{-1}), two blanks, and four calibration standards were enriched and measured as described in SI3-A2 with the following slight modifications. AcquireX was not used. The mass list comprised only the m/z of the prioritized suspects and nontargets. The dynamic exclusion time was reduced to 1 s to increase the number of MS/MS scans along a chromatographic peak.

Suspects and nontargets were confirmed based on matching MS/MS spectra and retention time in standard and sample with the following method. Using the R package MSnbase (Gatto and Lilley 2012), the EICs of the most intense adduct in standard, sample and spiked sample were extracted (mass window 5 ppm) and plotted to check the retention time. Then, the five most intense fragments in the standard were determined, and the EICs of these fragments (in standard and samples) were plotted. Head to tail plots were created with the R package MSMSsim (https://github.com/dutchjes/MSMSsim). The resulting plots are compiled in SI3-A12.

Concentrations were determined in the 60 samples by applying the calibration model determined later with the same LC-HRMS system. The calibration standards used for this calibration model were prepared with the same ILILS spike solution as was used for the first analysis. The quality of quantification was evaluated based on relative recoveries in spiked samples (ideally 80-120% in all spiked samples) and consistency of concentrations determined in samples, which were measured twice (i.e. first analysis and together with calibration standards). For some compounds, quantification was not satisfactory so that either no concentrations or concentration ranges were reported.

SI3-A8: Sample Classification based on Target Screening

The classification based on the target screening was consistent with the pre-classification based on long-term monitoring data for 53 out of 60 monitoring sites. For three sites pre-classified as urban impacted, the concentration sum of urban targets was (slightly) below the cut-off of 100 ngL^{-1} (i.e. 42, 53 and 99 ngL^{-1}). Two of these sites were classified as having high agricultural influence, one exhibited only low urban and agricultural influence. Four sites were pre-classified as having low anthropogenic impact but showed 140 to 640 ngL^{-1} of agricultural targets (concentration sum of urban targets <28 ngL^{-1}) resulting in a classification as sites with high agricultural influence.

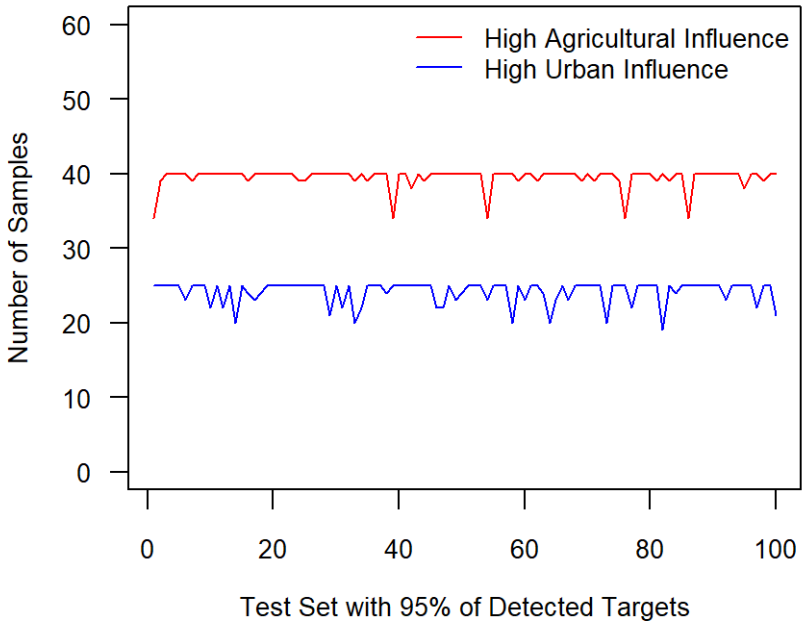

Figure SI3-A2: The 60 groundwater monitoring sites were classified using 100 randomly selected subsets of target compounds. Each subset comprised 95% of detected targets. The number of samples classified as having high agricultural or urban influence ranged from 34 to 40 and 19 to 25, respectively.

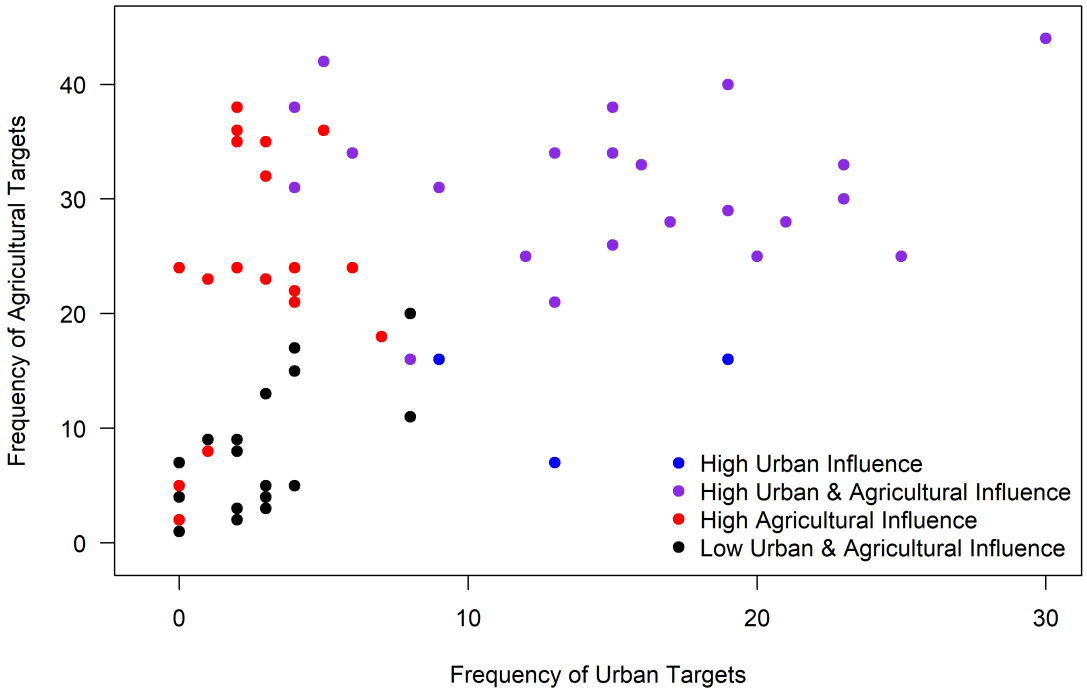

Figure SI3-A3: Detection frequency of agricultural targets versus detection frequency of urban targets at each monitoring site. The monitoring sites are coloured according to their classification based on concentration sums.

Table SI3-A7: Target compounds with detections ≥100 ngL^{-1}. The $logD_{OW\ pH7}$ (water-n-octanol distribution coefficient considering the speciation at pH 7) was predicted with JChem for Office, version 19.22.0.548, ChemAxon Ltd. LOQ (limit of quantification). c_{max} (maximum concentration) in the 60 groundwater samples.

Target Compound	**Classification**	**$LogD_{ow\ pH7}$**	**LOQ in ngL^{-1}**	**Detec-tions**	**c_{max} in ngL^{-1}**
Sum 4- &5-methyl-benzotriazole	Corrosion inhibitor	1.8	0.1	33	100
Benzotriazole	Corrosion inhibitor	1.3	0.2	40	220
Melamine	Industrial chemical	-2.5	5	14	690
Diatrizoate	Pharmaceutical	-0.6	1	17	240
N-N-Didesvenlafaxin	Pharmaceutical TP	-0.4	1.5	3	410
Acesulfame	Sweetener	-1.5	0.1	52	150
Sucralose	Sweetener	-0.5	100	2	230
N-N-Dimethylsulfamide	Pesticide/biocide TP	-1.5	1	30	470
Atrazine	Pesticide	2.2	0.1	52	160
Bentazone	Pesticide	-0.2	0.2	14	210
Cycluron	Pesticide	2	1	1	140
Mecoprop	Pesticide	-0.3	1	1	240
Atrazine-desethyl	Pesticide TP	1.5	0.1	51	100
Chloridazon-desphenyl	Pesticide TP	-0.7	1	33	1600
Chloridazon-methyl-desphenyl	Pesticide TP	-0.6	0.5	37	610
Chlorothalonil TP R417888	Pesticide TP	-0.7	0.5	50	940
Chlorothalonil TP R419492	Pesticide TP	-4.5	5	36	740
Chlorothalonil TP R471811	Pesticide TP	-1.7	3	60	2200
Chlorothalonil TP SYN507900	Pesticide TP	0.4	1	13	130
Metazachlor-OXA	Pesticide TP	-1	5	5	120
Metolachlor-ESA	Pesticide TP	-0.3	0.5	41	920
Metolachlor TP CGA 368208 (=Acetochlor sulfonic acid)	Pesticide TP	-0.5	2	22	280
Nicosulfuron TP UCSN	Pesticide TP	-2.3	1	38	140
Terbuthylazine TP CSCD648241	Pesticide TP	-2.5	0.2	44	120

SI3-A9: Characterization of Compounds

Natural organic matter (NOM): Naturally occurring compounds should be located in the centre of Figure 2 (see manuscript), either because the NOM molecules occur at each site or are randomly distributed. Therefore, we investigated the compounds located in the centre of Figure 2 with >40 detections and retention time >4 min in more detail. 40% of these compounds (profiles) were composed of several profiles (>2) grouped in the post-processing, i.e. these profiles were grouped together due to a similar m/z and retention time (<2 ppm, <30 s; section 2.5.1 in manuscript). These 106 compounds were detected in positive ionization mode and eluted after 10 min (except for one compound). In the whole dataset, only 328 compounds were composed of >2 profiles exported from enviMass and eluting after 10 min (319 compounds in positive mode, 9 compounds in negative mode). The EICs were manually checked and showed mostly a broadly-eluting peak (>5 min, Figure SI3-A4), which was found either in all samples or only in some samples (but not in blank samples). Such broad peaks cannot be correctly detected in peak picking algorithms so that several profiles are formed. Furthermore, these compounds had on average a more positive mass defect and higher m/z than the compounds from the remaining dataset (Figure SI3-A5). 24 profiles with a broadly-eluting peak were annotated using MetFrag and SIRIUS4/CSI:FingerID (SI-B2). The molecular formulae of the candidates comprised in most cases only C, H, O, and partially N, S, and Si atoms. Therefore, we speculate that these profiles represent NOM.

Cl-containing compounds: To get further evidence for an anthropogenic origin, the MS1 spectra of each compound were checked for characteristic isotope patterns such as Cl. Accordingly, at least 50 of the 488 compounds indicated the presence of one or more Cl atoms (SI-B2). However, 11 of the putatively mono-chlorinated compounds likely represented Cl adducts ($[M+Cl]^-$), which is supported by a co-eluting peak of the m/z of the corresponding $[M-H]^-$. Analogously, a nontarget compound classified as potential urban contaminant was finally elucidated as the $[M+Cl]^-$ of the target compound sucralose. The $[M+Cl]^-$ was ten times more intense than the $[M-H]^-$.

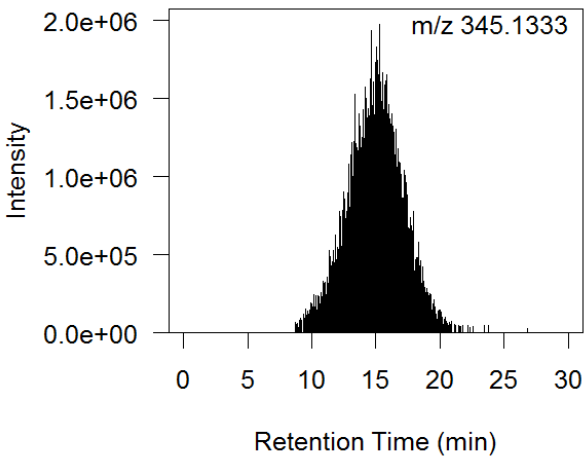

Figure SI3-A4: Extracted ion chromatograms of a grouped profile composed of four profiles exported from enviMass (positive ionization, m/z 345.1333). A broad peak was detected in all samples except for blank samples (enriched ultrapure water).

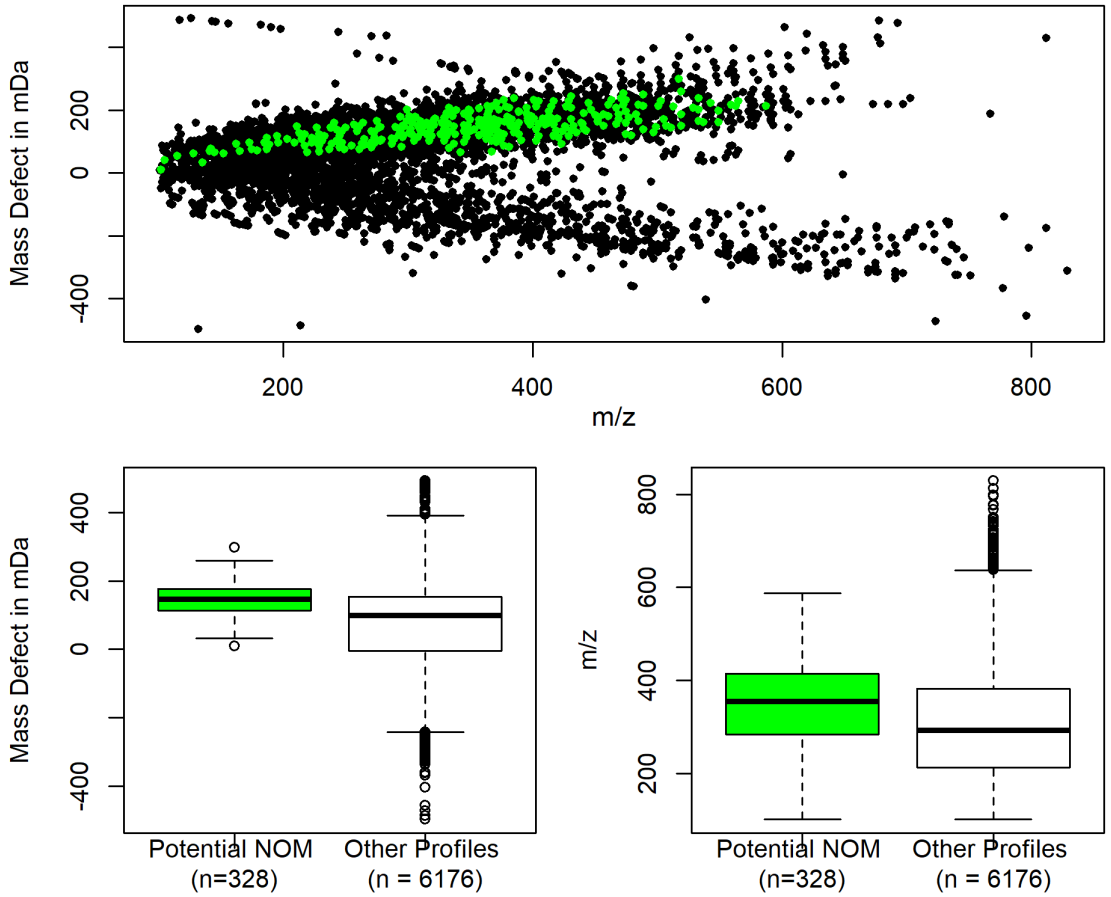

Figure SI3-A5: Mass defect and m/z range of the 328 profiles representing potential natural organic matter (NOM, green) and of the remaining 6176 profiles (black). The potential NOM profiles were extracted from the dataset by filtering for grouped profiles (composed of >2 profiles) with retention time >10 min.

SI3-A10: Evaluation of AcquireX

To investigate if AcquireX increased the MS/MS coverage, we compared the MS/MS coverage for the 488 nontargets (maximum intensity >5 × 10^6) and 695 suspects (maximum intensity >10^6) in the first replicate injections (mass list contained only precursor m/z of targets), with the MS/MS coverage in the second replicate injections (mass list contained precursor m/z of targets and features detected by AcquireX), and third replicate injections (precursor m/z which were triggered in second injection were shifted from mass list to exclusion list).

Assuming that without the use of AcquireX, MS/MS coverage would be in all three replicates similar, because always the most intense precursors are triggered, AcquireX increased the MS/MS coverage of nontargets by 39%, i.e. 28% more MS/MS were triggered in the second replicate injections than in the first injections and 11% additional MS/MS were triggered in the third injections compared to the first injections. In case of the suspects, AcquireX increased the MS/MS coverage by 73%, i.e. 56% more MS/MS were triggered in the second replicate injections than in the first injections and 17% additional MS/MS were triggered in the third injections compared to the first injections. Probably, AcquireX showed a smaller influence on the nontargets than on the suspects, because the nontargets were on average more intense and therefore also triggered without AcquireX (median of maximum intensity of nontargets vs. suspects: 1.2 × 10^7 vs. 1.7 × 10^6). Moreover, AcquireX improved the MS/MS coverage especially in positive ionization mode, possibly, because less compounds ionize in negative mode so that also without AcquireX a high MS/MS coverage is achieved.

SI3-A11: Characterization of Groundwater Monitoring Sites

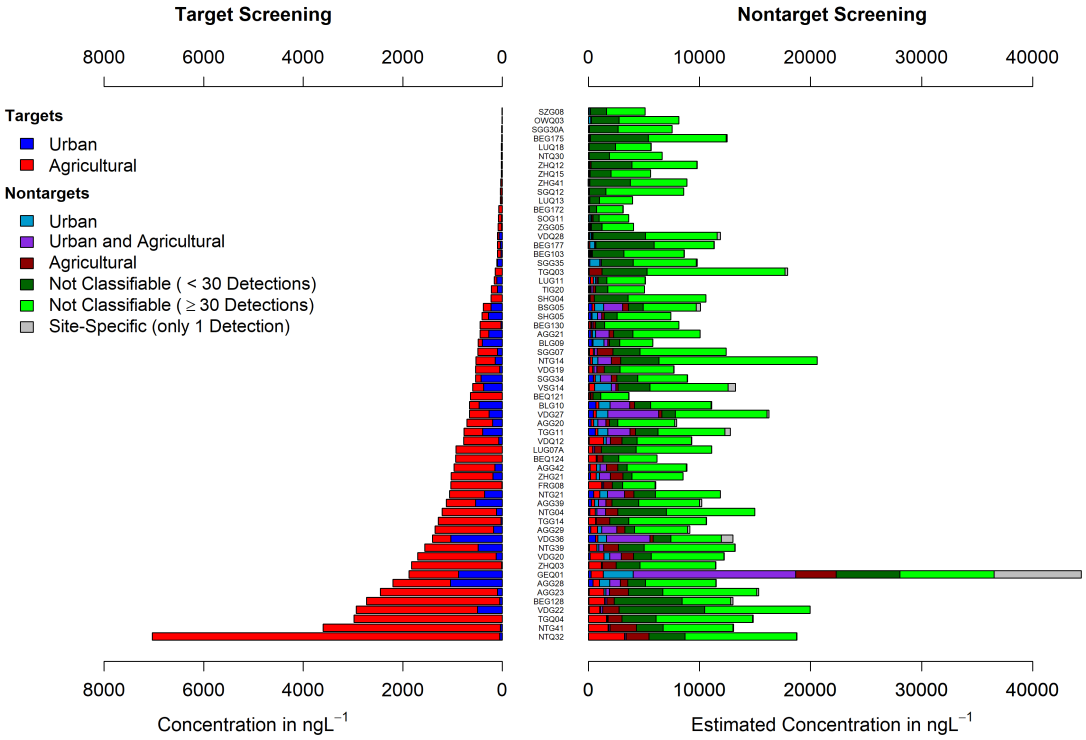

Figure SI3-A6: Total concentrations determined in the target screening (left) and estimated concentrations determined in the nontarget screening. In contrast to Figure 3 (manuscript), all compounds (profiles) are included.

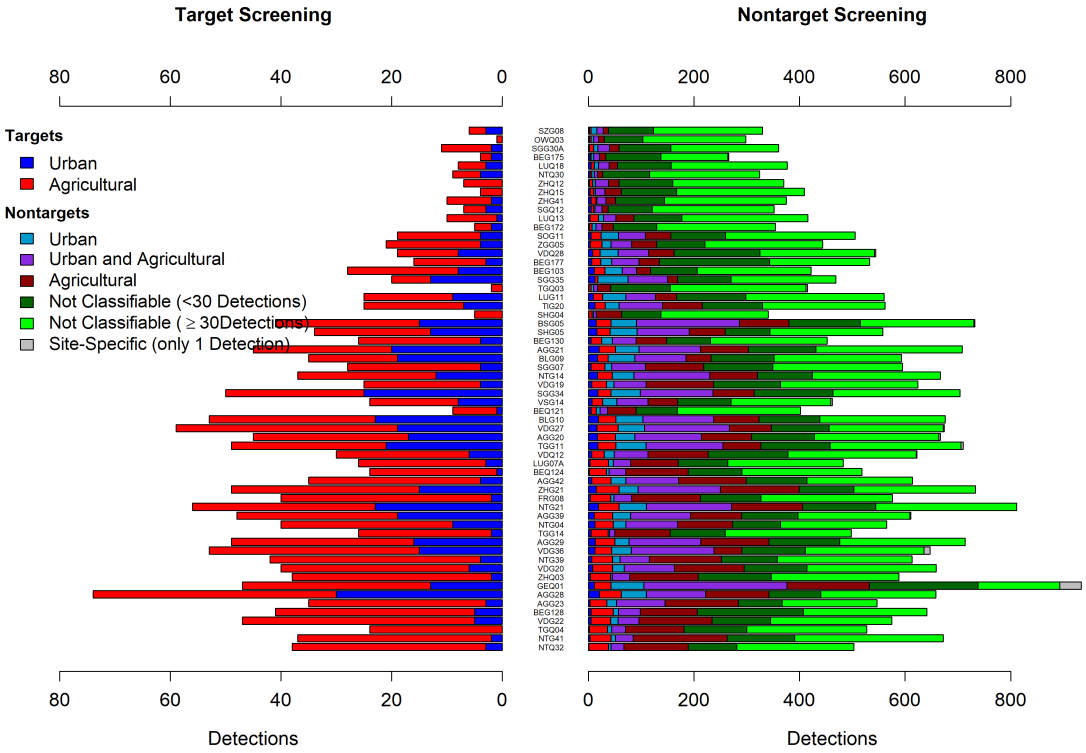

Figure SI3-A7: Number of detections in the target screening (left) and number of detected compounds (profiles) in the nontarget screening (right). Potential false positives (see manuscript) are not shown.

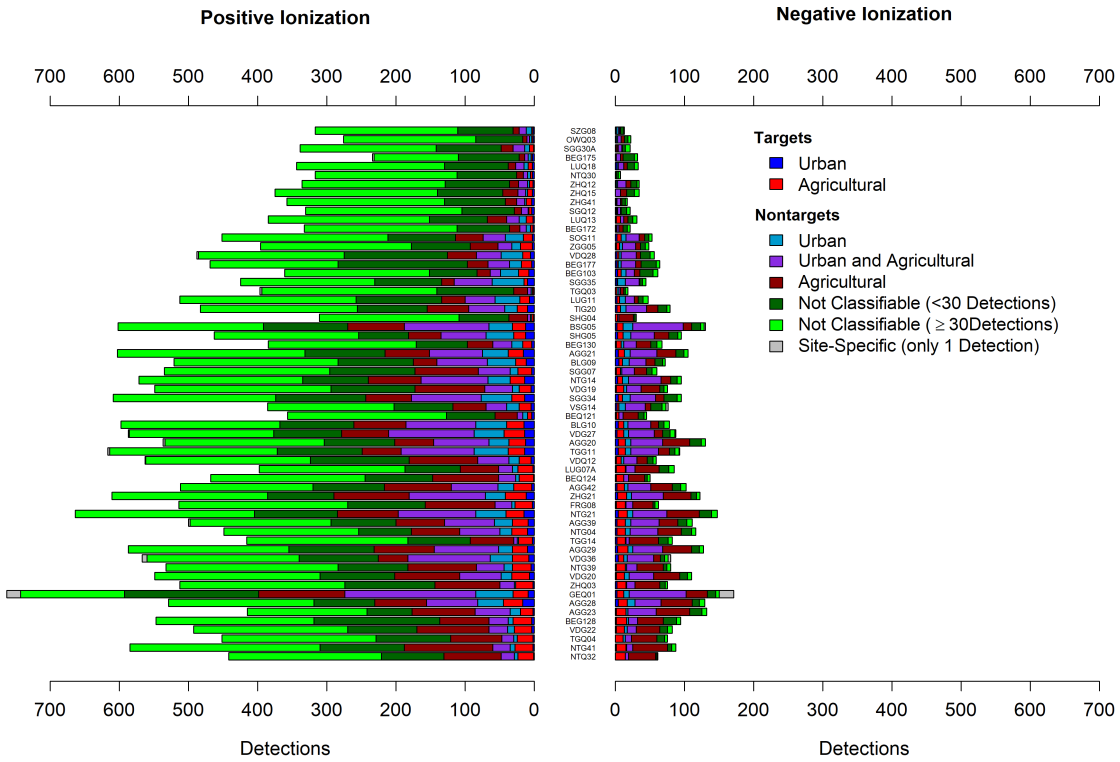

Figure SI3-A8: Number of detections in the nontarget screening in positive ionization mode (left) and negative ionization mode (right). Potential false positives (see manuscript) are not shown.

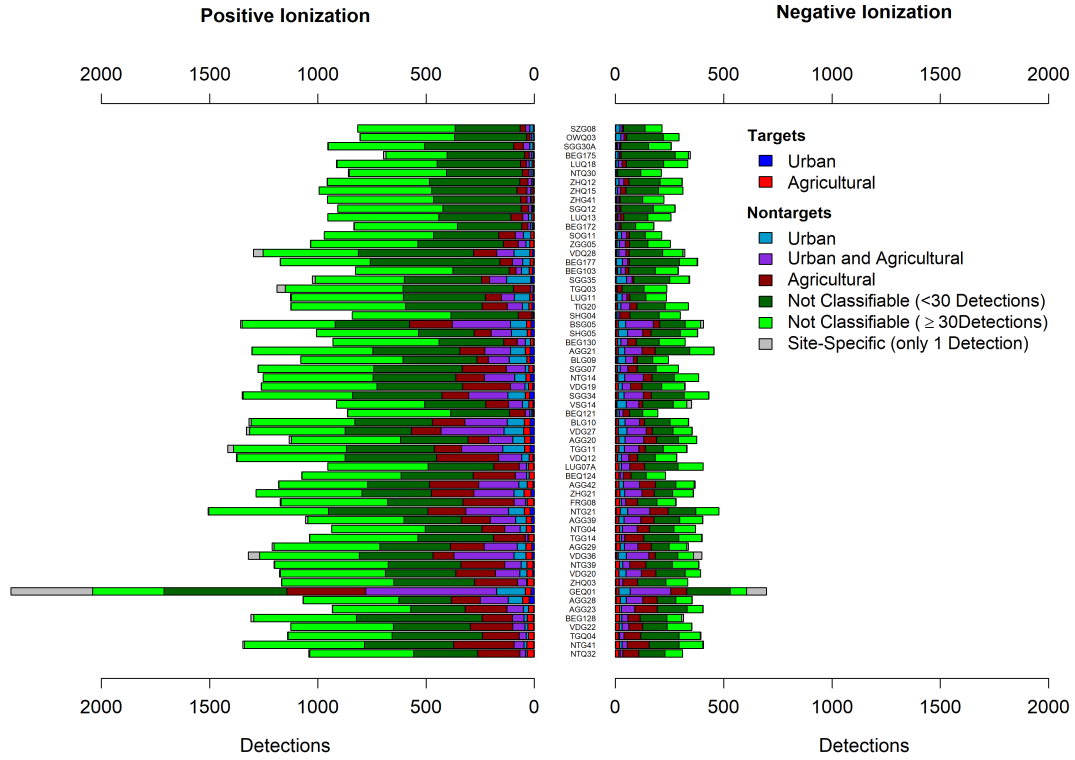

Figure SI3-A9: Number of detections in the nontarget screening in positive ionization mode (left) and negative ionization mode (right). All compounds (profiles) are shown.

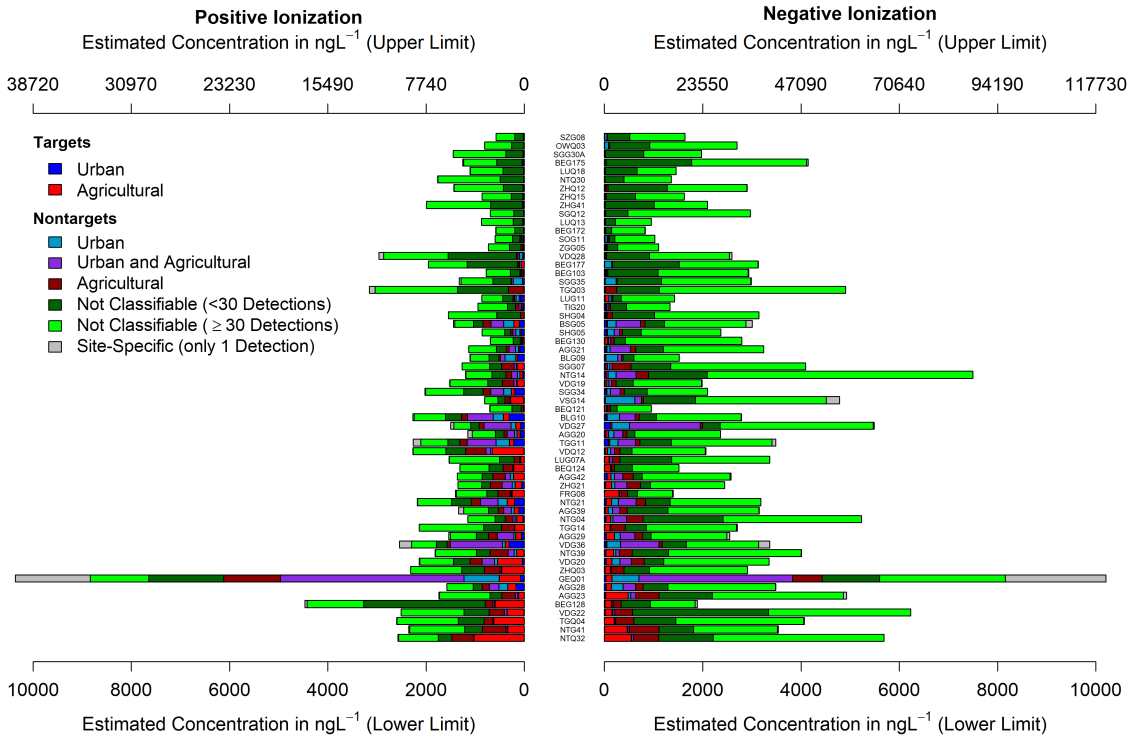

Figure SI3-A10: Upper (top x-axis) and lower (bottom x-axis) estimated concentrations of all compounds (profiles) detected in positive and negative ionization mode.

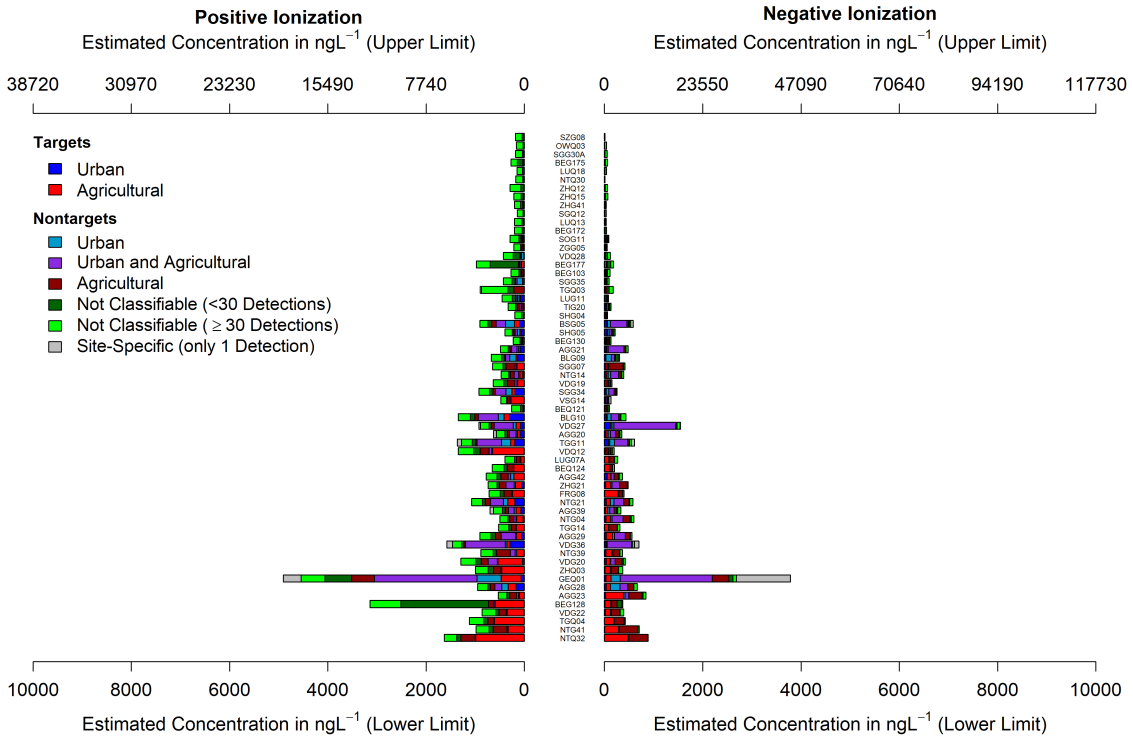

Figure SI3-A11: Upper (top x-axis) and lower (bottom x-axis) estimated concentrations of compounds (profiles) detected in positive and negative ionization mode. Potential false positives (see manuscript) are not shown.

SI3-A12: Confirmation of Suspects and Nontargets

The following figures illustrate the EICs of the precursor ion and of the five most intense MS/MS fragments in standards, samples, and spiked samples for suspects and nontargets identified unequivocally (Level 1). By comparing the EICs of the MS/MS ions and precursor ions, background ions (i.e. no true fragments of the precursor) can be identified (see e.g. 2-Acrylamido-2-methyl-1-propanesulfonic acid). Fragmentation was performed at three different NCEs (15, 30, 60), i.e. mix MS/MS spectra are shown. Using head to tail plots, MS/MS spectra of standard and sample are compared. In case of Level 2a candidates, MS/MS spectra are provided and fragments reported in literature (Kormos et al. 2009, Reemtsma et al. 2013, Schulz et al. 2008) or mzCloud (www.mzcloud.org) were marked. In case of Level 3 candidates, MS/MS spectra were annotated with structure proposals.

2,5-Dichlorobenzenesulfonic Acid
GEQ01, Level 1
[M-H]- 224.91854
(STD 100 ng/L)

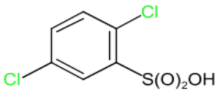

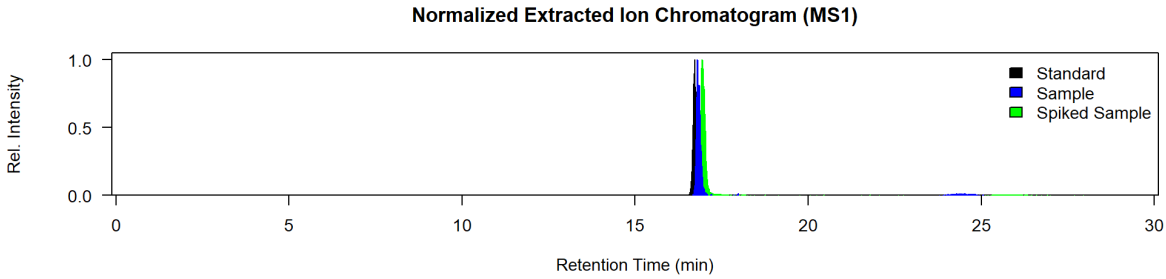

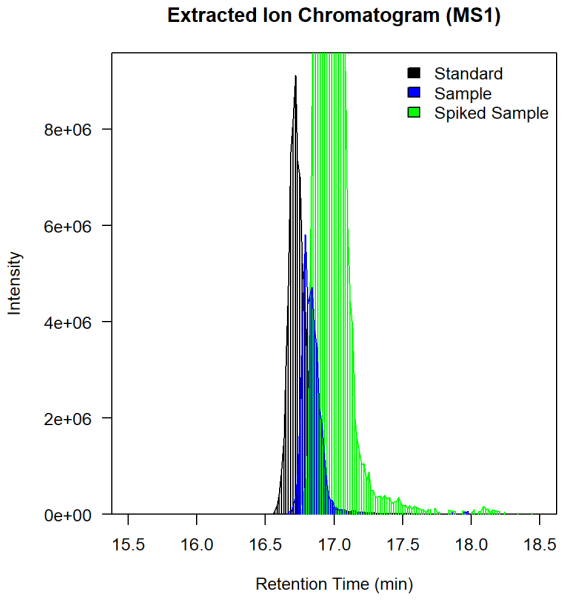

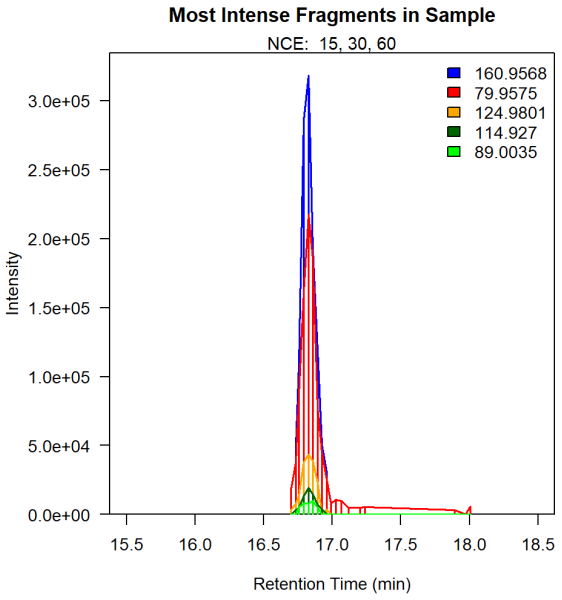

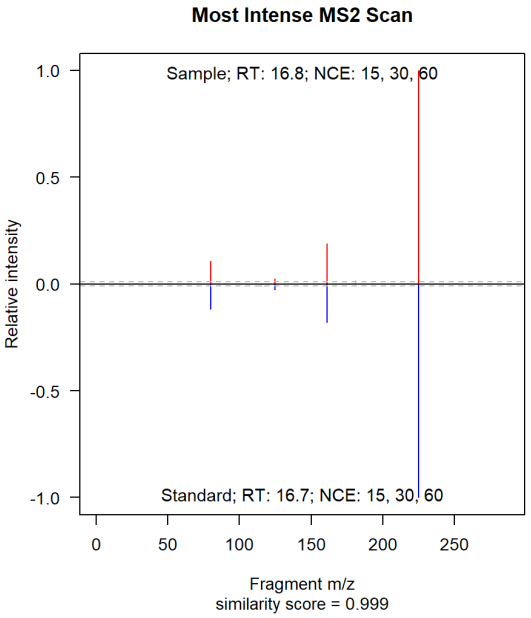

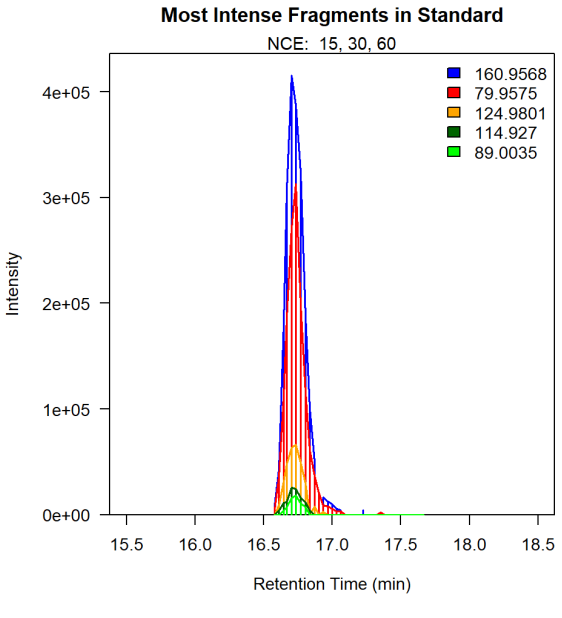

Phenylphosphonic Acid
VDG36, Level 1
[M+H]+ 159.02056
(STD 100 ng/L)

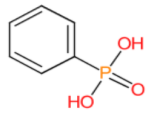

Normalized Extracted Ion Chromatogram (MS1)

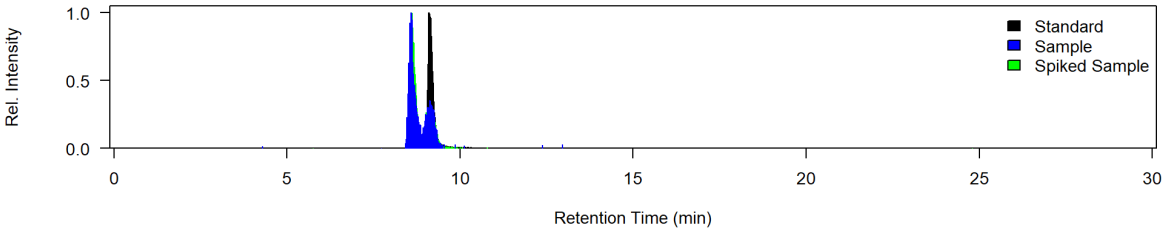

Extracted Ion Chromatogram (MS1)

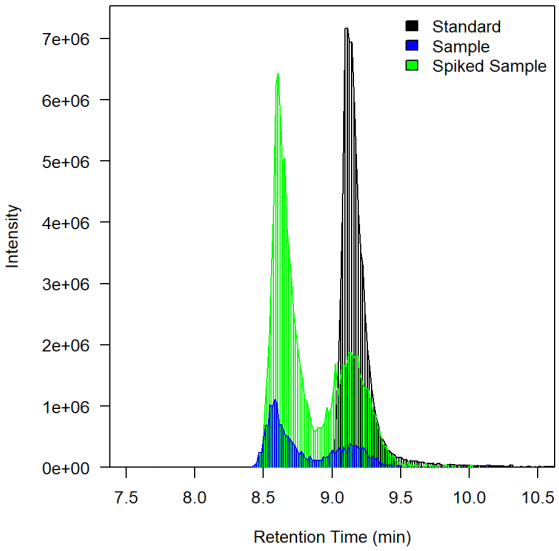

Most Intense Fragments in Sample

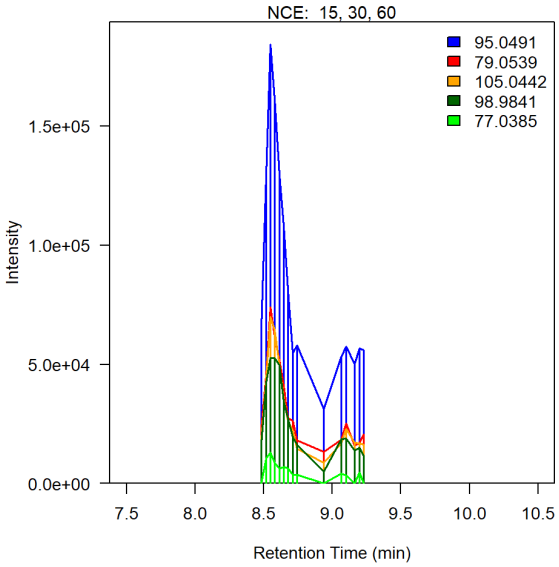

Most Intense MS2 Scan

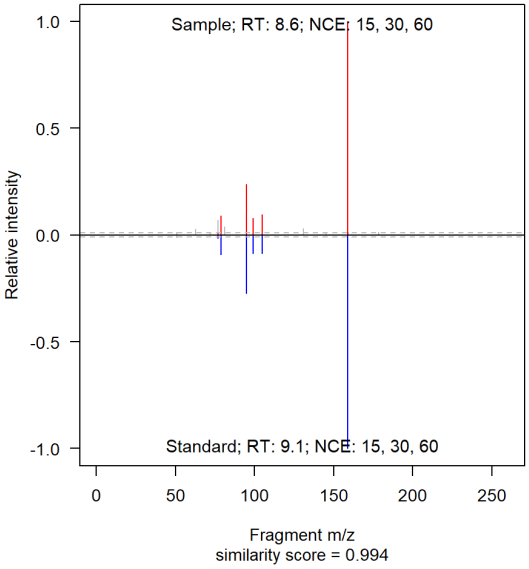

Most Intense Fragments in Standard

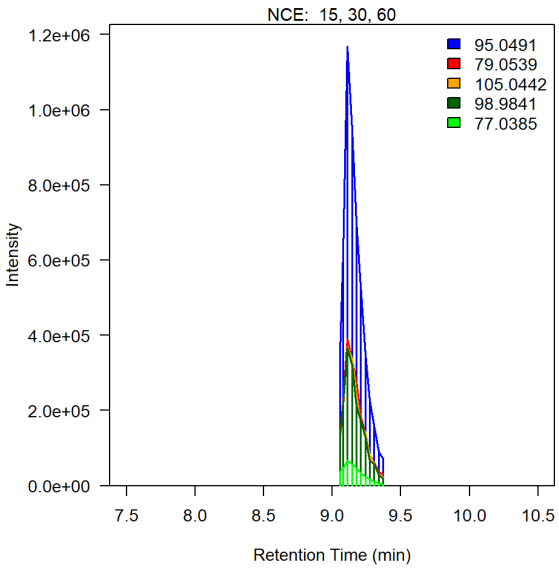

Triisopropanolamine borate
BLG10, Level 1
[M+H]+ 199.14888
(STD 100 ng/L)

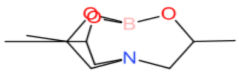

Normalized Extracted Ion Chromatogram (MS1)

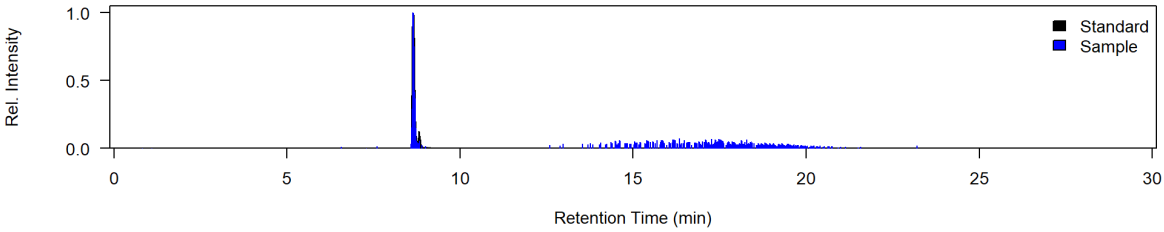

Extracted Ion Chromatogram (MS1)

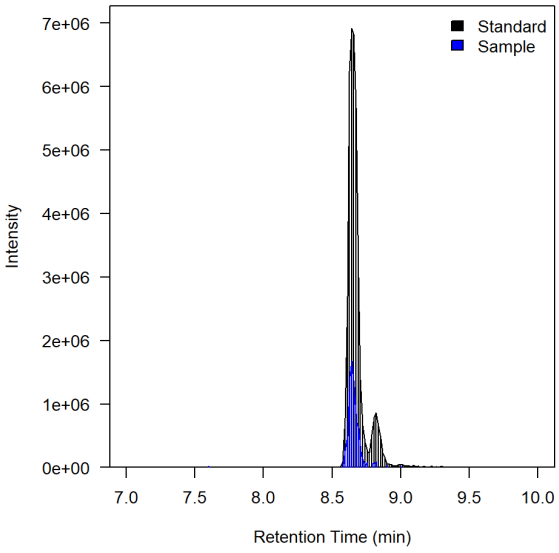

Most Intense Fragments in Sample

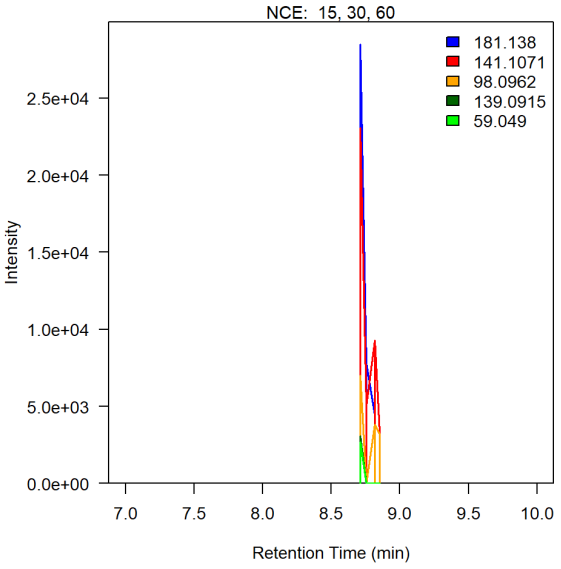

Most Intense MS2 Scan

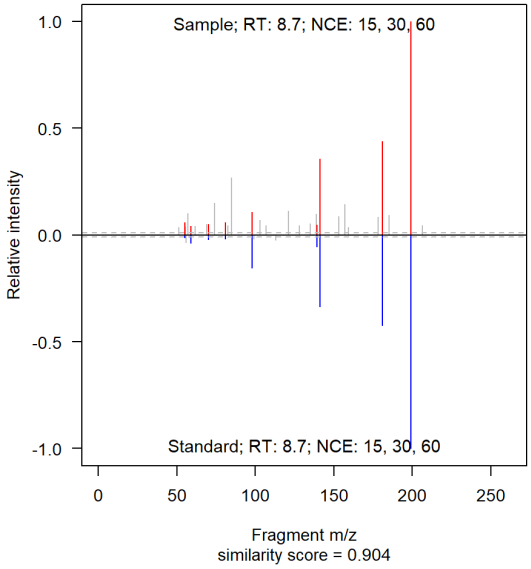

Most Intense Fragments in Standard

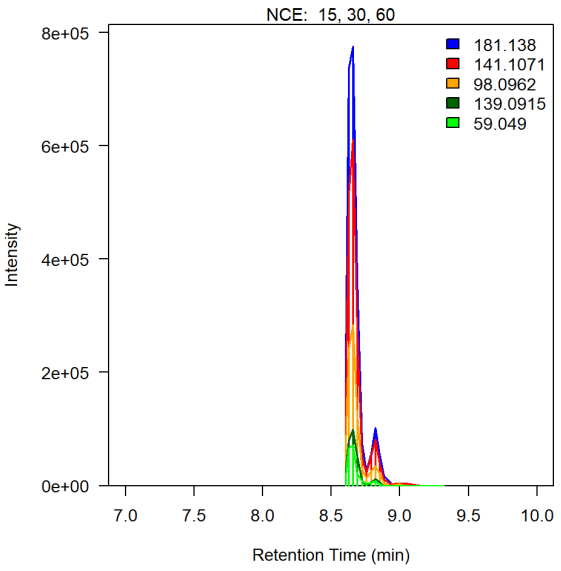

2-Methyl-5-Nitrobenzenesulfonic Acid
BSG05, Level 1
[M-H]- 215.99722
(STD 100 ng/L)

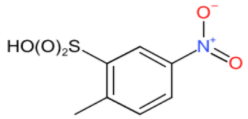

Normalized Extracted Ion Chromatogram (MS1)

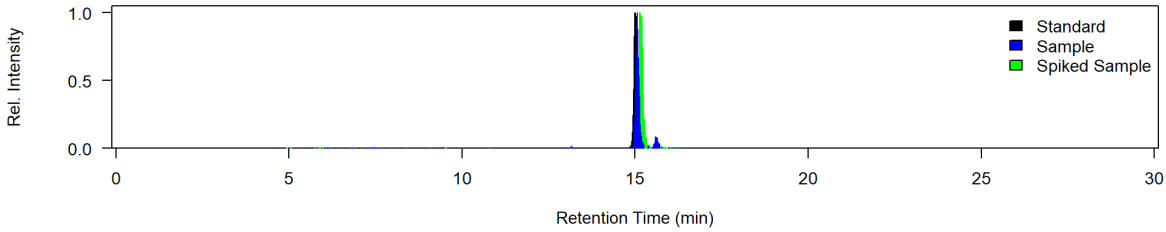

Extracted Ion Chromatogram (MS1)

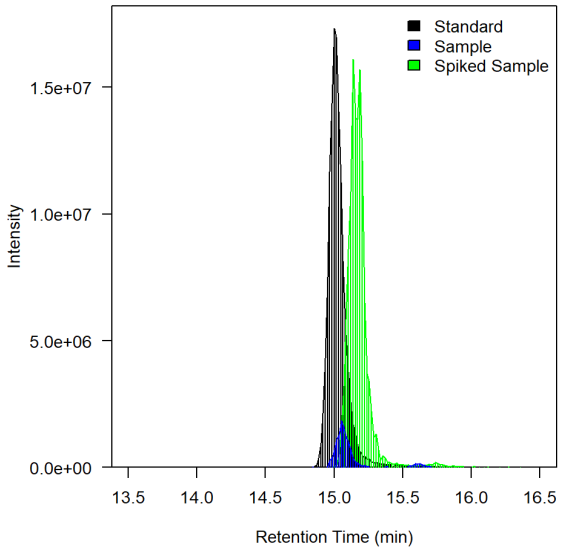

Most Intense Fragments in Sample

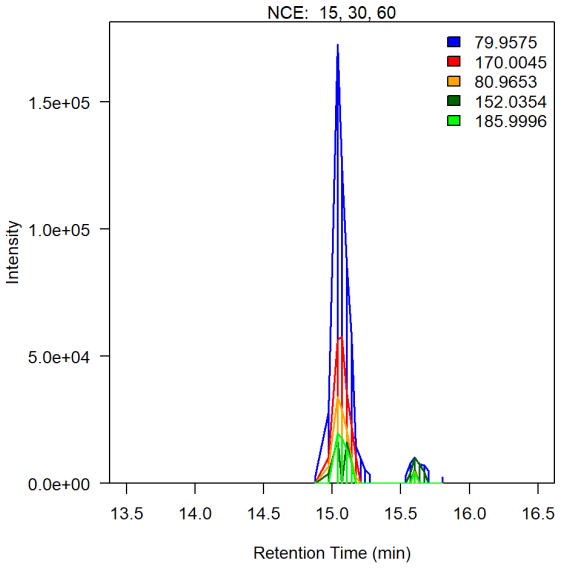

Most Intense MS2 Scan

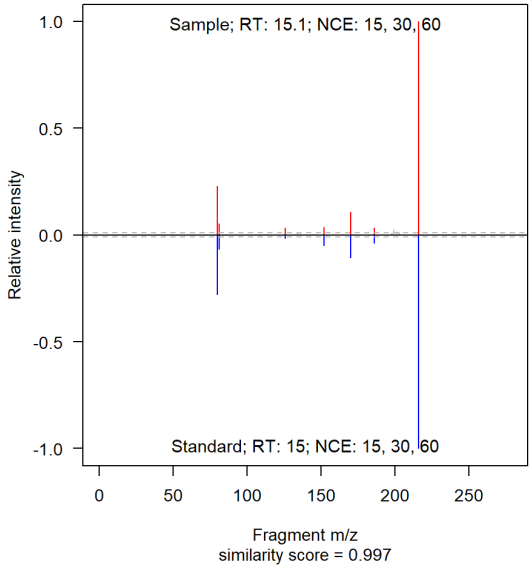

Most Intense Fragments in Standard

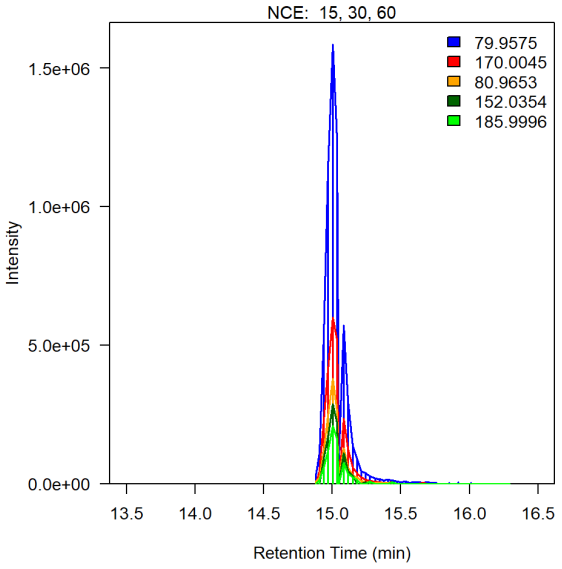

O-Des[2-aminoethyl]-O-carboxymethyldehydroamlodipine
BLG10, Level 1
[M+H]+ 422.10011
(STD 10 ng/L)

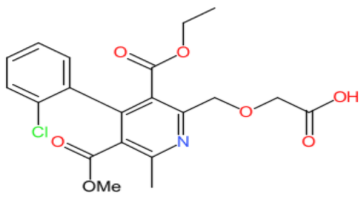

Normalized Extracted Ion Chromatogram (MS1)

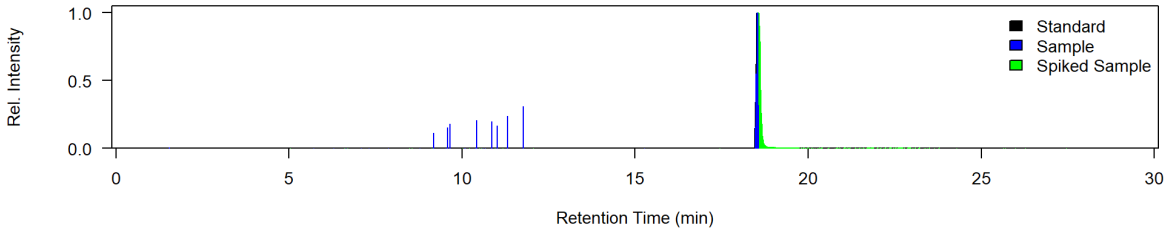

Extracted Ion Chromatogram (MS1)

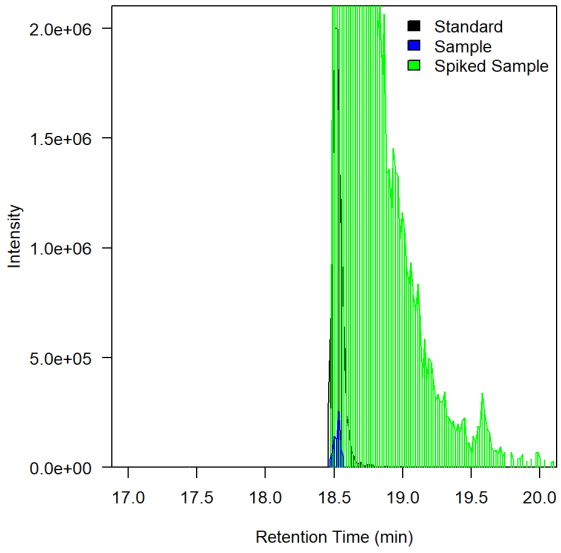

Most Intense Fragments in Sample

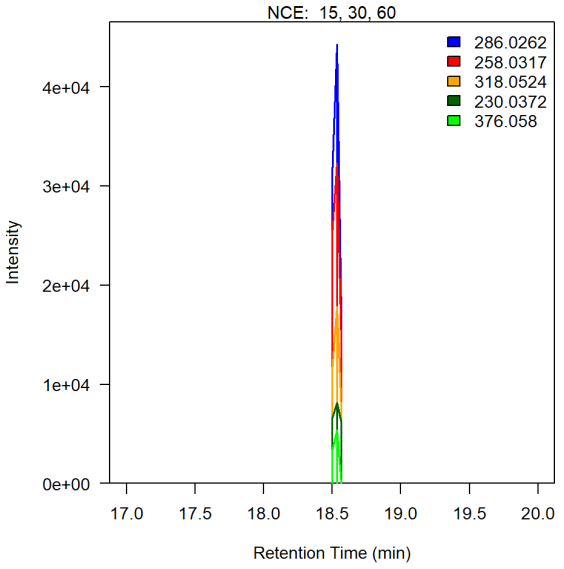

Most Intense MS2 Scan

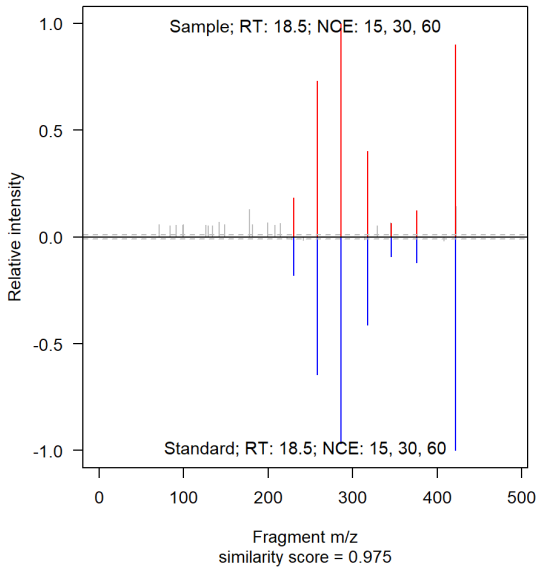

Most Intense Fragments in Standard

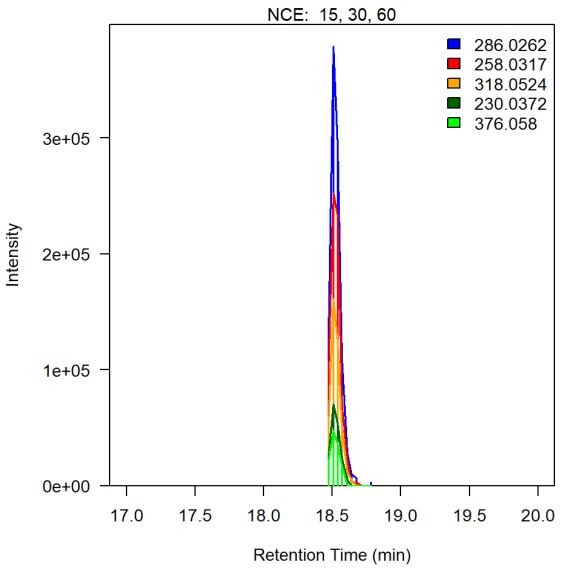

Xipamide
AGG39, Level 1
[M-H]- 353.03683
(STD 100 ng/L)

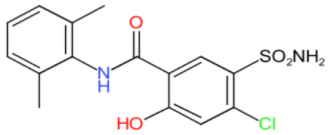

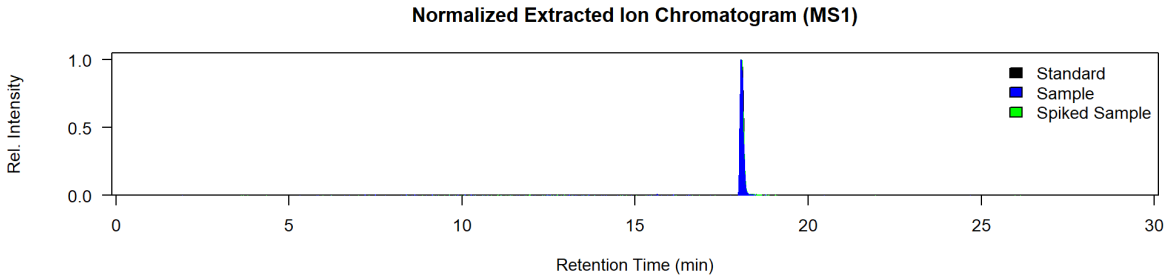

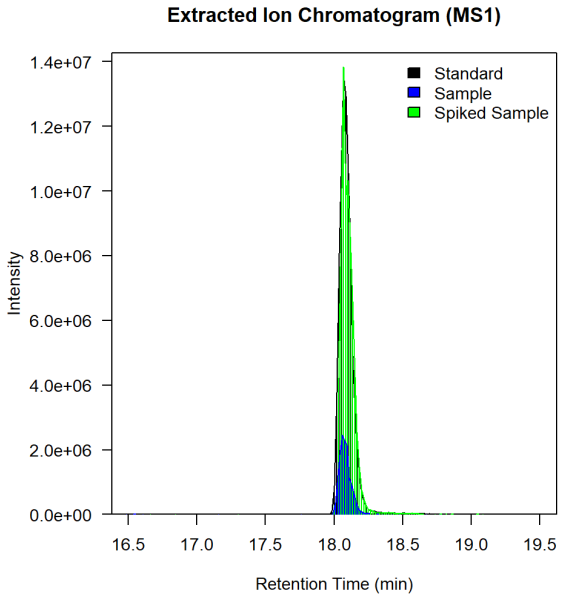

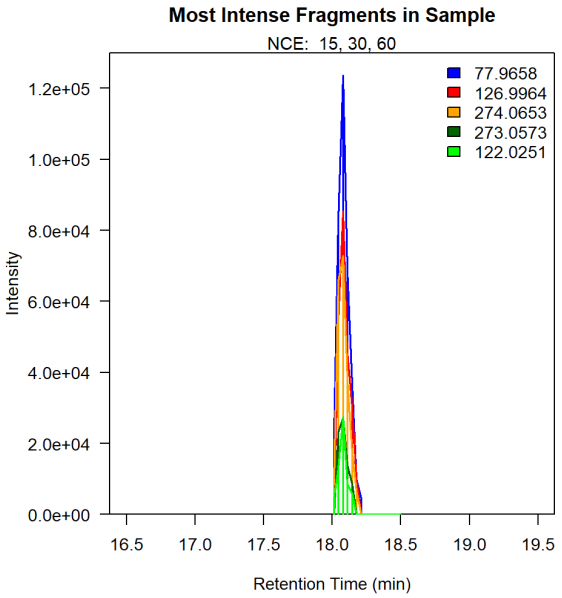

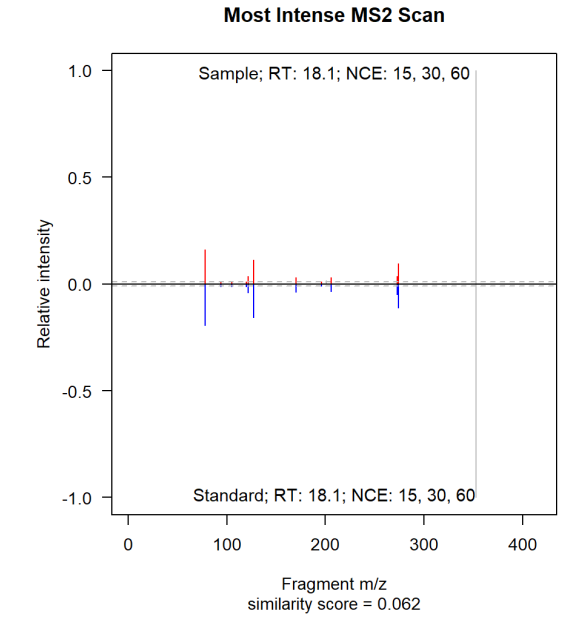

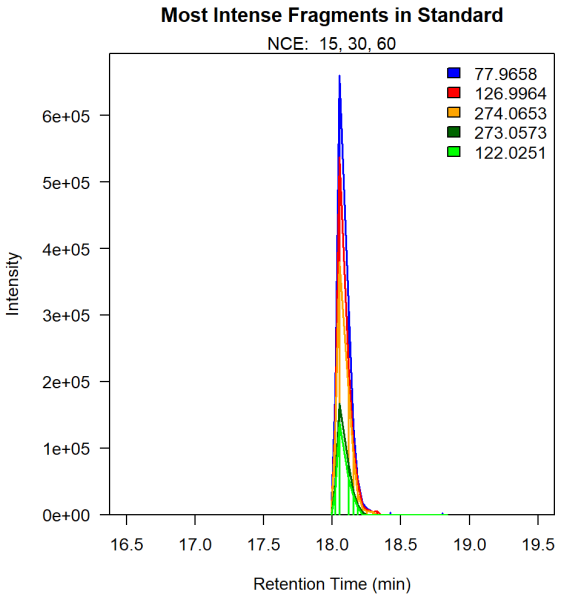

Metolachlor TP SYN542490
NTG41, Level 3
[M-H]- 342.10168

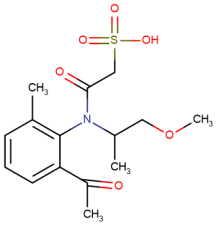

Extracted Ion Chromatogram (MS1)

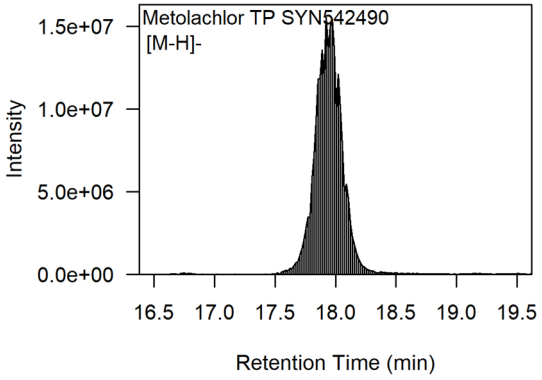

Most Intense Fragments in Sample

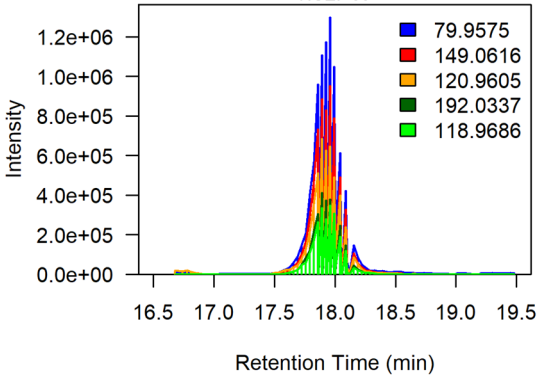

MS/MS Spectrum
Level 3

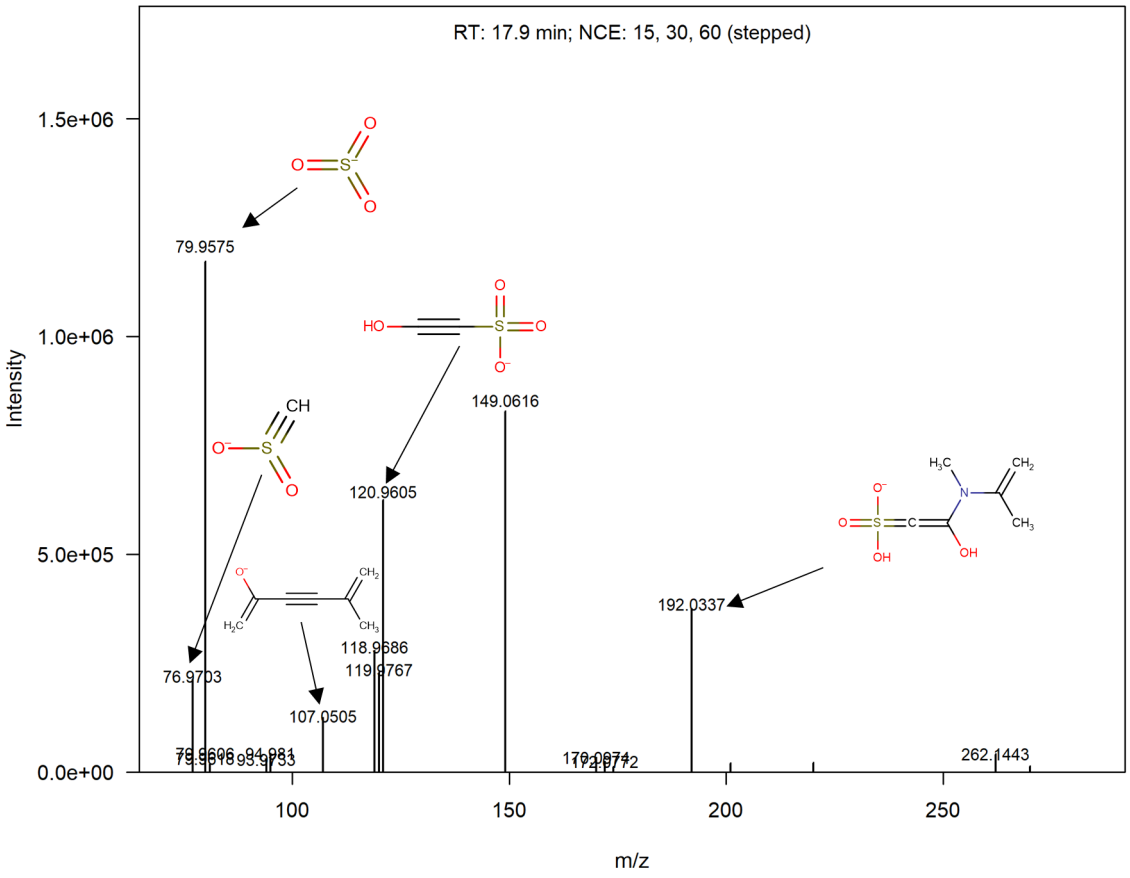

Metolachlor TP SYN547969 & SYN542488
NTG41, Level 3
[M-H]- 308.11396

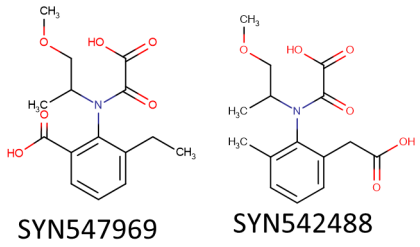

Extracted Ion Chromatogram (MS1)

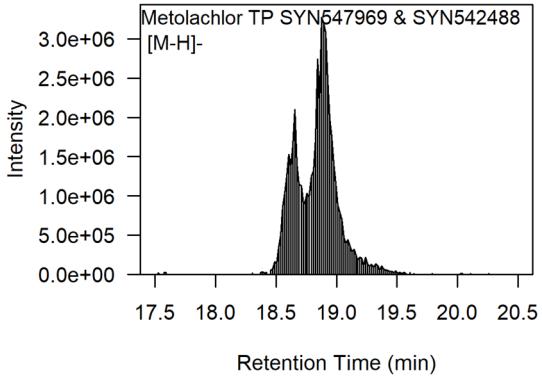

Most Intense Fragments in Sample

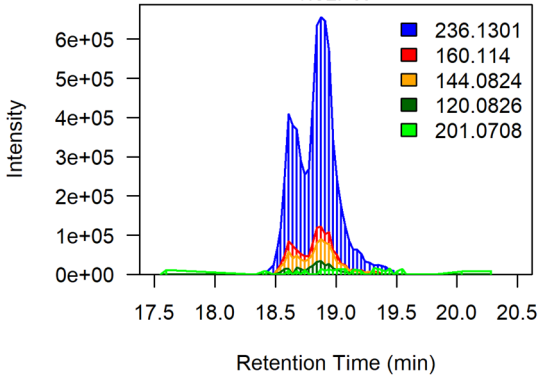

MS/MS Spectrum
Level 3

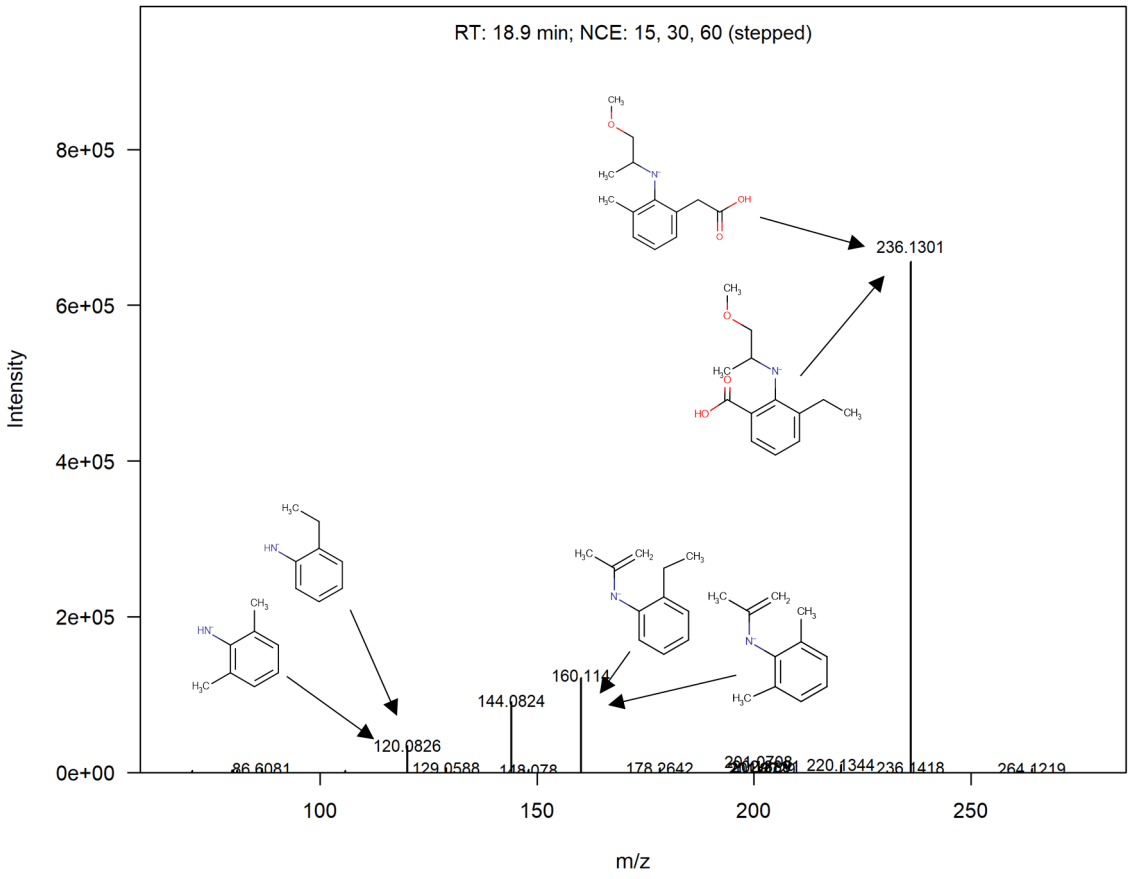

Metolachlor TP SYN547977
NTG41, Level 3
[M+H]+ 298.12045

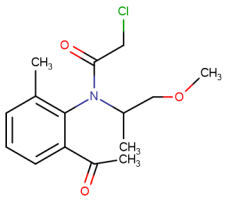

Extracted Ion Chromatogram (MS1)

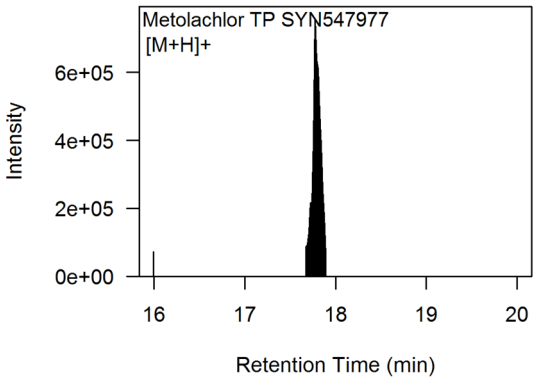

Most Intense Fragments in Sample

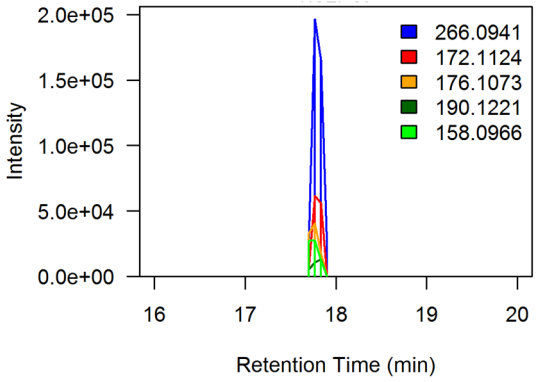

MS/MS Spectrum
Level 3

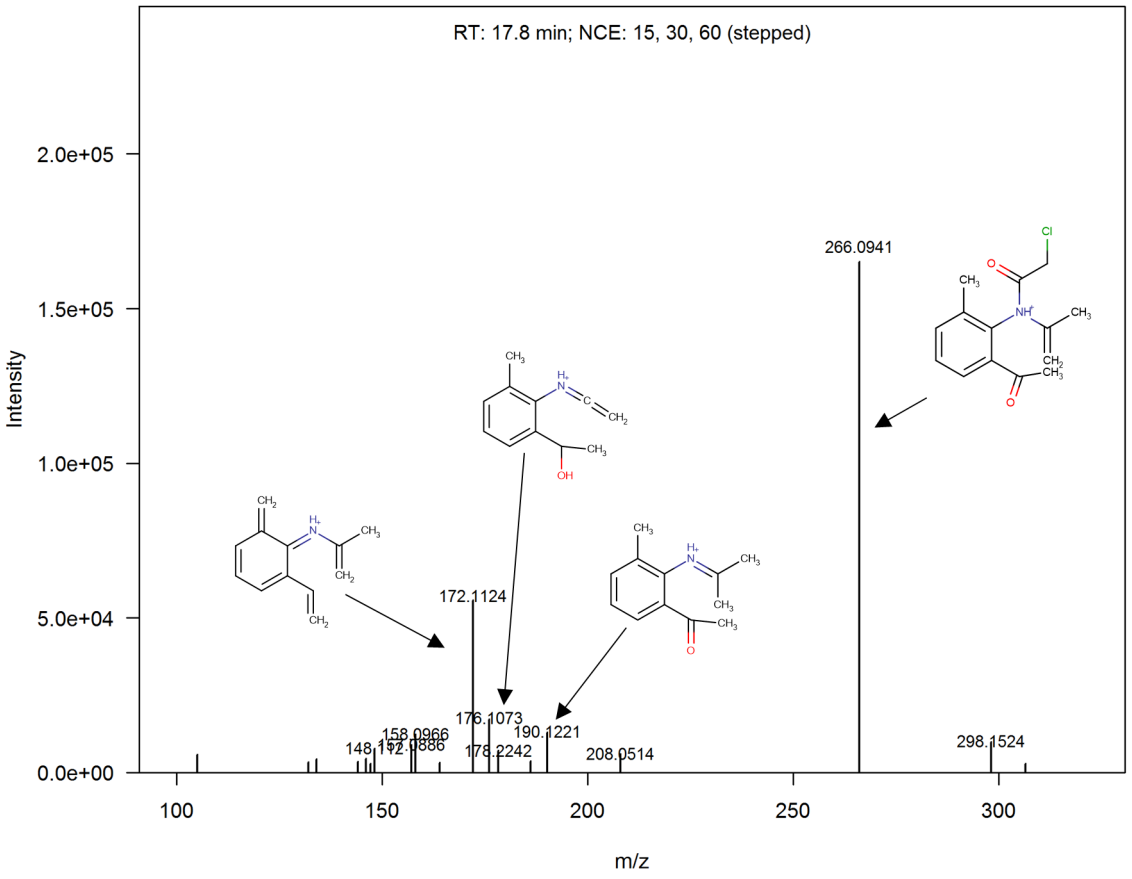

Metolachlor TP SYN542489
NTG41, Level 3
[M-H]- 294.1347

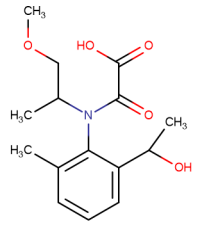

Extracted Ion Chromatogram (MS1)

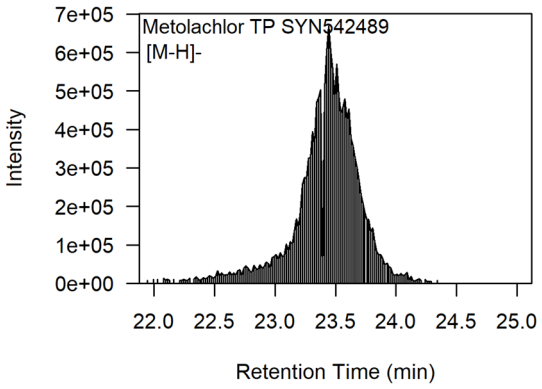

Most Intense Fragments in Sample

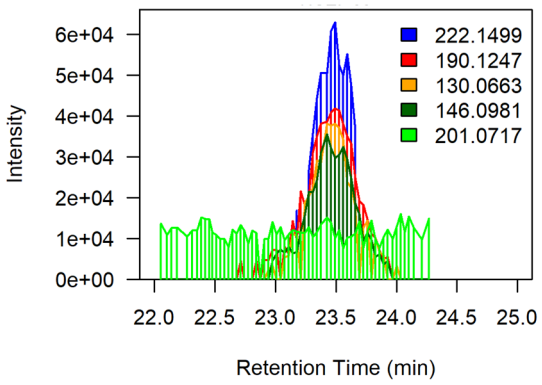

MS/MS Spectrum
Level 3

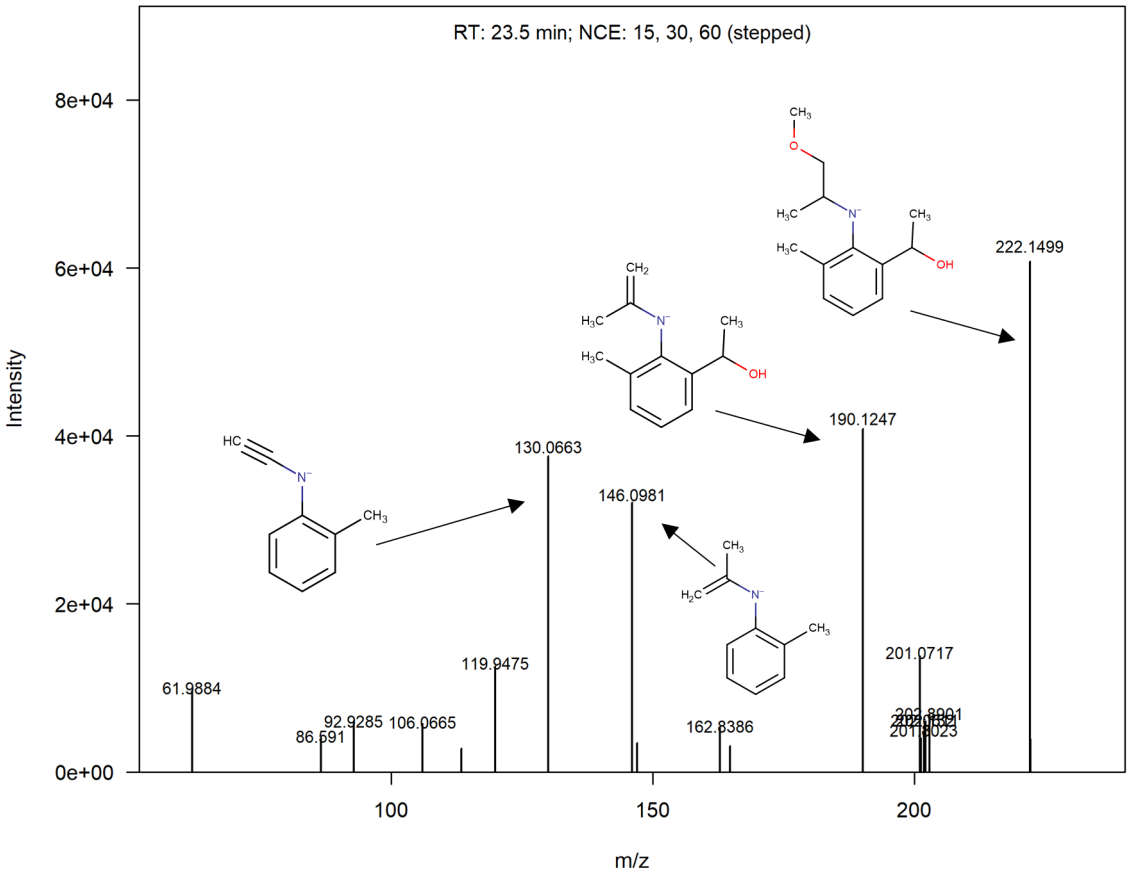

Metolachlor TP SYN542607
NTG41, Level 3
[M-H]- 344.11733

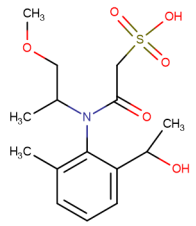

Extracted Ion Chromatogram (MS1)

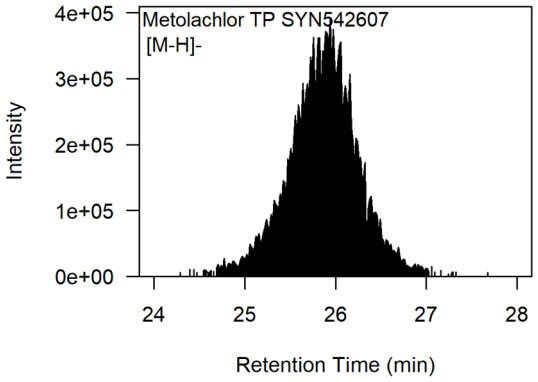

Most Intense Fragments in Sample

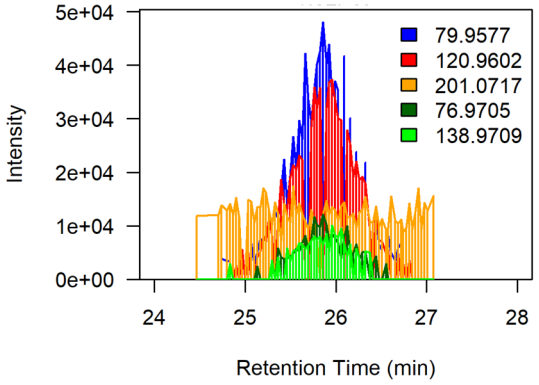

MS/MS Spectrum
Level 3

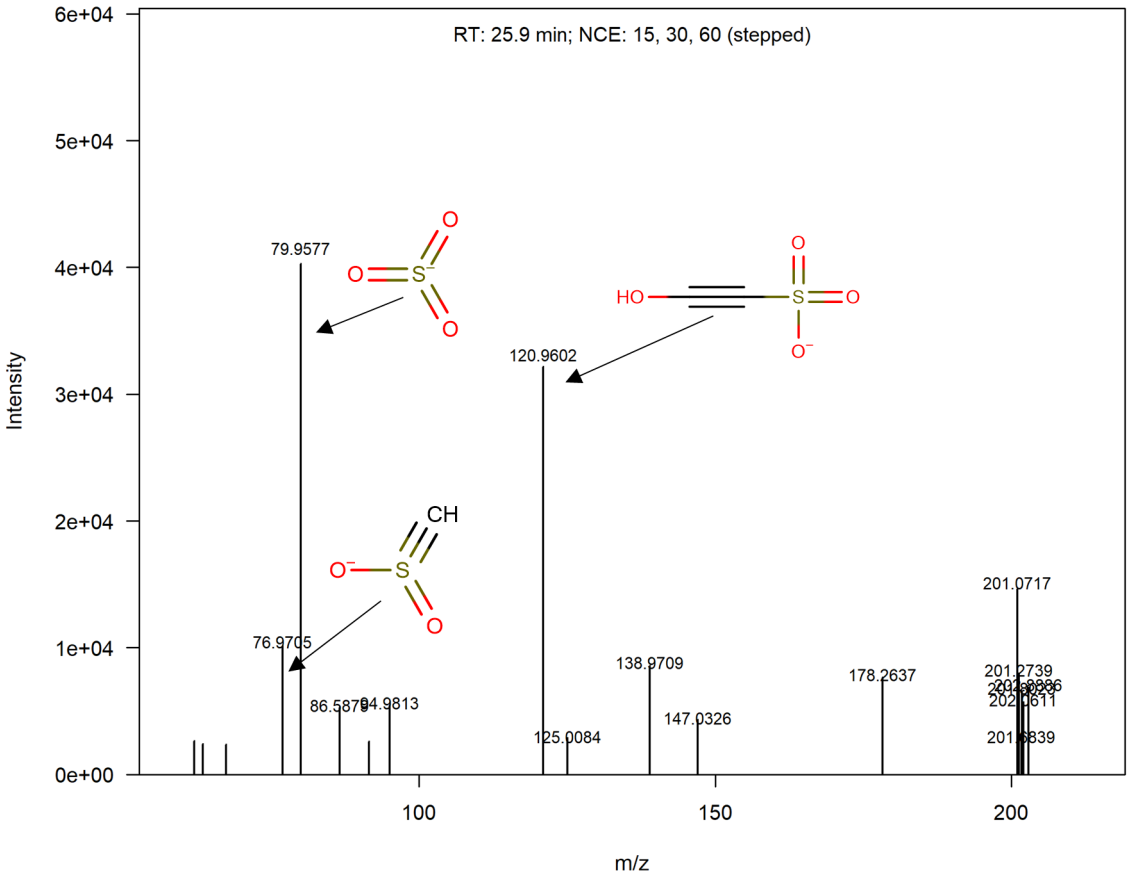

Metolachlor TP SYN542491
NTG41, Level 3
[M-H]- 294.09831

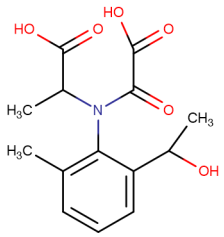

Extracted Ion Chromatogram (MS1)

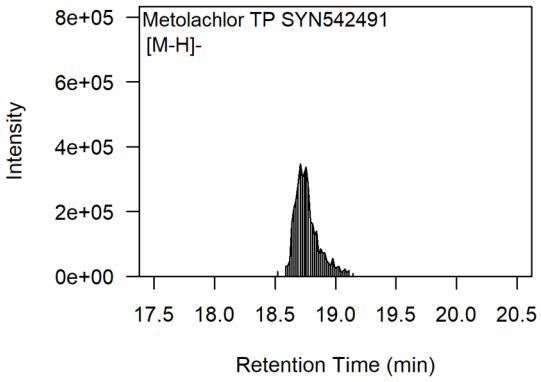

Most Intense Fragments in Sample

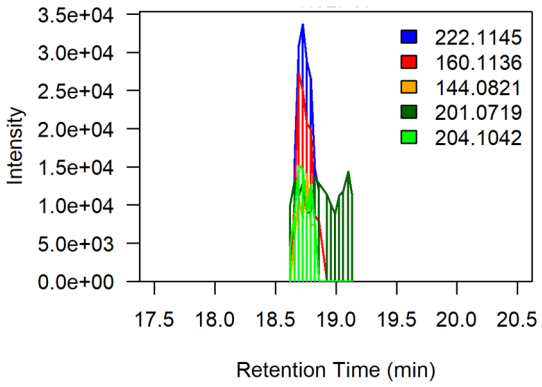

MS/MS Spectrum
Level 3

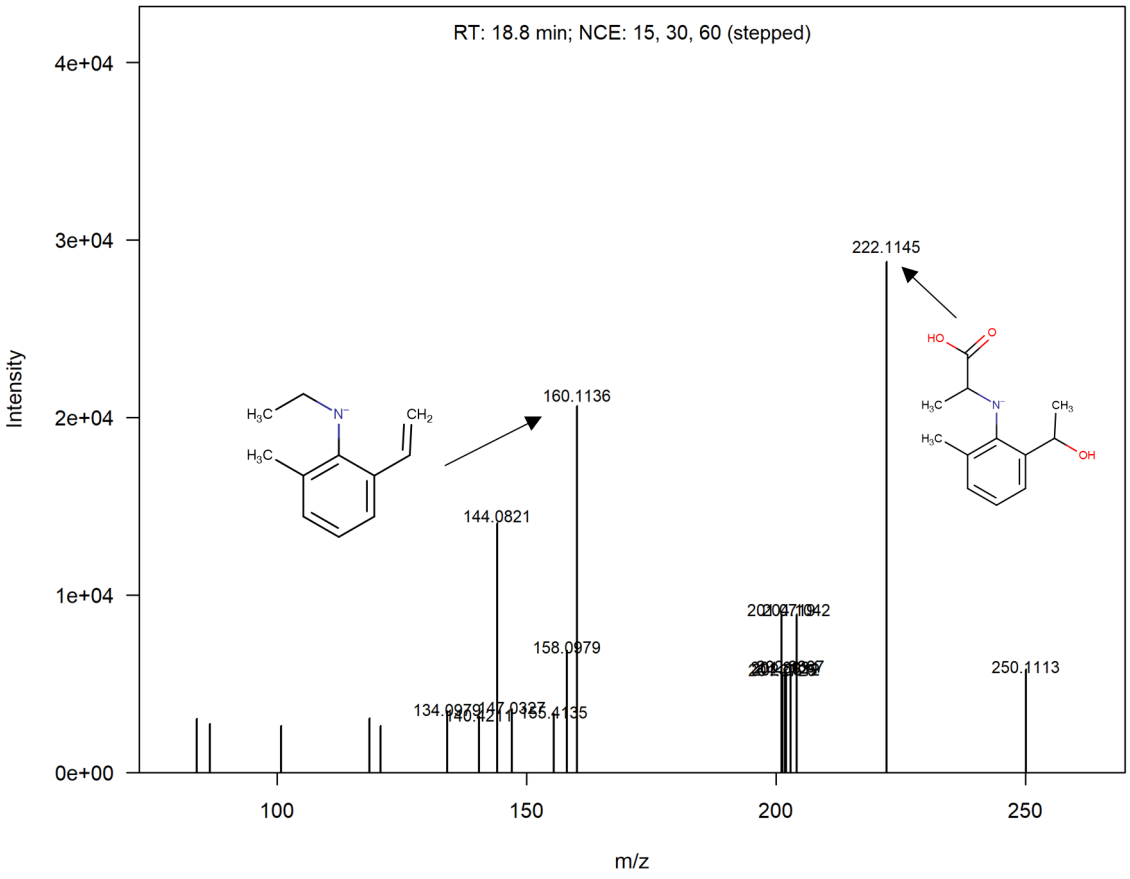

Pyroxsulam TP PSA
VDG27, Level 3
[M-H]- 255.98968

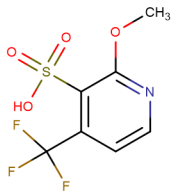

Extracted Ion Chromatogram (MS1)

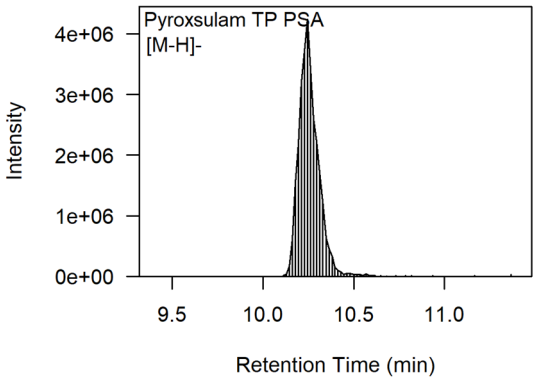

Most Intense Fragments in Sample

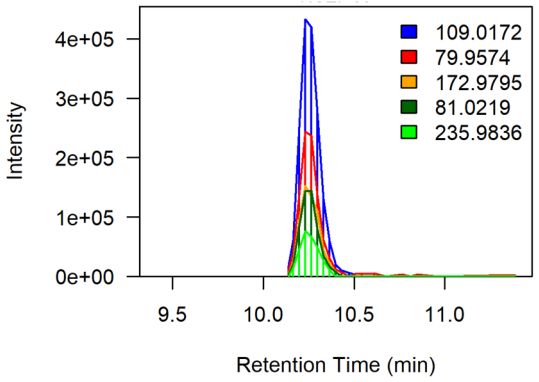

MS/MS Spectrum
Level 3

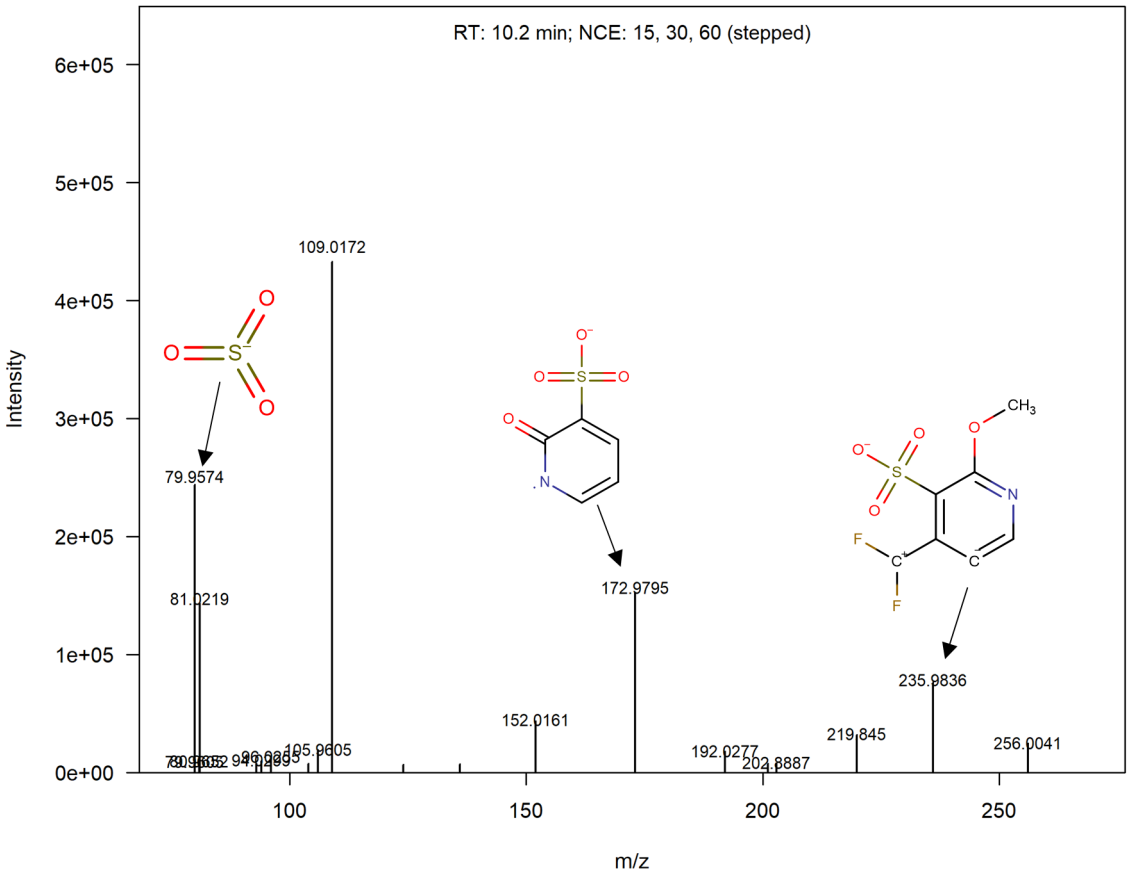

Trifluoroacetic acid
VDQ28, Level 1
[M-H]- 112.98559
(STD 1000 ng/L)

Normalized Extracted Ion Chromatogram (MS1)

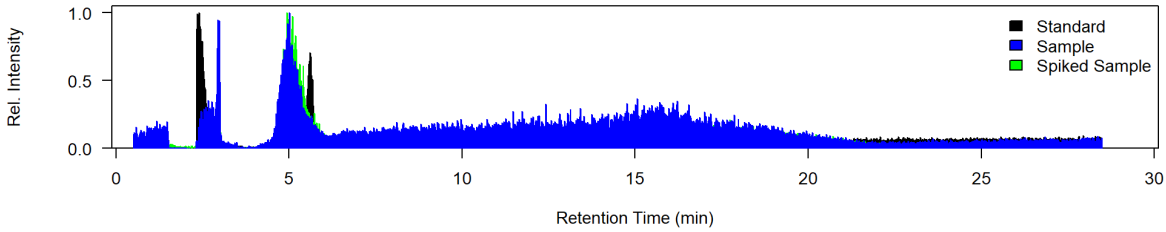

Extracted Ion Chromatogram (MS1)

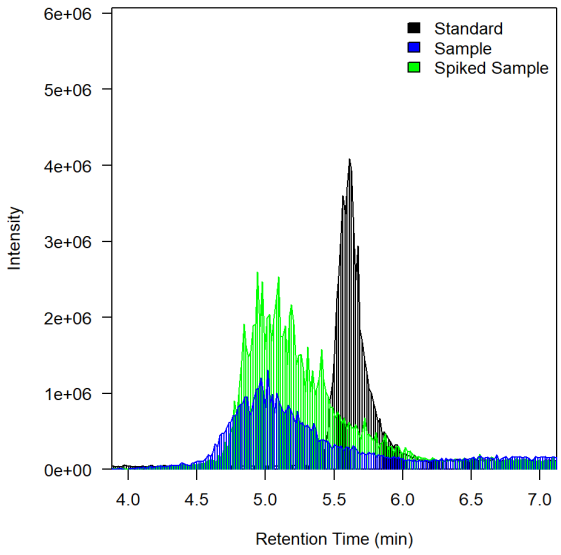

Most Intense Fragments in Sample

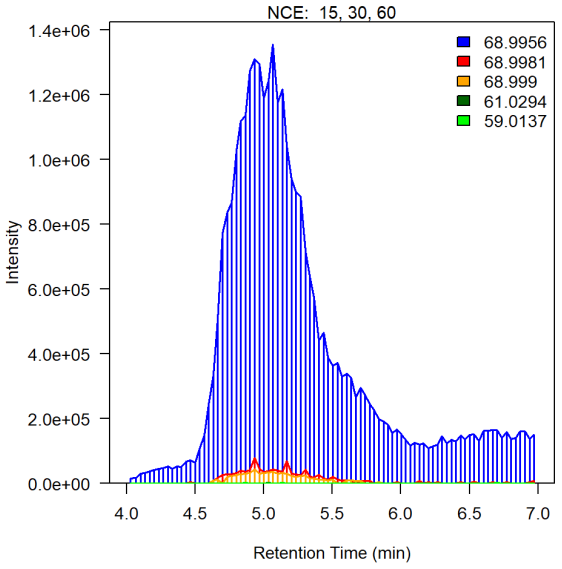

Most Intense MS2 Scan

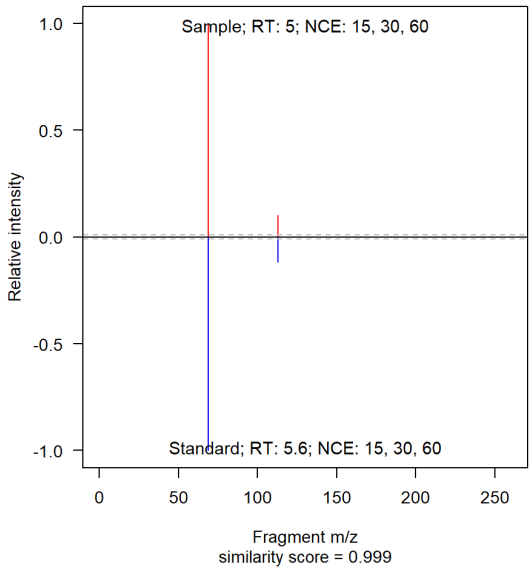

Most Intense Fragments in Standard

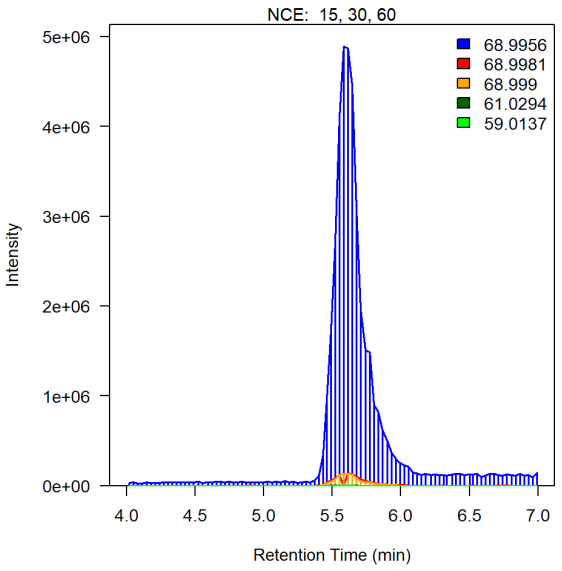

Trifluoromethanesulphonic acid
Pooled Sample, Level 1
[M-H]- 148.95257
(STD 100 ng/L)

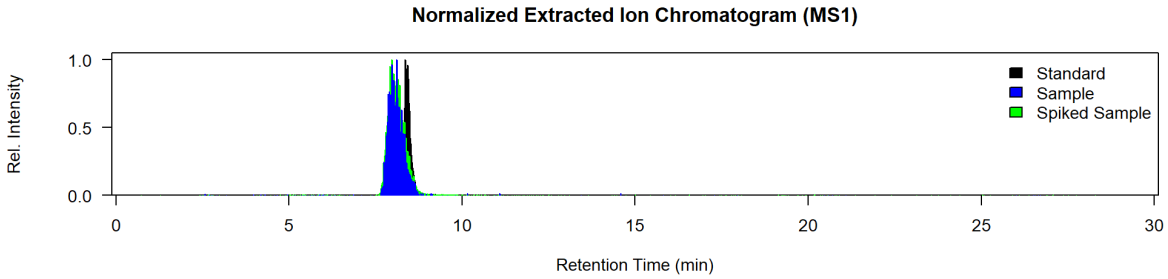

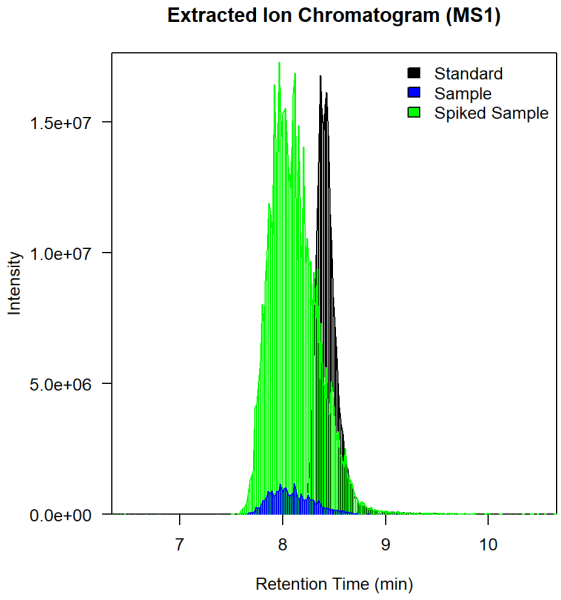

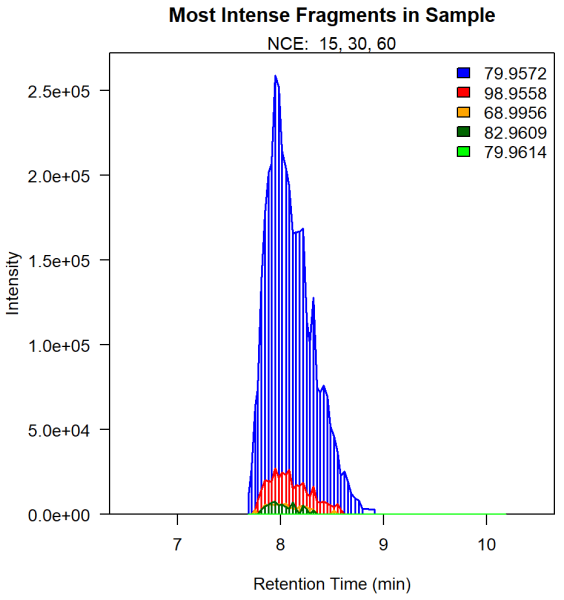

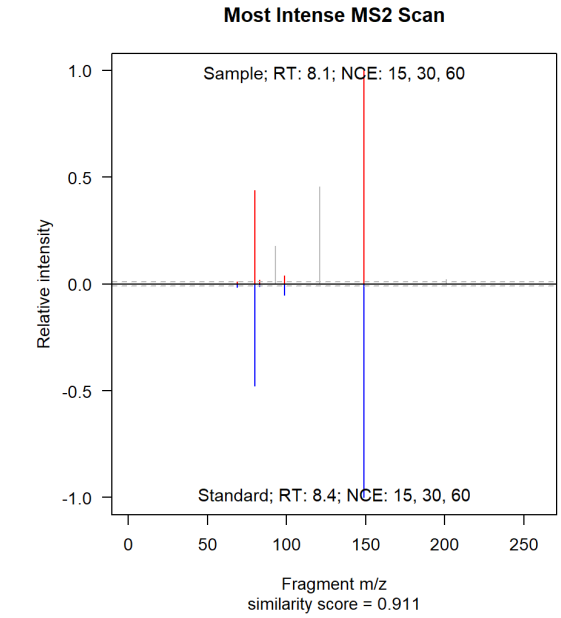

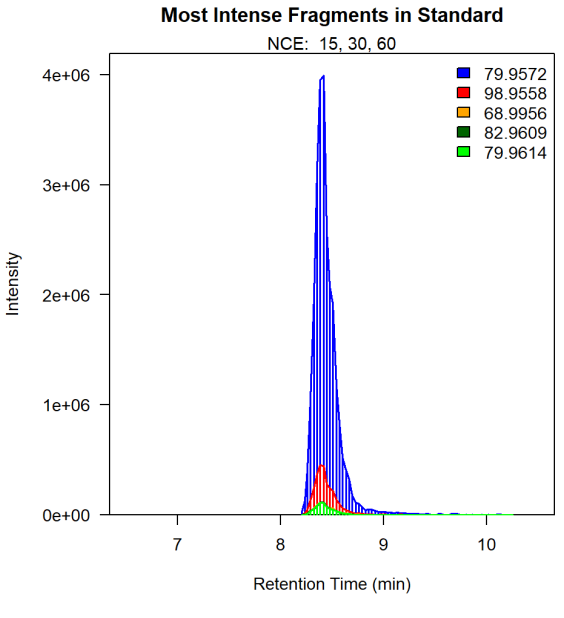

Atrazine-desethyl-desisopropyl
BSG05, Level 1
[M+H]+ 146.0228
(STD 100 ng/L)

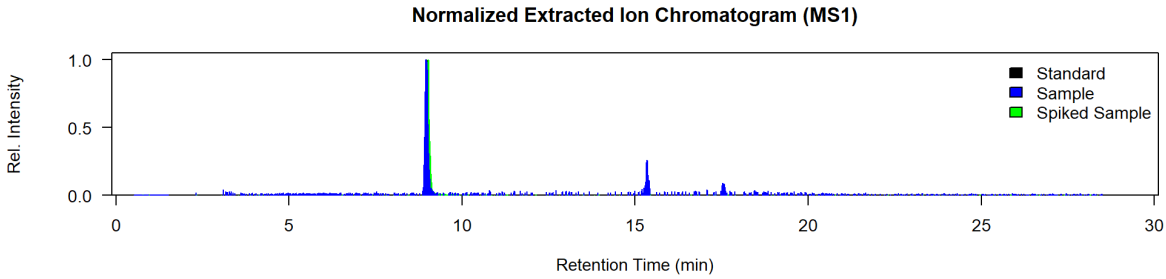

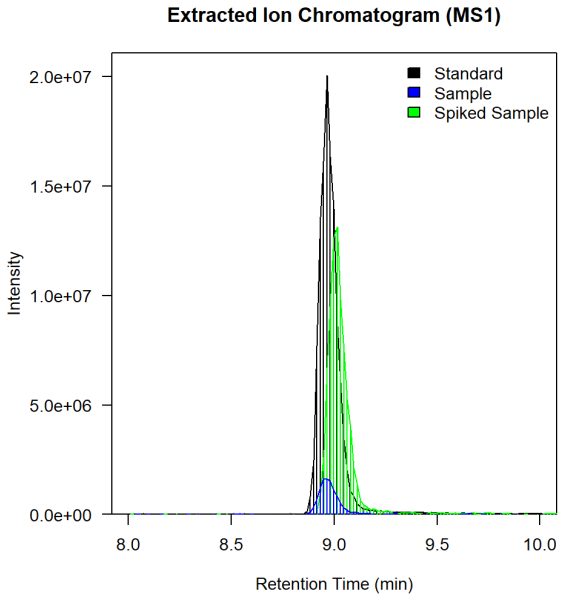

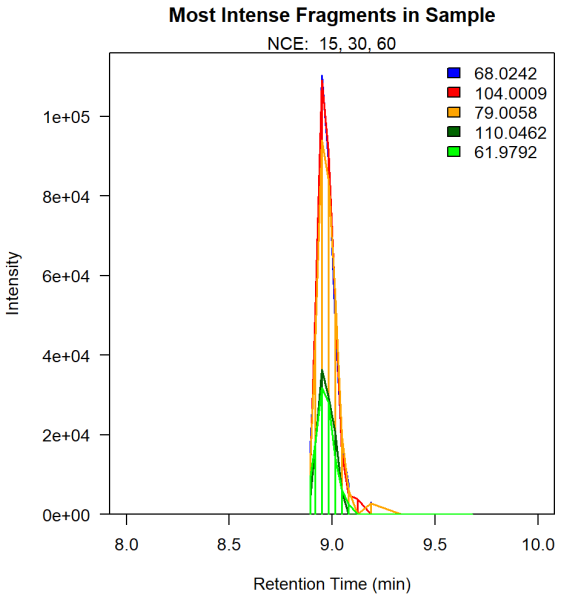

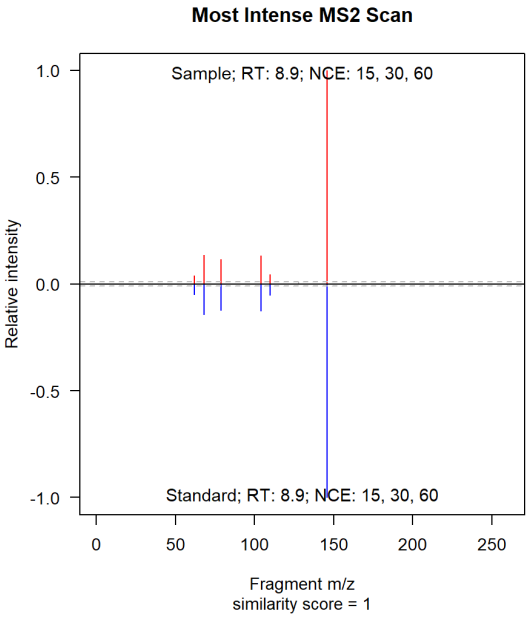

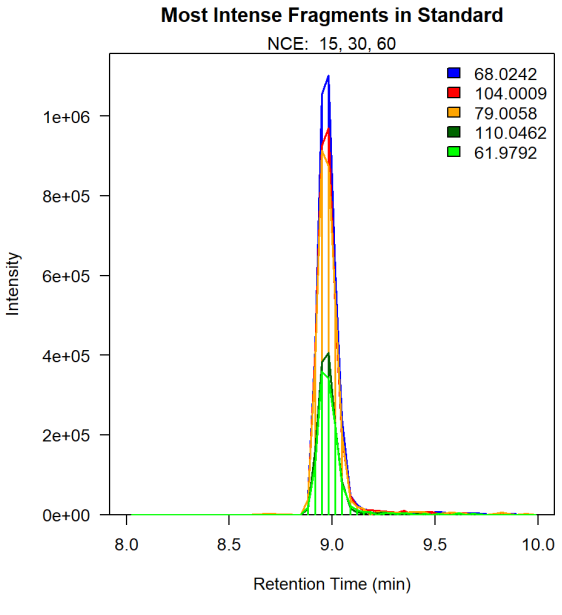

Perfluoropropanesulfonic Acid
BSG05, Level 1
[M-H]- 248.94619
(STD 100 ng/L)

Normalized Extracted Ion Chromatogram (MS1)

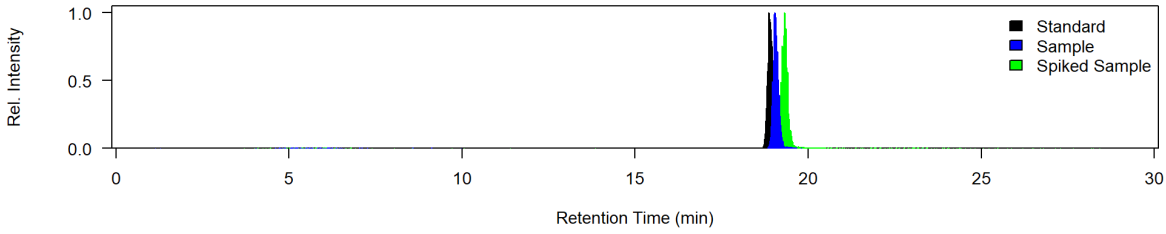

Extracted Ion Chromatogram (MS1)

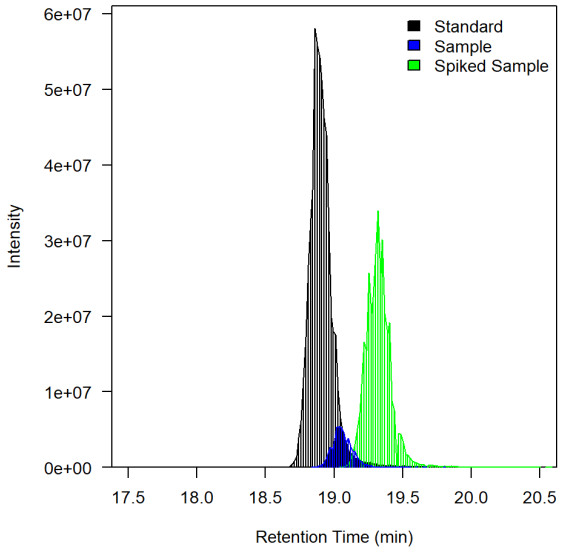

Most Intense Fragments in Sample

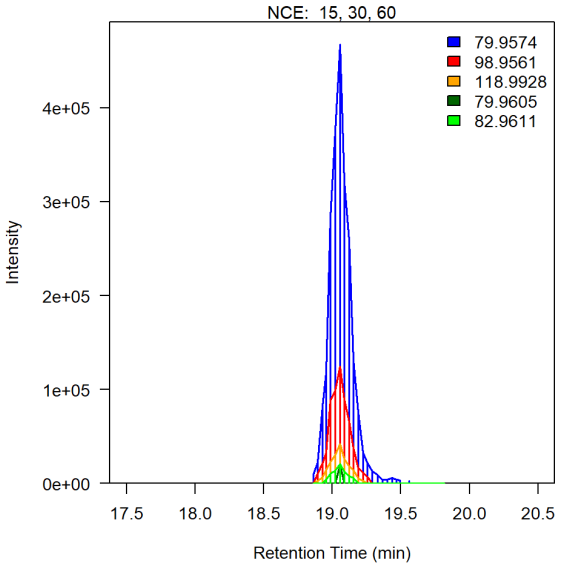

Most Intense MS2 Scan

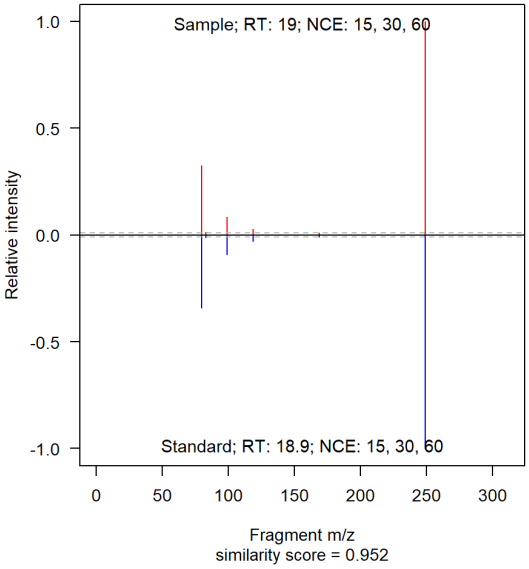

Most Intense Fragments in Standard

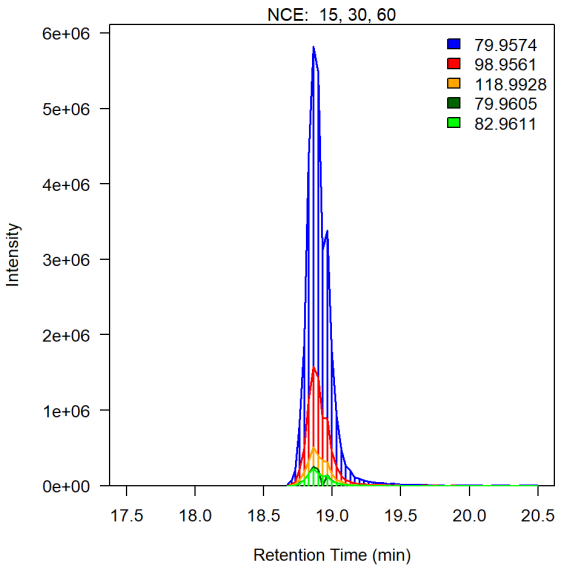

Oxypurinol
AGG28, Level 1
[M+H]+ 153.0407
(STD 1000 ng/L)

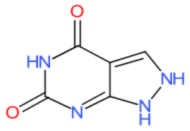

Normalized Extracted Ion Chromatogram (MS1)

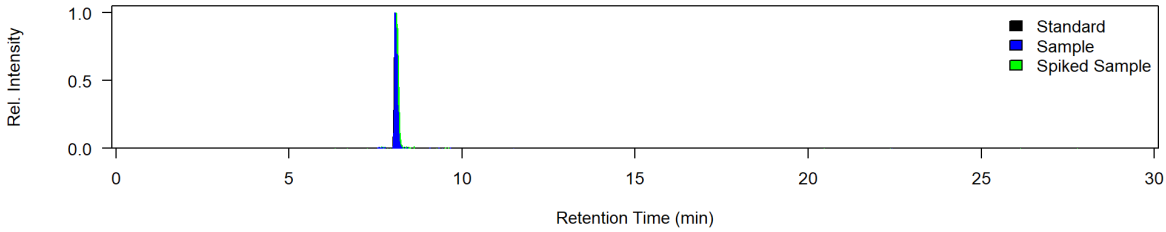

Extracted Ion Chromatogram (MS1)

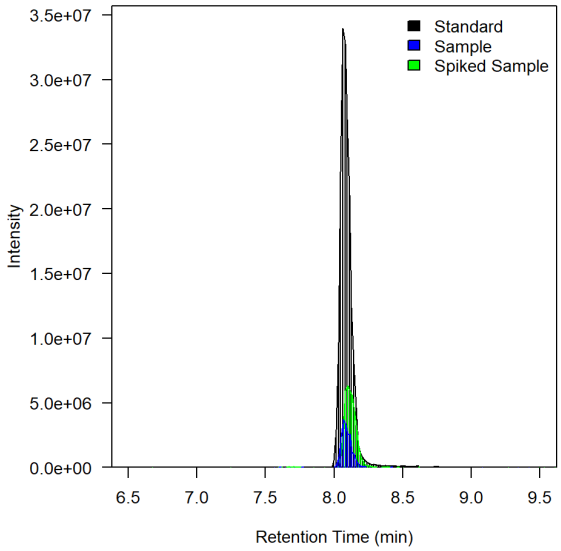

Most Intense Fragments in Sample

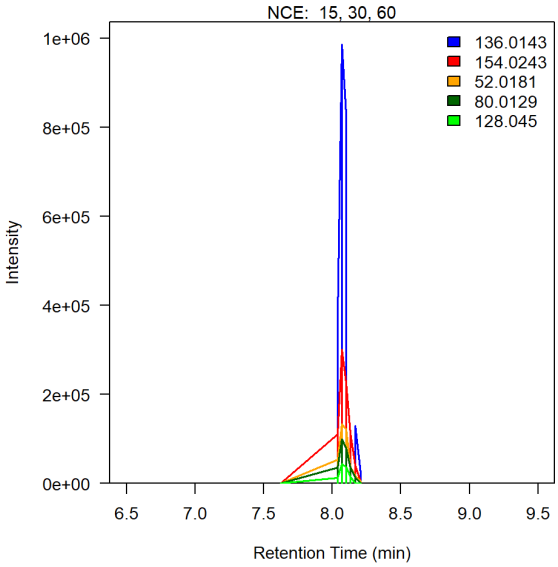

Most Intense MS2 Scan

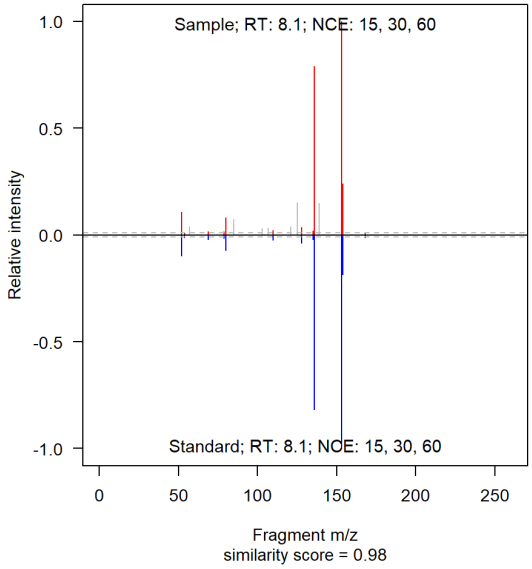

Most Intense Fragments in Standard

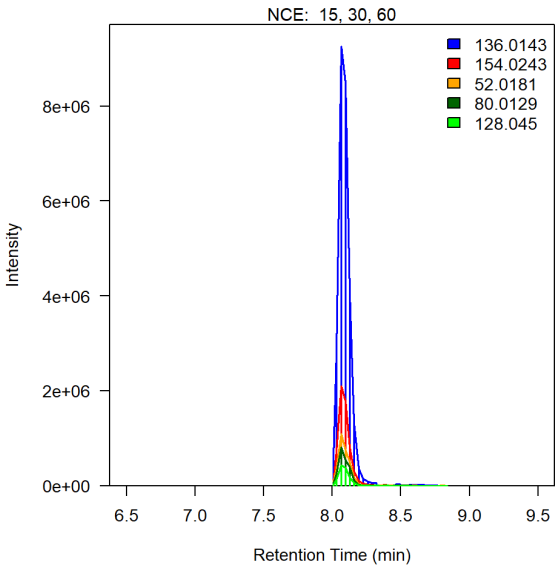

Oxypurinol
AGG28, Level 1
[M-H]- 151.02615
(STD 1000 ng/L)

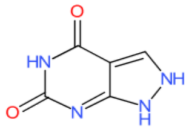

Normalized Extracted Ion Chromatogram (MS1)

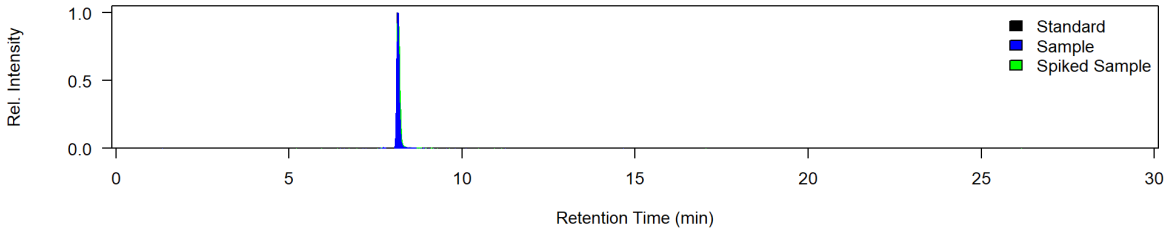

Extracted Ion Chromatogram (MS1)

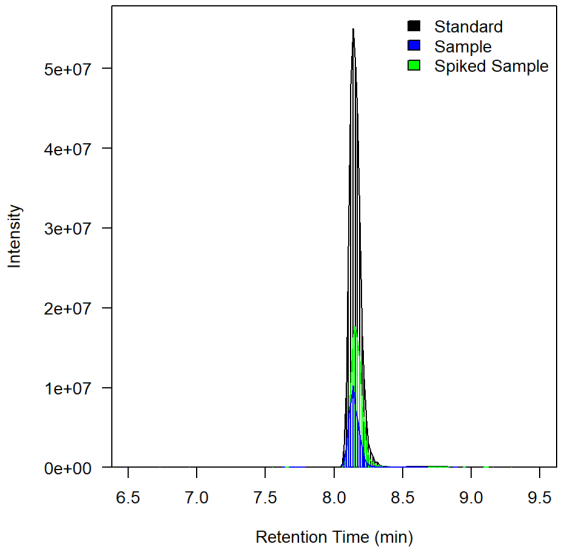

Most Intense Fragments in Sample

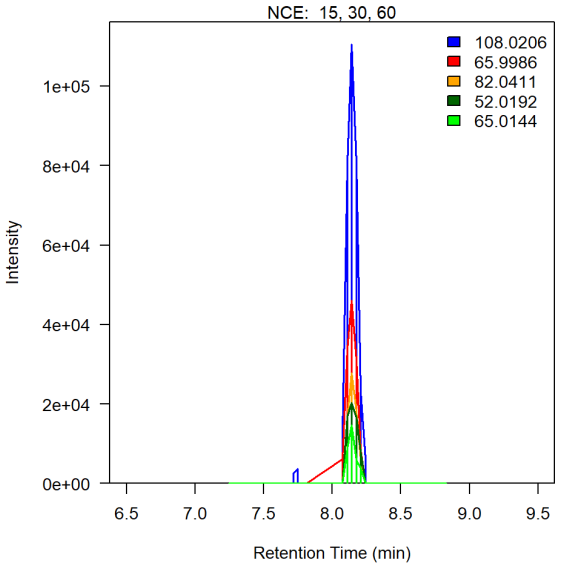

Most Intense MS2 Scan

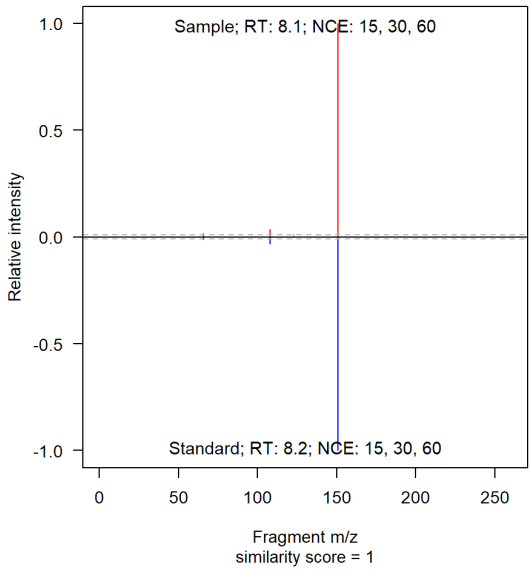

Most Intense Fragments in Standard

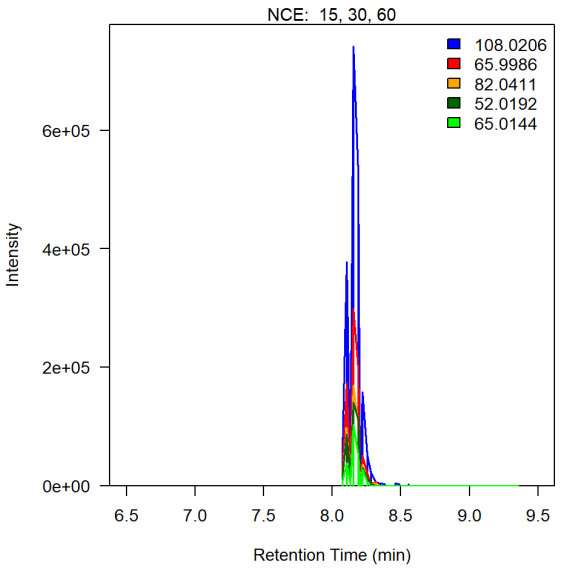

Methyldiphenylphosphine oxide
BLG10, Level 1
[M+H]+ 217.07768
(STD 0.1 mg/L, no enrichment)

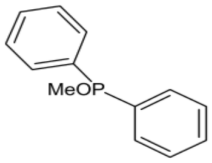

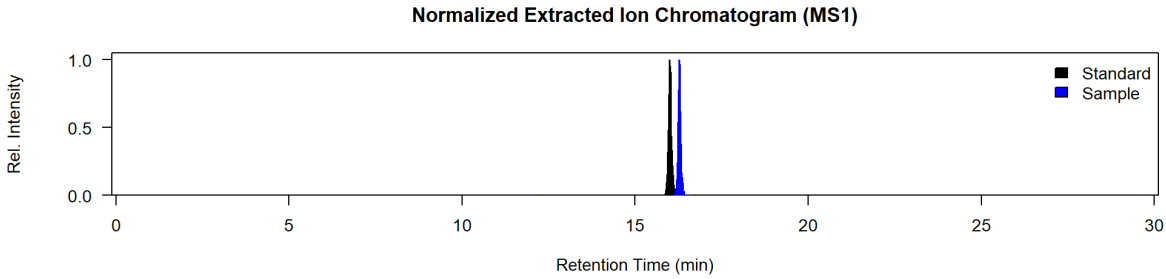

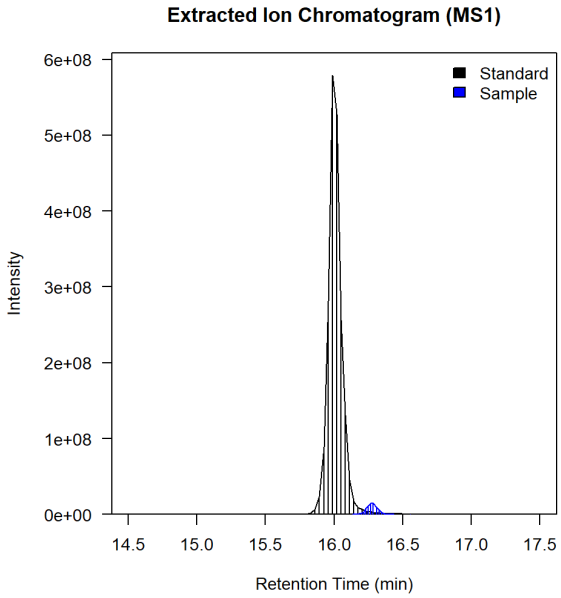

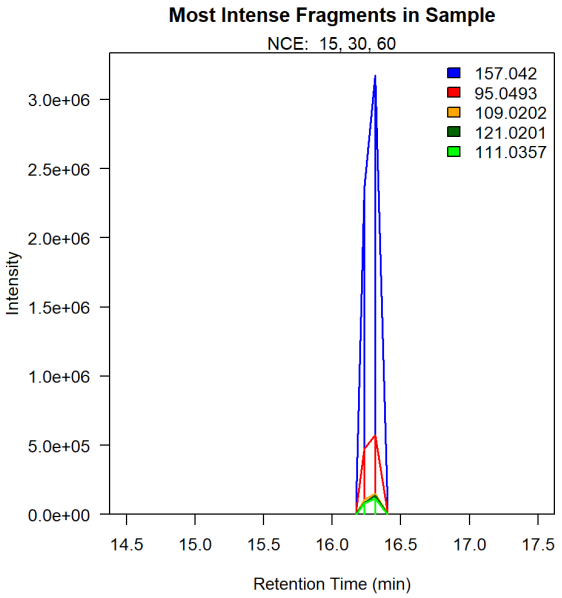

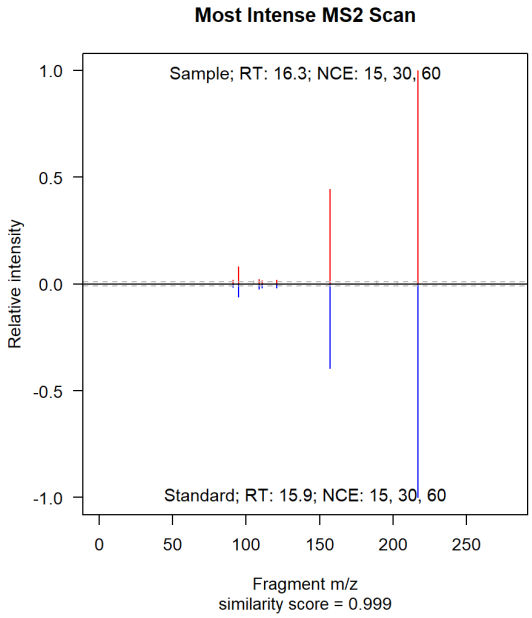

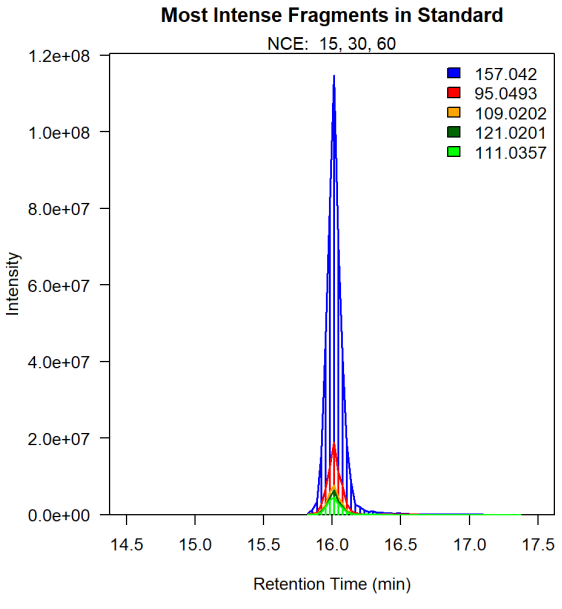

Sample and standard were injected in different sequences. Sample was not spiked.

Edetic acid (EDTA)
SHG05, Level 1
[M+H]+ 293.09794
(STD 100 ng/L)

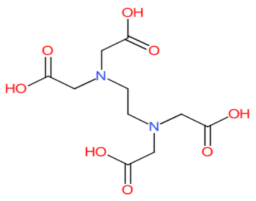

Normalized Extracted Ion Chromatogram (MS1)

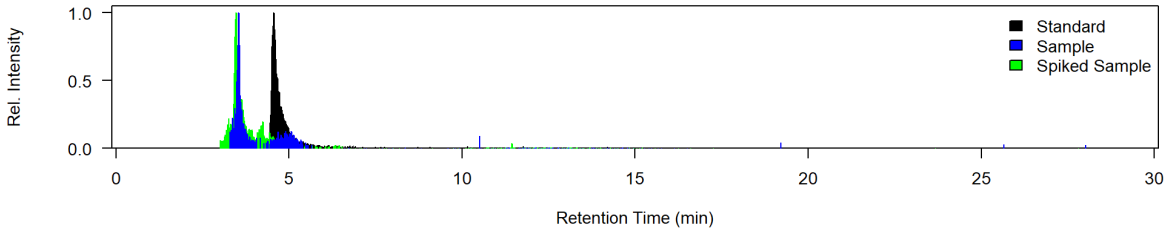

Extracted Ion Chromatogram (MS1)

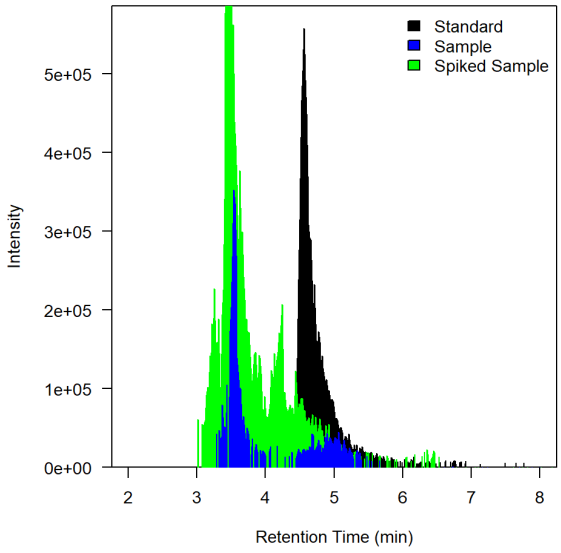

Most Intense Fragments in Sample

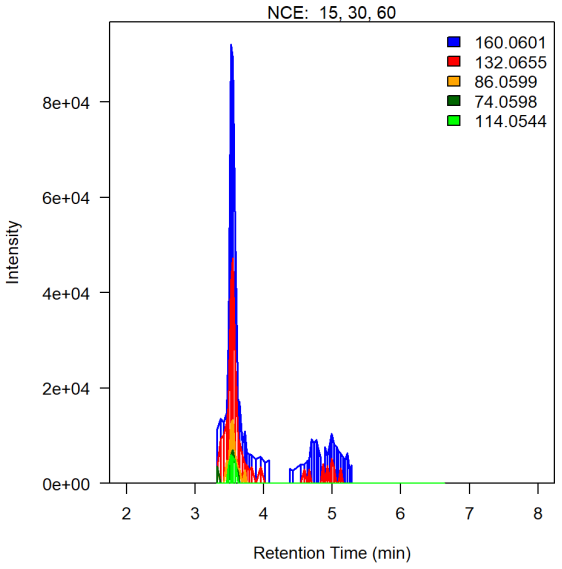

Most Intense MS2 Scan

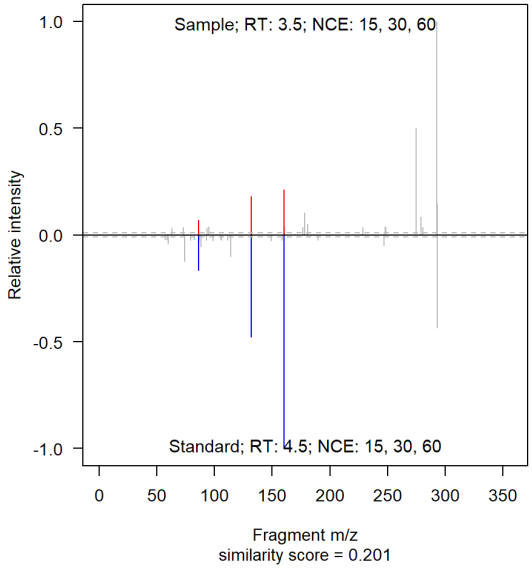

Most Intense Fragments in Standard

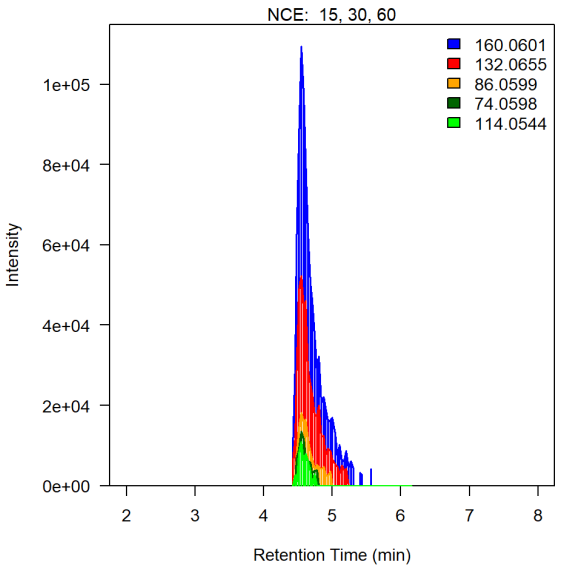

·Acrylamido-2-methyl-1-propanesulfonic acid (AMPS)
BSG05, Level 1
[M-H]- 206.04925
(STD 100 ng/L)

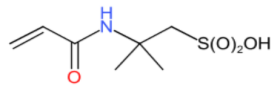

Normalized Extracted Ion Chromatogram (MS1)

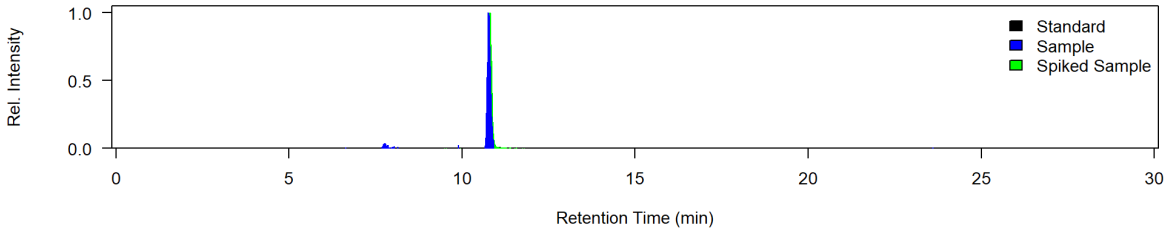

Extracted Ion Chromatogram (MS1)

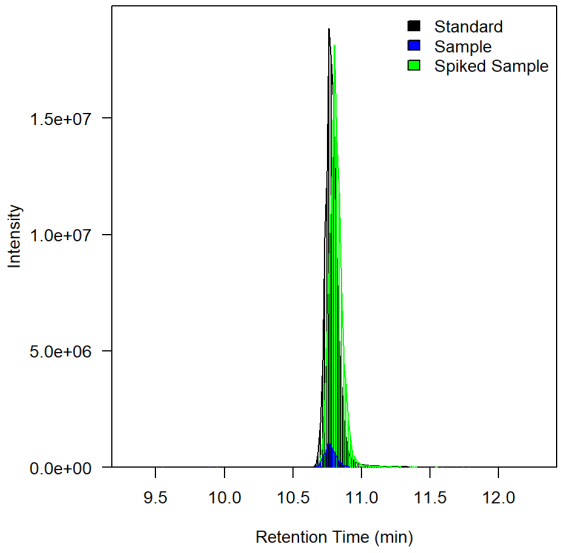

Most Intense Fragments in Sample

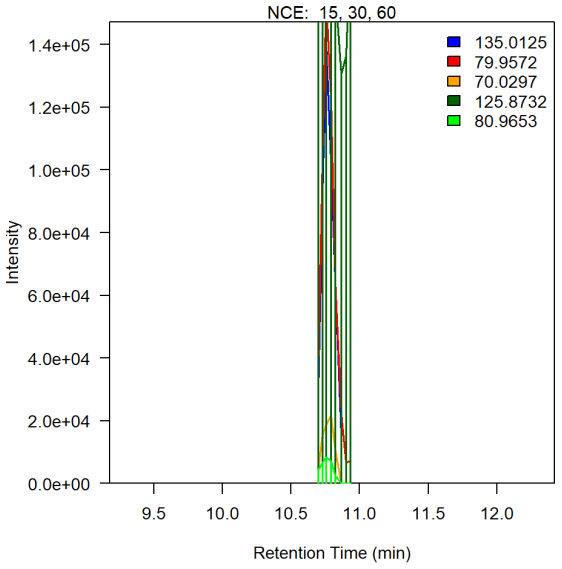

Most Intense MS2 Scan

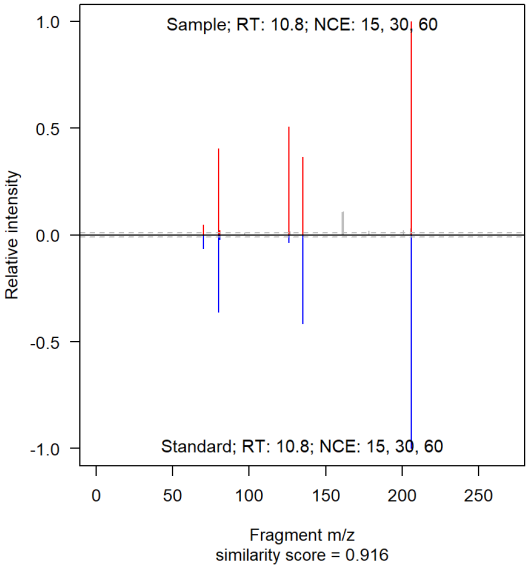

Most Intense Fragments in Standard

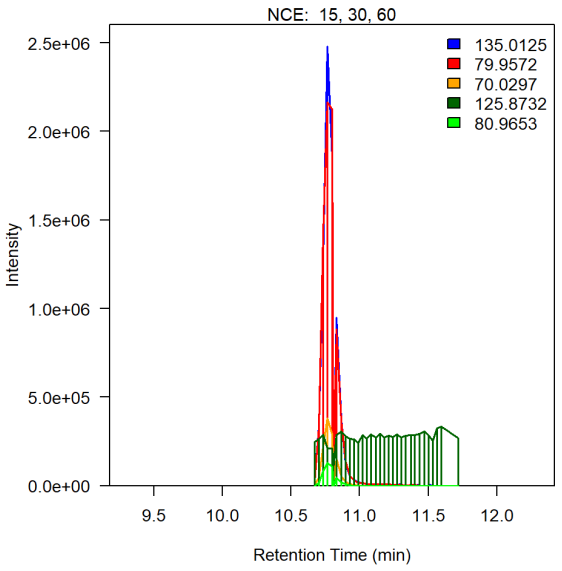

Perfluorobutylsulphonamide
Pooled Sample, Level 1
[M-H]- 297.95898
(STD 10 ng/L)

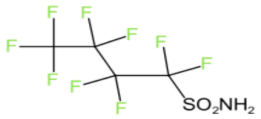

Normalized Extracted Ion Chromatogram (MS1)

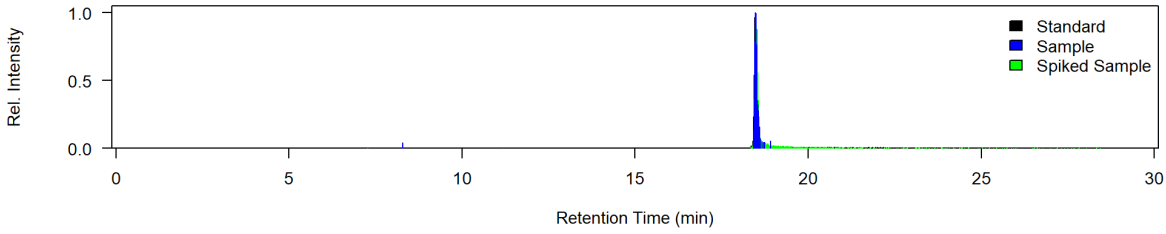

Extracted Ion Chromatogram (MS1)

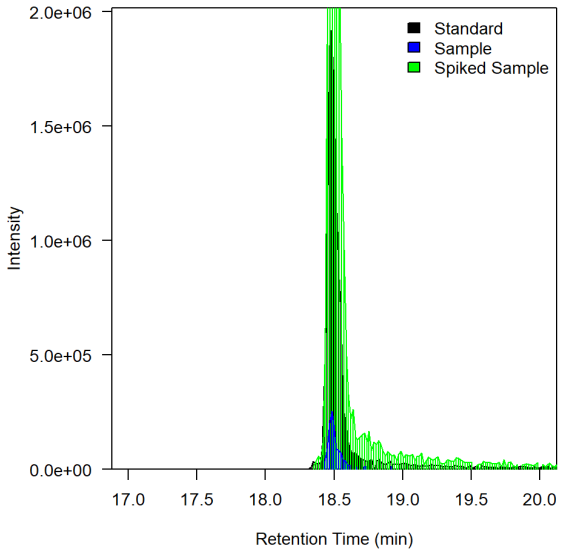

Most Intense Fragments in Sample

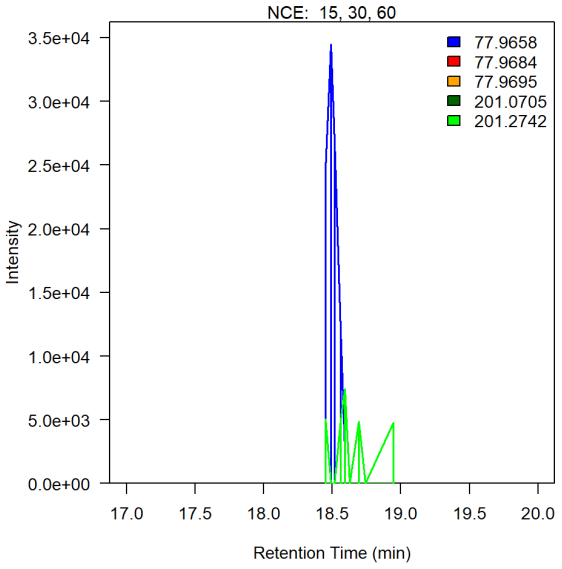

Most Intense MS2 Scan

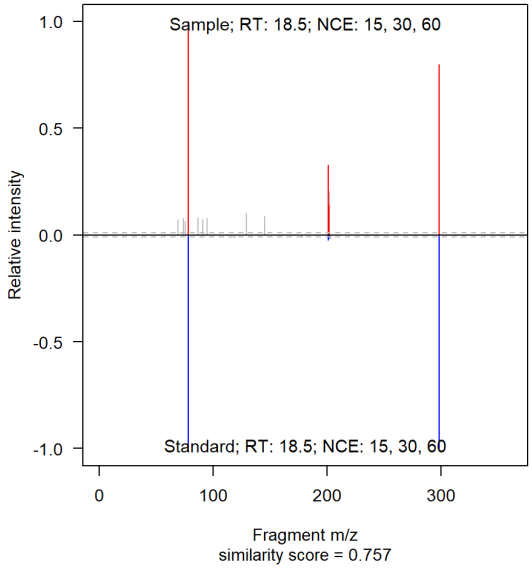

Most Intense Fragments in Standard

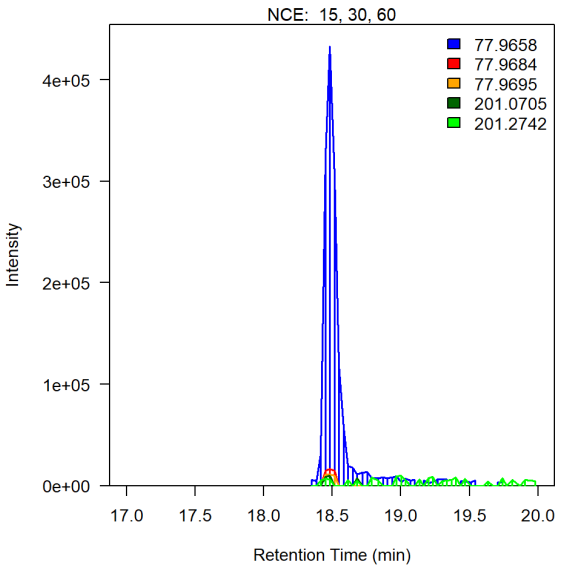

Methenamine
SHG05, Level 1
[M+H]+ 141.11347
(STD 100 ng/L)

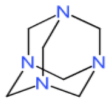

Normalized Extracted Ion Chromatogram (MS1)

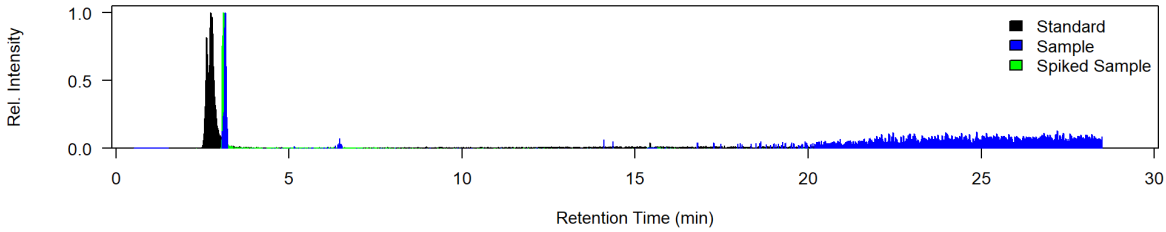

Extracted Ion Chromatogram (MS1)

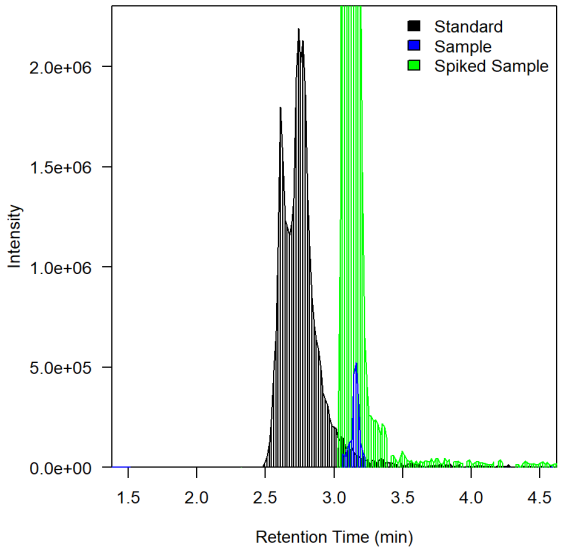

Most Intense Fragments in Sample

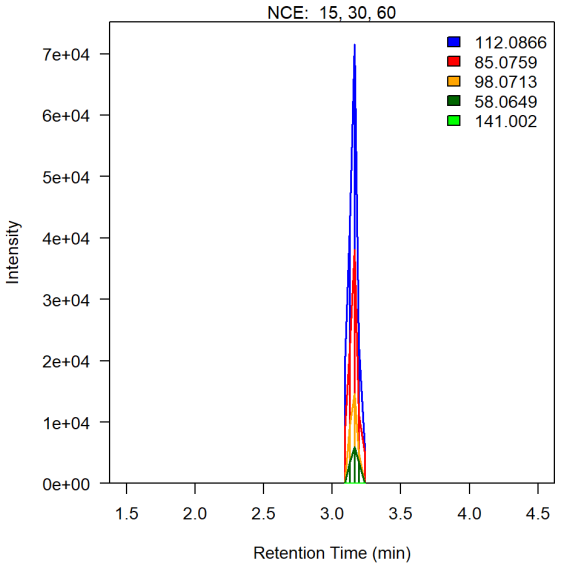

Most Intense MS2 Scan

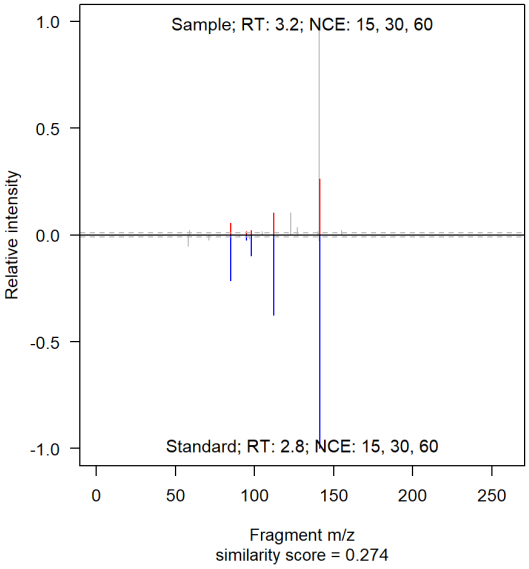

Most Intense Fragments in Standard

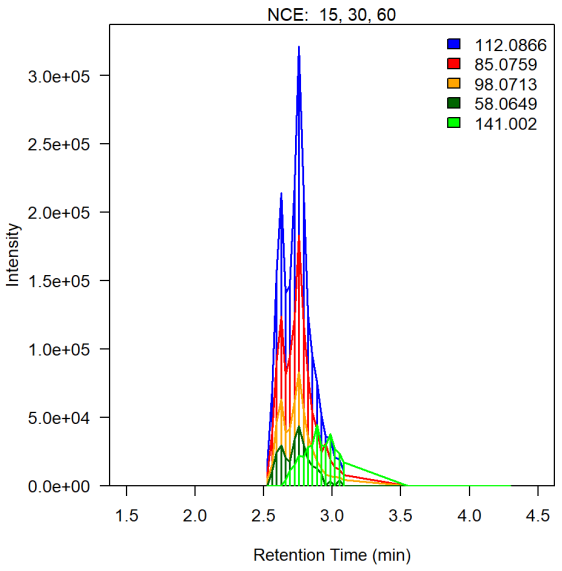

Dimethylbenzenesulfonic acid (isomers)
GEQ01, Level 1
[M-H]- 185.02779
(STD 100 ng/L)

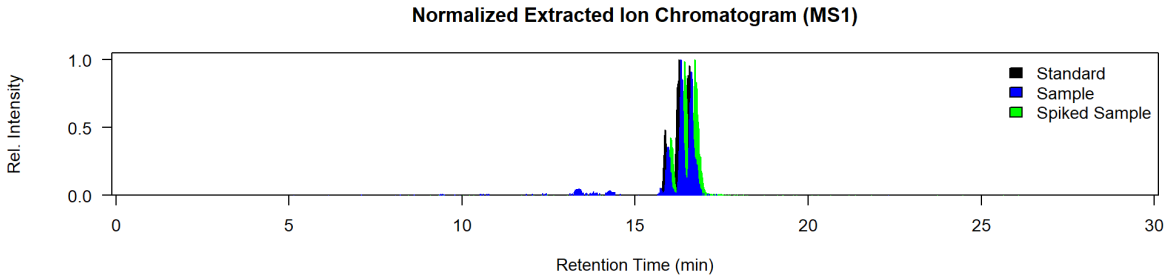

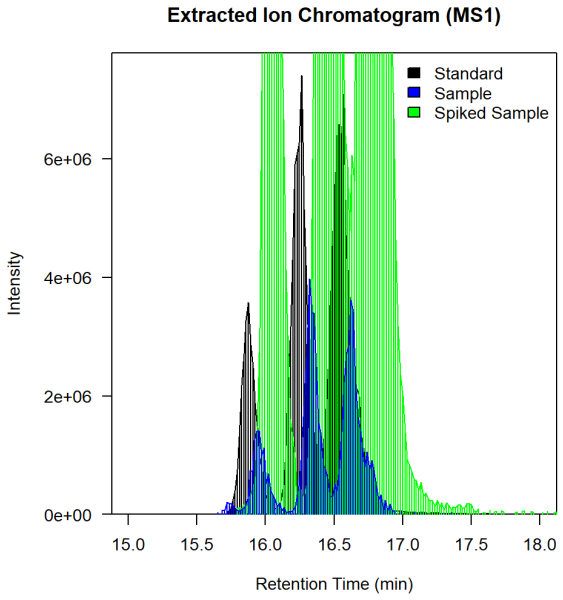

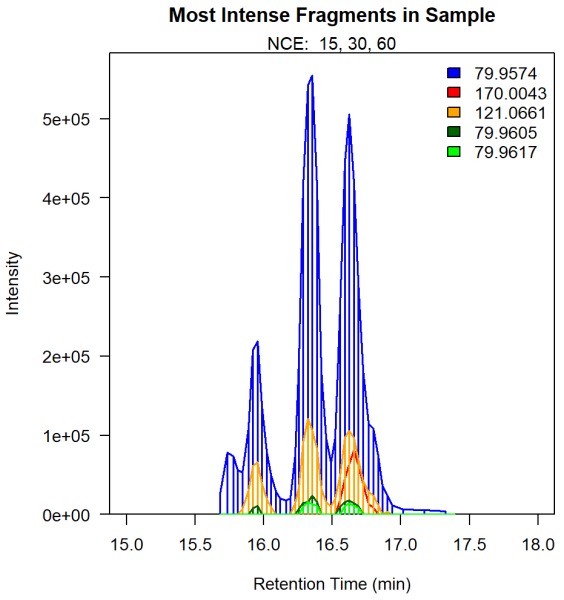

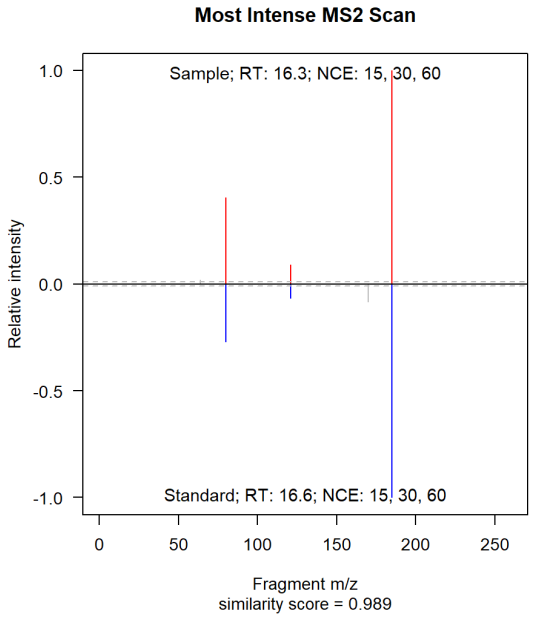

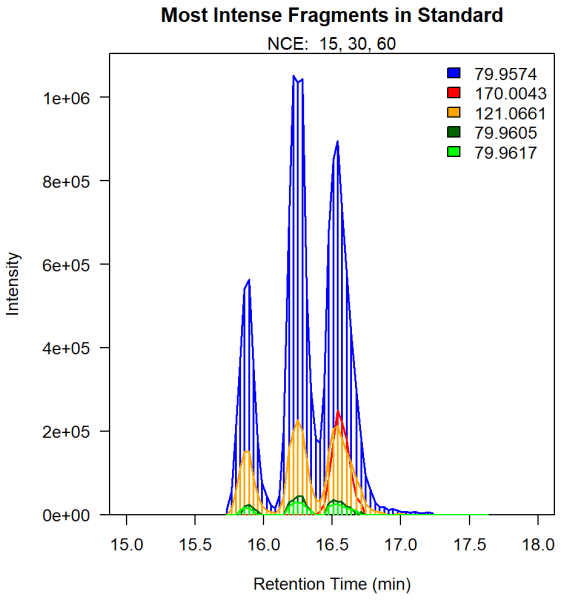

p-Toluenesulfonic acid
GEQ01, Level 1
[M-H]- 171.01214
(STD 1000 ng/L)

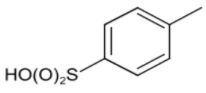

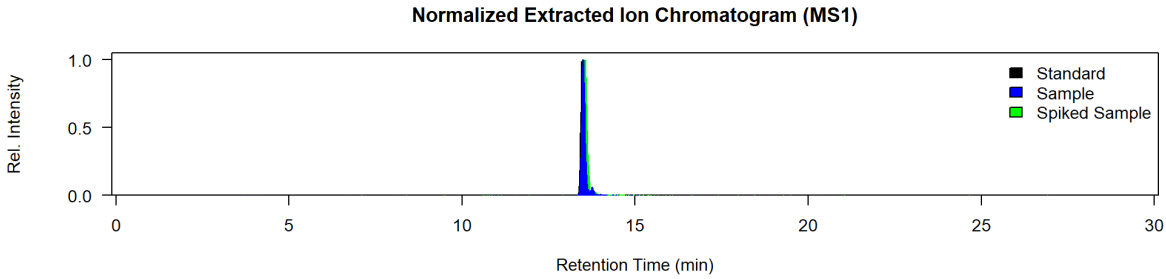

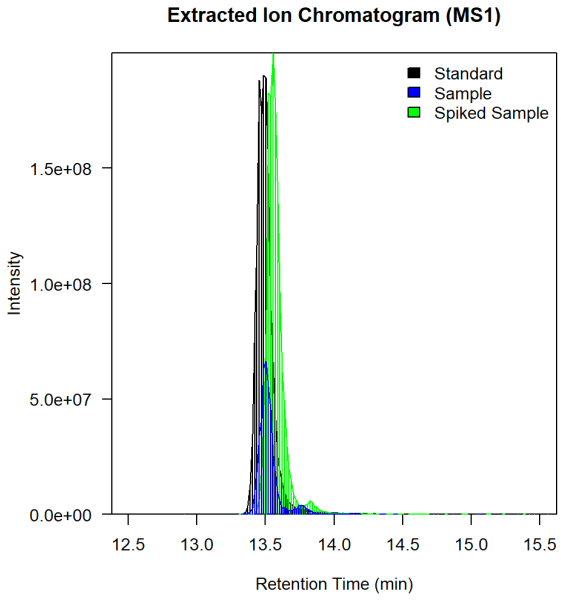

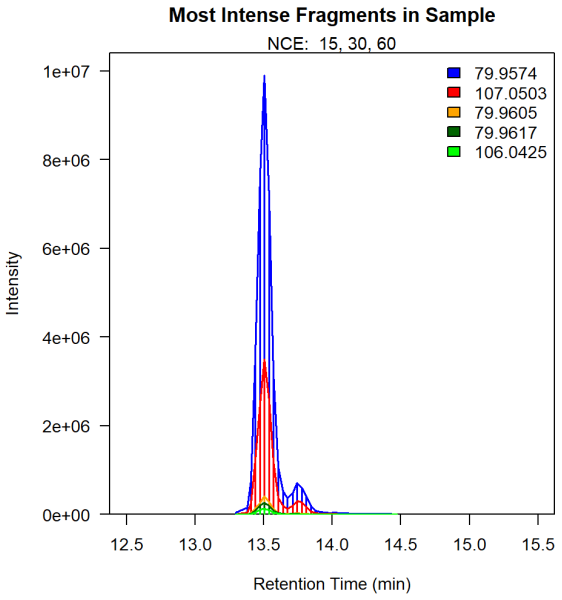

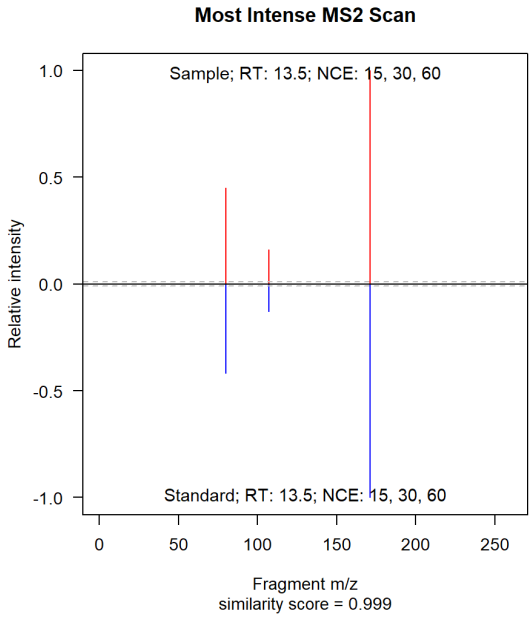

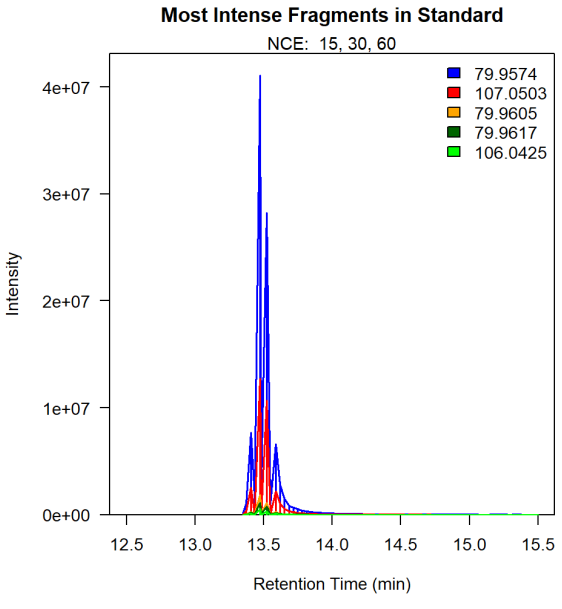

5-Methoxy-2H-benzotriazole
BLG10, Level 1
[M+H]+ 150.06619
(STD 100 ng/L)

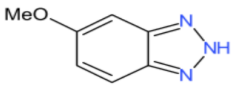

Normalized Extracted Ion Chromatogram (MS1)

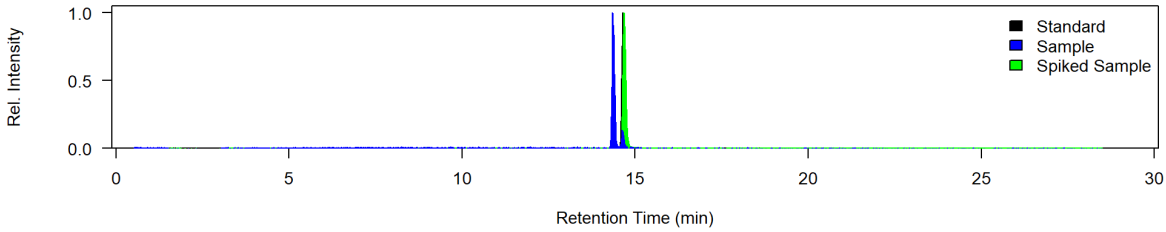

Extracted Ion Chromatogram (MS1)

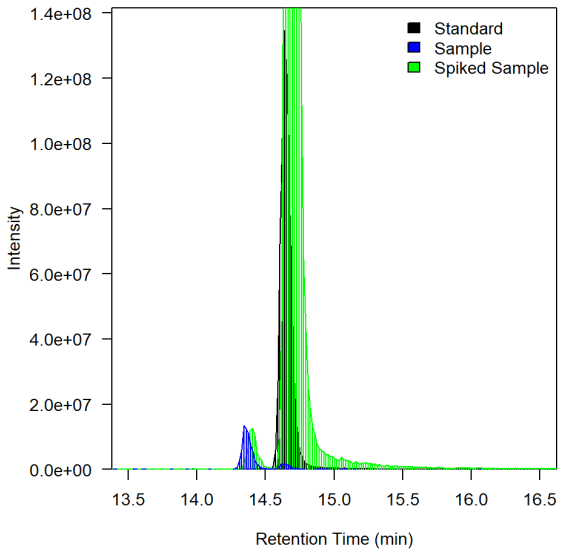

Most Intense Fragments in Sample

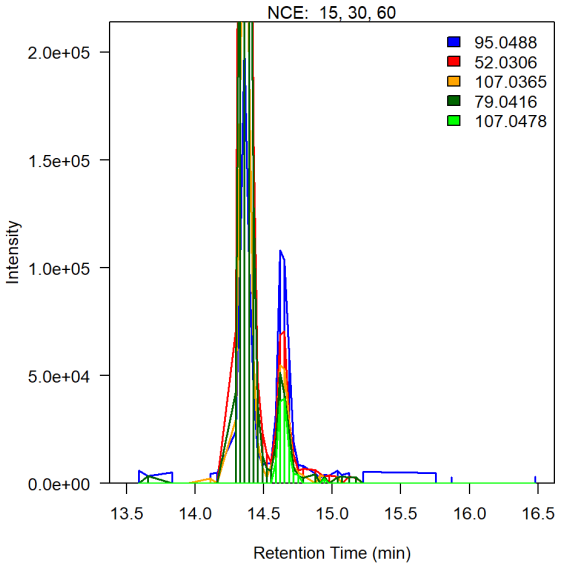

Most Intense MS2 Scan

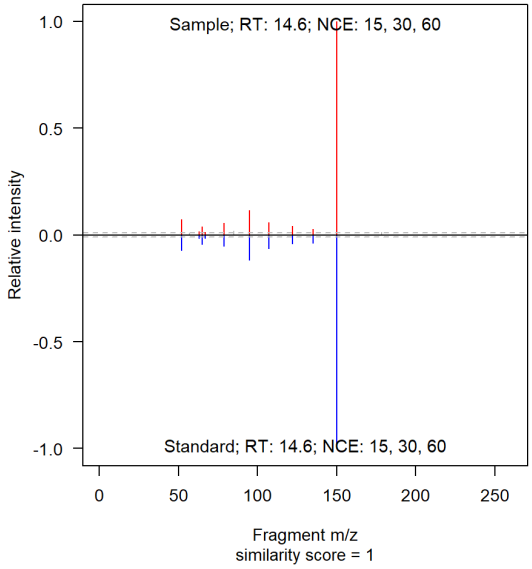

Most Intense Fragments in Standard

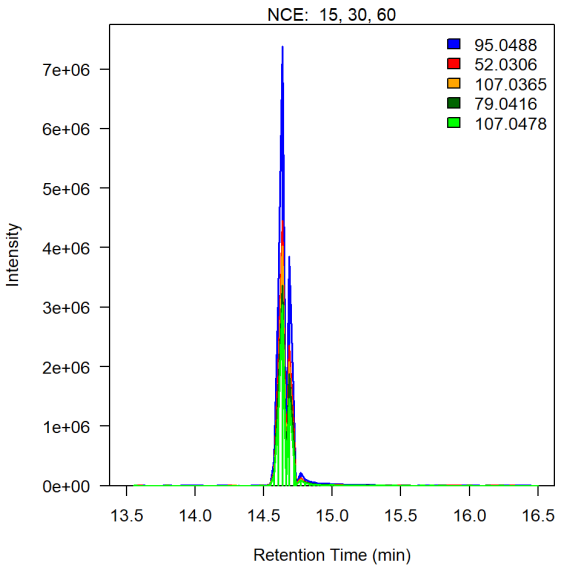

Isomer of 5-Methoxy-2H-benzotriazole
BLG10, Level 3
[M+H]+ 150.06619
(STD 100 ng/L)

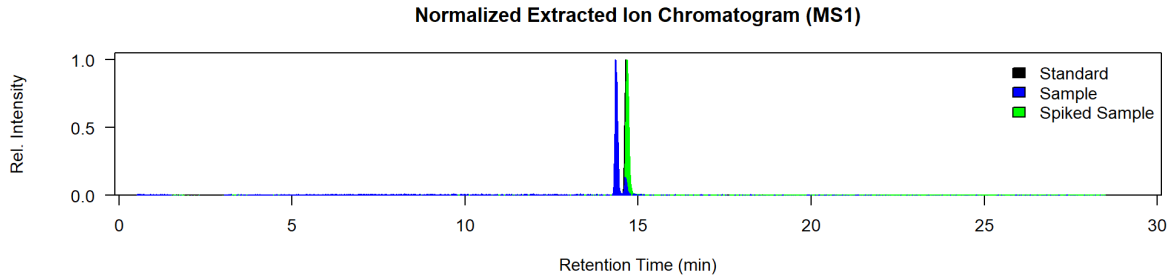

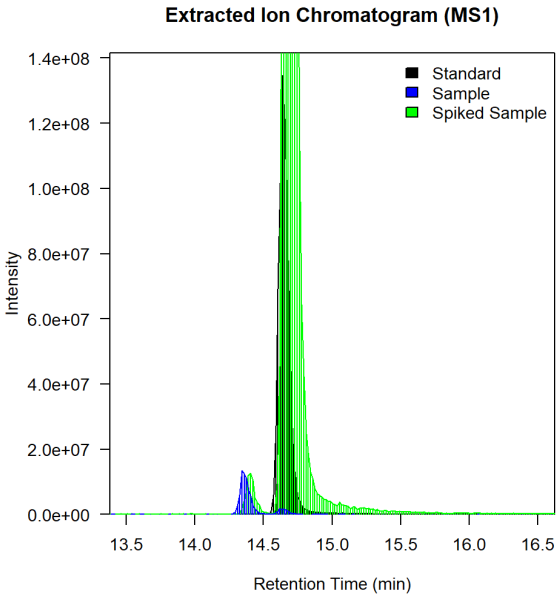

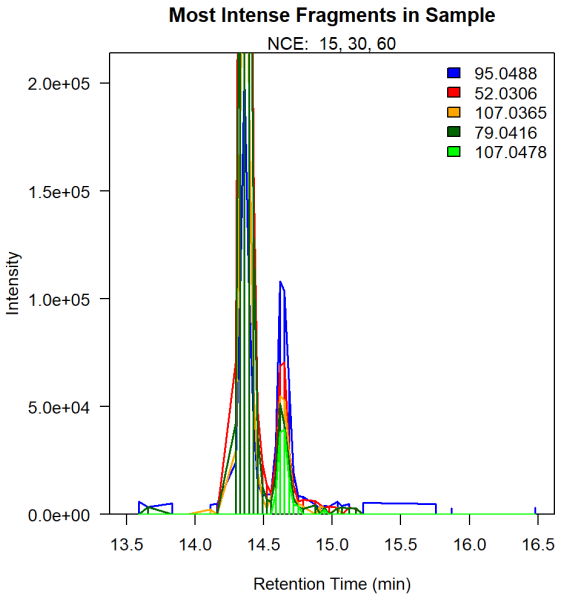

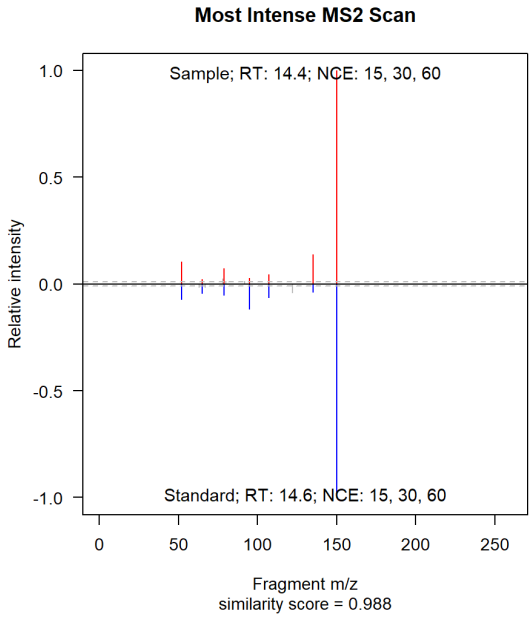

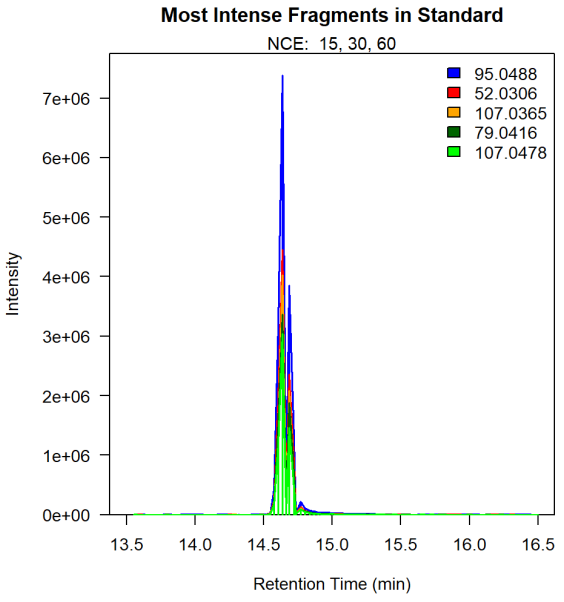

Propyphenazone
GEQ01, Level 1
[M+H]+ 231.14919
(STD 10 ng/L)

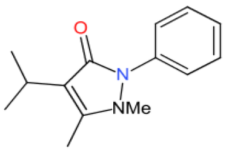

Normalized Extracted Ion Chromatogram (MS1)

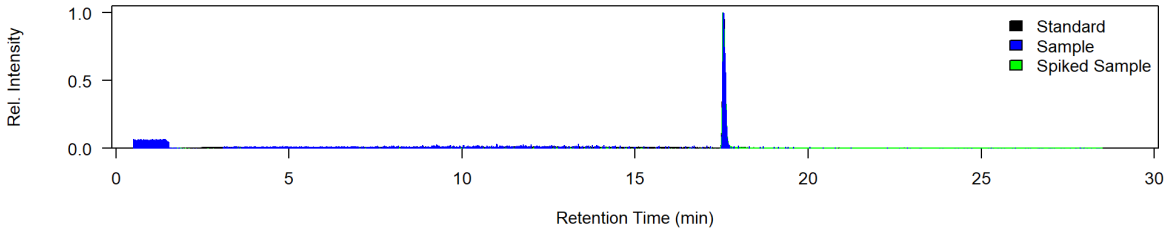

Extracted Ion Chromatogram (MS1)

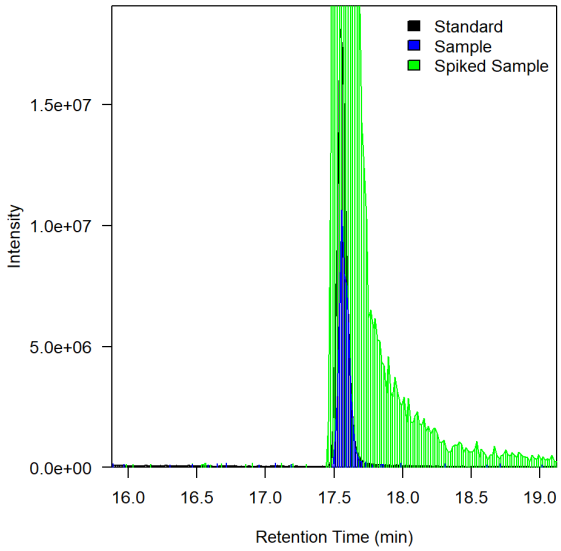

Most Intense Fragments in Sample

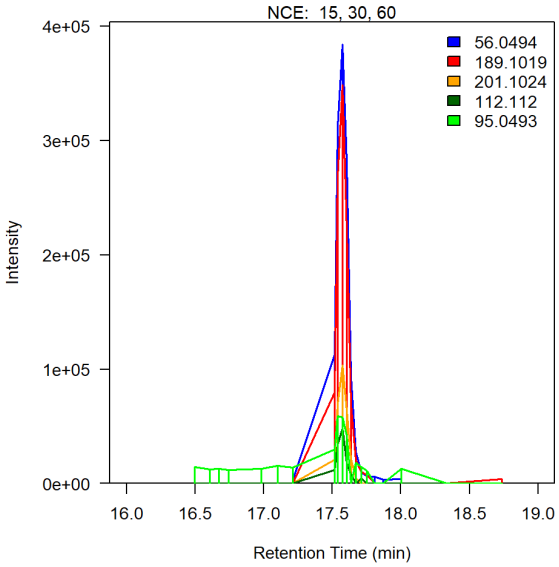

Most Intense MS2 Scan

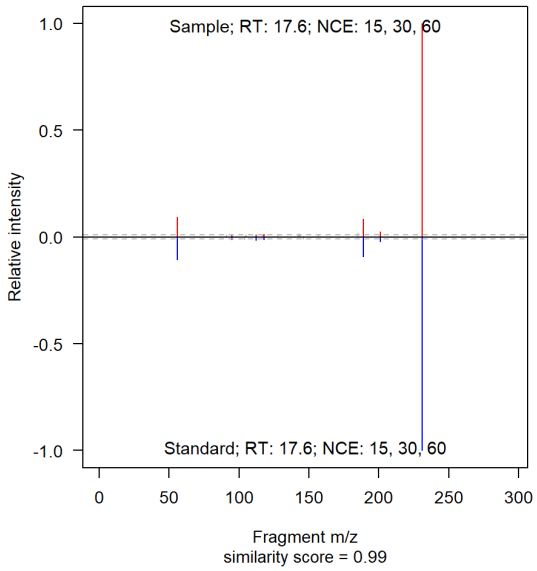

Most Intense Fragments in Standard

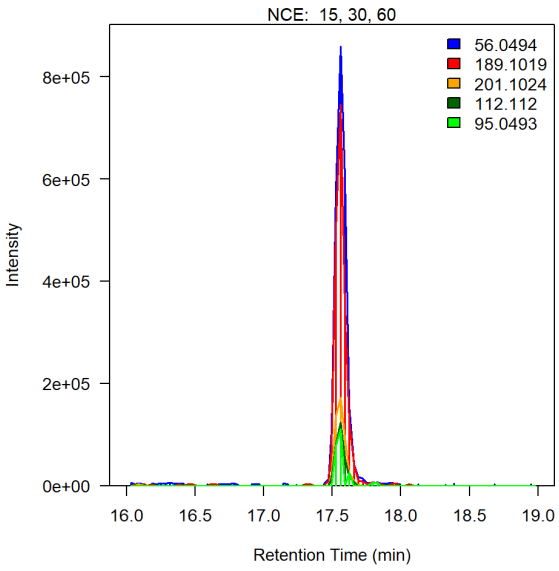

Pyrimidinol (2-Isopropyl-6-methyl-4-pyrimidone)
GEQ01, Level 1
[M+H]+ 153.1022395
(STD 100 ng/L)

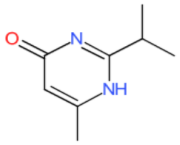

Normalized Extracted Ion Chromatogram (MS1)

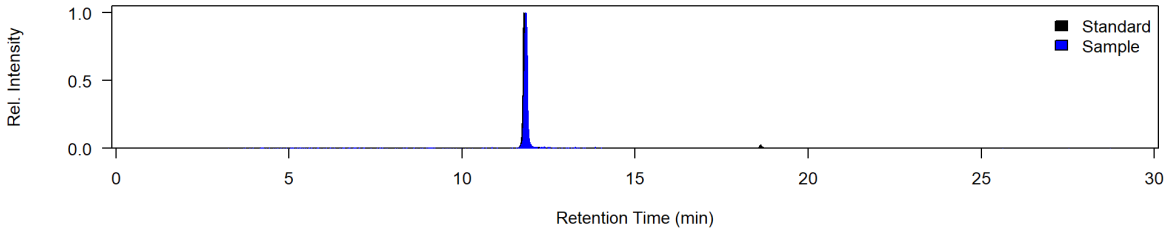

Extracted Ion Chromatogram (MS1)

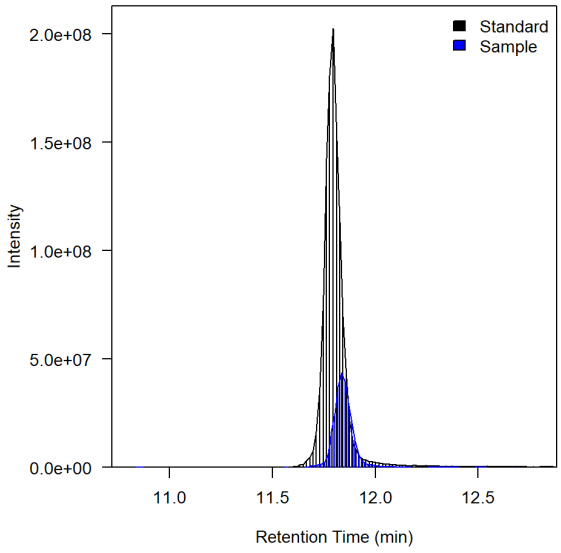

Most Intense Fragments in Sample

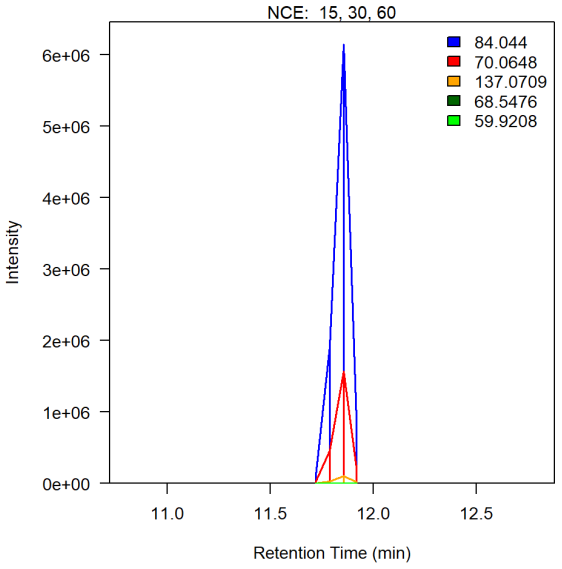

Most Intense MS2 Scan

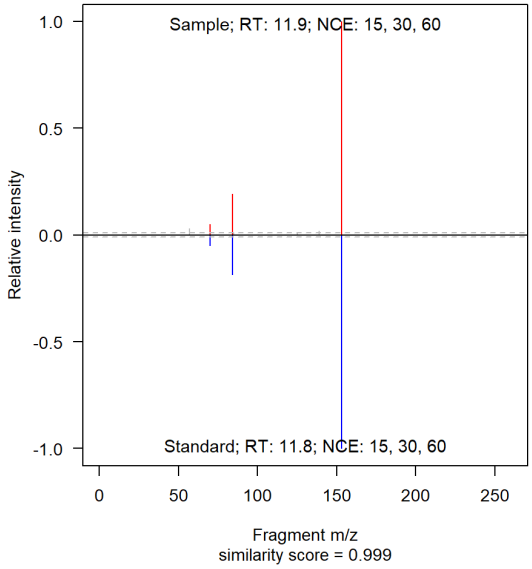

Most Intense Fragments in Standard

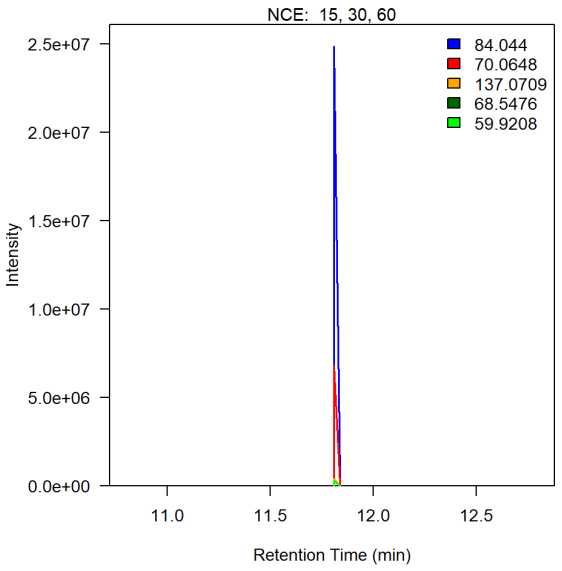

Fluometuron
VDG36, Level 1
[M+H]+ 233.08962
(STD 100 ng/L)

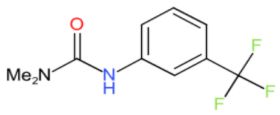

Normalized Extracted Ion Chromatogram (MS1)

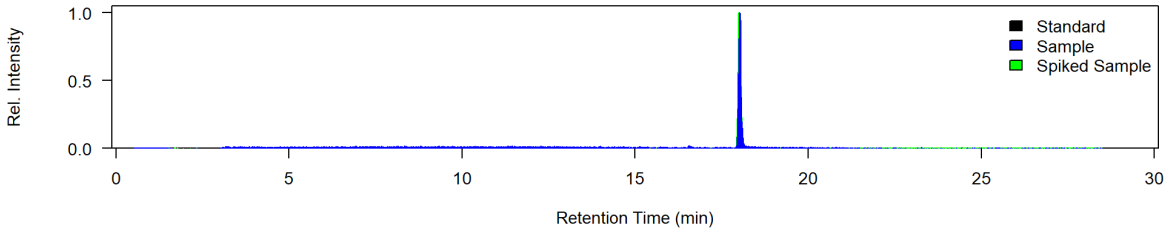

Extracted Ion Chromatogram (MS1)

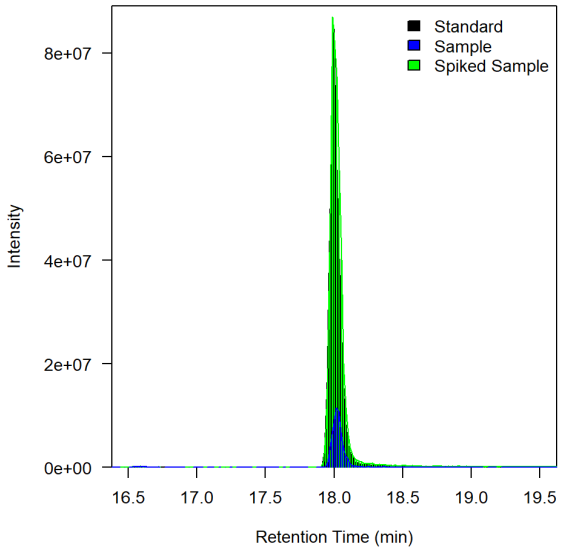

Most Intense Fragments in Sample

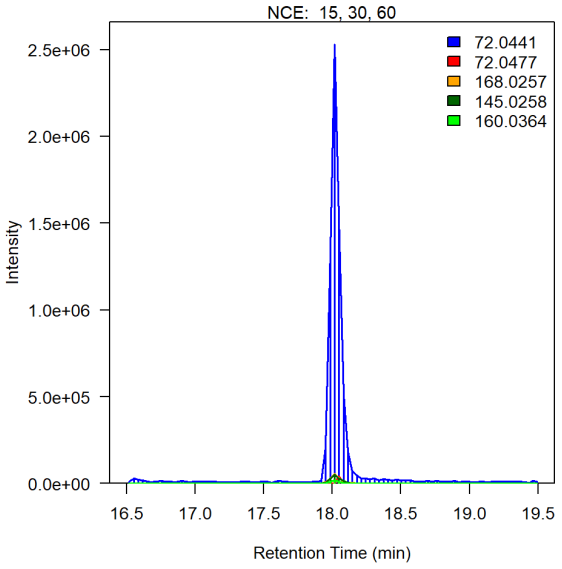

Most Intense MS2 Scan

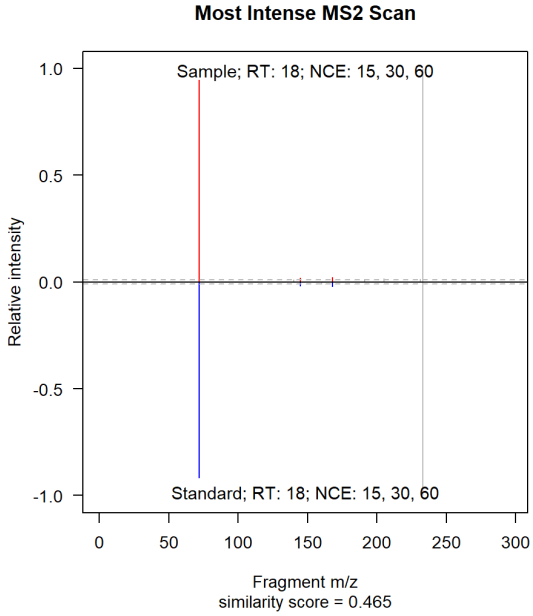

Most Intense Fragments in Standard

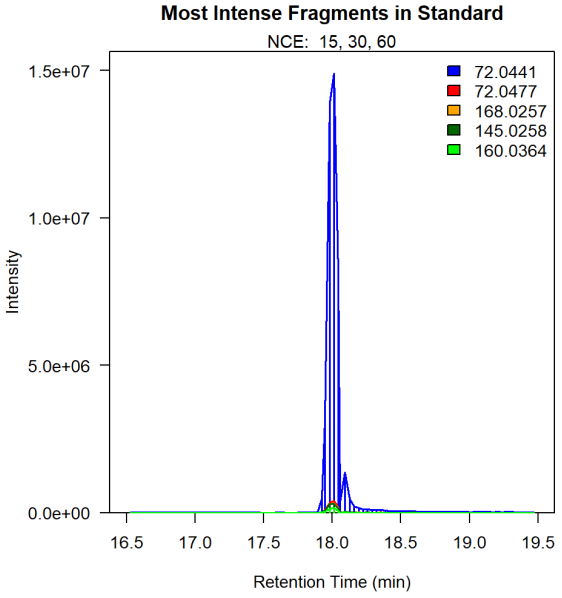

Sulisobenzone
Pooled Sample, Level 1
[M+H]+ 309.04274
(STD 100 ng/L)

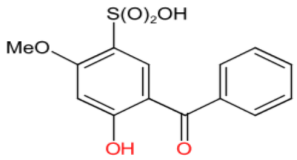

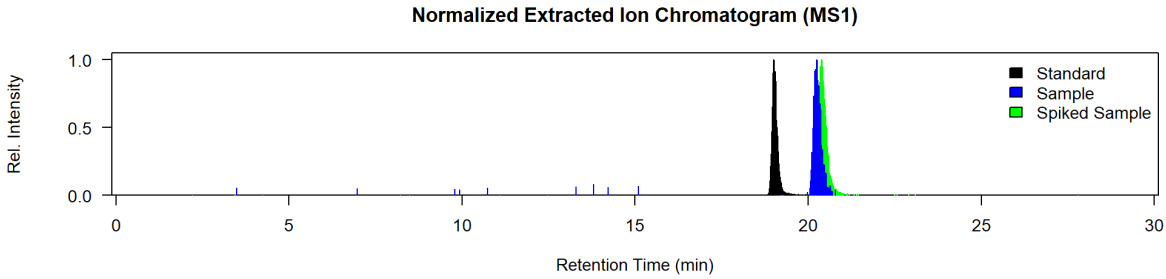

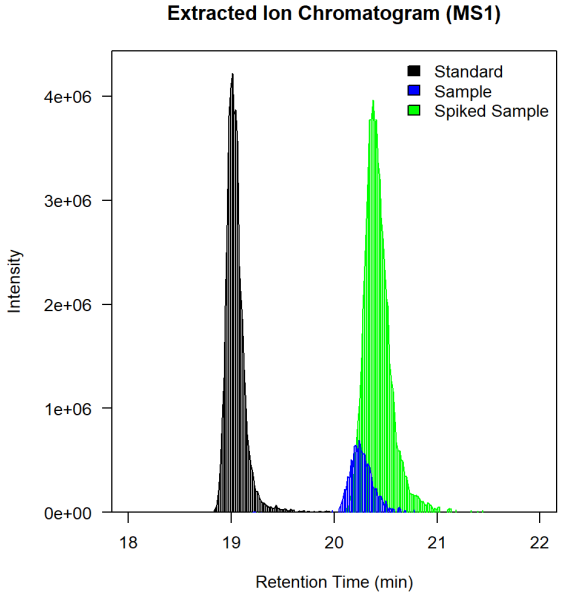

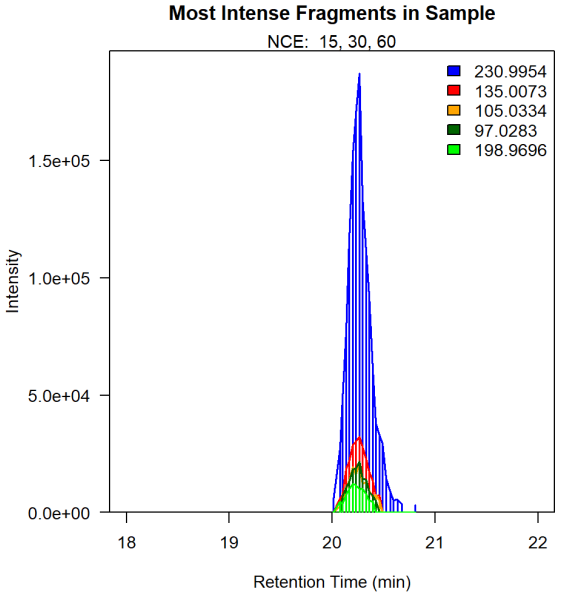

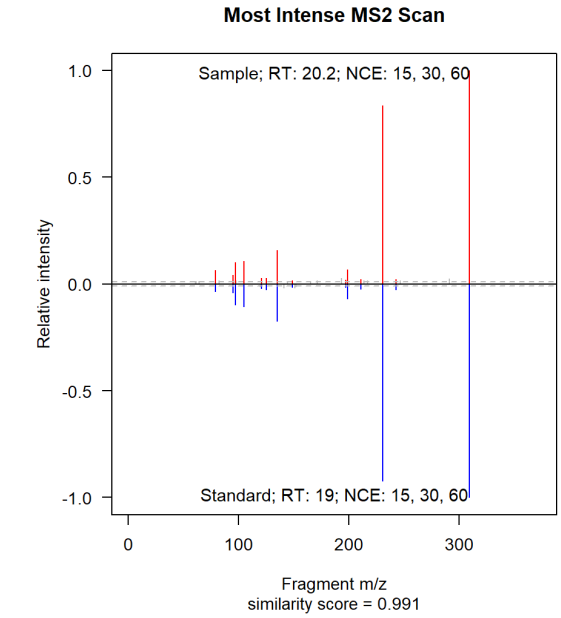

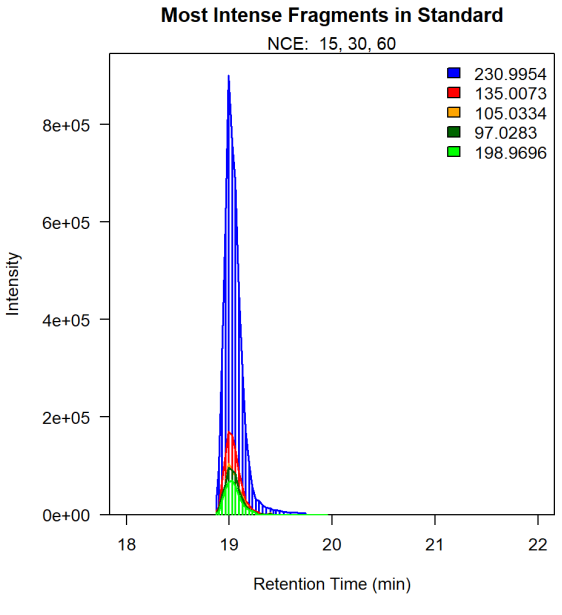

Sulisobenzone
Pooled Sample, Level 1
[M-H]- 307.02818
(STD 100 ng/L)

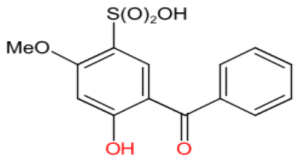

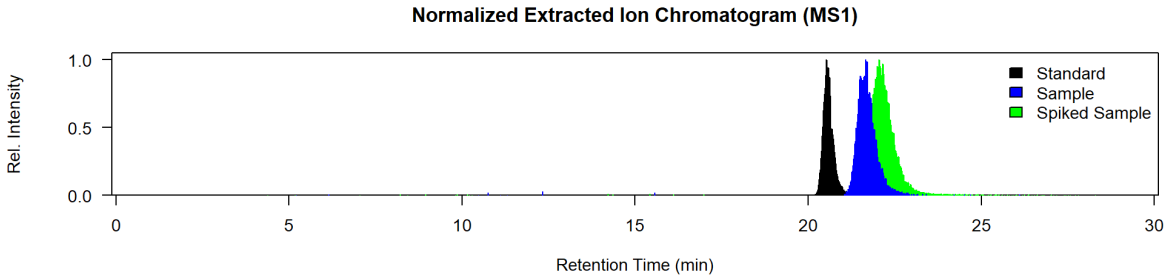

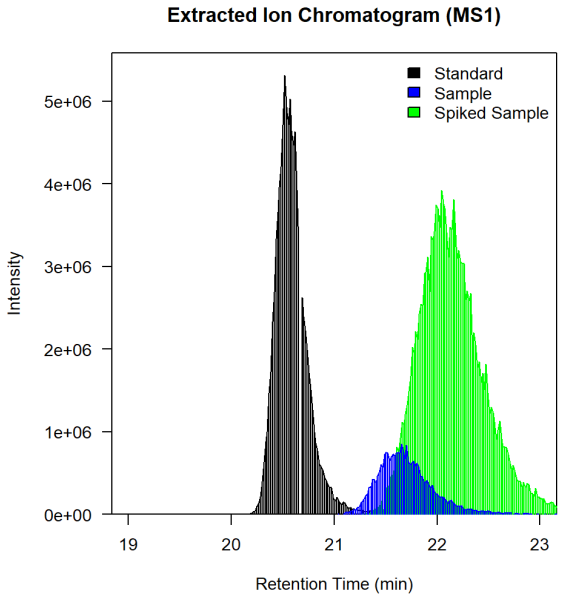

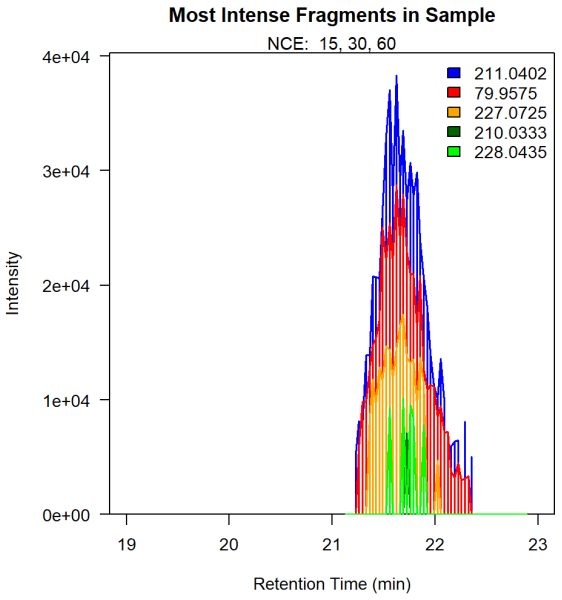

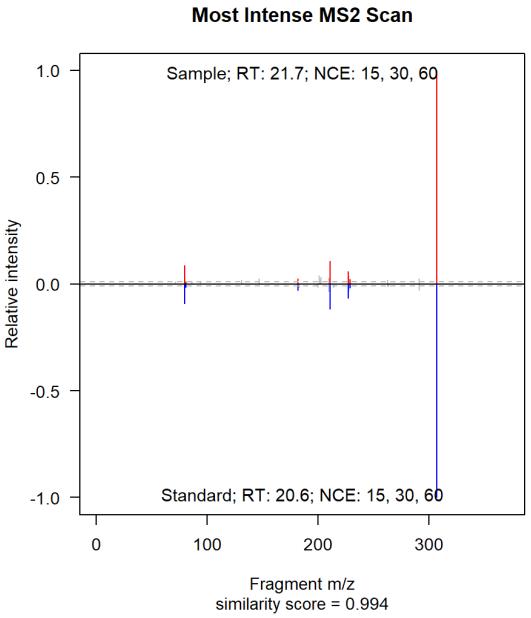

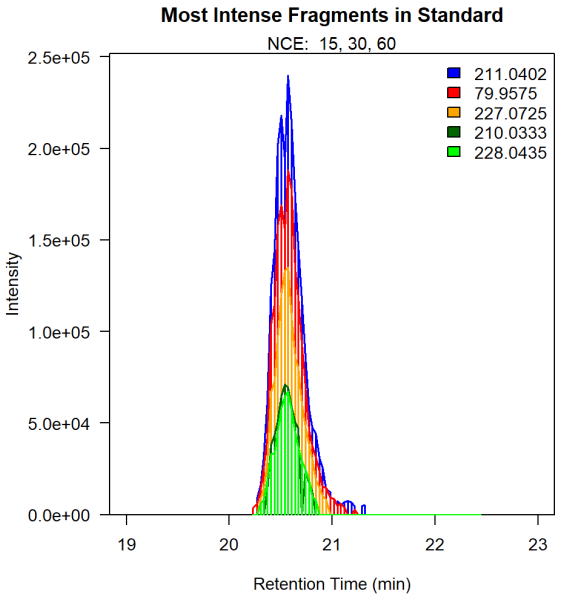

Iopromide TP 643
NTG41, Level 2a
[M+H]+ 643.80354

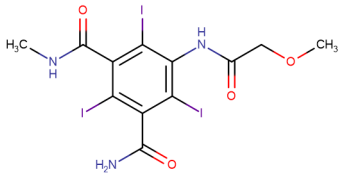

Extracted Ion Chromatogram (MS1)

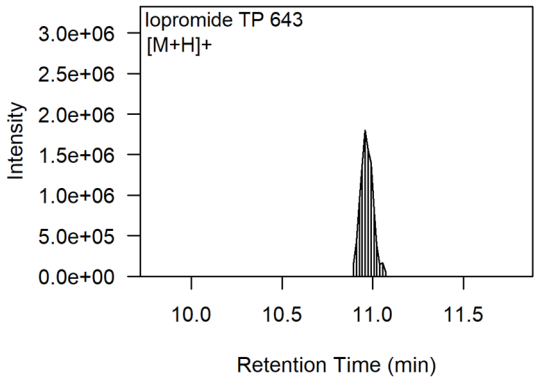

Most Intense Fragments in Sample

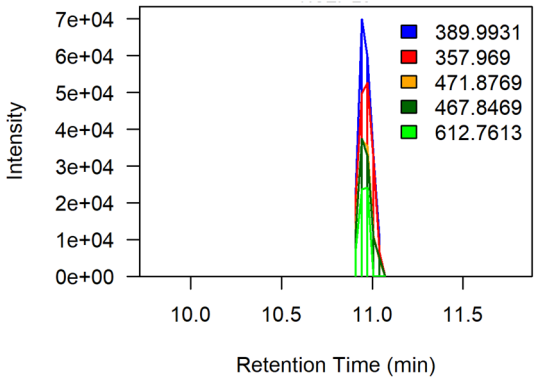

MS/MS Spectrum
Level 2a (Schulz et al. 2008, EST 42 (19))

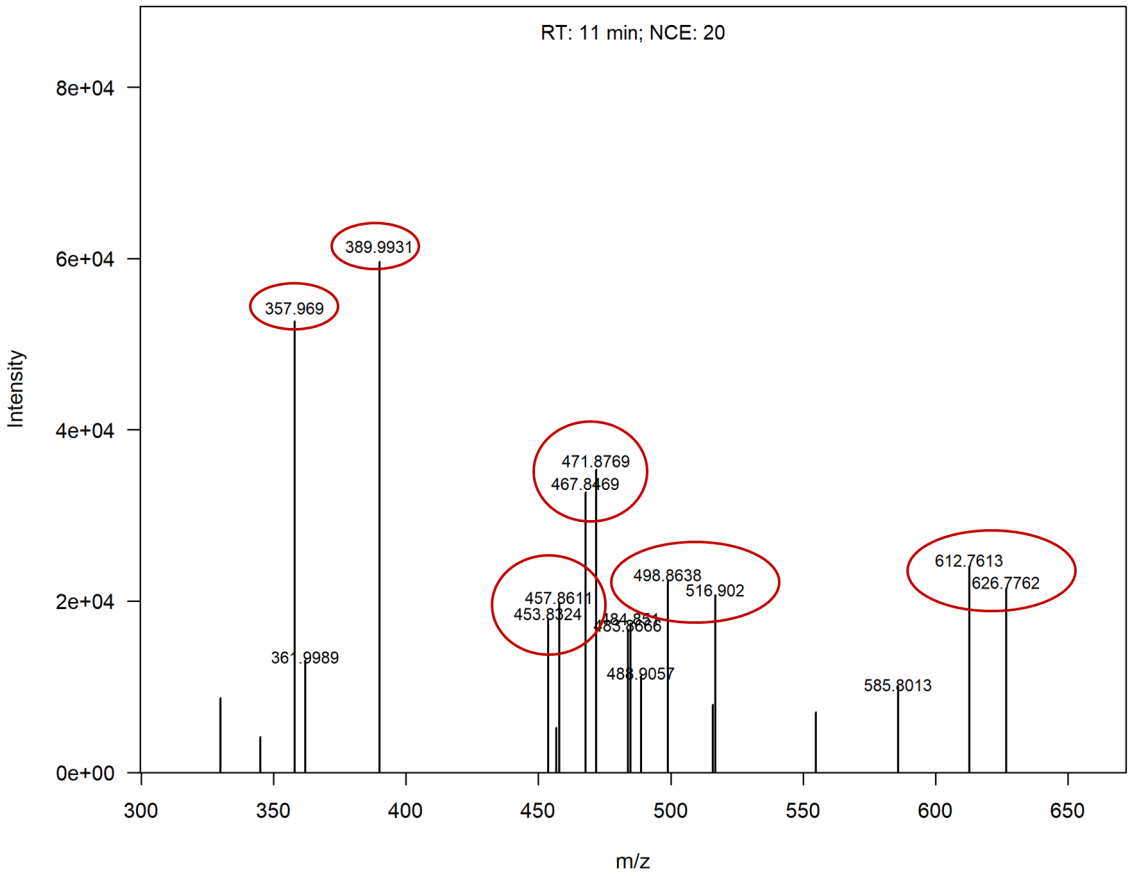

Iopromide TP 701 A
AGG28, Level 2a
[M+H]+ 701.80903

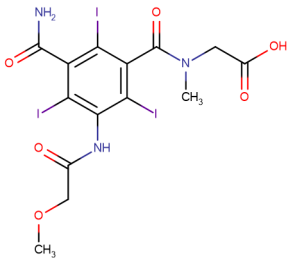

Extracted Ion Chromatogram (MS1)

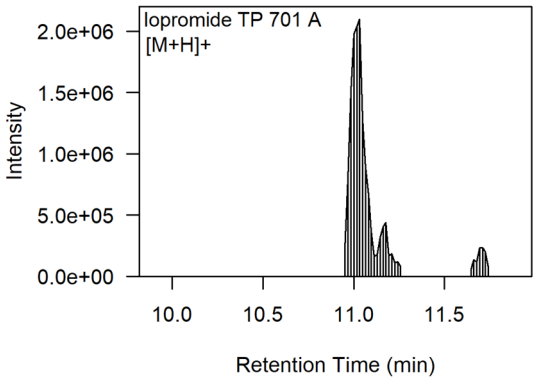

Most Intense Fragments in Sample

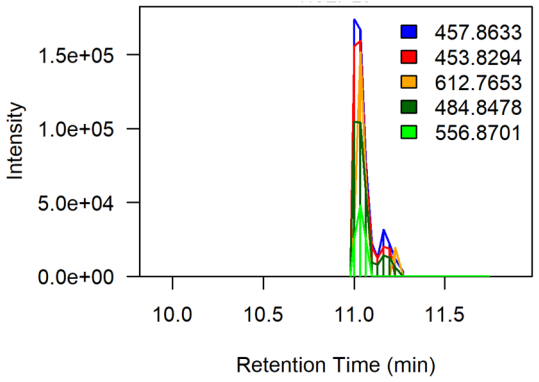

MS/MS Spectrum
Level 2a (Schulz et al. 2008, EST 42 (19))

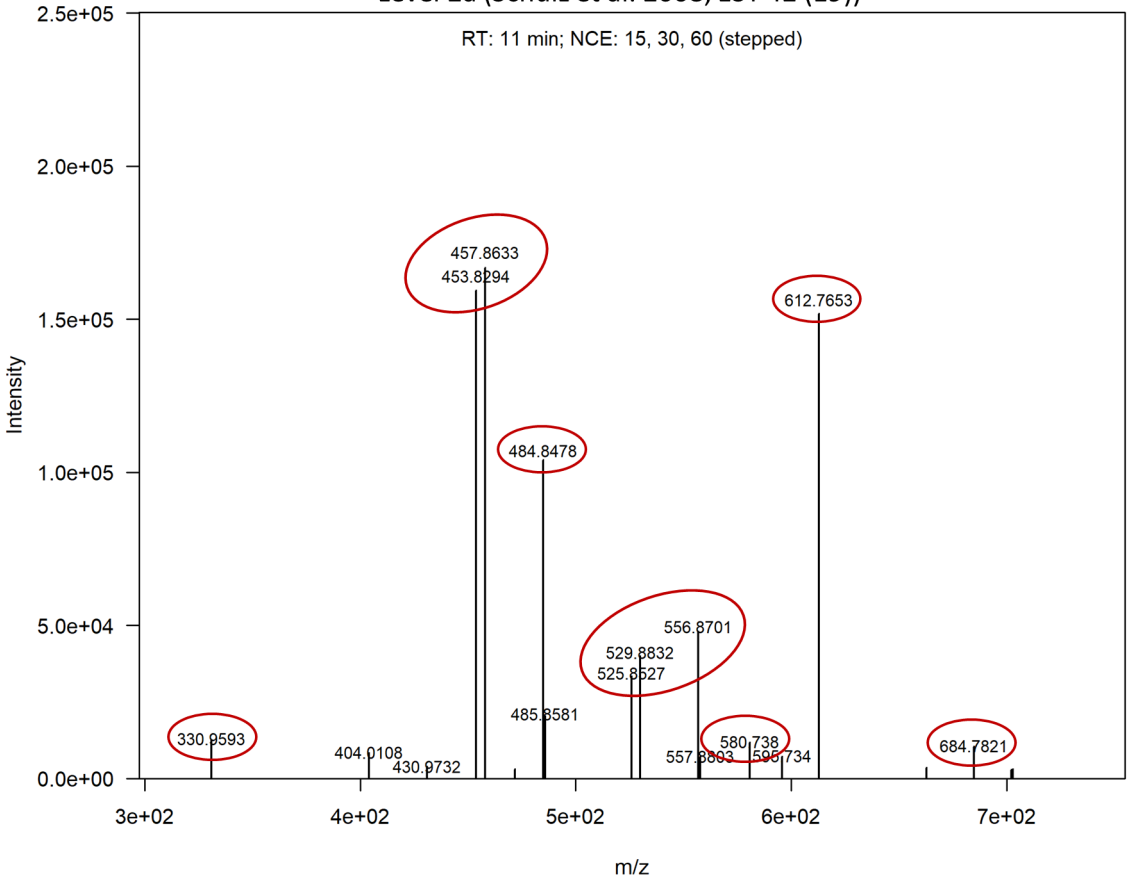

Iomeprol TP 629
SHG05, Level 2a
[M+H]+ 629.78786

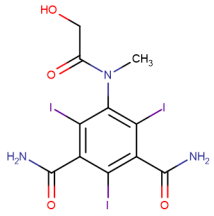

Extracted Ion Chromatogram (MS1)

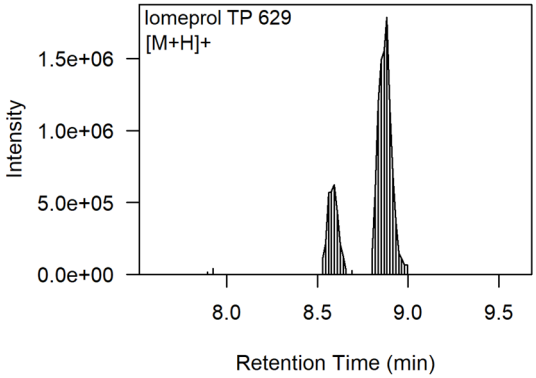

Most Intense Fragments in Sample

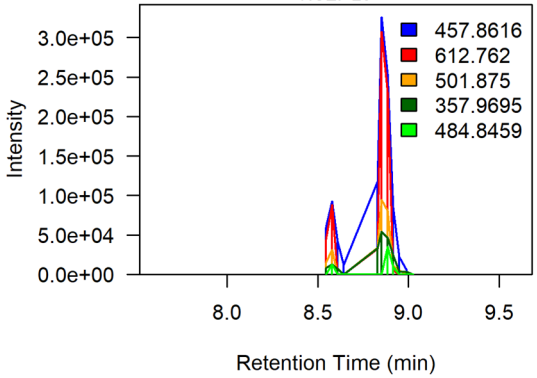

MS/MS Spectrum
Level 2a (Kormos et al. 2009, Anal Chem 81)

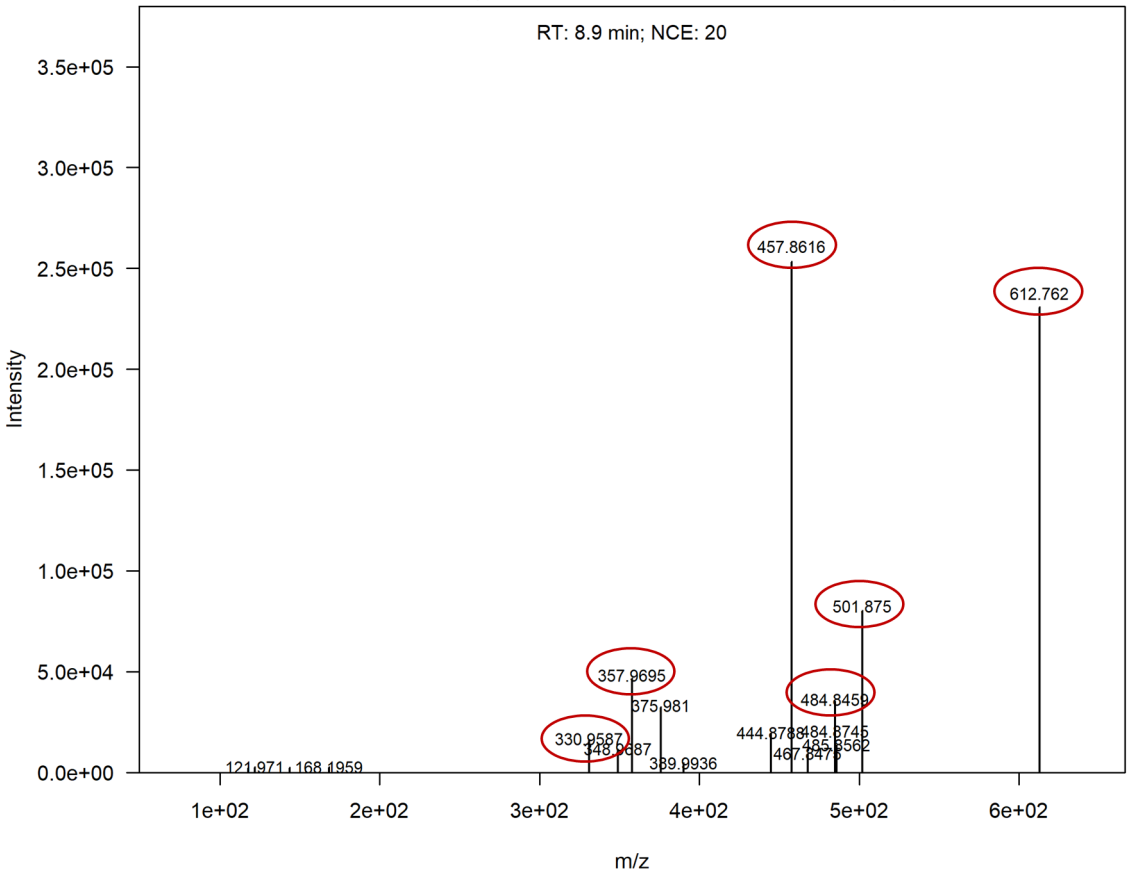

Triphenylphosphine oxide
AGG29, Level 2a
[M+H]+ 279.0933

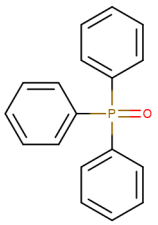

Extracted Ion Chromatogram (MS1)

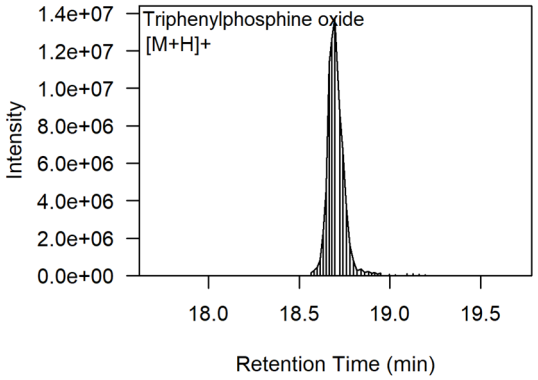

Most Intense Fragments in Sample

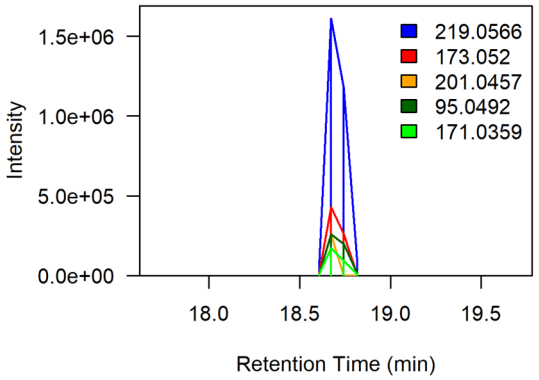

MS/MS Spectrum
Level 2a (library match mzCloud)

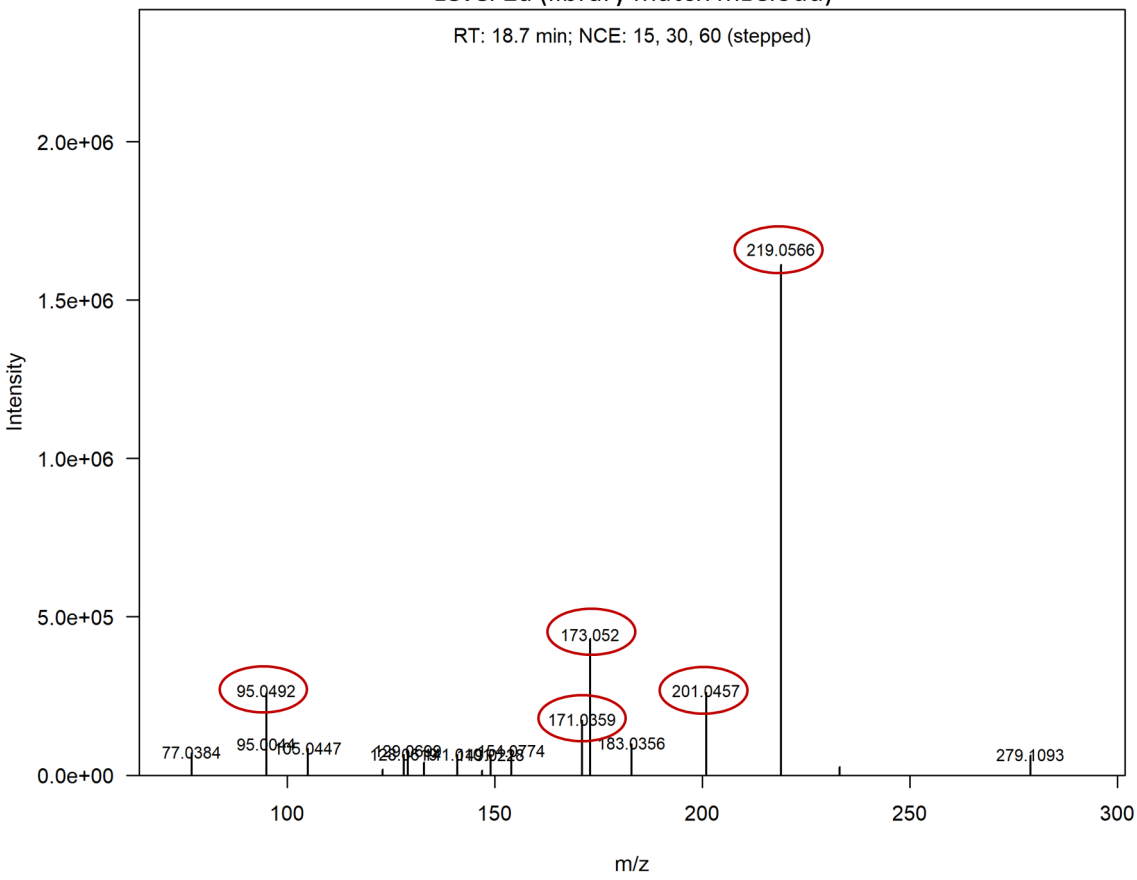

Hexa(methoxymethyl)melamine
VDG27, Level 2a
[M+H]+ 391.22996

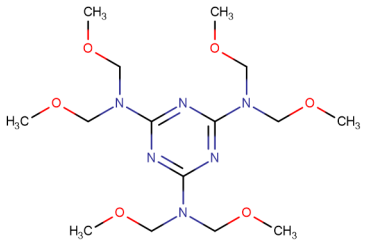

Extracted Ion Chromatogram (MS1)

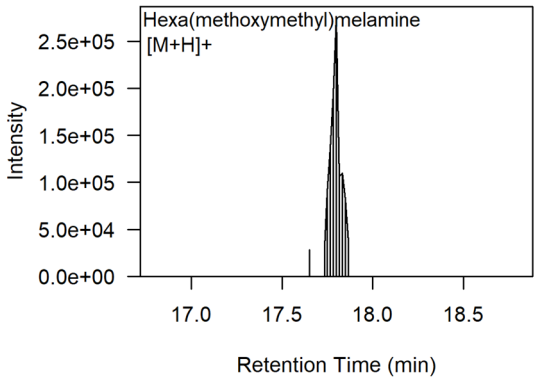

Most Intense Fragments in Sample

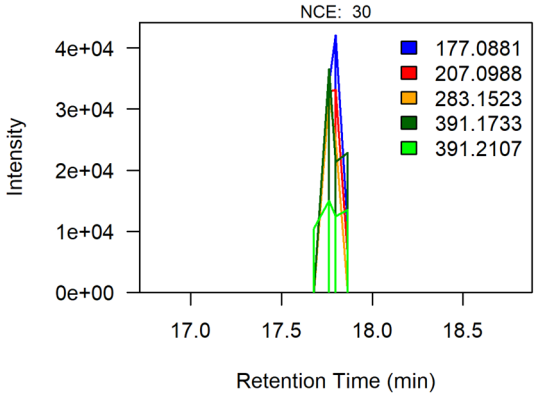

MS/MS Spectrum
Level 2a (library match mzCloud)

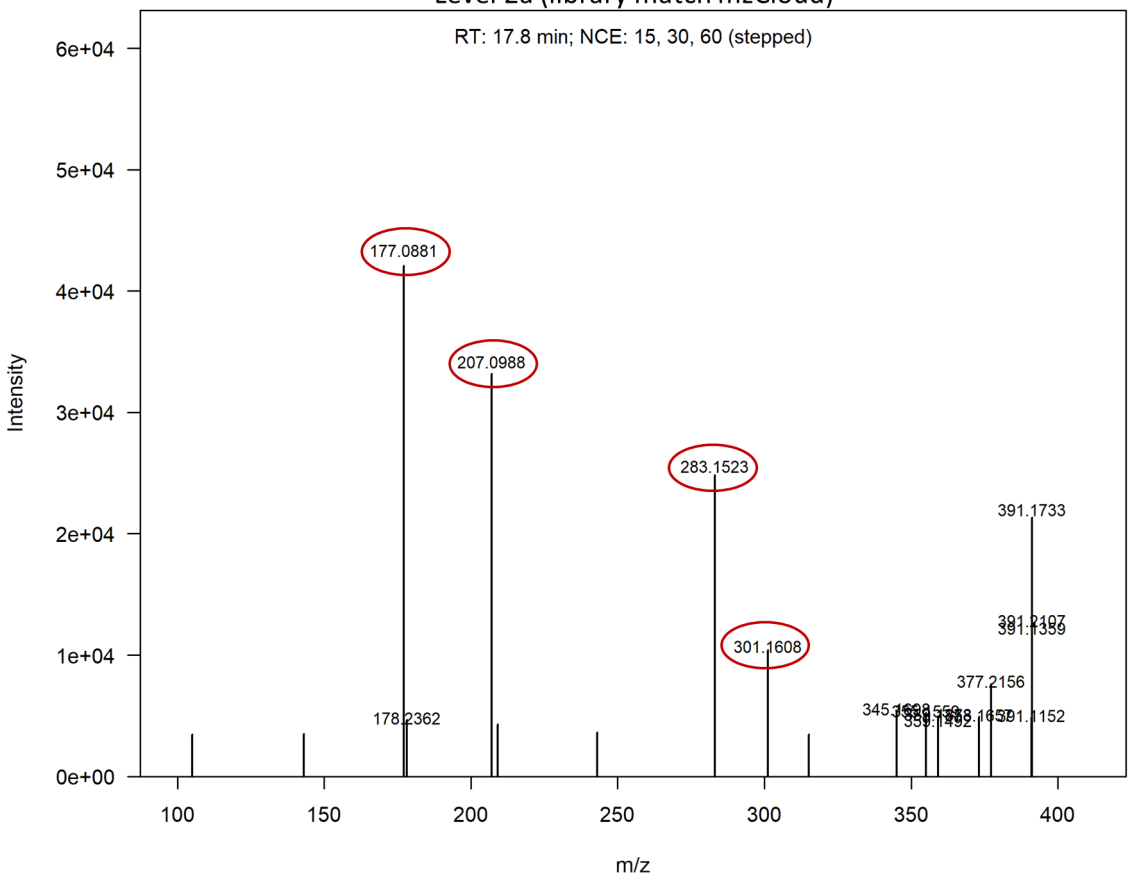

Metolachlor TP CGA357704
NTG41, Level 2a
[M-H]- 278.103396

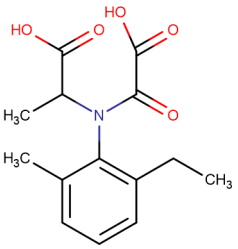

Extracted Ion Chromatogram (MS1)

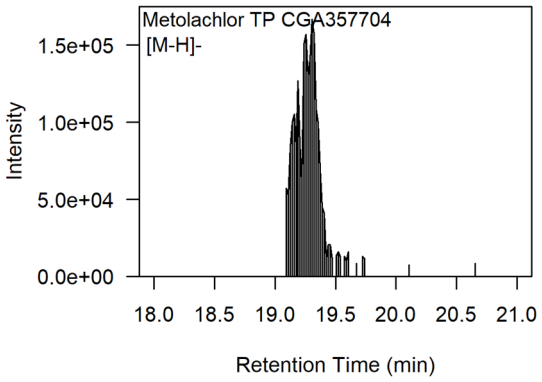

Most Intense Fragments in Sample

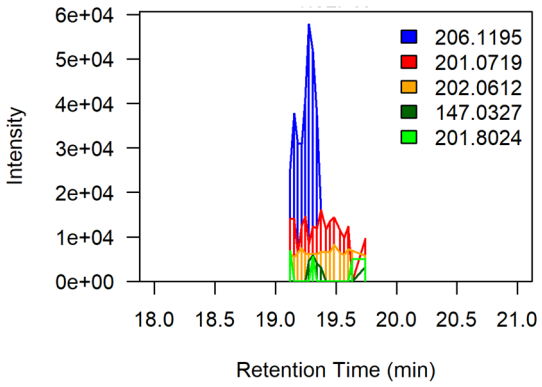

MS/MS Spectrum
Level 2a (Reemtsma et al. 2013, J. Chrom. A 1271 (1))

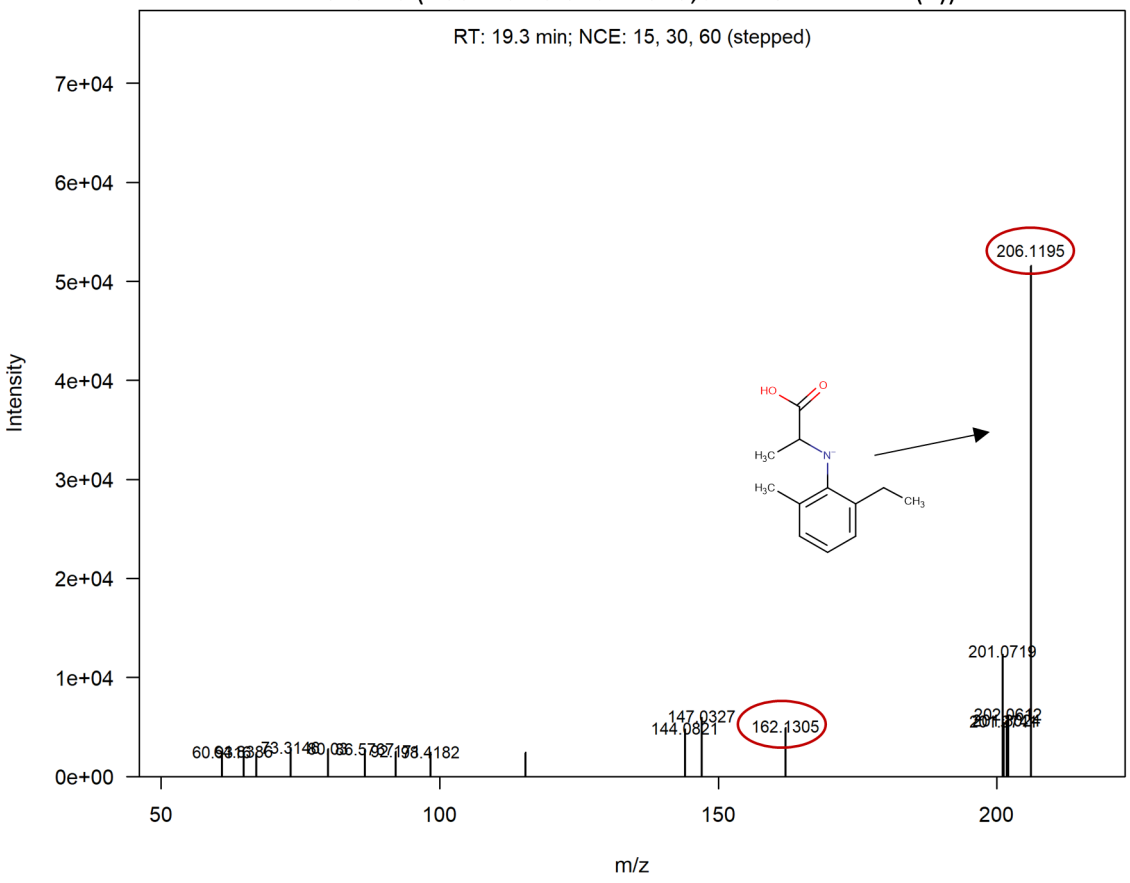

Chlorendic Acid
GEQ01, Level 2a
[M-H]- 384.8169

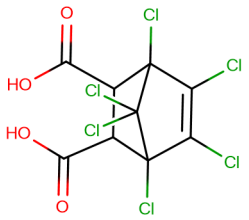

Extracted Ion Chromatogram (MS1)

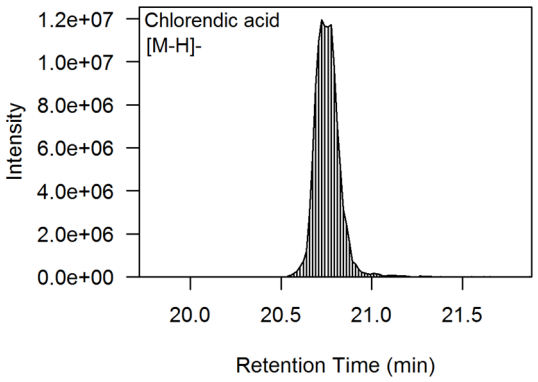

Most Intense Fragments in Sample

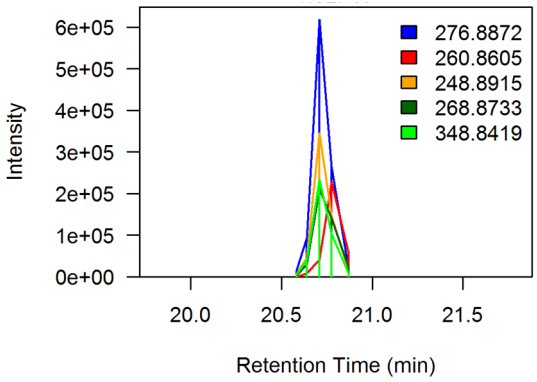

MS/MS Spectrum
Level 2a (library match mzCloud)

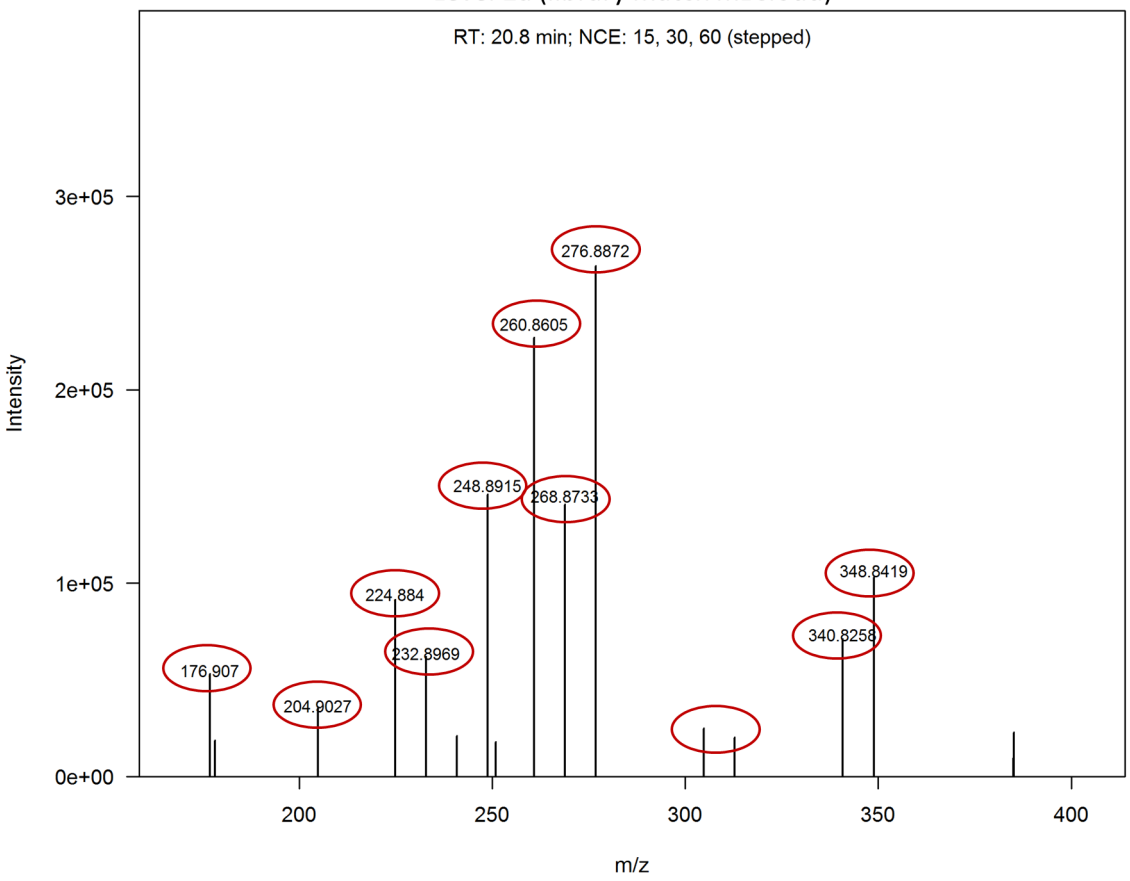

Isomer of 5,6-Dimethyl-2H-benzotriazole
BLG10, Level 3
[M+H]+ 148.08692
(STD 100 ng/L)

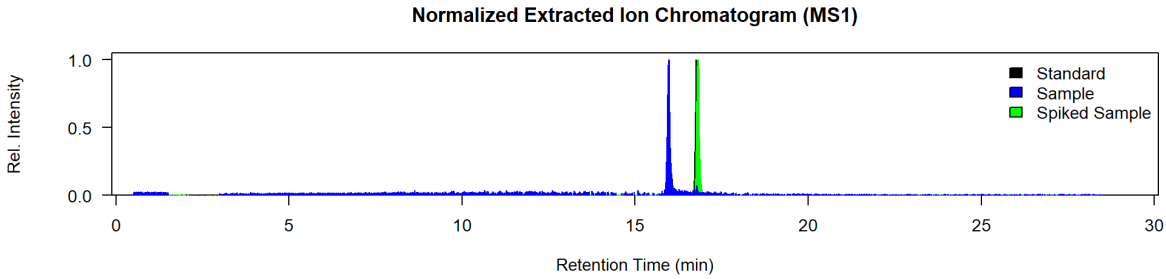

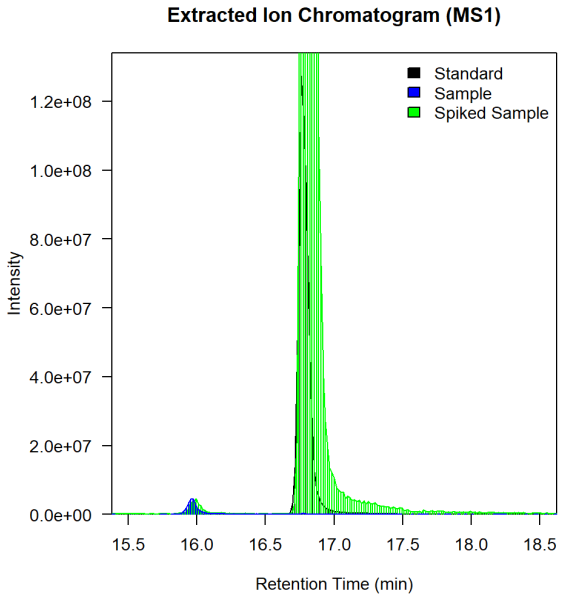

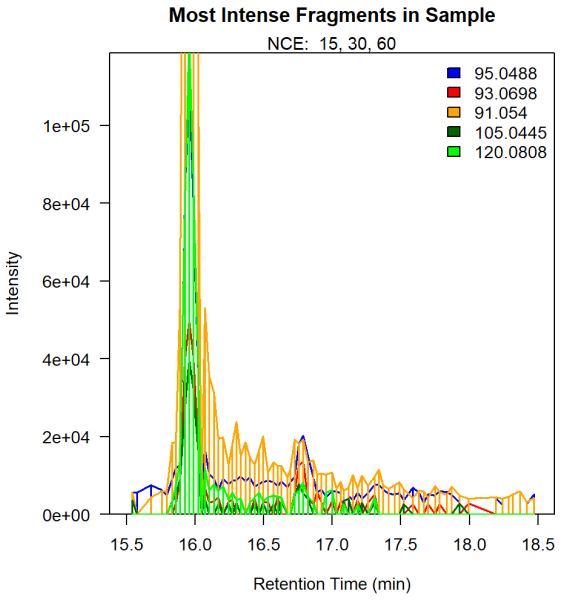

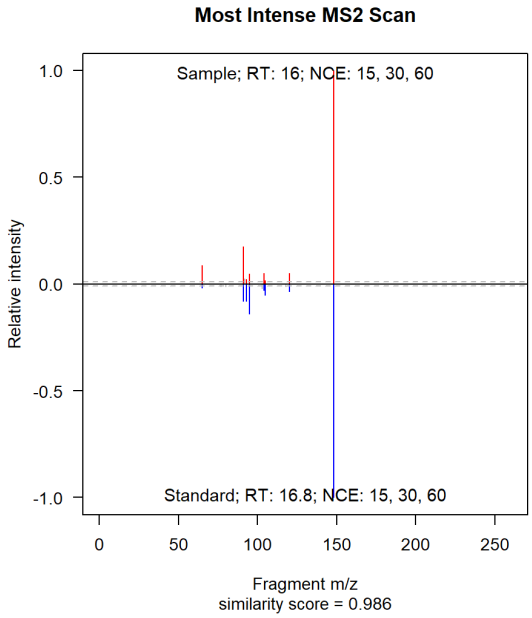

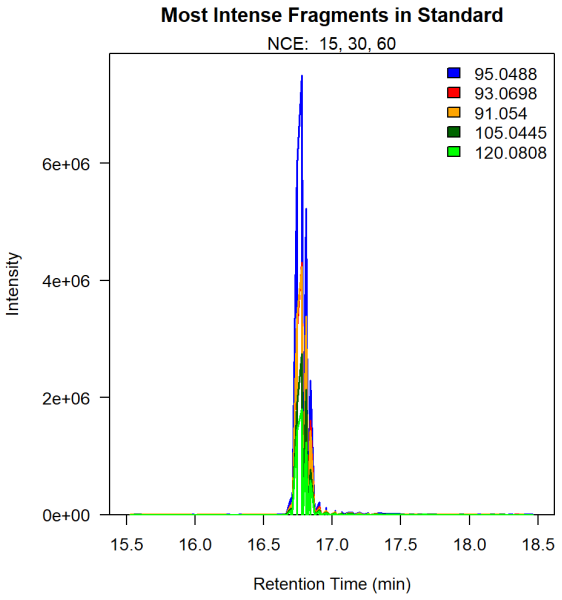

Naphthalenedisulfonic acid (isomers)
GEQ01, Level 3
[M-H]- 286.96895
(STD for 2 isomers: 1000 ng/L)

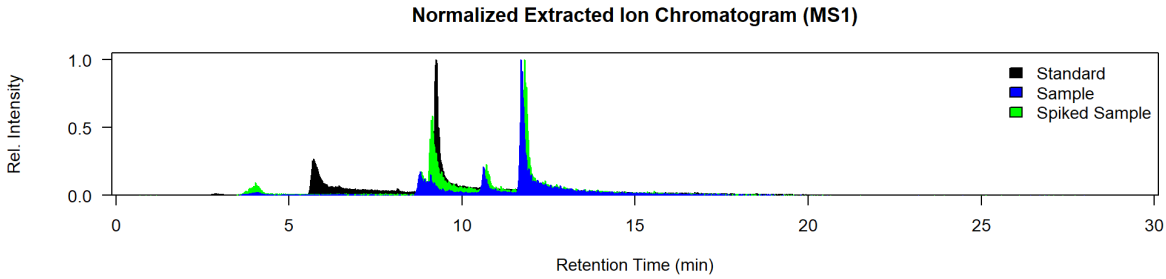

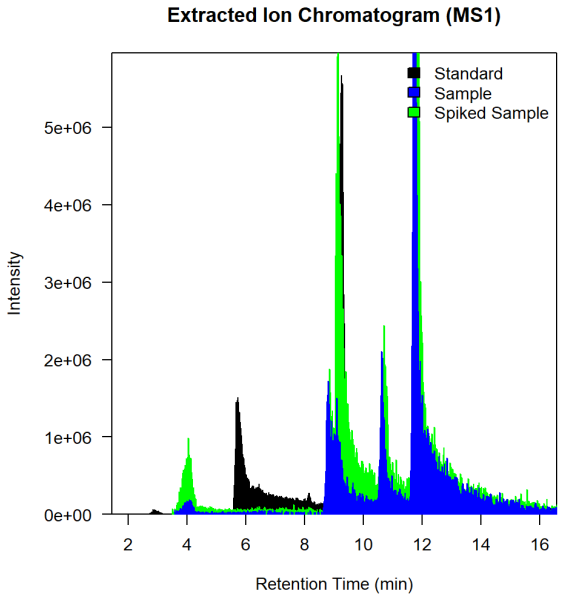

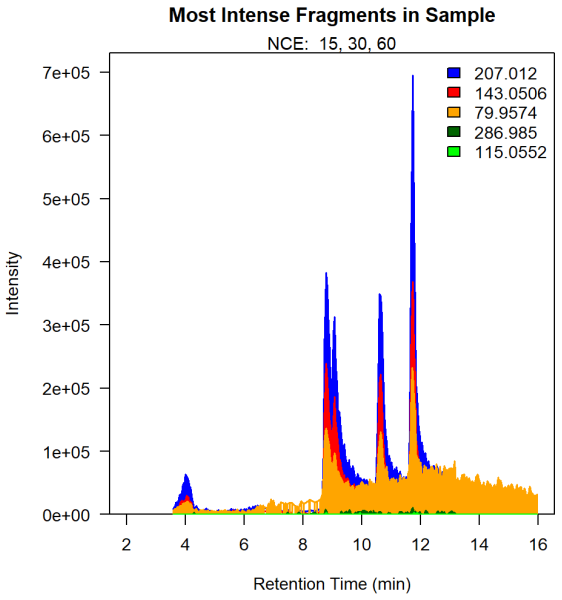

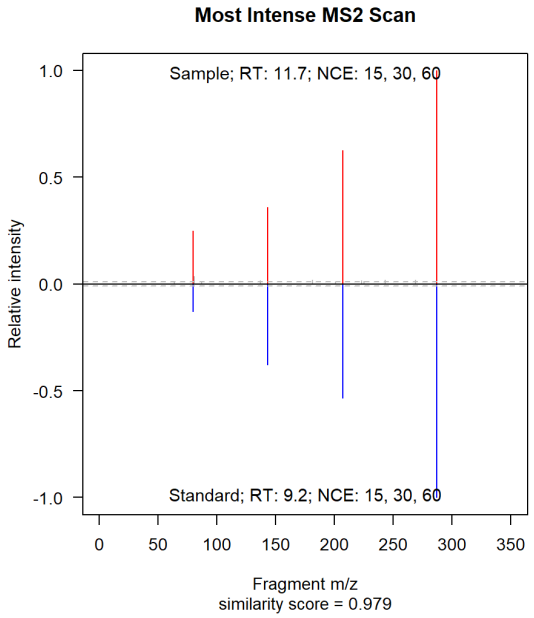

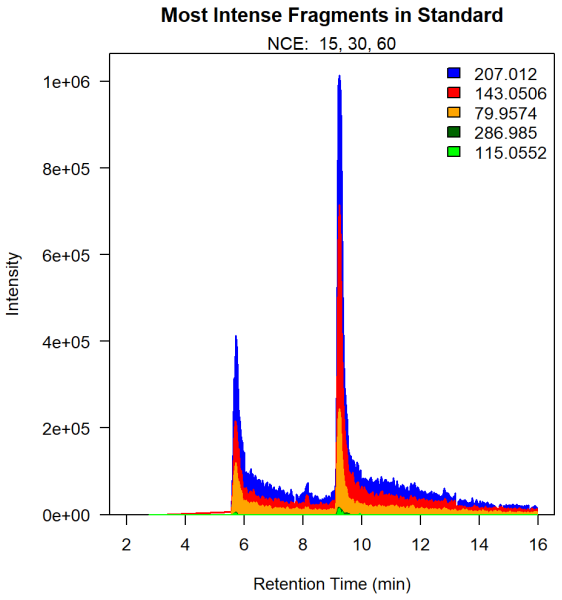

References

Arp, H.P. and Hale, S.E., 2020. S36 | UBAPMT | Potential Persistent, Mobile and Toxic (PMT) substances (Version NORMAN-SLE-S36.0.2.0) [Data set], Zenodo. http://doi.org/10.5281/zenodo.3637611.

Bolton, E. and Schymanski, E.L., 2020. PubChemLite tier0 and tier1 (Version PubChemLite.0.2.0) [Data set], Zenodo. http://doi.org/10.5281/zenodo.3611238.

Dührkop, K., Shen, H., Meusel, M., Rousu, J. and Bocker, S., 2015. Searching molecular structure databases with tandem mass spectra using CSI:FingerID. Proc Natl Acad Sci U S A 112(41), 12580-12585.

Dührkop, K., Fleischauer, M., Ludwig, M., Aksenov, A.A., Melnik, A.V., Meusel, M., Dorrestein, P.C., Rousu, J. and Bocker, S., 2019. SIRIUS 4: a rapid tool for turning tandem mass spectra into metabolite structure information. Nat Methods 16(4), 299-302.

Fischer, S., 2017. S17 | KEMIMARKET | KEMI Market List MS-ready (12/05/2017) (Version NORMAN-SLE-S17.0.1.3) [Data set], Zenodo. http://doi.org/10.5281/zenodo.3653175.

Gatto, L. and Lilley, K.S., 2012. MSnbase - an R/Bioconductor package for isobaric tagged mass spectrometry data visualization, processing and quantitation. Bioinformatics (28), 288-289.

Gerlich, M. and Neumann, S., 2013. MetFusion: integration of compound identification strategies. J Mass Spectrom 48(3), 291-298.

Kiefer, K., Müller, A., Singer, H. and Hollender, J., 2019. New Relevant Pesticide Transformation Products in Groundwater Detected Using Target and Suspect Screening for Agricultural and Urban Micropollutants with LC-HRMS. Water research 165.

Kiefer, K., Müller, A., Singer, H. and Hollender, J., 2020. S60 | SWISSPEST19 | Swiss Pesticides and Metabolites from Kiefer et al 2019 (Version S60.0.1.1) [Data set], Zenodo. http://doi.org/10.5281/zenodo.3766352.

Kormos, J.L., Schulz, M., Wagner, M. and Ternes, T.A., 2009. Multistep Approach for the Structural Identification of Biotransformation Products of Iodinated X-ray Contrast Media by Liquid Chromatography/Hybrid Triple Quadrupole Linear Ion Trap Mass Spectrometry and 1H and 13C Nuclear Magnetic Resonance. Analytical chemistry 81(22), 9216-9224.

Letzel, T., Grosse, S. and Sengel, M., 2017. S2 | STOFFIDENT | HSWT/LfU STOFF-IDENT Database of Water-Relevant Substances (Version NORMAN-SLE-S2.0.1.0) [Data set], Zenodo. http://doi.org/10.5281/zenodo.2621452.

Norman Network, Aalizadeh, R., Alygizakis, N.A., Schymanski, E.L., Slobodnik, J. and Fischer, S., 2020. S0 | SUSDAT | Merged NORMAN Suspect List: SusDat (Version NORMAN-SLE-S0.0.2.2) [Data set], Zenodo. http://doi.org/10.5281/zenodo.3695732.

Reemtsma, T., Alder, L. and Banasiak, U., 2013. A multimethod for the determination of 150 pesticide metabolites in surface water and groundwater using direct injection liquid chromatography-mass spectrometry. Journal of chromatography A 1271(1), 95-104.

Ruttkies, C., Schymanski, E.L., Wolf, S., Hollender, J. and Neumann, S., 2016. MetFrag relaunched: incorporating strategies beyond in silico fragmentation. Journal of Cheminformatics 8(3).

Ruttkies, C., Neumann, S. and Posch, S., 2019. Improving MetFrag with statistical learning of fragment annotations. BMC Bioinformatics 20(1), 376.

Schollée, J.E., 2018. TFAnalyzeR, version 1.0.1, Analysis of TraceFinder Target Screening, Zenodo, DOI: 10.5281/zenodo.3234748.

Schulz, M., Loffler, D., Wagner, M. and Ternes, T.A., 2008. Transformation of the X-ray contrast medium iopromide in soil and biological wastewater treatment. Environ Sci Technol 42(19), 7207-7217.

Schulze, S., Zahn, D., Montes, R., Rodil, R., Quintana, J.B., Knepper, T.P., Reemtsma, T. and Berger, U., 2019. Occurrence of emerging persistent and mobile organic contaminants in European water samples. Water Res 153, 80-90.

Schymanski, E.L., 2019. MetFrag Local CSV: CompTox (7 March 2019 release) Wastewater MetaData File (Version WWMetaData_4Oct2019) [Data set], Zenodo. http://doi.org/10.5281/zenodo.3472781.

Schymanski, E.L., 2020. ReSOLUTION: SOLUTIONS for High ReSOLUTION Mass Spectrometry. R package. https://rdrr.io/github/schymane/ReSOLUTION/.

Stravs, M.A., Schymanski, E.L., Singer, H.P. and Hollender, J., 2013. Automatic recalibration and processing of tandem mass spectra using formula annotation. J Mass Spectrom 48(1), 89-99.

Chapter 4: Chlorothalonil Transformation Products in Drinking Water Resources: Widespread and Challenging to Abate

Karin Kiefer[1,2], Tobias Bader[3], Nora Minas[1], Elisabeth Salhi[1], Elisabeth M.-L. Janssen[1], Urs von Gunten[1,2,4], Juliane Hollender[1,2]*

[1] Eawag, Swiss Federal Institute of Aquatic Science and Technology, 8600 Dübendorf, Switzerland
[2] Institute of Biogeochemistry and Pollutant Dynamics, ETH Zurich, 8092 Zurich, Switzerland
[3] Laboratory for Operation Control and Research, Zweckverband Landeswasserversorgung, 89129 Langenau, Germany
[4] School of Architecture, Civil and Environmental Engineering (ENAC), École Polytechnique Fédérale de Lausanne (EPFL), 1015 Lausanne, Switzerland

* Corresponding author: juliane.hollender@eawag.ch

Published in Water Research, DOI: 10.1016/j.watres.2020.116066

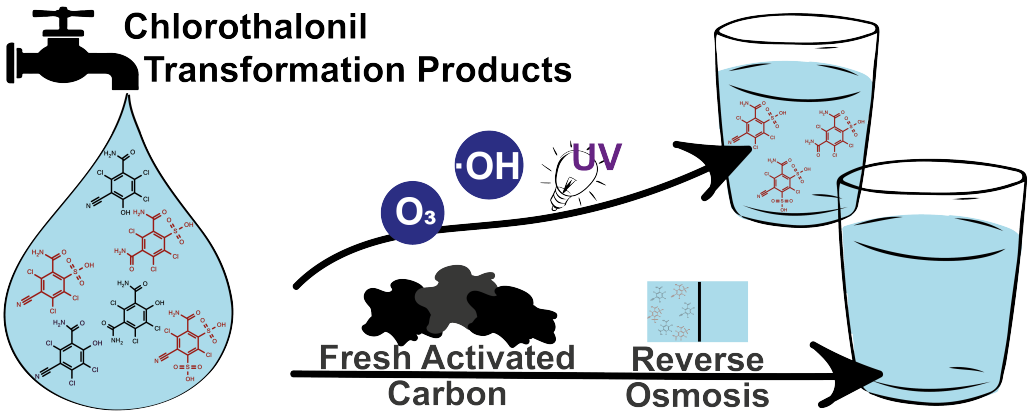

Abstract

Chlorothalonil, a fungicide applied for decades worldwide, has recently been banned in the European Union (EU) and Switzerland due to its carcinogenicity and the presence of potentially toxic transformation products (TPs) in groundwater. The spread and concentration range of chlorothalonil TPs in different drinking water resources was examined (73 groundwater and four surface water samples mainly from Switzerland). The chlorothalonil sulfonic acid TPs (R471811, R419492, R417888) occurred more frequently and at higher concentrations (detected in 65-100% of the samples, $\leq$2200 ngL^{-1}) than the phenolic TPs (SYN507900, SYN548580, R611968; detected in 10-30% of the samples, $\leq$30 ngL^{-1}). The TP R471811 was found in all samples and even in 52% of the samples above 100 ngL^{-1}, the drinking water standard in Switzerland and other European countries. Therefore, the abatement of chlorothalonil TPs was investigated in laboratory and pilot-scale experiments and along the treatment train of various water works, comprising aquifer recharge, UV disinfection, ozonation, advanced oxidation processes (AOPs), activated carbon treatment, and reverse osmosis. The phenolic TPs can be abated during ozonation (second order rate constant k_{O3} ~10^4 M^{-1}s^{-1}) and by reaction with hydroxyl radicals ($^{\cdot}$OH) in AOPs (k_{OH} ~10^9 M^{-1}s^{-1}). In contrast, the sulfonic acid TPs, which occurred in higher concentrations in drinking water resources, react only very slowly with ozone (k_{O3} <0.04 M^{-1}s^{-1}) and $^{\cdot}$OH (k_{OH} <5.0 $\times$ 10^7 M^{-1}s^{-1}) and therefore persist in ozonation and $^{\cdot}$OH-based AOPs. Activated carbon retained the very polar TP R471811 only up to a specific throughput of 25 m^{3}kg^{-1} (20% breakthrough), similarly to the X-ray contrast agent diatrizoic acid. Reverse osmosis was capable of removing all chlorothalonil TPs by $\geq$98%.

Keywords: pesticide; metabolite; water treatment; groundwater; ozonation; activated carbon

4.1 Introduction

Chlorothalonil, a broad-spectrum fungicide, has recently been banned in the EU and Switzerland because of its carcinogenic properties, the risks to fish and amphibians, and the expected contamination of groundwater with chlorothalonil TPs (BLW 2019a, European Commission 2019). In Switzerland, chlorothalonil had predominantly been used for grain and vegetable cultivation, but its use had also been approved for viticulture and non-agricultural land. Chlorothalonil has been applied in high amounts for decades (first registration in the USA in 1966) (EPA 1999), as shown by the sales data in Switzerland (45 t a^{-1}, 2017) and Germany (1000-2500 t a^{-1}, 2017), where chlorothalonil was among the ten most sold pesticides in 2017 (BLW 2019b, BVL 2018).

Due to the toxicity of the parent compound and insufficient toxicological data for the TPs, the European Food Safety Agency (EFSA) recommended to provisionally classify chlorothalonil TPs as relevant pesticide TPs in 2018 (EFSA 2018), implying an EU drinking water standard of 100 ngL^{-1} (European Commission 1998). To our knowledge, the EU member states have not yet decided on the drinking water relevance of chlorothalonil TPs; e.g. in Germany the previous classification as non-relevant or not evaluated still applies, resulting in a higher drinking water standard. However, some European countries, such as Denmark and France, apply the same drinking water standard of 100 ngL^{-1} to all pesticide TPs. Some non-European countries, e.g. Australia and the USA, define individual, risk-based thresholds, but so far only for a limited number of pesticides and TPs (Laabs et al. 2015). As recommended by the European Commission (2019), Switzerland recently classified chlorothalonil as carcinogen category 1B, thereby declaring all groundwater TPs as relevant (irrespectively of their toxicity), following the EU guidance document Sanco/221/2000 –rev.10- final (European Commission 2003).

To reduce drinking water contamination with organic micropollutants, various treatment processes exist, such as (i) managed aquifer recharge (Hollender et al. 2018, Maeng et al. 2011), (ii) activated carbon treatment (Delgado et al. 2012, Westerhoff et al. 2005), (iii) ozonation (Hübner et al. 2012, von Gunten 2003, von Sonntag and von Gunten 2012, Westerhoff et al. 2005), (iv) AOPs, e.g. UV/H_2O_2, O_3/H_2O_2, UV/Cl_2 (Chuang et al. 2017, Guo et al. 2018, Huber et al. 2003, Miklos et al. 2018, Stefan 2018, von Gunten 2018), and (v) membrane processes such as nanofiltration and reverse osmosis (Taheran et al. 2016). Treatment efficiency strongly depends on physical-chemical properties of a compound. Managed aquifer recharge is most effective for less polar and well-degradable compounds (Benotti et al. 2012, Maeng et al. 2011); similarly, activated carbon filtration retains especially semi- to non-polar micropollutants (Westerhoff et al. 2005). While the oxidant ozone (O_3) selectively transforms mainly electron-rich compounds (e.g. phenols), $^{\cdot}OH$ produced during ozone decomposition and in AOPs are less selective and react with a broader spectrum of organic compounds (von Sonntag and von Gunten 2012). While these oxidative methods may only partially abate the micropollutant load and can produce reaction products, reverse osmosis is capable of removing most micropollutants to a large extent. However, operational costs of reverse osmosis systems are high (Taheran et al. 2016) and the highly-concentrated reject water that is produced requires disposal (Umar et al. 2014).

In a recent suspect screening for more than 1000 pesticide TPs (including >25 chlorothalonil TPs) in Swiss groundwater, we have detected eight different chlorothalonil TPs, six of them reported for the first time (Kiefer et al. 2019). The chlorothalonil TP R471811 was even found in all 31

groundwater samples with concentrations up to 2700 ngL^{-1}. Due to the high usage of chlorothalonil worldwide, chlorothalonil TPs may be a widespread threat for drinking water quality. However, the efficiency of water treatment processes to abate chlorothalonil TPs from drinking water have not yet been evaluated.

Therefore, we aimed to investigate the abatement of sulfonic acid- and phenol-containing chlorothalonil TPs from water in full-scale waterworks, pilot plants, and laboratory experiments. Our hypothesis was that the more electron-poor and more polar sulfonic acid TPs (exhibiting at least one sulfonic acid group; R471811-SA, R419492-SA, R417888-SA, and two isomers of R417888-SA; "SA" for sulfonic acid) are probably more recalcitrant during oxidative or adsorptive treatment. In contrast, the less polar phenolic TPs (SYN507900-Ph, SYN548580-Ph, R611968-Ph, "Ph" for phenol) are probably abated more efficiently by oxidation or adsorption, as previously shown for other phenolic compounds (Kovalova et al. 2013a, Lee et al. 2005). First, chlorothalonil TPs were monitored in different drinking water resources such as in lakes, rivers, and groundwater to obtain more information on the scope of chlorothalonil TPs contamination. Second, the fate of chlorothalonil TPs in a full-scale water treatment train consisting of activated carbon, ozonation, and UV disinfection was investigated. Additional laboratory and pilot-scale experiments were carried out to supplement the full-scale observations regarding activated carbon, ozonation, and UV disinfection and to test additional advanced treatment processes (AOPs, reverse osmosis).

4.2 Materials and Methods

4.2.1 Drinking Water Resources and Waterworks

To investigate the fate of chlorothalonil TPs in water treatment, samples were taken along the treatment train of eight waterworks (Table SI4-A1) in February 2019. Waterworks A abstracts raw water from the river Rhine. Suspended matter is removed in a settling pond followed by a rapid sand filter. Then, the clarified water is infiltrated into the aquifer, abstracted again (average residence time: days to two months) and filtered via three granular activated carbon filters (specific throughput at the time of sampling: 25, 55, 305 m^3kg^{-1}). A final disinfection is performed with a medium pressure UV lamp. Waterworks B treats raw water from a karstic spring with ozonation (0.8 g O_3 g^{-1} DOC (dissolved organic carbon)) followed by two granular activated carbon filters (specific throughput at the time of sampling: 23, 215 m^3kg^{-1}). Waterworks C uses Lake Zurich water (abstraction point 30 m below the lake surface), which is ozonated in two steps (pre- and intermediate ozonation) with different specific ozone doses (0.3 and 0.6 g O_3 g^{-1} DOC). Ozonation is followed by twelve granular activated carbon filters (average specific throughput at the time of sampling: 1200 m^3kg^{-1}, i.e. mainly biological and not adsorptive filters) and slow sand filtration. Waterworks D abstracts river bank filtrate from the river Limmat (outflow of Lake Zurich, Switzerland). The bank filtrate is disinfected (Cl_2/ClO_2), infiltrated into the aquifer and abstracted again. In addition, seven groundwater abstraction wells and four springs were sampled in Switzerland. The water from these wells or springs is delivered to the consumer as drinking water either without further treatment, with only minor treatment (UV disinfection), or after mixing with water from other sources (Table SI4-A1, waterworks E-I).

Samples were collected in laboratory glass bottles (previously annealed at 500 °C; 500 mL bottles, SIMAX Kavalier, Czech Republic) in February 2019 and then frozen at -20 °C until sample enrichment and measurement. Six field blanks, consisting of ultrapure water (>18 MΩcm, Barnstead Nanopure Diamond system and Elga Purelab Chorus) filled in sampling bottles, transferred to a second bottle during sampling, and frozen until enrichment and measurement, did not show detectable concentrations of the target analytes, demonstrating that no contamination occurred during sample handling and analysis. Furthermore, rain water from Dübendorf (vicinity of Zurich, 431 m above sea level, Switzerland) and Jungfraujoch (3571 m above sea level, Switzerland) was collected and analysed as background controls from hypothetically uncontaminated field sources. Since evian® water is used in many laboratories for calibration standard preparation, additionally evian® water (bottled in polyethylene terephthalate, PET) was enriched and analysed as a blank sample.

To investigate the occurrence of chlorothalonil TPs in groundwater (the major drinking water resource in Switzerland), we also present semi-quantitative data for 60 groundwater samples, collected in May and August 2018 within the Swiss National Groundwater Monitoring NAQUA (www.bafu.admin.ch/naqua). The 60 groundwater monitoring sites were selected based on long-term monitoring data. Twenty sites were known to have very low overall micropollutant concentrations, whereas 40 sites were chosen because micropollutants from urban or agricultural sources had been detected in the past. These samples were analysed using a comparable analytical method as described in section 4.2.4.

4.2.2 Stock Solutions and Chemicals

Stock solutions for liquid chromatography high-resolution tandem mass spectrometry (LC-HRMS/MS) analyses were prepared depending on compound solubility in ethanol, methanol or ethanol/water (1:1, volumetrically) at a concentration of 0.1 or 1 gL^{-1}. As organic solvents may influence ozonation and photodegradation experiments, stock solutions for laboratory experiments (except for activated carbon) were prepared in water (20-100 µM corresponding to 0.005-0.035 gL^{-1}). For details, see SI4-A2.

Six chlorothalonil TPs (Figure 4-1), reported by Kiefer et al. (2019) in groundwater and for which reference material was available (ASCA GmbH, Germany; Syngenta, Switzerland), were analysed in the environmental water samples (section 4.2.1). The TPs differ in their functional groups (Figure 4-1). All TPs contain at least one amide group, three of the TPs have at least one hydroxyl group (phenolic TPs), whereas the other three TPs are characterized by at least one sulfonic acid group (sulfonic acid TPs). For the laboratory experiments, two phenolic TPs (R611968-Ph, SYN507900-Ph) and two sulfonic acid TPs (R471811-SA, R417888-SA) were selected as test compounds and it was assumed that structurally related TPs would behave similarly during water treatment. The four TPs were selected due to lower measurement uncertainty compared to R419492-SA and SYN548580-Ph.

4.2.3 Laboratory and Pilot-Scale Experiments

Abatement of micropollutants with ozone or to a lesser extent with ·OH or degradation by UV photolysis can depend on the speciation of organic compounds such as phenols. For the phenolic TPs considered here (R611968-Ph and SYN507900-Ph), experimentally determined acid-base equilibrium constants (pK_a) were not available, so the exact speciation under environmentally relevant pH values is not known. However, the predicted pK_a values (4.1 and 4.7, Figure 4-1; predicted with JChem for Office, version 17.1.2300.1455, ChemAxon Ltd.) are more than two

units below environmentally relevant pH values, indicating the dominance of the anionic phenolate species (>99%). To obtain data applicable to most waterworks, all laboratory experiments were conducted at pH 7.5 using a 5 mM phosphate buffer, unless stated otherwise. Laboratory experiments were performed individually for each compound, unless stated otherwise. Samples from laboratory or pilot-scale experiments were analysed without prior enrichment.

4.2.3.1 UVC Irradiation

Photodegradation under UVC irradiation (four RPR-2537A lamps centered around 254 nm, Rayonet, Southern New England Ultraviolet Company, Branford, USA, emission spectrum in Figure SI4-A1) was carried out in a merry-go-round photoreactor (Rayonet, Southern New England Ultraviolet Company, Branford, USA) and by back-to-front light exposure. Temperature was kept constant (12±2 °C, typical for groundwater in Central Europe). Depending on the reactivity, TPs (0.1 µM, pH 7.5) were irradiated for 40-150 min in quartz test tubes (diameter: 1.3 cm, length: 7 cm). Photon fluence rates were determined by chemical actinometry using atrazine as described by Zepp (1978) (pH 7.0, 5 mM phosphate buffer; quantum yield: 0.046 $molE^{-1}$, Hessler et al. (1993), molar absorption coefficient: 3860 $M^{-1}cm^{-1}$ at 254 nm, Nick et al. (1992)). Atrazine shows similar phototransformation rates as the phenolic TPs, is easy to handle and analyse, and was successfully tested and compared to the actinometer hydrogen peroxide by Canonica et al. (2008). The photon fluence rate was 4.0 to 5.3 $\times$ 10^{-5} $Em^{-2}s^{-1}$ (determined on different days). For details, including light emission spectra and absorbance spectra of chlorothalonil TPs and data analysis for photon fluence rates, quantum yields, and photon fluence-based rate constants, see SI4-A5.

4.2.3.2 Ozonation

To determine the second order rate constant (k_{O3}) for the reaction of ozone with the slowly-reacting sulfonic acid TPs (R471811-SA, R417888-SA), TPs were exposed to ozone in excess at pH 2.3 (0.1 µM TP, 100 µM ozone, 10 mM phosphoric acid, 10 mM tert-butanol to scavenge $^{\cdot}OH$) in a 250 mL glass bottle with a dispenser system (Hoigné and Bader 1994). Acidic conditions were selected as ozone is more stable at low pH (von Sonntag and von Gunten 2012) and the sulfonic acid TPs do not change their speciation over a wide pH range (predicted pK_a -4.3, Figure 4-1). The ozone concentration and TP abatement were monitored over 15 h (for details, see SI4-A6).

The reaction kinetics for the faster reacting phenolic TPs (SYN507900-Ph, R611968-Ph) were investigated by competition kinetics using salicylic acid as a competitor (k_{O3} = 2.8 $\times$ 10^4 $M^{-1}s^{-1}$, Hoigné and Bader (1983)). Phenolic TPs (1 µM) and salicylic acid (1 µM) were exposed to varying ozone doses (0-4.5 µM) at pH 7.5 in 10 mL glass vials in presence of tert-butanol (50 mM, to scavenge $^{\cdot}OH$) (for details, see SI4-A7). Other compounds for which reliable second order rate constants were reported (e.g. carbamazepine, clarithromycin) were also tested or considered as competitors but finally not used, either due to higher reactivity with ozone (carbamazepine, k_{O3} = 3 $\times$ 10^5 $M^{-1}s^{-1}$, Huber et al. (2003)) or analytical problems (clarithromycin). Direct measurement of the second order rate constant with ozone (similar approach as for the sulfonic acid TPs) was not feasible for the phenolic TPs because these reactions are too fast to be observed in batch reactors at environmentally relevant pH values.

4.2.3.3 Advanced Oxidation

To evaluate the potential of AOPs, the second order rate constants were determined for the reactions of ·OH (k_{OH}) with the TPs. ·OH can be produced by a combination of hydrogen peroxide (H_2O_2) with UV irradiation or ozone, or at high pH directly from ozone (Rosenfeldt and Linden 2004, Staehelin and Hoigne 1982). Here, TPs (0.1 µM) were exposed to H_2O_2 (1 mM) at pH 7.5 in a comparable reactor set-up as for UVC photodegradation experiments (section 4.2.3.1; here: UVA light with emission peak at 367 nm). To reduce the experimental effort, R471811-SA and SYN507900-Ph, and R417888-SA and R611968-Ph, respectively, were exposed to UVA/H_2O_2 in the same vials. The second order rate constant k_{OH} was determined by competition kinetics using benzoic acid as a reference compound exhibiting similar reactivity as the TPs (10 µM, k_{OH} = 5.9 $\times$ 10^9 M^{-1} s^{-1}, Buxton et al. (1988)) (for details, see SI4-A9).

Using this experimental set-up, the sulfonic acid TPs showed no degradation, probably because the ·OH concentration was too low (10^{-15} M). Thus, the second order rate constants for sulfonic acid TPs were determined by exposure to higher ·OH concentrations produced from ozone (0-80 µM) under alkaline conditions (pH ~10, 0.3 mM NaOH), with the X-ray contrast agent diatrizoic acid as a competitor. Diatrizoic acid was selected as a competitor due to its low reactivity (k_{OH} = 5.4 $\times$ 10^8 $M^{-1}s^{-1}$, Real et al. (2009)), which is of similar order of magnitude as that expected for the sulfonic acid TPs. Degradation by ozone could be excluded due to the low stability of ozone at pH ~10 and the very low ozone reactivity of both diatrizoic acid (k_{O3} 0.05 $M^{-1}s^{-1}$, Real et al. (2009)) and sulfonic acid TPs (<0.04 $M^{-1}s^{-1}$, see section 4.3.3.1 and Table 4-1). For details, see SI4-A8.

4.2.3.4 Activated Carbon

The potential of adsorption to activated carbon was evaluated by conducting powdered activated carbon batch experiments. As the experimental set-up does not take into account kinetic effects, adsorption might be overestimated compared to granular activated carbon filters. In order to compare not only the adsorption behaviour between the chlorothalonil TPs but also relative to other micropollutants present in many waterworks, the herbicide atrazine and the X-ray contrast agent diatrizoic acid were also included in the experiments as reference compounds. Adsorption to activated carbon is affected by the water matrix and micropollutant concentration (Delgado et al. 2012, Knappe et al. 1998). To simulate real water conditions as closely as possible, groundwater (DOC 1.1 mgL^{-1}, electrical conductivity 840 μScm^{-1}) was spiked to a target concentration of ~500 ngL^{-1} for each TP (test solution <0.05% MeOH). Adsorption experiments were not performed for each chlorothalonil TP individually because it was assumed that the competition for adsorption sites between the chlorothalonil TPs and natural organic matter (NOM; low mgL^{-1} range) and further anthropogenic micropollutants affects the adsorption to a larger extent than the competition between the individual chlorothalonil TPs (ngL^{-1} range). The test solution (17 mL spiked groundwater, 34-680 µL activated carbon suspension, 0-646 µL ultrapure water) was stirred for 42 h in closed glass vials with varying powdered activated carbon doses (0-40 mgL^{-1}, Eurocarb CC PHO 8x30, added as suspension). The chlorothalonil TP concentration in the supernatant solution was determined after filtration (Chromafil® Xtra RC-20/13, 0.2 µm).

4.2.3.5 Reverse Osmosis

Reverse osmosis was investigated in a pilot-scale experiment at the waterworks E (Table SI4-A1). Raw water originated from groundwater that was highly contaminated with chlorothalonil

TPs (total concentration ~2000 ngL^{-1}). The raw water was pumped through a spiral wound reverse osmosis membrane (TMG20D-400, Toray Membrane Europe AG, Switzerland) with a pre-filter (PP95BL5L2005, Everblue, Italy), recovering 38-65% as permeate (permeate flow rate 12.9-14.0 $Lmin^{-1}$, for details, see SI4-B10). Within a period of fourteen weeks, five raw water, five permeate, and three reject water samples were taken. Between sampling campaign two and three, the membrane was exchanged due to clogging because the antiscalant (ROPUR RPI-3000A, Toray Membrane Europe AG, Switzerland) had not correctly been dosed.

4.2.4 Analytical Methods

4.2.4.1 Enrichment of Environmental Samples

Environmental samples were enriched via vacuum-assisted evaporative concentration using a Syncore® Analyst (BÜCHI, Switzerland) according to the method validated by Mechelke et al. (2019) with slight modifications. A sample volume of 120 mL was spiked with 221 isotope-labelled internal standards (100 ngL^{-1}) and evaporated into BÜCHI glass vials (1 mL appendix cooled at 7-10 °C) at 20 mbar and 45 °C to ~1 mL using a back-flush unit. The sample volume was adjusted to 1.2 mL with ultrapure water. To reduce analyte loss by sorption to the glass surface, the BÜCHI vials were rinsed thoroughly with the sample. Then, the sample was centrifuged at 3720 g (Heraeus Megafuge 1.0 R, Thermo Fisher Scientific, U.S.) for 15 min in annealed centrifuge vials. The supernatant was transferred to 1.5 mL vials (with screw caps; BGB Analytik AG, Switzerland) and kept at 8 °C until measurement. Analogous to the environmental samples, 17 calibration standards (0.1-2000 ngL^{-1} in ultrapure water), seven laboratory and field blank samples, one evian®, two rain water samples, and nine spiked samples (10, 100, 250, 500 ngL^{-1}) were prepared and analysed.

4.2.4.2 HPLC-MS/MS and HPLC-UV Analyses

Environmental samples: Analytes were separated with high-performance LC (HPLC) on a reverse phase C18 column (Atlantis® T3 3 µm, 3.0x150 mm; Waters, Ireland) with water and methanol as eluents, both modified with 0.1% concentrated formic acid. The injection volume was 150 µL corresponding to 15 mL of the original water sample. Samples were analysed in sequence, first in negative, then in positive electrospray ionization mode (-2.5/3.5 kV) on an Orbitrap high-resolution mass spectrometer (Fusion Lumos, Thermo Fisher Scientific, U.S.).

Laboratory and pilot experiments: Samples from ozonation, UV irradiation and advanced oxidation experiments were spiked with isotope-labelled internal standards (2500 ngL^{-1}) and then measured with the same analytical method as the environmental samples, except for a lower injection volume (100 µL). Additionally, the first five minutes of the HPLC run were directed to the waste to reduce interferences from the phosphate buffer. Samples from experiments conducted at elevated TP concentration (1 µM) were diluted by a factor of ten.

The adsorption experiments with activated carbon (section 4.2.3.4) were measured with another analytical method at the Laboratory for Operation Control and Research (Zweckverband Landeswasserversorgung, Germany). For chromatographic separation an Ultra Aqueous C18 column (5 µm, 4.6x250 mm; Restek, U.S.) was used with an injection volume of 100 µL and with water and acetonitrile as eluents, each acidified with 0.1% concentrated formic acid. Analytes were ionized using electrospray (4.5/-4.5 kV) in switching mode and detected with a triple quadrupole mass spectrometer (API 5500 Qtrap, Sciex, U.S.).

Samples from the reverse osmosis pilot plant were analysed at the Water and Soil Protection Laboratory (Office of Water and Waste Management of the Canton of Berne) for four pesticide TPs with high concentrations (chlorothalonil TPs R471811-SA and R417888-SA, chloridazon-desphenyl, chloridazon-desphenyl-methyl) using a comparable LC-HRMS/MS method (injection volume 100 µL; Atlantis® T3 3 µm, 3.0x150 mm; Waters, Ireland; QExactive, Thermo Fisher Scientific, U.S.). Selected samples were additionally measured at Eawag (comparable method to environmental samples, without enrichment). Major cations and anions were analysed at the Eawag apprenticeship laboratory.

The actinometer atrazine (section 4.2.3.1) was analysed on a Dionex UltiMate 3000 RS HPLC system coupled to a diode array detector (Thermo Fisher Scientific, U.S.) using a reverse phase C18 column (Atlantis® T3 3 µm, 3.0x150 mm; Waters, Ireland). Data was processed with the Chromeleon 7.2.1 Software. For details on HPLC-MS/MS and HPLC-UV analyses, see SI4-A3.

4.2.4.3 Quantification

Samples measured with HPLC-MS/MS were quantified using TraceFinder 4.1 (Thermo Fisher Scientific, U.S.) and MultiQuant 3.0.3 (Sciex, U.S.), as appropriate. For each analyte and measurement, an isotope-labelled internal standard was selected for quantification that eluted at a similar retention time as the analyte and resulted in a relative recovery close to 100% and high reproducibility across different spiked samples (for more details, see Kiefer et al. (2019) or SI4-A4). Quantification results including limits of quantification (LOQs, 0.2-10 ngL^{-1} in environmental samples), relative recoveries (average 85-110% and relative standard deviation <20% across spiked samples in environmental samples) and isotope-labelled internal standards are provided in SI4-B1 and SI4-B2.

The chlorothalonil TPs R419492-SA and SYN548580-Ph were quantified retrospectively because reference material was received after analysis. For quantification and quality control, eleven calibration standards, one blank sample, six samples from drinking water treatment and six corresponding spiked samples were enriched and analysed (section 4.2.4.1 and 4.2.4.2). This calibration model was applied to the previously measured samples. The concentration of SYN548580-Ph deviated less than 20% in the six samples, which were measured twice. However, in case of R419492-SA, the concentration results differed by a factor of two. Due to the early retention time of R419492-SA, a suitable internal standard was not available. Therefore, R419492-SA concentrations were multiplied by two in the retrospectively quantified samples. It should be noted that measurement uncertainty for R419492 is expected to be higher (~0.5-2 × reported concentration) than in case of the other chlorothalonil TPs (~0.7-1.5 × reported concentration). The abatement of chlorothalonil TPs in the waterworks was compared to the abatement of the sweetener acesulfame and the X-ray contrast agent diatrizoic acid. In contrast to acesulfame, diatrizoic acid could not be quantified because reference material for diatrizoic acid was not included in the multi-component standard solution for quantification of the environmental samples. However, abatement was calculated from differences in the response ratios of diatrizoic acid and its structurally identical isotope-labelled internal standard before and after treatment.

To estimate the error of the calculated abatement efficiencies in water treatment due to measurement uncertainty, each sample taken along the treatment train was measured in triplicate. The uncertainty in removal was calculated based on the standard deviation of the measurement triplicates using Gaussian error propagation. In addition, three samples were

enriched and measured in triplicate to assess the reproducibility of sample enrichment. The standard deviations of the triplicate measurement concentrations and the enrichment triplicates was comparable.

To determine the extent of chlorothalonil TPs in groundwater, concentrations were quantified in 60 groundwater samples (section 4.2.1) that have been analysed using a comparable method as the one used for the environmental samples in this study. The major differences were a lower enrichment factor (75 instead of 100) and a lower injection volume (140 instead of 150 µL), corresponding to 10.5 mL of the original sample (instead of 15 mL). Additionally, only 35 isotope-labelled internal standards were spiked. The samples were analysed together with four calibration standards (1, 10, 100, 1000 ngL^{-1}) and three spiked samples (10, 100, 250 ngL^{-1}), containing among other compounds the chlorothalonil TPs R471811-SA, R417888-SA, SYN507900-Ph and R61198-Ph. The concentrations of the chlorothalonil TPs R419492-SA and SYN545850-Ph were estimated based on the calibration standards measured separately (see above).

4.3 Results and Discussion

4.3.1 Chlorothalonil TPs in Drinking Water Resources

Figure 4-1 illustrates the concentration ranges of the chlorothalonil TPs in different drinking water resources. In addition to the TPs presented in Figure 4-1, the TPs R611965 (carboxylic acid) and R418503-SA were investigated with reference material (LOQ 10 ngL^{-1}) but never detected. SYN548581-SA, which is the R417888-SA isomer that we previously identified only tentatively based on comparison of the isotope pattern, predicted MS/MS spectrum and retention time (Kiefer et al. 2019), was now confirmed with reference material (Figure SI4-A9). As expected, none of the TPs were found above the LOQ of 0.2 to 10 ngL^{-1} in rain water or ultrapure water. TP R471811-SA was detected in all other samples, even in groundwater with very low anthropogenic impact, in surface water (river Rhine: 53 ngL^{-1}, Lake Zurich: 5 ngL^{-1}), and in bottled water (evian® water: 6 ngL^{-1}). The two other sulfonic acid TPs, R417888-SA and R419492-SA, were detected in 86% and 65% of samples (without rain and ultrapure water), whereas the phenols (R611968-Ph, SYN507900-Ph, SYN548580-Ph) were detected less frequently (in 10-30% of the samples) and at lower concentrations (Figure 4-1). In the four surface waters investigated (3 rivers, 1 lake), all TPs had concentrations below 100 ngL^{-1}; whereas at least one TP was above 100 ngL^{-1} in 40 out of 73 groundwater samples. It should be noted that concentrations in rivers may be subject to stronger seasonal fluctuations compared to concentrations in groundwater (for a compilation of all quantitative data, refer to SI4-B1 and SI4-B2).

Based on long-term monitoring data, the 60 groundwater monitoring sites were pre-classified as influenced by agricultural micropollutants (20 sites), micropollutants from wastewater (20 sites, often influenced by river bank filtration), or with only low anthropogenic influence (20 sites, section 4.2.1). As expected, the median concentration of the chlorothalonil TPs was higher in groundwater samples influenced by agriculture (515 ngL^{-1}) than in groundwater samples pre-classified as wastewater-impacted (99 ngL^{-1}) or in samples with only low anthropogenic influence (19 ngL^{-1}). The phenols play a minor role for the drinking water quality, since they exceeded 100 ngL^{-1} in only 3% of samples, whereas the sulfonic acids R471811-SA, R417888-SA, and R419492-SA exceeded 100 ngL^{-1} in 52%, 14%, and 14% of samples, respectively.

The concentration ratios between the TPs vary strongly from sample to sample (SI4-B1). For example, TP R471811-SA was found at 2-50 times (median: 7.4) higher concentrations compared to its direct precursor compound, TP R417888-SA. These differences could be related to a different formation rate and/or transport behavior. The less polar TP R417888-SA is more affected by sorption than the more polar TP R471811-SA. Therefore, in case of TP R417888-SA, the degree of retardation during transport through the unsaturated zone might depend more strongly on the site-specific soil/sediment characteristics (e.g. organic carbon) than in the case of TP R471811-SA. In addition, more R417888-SA will be oxidized to R471811-SA with increasing residence time (depending e.g. on size of soil/sediment particles) in the biologically more active aerobic top soil. Therefore, we speculate that the concentration ratio between the TPs R471811-SA and R417888-SA will increase with increasing organic carbon content and residence time in the unsaturated zone.

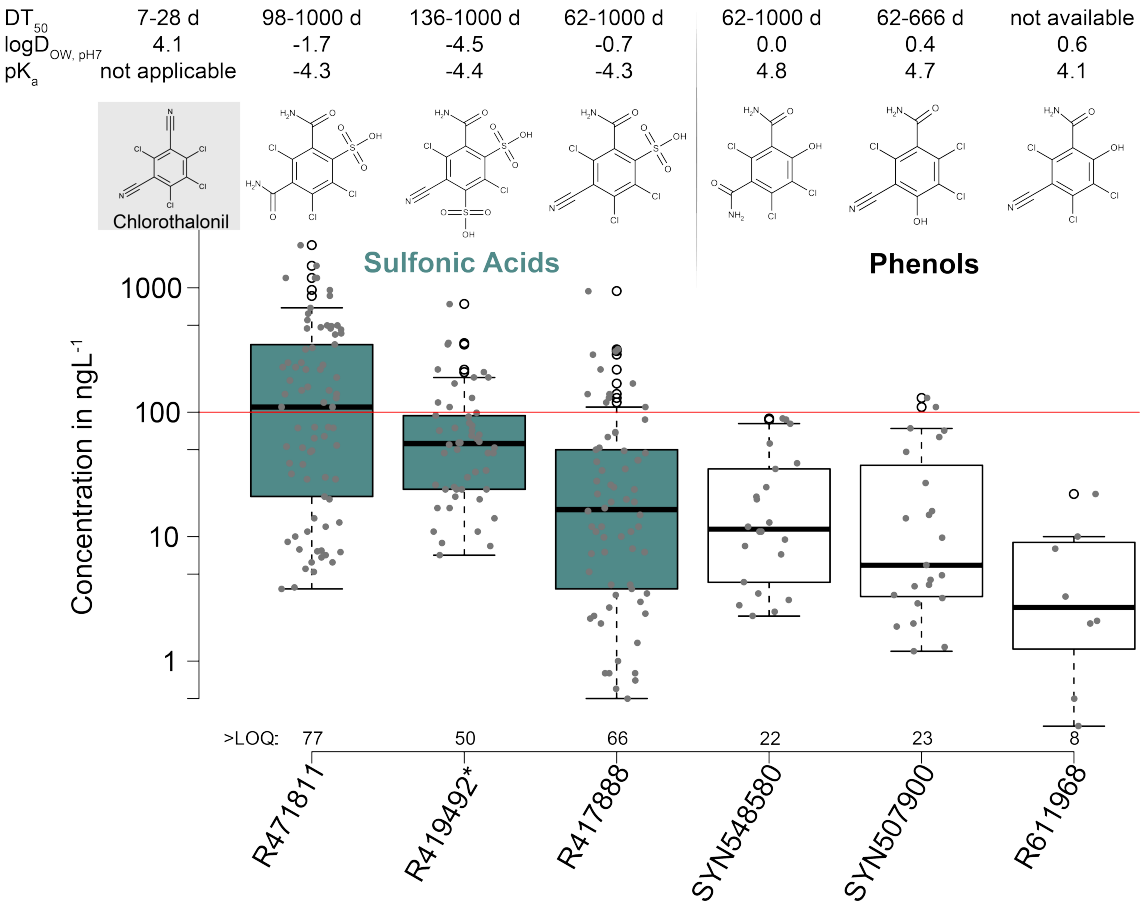

Figure 4-1: Concentration distribution of different chlorothalonil TPs in 77 samples (73 x groundwater, 4 x surface water). Non-detects (LOQs: 0.2-5 ngL-1) are not included in the boxplots. The sulfonic acid-containing TPs (on the left in green) were more frequently detected and at higher concentrations than the phenol-containing TPs (on the right in white). The red line marks the Swiss drinking water standard. The open circles represent outliers. The gray solid circles show the concentrations of individual samples. Dissipation time DT_{50} from EFSA (2018), $logD_{OW, pH7}$ (water-n-octanol distribution coefficient considering the speciation at pH 7) and pKa (acid dissociation constant) were predicted with JChem for Office (Version 17.1.2300.1455; ChemAxon Ltd.). *R419492: high measurement uncertainty (~0.5-2 × reported concentration).

4.3.2 Abatement of Chlorothalonil TPs during Drinking Water Treatment

Figure 4-2 provides an overview of the abatement by granular activated carbon filtration, ozonation and UV disinfection in different waterworks, while Figure 4-3 illustrates the abatement of the three sulfonic acid TPs along the treatment train of waterworks A and B (phenolic TPs were not detected). Waterworks C and D showed only very low concentrations of chlorothalonil TPs in the raw water and were therefore not discussed in detail (Lake Zurich and river Limmat both ≤7 ngL^{-1}, see SI4-B2 for all quantitative data). Sand filtration and subsequent infiltration to the aquifer followed by abstraction did not lead to a decrease of the concentrations (Figure 4-3, left), which is in accordance with the high mobility and persistence of the sulfonic acid TPs (EFSA 2018).

Whereas the sulfonic acid TPs were stable during ozonation and UV disinfection, granular activated carbon filtration led to an abatement (Figure 4-3). However, only very fresh activated carbon (specific throughput 23 and 25 m^3kg^{-1}, waterworks A and B) was capable of sufficiently abating all sulfonic acid TPs (R471811-SA: 80% abatement; R417888-SA, R419492-SA: below LOQ). For slightly older activated carbon (specific throughput 55 m^3kg^{-1}, waterworks A), no retention of R471811-SA was observed, whereas R419492-SA was still abated by 55% and R417888-SA was below LOQ. An activated carbon filter with a specific throughput of 215 m^3kg^{-1} (waterworks B) retained only the sulfonic acid TP with the highest water-n-octanol distribution coefficient considering the speciation at pH 7 (log $D_{OW\ pH7}$; R417888-SA, 58% abatement). The oldest activated carbon filter (specific throughput 305 m^3kg^{-1}, waterworks A) had higher effluent than influent concentrations for all sulfonic acid TPs, indicating slight leaching from the filter.

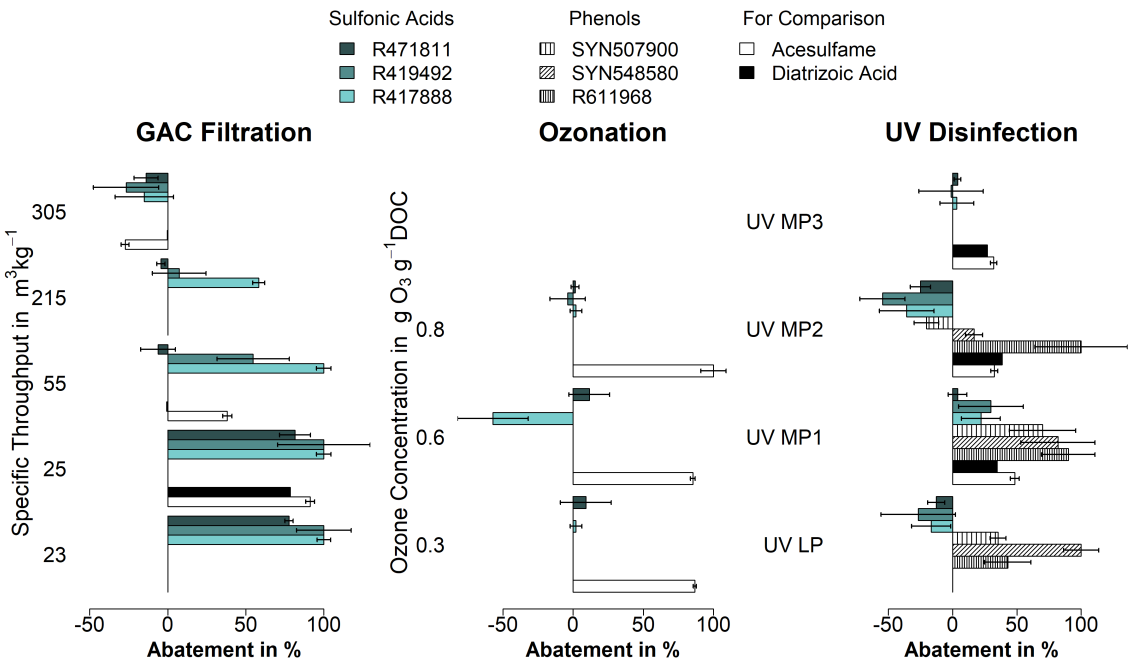

Figure 4-2: Abatements of chlorothalonil TPs by different treatment processes across multiple waterworks; for comparison acesulfame and diatrizoic acid are also included. Error bars indicate measurement uncertainty propagated from standard deviation of measurement triplicates (no triplicate measurements for diatrizoic acid). Uncertainty from sampling is not included. Abatement <LOQ is reported as 100%. The apparent formation of R417888-SA in ozonation was only observed in one sample with concentrations close to the LOQ (SI4-B2) and is probably related to measurement uncertainty. GAC: granular activated carbon; LP: low pressure Hg lamp; MP: medium pressure Hg lamp; MP1&2: waterworks E, MP3: waterworks A, see Table SI4-A1.

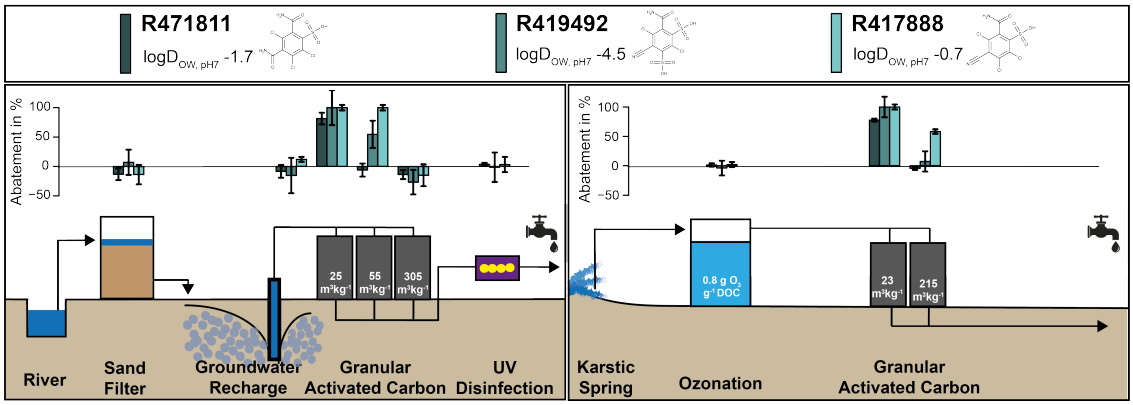

Figure 4-3: Abatement of sulfonic acid chlorothalonil TPs along the treatment train of waterworks A (left) and B (right; calculated from one step to the next step). The UV disinfection system was equipped with a medium pressure Hg lamp. Phenolic TPs were not detected. $logD_{OW, pH7}$ (water-n-octanol distribution coefficient considering the speciation at pH 7) predicted with JChem for Office (Version 17.1.2300.1455; ChemAxon Ltd.).

The poor retention behaviour for R471811-SA was comparable to the breakthrough behaviour of the X-ray contrast agent diatrizoic acid (Figure 4-2). Whereas both compounds were still abated by 80% by fresh activated carbon (specific throughput 25 m^3kg^{-1}), neither R471811-SA nor diatrizoic acid were abated by slightly older activated carbon (specific throughput 55 and 305 m^3kg^{-1}; diatrizoic acid was not present in the raw water of waterworks B). It should be noted that the results from the two waterworks A and B are in good agreement, although different granular activated carbons were used (waterworks A: bituminous coal, Filtrasorb® 400, Calgon Carbon Corporation; waterworks B: bituminous coal, Hydraffin® XC 30, Donau Carbon).

In intensively used agricultural areas, managed aquifer recharge can decrease groundwater contamination with chlorothalonil TPs by dilution because surface waters are usually less polluted with chlorothalonil TPs (section 4.3.1). Three of the investigated groundwater abstraction wells were close to a river (40-730 m), which was only slightly contaminated (concentration sum of chlorothalonil TPs 100 ngL^{-1} in a grab sample). With increasing distance to the river, the concentration sum of the chlorothalonil TPs in the abstracted groundwater increased (2 abstraction wells 40 m from river: 85 and 220 ngL^{-1}, concentrations may differ due to a different pumping regime before sampling, leading to different proportions of river water in the abstracted sample; abstraction well 730 m from river: 420 ngL^{-1}; SI4-B2). However, managed aquifer recharge may introduce other organic micropollutants such as wastewater-derived compounds (Hollender et al. 2018). Accordingly, we observed higher concentrations of the sweetener acesulfame in abstraction wells close to the river compared to an abstraction well with larger distance to the river (grab sample in river: 280 ngL^{-1}; 2 abstraction wells 40 m from river: 120 and 34 ngL^{-1}, concentrations may differ due to a different pumping regime before sampling; abstraction well 730 m from river: 11 ngL^{-1}; SI4-B2).

The phenolic TPs were partly abated by UV disinfection with a large variability (57±43%, Figure 4-2, SI4-B3, waterworks E and F). No clear difference in abatement between the UV disinfection systems with low pressure Hg lamps (monochromatic UV light, 254 nm) or medium pressure Hg lamps (polychromatic UV light) was observed (Figure 4-2). UV systems at waterworks are usually installed for disinfection, requiring only low fluences, i.e. ≥400 Jm^{-2} according to German,

Austrian and Swiss legislation (DVGW 2006, ÖNORM 2001, SVGW 2010). Despite the low fluences, abatement of some organic micropollutants has been reported. Scheurer et al. (2014) observed 30% abatement of the sweetener acesulfame at a waterworks in Basel, Switzerland, and similar acesulfame abatement (30-50%, Figure 4-2) was observed at the UV disinfection systems in this study. In addition to acesulfame, we also observed partial abatement of diatrizoic acid (30-40%, Figure 4-2). In contrast, UV disinfection did not affect the concentration of the sulfonic acid TPs (waterworks A, Figure 4-3). The slight abatement or formation observed at three other UV systems (Figure 4-2) likely reflects uncertainty from sampling and sample analysis.

It can be asked whether the investigated TPs may also be formed in the waterworks from chlorothalonil or chlorothalonil TPs. Chlorothalonil itself was not analysed in this study as it does not ionize sufficiently in electrospray. However, based on laboratory and lysimeter experiments performed within the EU pesticide registration process (EFSA 2018) and a German groundwater monitoring program (LUBW 2011), the presence of chlorothalonil in the raw waters in relevant concentrations is unlikely. Accordingly, the water supplier operating waterworks B regularly checks for chlorothalonil in the raw water using gas chromatography electron ionization mass spectrometry, but has never detected this compound (LOQ = 20 ngL^{-1}). Furthermore, a formation of one target TP from another target TP was only observed in small amounts in the laboratory experiments, i.e. 2% R471811-SA was formed from R417888-SA at pH 10 (for each ozone dose, including the control without ozone, SI4-A8), indicating very slow basic hydrolysis (section 4.3.3). Therefore, we expect that the results of our study are not influenced by chlorothalonil TPs formed in the waterworks.

4.3.3 Laboratory Experiments

Table 4-1 provides the results from laboratory experiments with ozone, UV and AOPs and corresponding literature data for common micropollutants for comparison. SI4-B4 to SI4-B10 show the experimental data, SI4-A5 to SI4-A10 describe the calculations of the reported values.

Table 4-1: Rate constants and photochemical parameters determined in laboratory experiments in this study (chlorothalonil TPs) or from literature (other micropollutants): second order rate constant for the reactions of target compounds with ozone (k_{O3}) or $^{\cdot}OH$ (k_{OH}), photon fluence-based rate constant k_E, molar absorptivity ε_{254nm} , and the quantum yield Φ; ± standard deviation or as reported in respective study.

Compound	Ozone k_{O3} in $M^{-1}s^{-1}$	$^{\cdot}OH$ k_{OH} in $M^{-1}s^{-1}$	UVC k_E in m^2einstein^{-1}	UVC ε_{254nm} in M^{-1} cm^{-1}	UVC Φ in mol einstein^{-1}
R471811-SA	< 0.04	$< 5.0 \times 10^7$	1.1±0.1	710	$(0.7\pm0.1) \times 10^{-2}$
R417888-SA	< 0.04	$< 5.0 \times 10^7$	1.9±0.1	8000	$(0.10\pm0.01) \times 10^{-2}$
SYN507900-Ph	4.1×10^4*	not determined	30±1	6900	$(1.8\pm0.1) \times 10^{-2}$
R611968-Ph	$(2.6\pm0.3) \times 10^4$*	$(2.7\pm0.6) \times 10^9$	17±1	5400	$(1.4\pm0.1) \times 10^{-2}$
Acesulfame	88 (a)	4.55×10^9 (a); $(3.8 \pm 0.3) \times 10^9$ (b)	130** (c)	not reported	26-33 (d)
Atrazine	6 (e)	3×10^9 (e)	41±1	3860 (f)	$(4.6\pm0.4) \times 10^{-2}$ (g)
Carbamazepine	~3×10^5 (h)	$(8.8\pm1.2) \times 10^9$ (h)	1.0 (i)	6070 (i)	0.06×10^{-2} (i)
Diatrizoic Acid	0.05±0.01 (j)	$(5.4\pm0.3) \times 10^8$ (j)	251±22 (j)	31200 (j)	$(3.5\pm0.3) \times 10^{-2}$ (j)

* Value might be smaller (factor 10) due to conflicting values for k_{O3} of the competitor salicylic acid in Hoigné and Bader (1983), for details see SI4-A7; ** calculated according to equation (SI4-9) using values from Fu et al. (2019); references: (a) Kaiser et al. (2013), (b) Toth et al. (2012), (c) Fu et al. (2019) (d) Scheurer et al. (2014), (e) Acero et al. (2000), (f) Nick et al. (1992), (g) Hessler et al. (1993), (h) Huber et al. (2003), (i) Pereira et al. (2007), (j) Real et al. (2009)

4.3.3.1 UV Irradiation

In full-scale water treatment, the phenolic TPs were partially abated by UV disinfection (57±43%), whereas the sulfonic acid TPs were persistent (section 4.3.2, Figure 4-2). The UVC irradiation experiments confirmed the higher photodegradability at 254 nm of the phenolic TPs, exhibiting higher photon fluence-based rate constants (Table 4-1). The fast decay of the phenolic TPs relates to their higher quantum yields compared to the sulfonic acid TPs, while all TPs have moderate to high molar absorptivities (Table 4-1, Figures SI4-A1 and SI4-A2). Using the photon fluence-based rate constants determined, we calculated the theoretical abatement by UV disinfection (SI4-A5), assuming an applied UV dose of 400 Jm^{-2} as prescribed in Switzerland, Germany and Austria (DVGW 2006, ÖNORM 2001, SVGW 2010). Theoretically, <0.2% of the sulfonic acids and <2.5% of the phenols should be abated under such UV disinfection conditions (Table SI4-A10). However, abatement in full-scale treatment (Figure 4-2) was higher compared to the estimates from UVC treatment alone. This difference might be explained by indirect phototransformation due to production of reactive intermediates that can contribute to the removal of micropollutants, i.e. reactions with radicals or triplet states generated by photoexcitation of dissolved organic matter or nitrate (Canonica et al. 1995, Mark et al. 1996, Zepp et al. 1987). Especially nitrate may play an important role, because groundwater polluted with chlorothalonil TPs often has elevated nitrate concentrations, since both originate from mainly agricultural sources (median of nitrate concentration in groundwater samples with phenolic TPs: 20 mgL^{-1}, SI4-B1). In contrast, dissolved organic matter concentrations are usually low in groundwater (DOC in the 60 groundwater samples ≤2.1 mgL^{-1}). Indirect phototransformation is especially important for compounds susceptible to oxidation such as phenols (Canonica et al. 2008).

In addition to disinfection, UV irradiation is used to generate ·OH in UV-based AOPs. The fluence applied in UV-based AOPs (5000-10000 Jm^{-2}, Chuang et al. (2017)) are about 10-25 times higher compared to UV disinfection, so also direct phototransfomation can become relevant in case of the phenols. An abatement of 24% for R611968-Ph and 37% for SYN507900-Ph is estimated for a UV dose of 7500 Jm^{-2} and the respective rate constants. For 90% abatement of the phenolic TPs by direct photolysis, 38000-64000 Jm^{-2} would be required; for the sulfonic acid TPs UV doses would need to be even ten times higher (Table SI4-A10).

4.3.3.2 Ozonation

In the ozonation step of waterworks B, the sulfonic acid TPs were not degraded (section 4.3.2). This is in agreement with the very low second order rate constant for the reaction with ozone (k_{O3} <0.04 $M^{-1}s^{-1}$, Table 4-1). Only micropollutants with second order rate constants >>10 $M^{-1}s^{-1}$ are significantly abated during ozonation (von Sonntag and von Gunten 2012); e.g. acesulfame (k_{O3} = 88 $M^{-1}s^{-1}$, Table 4-1) was abated by >85% during ozonation (waterworks B and C; Figure 4-2). The measured second order rate constants support our hypothesis that ozone only minimally reacts with the sulfonic acid TPs, because the benzene rings have six electron-withdrawing substituents such as chlorine, sulfonic acid, cyano- and/or amide-groups (Figure 4-1). Ozone-refractory compounds (e.g. atrazine, Table 4-1) are mostly abated by ·OH that are formed from ozone decay and ozone reactions with dissolved organic matter as secondary oxidants (von Sonntag and von Gunten 2012). However, the sulfonic acid-containing TPs are also very refractory against ·OH (k_{OH} <5.0 × 10^7 $M^{-1}s^{-1}$, Table 4-1), explaining why no abatement was observed in waterworks B for these compounds.

In contrast, the more electron-rich phenolic TPs are clearly more reactive, as expected, both with ozone and ·OH (k_{O3} > 10^4 $M^{-1}s^{-1}$, Table 4-1). To what extent the phenolic TPs will be abated in full-scale treatment cannot be concluded from the data presented here because the concentrations of the phenolic TPs were <LOQ in the raw water of waterworks B and C. However, Hollender et al. (2009) showed for a wastewater treatment plant with 5.2±0.6 mgL^{-1} DOC and hydraulic retention times of 3.7 to 10.1 min in the ozone reactor that micropollutants with k_{O3} >10^4 $M^{-1}s^{-1}$ are fully abated at ozone doses >0.4 g ozone g^{-1} DOC. Therefore, we assume that the phenols will be fully abated in waterworks B (0.8 g O_3 g^{-1} DOC, contact time >10 min) and C (pre-ozonation: 0.3 g O_3 g^{-1} DOC, contact time >25 min; intermediate ozonation 0.6 g O_3 g^{-1} DOC; contact time >10 min).

For phenolic compounds, Lee and von Gunten (2012) developed quantitative structure-activity relationships (QSARs) based on substituent descriptors (Hammett constants) to predict the second order rate constants for the reactions with ozone. The proposed QSAR was applied to predict the second order rate constants of R611968-Ph and SYN507900-Ph, and in addition, of the phenolic TP, which was not investigated in laboratory experiments (SYN548580-Ph, see SI4-A7). The second order rate constants of R611968-Ph and SYN507900-Ph predicted by QSAR were on average 2.4 times higher than the measured values. A factor 2.4 is within the uncertainty described by Lee and von Gunten (2012). The predicted second order rate constant of SYN548580-Ph was three to five times higher than the predicted second order rate constants of SYN507900-Ph and R611968-Ph, indicating higher abatement.

4.3.3.3 Advanced Oxidation

Overall, a broader range of micropollutants can be transformed in AOPs compared to ozonation because the ·OH generated in AOPs is a less selective oxidant (von Gunten 2018). Moreover,

direct phototransformation by UV irradiation can contribute to micropollutant abatement depending on the AOP applied (e.g. UV/ H_2O_2, UV/free chlorine) (Katsoyiannis et al. 2011).

The second order rate constant for the reaction of R611968-Ph with ·OH was (2.7±0.6) × 10^9 $M^{-1}s^{-1}$, which is similar to e.g. atrazine and many other micropollutants (Table 4-1; von Sonntag and von Gunten (2012)). For SYN507900-Ph, the second order rate constant could not be determined because it was already reacting by direct photochemical reactions during UVA irradiation and an enhancement of the decay rates could not be observed in UVA/H_2O_2 (SI4-A9, SI4-B8). However, because of their similar structures, we assume that the second order rate constant for the reaction of SYN507900-Ph with ·OH is in the same range as for R611968-Ph. For a treatment plant with reverse osmosis followed by UV/H_2O_2, Marron et al. (2019) calculated pollutant abatement depending on their second order rate constants for the reaction with ·OH, whereby they assumed that the UV/H_2O_2 reactor is designed to remove 1,4-dioxane by 70% through reactions with ·OH (i.e. 4 × 10^{-10} Ms ·OH exposure). Under these comparably favourable conditions (low ·OH scavenging due to low DOC: <0.5 mgL^{-1}), R611968-Ph (k_{OH} (2.7±0.6) × 10^9 $M^{-1}s^{-1}$) would be abated by 60-70% due to reaction with ·OH. In contrast to the phenolic TPs, the abatement of the sulfonic acids (k_{OH} < 5.0 × 10^7 $M^{-1}s^{-1}$) is expected to be negligible in O_3/H_2O_2 or UV/H_2O_2. Based on these low reactivities both with the rather unselective oxidant ·OH and the selective oxidant ozone, it is likely that sulfonic acids are also persistent towards other oxidants such as HOCl, ClO_2 or sulfate radicals.

4.3.3.4 Activated Carbon

Adsorption to powdered activated carbon was investigated in a natural groundwater (DOC 1.1 mgL^{-1}) spiked with four chlorothalonil TPs and, for comparison, with diatrizoic acid (anionic at pH 7; predicted log $D_{OW\ pH7}$ -0.6) and atrazine (neutral at pH 7; predicted log $D_{OW\ pH7}$ 2.2), two micropollutants with well-known adsorption behaviour. Figures SI4-A7 and SI4-A8 show the abatement as a function of the powdered activated carbon dose. According to this, the affinity to activated carbon decreases in the following order: atrazine > R611968-Ph > R417888-SA ≈ SYN507900-Ph > R4718111-SA ≈ diatrizoic acid.

The laboratory experiments showed a higher activated carbon affinity of R417888-SA compared to R471811-SA, which was confirmed by the better retention of R417888-SA in the waterworks (section 4.3.2) and is in accordance with the higher hydrophobicity (Figure 4-1, higher log $D_{OW\ pH7}$). However, hydrophobicity is not the only parameter governing adsorption to activated carbon (Kovalova et al. 2013b). Diatrizoic acid, which has a predicted log $D_{OW\ pH7}$ comparable to R417888-SA, showed similar adsorption behaviour to R471811-SA. This was observed as well in full-scale (section 4.3.2), i.e. diatrizoic acid can be used in waterworks as predictor for the expected breakthrough of R471811-SA.

4.3.3.5 Reverse Osmosis

The reverse osmosis pilot plant was sampled five times over a period of fourteen weeks. The corresponding results are summarized in SI4-B10. Chemical analyses focused on the two chlorothalonil TPs with the highest concentrations (R471811-SA, R417888-SA). Two additional pesticide TPs (chloridazon-desphenyl, log $D_{OW\ pH7}$ -0.8; chloridazon-desphenyl-methyl, log $D_{OW\ pH7}$ -0.6) and nitrate, which are typical groundwater contaminants in many agricultural areas, were also investigated.

The phenolic TPs were completely removed (not detectable in permeate, i.e. <10 ng/L, raw water: ~30-100 ng/L). Furthermore, the chlorothalonil TP R417888-SA and chloridazon-desphenyl-methyl were not detectable in the permeate (raw water: 200-280 ngL^{-1} and 30-33 ngL^{-1}), whereas the chlorothalonil TP R471811-SA was abated by ≥98% (raw water: 1200-2100 ngL^{-1}; permeate: 15-20 ngL^{-1}), nitrate by 95-98% (raw water: 16.5-18.6 mgL^{-1}; permeate: 0.4-0.9 mgL^{-1}), and the pesticide TP chloridazon-desphenyl was only abated by 87-94% (raw water: 440-560 ngL^{-1}; permeate: 30-63 ngL^{-1}). The lower removal of chloridazon-desphenyl compared to the chlorothalonil TPs may be related to differences in the molecular properties. In contrast to the chlorothalonil TPs, chloridazon-desphenyl is uncharged and has a smaller molecular mass and volume (R471811-SA: 348 $gmol^{-1}$, 23 nm^3; chloridazon-desphenyl: 146 $gmol^{-1}$, 11 nm^3; predicted by JChem for Excel, Version 17.1.2300.1455, ChemAxon Ltd.).

4.3.4 Practical Implications

The sulfonic acid TPs are detected more frequently in drinking water resources than the phenolic TPs and exhibit higher concentrations, often exceeding the Swiss drinking water standard of 100 ngL^{-1}. Chlorothalonil has recently been banned in the EU and in Switzerland (BLW 2019a, European Commission 2019), so chlorothalonil will no longer be applied in large parts of Europe. However, it is difficult to predict how long these TPs will continue to be present in groundwater and for how long water suppliers will face raw water polluted with chlorothalonil TPs. The duration depends on various factors such as the exact dissipation time, groundwater recharge rate, groundwater residence time, and dilution with other water sources in the respective aquifer. Experience from other pesticides with similar properties related to biodegradability and application periods and polar TPs is scarce. However, studies in Germany and Switzerland showed no concentration decline for the TPs of the herbicide chloridazon within five years after the last application in two shallow aquifers with average groundwater residence times <15-20 years (Hintze and Hunkeler 2019, Neukum and Meyer 2019). Model predictions are uncertain but indicate that a decrease in chloridazon TP concentration by 90% will take more than 20 years (Neukum and Meyer 2019).

Both sampling along water treatment trains and laboratory experiments indicate that the sulfonic acid TPs of chlorothalonil are persistent in most water treatment processes. Photochemical and oxidative processes (UV irradiation, ozonation, and AOPs based on $^{\cdot}OH$) are not able to abate the sulfonic acid-containing TPs. In contrast, activated carbon may offer a chance to abate the sulfonic acid TPs to a certain extent, but efficiency varies strongly among TPs. To remove all chlorothalonil TPs, activated carbon needs to be exchanged or regenerated very frequently, approximately as often as for the removal of the X-ray contrast agent diatrizoic acid, causing high economic and ecological costs. Reverse osmosis abated ≥98% of chlorothalonil TPs; however, this is an energy intensive process and the reject water (20-30% of treated water) needs to be treated or disposed. Efficient post-treatment processes are not known and disposal to lakes and rivers is questionable because the pollutants are returned to the water cycle.

4.4 Conclusions

- Chlorothalonil TPs are widespread in drinking water resources. One TP (R471811-SA) was detected in all 77 samples, even in groundwater with low anthropogenic impact. The sulfonic acid containing TPs (R471811-SA, R419492-SA, R417888-SA) exceeded concentrations of 100 ngL^{-1} in 14-52% of the samples, while the phenol-containing TPs (SYN507900-Ph, SYN548580-Ph, R611968-Ph) were less frequently detected; in 97% of samples the phenol-containing TPs were below concentrations of 100 ngL^{-1}.
- Although chlorothalonil has recently been banned in Europe, the TPs of chlorothalonil are expected to challenge drinking water suppliers for many years due to their persistence in the environment and in water treatment processes.
- The phenolic TPs can be removed by various treatment techniques such as ozonation, AOPs, and activated carbon. Even UV disinfection may lead to a certain extent of removal.
- In contrast to the phenolic TPs, the less electron-rich sulfonic acids are more persistent and can be removed neither by ozonation nor by $^{\cdot}OH$-based AOPs under typical water treatment conditions. The sulfonic acids adsorb to activated carbon to varying extents, depending on their polarity. For an efficient removal of the TP with the highest concentrations, granular activated carbon needs to be exchanged more frequently than for other common micropollutants.
- Reverse osmosis was able to abate the chlorothalonil TPs by ≥98%. However, the reject water needs to be disposed.

Acknowledgements

We thank all water suppliers, the Federal Office for the Environment (FOEN), and the cantonal authorities for providing samples, the Eawag apprenticeship laboratory for analysing DOC and nitrate as well as Heinz Singer and Philipp Longrée, Eawag, for discussion of the analytical methods. We acknowledge Miriam Reinhardt, FOEN, for selecting the 60 NAQUA groundwater monitoring sites and accompanying the project. We especially thank Roman Wiget, Seeländische Wasserversorgung, Jean-Julien Dessimoz, membratec, Marcel Leemann, Wasserversorgung Zürich, and Thomas Gabriel, Hardwasser AG, for providing detailed information on the reverse osmosis pilot plant or waterworks as well as Claudia Minkowski and Matthias Ruff (Water and Soil Protection Laboratory, Office of Water and Waste Management of the Canton of Berne) for analysing samples from the reverse osmosis pilot plant. Syngenta offered reference material if commercially not available. We acknowledge Jennifer Schollée, Eawag, for critically proofreading the manuscript. This project was partially funded by the FOEN.

References

Acero, J.L., Stemmler, K. and von Gunten, U., 2000. Degradation Kinetics of Atrazine and Its Degradation Products with Ozone and OH Radicals: A Predictive Tool for Drinking Water Treatment. Environmental science & technology 34(4), 591-597.

Benotti, M.J., Song, R., Wilson, D. and Snyder, S.A., 2012. Removal of pharmaceuticals and endocrine disrupting compounds through pilot- and full-scale riverbank filtration. Water science and technology: water supply 12(1), 11-23.

BLW, 2019a. Approval for chlorothalonil is withdrawn with immediate effect (Zulassung für Chlorothalonil wird mit sofortiger Wirkung entzogen). https://www.blw.admin.ch/blw/de/home/services/medienmitteilungen.msg-id-77491.html. Accessed: 17/12/2019.

BLW, 2019b. Sales per active ingredient (Verkaufsmengen je Pflanzenschutzmittel-Wirkstoff). Federal Office for the Agriculture. https://www.blw.admin.ch/blw/de/home/nachhaltige-produktion/pflanzenschutz/pflanzenschutzmittel/verkaufsmengen-der-pflanzenschutzmittel-wirkstoffe.html. Accessed: 06/01/2020.

Buxton, G.V., Greenstock, C.L., Helman, W.P. and Ross, A.B., 1988. Critical Review of rate constants for reactions of hydrated electrons, hydrogen atoms and hydroxyl radicals (·OH/·O− in Aqueous Solution. 17(2), 513-886.

BVL, 2018. Sales of plant protection products in the Federal Republic of Germany, Results of the notifications according to § 64 Plant Protection Act for the year 2017 (Absatz an Pflanzenschutzmittelen in der Bundesrepublik Deutschland, Ergebnisse der Meldungen gemäß § 64 Pflanzenschutzgesetz für das Jahr 2017). Federal Office of Consumer Protection and Food Safety. www.bvl.bund.de/psmstatistiken.html. Accessed: 21/08/2019.

Canonica, S., Jans, U., Stemmler, K. and Jürg, H., 1995. Transformation Kinetics of Phenols in Water: Photosensitization by Dissolved Natural Organic Material and Aromatic Ketones. Environmental science & technology 29, 1822-1831.

Canonica, S., Meunier, L. and von Gunten, U., 2008. Phototransformation of selected pharmaceuticals during UV treatment of drinking water. Water research 42, 121-128.

Chuang, Y.H., Chen, S., Chinn, C.J. and Mitch, W.A., 2017. Comparing the UV/Monochloramine and UV/Free Chlorine Advanced Oxidation Processes (AOPs) to the UV/Hydrogen Peroxide AOP Under Scenarios Relevant to Potable Reuse. Environ Sci Technol 51(23), 13859-13868.

Delgado, L.F., Charles, P., Glucina, K. and Morlay, C., 2012. The removal of endocrine disrupting compounds, pharmaceutically activated compounds and cyanobacterial toxins during drinking water preparation using activated carbon--a review. Sci Total Environ 435-436, 509-525.

DVGW, 2006. W 294-2 Worksheet 06/2006: UV devices for disinfection in water supply; part 2: testing the quality, function and effectiveness of disinfection (W 294-2 Arbeitsblatt 06/2006: UV-Geräte zur Desinfektion in der Wasserversorgung; Teil 2: Prüfung von Beschaffenheit, Funktion und Desinfektionswirksamkeit).

EFSA, 2018. Peer review of the pesticide risk assessment of the active substance chlorothalonil. EFSA Journal 16(1), 1-40.

EPA, 1999. Reregistration Eligibility Decision (RED) Chlorothalonil. United States Environmental Protection Agency. https://archive.epa.gov/pesticides/reregistration/web/pdf/0097red.pdf.

European Commission, 1998. Council Directive 98/83/EC of 3 November 1998 on the quality of water intended for human consumption. Official Journal of the European Communities (L330).

European Commission, 2003. Guidance document on the assessment of the relevance of metabolites in groundwater of substances regulated under council directive 91/414/EEC. Sanco/221/2000 –rev.10- final.

European Commission, 2019. Commission implementing regulation (EU) 2019/677 of 29 April 2019 concerning the non-renewal of the approval of the active substance chlorothalonil, in accordance with Regulation (EC) No 1107/2009 of the European Parliament and of the Council concerning the placing of plant protection products on the market, and amending Commission Implementing Regulation (EU) No 540/2011. Official Journal of the European Union.

Fu, Y., Wu, G., Geng, J., Li, J., Li, S. and Ren, H., 2019. Kinetics and modeling of artificial sweeteners degradation in wastewater by the UV/persulfate process. Water Res 150, 12-20.

Guo, K., Wu, Z., Yan, S., Yao, B., Song, W., Hua, Z., Zhang, X., Kong, X., Li, X. and Fang, J., 2018. Comparison of the UV/chlorine and UV/H2O2 processes in the degradation of PPCPs in simulated drinking water and wastewater: Kinetics, radical mechanism and energy requirements. Water Res 147, 184-194.

Hessler, D.P., Gorenflo, V. and Frimmel, F.H., 1993. Degradation of Aqueous Atrazine and Metazachlor Solutions by UV and UV/H202 - Influence of pH and Herbicide Concentration. Acta hydrochimica et hydrobiologica 21(4), 209-214.

Hintze, S. and Hunkeler, D., 2019. Long-term behaviour of PPP metabolites in groundwater (Langzeitverhalten von PSM-Metaboliten im Grundwasser). Aqua & Gas 99(11), 24-29.

Hoigné, J. and Bader, H., 1983. Rate constants of reactions of ozone with organic and inorganic compounds in water—II: Dissociating organic compounds. Water research 17(2), 185-194.

Hoigné, J. and Bader, H., 1994. Characterization Of Water Quality Criteria for Ozonation Processes. Part II: Lifetime of Added Ozone. Ozone: Science & Engineering 16(2), 121-134.

Hollender, J., Rothardt, J., Radny, D., Loos, M., Epting, J., Huggenberger, P., Borer, P. and Singer, H., 2018. Comprehensive micropollutant screening using LC-HRMS/MS at three riverbank filtration sites to assess natural attenuation and potential implications for human health. Water Research X 1, 1-12.

Hollender, J., Zimmermann, S.G., Koepke, S., Krauss, M., McArdell, C.S., Ort, C., Singer, H., von Gunten, U. and Siegrist, H., 2009. Elimination of Organic Micropollutants in a Municipal Wastewater Treatment Plant Upgraded with a Full-Scale Post-Ozonation Followed by Sand Filtration. Environmental science & technology 43(20), 7862-7869.

Huber, M.M., Canonica, S., Park, G.-Y. and von Gunten, U., 2003. Oxidation of Pharmaceuticals during Ozonation and Advanced Oxidation Processes. Environmental science & technology 37(5), 1016-1024.

Hübner, U., Miehe, U. and Jekel, M., 2012. Optimized removal of dissolved organic carbon and trace organic contaminants during combined ozonation and artificial groundwater recharge. Water research 46(18), 6059-6068.

Kaiser, H.-P., Köster, O., Gresch, M., Périsset, P.M.J., Jäggi, P., Salhi, E. and von Gunten, U., 2013. Process Control For Ozonation Systems: A Novel Real-Time Approach. Ozone: Science & Engineering 35(3), 168-185.

Katsoyiannis, I., Canonica, S. and von Gunten, U., 2011. Efficiency and energy requirements for the transformation of organic micropollutants by ozone, O3/H2O2 and UV/H2O2. Water research 45(13), 3811-3822.

Kiefer, K., Müller, A., Singer, H. and Hollender, J., 2019. New Relevant Pesticide Transformation Products in Groundwater Detected Using Target and Suspect Screening for Agricultural and Urban Micropollutants with LC-HRMS. Water research 165.

Knappe, D.R.U., Matsui, Y., Snoeyink, V.L., Roche, P., Prados, M.J. and Bourbigot, M.-M., 1998. Predicting the Capacity of Powdered Activated Carbon for Trace Organic Compounds in Natural Waters. Environmental science & technology 32(11), 1694-1698.

Kovalova, L., Knappe, D.R., Lehnberg, K., Kazner, C. and Hollender, J., 2013a. Removal of highly polar micropollutants from wastewater by powdered activated carbon. Environ Sci Pollut Res Int 20(6), 3607-3615.

Kovalova, L., Siegrist, H., von Gunten, U., Eugster, J., Hagenbuch, M., Wittmer, A., Moser, R. and McArdell, C.S., 2013b. Elimination of micropollutants during post-treatment of hospital wastewater with powdered activated carbon, ozone, and UV. Environ Sci Technol 47(14), 7899-7908.

Laabs, V., Leake, C., Botham, P. and Melching-Kollmuss, S., 2015. Regulation of non-relevant metabolites of plant protection products in drinking and groundwater in the EU: Current status and way forward. Regul Toxicol Pharmacol 73(1), 276-286.

Lee, Y. and von Gunten, U., 2012. Quantitative structure-activity relationships (QSARs) for the transformation of organic micropollutants during oxidative water treatment. Water Res 46(19), 6177-6195.

Lee, Y., Yoon, J. and von Gunten, U., 2005. Kinetics of the Oxidation of Phenols and Phenolic Endocrine Disruptors during Water Treatment with Ferrate (Fe(VI)). Environmental science & technology 39(22), 8978-8984.

LUBW, 2011. Groundwater monitoring programme - results from sampling campaign 2010 (Grundwasserüberwachungsprogramm - Ergebnisse der Beprobung 2010). Reihe Grundwasserschutz. 42, 1-98. http://www4.lubw.baden-wuerttemberg.de/servlet/is/208632/.

Maeng, S.K., Sharma, S.K., Lekkerkerker-Teunissen, K. and Amy, G.L., 2011. Occurrence and fate of bulk organic matter and pharmaceutically active compounds in managed aquifer recharge: a review. Water Res 45(10), 3015-3033.

Mark, G., Korth, H.-G., Schuchmann, H.-P. and von Sonntag, C., 1996. The photochemistry of aqueous nitrate ion revisited. Journal of Photochemistry and Photobiology A: Chemistry 101(2), 89-103.

Marron, E.L., Mitch, W.A., Gunten, U.V. and Sedlak, D.L., 2019. A Tale of Two Treatments: The Multiple Barrier Approach to Removing Chemical Contaminants During Potable Water Reuse. Acc Chem Res 52(3), 615-622.

Mechelke, J., Longree, P., Singer, H. and Hollender, J., 2019. Vacuum-assisted evaporative concentration combined with LC-HRMS/MS for ultra-trace-level screening of organic micropollutants in environmental water samples. Analytical and Bioanalytical Chemistry 411, 2555–2567.

Miklos, D.B., Remy, C., Jekel, M., Linden, K.G., Drewes, J.E. and Hübner, U., 2018. Evaluation of advanced oxidation processes for water and wastewater treatment – A critical review. Water research 139, 118-131.

Neukum, C. and Meyer, K., 2019. Chloridazon-metabolites in groundwater: Coupled modelling for long-term estimation of transport behavior and concentration development in groundwater of a drinking water abstraction (Chloridazon-Metaboliten im Grundwasser: Gekoppelte Modellierung zur langfristigen Abschätzung des Transportverhaltens und der Konzentrationsentwicklung im Grundwasser einer Trinkwassergewinnungsanlage). Grundwasser 24(1), 73-81.

Nick, K., Schöler, H.F., Mark, G., Söylemez, T., Akhlaq, M.S., Schuchmann, H.-P. and Von Sonntag, C., 1992. Degradation of some triazine herbicides by UV radiation such as used in the UV disinfection of drinking water. J. Water Supply Res. Technol. Aqua 41(2), 82-87.

ÖNORM, 2001. M 5873-1: Water disinfection systems using ultraviolet rays - requirements and testing (Anlagen zur Desinfektion von Wasser mittels Ultraviolett-Strahlen - Anforderungen und Prüfung).

Pereira, V.J., Weinberg, H.S., Linden, K.G. and Singer, P.C., 2007. UV Degradation Kinetics and Modeling of Pharmaceutical Compounds in Laboratory Grade and Surface Water via Direct and Indirect Photolysis at 254 nm. Environmental science & technology 41(5), 1682-1688.

Real, F.J., Benitez, F.J., Acero, J.L., Sagasti, J.J.P. and Casas, F., 2009. Kinetics of the Chemical Oxidation of the Pharmaceuticals Primidone, Ketoprofen, and Diatrizoate in Ultrapure and Natural Waters. Industrial & Engineering Chemistry Research 48(7), 3380-3388.

Rosenfeldt, E.J. and Linden, K.G., 2004. Degradation of Endocrine Disrupting Chemicals Bisphenol A, Ethinyl Estradiol, and Estradiol during UV Photolysis and Advanced Oxidation Processes. Environmental science & technology 38(20), 5476-5483.

Scheurer, M., Schmutz, B., Happel, O., Brauch, H.J., Wulser, R. and Storck, F.R., 2014. Transformation of the artificial sweetener acesulfame by UV light. Sci Total Environ 481, 425-432.

Staehelin, J. and Hoigne, J., 1982. Decomposition of ozone in water: rate of initiation by hydroxide ions and hydrogen peroxide. Environmental science & technology 16(10), 676-681.

Stefan, M.I. (ed) 2018. Advanced Oxidation Processes for Water Treatment: Fundamentals and Applications, IWA Publishing, London.

SVGW, 2010. W13d: Guideline for UV disinfection in water supply (Richtlinie zur UV-Desinfektion in der Wasserversorgung). Schweizerischer Verein des Gas- und Wasserfaches.

Taheran, M., Brar, S.K., Verma, M., Surampalli, R.Y., Zhang, T.C. and Valero, J.R., 2016. Membrane processes for removal of pharmaceutically active compounds (PhACs) from water and wastewaters. Sci Total Environ 547, 60-77.

Toth, J.E., Rickman, K.A., Venter, A.R., Kiddle, J.J. and Mezyk, S.P., 2012. Reaction kinetics and efficiencies for the hydroxyl and sulfate radical based oxidation of artificial sweeteners in water. J Phys Chem A 116(40), 9819-9824.

Umar, M., Roddick, F. and Fan, L., 2014. Recent Advancements in the Treatment of Municipal Wastewater Reverse Osmosis Concentrate—An Overview. Critical Reviews in Environmental Science and Technology 45(3), 193-248.

von Gunten, U., 2003. Ozonation of drinking water: Part I. Oxidation kinetics and product formation. Water research 37(7), 1443-1467.

von Gunten, U., 2018. Oxidation Processes in Water Treatment: Are We on Track? Environ Sci Technol 52(9), 5062-5075.

von Sonntag, C. and von Gunten, U., 2012. Chemistry of Ozone in Water and Wastewater Treatment: From Basic Principles to Applications, IWA Publisher, London.

Westerhoff, P., Yoon, Y., Snyder, S. and Wert, E., 2005. Fate of Endocrine-Disruptor, Pharmaceutical, and Personal Care Product Chemicals during Simulated Drinking Water Treatment Processes. Environmental science & technology 39, 6649-6663.

Zepp, R.G., 1978. Quantum yields for reaction of pollutants in dilute aqueous solution. Environmental science & technology 12(3), 327-329.

Zepp, R.G., Hoigne, J. and Bader, H., 1987. Nitrate-induced photooxidation of trace organic chemicals in water. Environmental science & technology 21(5), 443-450.

Chapter SI4: Supporting Information to Chapter 4 Chlorothalonil Transformation Products in Drinking Water Resources: Widespread and Challenging to Abate

SI4-B can be found under:
doi.org/10.1016/j.watres.2020.116066

SI4-A1: Selected Waterworks

Table SI4-A1: Investigated waterworks and details on treatment steps.

Waterworks	Raw Water	Treatment Steps
A	River Rhine	1) Rapid sand filter 2) Granular activated carbon filtration (GAC) in parallel ○ GAC 1: specific throughput 25 m^3kg^{-1} GAC ○ GAC 2: specific throughput 55 m^3kg^{-1} GAC ○ GAC 3: specific throughput 305 m^3kg^{-1} GAC 3) UV disinfection (medium pressure lamp, Berson Inline, > 400 Jm^{-2})
B	Groundwater (karstic spring)	1) Ozonation (0.8 g O_3 g^{-1} DOC) 2) Multi-layer filtration (no sampling) 3) GAC filtration in parallel ○ GAC 1: specific throughput 23 m^3kg^{-1} GAC ○ GAC 2: specific throughput 216 m^3kg^{-1} GAC ○ 2 more GAC filters (no sampling) 4) ClO_2 disinfection (no sampling)
C	Lake water	1) Pre-Ozonation (0.3 g O_3 g^{-1} DOC) 2) Rapid sand filtration (no sampling) 3) Intermediate ozonation (0.6 g O_3 g^{-1} DOC) 4) GAC filtration: specific throughput 1200 m^3kg^{-1} GAC 5) Slow sand filtration
D	River water	1) River bank filtration 2) Cl_2/ClO_2 disinfection (0.3-0.4 mgL^{-1}) 3) Artificial recharge and abstraction
E	Groundwater	• 2 abstraction wells influenced by river bank filtration ○ Distance to river: 40 m ○ UV disinfection (medium pressure lamp, Barrier® M, > 400 Jm^{-2}) • 1 abstraction well (no further treatment) ○ Distance to river: 730 m • 1 abstraction well ○ Not influenced by river ○ Reverse osmosis pilot plant
F	Groundwater	• 1 abstraction well (no further treatment) • 2 springs (no further treatment) • 1 spring ○ UV disinfection (low pressure lamp, Aquafides 1 AF300 T, > 400 Jm^{-2})
G	Groundwater	• 1 Groundwater abstraction well (no further treatment) • 1 Groundwater spring (no further treatment)
I	Groundwater	• Groundwater abstraction well (no further treatment) • Water is mixed (ratio 1:1, v:v) with groundwater from area with low agricultural impact

SI4-A2: Stock Solutions

Analyte stock solutions for LC-MS/MS analysis: Reference material was dissolved depending on solubility and stability (Table SI4-A2). Then, mixed solutions were prepared in ethanol at different concentrations.

Table SI4-A2: Analyte stock solutions in organic solvent.

Analyte	Solvent	Concentration
Chlorothalonil TP R471811-SA	Ethanol:Water (1:1, v:v)	1000 mgL^{-1}
Chlorothalonil TP R417888-SA	Methanol	1000 mgL^{-1}
Chlorothalonil TP R419492-SA	Ethanol:Water (1:1, v:v)	100 mgL^{-1}
Chlorothalonil TP SYN507900-Ph	Ethanol:Water (1:1, v:v)	100 mgL^{-1}
Chlorothalonil TP R611968-Ph	Ethanol	1000 mgL^{-1}
Chlorothalonil TP SYN5458580-Ph	Ethanol:Water (1:1, v:v)	100 mgL^{-1}
Acesulfame	Ethanol:Water (1:1, v:v)	1000 mgL^{-1}
Diatrizoic acid	Ethanol	1000 mgL^{-1}
Salicylic acid	Acetonitrile	1000 mgL^{-1}

Isotope-labelled internal standards: Isotope-labelled internal standards were dissolved in ethanol, methanol, acetonitrile, ethanol/water mix, methanol/water mix, dimethyl sulfoxide, ethyl acetate, toluene, acetone, water at concentrations ranging from 100 to 1000 mgL-1, depending on the solubility and stability. Then, mixed solutions were prepared in ethanol or acetonitrile at 10 mgL-1, which were combined for the final spike solution (0.1 mgL-1).

Aqueous stock solutions for laboratory experiments: Aqueous stock solutions (20-100 µM) were prepared using the stock solutions described in Table SI4-A2. The organic solvent was evaporated under a gentle nitrogen stream. Then, the precipitate was dissolved in ultrapure water at room temperature within one to two days. The aqueous stock solution was stored until the experiment (up to seven days) at 4 °C.

SI4-A3: LC-MS/MS and LC-UV Settings

Environmental samples were enriched using vacuum-assisted evaporative concentration, whereas samples from laboratory experiments were analysed without enrichment. Table SI4-A3 and Table SI4-A4 describe the HPLC-HRMS/MS method used for the environmental samples and samples from experiments with UV irradiation, ozone and hydroxyl radicals ($^{\cdot}OH$). The adsorption experiment with activated carbon was performed at the Laboratory for Operation Control and Research (Zweckverband Landeswasserversorgung) and samples were subsequently measured onsite with a different HPLC-MS/MS method (Table SI4-A5, Table SI4-A6, and Table SI4-A7). The actinometer atrazine used for the photodegradation experiments was analysed by HPLC-UV (Table SI4-A8).

Table SI4-A3: HPLC method for environmental samples and samples from experiments with UV irradiation, ozone and ·OH.

Autosampler: PAL RTC (CTC Analytics, Switzerland) **Pump: Dionex UltiMate3000 RS (Thermo Fisher Scientific, U.S.)** **Column: Atlantis T3 3 µm, 3.0 x 150 mm (Waters, Ireland)**	
Injection volume	150 µL (environmental samples) 100 µL (laboratory samples)
Flow rate	0.3 mL min^{-1}
Eluent A	Water + 0.1% concentrated formic acid
Eluent B	Methanol + 0.1% concentrated formic acid
Gradient	0 min: 100% eluent A, 0% eluent B 1.5 min: 100% eluent A, 0% eluent B 18.5 min: 5% eluent A, 95% eluent B 28.5 min: 5% eluent A, 95% eluent B 29 min: 100% eluent A, 0% eluent B 33 min: 100% eluent A, 0% eluent B

Table SI4-A4: ESI-HRMS/MS settings for environmental samples and samples from experiments with UV irradiation, ozone and ·OH.

Mass spectrometer: Fusion Lumos (Thermo Fisher Scientific, U.S.)	
Spray voltage (kV)	3.5 / -2.5
Capillary temperature (°C)	300
Sheath gas (AU)	40
Auxiliary gas (AU)	10
S-lens RF level (AU)	60
Automatic gain control (AGC) target MS1	5×10^4
Maximum injection time MS1 (ms)	50
Scan range MS1 (m/z)	100 - 1000
Resolution MS1 (at m/z 200)	240 000
Internal calibration	Yes (Easy-IC)
Cycle time	1 s
MS/MS activation type	Higher energy collisional dissociation (HCD)
Data-dependent trigger	Ions of target compounds; if idle pick most intense
Isolation window (m/z)	1
Resolution MS2 (at m/z 200)	30 000
Automatic gain control (AGC) target MS2	1×10^4
Maximum injection time MS2 (ms)	54
Dynamic exclusion time (s)	3
Normalized collision energy (NCE)	Stepped: 20, 40, 60 or 20, 30, 40

Table SI4-A5: HPLC method for samples from laboratory experiments with activated carbon.

Autosampler: Nexera X2 SIL-30AC (Shimadzu, Japan) **Pump: Nexera X2 LC-30AD** **Column: Ultra Aqueous C18 5 µm, 4.6x250 mm (Restek, U.S.)**	
Injection volume	100 µL
Flow rate	0.8 $mLmin^{-1}$
Eluent A	Water + 0.1% concentrated formic acid
Eluent B	Acetonitrile + 0.1% concentrated formic acid
Gradient	0 min: 98% eluent A, 2% eluent B 7 min: 20% eluent A, 80% eluent B 12 min: 20% eluent A, 80% eluent B 12.1 min: 98% eluent A, 2% eluent B 17 min: 98% eluent A, 2% eluent B

Table SI4-A6: Parameter settings for triple quadrupole measurement for samples from laboratory experiments with activated carbon.

Mass spectrometer: API 5500 Qtrap (Sciex, U.S.)	
Ion Spray Voltage	4500 / -4500
Curtain Gas	30
Collision Gas	Medium
Temperature	700
Ion Source Gas 1	50
Ion Source Gas 2	60
Entrance Potential	10 / -10

Table SI4-A7: Parameter settings for triple quadrupole measurement for samples from laboratory experiments with activated carbon.

Analyte	**Q1 → Q3 in Da**	**Dwell time in ms**	**DP in V**	**CE in V**	**CXP in V**
Chlorothalonil TP	345 → 302	50	-100	-40	-12
R471811-SA	345 → 238	50	-100	-40	-12
Chlorothalonil TP	327 → 220	50	-60	-36	-9
R417888-SA	327 → 284	50	-60	-26	-13
Chlorothalonil TP	263 → 35	50	-135	-70	-17
SYN507900-Ph	263 → 184	50	-135	-40	-11
	283 → 220	50	-135	-28	-11
Chlorothalonil TP	263 → 35	50	-45	-78	-17
R611968-Ph	263 → 156	50	-45	-46	-7
	263 → 184	50	-45	-34	-11
Diatrizoic acid	615 → 361	30	101	47	18
	615 → 233	30	101	55	12
Atrazine	216 → 174	30	46	27	8
	216 → 104	30	46	27	8

Table SI4-A8: HPLC-UV method for actinometry with atrazine.

Autosampler: Dionex UltiMate3000 RS (Thermo Fisher Scientific, U.S.) **Pump: Dionex UltiMate3000 RS (Thermo Fisher Scientific, U.S.)** **Column: Atlantis T3 3 µm, 3.0 x 150 mm (Waters, Ireland)** **Detector: Diode Array, Dionex UltiMate3000 RS (Thermo Fisher Scientific, U.S.)**	
Injection volume	100 µL
Flow rate	0.3 $mLmin^{-1}$
Eluent A	Water + 0.1% concentrated formic acid
Eluent B	Acetonitrile + 0.1% concentrated formic acid
Gradient	0 min: 50% eluent A, 50% eluent B 7 min: 5% eluent A, 95% eluent B 9 min: 5% eluent A, 95% eluent B 9.5 min: 50% eluent A, 50% eluent B 13.5 min: 50% eluent A, 50% eluent B
Wavelength	265 nm

SI4-A4: Quantification

SI4-B1 and SI4-B2 summarize quantification results and various analytical information such as limit of quantification (LOQ), isotope-labelled internal standards (ILIS), or relative recoveries for the environmental samples. For other samples (laboratory experiments, pilot plant reverse osmosis), LOQ, ILIS and relative recovery may differ (e.g. due to different analytical methods).

ILIS Selection: Quantification was based on the peak area ratio of analyte and ILIS. If a structurally identical ILIS was not available (i.e. for all chlorothalonil TPs), ILIS selection was supported by an internal R script using the R functions available on Zenodo (Schollée 2018). First, the TraceFinder 4.1 export was imported to R (R Core Team 2016) and all ILIS co-eluting with the analyte within the given RT window (±2.5 min) were selected (function selectISTDs()). Then, a linear calibration model was calculated for each combination of analyte and ILIS (function calibrationCalc()), and finally, sample concentrations were determined based on each calibration model (function predictConc()). Using the concentration c in the spiked / not spiked samples and the theoretical spike level, relative recoveries as defined in equation (SI4-1) were calculated,

$$\text{Relative Recovery} = \frac{\left(c_{\text{spiked sample}} - c_{\text{not spiked sample}}\right)}{\text{Theoretical Spike Level}} \quad \text{(SI4-1)}$$

if the following equation was true (function recoveryCalc()):

$$c_{\text{not spiked sample}} < \left(c_{\text{spiked sample}} - c_{\text{not spiked sample}}\right) \cdot 1.7 \quad \text{(SI4-2)}$$

This check ensured that relative recoveries were only determined if the concentration difference in the spiked and not spiked samples was large enough, to avoid cases where the relative recoveries were dominated by measurement uncertainty, and therefore, misleading. Finally, an ILIS was selected for which the mean relative recovery was close to 100% and the standard deviation of the relative recoveries across the spiked samples was low. Final analyte concentrations were corrected by the relative recovery, if a structurally identical ILIS was not available.

Limit of Quantification (LOQ): The LOQ in ultrapure water ($LOQ_{Ultrapure}$) was defined as the lowest calibration standard with at least five data points along the chromatographic peak (MS1 full scan mode) and a peak area ratio (analyte vs. ILIS) of at least twice the peak area ratio in all blank samples. To estimate the LOQ in matrix (LOQ_{Matrix}), the $LOQ_{Ultrapure}$ was divided by the absolute recovery:

$$LOQ_{Matrix} = \frac{LOQ_{Ultrapure}}{\text{Absolute Recovery}} \quad \text{(SI4-3)}$$

If the sample concentration was in the range of the LOQ_{Matrix}, the so-defined LOQ_{Matrix} was lowered if the chromatographic peaks in the samples were defined by at least five data points.

Absolute recoveries were determined for each analyte by comparing the peak area in the matrix to the peak area in ultrapure water, as described in the following. If a structurally identical ILIS was available (i.e. for acesulfame), the peak area of the ILIS in the matrix (environmental samples) was divided by the peak area of the ILIS in ultrapure water (median of all enriched calibration standards) according to equation 4:

$$\text{Absolute Recovery}_{\substack{\text{Identical}\\\text{ILIS}}} = \text{Median}\,\frac{\text{Peak Area ILIS}_{\text{Matrix}}}{\text{Median (Peak Area ILIS}_{\text{Ultrapure}})} \quad \text{(SI4-4)}$$

If a structurally identical ILIS was not available (i.e. all chlorothalonil TPs), the peak area of the analyte in the spiked sample (after subtracting the peak area in the not spiked sample) was compared to the peak area of the analyte in the calibration standard that corresponded to the spike level:

$$\text{Absolute Recovery}_{\substack{\text{No Identical}\\\text{ILIS}}} = \frac{\text{Peak Area}_{\substack{\text{Spiked}\\\text{Sample}}} - \text{Peak Area}_{\substack{\text{Not Spiked}\\\text{Sample}}}}{\text{Peak Area}_{\substack{\text{Calibration}\\\text{Standard}}}} \quad \text{(SI4-5)}$$

SI4-A5: UVC Irradiation

Figure SI4-A1 illustrates the absorbance spectra of the chlorothalonil TPs and the emission spectrum of the UVC lamps. UVC irradiation experiments were conducted in triplicate at pH 7.5 (actinometer atrazine: pH 7.0). The experiments with the phenolic TPs were repeated with shorter irradiation time to capture more data points for the assessment of the phototransformation rate for these fast degrading compounds. The determined photon fluence rates at the two different days differed by 25% (4.0×10^{-5} and 5.3×10^{-5} E m^{-2} s^{-1}), which can be the result of small variations of performance of the lamps, temperature in the reactor, distance of the vials to the lamps, etc.

The reported phototransformation data (Table SI4-A9) was determined as follows. First, the pseudo-first-order phototransformation rate constants k_{obs} (s^{-1}) for each TP and for the actinometer atrazine were determined from a linear regression (Figure SI4-A2) according to equation (SI4-6):

$$\ln\left(\frac{[TP]_T}{[TP]_0}\right) = -\,k_{obs}t \quad \text{(SI4-6)}$$

Then, the photon fluence rate E was calculated from k_{obs} of the actinometer atrazine according to:

$$E = \frac{k_{obs}^{atr}}{2.303\;\Phi_{atr}\;\varepsilon_{atr\;254nm}}\ \text{(einstein } m^{-2}s^{-1}\text{)}, \quad \text{(SI4-7)}$$

where Φ_{atr} and $\varepsilon_{atr\;254nm}$ are the quantum yield (0.046 mol E^{-1}, Hessler et al. (1993)) and molar absorptivity at wavelength 254 nm (3860 M^{-1} cm^{-1} Nick et al. (1992) of atrazine.

The quantum yield Φ_{TP} of each TP was obtained according to equation (SI4-8)

$$\Phi_{TP} = \Phi_{atr}\,\frac{k_{obs}^{TP}}{k_{obs}^{atr}}\,\frac{\varepsilon_{254\;nm}^{atr}}{\varepsilon_{254\;nm}^{TP}}\ \text{(mol einstein}^{-1}\text{)} \quad \text{(SI4-8)}$$

In addition, the photon fluence based rate constants k_E^{TP} were calculated:

$$k_E^{TP} = \frac{k_{obs}^{TP}}{E} \ (m^2 \ einstein^{-1}) \qquad (SI4\text{-}9)$$

Photon fluence based rate constants are independent of the experimental set-up and allow therefore a comparison with other studies (Canonica et al. 2008).

Furthermore, we calculated the relative abatement in UV disinfection and UV/H_2O_2 assuming only direct photolysis and a UV dose of 400 Jm^{-2} (=8.49 10^{-4} einstein m^{-2}) and 7500 Jm^{-2} (=1.59 10^{-2} einstein m^{-2}), respectively (Canonica et al. 2008):

$$\text{relative abatement (254 nm, 400 Jm}^{-2}) = 1 - \exp\left(-k_E^{TP}\ 8.49\ 10^{-4}\ \text{einstein m}^{-2}\right) \qquad (SI4\text{-}10)$$

$$\text{relative abatement (254 nm, 7500 Jm}^{-2}) = 1 - \exp\left(-k_E^{TP}\ 1.59\ 10^{-2}\ \text{einstein m}^{-2}\right) \qquad (SI4\text{-}11)$$

Additionally, we determined the UV dose necessary to remove 90% of the TPs (Table SI4-A10) as described by Bahnmüller et al. (2015):

$$\text{UV dose (90\% abatement)} = \frac{-\ln(0.1)}{k_E^{TP}}\ 4.75 \times 10^5\ \text{J einstein}^{-1}\ \ (\text{J m}^{-2}) \qquad (SI4\text{-}12)$$

The factor 4.75×10^5 is the photon to energy conversion factor for 254 nm.

Table SI4-A9: Determined photochemical data: observed pseudo-first-order phototransformation rate constants of the actinometer atrazine or the chlorothalonil TP (k_{obs}^{atr}, k_{obs}^{TP}), photon fluence rate E, molar absorptivity $\varepsilon_{254\,nm}^{TP}$, and the quantum yield Φ_{TP}. Standard deviation of quantum yields consider the propagated standard deviation of the measured rates of the actinometer and of the TPs, potential standard error of the absorbance spectra were not considered.

	R471811-SA	**R417888-SA**	**R611968-Ph**	**SYN507900-Ph**
k_{obs}^{atr} in s^{-1}	$(2.2\pm0.1) \times 10^{-3}$	$(2.2\pm0.1) \times 10^{-3}$	$(1.6\pm0.1) \times 10^{-3}$	$(1.6\pm0.1) \times 10^{-3}$
E in einstein $m^{-2}s^{-1}$	$(5.3\pm0.1) \times 10^{-5}$	$(5.3\pm0.1) \times 10^{-5}$	$(4.0\pm0.1) \times 10^{-5}$	$(4.0\pm0.1) \times 10^{-5}$
k_{obs}^{TP} in s^{-1}	$(6.0\pm0.3) \times 10^{-5}$	$(9.9\pm0.2) \times 10^{-5}$	$(6.9\pm0.1) \times 10^{-4}$	$(11.6\pm0.1) \times 10^{-4}$
k_E^{TP} in m^2einstein^{-1}	1.1±0.1	1.9±0.1	17±1	29±1
$\varepsilon_{254\,nm}^{TP}$ in $M^{-1}cm^{-1}$	710	8000	5400	6900
Φ_{TP} in mol einstein^{-1}	$(0.7\pm0.1) \times 10^{-2}$	$(0.10\pm0.01) \times 10^{-2}$	$(1.4\pm0.1) \times 10^{-2}$	$(1.8\pm0.1) \times 10^{-2}$
Rel. Abatement in % at 254 nm, 400 Jm^{-2}	0.1	0.2	1.5	2.4

Table SI4-A10: Relative abatement for different fluence doses applied for UV disinfection (400 Jm^{-2}) and UV-based AOPs (7500 Jm^{-2}), as well as calculated fluence doses required to remove 90% of chlorothalonil TPs by UVC treatment in water without organic matter and nitrate.

	Relative abatement for 400 Jm^{-2} in %	**Relative abatement for 7500 Jm^{-2} in %**	**UV dose for 90% abatement in Jm^{-2}**
R471811-SA	0.1	1.8	968000
R417888-SA	0.2	2.9	588000
SYN507900-Ph	2.4	37	38000
R611968-Ph	1.5	24	64000

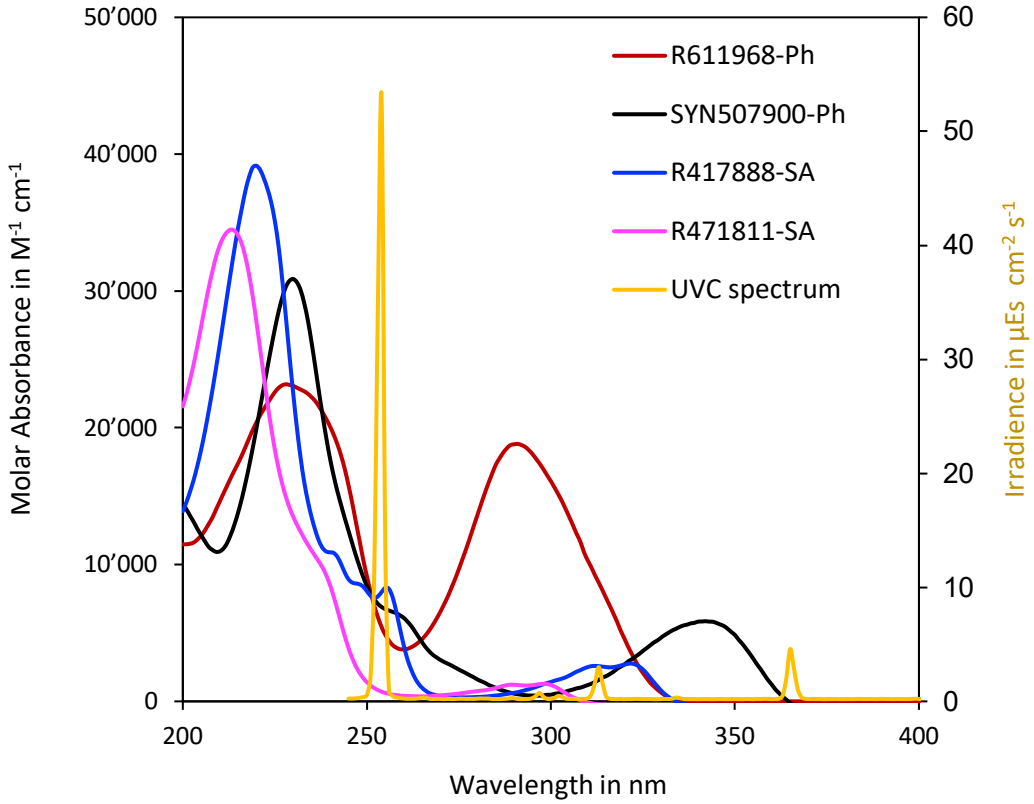

Figure SI4-A1: Absorbance spectra of the chlorothalonil TPs (R611968-Ph: 20 µM, SYN507900-Ph: 20 µM, R417888-SA: 50 µM, R471811-SA: 50 µM, path length: 1 cm) and emission spectrum of the UVC lamps with peak emission at 254 nm.

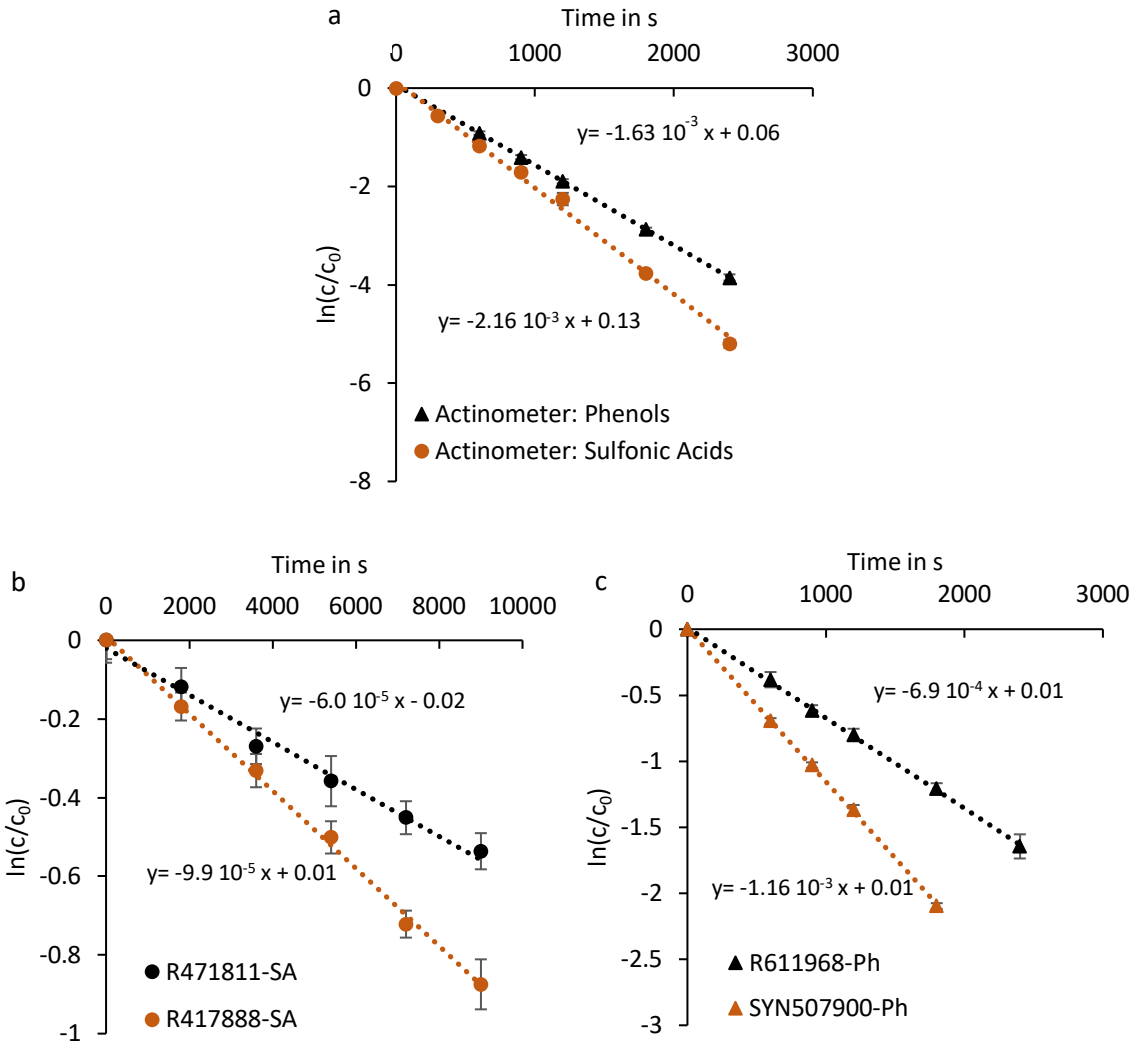

Figure SI4-A2: Phototransformation observed in UVC experiments (a) of the actinometer atrazine in experiments with phenolic TPs and sulfonic acid TPs, (b) of the sulfonic acids R471811-SA and R417888-SA, and (c) of the phenolic TPs R611968-Ph and S YN507900-Ph. Error bars indicate standard deviations of triplicates. Temperature: 12±2 °C. pH: 7.5 for chlorothalonil TPs and 7.0 for actinometer atrazine (phosphate buffer). Chlorothalonil TPs: 0.1 µM. Atrazine: 5 µM.

SI4-A6: Ozone Experiments with Sulfonic Acids

Ozone stock solutions were prepared by sparging an ozone/oxygen gas mixture produced by an ozone generator from pure oxygen (BMT 803 BT, BMT Messtechnik GmbH, Germany) into ice-cooled ultra-purified water (Bader and Hoigné 1981). The ozone concentration was determined either with the indigo method (Bader and Hoigné 1981) or spectrophotometrically using the absorbance at 260 nm (ε = 3200 $M^{-1}cm^{-1}$) (von Sonntag and von Gunten 2012). To determine the second order rate constant (k_{O3}) for the reaction of ozone with the slowly-reacting sulfonic acid TPs (R471811-SA, R417888-SA), the TPs were exposed to ozone in excess at pH 2.3 (0.1 µM TP, 100 µM ozone, 10 mM phosphoric acid) in a 250 mL glass bottle with a dispenser system (Hoigné and Bader 1994). Acidic conditions were selected as ozone is more stable at low pH (von Sonntag and von Gunten 2012) and the sulfonic acid TPs do not change their speciation over a wide pH range (predicted pK_a -4.3). To scavenge $^{\cdot}OH$, *tert*-butanol (10 mM) was added to the solution. To monitor TP abatement and the ozone concentration, eleven samples were collected at various

time points over 15 h. Directly after sampling, ozone was quenched using 3-buten-2-ol (210 µM, to determine the TP concentration) or indigo trisulfonate (100 µM, to determine the ozone concentration).

The ozone concentration decreased exponentially, whereas the TPs were stable (Figure SI4-A3). The second order rate constant k_{O3}^{TP} was estimated from the ozone exposure ($\int[O_3]\,dt$) according to equation (SI4-13) (von Gunten and Hoigne 1994) and assuming that TP degradation was $\leq$ 10%:

$$\ln\left(\frac{[TP]_t}{[TP]_0}\right) = -k_{O3}^{TP} \int [O_3]\,dt \qquad \text{(SI4-13)}$$

$$\Leftrightarrow \quad k_{O3}^{TP} < -\frac{\ln(0.9)}{\int_0^{53520} 111\, e^{-4\,10^{-5}t}\,dt} \approx -\frac{\ln(0.9)}{2.4\,10^6\ \mu M\ s} \approx 0.04\ M^{-1}s^{-1} \qquad \text{(SI4-14)}$$

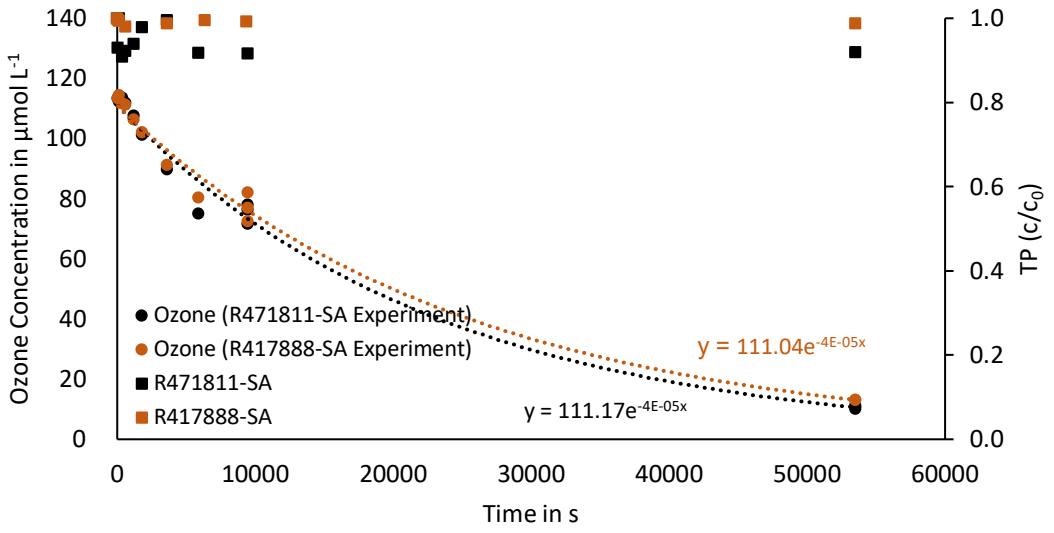

Figure SI4-A3: Decrease of ozone (circles) in ozonation batch experiment with the sulfonic acids R471811-SA and R417888-SA. The concentration of R471811-SA and R417888-SA was constant within measurement uncertainty. Temperature: 23 ± 2 °C. pH: 2.3. Concentration of TPs: 0.1 µM.

SI4-A7: Ozone Experiments with Phenols

Determination of second order rate constants: The kinetics of the reactions of the faster reacting phenolic TPs (SYN507900-Ph, R611968-Ph) were investigated by competition kinetics using salicylic acid as competitor. The phenolic TPs (1 µM) and salicylic acid (1 µM) were exposed in three independent experiments to varying ozone doses (0-2 µM, 0-4.5 µM and 0-6 µM) at pH 7.5 in 10 mL glass vials. To scavenge $^{\cdot}OH$, 50 mM *tert*-butanol was added before the experiment. The rate constant was derived from linear regression according to equation (SI4-15):

$$\ln\left(\frac{[TP]_x}{[TP]_0}\right) = \frac{k_{O3}^{TP}}{k_{O3}^{competitor}} \ln\left(\frac{[competitor]_x}{[competitor]_0}\right) \qquad \text{(SI4-15)}$$

where $[TP]_x$, $[TP]_0$, $[competitor]_x$ and $[competitor]_0$ are the concentration of the chlorothalonil TP or competitor at varying ozone doses or without ozone, respectively, and k are the second

order rate constants for the reaction of ozone with the TP or the competitor. The second order rate constant for salicylic acid was obtained from Hoigné and Bader (1983). It should be noted that Hoigné and Bader (1983) reported conflicting values (Table 1: (2.8±3) × 10^3 $M^{-1}s^{-1}$, Table 2: (3.0±1.0) × 10^4 $M^{-1}s^{-1}$; Figure 4: ~3 × 10^3 $M^{-1}s^{-1}$). For the calculations in this study, we used k_{O3} = 2.8 × 10^4 $M^{-1}s^{-1}$, because it is reported both in a Table and a Figure. However, the uncertainty in the second order rate constant may affect the determined second order rate for the reaction of ozone with the phenolic TPs by a factor of 10.

The reported rate constant and uncertainty is the average and standard deviation of the rate constants calculated from the three experiments (Table SI4-A11). In case of SYN507900-Ph, one rate constant was considered as outlier (factor 2.8 lower) and therefore was not used to calculate the final second order rate constant. This discrepancy can be explained by the fact that the experimental conditions were not optimized at that point (ozone doses too low, 0-2 µM).

Table SI4-A11: Second order rate constants calculated from experiments conducted with varying ozone doses (0-2 µM, 0-4.5 µM and 0-6 µM); *outlier.

TP	Rate Constant 1 in $M^{-1}s^{-1}$	Rate Constant 2 in $M^{-1}s^{-1}$	Rate Constant 3 in $M^{-1}s^{-1}$	**Average Rate Constant in $M^{-1}s^{-1}$**
R611968-Ph	2.43 × 10^4	3.01 × 10^4	2.40 × 10^4	(2.6 ± 0.3) × 10^4
SYN507900-Ph	1.50 × 10^4 *	4.22 × 10^4	4.05 × 10^4	4.1 × 10^4

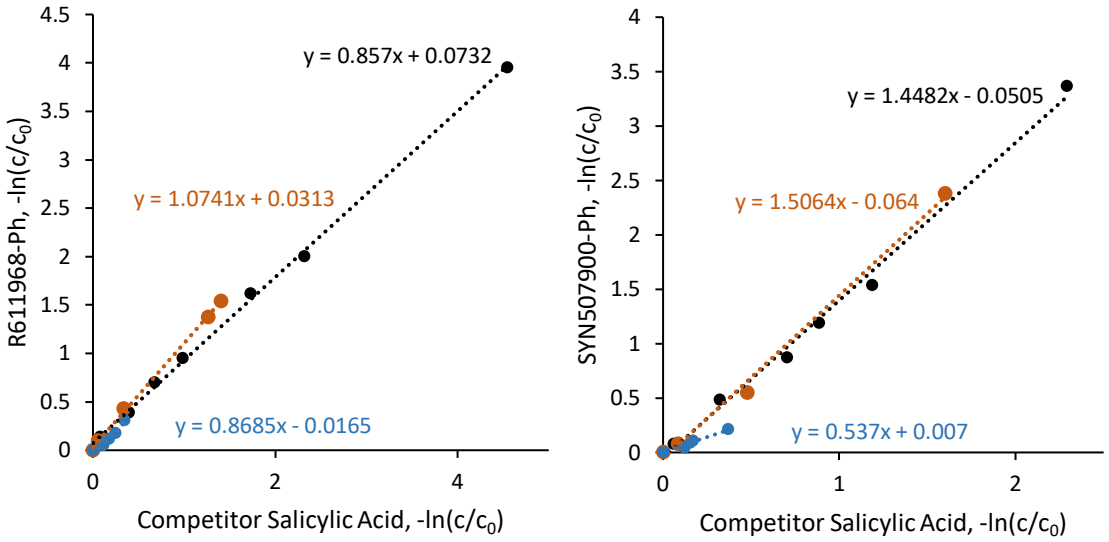

Figure SI4-A4: Competition kinetics plots for the phenolic TPs and the competitor salicylic acid in presence of ozone; orange: 0-6 µM ozone; black: 0-4.5 µM ozone; blue: 0-2 µM ozone. Temperature: 23 ± 2 °C. pH: 7.5 (5 mM phosphate buffer). Concentrations of TPs and competitor: 1 µM.

Estimation of second order rate constants with QSAR: Lee and von Gunten (2012) developed quantitative structure-activity relationships (QSARs) to predict second order rate constants for the reactions of ozone with e.g. phenols based on substituent descriptors (Hammett constants σ, σ^+, σ^-). For phenols (PhOH) and phenolates (PhO^-), Lee and von Gunten (2012) proposed the QSAR equations (SI4-16) and (SI4-17):

$$\log k_{O3}^{PhOH} = 3.53\ (\pm 0.25) - 3.24(\pm 0.69) \sum \sigma_{o,m,p}^{+} \quad \text{(SI4-16)}$$

$$\log k_{O3}^{PhO^-} = 8.80\ (\pm 0.16) - 2.27(\pm 0.30) \sum \sigma_{o,m,p}^{+} \quad \text{(SI4-17)}$$

Using the Hammett constants collected by Lee and von Gunten (2012) and references therein for the substituents of the phenolic chlorothalonil TPs (Table SI4-A12), second order rate constants were predicted (Table SI4-A13). The predicted rate constants for the dissociated phenolic TPs, which are the major form (> 99%) at pH 7.5 due to the low predicted pK_a values (4.1-4.7; JChem for Office, Version 17.1.2300.1455, ChemAxon Ltd.) were higher by a factor of 2.3-2.5 compared to the measured values. This is in the range of the uncertainties described by Lee and von Gunten (2012). The phenolic TP SYN548580-Ph was not investigated in laboratory experiments. The second-order rate constant predicted by QSAR was 2.9×10^5 $M^{-1}s^{-1}$.

Table SI4-A12: Hammett constants for ortho, meta and para position. *σ^+ values were not available and therefore replaced by σ values. σ^+ (vs. σ) accounts for resonance effects (Lee and von Gunten 2012).

Substituents	σ^+_o	σ^+_m	σ^+_p
-Cl	0.07	0.40	0.11
-CN	0.44	0.56	0.66
-CONH2	0.24*	0.28*	0.36*

Table SI4-A13: Substituents of the phenolic TPs, measured k_{O3} (pH 7.5) and predicted k_{O3} for the phenol (PhOH) and the dissociated phenol (PhO^-).

TP	ortho	meta	para	$\sum \sigma^+_{o,m,p}$	k_{O3} pH 7.5	k_{O3}^{PhOH}	$k_{O3}^{PhO^-}$
R611968-Ph	Cl, CONH2	Cl, Cl	CN	1.77	2.61×10^4	6.23×10^{-3}	6.10×10^4
SYN507900-Ph	Cl, CN	Cl, Cl	CONH2	1.67	4.14×10^4	1.33×10^{-2}	1.04×10^5
SYN548580-Ph	Cl, CONH2	Cl, Cl	CONH2	1.47		5.84×10^{-2}	2.92×10^5

SI4-A8: Advanced Oxidation Experiments with Sulfonic Acids

To generate sufficiently high $^{\cdot}OH$ concentrations, the relatively stable sulfonic acid TPs were exposed to ozone (0-80 µM) at pH ~10 (0.3 mM NaOH). It should be noted that R417888-SA was not completely stable at pH ~10, i.e. a slight formation of R471811-SA (2%) was observed (for each ozone dose, including the control without ozone addition). However, this did not affect the interpretation of the experiments because each sample (with corresponding ozone dose) was affected to the same extent.

Diatrizoic acid (k_{OH} 5.4 x 10^8 $M^{-1}s^{-1}$, Real et al. (2009)) was used as competitor. In addition, one experiment was performed in which the two TPs R471811-SA and R417888-SA were exposed to ozone (0-210 µM) together (R471811-SA as competitor instead of diatrizoic acid, Figure SI4-A5). The second order rate constants were calculated according to equation (SI4-18) and are summarized in Table SI4-A14:

$$\ln\left(\frac{[TP]_x}{[TP]_0}\right) = \frac{k_{OH}^{TP}}{k_{OH}^{competitor}} \ln\left(\frac{[competitor]_x}{[competitor]_0}\right) \quad \text{(SI4-18)}$$

The competitor diatrizoic acid reacts approximately ten times faster than the sulfonic acids, leading to higher uncertainties, but experiments conducted with both TPs together confirmed the results.

Table SI4-A14: Second order rate constants *k* calculated from experiments conducted with varying ozone doses.

TP	Competitor	$k_{competitor}$ in $M^{-1}s^{-1}$	$k_{target\ compound}$ in $M^{-1}s^{-1}$	**Reported $k_{target\ compound}$ in $M^{-1}s^{-1}$**
R471811-SA	Diatrizoic acid	5.4×10^8	$\sim 3.0 \times 10^7$	$< 5.0 \times 10^7$
R417888-SA	Diatrizoic acid	5.4×10^8	$\sim 1.7 \times 10^7$	$< 5.0 \times 10^7$
R417888-SA	R471811-SA	$\sim 3.0 \times 10^7$	$\sim 1.7 \times 10^7$	$< 5.0 \times 10^7$

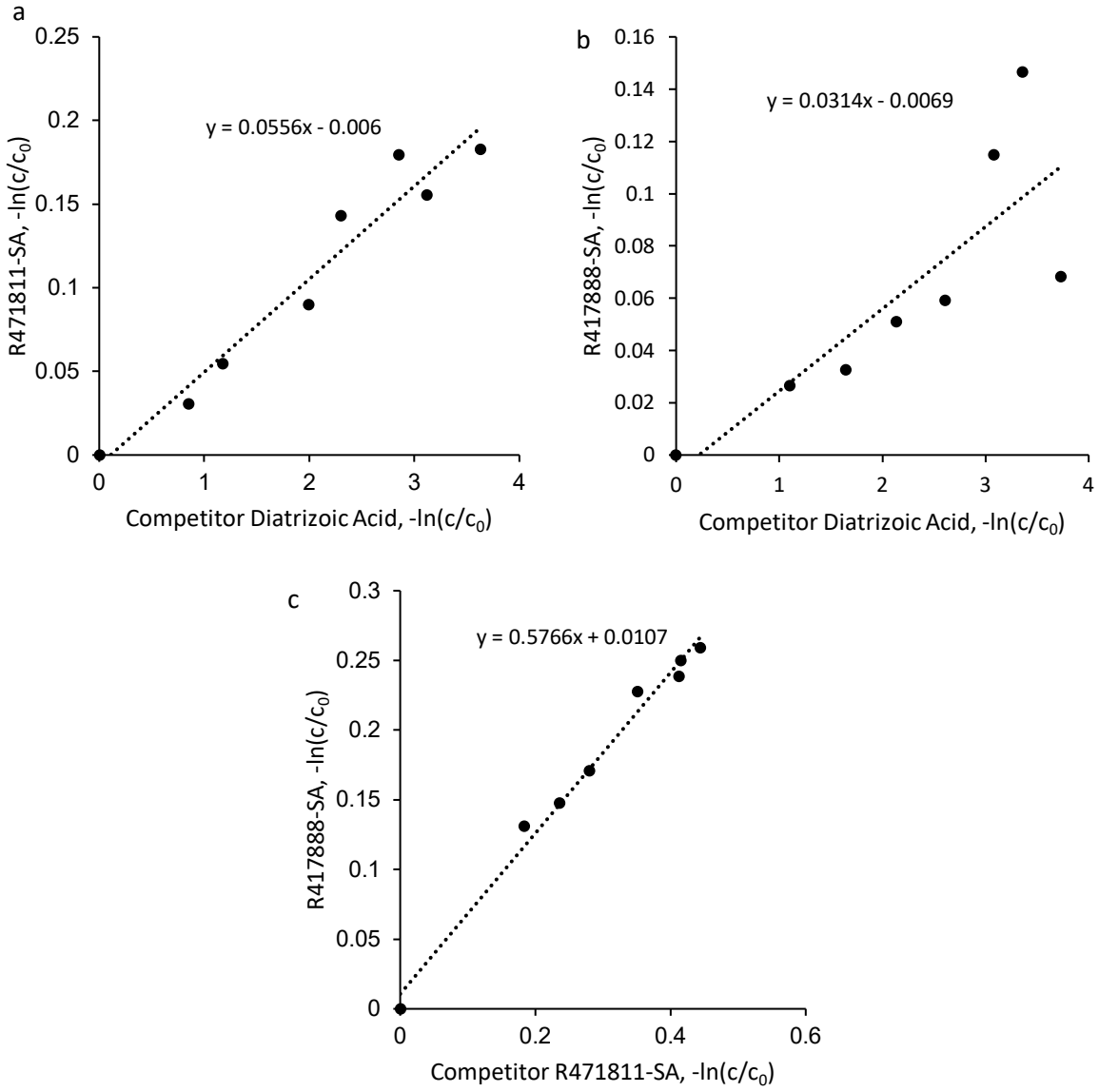

Figure SI4-A5: Competition kinetics plot (a, b) for the sulfonic acid TPs and the competitor diatrizoic acid and (c) for the two sulfonic acid TPs during ozonation at pH ~10 (reaction by ·OH). Temperature: 23 ± 2 °C. Concentration of TPs and competitor: 1 µM.

SI4-A9: Advanced Oxidation Experiments with Phenols

Degradation of the phenolic TPs by advanced oxidation was investigated using the UVA/H_2O_2 method. The phenolic TPs (0.1 µM) were exposed to UVA irradiation (350-410 nm, emission peak 367 nm, eight lamps) in a merry-go-round photoreactor (Rayonet, Southern New England Ultraviolet Company, Branford, USA) for 180 min together with the competitor benzoic acid (10 µM, $k_{OH} = 5.9 \times 10^9\ M^{-1}\ s^{-1}$, Buxton et al. (1988)) in presence of H_2O_2 (1 mM). In addition, the TPs were irradiated without H_2O_2 and benzoic acid to quantify direct photodegradation. Experiments were conducted in triplicate. Controls with H_2O_2 in the dark were stable, but the phenolic TPs were transformed during UVA irradiation in the absence of H_2O_2. The TP R611968-Ph was degraded faster by UVA/H_2O_2 than by UVA irradiation, whereas, the TP SYN507900-Ph was degraded approximately as fast by UVA irradiation as by UVA/H_2O_2 (Figure SI4-A6). Therefore, the second order rate constant k_{OH} could not be determined for SYN507900-Ph.

In case of R611968-Ph, first the degradation by ·OH was determined according to equation (SI4-19):

$$\frac{[TP]_t}{[TP]_{0\ \underset{Radicals}{OH}}} = 1 - \left(\frac{[TP]_t}{[TP]_{0\,UVA}} - \frac{[TP]_t}{[TP]_{0\,UVA/H2O2}} \right) \qquad \text{(SI4-19)}$$

where [TP] describes the concentration of R611968-Ph at different time points. Competition kinetics plots were generated by plotting the logarithmically normalized decrease of TPs, $\ln(C/C_0)$, against the logarithm of the relative residual concentration of benzoic acid and k_{OH}^{TP} was determined from the slope of the linear regression model:

$$\ln\left(\frac{[TP]_t}{[TP]_{0\ \underset{Radicals}{OH}}} \right) = \frac{k_{OH}^{TP}}{k_{OH}^{benzoic\ acid}} \ln\left(\frac{[benzoic\ acid]_t}{[benzoic\ acid]_0} \right) \qquad \text{(SI4-20)}$$

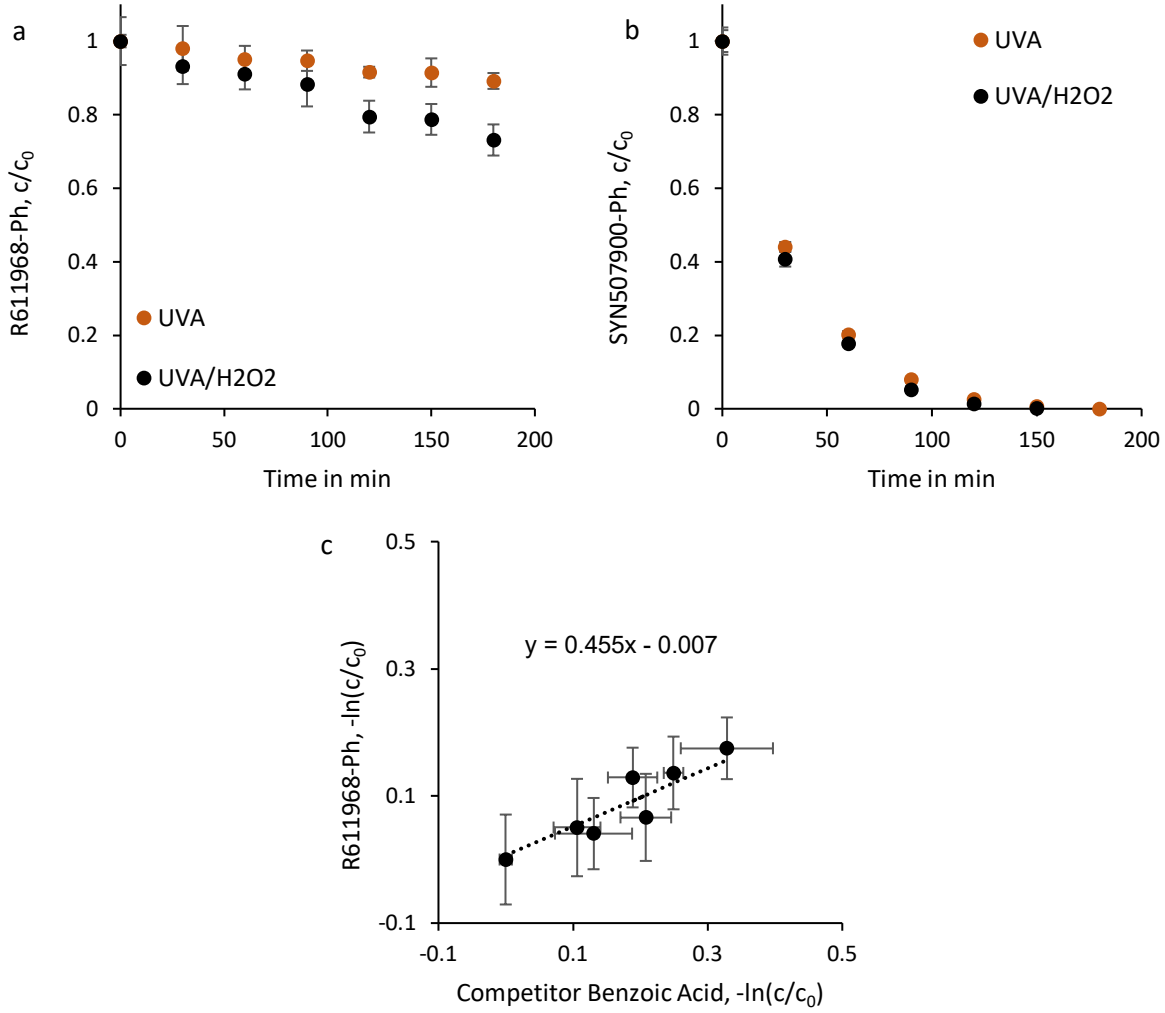

Figure SI4-A6: Degradation of (a) R611968-Ph and (b) SYN507900-Ph by UVA and UVA/H_2O_2. (c) Competition kinetics plot for R611968-Ph and the competitor benzoic acid in the UVA/H_2O_2 process ($^{\cdot}OH$). Degradation of R611968-Ph was corrected for abatement by UVA irradiation only. Error bars indicate the standard deviation of experimental triplicates. Temperature: 12 ± 2 °C. pH: 7.5 (5 mM phosphate buffer). Chlorothalonil TPs: 0.1 µM.

SI4-A10: Adsorption on Activated Carbon

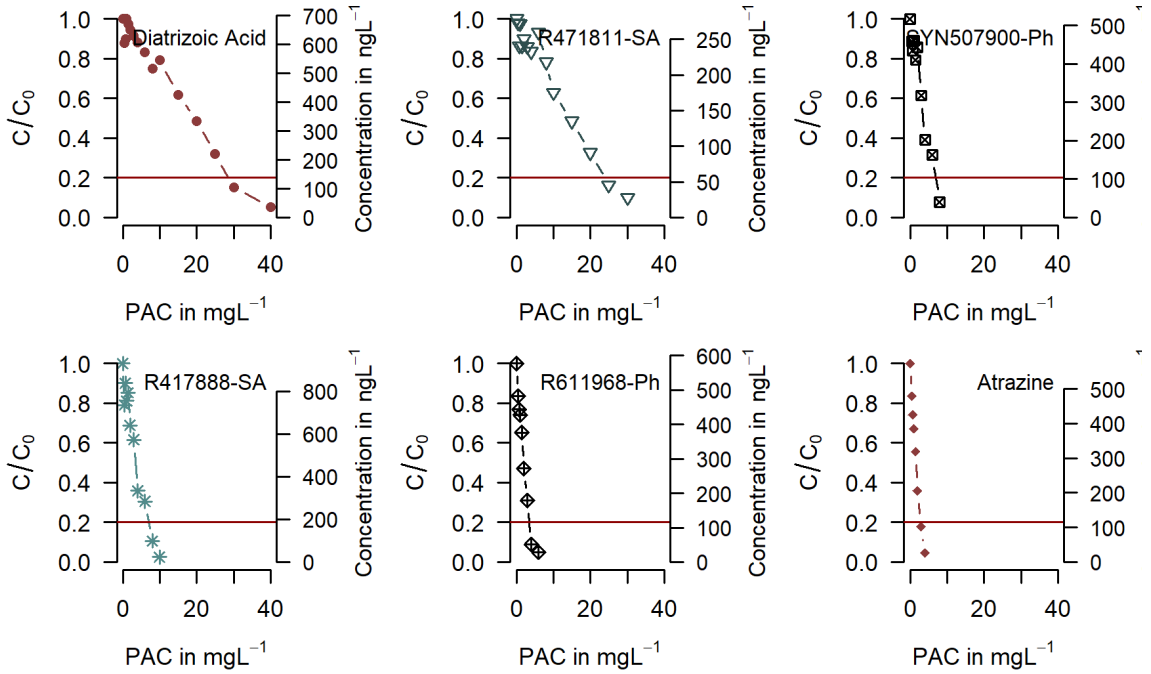

Figure SI4-A7: Abatement of chlorothalonil TPs, diatrizoic acid, and atrazine as a function of powdered activated carbon (PAC) dosed into natural groundwater (multi-component system) after 42 h. Red line marks 80% removal. Powdered activated carbon: Eurocarb CC PHO 8x30 produced from coconut shell. Temperature: 22 °C. Dissolved organic carbon content: 1.1 mgL^{-1}. Electrical conductivity: 840 μScm^{-1}.

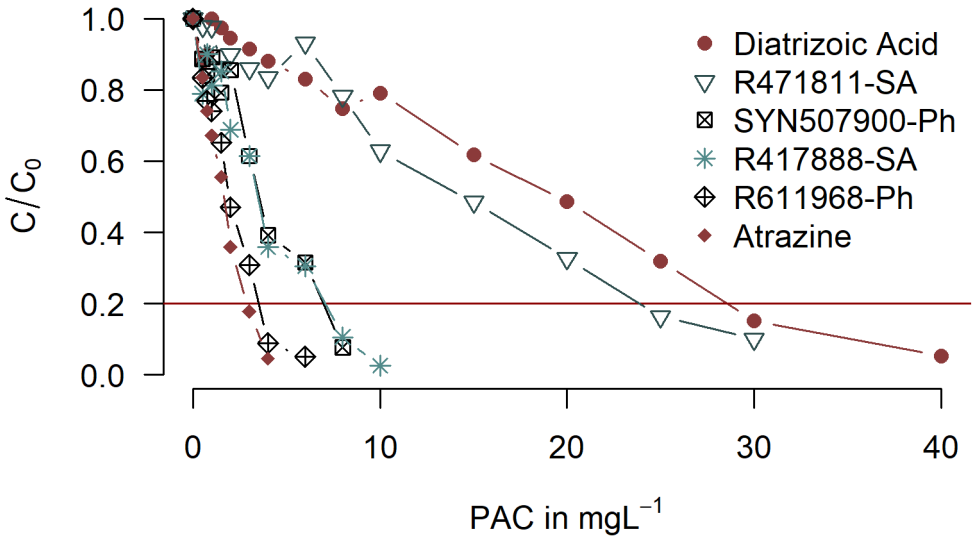

Figure SI4-A 8: Abatement of chlorothalonil TPs, diatrizoic acid, and atrazine by different powdered activated carbon (PAC) dosed into natural groundwater (multi-component system) after 42 h. Red line marks 80% removal. Powdered activated carbon: Eurocarb CC PHO 8x30. Temperature: 22 °C. Dissolved organic carbon content: 1.1 mgL^{-1}. Electrical conductivity: 840 μScm^{-1}.

SI4-A11: Confirmation of the R417888-SA isomer: SYN548581-SA

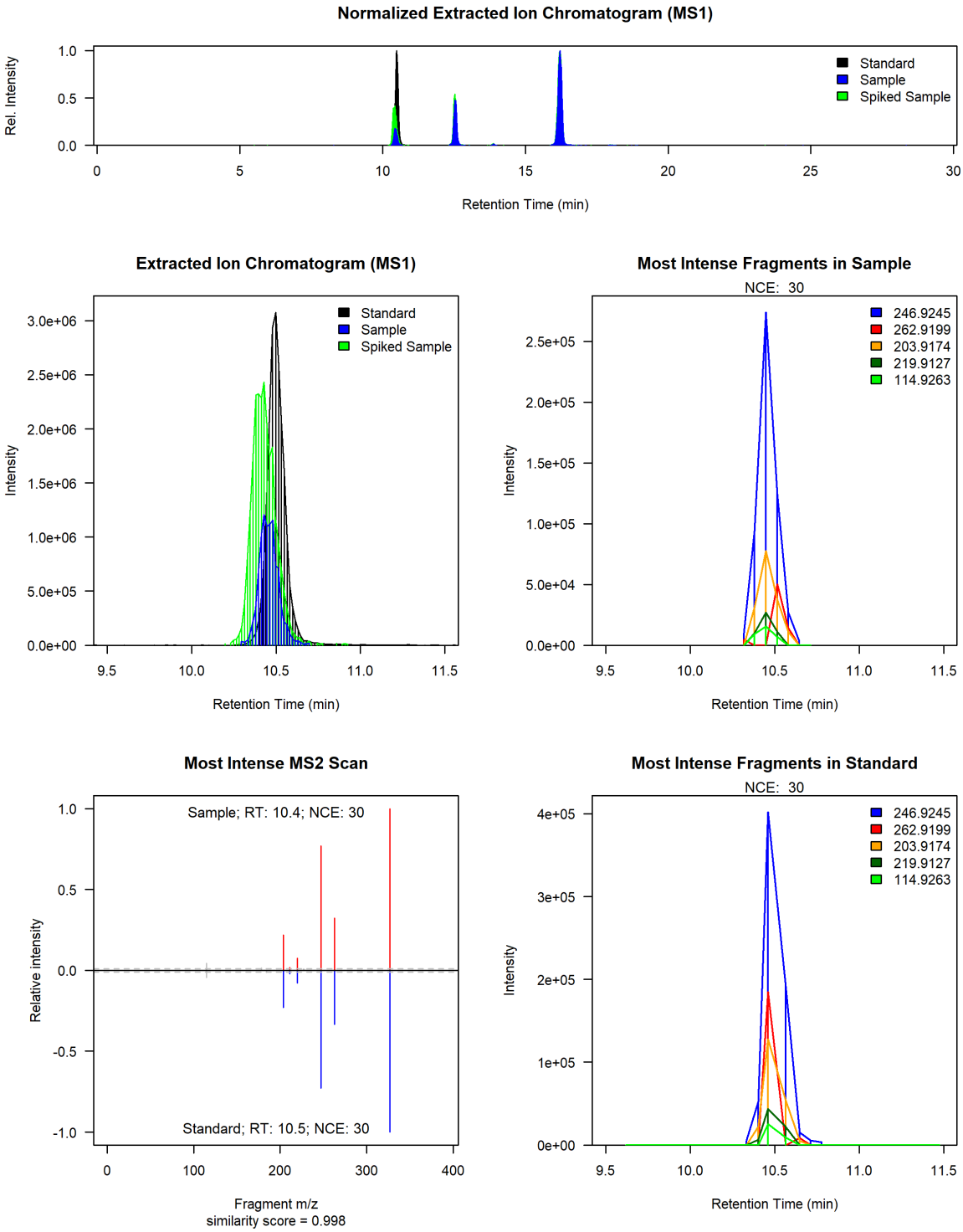

Figure SI4-A9: SYN548581 (isomer of R417888-SA) was confirmed with reference material. The normalized extracted ion chromatogram (m/z 326.88063, 5 ppm window) shows three chromatographic peaks in the sample (blue). The sample was spiked with SYN548581 (green) so that the first peak (retention time 10.5 min) was identified as SYN548581. MS/MS fragments confirm the identification. R417888-SA elutes at 16 min. The compound eluting at 12.5 min is assumed to be another isomer of R417888-SA, which so far could not be confirmed.

References

Bader, H. and Hoigné, J., 1981. Determination of ozone in water by the indigo method. Water research 15(4), 449-456.

Bahnmüller, S., Loi, C.H., Linge, K.L., Gunten, U. and Canonica, S., 2015. Degradation rates of benzotriazoles and benzothiazoles under UV-C irradiation and the advanced oxidation process UV/H2O2. Water Res 74, 143-154.

Buxton, G.V., Greenstock, C.L., Helman, W.P. and Ross, A.B., 1988. Critical Review of rate constants for reactions of hydrated electrons, hydrogen atoms and hydroxyl radicals (·OH/·O− in Aqueous Solution. 17(2), 513-886.

Canonica, S., Meunier, L. and von Gunten, U., 2008. Phototransformation of selected pharmaceuticals during UV treatment of drinking water.

Hessler, D.P., Gorenflo, V. and Frimmel, F.H., 1993. Degradation of Aqueous Atrazine and Metazachlor Solutions by UV and UV/H202 - Influence of pH and Herbicide Concentration. Acta hydrochimica et hydrobiologica 21(4), 209-214.

Hoigné, J. and Bader, H., 1983. Rate constants of reactions of ozone with organic and inorganic compounds in water—II: Dissociating organic compounds. Water research 17(2), 185-194.

Hoigné, J. and Bader, H., 1994. Characterization Of Water Quality Criteria for Ozonation Processes. Part II: Lifetime of Added Ozone. Ozone: Science & Engineering 16(2), 121-134.

Lee, Y. and von Gunten, U., 2012. Quantitative structure-activity relationships (QSARs) for the transformation of organic micropollutants during oxidative water treatment. Water Res 46(19), 6177-6195.

Nick, K., Schöler, H.F., Mark, G., Söylemez, T., Akhlaq, M.S., Schuchmann, H.-P. and Von Sonntag, C., 1992. Degradation of some triazine herbicides by UV radiation such as used in the UV disinfection of drinking water. J. Water Supply Res. Technol. Aqua 41(2), 82-87.

R Core Team, 2016. R: A language and environment for statistical computing. R Foundation for Statistical Computing, Vienna, Austria. https://www.R-project.org/.

Real, F.J., Benitez, F.J., Acero, J.L., Sagasti, J.J.P. and Casas, F., 2009. Kinetics of the Chemical Oxidation of the Pharmaceuticals Primidone, Ketoprofen, and Diatrizoate in Ultrapure and Natural Waters. Industrial & Engineering Chemistry Research 48(7), 3380-3388.

Schollée, J.E., 2018. TFAnalyzeR, version 1.0.1, Analysis of TraceFinder Target Screening, Zenodo, DOI: 10.5281/zenodo.3234748.

von Gunten, U. and Hoigne, J., 1994. Bromate Formation during Ozonization of Bromide-Containing Waters: Interaction of Ozone and Hydroxyl Radical Reactions. Environmental science & technology 28(7), 1234-1242.

von Sonntag, C. and von Gunten, U., 2012. Chemistry of Ozone in Water and Wastewater Treatment: From Basic Principles to Applications, IWA Publisher, London.

Chapter 5: Conclusions and Outlook

5.1 Comprehensive Screening for Micropollutants and its Limitations

This work contributed to a more comprehensive inventory of micropollutants (MPs) in groundwater, the major drinking water resource in Switzerland and many other countries. We assumed that polar and therefore mobile compounds, originating primarily from pesticide application and wastewater impacted surface waters, impair groundwater quality. In chapter 2, we specifically targeted **pesticides and their transformation products (TPs)** using target and suspect screening. This screening was, to our knowledge, the most comprehensive pesticide TP screening performed so far, including more than 300 pesticides and more than 1100 pesticide TPs, most of which had only previously been observed experimentally within the European pesticide registration. The suspect screening revealed 26 pesticide TPs (21 TPs unequivocally identified, Level 1; 5 TPs tentatively identified, Level 2/3); 13 of the 26 pesticide TPs have not previously been reported in groundwater. The TP R471811 of the fungicide chlorothalonil was the only contaminant detected in all samples, with concentrations ranging from 3 to 2700 ngL^{-1}. The widespread occurrence and high concentrations of R471811 and other chlorothalonil TPs were confirmed in chapter 4. The screening supported also previous observations that pesticide TPs often contribute far more to groundwater contamination than the parent pesticides (Buttiglieri et al. 2009, Kolpin et al. 1998).

In chapter 3, we expanded the screening to **MPs of urban origin**. Using a broad target screening, 60 monitoring sites were characterized with regard to their anthropogenic influence. Detected compounds were then classified regarding their potential origin based on their detection pattern in the samples. This classification approach indicated that many agricultural MPs might still be unknown. Unfortunately, it was not possible to determine if the investigated sites were more affected by agricultural or urban activities because many nontargets could not be unambiguously assigned to either urban or agricultural sources. The identification workflow, focusing on urban MPs, was highly automated, combining two in silico fragmentation tools, and resulted in 22 unequivocal (Level 1) and 18 tentative identifications (Level 2/3); 13 of these compounds have not previously been reported in environmental samples.

Although we were able to elucidate several compounds, still a substantial number of potential agricultural and urban MPs remained unknown, both in terms of absolute numbers of MPs and of estimated concentrations. On the one hand, the compound classification (chapter 3) might be erroneous; on the other hand, gaps in the presented groundwater screening are very likely, e.g. due to incomplete databases or issues related to analytics and data analysis, as described in the following.

Erroneous compound classification: For most of the identified compounds presented in chapter 3, their assigned classification corresponded to their expected usage, validating the classification approach. However, the number of elucidated compounds, which were used to evaluate the classification approach, was relatively small (40 elucidated compounds). The following aspects could also reduce the reliability of the classification. First, sample classification was based on a limited number of detected targets (52 urban targets, 87 agricultural targets), often with very low concentrations. Second, some of these targets, such as melamine, might originate from urban and agricultural sources; for classification, we used their pre-dominating source. Third, the number of monitoring sites with high urban but low agricultural influence was rather small. Fourth, we investigated only 60 monitoring sites due to the time-consuming enrichment and analysis (six injections per sample). A larger number of samples would probably increase the

reliability of this classification approach. Accordingly, we can assume that this classification approach is more reliable for compounds detected at many sites than for compounds detected at few sites. Therefore, our conclusions of still unknown groundwater contamination should be seen as estimations.

Gaps due to incomplete compound databases: Some pesticide TPs might have been overlooked because the suspect list with pesticide TPs was incomplete (chapter 2). For 26% of the pesticides approved from 2005 to 2017, no transformation data was available. In the case of the remaining pesticides, as for example metolachlor, the suspect list often included only few TPs. For the screening presented in chapter 3, we had further information about metolachlor TPs, and could tentatively identify six additional metolachlor TPs. One of these metolachlor TPs was among the 14 nontargets classified as potential agricultural MP and prioritized for elucidation due to a very high peak intensity and detection frequency. The remaining five metolachlor TPs were only found after searching the extracted ion chromatograms, demonstrating that suspect screening can be more sensitive than nontarget screening. This is especially true for suspect lists with a limited number of compounds, because the smaller number of compounds of interest means the analyst can also consider less intense peaks, often representing lower concentrations. The detection of additional metolachlor TPs highlights that the data collected within the pesticide registration is (i) extremely valuable for monitoring, but (ii) needs to be published in an easily accessible format and include all known TPs from pesticides approved in the past and present.

However, for other compounds such as pharmaceuticals or especially industrial chemicals, transformation data is very scarce or not available at all. Considering the high importance of pesticide TPs for groundwater quality, it is likely that TPs of other compound classes also play a major role. To address this gap, TPs can be assessed in laboratory experiments (Kormos et al. 2009, Schulz et al. 2008, Zahn et al. 2019), or TPs can be predicted using in silico prediction systems such as enviPath (Wicker et al. 2016). While the experimental approach is very time-consuming, it also provides high quality data. In contrast, prediction is fast but likely produces many false positives (Bletsou et al. 2015). In silico TP prediction was not used for the pesticide TP screening, as we had access to an extensive experimental, high-quality dataset (chapter 2.2.6.1), but might be valuable for other compound classes.

Gaps due to analytical reasons: The amount of MPs that were either not detected at all or not in sufficient quality (poor peak shape, low intensity) is unknown. These MPs likely consist of (i) very polar compounds and (ii) more hydrophobic/volatile compounds not captured by the enrichment and chromatography, (iii) compounds not ionizable/stable in ESI, and (iv) compounds with a mass <100 Da or >1000 Da. Compounds outside the analytical mass range can be tackled by an adapted MS method. Additional chromatographic approaches and enrichment methods might open the analytical window to very polar compounds or to more hydrophobic/volatile compounds. As discussed in chapter 1.2, ion-exchange chromatography (IC), hydrophilic interaction liquid chromatography (HILIC), supercritical fluid chromatography (SFC), or mixed mode liquid chromatography (MMLC) might capture very polar compounds. However, a generic approach for all very polar compounds does not currently appear to exist, as shown recently by a target screening study for 64 PMOCs using HILIC, SFC, MMLC, and reversed-phase (RP) LC (Schulze et al. 2019). More hydrophobic compounds could be covered by solid-phase extraction followed by RP columns, retaining less polar compounds, possibly

combined with atmospheric pressure chemical ionization. Liquid-liquid extraction and gas chromatography might be an option for even more hydrophobic/volatile compounds.

This work focused on polar compounds because polar compounds are likely to occur ubiquitously due to their high mobility, but it should be kept in mind that more hydrophobic/volatile compounds have also been reported in groundwater at high concentrations, probably due to high production volumes or contaminated sites (Postigo and Barcelo 2015). The combination of several chromatographic approaches can close some of the current analytical gaps, but be limited by time constraints and will challenge the subsequent data analysis workflow. To reduce structure elucidation efforts and to avoid overestimating the amount of unknown MPs, the overlap of compounds detected by several chromatographic approaches needs to be determined, which might be difficult due to differences in retention time and adduct formation (Erngren et al. 2019).

Gaps due to data analysis issues: Using two in silico fragmenters in an automated way for structure annotation proved to be very useful for identification (chapter 3). However, many nontargets were not pursued with reference material because of (i) the lack of reference material, (ii) the large number of annotated candidates (partially with similar structure), and/or (iii) contradicting results from the two in silico fragmenters. Contradicting results point to the different strengths of the two in silico fragmenters. Whereas SIRIUS4/CSI:FingerID has been shown to clearly outperform MetFrag if evaluated only based on in silico prediction, MetFrag results can be significantly improved by using metadata such as reference counts in databases (Dührkop et al. 2019, Schymanski et al. 2017). Possibly, identification could be further supported by using additional in silico fragmentation tools such as CFM-ID (Allen et al. 2014) or MS-Finder (Tsugawa et al. 2016), as was shown in the CASMI (Critical Assessment of Small Molecule Identification) Contest (Schymanski et al. 2017). However, these software are only capable of proposing structures that are present in the used databases.

So far, structure annotation was based only on one MS/MS spectrum, i.e. the MS/MS scan triggered closest to the peak apex and in the sample with highest precursor intensity. Alternatively, all MS/MS spectra triggered for the precursor within the measurement sequence could be combined keeping only fragments, which were reproducibly measured. This may increase the confidence in the quality of the MS/MS spectrum.

Structure annotation depended not only on a single MS/MS spectrum but also on the assumption that the nontarget compound is represented by the (de)protonated molecular ion. The enviMass workflow (envibee GmbH, Switzerland) groups peaks originating from the same compound (i.e. isotopologues, adducts, in-source fragments) based on intensity and peak shape correlations and resolution-dependent mass differences within a sample and across samples. The grouped peaks (in chapter 3, called profile or compound) are then represented by the species with highest intensity, whereby enviMass provides a suggestion of which species it is, based on mass differences within the peak group. However, for some targets this suggestion was incorrect, demonstrating that peak relationships often are ambiguous, i.e. many peaks can be linked to various peak groups. Due to the uncertainty of the true nature of the species and to facilitate automation in structure annotation, we assumed that the compound was represented by the (de)protonated molecular ion, which might have led in some cases to no or incorrect annotations. Accordingly, a wrongly annotated nontarget was finally elucidated as $[M+Cl]^-$ of the target compound sucralose (see chapter 3, SI3-A9).

The formation of salt/solvent adducts and in-source fragments depends on various factors such as sample matrix, enrichment method, eluents, ionization conditions, or structure (Broeckling et al. 2016, Lynn et al. 2015) and might explain a substantial proportion of detected peaks (Domingo-Almenara et al. 2019). Therefore, a reliable peak grouping is essential to exclude an overestimation of detected compounds in groundwater. To assess if peak grouping was sufficient, the final compound table could be screened for all known species possibly formed by the target compounds, i.e. adducts, isotopologues, and in-source fragments. In-source fragments usually are unknown, but MS/MS fragments, detected at low collision energy, have also been observed in the MS1 scan (Domingo-Almenara et al. 2019) and can alternatively be used to provide an estimate of the number of redundantly reported compounds. Furthermore, the annotated peak groups could be analysed in detail, to make estimates on the extent of in-source fragmentation and adduct formation. Broeckling et al. (2016) suggested that not only in-source fragmentation but also adduct formation is related to the chemical structure, and could be used to support structure elucidation.

5.2 Chlorothalonil TPs: Widespread and Challenging to Abate

As a consequence of the re-evaluation of chlorothalonil in the European Union (EU), the European Commission (2019) recommended that chlorothalonil be classified as a carcinogen category 1B. Switzerland followed this recommendation and subsequently declared all TPs as relevant, implying a drinking water standard of 100 ngL^{-1} (EDI 2016). In chapter 4, we showed the widespread occurrence of chlorothalonil TPs in Swiss groundwater. In 40 of 73 groundwater samples, at least one chlorothalonil TP exceeded 100 ngL^{-1}. The sulfonic acid TPs (R471811, R419492, R417888) were detected more frequently and at higher concentrations than the phenolic TPs (SYN507900, SYN548580, R611968). Not only could the occurrence of chlorothalonil TPs in groundwater be related to their structural class (sulfonic acid TPs, phenolic TPs), but also the fate in water treatment was linked to the TP structure. Whereas the phenolic TPs could be (partially) abated by UV disinfection, ozonation, and advanced oxidation processes (AOPs), the sulfonic acid TPs were persistent in these treatment processes under typical conditions. Activated carbon and reverse osmosis were found to abate all TPs. However, activated carbon needs to be exchanged or regenerated very frequently to sufficiently abate the TP with highest concentrations (R471811) and the reverse osmosis produces large volumes of reject water.

Under environmentally relevant pH values, the investigated chlorothalonil TPs are anionic (chapter 4). Therefore, further investigations might include anion exchange filters, either for direct treatment of the raw water or as post-treatment of the reject water from membrane filtration, as suggested for perfluoroalkyl substances (Franke et al. 2019). The anion exchange filters can then be incinerated to avoid the disposal of reject water to surface waters. As an alternative to reverse osmosis, nanofiltration with a small molecular weight cutoff (<300-400) could be considered, as it requires less energy and is therefore more cost-efficient (Garg and Joshi 2014, Taheran et al. 2016). Upgrading water treatment plants with the discussed treatment techniques is associated both with high ecological and economic burdens. Therefore, the treatment processes should be compared based on multiple criteria, including installation and operational costs, energy consumption, and ecological and social impacts related to activated carbon production and reject water disposal (Joseph et al. 2020, Teodosiu et al. 2018).

Although chlorothalonil has been recently banned in Europe, the TPs may persist for years or decades in the environment. However, decisions on upgrading water treatment or investigating alternative water resources require a better understanding of the long-term fate of chlorothalonil TPs. As discussed in chapter 4, compound concentrations over time in the respective aquifer depends on various factors such as the amount of chlorothalonil applied in the catchment, exact dissipation time, groundwater residence time, groundwater recharge rate, and dilution with up gradient groundwater. In soil, chlorothalonil is transformed relatively fast (DT_{50} 7.4-28 days) forming highly persistent TPs (DT_{50} >62-1000 days, Figure 2.2). Therefore, the crucial question is how fast are the TPs "washed out" of the system, i.e. the unsaturated and saturated zone. A key parameter determining this "wash out" time is transport; the faster TPs are transported, the faster TPs will leave the system. As hypothesized in chapter 4, transport velocity or residence time might be reflected in the concentration ratio between TP R471811 and its precursor TP, R417888, i.e. the higher the TP ratio, the higher the residence time, and the slower the transport. Similar suggestions were made for atrazine and its TP atrazine-desethyl (Adams and Thurman 1991, Lerch et al. 2018). The underlying assumptions are that with increasing residence time, (i) more R417888 is transformed to R471811 (primarily in the microbiologically active topsoil) and (ii) the less polar R417888 is more strongly retained compared to R471811 due to sorption during transport through the unsaturated and saturated zone. Accordingly, a large TP ratio would mean a slow "wash out" and slow concentration decline and a small TP ratio would mean a fast "wash out" and fast concentration decline. However, this might be superseded by other factors such as different formation rates of TPs from site to site, e.g. due to different microbial activity. These hypotheses could be investigated at selected monitoring sites with a wide range of TP ratios. Monthly sampling would show how much the TP ratios fluctuate. Furthermore, the catchments would need to be characterized including size, historical application amounts of chlorothalonil, and soil and sediment characteristics (e.g. particle size distribution, organic carbon content). Soil column experiments in the laboratory and numerical modelling could complement field investigations. The long-term monitoring will finally show if pesticide TP ratios can be used as a predictor for concentration decline.

5.3 Practical Implications and General Outlook

By combining target, suspect, and nontarget screening approaches, this work presented a much more comprehensive picture of groundwater quality regarding polar MPs compared to classical routine monitoring efforts. Furthermore, the screening drew attention to several widespread and novel MPs in the research community and public. The presented concentration data for more than 500 MPs including novel identified compounds are highly valuable to authorities and water suppliers to revise and complement their monitoring programs. In addition, the applied workflows can act as an example for commercial laboratories and water suppliers, supporting the implementation of broad screenings in the practice. To facilitate future monitoring efforts in research and practice, MS/MS spectra of novel MPs were uploaded to the European MassBank (Horai et al. 2010, Schulze et al. 2012), all collected pesticide TP structures were made available in an easily accessible format (Kiefer et al. 2020) and were added to the online database PubChem (Kim et al. 2019), if not yet included.

Major drivers of groundwater contamination were several TPs of the pesticides chlorothalonil, chloridazon, metolachlor, atrazine, terbuthylazine, and nicosulfuron, the parent pesticides bentazone and atrazine, the biocide or pesticide TP N,N-dimethylsulfamide, the sweetener acesulfame, the industrial chemicals 2,5-dichlorobenzenesulfonic acid, benzotriazole, and 4/5-methyl-benzotriazole, the pharmaceutical TP oxypurinol, and trifluoroacetic acid, a pollutant with multiple sources (all ≥100 ngL^{-1} and detections in >30% of samples). Some of the pesticides mentioned have been banned in Switzerland and the EU (i.e. chlorothalonil, chloridazon, atrazine).

However, this work also demonstrated that many MPs in groundwater probably remain unknown. Despite enormous progress in the automation of data processing within the last years, structure elucidation remains a major bottleneck and identification of all detected compounds is unfeasible. This raises the question, if other prioritization strategies need to be included, e.g. using effect-directed analysis to focus elucidation efforts more on toxicologically relevant MPs. In effect-directed analysis, the sample is first fractionated by a chromatographic approach and in a next step, the individual fractions are tested for their toxic potential. In this way, structure elucidation can be limited to toxicologically relevant fractions (Brack et al. 2016). However, the selection of appropriate toxicity tests remains a challenge, since any selected bioassay will probably not cover all potential effects of each compound, so that some toxicologically relevant MPs might still be overlooked.

The example of chlorothalonil illustrated that (i) the relevance evaluation in the regulatory context can suddenly change and (ii) that MP abatement in water treatment can be highly challenging and can sometimes lead to new problems. Further progress in analytics will likely reveal more and more MPs in the water cycle. Compounds, considered today as not posing severe risks, might be evaluated differently in the future due to new insights in the effects of MPs on ecosystems and human health. Therefore, precautionary measures to effectively prevent the release of chemicals into the environment are crucial to preserving groundwater resources.

References

Adams, C.D. and Thurman, E.M., 1991. Formation and Transport of Deethylatrazine in the Soil and Vadose Zone. Journal of Environmental Quality 20(3), 540-547.

Allen, F., Greiner, R. and Wishart, D., 2014. Competitive fragmentation modeling of ESI-MS/MS spectra for putative metabolite identification. Metabolomics 11(1), 98-110.

Bletsou, A.A., Jeon, J., Hollender, J., Archontaki, E. and Thomaidis, N.S., 2015. Targeted and non-targeted liquid chromatography-mass spectrometric workflows for identification of transformation products of emerging pollutants in the aquatic environment. TrAC Trends in Analytical Chemistry 66, 32-44.

Brack, W., Ait-Aissa, S., Burgess, R.M., Busch, W., Creusot, N., Di Paolo, C., Escher, B.I., Mark Hewitt, L., Hilscherova, K., Hollender, J., Hollert, H., Jonker, W., Kool, J., Lamoree, M., Muschket, M., Neumann, S., Rostkowski, P., Ruttkies, C., Schollée, J., Schymanski, E.L., Schulze, T., Seiler, T.B., Tindall, A.J., De Aragao Umbuzeiro, G., Vrana, B. and Krauss, M., 2016. Effect-directed analysis supporting monitoring of aquatic environments--An in-depth overview. Sci Total Environ 544, 1073-1118.

Broeckling, C.D., Ganna, A., Layer, M., Brown, K., Sutton, B., Ingelsson, E., Peers, G. and Prenni, J.E., 2016. Enabling Efficient and Confident Annotation of LC-MS Metabolomics Data through MS1 Spectrum and Time Prediction. Anal Chem 88(18), 9226-9234.

Buttiglieri, G., Peschka, M., Fromel, T., Muller, J., Malpei, F., Seel, P. and Knepper, T.P., 2009. Environmental occurrence and degradation of the herbicide n-chloridazon. Water research 43(11), 2865-2873.

Domingo-Almenara, X., Montenegro-Burke, J.R., Guijas, C., Majumder, E.L., Benton, H.P. and Siuzdak, G., 2019. Autonomous METLIN-Guided In-source Fragment Annotation for Untargeted Metabolomics. Anal Chem.

Dührkop, K., Fleischauer, M., Ludwig, M., Aksenov, A.A., Melnik, A.V., Meusel, M., Dorrestein, P.C., Rousu, J. and Bocker, S., 2019. SIRIUS 4: a rapid tool for turning tandem mass spectra into metabolite structure information. Nat Methods 16(4), 299-302.

EDI, 2016. Swiss regulation No. 817.022.11 concerning drinking water and water in public swimming pools and shower facilities (Verordnung des EDI über Trinkwasser sowie Wasser in öffentlich zugänglichen Bädern und Duschanlagen (TBDV) vom 16. Dezember 2016 (Stand am 1. Mai 2018)), Eidgenössisches Departement des Innern.

Erngren, I., Haglof, J., Engskog, M.K.R., Nestor, M., Hedeland, M., Arvidsson, T. and Pettersson, C., 2019. Adduct formation in electrospray ionisation-mass spectrometry with hydrophilic interaction liquid chromatography is strongly affected by the inorganic ion concentration of the samples. J Chromatogr A 1600, 174-182.

European Commission, 2019. Commission implementing regulation (EU) 2019/677 of 29 April 2019 concerning the non-renewal of the approval of the active substance chlorothalonil, in accordance with Regulation (EC) No 1107/2009 of the European Parliament and of the Council concerning the placing of plant protection products on the market, and amending Commission Implementing Regulation (EU) No 540/2011. Official Journal of the European Union.

Franke, V., McCleaf, P., Lindegren, K. and Ahrens, L., 2019. Efficient removal of per- and polyfluoroalkyl substances (PFASs) in drinking water treatment: nanofiltration combined with active carbon or anion exchange. Environmental Science: Water Research & Technology 5(11), 1836-1843.

Garg, M.C. and Joshi, H., 2014. Optimization and economic analysis of small scale nanofiltration and reverse osmosis brackish water system powered by photovoltaics. Desalination 353, 57-74.

Horai, H., Arita, M., Kanaya, S., Nihei, Y., Ikeda, T., Suwa, K., Ojima, Y., Tanaka, K., Tanaka, S., Aoshima, K., Oda, Y., Kakazu, Y., Kusano, M., Tohge, T., Matsuda, F., Sawada, Y., Hirai, M.Y., Nakanishi, H., Ikeda, K., Akimoto, N., Maoka, T., Takahashi, H., Ara, T., Sakurai, N., Suzuki, H., Shibata, D., Neumann, S., Iida, T., Tanaka, K., Funatsu, K., Matsuura, F., Soga,

T., Taguchi, R., Saito, K. and Nishioka, T., 2010. MassBank: a public repository for sharing mass spectral data for life sciences. Journal of Mass Spectrometry 45(7), 703-714.

Joseph, B., Kaetzl, K., Hensgen, F., Schäfer, B. and Wachendorf, M., 2020. Sustainability assessment of activated carbon from residual biomass used for micropollutant removal at a full-scale wastewater treatment plant. Environmental Research Letters 15(6).

Kiefer, K., Müller, A., Singer, H. and Hollender, J., 2020. S60 | SWISSPEST19 | Swiss Pesticides and Metabolites from Kiefer et al 2019 (Version S60.0.1.1) [Data set], Zenodo. http://doi.org/10.5281/zenodo.3766352.

Kim, S., Chen, J., Cheng, T., Gindulyte, A., He, J., He, S., Li, Q., Shoemaker, B.A., Thiessen, P.A., Yu, B., Zaslavsky, L., Zhang, J. and Bolton, E.E., 2019. PubChem 2019 update: improved access to chemical data. Nucleic Acids Res 47(D1), D1102-D1109.

Kolpin, D.W., Thurman, E.M., Linhart, S.M.J.A.o.E.C. and Toxicology, 1998. The Environmental Occurrence of Herbicides: The Importance of Degradates in Ground Water. 35(3), 385-390.

Kormos, J.L., Schulz, M., Wagner, M. and Ternes, T.A., 2009. Multistep Approach for the Structural Identification of Biotransformation Products of Iodinated X-ray Contrast Media by Liquid Chromatography/Hybrid Triple Quadrupole Linear Ion Trap Mass Spectrometry and 1H and 13C Nuclear Magnetic Resonance. Analytical chemistry 81(22), 9216-9224.

Lerch, R.N., Groves, C.G., Polk, J.S., Miller, B.V. and Shelley, J., 2018. Atrazine Transport through a Soil-Epikarst System. J Environ Qual 47(5), 1205-1213.

Lynn, K.S., Cheng, M.L., Chen, Y.R., Hsu, C., Chen, A., Lih, T.M., Chang, H.Y., Huang, C.J., Shiao, M.S., Pan, W.H., Sung, T.Y. and Hsu, W.L., 2015. Metabolite identification for mass spectrometry-based metabolomics using multiple types of correlated ion information. Anal Chem 87(4), 2143-2151.

Postigo, C. and Barcelo, D., 2015. Synthetic organic compounds and their transformation products in groundwater: occurrence, fate and mitigation. Science of The Total Environment 503-504, 32-47.

Schulz, M., Loffler, D., Wagner, M. and Ternes, T.A., 2008. Transformation of the X-ray contrast medium iopromide in soil and biological wastewater treatment. Environ Sci Technol 42(19), 7207-7217.

Schulze, S., Zahn, D., Montes, R., Rodil, R., Quintana, J.B., Knepper, T.P., Reemtsma, T. and Berger, U., 2019. Occurrence of emerging persistent and mobile organic contaminants in European water samples. Water Res 153, 80-90.

Schulze, T., Schymanski, E., Stravs, M.A., Neumann, S., Krauss, M., Singer, H., Hug, C., Gallampois, C.M., Hollender, J., Slobodnik, J. and Brack, W., 2012. NORMAN MassBank: Towards a community-driven, open-access accurate mass spectral database for the identification of emerging pollutants. Norman Network Bulletin, www.norman-network.net (3), 9-11.

Schymanski, E.L., Ruttkies, C., Krauss, M., Brouard, C., Kind, T., Dührkop, K., Allen, F., Vaniya, A., Verdegem, D., Böcker, S., Rousu, J., Shen, H., Tsugawa, H., Sajed, T., Fiehn, O., Ghesquière, B. and Neumann, S., 2017. Critical Assessment of Small Molecule Identification 2016: automated methods. Journal of Cheminformatics 9(1).

Taheran, M., Brar, S.K., Verma, M., Surampalli, R.Y., Zhang, T.C. and Valero, J.R., 2016. Membrane processes for removal of pharmaceutically active compounds (PhACs) from water and wastewaters. Sci Total Environ 547, 60-77.

Teodosiu, C., Gilca, A.-F., Barjoveanu, G. and Fiore, S., 2018. Emerging pollutants removal through advanced drinking water treatment: A review on processes and environmental performances assessment. Journal of Cleaner Production 197, 1210-1221.

Tsugawa, H., Kind, T., Nakabayashi, R., Yukihira, D., Tanaka, W., Cajka, T., Saito, K., Fiehn, O. and Arita, M., 2016. Hydrogen Rearrangement Rules: Computational MS/MS Fragmentation and Structure Elucidation Using MS-FINDER Software. Anal Chem 88(16), 7946-7958.

Wicker, J., Lorsbach, T., Gutlein, M., Schmid, E., Latino, D., Kramer, S. and Fenner, K., 2016. enviPath--The environmental contaminant biotransformation pathway resource. Nucleic Acids Res 44(D1), D502-508.

Zahn, D., Mucha, P., Zilles, V., Touffet, A., Gallard, H., Knepper, T.P. and Fromel, T., 2019. Identification of potentially mobile and persistent transformation products of REACH-registered chemicals and their occurrence in surface waters. Water Res 150, 86-96.

Acknowledgements

Mein besonderer Dank richtet sich an Juliane Hollender, für ihre Offenheit Grundwasser zu screenen statt Biota, wie anfänglich angedacht, für ihre hervorragende Unterstützung während der vergangenen vier Jahre und ihre gelassene und offene Art, die ich sehr geschätzt habe. Ausserdem danke ich Heinz Singer für kritische Fragen und den etwas anderen Blickwinkel. Weiterhin möchte ich Urs von Gunten danken, ohne dessen Unterstützung die Untersuchung des Verhaltens der Chlorothalonil-TPs in der Wasseraufbereitung so nicht möglich gewesen wäre sowie für das Begutachten dieser Dissertation. Zudem danke ich Bernhard Wehrli und Thorsten Reemtsma für ihr Interesse am Thema sowie ihre Bereitschaft diese Arbeit zu begutachten.

Weiterhin danke ich all denjenigen, die auf irgendeine Weise zum Gelingen dieser Arbeit beigetragen haben: Miriam Reinhardt und Ronald Kozel, welche das Projekt von Seiten des BAFUs begleitet haben; den zahlreichen Personen, die an der Probenahme beteiligt waren; Adrian Müller, Nora Minas, Letian Du und Benedikt Lauper, die als wissenschaftliche Assistenten oder Masterstudenten mich bei der Laborarbeit tatkräftig unterstützt und zahlreiche Peaks begutachtet haben; Philipp Longrée für die detaillierte Einführung am Messgerät und Support in vielerlei Hinsicht; Bernadette Vogler und Birgit Beck für die kompetenten Auskünfte bei mancherlei Fragen; Elisabeth Salhi für die Durchführung der Ozon-Versuche; Elisabeth Janssen für die Unterstützung bei den Photochemie-Versuchen; Tobias Bader für die Durchführung der Aktivkohle-Versuche und den Austausch zu manchem Spurenstoff; Jennifer Schollée für die zahlreichen Hilfestellungen im Bereich Nontarget-Screening und das Korrekturlesen (fast) meiner gesamten Diss; Michael Stravs für den Austausch zu Datenauswertungsfragen; Emma Schymanski für ihre Unterstützung beim Zusammenstellen verschiedener Substanzlisten; Martin Loss für die Hilfe mit enviMass.

Besonders positiv bleibt mir die gute Atmosphäre in der Abteilung Uchem in Erinnerung, die vielen Apéros, die gemeinsamen Mittags- und Kaffeepausen, die Ausflüge mit Skiern oder Wanderschuhen (in Zeiten vor Corona). Zudem erinnere ich mich gerne an die gemeinsame Bürozeit mit Urs, Nicole und anderen, an die FlyAware-Aktion mit Philipp, Andrea und anderen, an die Sekt- und Schwimmabende mit Andrea, an die meist sehr ironiereichen Unterhaltungen mit Jonas, die vielen Gespräche mit Philipp, den Austausch mit Stefan bezüglich aufregender Wanderungen…

Zuletzt möchte ich mich bei verschiedenen Menschen bedanken, die mein Leben ausserhalb der Eawag begleitet haben: Zunächst den Göks für die lustigen Mädelsrunden in Stuttgart und Karlsruhe; Andreas für seine kleinen und grossen Ratschläge sowie seine exzellente Einführung ins Freizeitparadies Schweiz; Tobias, der auf halber Strecke hinzugestossen ist und mein Leben in vielerlei Hinsicht bunter gemacht hat; und schliesslich meinen Eltern, Hedwig und Erich, auf deren Unterstützung ich stets zählen konnte.

Karin Kiefer

Date of Birth: 25th October 1989
Nationality: German

Education

12/2016 – 12/2020	Doctoral candidate Swiss Federal Institute of Aquatic Science and Technology (Eawag), Department of Environmental Chemistry, Dübendorf, Switzerland; Institute of Biogeochemistry and Pollutant Dynamics, ETH Zurich, Switzerland
10/2013 – 11/2016	Geoecology, Master of Science (Geoökologie M.Sc.) Karlsruhe Institute of Technology (KIT), Germany
10/2010 – 09/2013	Geoecology, Bachelor of Science (Geoökologie B.Sc.) Karlsruhe Institute of Technology (KIT), Germany
07/2009	Abitur Theodor-Heuss-Gymnasium, Schopfheim, Germany

Practical Experiences

04/2014 – 08/2014	Intern at Agency for the Environment and Energy, Basel-City, Switzerland Department of Water and Soil / Section Groundwater
10/2013 – 02/2014	Intern at University of Queensland, Brisbane, Australia Centre for Mined Land Rehabilitation (CMLR)
09/2009 – 07/2010	Voluntary service at a daycare facility for children Hogar de Tablada, Lima, Peru